CRANFIELD UNIVERSITY

SCHOOL OF ENGINEERING

COLLEGE OF AERONAUTICS

"DESIGN METHODOLOGY FOR WING TRAILING EDGE DEVICE MECHANISMS"

RUI MIGUEL MARTINS PIRES

PhD Thesis

April 2007

CRANFIELD UNIVERSITY

SCHOOL OF ENGINEERING

COLLEGE OF AERONAUTICS

PhD Thesis

RUI MIGUEL MARTINS PIRES

"DESIGN METHODOLOGY FOR WING TRAILING EDGE DEVICE MECHANISMS"

Supervisor: Prof. John Fielding

April 2007

This thesis is submitted in partial fulfilment of the requirements for the degree of Doctor of Philosophy

Guidance on the Future Use of this Thesis

"This thesis has been assessed as a satisfactory standard for the award of a Doctor of Philosophy degree in Aerospace Engineering. Readers must be aware that the work contained is not necessarily 100% correct, and caution should be exercised if this thesis, or data it contains, is used for future work. If in doubt, please refer to the supervisor named in the thesis, or the Department of Aerospace Technology"

Abstract

Over the last few decades the design of high lift devices has become a very important part of the total aircraft design process. Reviews of the design process are performed on a regular basis, with the intent to improve and optimize the design process.

This thesis describes a new and innovative methodology for the design and evaluation of mechanisms for Trailing Edge High-Lift devices. The initial research reviewed existing High-Lift device design methodologies and current flap systems used on existing commercial transport aircraft. This revealed the need for a design methodology that could improve the design process of High-Lift devices, moving away from the conventional "trial and error" design approach, and cover a wider range of design attributes. This new methodology includes the use of the innovative design tool called SYNAMEC. This is a state-of-the-art engineering design tool for the synthesis and optimizations of aeronautical mechanisms. The new multidisciplinary design methodology also looks into issues not usually associated with the initial stages of the design process, such as Maintainability, Reliability, Weight and Cost.

The availability of the SYNAMEC design tool and its ability to perform Synthesis and Optimization of mechanisms led to it being used as an important module in the development of the new design methodology. The SYNAMEC tool allows designers to assess more mechanisms in a given time than the traditional design methodologies.

A validation of the new methodology was performed and showed that creditable results were achieved.

A case study was performed on the ATRA – Advance Transport Regional Aircraft, a Cranfield University design project, to apply the design methodology and select from within a group of viable solutions the most suitable type of mechanism for the Variable Camber Wing concept initially defined for the aircraft. The results show that the most appropriate mechanism type for the ATRA Variable Camber Wing is the Link /Track Mechanism. It also demonstrated how a wide range of design attributes can now be considered at a much earlier stage of the design.

Keywords:

High-Lift device, flap, mechanism, aircraft, maintainability, reliability, cost estimation, weight estimation, fairing drag, design methodology, variable camber.

Acknowledgements

The author would like to express his gratitude to his supervisor, Professor **John Fielding**, for his guidance and useful comments during the development and preparation of this thesis.

Many thanks to Mr **Vincent Lajux** and Mr **Otsin Nilubol**, my office colleagues, for their friendship and support.

My gratitude goes to my amazing wife **Cristina** and my beautiful children **Catarina** and **Miguel** for their patient and never ending supply of love and encouragement.

And finally, I would also like to thank my parents and brothers for their encouragement and support. For always being there and never letting me slip.

Table of Contents

List of Figures

List of Tables

Notations

AR	Aspect Ratio
A	Area, [mm^2]
b	Span
c	Chord
C_D	Drag Coefficient
C_L	Lift Coefficient
C_m	Moment Coefficient
C_p	Pressure Coefficient
D	Drag
E	Modulus of Elasticity (Young's Modulus), [N/mm^2]
e	Strain
E_T	Tangential Modulus of the material), [N/mm^2]
F	Force, [N]
f_b	Allowable Bending Stress, [N/mm^2]
F_{bu}	Ultimate Bearing Strength of Material, [N/mm^2]
f_s	Allowable Shear Stress, [N/mm^2]
f_{su}	Ultimate Shearing Strength of Material, [N/mm^2]
f_t	Allowable Tensile Stress, [N/mm^2]
f_{tu}	Ultimate Tensile Strength of Material, [N/mm^2]
G	Shear Modulus, [N/mm^2]
I_{NA}	Moment of inertia about the Neutral axis, [$Kg.m^2$]
I_{uu}	Moment of inertia about the principal axis uu, [$Kg.m^2$]
I_{vv}	Moment of inertia about the principal axis vv, [$Kg.m^2$]
I_{xx}	Moment of inertia about xx-axis, [$Kg.m^2$]
I_{yy}	Moment of inertia about yy-axis, [$Kg.m^2$]
L	Lift
M	Bending Moment, [Nmm]
S	Wing Area [m]
t	Thickness [m]
T	Torque, [Nmm]
t	Thickness, [mm]
V	Shear Force, [N]
V_2	Safe Climb Speed [m/s]

V_{LO}	Lift off Speed [m/s]
V_{MC}	Minimum Control Speed [m/s]
V_{MU}	Minimum unstick speed (minimum speed with which the airplane can safely take off with one engine inoperative) [m/s]
V_S	Dynamic Stall Speed [m/s]
X_{cg}	Position of the centre of gravity of the aircraft, [m]
W	Weight, [kg]
$_z\bar{c}$	Aerodynamic Mean Chord [m]
$_z\alpha$	Angle of Attack, [°]
φ	Climb Angle, [°]
$_z\lambda$	Taper Ratio
$_z\theta$	Wing Twist Angle, [°]
$_z\Lambda$	Wing Sweep Angle, [°]
ρ	Density [kg/m^3]
ν	Poisson's Ratio
nm	Nautical Mile
US Gal.	USA Gallon
Re	Reynolds Number

Abbreviations

2D	Two-Dimensional
3D	Three-Dimensional
ATRA	Advanced Transport Regional Aircraft
CAD	Computer Aided Design
CFD	Computer Fluid Dynamics
COA	College of Aeronautics
FEA	Finite Element Analysis
HLFC	Hybrid Laminar Flow Control
L/D	Lift to Drag Ratio
MTOW	Maximum Take-Off Weight
OEW	Operating Empty Weight
R&M	Reliability and Maintenability
VC	Variable Camber
VCW	Variable Camber Wing
AVD	Aerospace Vehicle Design
CofG	Centre of Gravity
BM	Bending Moment
FEA	Finite Element Analysis
Stn	Station
MBB	Messerschmitt-Bölkow-Blohm GmbH
RS	Rear Spar
FS	Front Spar
TE	Trailing Edge
LE	Leading Edge
HL	High Lift
ESDU	Engineering Sciences Data Units
TO	Take-Off

All other notations used on this thesis are explained before use if they are not described above.

CHAPTER 1

INTRODUCTION

1.1. GENERAL

Early transport aircraft used simple high lift devices to provide better control of the aircraft and to improve pilot vision by producing low-speed flight [85]. The introduction and development of more complex high lift devices in transport aircraft was mainly due to the development of more powerful engines, which increased substantially the speed and the wing loading of the aircraft, and the limitations on runaway lengths. Due to economical considerations the wing profiles were optimised for cruise flight efficiency, but at low speeds they are rather inefficient, needing lots of lift to achieve the required L/D. Hence, in order to cope with the high wing loadings and to achieve the required additional lift for takeoff and landing it was necessary to introduce high lift devices.

The design of high lift systems plays an important part in the process of defining the size and performance of modern aircraft and has taken a very important role in the total aircraft design process. The design process of High-Lift devices has been heavily scrutinized and has become of great importance for aircraft manufacturers. For typical subsonic transports, the high lift systems are about 5 to 11% of the total cost of the aircraft, and they have a large impact on the performance of the aircraft. As an example, for a typical long-range twin-engine subsonic transport, an increase of 1% in takeoff L/D can result in a 150nm increase in range or a payload increase of 2800lb [105]. The commercial transport market has become so competitive that an enormous and constant effort is expended on ways to reduce the direct operation costs. When it comes to High-lift devices, aircraft manufactures focus in the improvement and optimization of the currently used High-Lift device concepts.

The introduction of High-Lift devices in the leading and trailing edge of the wing provides the aircraft with the means to adjust and comply with the low speed requirements for take-off and landing, while maintaining the "optimized" wing profile for cruise flight efficiency. Though, because the wing profile is set during cruise, without the possibility of variations, in specific occasions the wing might not be working in optimum conditions, incurring higher levels of drag and ultimately consuming more fuel. The Variable Camber Wing (VCW) concept provides a solution to this problem by allowing the wing to adapt to the different flight cruise conditions, hence improving the performance of the aircraft.
The advantages of the Variable Camber Wing concept have been acknowledged, but no feasible practical design has yet been achieved or developed in the area of commercial transport. Current improvements in computational capabilities, development of new design tools and the introduction of new technologies provide the means for a possible improvement of the traditional design methodologies and/or a breakthrough in the design of Variable Camber Wing concepts.

1.2. RESEARCH BACKGROUND

In the subject of High-Lift devices and Variable Camber Wing there has been considerable research work performed inside the College of Aeronautics at Cranfield University. A brief description of the most relevant is presented below.

Mr S. H. M. MACCI PhD's Thesis (1992) [53]

"Structural and Mechanical Feasibility Study of a Variable Camber Wing (VCW) for a Transport Aircraft"

Mr Macci investigated the structural and mechanical feasibility of introducing VC to supercritical airfoil sections of different characteristics. The validation of the research was made for a modern transport aircraft wing, and the results showed that it was feasible to apply the VC concept to the trailing edge, but further research was recommended for the leading edge.
As part of the research a half-scale structural model of one trailing edge segment was manufactured and tested.
Mr Macci recommended further investigation on the implications of VCW on transport aircraft in terms of overall aerodynamics, mass and cost.

Mr A. V. MACKINNON PhD's Thesis (1993) [55]

"An Experimental Study of a Variable Camber Wing (VCW)"
Mr MacKinnon, working alongside Mr Macci, researched the application of a novel concept of varying the wing camber, the Variable Camber Wing. The concept was applied to a supercritical aerofoil and the research included the manufacturing of a 3D, half wing, wind tunnel model. The tests looked at local and spanwise variation of camber, but only for the trailing edge. The results were not totally satisfactory, showing that a bigger wind tunnel model was required. Mr MacKinnon recommended that a bigger model should be used, including leading edge camber variation.

Mr PRASETYO EDI PhD's Thesis (1995-1998) [20]

"Investigation of the Application of Hybrid Laminar Flow Control and Variable Camber Wing Design for Regional Aircraft"

Mr. Edi investigated the feasibility of introducing a combined HLFC-VCW concept in a regional aircraft family to improve the overall efficiency, flexibility and reduce weight. The aircraft used to validate the research was the ATRA – Advanced Transport Regional Aircraft.
This research showed that the combined HLFC-VCW concept is feasible for this class and size of aircraft. It was proved that the VCW concept could be optimised to increase the lift to the desired range. Although, Mr. Edi recommended a further multidisciplinary investigation in order to improve the potential of these concepts. The work on the VCW focused mainly in the trailing edge devices.

Mr MOHD S. AMMOO PhD's Thesis (1997-2002) [1]

"Development of a Design Methodology for Transport Aircraft Variable Camber Flaps Suitable for Cruise and Low-Speed Operations"

Mr Ammoo developed a design methodology for variable camber flaps based on the design methodology applied to conventional high lift devices. A computer-based analysis was performed on the transport aircraft ATRA to validate the design methodology. The case study used MSES-code (CFD) to analyse aerodynamic characteristics, along with ESDU datasheets. For layout and simulation Mr. Ammoo used CATIA and for Structural analysis PATRAN/NASTRAN.
The conclusions were that it is feasible to apply the proposed high lift device. Although, it was suggested that the 3D wing lift coefficient should be determined in order to have more precise aerodynamic loads. This could be obtained through a dedicated 3D CFD analysis and/or wind tunnel testing. This research focused primarily on trailing edge devices.

1.3. RESEARCH OBJECTIVE

The objective of this research is to develop a comprehensive design methodology for mechanisms of wing trailing edge High-Lift devices, so that the overall performance requirements can be met. The methodology will include a step-by-step multidisciplinary analysis of the process, from initial requirements to preliminary structural definition, with special focus on Synthesis & Optimization of Mechanisms, Preliminary Sizing Methods, Weight Estimation, Reliability & Maintainability Assessments and Cost estimation. This has the objective of enabling the designer to choose the best solution to meet the requirements from a group of viable mechanism types.
The methodology will be validated and a case study performed on the ATRA with the application of the innovative VCW concept. It will use the aircraft configuration from Edi's Thesis [20] and the loads from Ammoo's thesis [1].

1.4. RESEARCH METHOD

The method used in this research study and development of the design methodology is presented below.

Review of Existing High-Lift Device Systems and Design Methodologies

The initial step of this research study was an extensive review of existing trailing edge high-lift devices. It also includes a review of the most relevant design parameters involved in the design of High-lift devices.

Development of a Design Methodology

Prior to the development of the new design methodology, a review of current design methodologies for high-lift devices was carried out. The new methodology mainly covers the initial stages of the design process and incorporates synthesis and optimization, preliminary sizing, CAD design, aerodynamics, reliability & maintainability and cost. New specific tools were developed to improve the design process.

Validation of the Design Methodology

The different areas of the methodology are validated against theoretical results obtained by experts in these fields of research or by direct comparison with existing applications.

Case Study

A case study was performed on the ATRA – Advanced Transport Regional Aircraft, to verify the applicability of the methodology and develop new knowledge about High-Lift devices and Variable Camber flaps.

Discussion

The results of the case study results were analysed and discussed.

Conclusions and Recommendations

The conclusions related with the whole research project were drawn and recommendations for future work are presented.

CHAPTER 2

LITERATURE REVIEW

2.1. INTRODUCTION

High lift devices are a very important component of an aircraft and have a strong effect on its size and performance. This chapter presents a general description of the transport aircraft design objectives and constraints which guide the design of high-lift systems. As part of a bigger component of the aircraft, the design of these devices is dependent on a great number of wing design parameters. The aircraft wing has to be capable of providing cruise efficiency and adequately meet the take-off and landing requirements. There is a big difference between a wing designed for high-speed flight and a wing designed for Take-off and Landing only. A wing designed for Take-off and Landing requires high C_{Lmax} at low speeds, usually provided by increased wing area. This increased wing area (and the associated weight and drag) is not desirable in cruise. To achieve the best results for these two requirements, designers generally optimize the wing for cruise performance and make use of a variety of trailing and leading edge high lift devices to allow the aircraft to meet the low speed requirements safely and reliably.

This chapter presents the most relevant wing design parameters for the design of High Lift devices, and a description of a wide range of trailing edge high lift devices and mechanisms that can be found in today's commercial aircraft, new systems and the Variable Camber High Lift device.

The final references are for the pertinent issue of Noise.

2.2. AIRCRAFT DESIGN OBJECTIVES AND CONSTRAINTS

Before entering the high lift device subject, is important to make reference to the overall objectives and constraints involved in the design of civil transport aircraft. The general design objectives and constraints present in the aircraft design and that may ultimately influence the designer's choice regarding the high lift system are presented in Table 2.1.

Table 2.1 – Medium and Long Range Transport Aircraft Design Objectives and Constraints [16]

Issues	Civil Transport Aircraft
Dominant Design Criteria	▪ Economics and safety
Performance	▪ Maximum economic cruise ▪ Minimum-off design penalty in wing design
Airfield Environment	▪ Moderate to long runways ▪ Paved runways ▪ High-level ATC and landing aids ▪ Adequate space for ground manoeuvre and parking
System complexity and Mechanical Design	▪ Low maintenance-economic issue ▪ Low system cost ▪ Safety and reliability ▪ Long service life
Government regulations and community acceptance	▪ Must be certifiable (FAA, etc...) ▪ Low noise mandatory

As can be seen on the previous table, the design of civil transport aircraft is mainly driven by economic considerations with equal concerns for safety.

For the designer of high lift devices, the above objectives and constraints can be presented as the following most relevant factors [82]:

a) **High Lift Requirements.**
b) **Trim considerations**
c) **Drag Considerations.**
d) **Mass.**
e) **Cost, Complexity and Maintenance.**

2.3. HIGH LIFT DEVICE BASICS

The use of high lift devices has the main objective of providing the aircraft with means for achieving adequate Take-Off and Landing performances (Figure 2.1 and Figure 2.2). In the majority of the cases the important factor for take-off is climb rate and for landing, approach and landing speeds, which are dominated by wing loading and C_{LMax}.

a) Take-Off Requirements

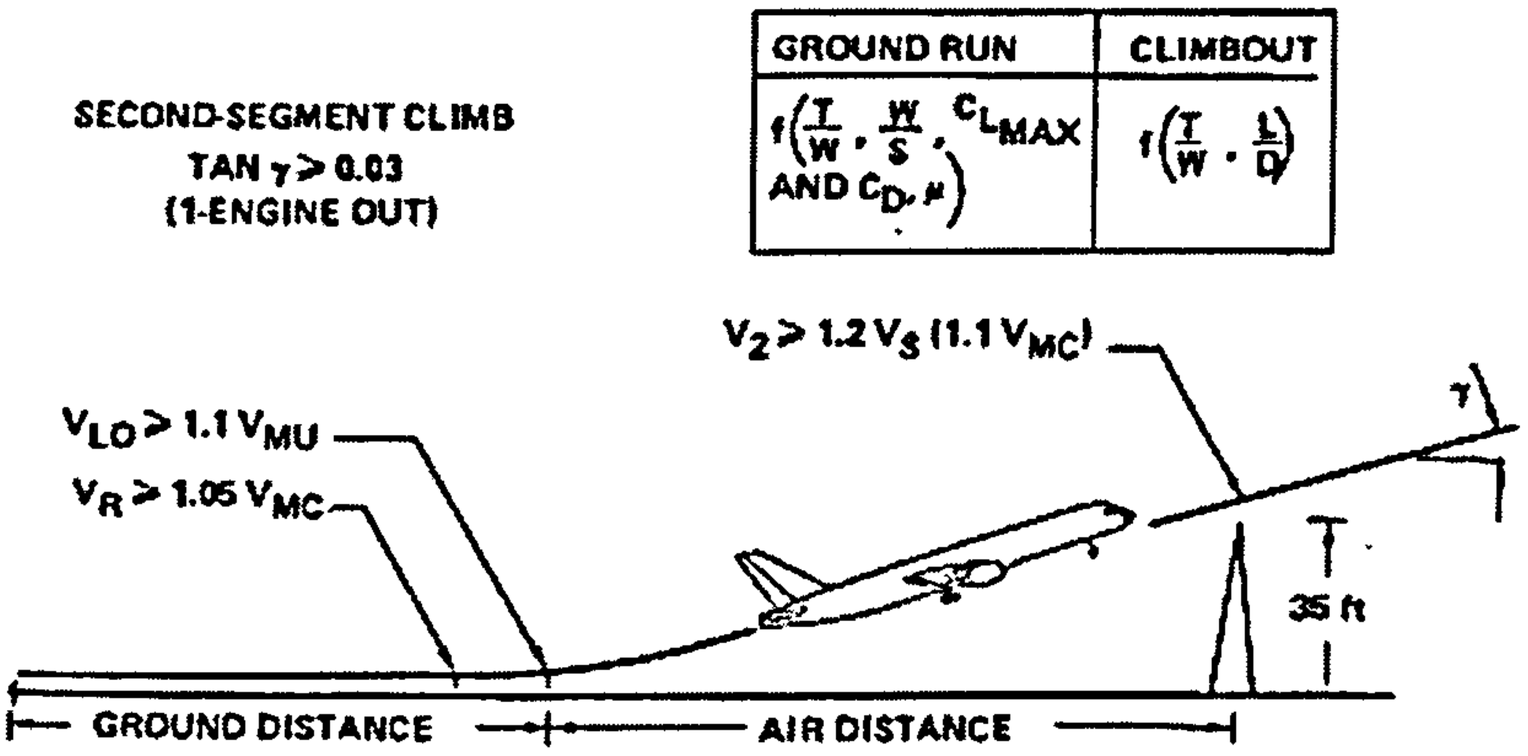

Figure 2.1 - Take of profile [16]

Take-off field length – the total ground roll distance to lift off plus the airborne distance to over fly a 35-foot obstacle.

Second-segment climb with one engine failed:
Tan $\gamma \geq 0.03$ (4 engine A/C)
Tan $\gamma \geq 0.023$ (Twin engine A/C)

The climb rate is a function of the thrust-to-weight ratio (T/W) and L/D defined by the following equation:

$$R/C = T/W - (L/D)^{-1}$$ Equation 2.1

b) Landing Requirements

APPROACH	GROUND RUN	GO-AROUND
f ($C_{L_{MAX}}$, W/S AND L/D)	f ($C_{L_{MAX}}$, W/S AND C_D, μ, T_{REV})	$f\left(\frac{T}{W} \cdot \frac{L}{D}\right)$

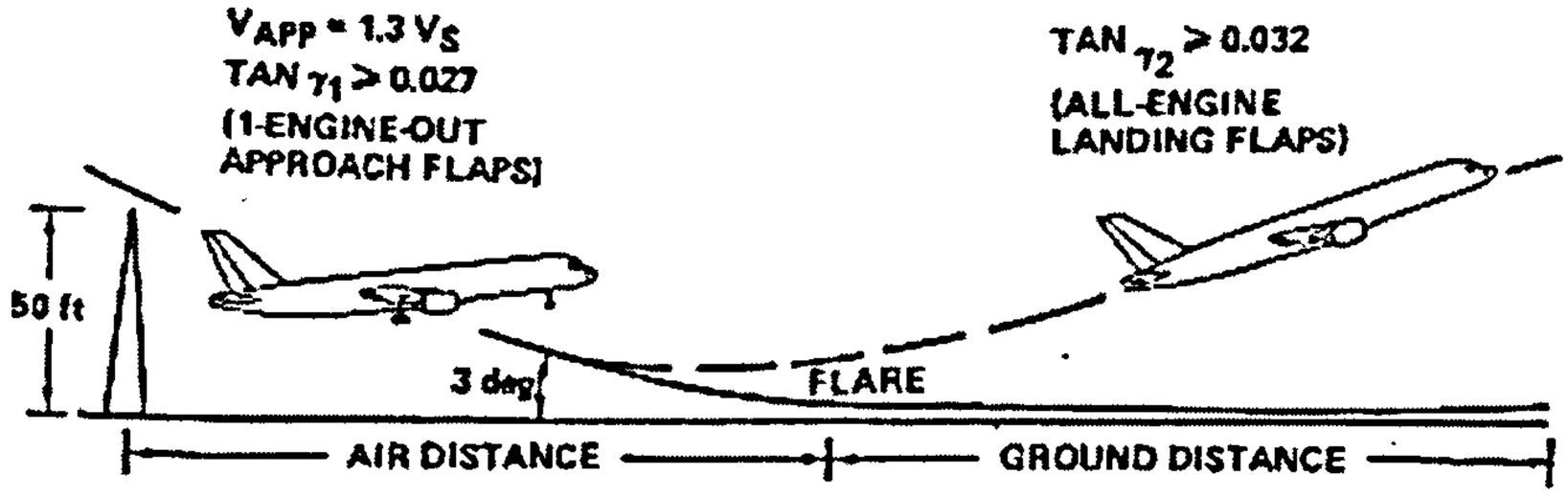

Figure 2.2 - Landing Profile [16]

Because the stalling speed is related to wing parameters by Equation 2.2, one of the ways used to reduce stalling speed is by increasing wing C_{Lmax}, usually by means of High Lift devices.

$$V_S = \left(\frac{2 \cdot W}{S \cdot \rho \cdot C_{Lmax}}\right) \qquad \text{Equation 2.2}$$

There is a correlation between the landing accident rate and the approach speed, as can be seen in Figure 2.3 [16]. Typical approach speeds on today's civil transport aircraft are between 120 and 150 knots [85].

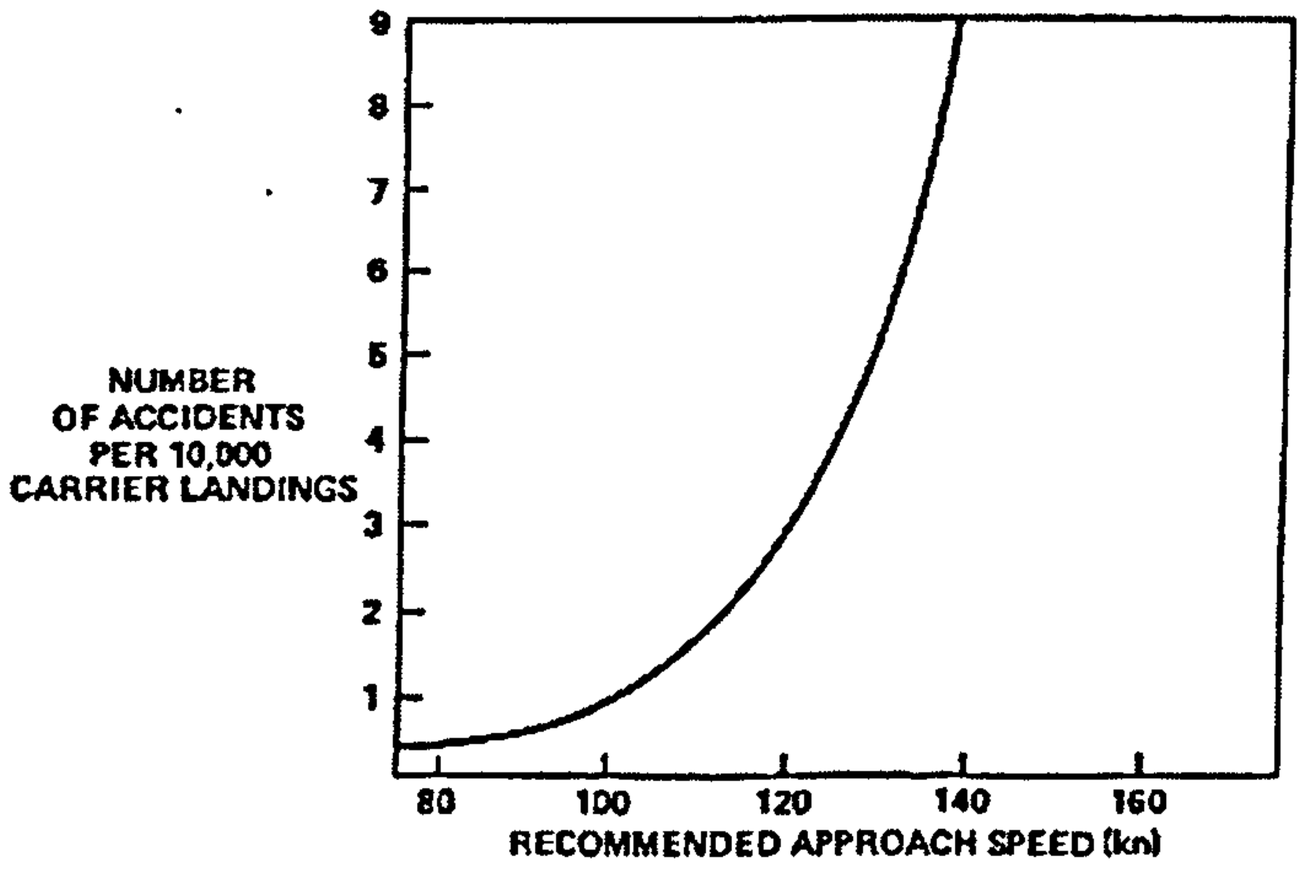

SOURCE: AIRCRAFT RECOVERY BULLETIN NO. 26-12A NAEL-SE-731

Figure 2.3 – Influence of A/C Approach Speed on Landing Accidents

c) How to Achieve Additional Lift

There are basically 3 ways of achieving additional lift through the use of high lift devices [48][77].

Change in Camber – This is achieved with the deflection of the trailing edge, and possibly the leading edge airfoil, increasing the camber. The increase in lift is obtained at the expense of more drag and pitching moment

Increase in the Effective Wing Area – With the extension of the trailing edge, and possibly the leading edge airfoil, an effective increase in the wing area is achieved. In this case, the increase in lift is obtained with relatively small drag penalties.

Boundary Layer Control – Introducing slots between the lower and upper wing surfaces results in an enhancement of the upper surface flow delaying separation. It improves pressure distribution, re-energizing the upper flow through the elimination of low energy boundary layers.

The use of high lift devices has a direct impact on the lift curve of the wing. Figure 2.4 illustrates the effect that the high lift devices have on the lift curve of the wing.

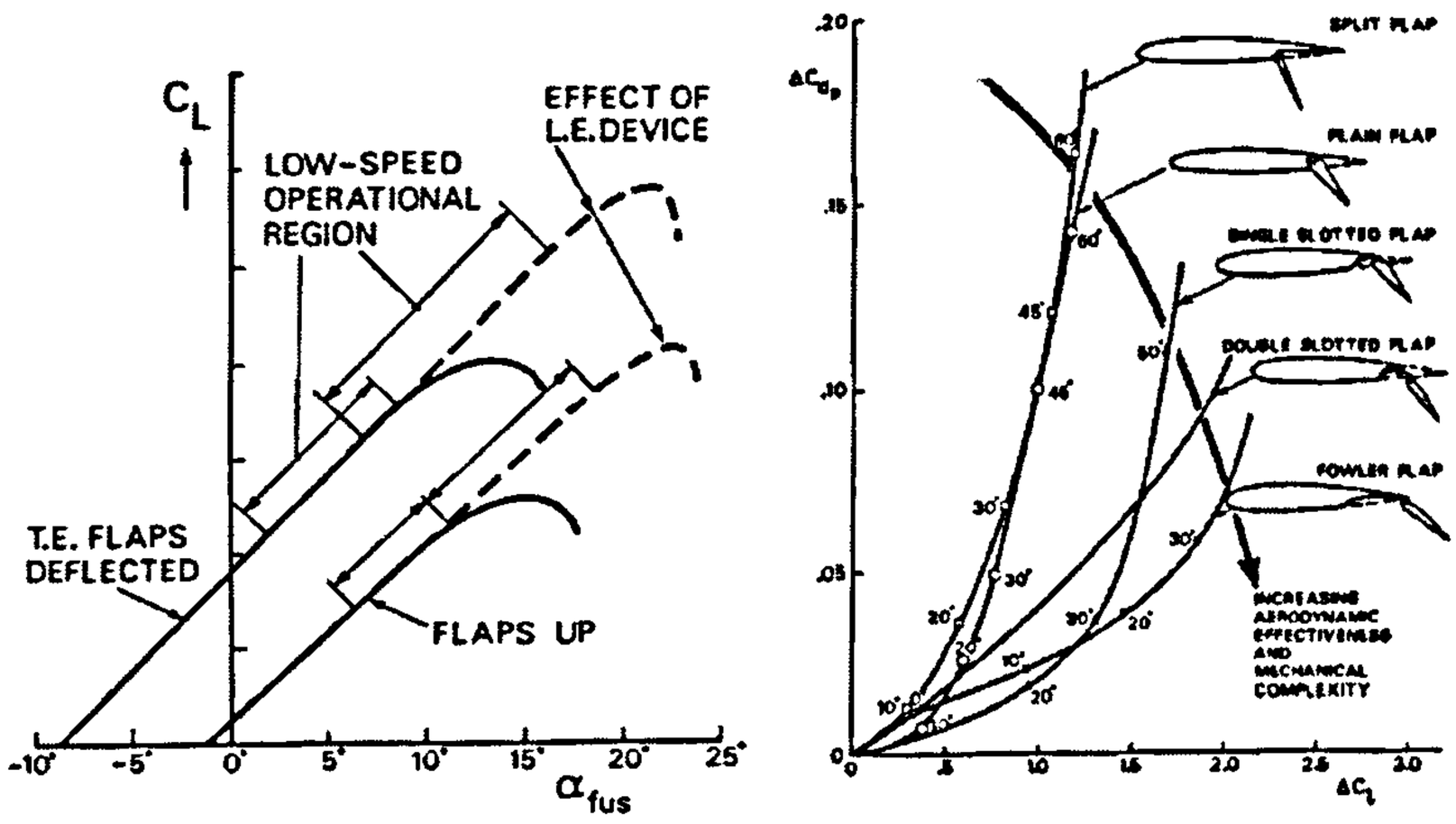

Figure 2.4 – Effects of High Lift devices on the lift curve [104]

As it can be seen, and although they increase the lift, aft flaps tend to decrease the stall angle. The flap deflection promotes a pressure drop in the upper surface, which leads to flow separation and earlier stall. In order to solve this problem leading edge devices are usually used, which increase the stall angle, as shown in Figure 2.4.
The flaps that increase camber also increase the maximum lift but they move the zero lift point to the left. The slope of the curve does not change, meaning that the angle of stall is somewhat reduced. The flaps that increase the area cause the same effect on the zero-lift angle and stall angle, the difference is that they produce more lift than the flaps that only change the camber.

Table 2.2 presents the approximate lift contributions for the different types of high lift devices.

Table 2.2 – Approximate lift contributions of high lift devices [48]

Device	Max. increment in lift coefficient*	
	2- dim. potential	Typical 3- dim. value*
Basic aerofoil - subsonic	1.6	1.50
Basic aerofoil - sharp nose	1.0	0.95
Plain trailing edge flap: 20% chord	0.80	0 55
40% chord	1 10	0.75
Split flap (no gap) (t/c) = 0.15; 20% chord	0.9	0.60
40% chord	1 4	0.95
Single-slotted flap: 20% chord	1.2	0 80
40% chord	1 8	1.20
Double-slotted flap: 40% (+26%) chord	2.5	1.65
Triple-slotted flap: 40% chord overall	2 9	1 90
Fowler flaps: 20% chord	1.2	0 80
40% chord	1.8	1.2
Fowler plus split flap: 40% chord	2.2	1.45
Plain leading edge flap: 15% chord	0.5	0.4
Vented slat: 18% chord	1.0	0.85
Kruger flap: 20% chord	0 8	0 65
Vented Kruger flap: 20% chord	1.0	0.85

* Notes: 1) Typical 3-dimension values are for moderate to high aspect ratio unswept wings, allowing for part span effects. Multiply by ($cos\Lambda_{1/4}$) for swept case. A typical corresponding value for plain/single-slotted flaps on a low aspect ratio wing is 0.25.

2) Take-off lift coefficient values are usually 50 to 60% of maximum (landing) values quoted, see Chapter 6, paragraph 6.2.4.4.

2.4. WING DESIGN PARAMETERS

2.4.1. Basic Wing Geometry

The basic geometry of the wing, or "reference" wing, used for initial layout and the key geometric parameters are shown in Figure 2.5 and Figure 2.6.

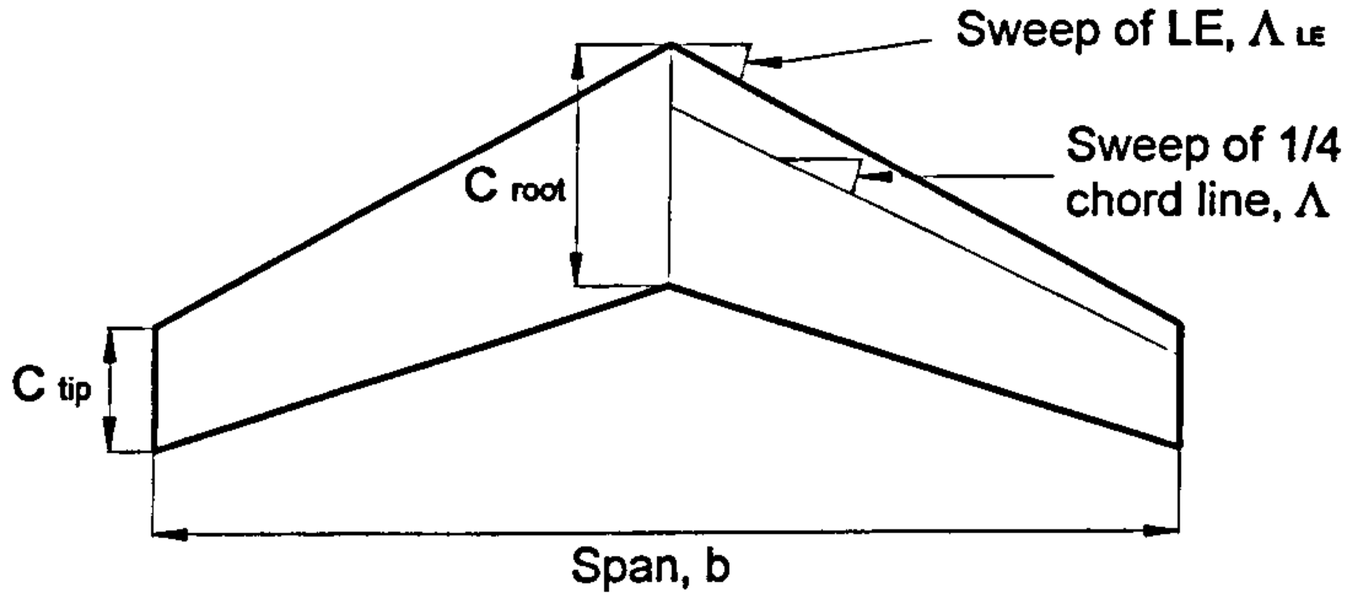

Figure 2.5 – Wing Planform [124]

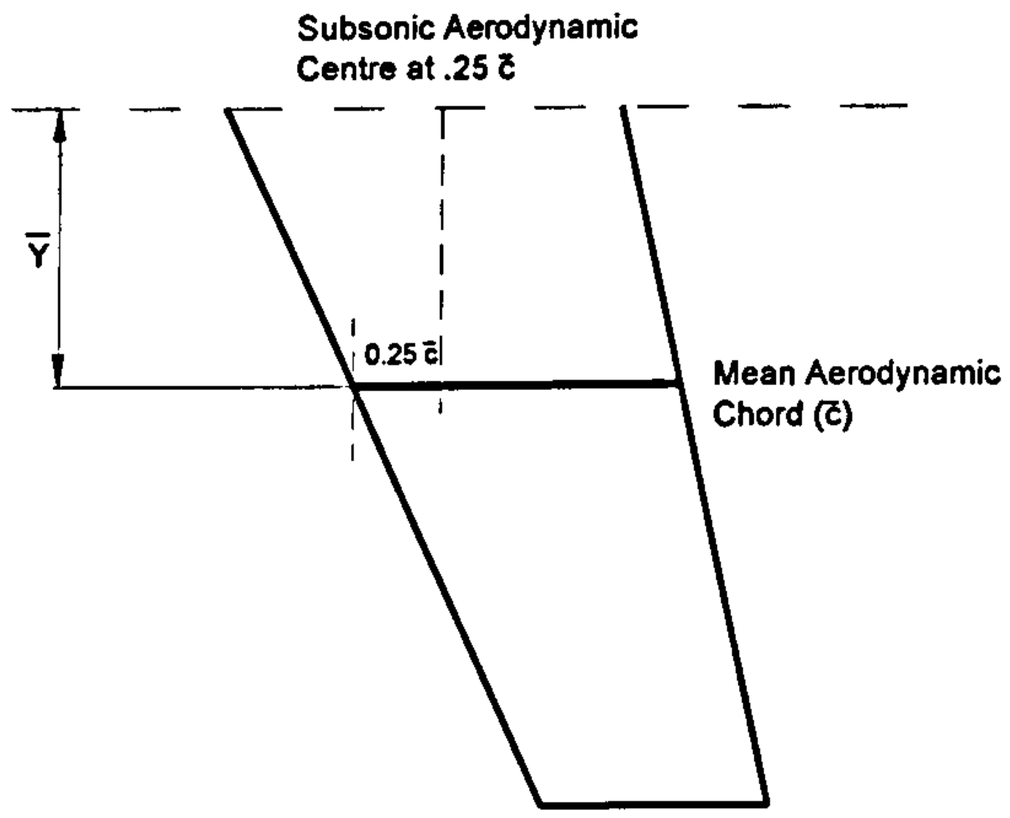

Figure 2.6 – Mean aerodynamic chord [77]

Where:

S = Wing area

A = Aspect Ratio, given by: $A = \frac{b^2}{S} = \frac{b}{\bar{c}}$

λ = Taper Ratio, given by: $\lambda = \frac{C_{tip}}{C_{root}}$

Λ = Sweep of ¼ chord line

θ = Wing Twist Angle

$\bar{c}$ = Mean aerodynamic chord, given by:

$\bar{c} = (2/3) \cdot c_{root} \cdot (1 + \lambda + \lambda^2)/(1 + \lambda)$ [77]

$\overline{Y}$ = Distance of $\overline{c}$ from centreline, given by:

$$\overline{Y} = (b/6)\cdot[(1+2\cdot\lambda)\cdot(1+\lambda)] \quad [77]$$

Typical, Wing Aerodynamic Centre = 0.25 $\overline{c}$ Subsonic

0.40 $\overline{c}$ Supersonic [77]

2.4.2. Main Wing Design Parameters

Airfoil

Airfoil design is one of the major tasks in aerodynamics. Nowadays, airfoils are purposely designed for specific applications using computational fluid dynamics. It is possible to design different airfoil profile sections along the wing span of an aircraft to optimize the aerodynamic conditions at every specific position [125].
The main task in the airfoil design to achieve the highest lift coefficient consistent with suitable drag and moment characteristics is to guarantee that the pressure in the lower side of the airfoil is as high as possible, and that the pressure in the upper side is as low as possible. The parameters that have most influence in the airfoil lift coefficient are the Camber, Thickness distributions, Leading edge radius and trailing edge angle [77].

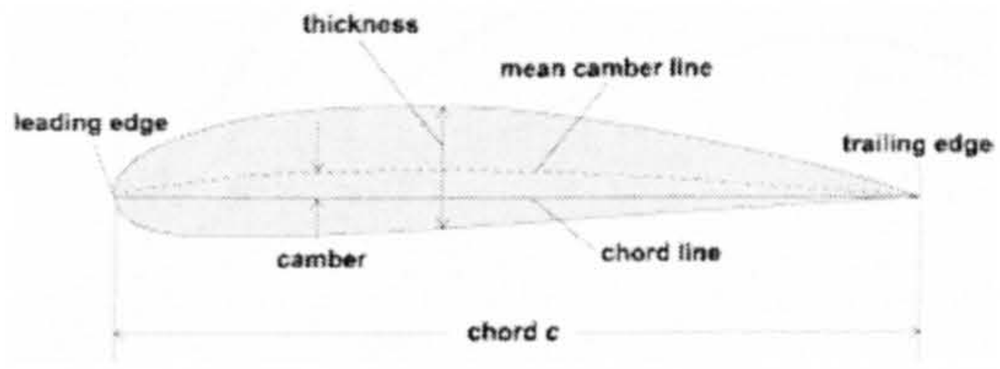

Figure 2.7 – Airfoil Configuration [125]

Span

In the wing design process, one of the most basic decisions is the selection of the wingspan. For commercial aircraft this parameter is usually constrained to hangar size or ground facilities and to structural dynamic constraints (flutter). However, with the increase of span, the structural weight will also increase.
One of the parameters influenced by the wingspan is the induced drag. This type of drag depends on the lift and in some cases it can be as much as 70 to 80 % of the total drag [124]. Hence, trade-off studies are required to optimise the relation between the weight and the induced drag savings.
It must be noticed that the wing span selection is not only made with the analysis of the structural weight and the induced drag. This is just to achieve a reasonable value to start the iterative process of designing a wing.

Planform

The wing planform plays an important role in the design of a wing and it is basically defined as the shape of the wing when view from directly above. It relates directly with the Aspect Ratio and Taper and it has a direct influence on the Induced drag coefficient and the stalling characteristics of the wing [104]. The selection of the wing planform also affects other parameters such as the structural weight and the fuel volume. Due to the iterative nature of the design process, the

selection of the wing planform is based in combinations of the parameters referred previously, which are in constant review during the design process.

Aspect Ratio

The wing Aspect Ratio, A, is another important parameter in the wing design procedure. It affects not only the Induced Drag and the weight, but also the stalling angle of the wing. When compared with low Aspect Ratio wings, the high Aspect Ratio wings achieve larger values of L/D, approximately by the square root of an increase of Aspect Ratio (for constant wing area and S_{wet}/S_{ref}). This is because they tend to have lower induced drag.
High aspect ratio wings tend to have high lift curve slopes, this is mainly due to the reduced effective angle of attack at the tips. Figure 2.8 shows that high aspect ratio wings stall at lower angles of attack than the lower aspect ratio wings [77].
The Aspect Ratio will also be determined later in the design process by trade-off studies between the aerodynamic advantages and the weight.

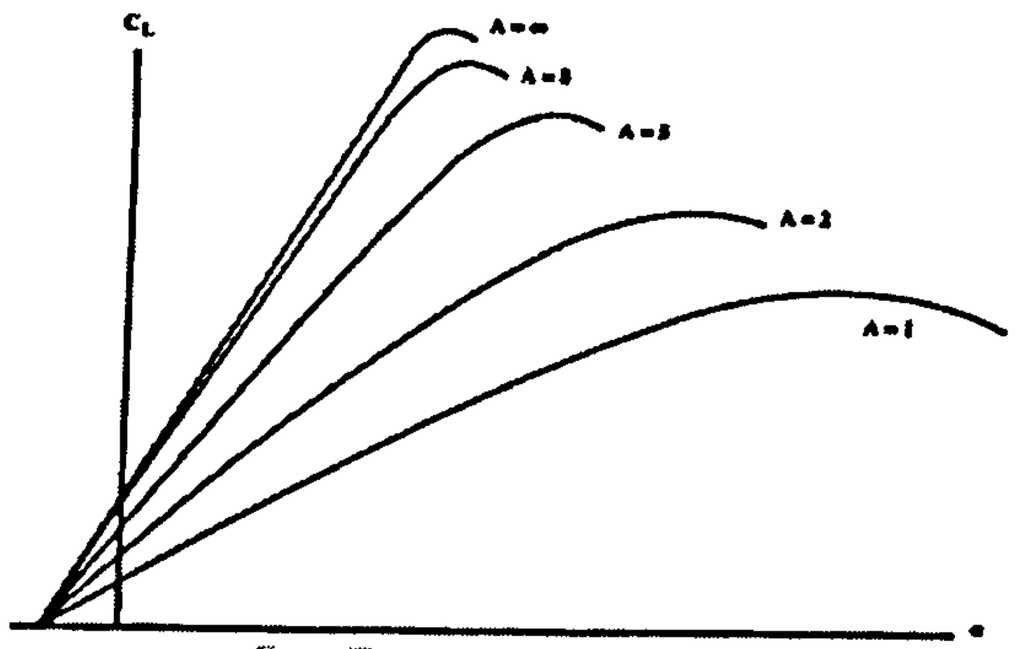

Figure 2.8 – Effect of aspect ratio on lift [77]

Thickness Ratio

The thickness ratio is the wing maximum thickness divided by the wing chord. This parameter primarily affects the Drag, the maximum Lift, stalling characteristics, the weight and the fuel volume. Table 2.3 presents a summary of the effect of the thickness ratio on these parameters.

Table 2.3 – Summary of the effect of thickness ratio [82]

Item	Effect of Thickness	
	Low t/c	High t/c
Wing Weight	High	Low
Wing Drag: Subsonic Supersonic	Low Acceptable	High Very High
Wing Fuel Volume	Poor	Good
Maximum Lift	Poor	Good (Up to 12-14% depends on airfoil)

For a wing of fairly high Aspect ratio and moderate sweep, the nose shape is related to the thickness ratio, increasing with it. This affects the maximum lift and stall characteristics. A larger nose radius provides higher stall angles and greater maximum lift coefficient [77]. The effect of thickness ratio in the maximum lift is shown in Figure 2.9.

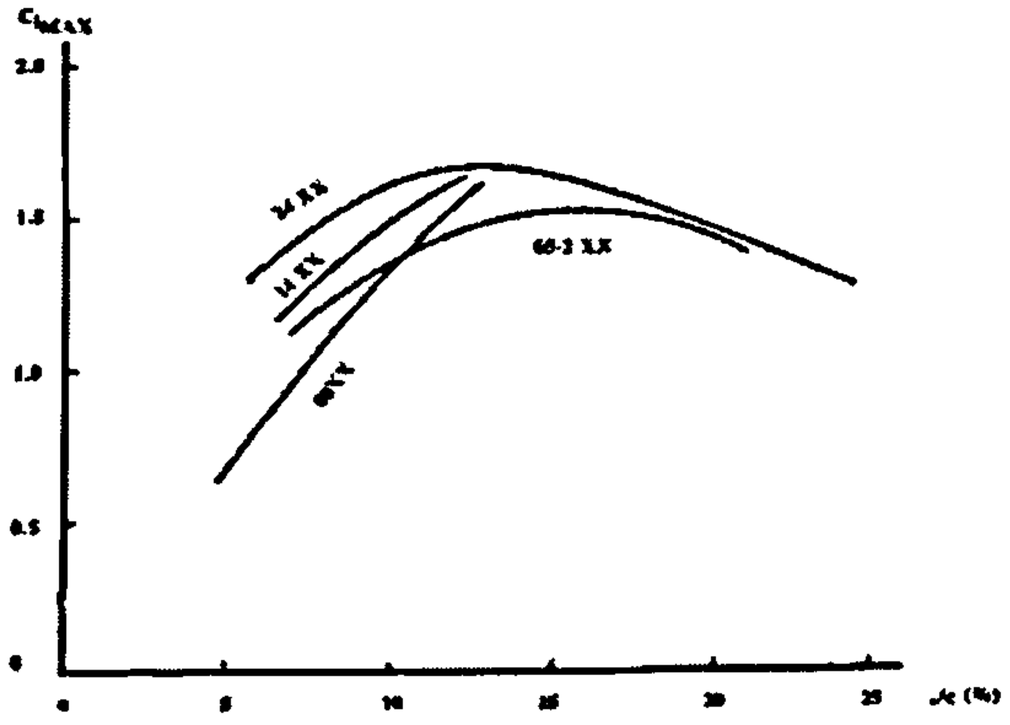

Figure 2.9 – Effect of t/c on maximum lift [77]

The thickness ratio also affects the structural weight of the wing and it has been shown by statistical equations that the wing structural weight varies approximately inversely with the square root of the thickness ratio [77].
At the intersection of the wing and the fuselage, the thickness of the root airfoil can be as much as 20 to 60% thicker than the tip airfoil. This results in more volume for fuel and the landing gear. This variation of thickness from root to tip doesn't have a great influence in the drag [77].

Taper Ratio

The taper ratio is defined as the ratio between the tip chord and the centreline root chord, measured in the stream wise direction. It affects directly the spanwise lift distribution in the wing, as can be seen in Figure 2.10. By lowering the taper ratio (increasing taper) the position of the centre of pressure is moved inboard. This decreases the bending moment due to lift at the root, which may lead to weight savings. Higher taper ratios will produce a heavier wing and more fuel volume than a small taper ratio. Table 2.4 presents a summary of the effect of the taper ratio on wing design.

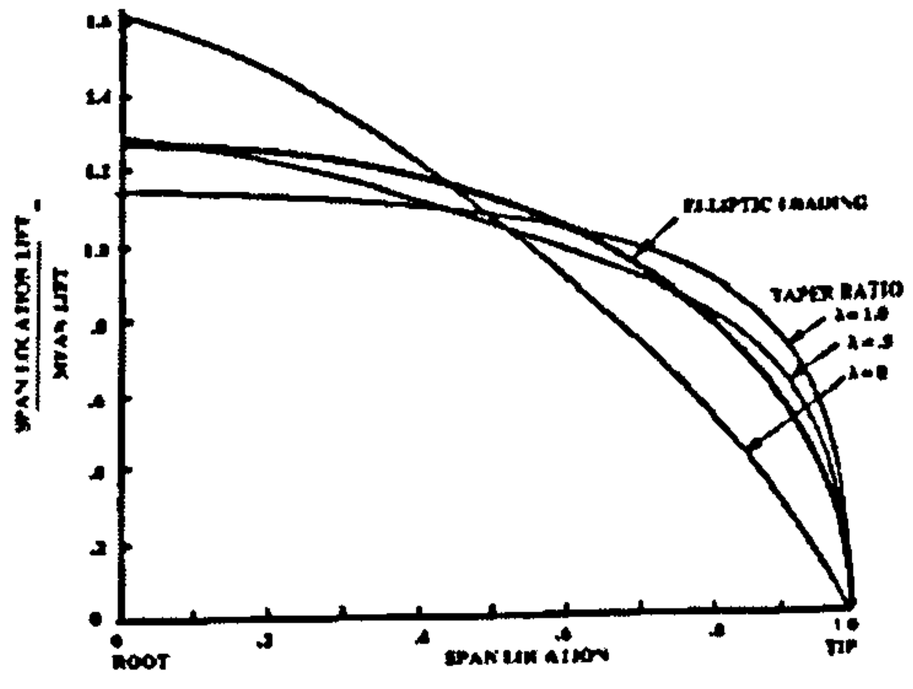

Figure 2.10 – Effect of taper on lift distribution [77]

Table 2.4 – Summary of the effect of taper ratio [82]

Item	Effect of Taper Ratio	
	High Taper	**Low Taper**
Wing Weight	High	Low
Tip Stall	Good	Poor
Wing Fuel Volume	Good	Poor

Howe [48] suggests that for initial studies the taper ratio, λ, should not be less than:

$$\lambda \geq 0.2 \cdot A^{1/4} \cdot \cos^2 \Lambda_{1/4}$$

Sweep

With the increase of aircraft speed provided by the development of more powerful engines new problems started to arise at cruising speeds of M=0.75 to 0.80. At these speeds the compressibility problems have a great impact in the wave drag. To cope with this problem it is desirable to use sweepback (or sweep forward). Sweep will postpone the effects of critical compressibility to a certain extent.
The use of sweep also has a significant effect on the lift-curve slope, as shown in Figure 2.11. It provides better pitch attitude at low speed, and hence better runway visibility and during turbulence it provides better ride characteristics.

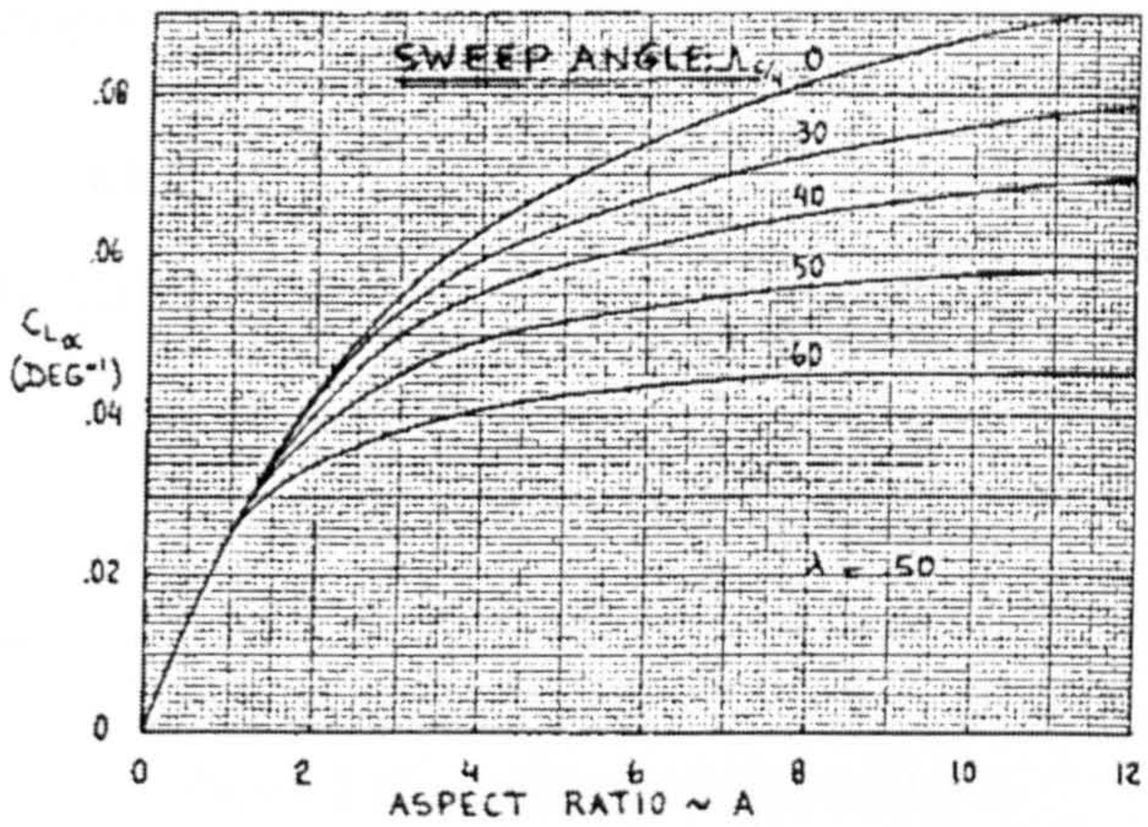

Figure 2.11 – Effect of sweep on the lift curve slope [82]

Other factors that can lead to the use of sweep are layout considerations and C.G balance. It can be used to provide stowage volume for a retracted landing gear and to balance the aircraft when fuselage layout requirements don't allow the wing to be placed in the required place.
There are two ways of defining the sweep angle, as shown in Figure 2.5, the leading edge and the ¼ chord line. The leading edge sweep angle is usually defined for supersonic flight and it is common to sweep the wing so that it is inside

the Mach cone. The ¼ chord line sweep angle is usually associated with subsonic flight. For initial wing layout the trend line of Figure 2.12 is reasonable.

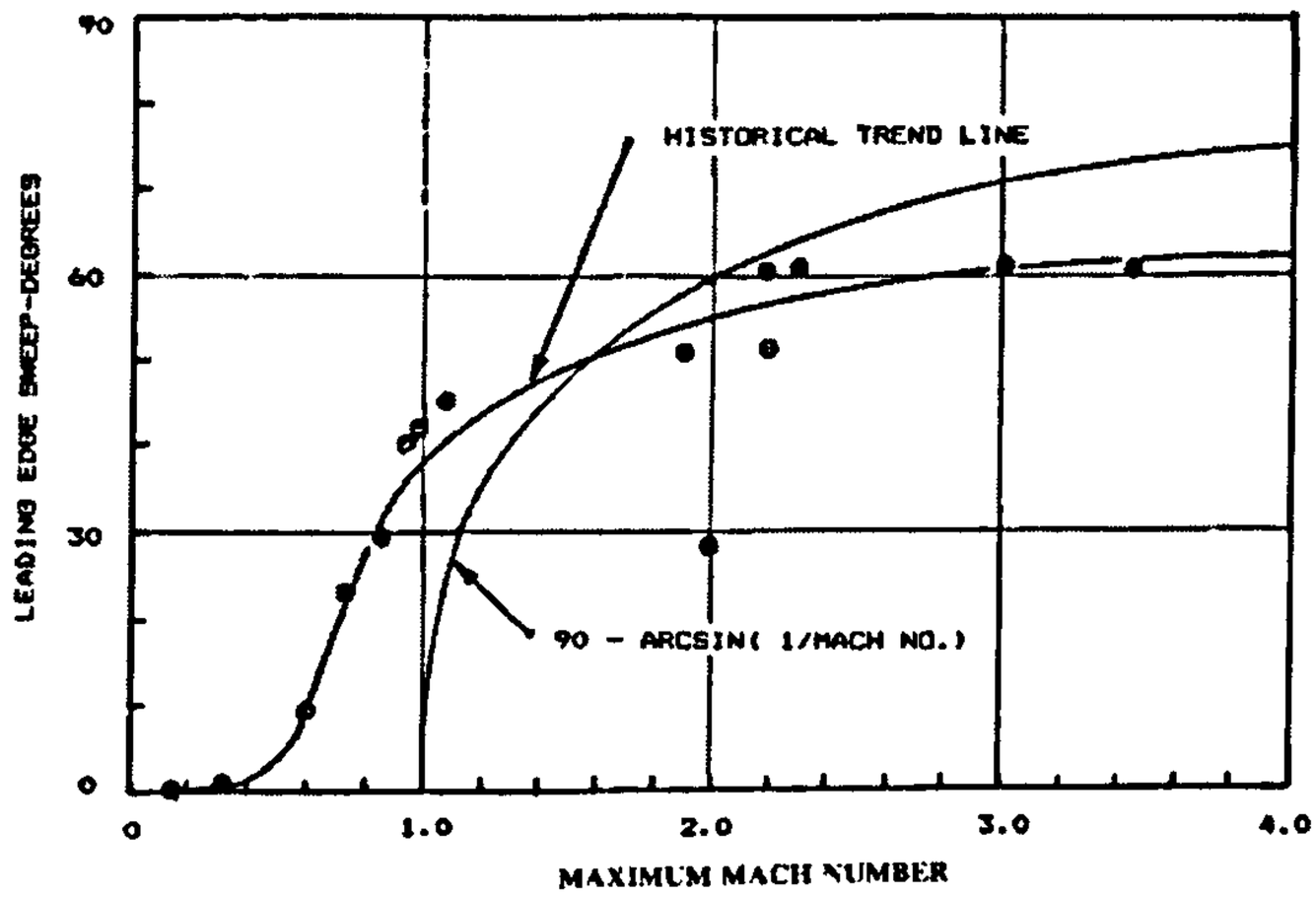

Figure 2.12 – Wing Sweep historical trend [77]

Twist

The wing twist is defined as the change in the airfoil angle of incidence with respect to the root airfoil angle of incidence. If the wing tip airfoil has a negative angle (nose-down) when relative to the root airfoil it is said to have "wash-out". Figure 2.13 shows the definition of the wing twist.

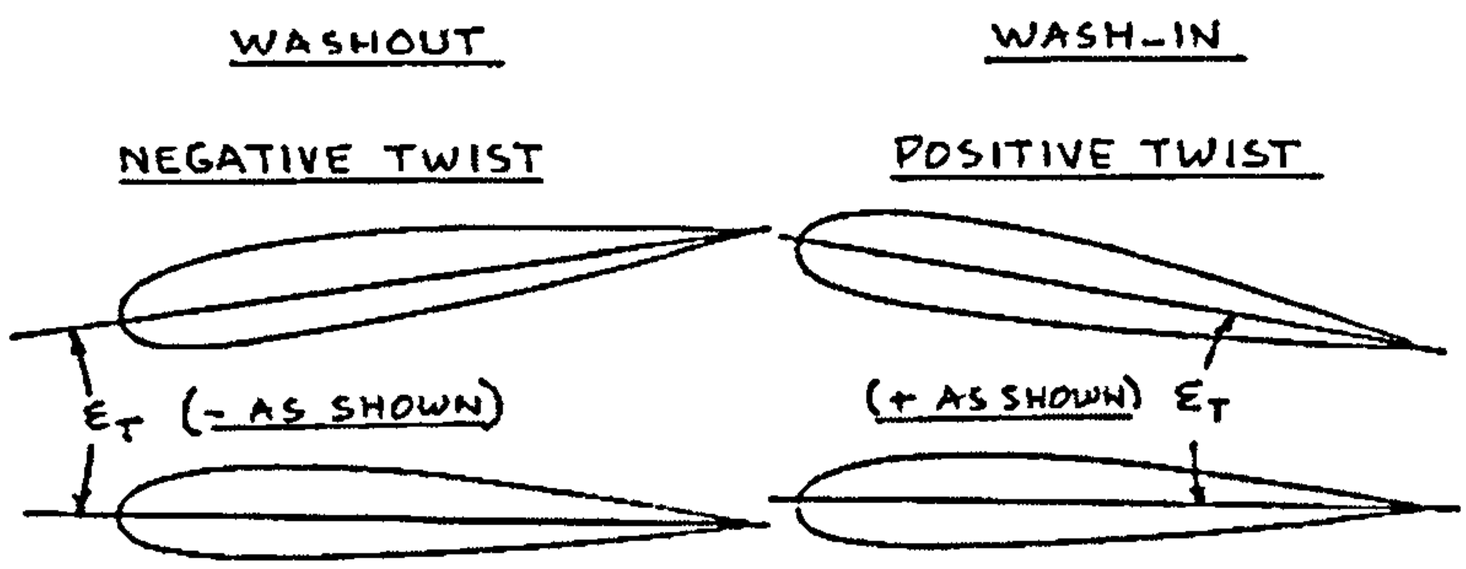

Figure 2.13 – Definition of wing twist [82]

This feature is mainly included in the wing with the objective of preventing tip stall and to move the wing centre of pressure inboard. This has a direct impact on the moment distribution over the wing, reducing the wing root bending moment, and hence allowing a decrease in weight [77] [124]. Table 2.5 presents a summary of the effects of twist.

Table 2.5 – Summary of the effect of twist [82]

Item	Effect of Twist Angle (Washout)	
	Large	Small
Induced Drag	High	Small
Tip Stall	Good	Poor
Wing Weight	Mildly Lower	Mildly Higher

Dihedral

The wing Dihedral is defined as the angle of the wing with respect to the horizontal when view directly from the front, as shown in Figure 2.14. If the dihedral angle is negative it is then called Anhedral.

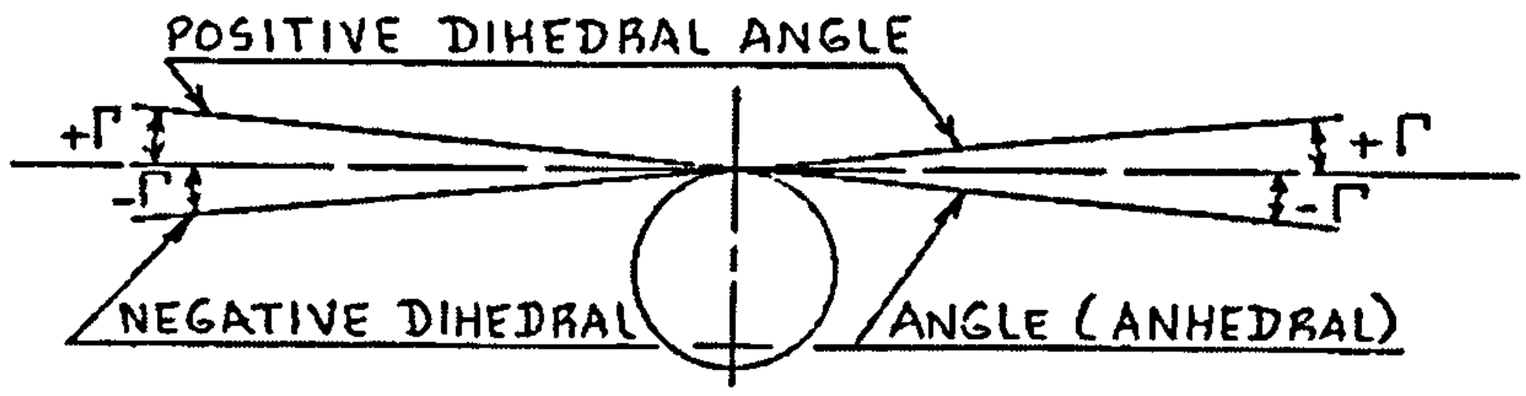

Figure 2.14 – Definition of wing dihedral angle [82]

The dihedral angle affects the natural lateral stability of the aircraft. It influences the Spiral and Dutch roll stability of the aircraft, and because they vary inversely with the dihedral angle, a compromise must be achieved in order to obtain a good natural lateral stability.
The dihedral angle can also be used due to layout requirements, such as ground clearance for engines and stores, or fuel system design [48]. In some cases, airplanes with swept wings will have too much natural dihedral in flight due to sweep, and in some cases that is the reason why negative dihedral (Anhedral) is used.

Table 2.6 – Summary of the effect of wing dihedral angle [82]

Item	Effect of Wing Dihedral Angle	
	Positive	Negative
Spiral Stability	Increased	Decreased
Dutch Roll Stability	Decreased	Increased
Ground Clearance of Wing, Nacelle, propeller or Landing Gear	Increased	Decreased

2.4.3. Wing Structural Layout

At the start of the wing design process of a civil transport aircraft there are several restrictions, which generate three distinct regions on the wing [123]. This is mainly to provide the wing with space for the control and high lift devices. The referred regions are (See Figure 2.15):

Leading Edge – In this region it is common to see flaps, de-icing systems, engine controls and fuel systems. It usually takes about 10-15 % of the chord and most of the Span.

Trailing Edge – Usually flaps, ailerons and control runs occupy this region. In swept wing aircraft it is common to see undercarriage stowage. The ailerons use about 25-30 % Chord and 35 % Span. The flaps take about the same value of the chord as the ailerons, but as much as 65 % Span.

Main Torsion Box – This region is basically a load carrying structure that should be maintained unbroken to avoid severe weight penalties. It is normally restricted to 50% of the chord and can be used as a fuel tank, stow the undercarriage, etc...

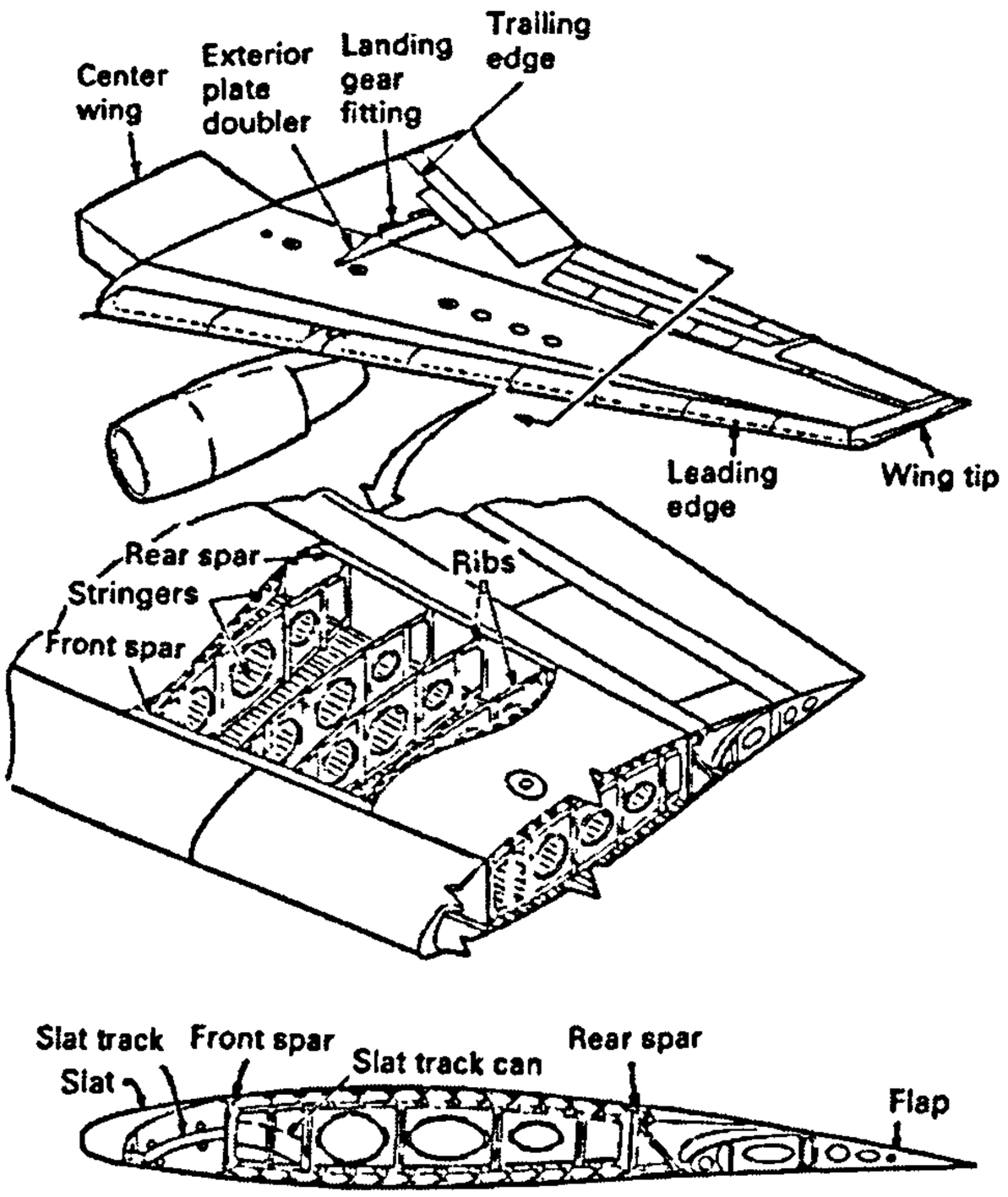

Figure 2.15 – Typical Transport Wing [67]

Also, Figure 2.16 shows a typical arrangement of the main control surfaces that can be seen on modern civil transport aircraft.

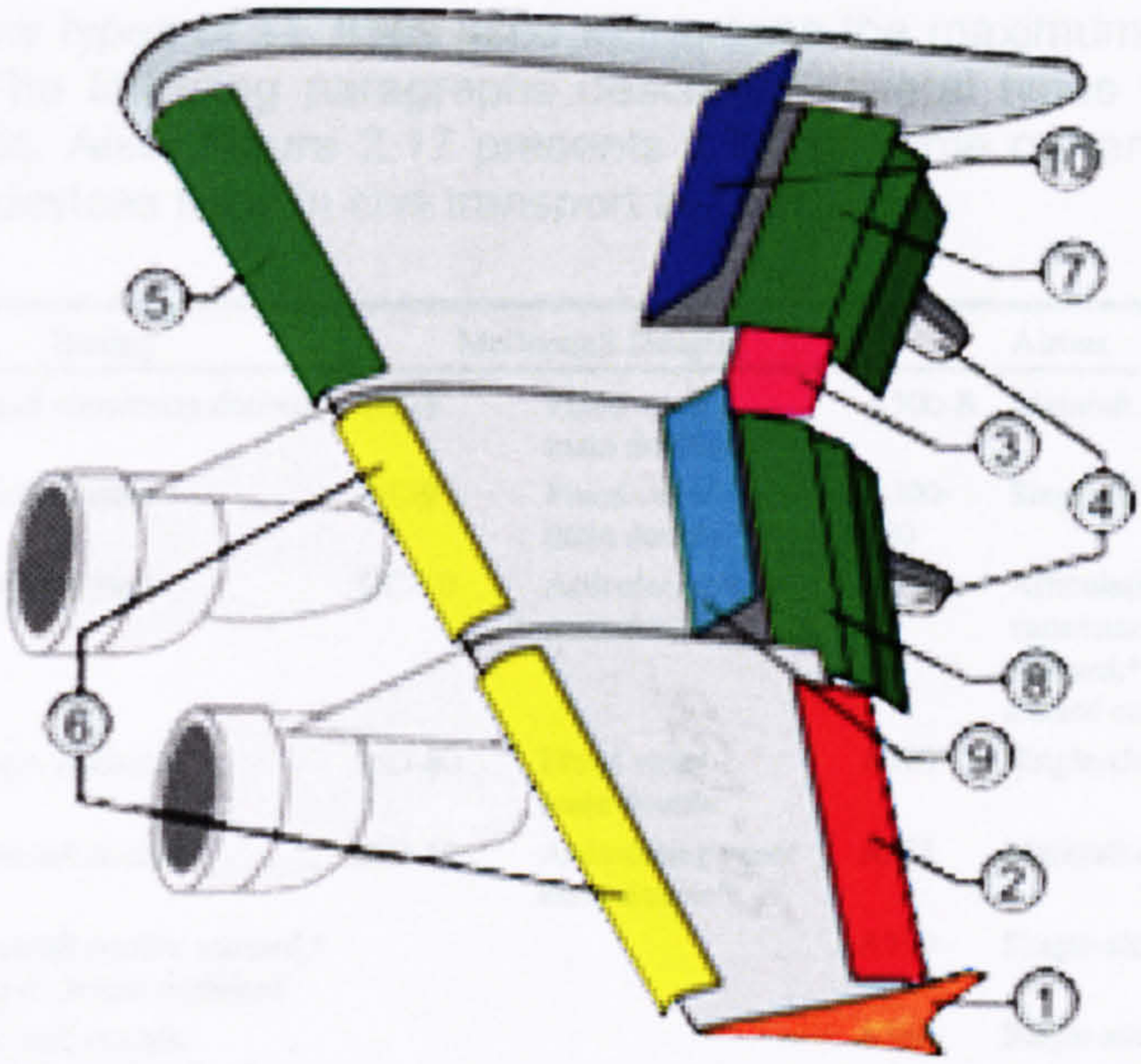

Figure 2.16 – Typical Transport Wing Main Control Surfaces [125]

1. **Winglet**
   A vertical or angled extension at the tips of each wing used to improve the efficiency of the aircraft by decreasing the lift induced drag caused by wing tip vortices.
2. **Low-Speed Aileron**
   Movable flaps used to control the aircraft rolling and banking movements.
3. **High-Speed Aileron**
4. **Flap track fairing**
5. **Krueger flaps**
6. **Slats**
   Small aerodynamic surfaces on the leading edge of the wings that when deployed allow the wing to operate at higher angles of attack.
7. **Inner flaps**
   Hinged surfaces that when deployed increase the lift and drag of a wing.
8. **Outer flaps**
9. **Spoilers**
   Spoilers are hinged plates on the top surface of a wing which can be rotated upwards into the airflow reducing lift in an aircraft. When actuated, the spoiler creates a carefully controlled stall over the portion of the wing behind it, rapidly reducing lift.
10. **Air brakes**
    Flight control surface used to reduce speed during landing. Air brakes are designed to increase drag while making little change to lift.

2.5. CONVENTIONAL TRAILING EDGE HIGH LIFT DEVICES

There are many types of TE flaps used to increase the maximum lift coefficient at low speeds. The following paragraphs described several types of trailing edges high lift devices. Also, Figure 2.17 presents a list of some current applications of Trailing Edge devices flaps in civil transport aircraft.

Boeing		McDonnell Douglas		Airbus	
707	Fixed vane/main double	DC-8	Fixed vane/ main double	A300-B	Main/aft double
727	Triple-slotted	DC-9	Fixed vane/ main double	A300-600	Single-slotted*
737	Triple-slotted	DC-10	Articulating vane/ main double	A310	Articulating vane/main inboard,* single-slotted outboard
747	Triple-slotted	MD-80	Fixed vane/ main double	A320	Single-slotted
757	Main/aft double	MD-11	Articulating vane/ main double*	A321	Main/aft double
767	Main/aft double inboard,* single-slotted outboard			A330	Single-slotted**
777	Main/aft double inboard,*** single-slotted outboard			A340	Single-slotted**

*Drooped inboard aileron. **Drooped outboard aileron. ***Drooped and slotted inboard aileron.

Figure 2.17 – Applications of Trailing Edge Flaps [85]

2.5.1. Plain Flaps

The Plain flap (Figure 2.18) is a simple hinged part of the wing trailing edge that pivots in a chord line. This allows the trailing edge to be deployed by downward rotation leading to an increase of the local wing camber and, hence an increase in lift.

The flap deployment is limited to an angle of about 20°. This limitation is due to the fact that at higher angles the flow separates on the upper surface.

The plain flap is also a mechanically simple device, but due to the deployment angle limitation it hasn't been used on any modern airliner [85].

This type of flap has been used as a flaperon, an aileron drooped at low speed.

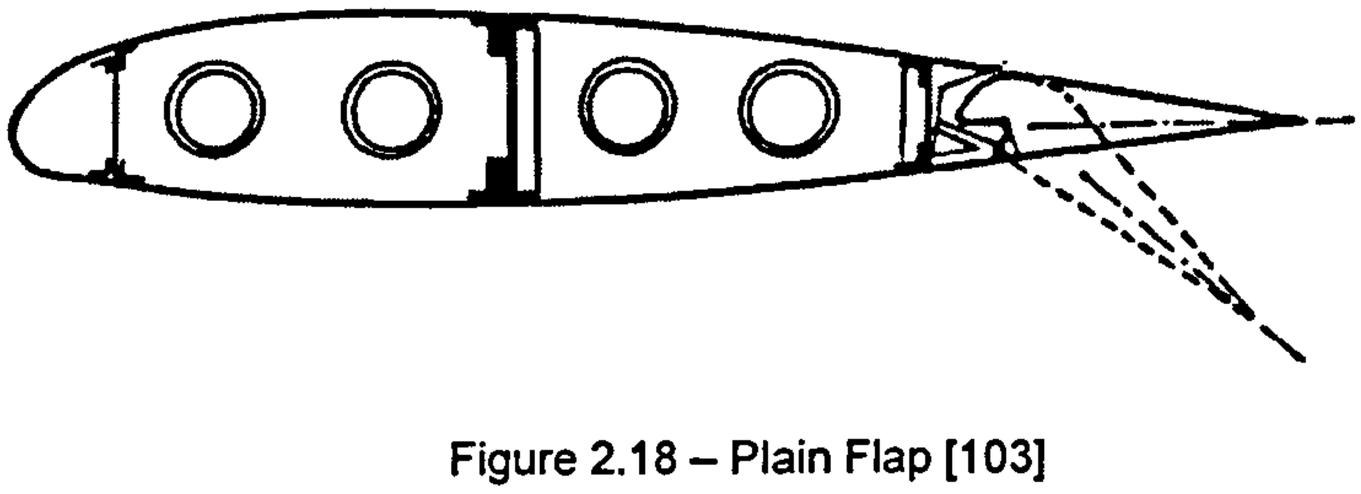

Figure 2.18 – Plain Flap [103]

2.5.2. Split Flaps

The Split flap (Figure 2.19) consists of a simple stiffened plate hinged in the wing lower surface, which deflects downwards and effectively changes the local camber of the wing section. When this device is deployed, the flow is always separated. It is structurally and mechanically simple and with low weight.
This type of flap produces a slightly greater increase in lift than the plain flap. The downside is that it generates more drag.
In the early days, it was commonly used in military aircraft. The low efficiency associated has made its use rare and it has not been used in any modern airliner. Nowadays its usual application is as a landing flap in unsophisticated aircraft [48].

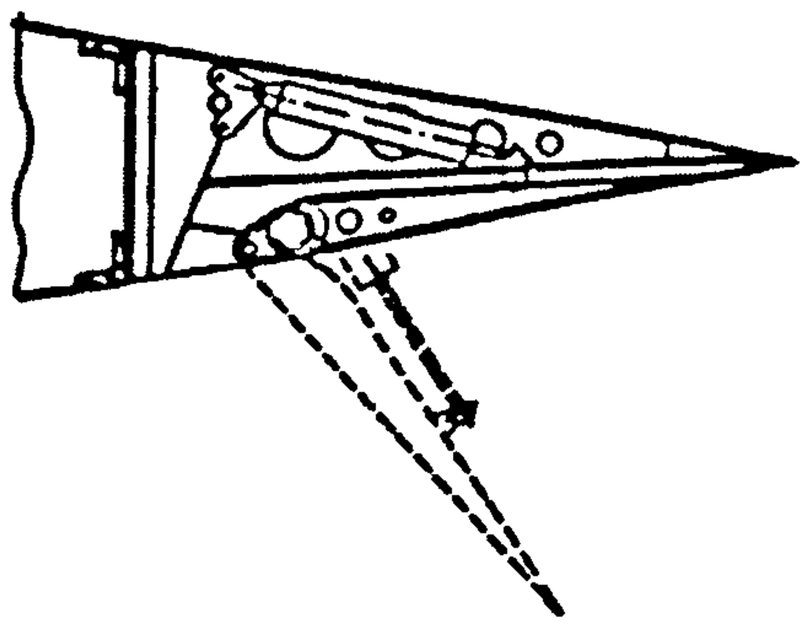

Figure 2.19 – Split Flap [67]

2.5.3. Simple Slotted Flap

The Simple Slotted flap (Figure 2.20) is similar to the plain flap. The major difference is the introduction of a slot between the main wing surface and the flap's leading edge when the device is deployed. This will allow high-pressure air from the lower surface to be introduced in the upper surface, re-energizing and stabilizing the boundary layer. This delays the flow separation problem characteristic of the previous devices and causes much greater increases in lift. The newly stabilized boundary layer will allow flap deflections of up to about 30-35°. The performance of this device is sensitive to the slot shape requiring a careful aerodynamic design for the flap leading edge. The introduction of the slot also introduces an increase in mechanical complexity.
The deployment of the device also generates a small wing area increase, but the lift increment due to this is also small, that is why its use is not made on many modern airliners.

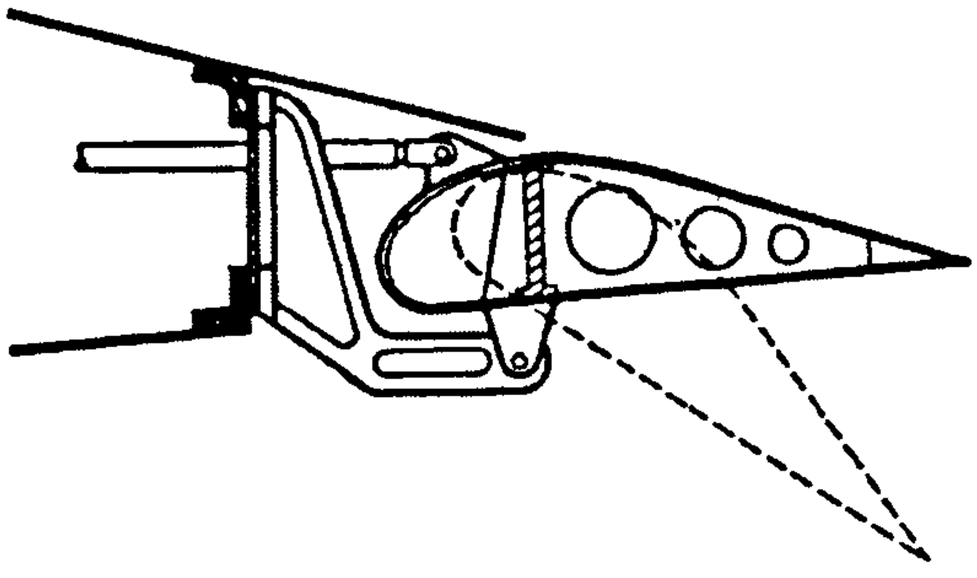

Figure 2.20 – Simple Slotted Flap [104]

2.5.4. Single Slotted Fowler Flap

The Fowler flap is similar to the Simple Slotted flap. The difference comes from the fact that this device is not only rotated, but it also travels rearward. This movement generates an increase in camber as well as a significant increase in wing area. As the simple slotted flap it requires a careful aerodynamic design of the flap leading edge in order to obtain good performance.
It has a very good efficiency because it yields a large increase in lift for very little changes in drag. This is the main reason why this device is so popular in transport aircraft and it is used in almost all airliners on the wing trailing edge or only on the outboard wing.
The Fowler flap can be deployed to about 40°, but from this point onwards the flap loses effectiveness. The initial deployment of the Fowler flaps is characterized by an increase in wing area with small variation of camber, which is good for takeoff. As the deployment continues the required landing characteristics are achieved with further increase of wing area and camber.
Simple hinges below the wing, or by means of a track carriage assembly can actuate the Fowler flap. Figure 2.21 shows two different ways of actuating the Fowler flap.

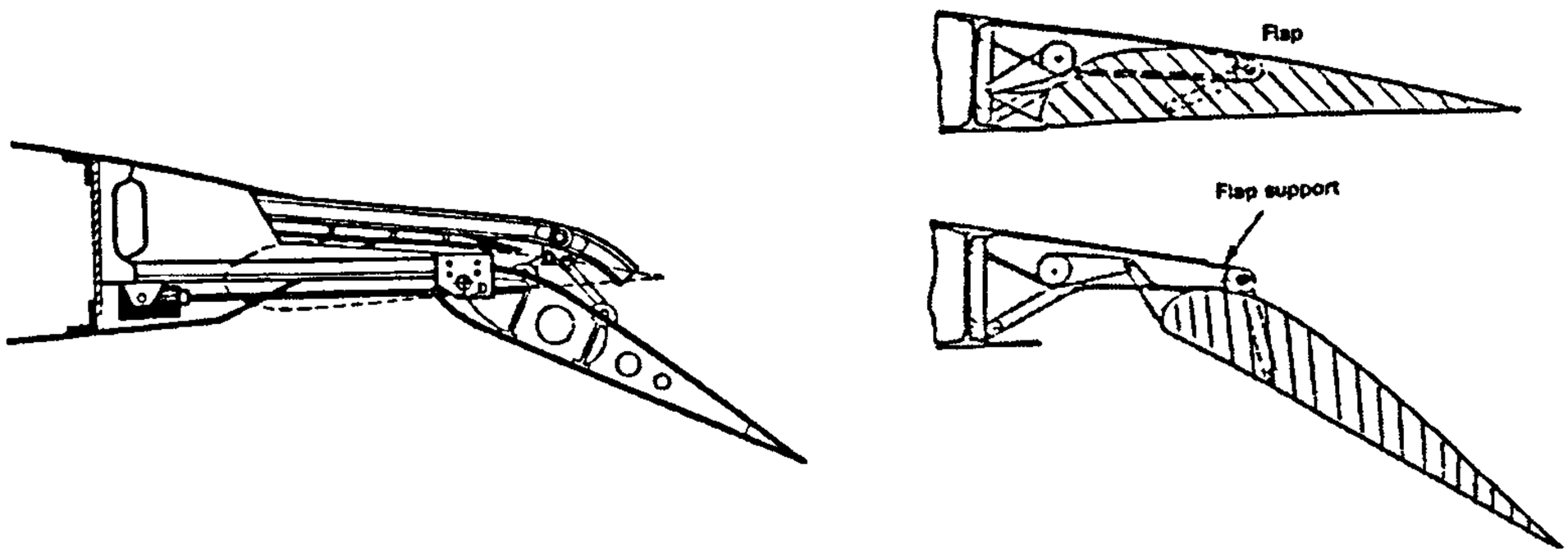

(a) Track Carriage [104] (b) Hinge [85]

Figure 2.21 – Single-Slotted Fowler Flap

2.5.5. Double Slotted Flap

To further take advantage of the Fowler flap good qualities, double – and even triple – slotted flaps are used in some airliners. The use of more than one slot will make the re-energizing of the airflow over the upper surface of the wing much more effective and will allow even larger flap deflection angles. However the introduction of one or two more slots will introduce growing mechanical complexity. Three of the ways of using double slotted flaps are described below.

Fixed Vane/Main Double-Slotted Flap

The Fixed Vane/Main Double-Slotted flap (Figure 2.22) is divided in two distinct parts, the vane and the main body of the flap. The vane is an aerodynamically designed shape rigidly attached forward to the main body of the flap, forming a fixed geometry slot. The fact that the slot is fixed it may cause high profile drag during takeoff, when the flap deflections are small.

This type of flap allows deflections of up to about 55°, producing a little more lift than the single-slotted flap.
This flap is still structurally simple when compared to the single-slotted flap, but its cost and weight are a little higher [85].

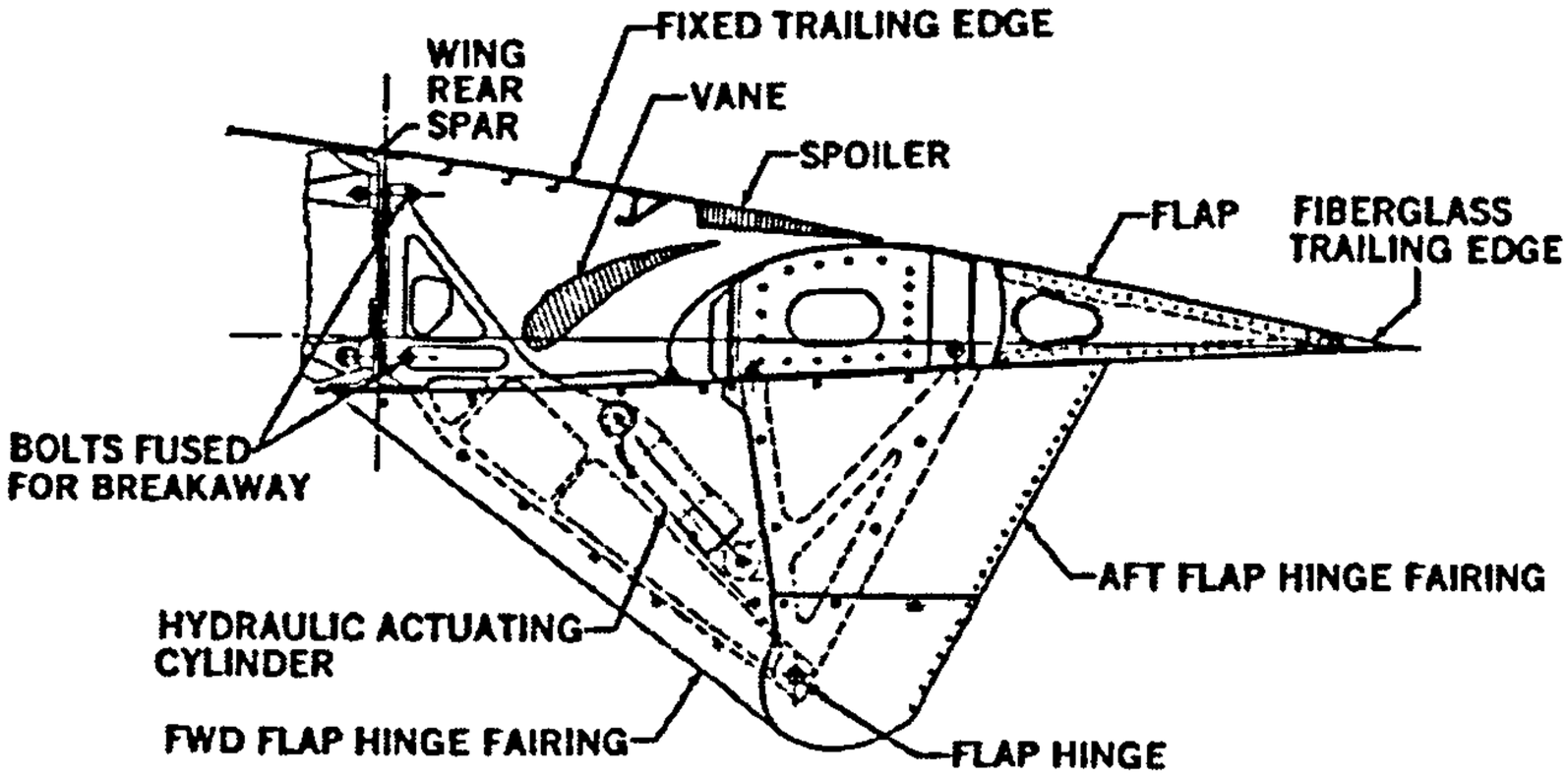

Figure 2.22 – Fixed Vane/Main Double-Slotted Flap [82]

Articulating Vane/Main Double-Slotted Flap

The Articulating Vane/Main Double-Slotted flap (Figure 2.24) has the same configuration as the previous one, the only difference is that the vane is now made movable. This solution was one way of resolving the high profile drag associated with the fixed vane/main double-slotted flap during takeoff i.e. at small angle deflections. By maintaining the vane in contact with the main body of the flap during takeoff, and effectively making it single-slotted, a better L/D can be achieved.
However, the introduction of a moving vane makes the mechanism design a lot more complex.

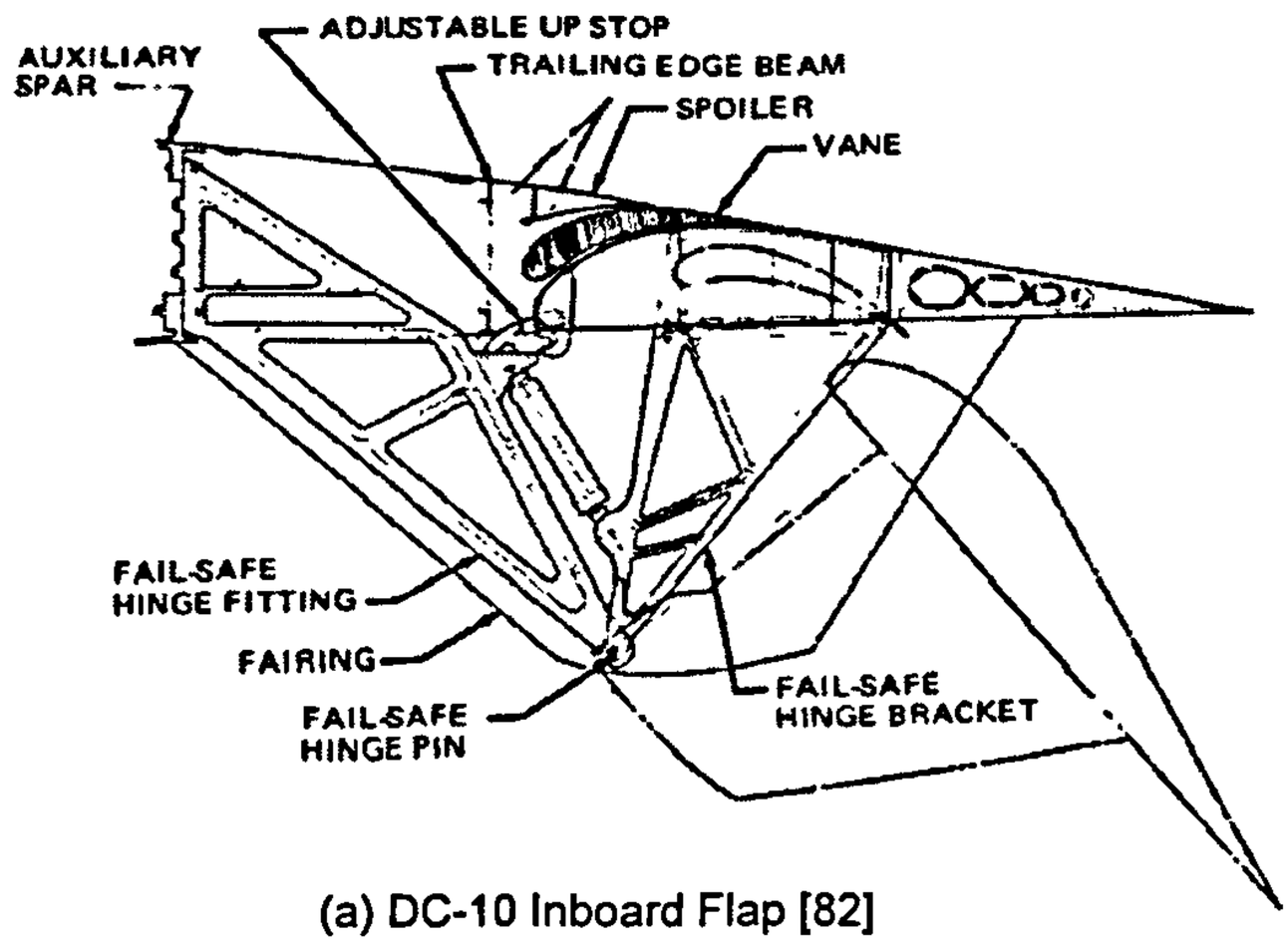

(a) DC-10 Inboard Flap [82]

Figure 2.23 – Articulating Vane/Main Double-Slotted Flap – Simple Hinge Mechanism

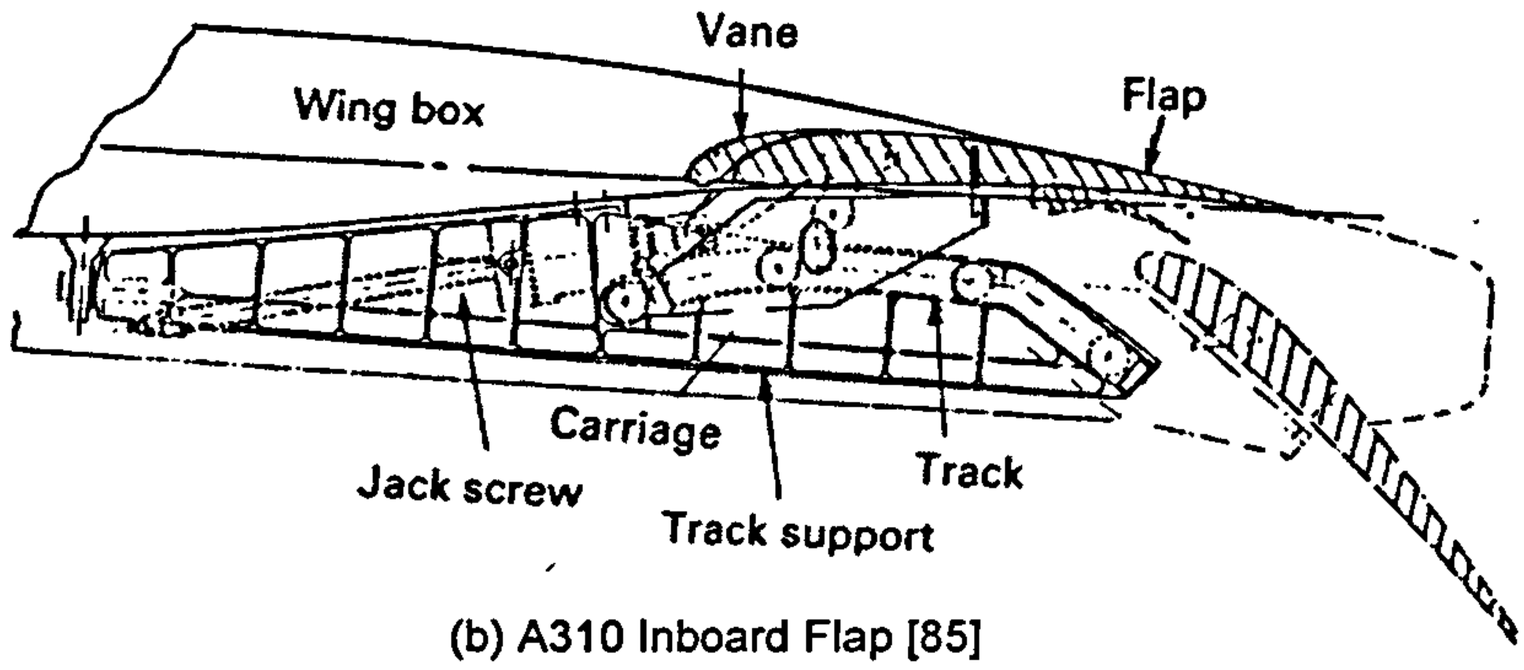

(b) A310 Inboard Flap [85]

Figure 2.24 – Articulating Vane/Main Double-Slotted Flap – Track Mechanism

Main/Aft Double-Slotted Flap

The Main/Aft Double-Slotted flap is also composed of two distinct parts, but instead of introducing a vane forward to the main body of the flap, it is now positioned aft of the main body of the flap, as shown in Figure 2.25. This makes this device even more complex than the previous ones.

From the double-slotted flaps presented, and considering the same stowed chord length for the flaps, this is the one that generates more lift.

The deflections that are typical in this type of devices are of about 60° to 65° [85].

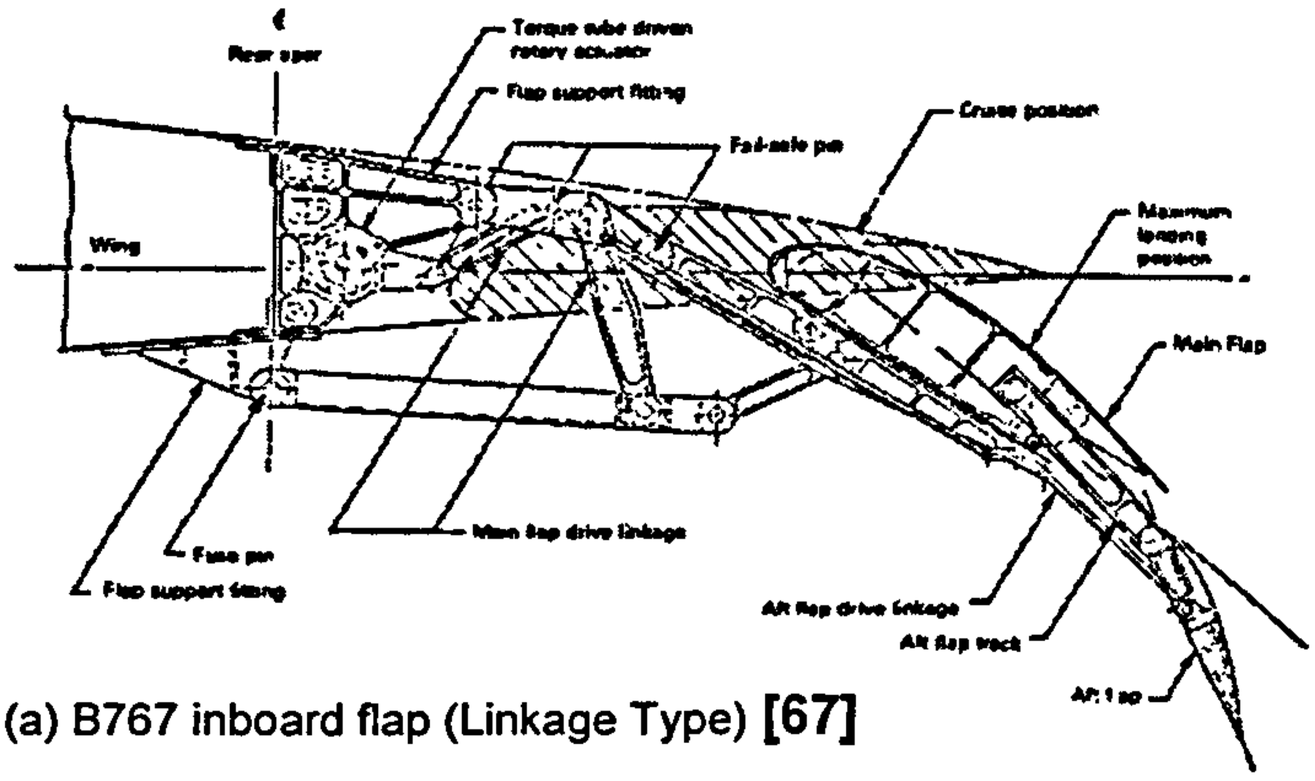

(a) B767 inboard flap (Linkage Type) **[67]**

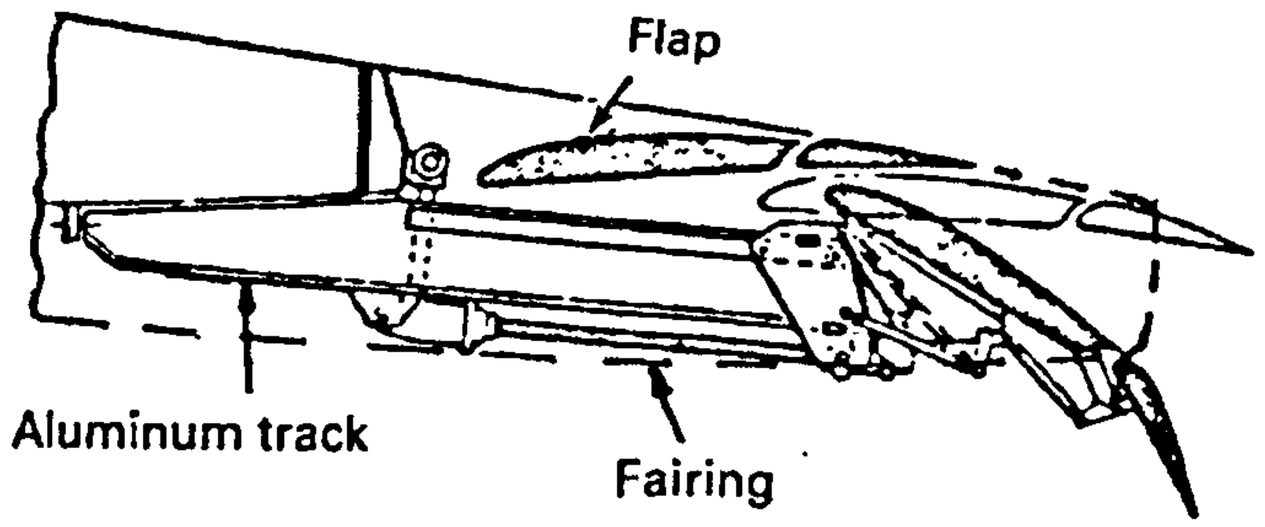

(b) A300 flap **[67]**

Figure 2.25 – Main/Aft Double-Slotted Flap

2.5.6. Triple Slotted Flap

The triple slotted flap is a combination of the articulating vane/main and the main/aft double-slotted flaps. This device is composed of a vane, a main flap body, and a small aft flap, as shown in Figure 2.26.

This device achieves extremely high Fowler motion, which can result in a flap defection of up to about 80° [85].

Aircraft with very high wing loadings are usually the candidates for the use of this type of flap. When compared with all the other flaps, this is the one that provides the highest sectional lift. However, the high edge losses due to tip vortex at each flap panel edge, and the higher nose-down pitching moment associated, reduce its benefits.

With the introduction of another moving part the mechanical complexity is increased even more, and it has been claimed that the penalties associated with the complexity outweigh the aerodynamic gains [74]. It requires complicated flap supports and controls, making it a heavy mechanism.

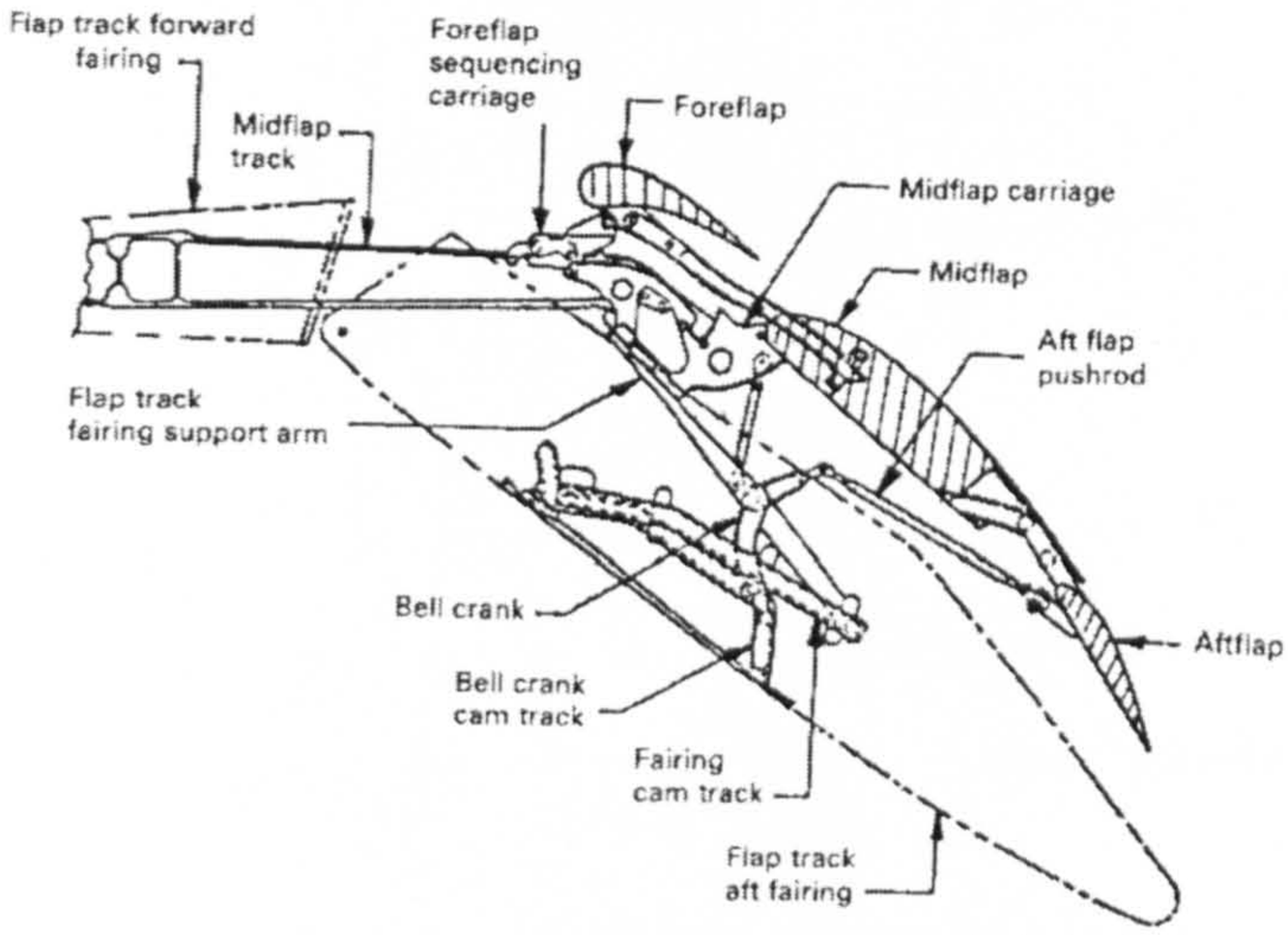

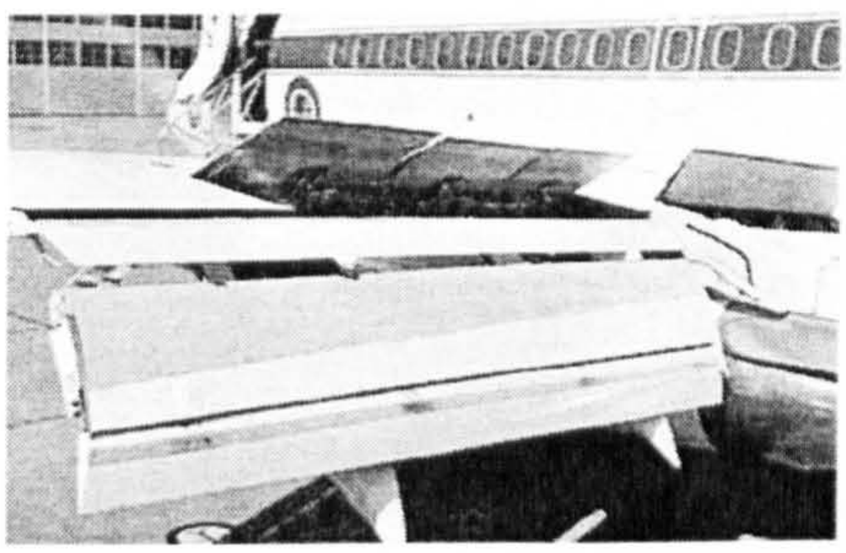

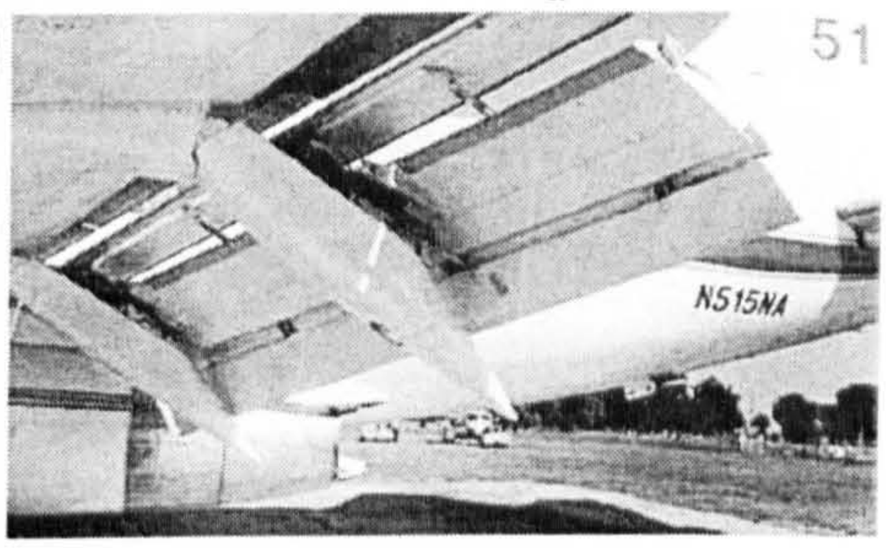

Figure 2.26 – B737 Triple Slotted Flap [67], [119]

2.6. POWERED TRAILING EDGE HIGH LIFT DEVICES

The limits of achievable lift for mechanical high lift devices have been reached as shown in Figure 2.27.
Further improvements have been achieved by the use of powered high lift devices.

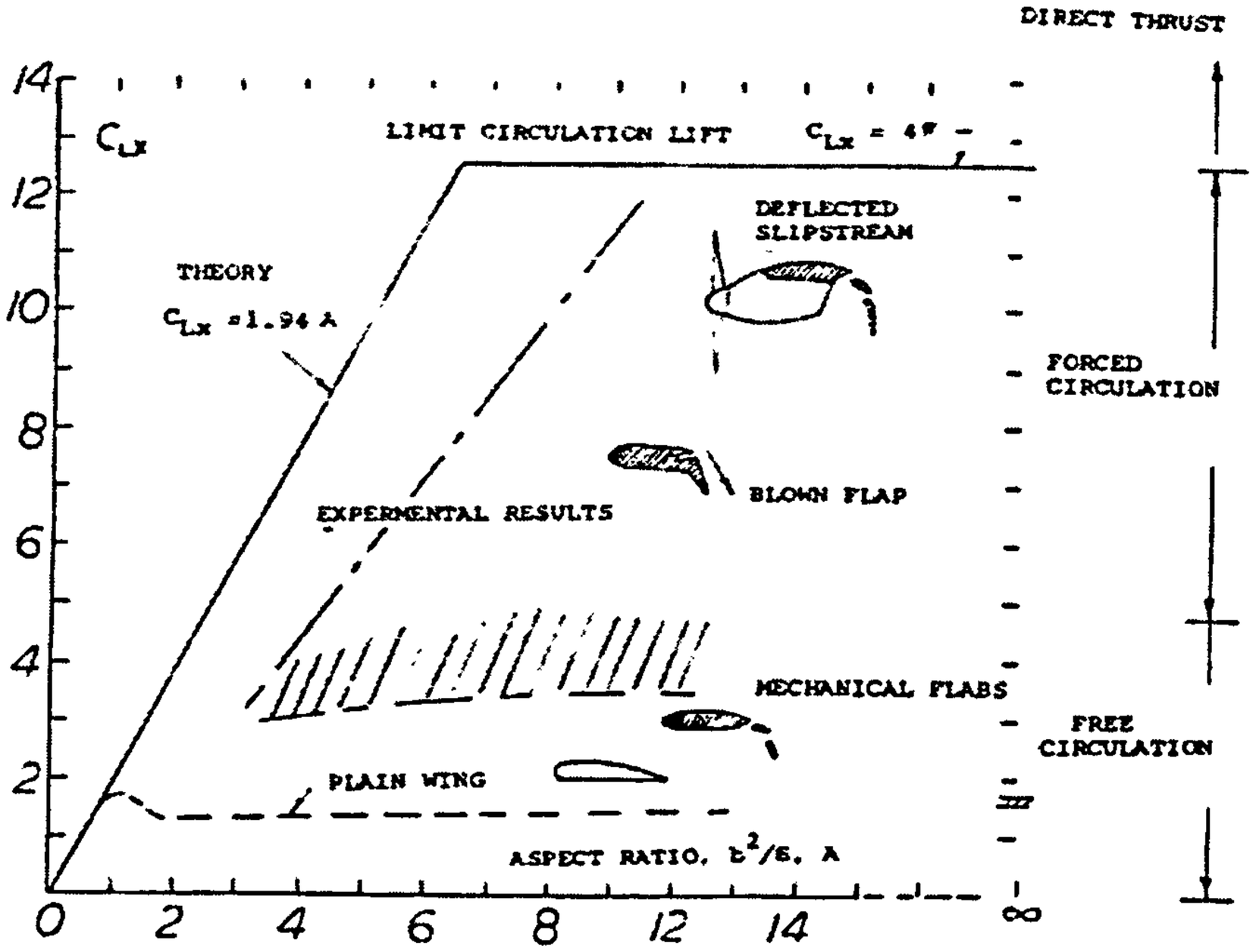

Figure 2.27 – Powered High-Lift Performance [87]

Table 2.7 and Figure 2.28 present a summary of approximate C_L ranges of powered high-lift systems used in V/STOL aircraft.

Table 2.7 – Summary of CL ranges for powered high-lift systems [114]

SYSTEM	C_{Lmax}
Internally Blown Flap	9
Upper Surface Blowing	8
Externally Blown Flap	7
Augmentor Flap	7
Vectored Thrust	3

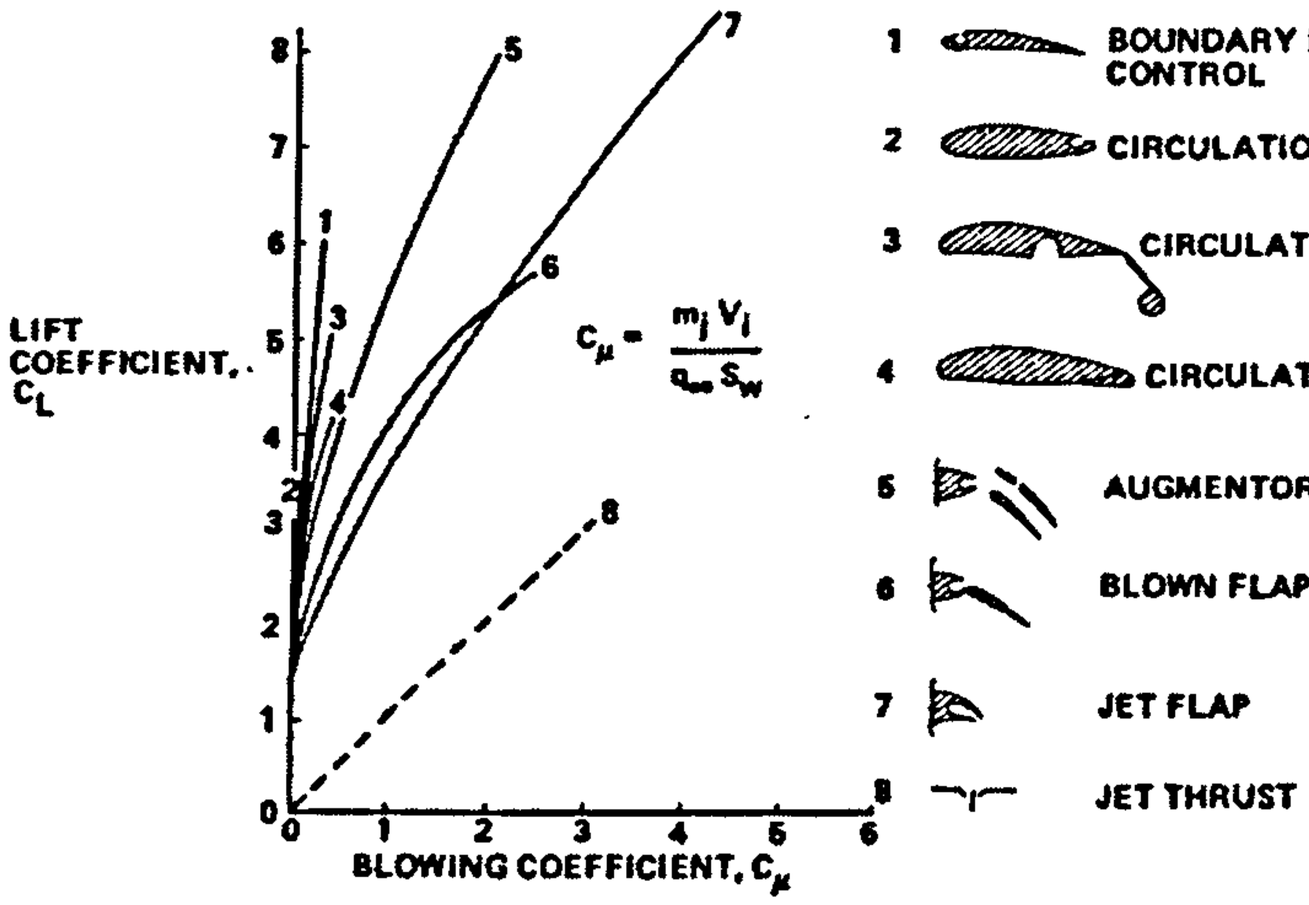

Figure 2.28 – Powered High-Lift Performance [16]

Powered High-lift Systems can be separated in two categories, the Power Augmented Boundary Layer/ Circulation Control and Powered Lift [16].

2.6.1. Power Augmented Boundary Layer / Circulation Control

These types of devices achieve better lift performance by channelling small amounts of auxiliary power to reduce the skin friction drag and delay the flow separation over the airfoil, and ultimately increase the C_{Lmax}.
Boundary layer control can be achieved in two different ways, by blowing air to increase the energy of the boundary layer, or by removing all or part of the boundary layer by suction.

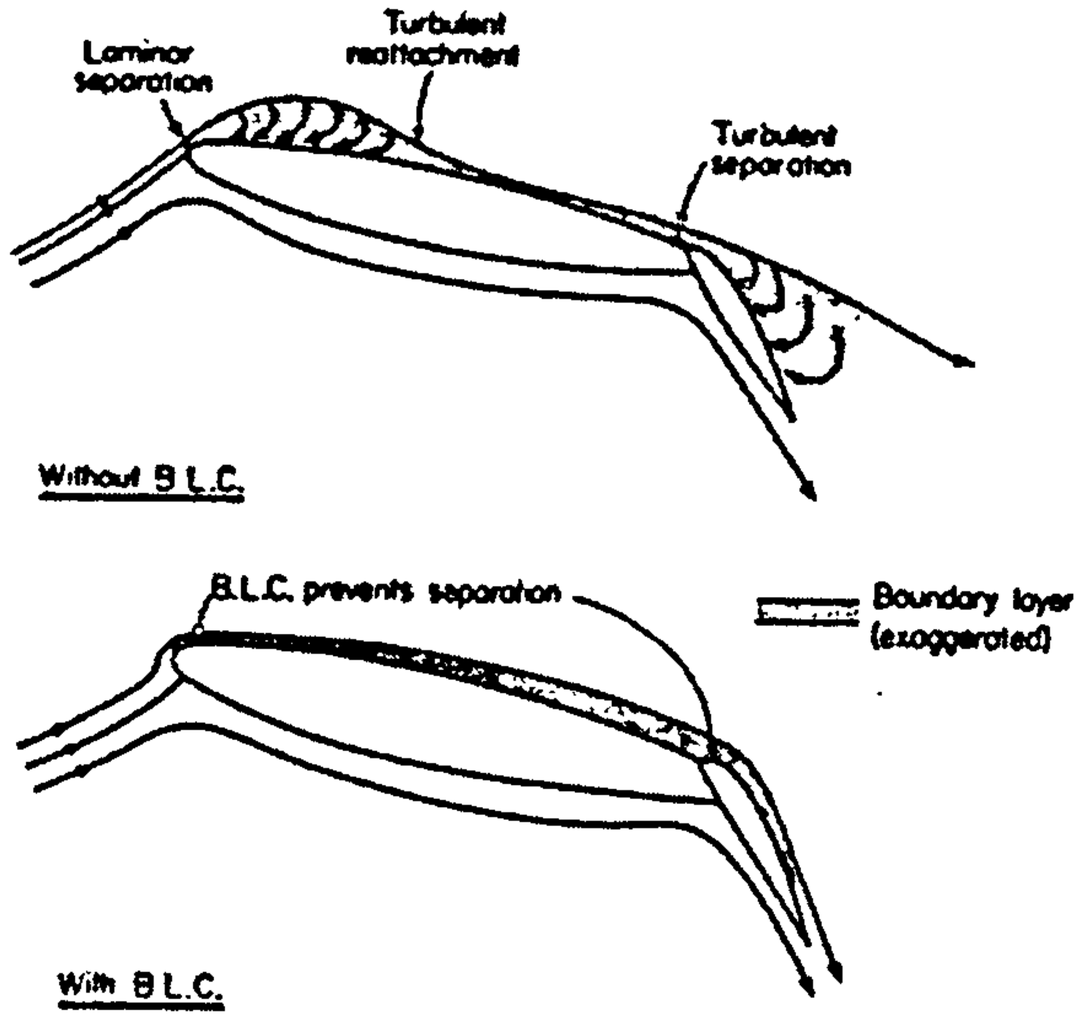

Figure 2.29 – Boundary Layer Control [16]

a) Boundary Layer Control by Suction

This system uses a powered system to suck the boundary layer flow from over the aircraft surface through closely spaced perforations.
When tested, this system has achieved considerable reductions in take-off and landing distances, though it has never been built in production aircraft. This is mainly due to the disadvantages that it holds when compared with the blowing system. Figure 2.30 presents several suction BLC concepts. The main disadvantages of this system are [108]:

- Complex system to develop and optimize;
- Requires an additional pump;
- Requires thick ducts due to the low pressure involved;
- Perforations are difficult to manufacture.
- Contamination due to insects, ice, dirt, etc...

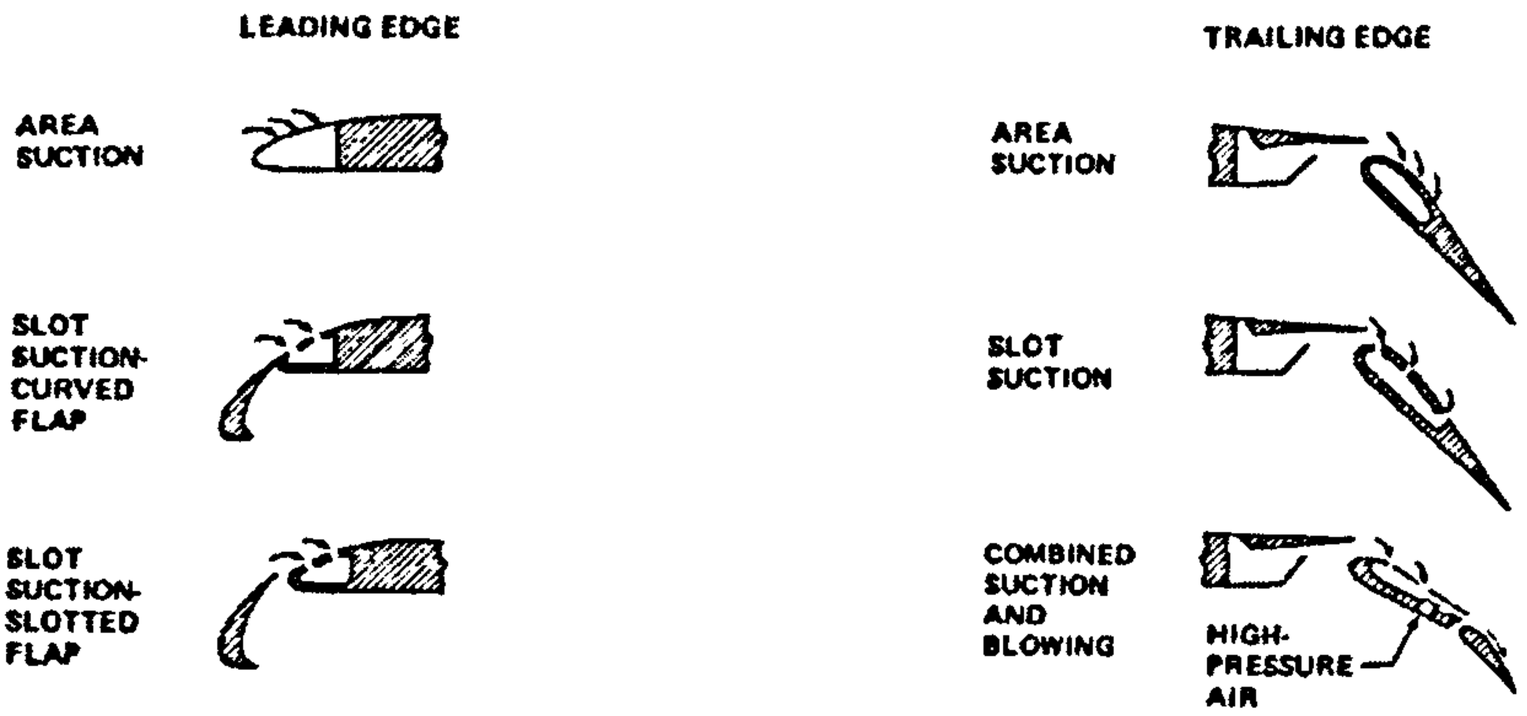

Figure 2.30 – LE and TE Suction BLC Concepts [16]

b) Boundary Layer Control by Blowing

This boundary layer control system uses a powered system to blow high pressure air to the boundary layer flow also to prevent flow separation.
Contrary to the previous system, there are not so many disadvantages, particularly for jet powered aircraft, where the high pressure air can be supplied directly from the jet engine compressor and can be used for de-icing. Due to its relative simplicity and reliability it has been used in military aircraft [108].
Figure 2.31 presents several suction BLC concepts.

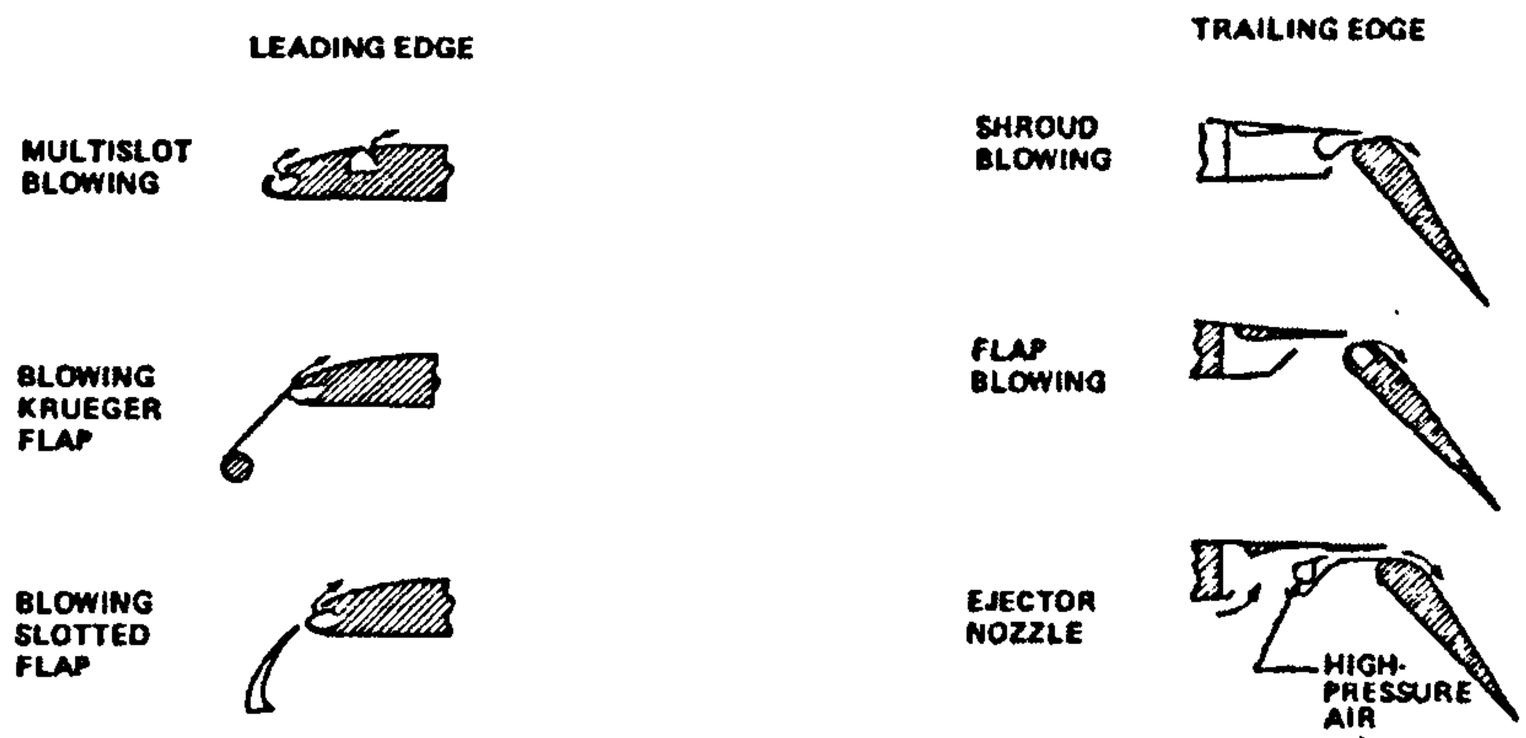

Figure 2.31 – LE and TE Blowing BLC Concepts [16]

2.6.2. Powered Lift Concepts

The main characteristic of powered lift devices is that the propulsion system is an integrated part of the High Lift system, as can be seen in Figure 2.32.

These high lift systems can also be separated in two different types, the main difference is the fact that one provides only direct lift and the other combines the propulsion and the circulation lift systems [108].

There are currently VSTOL and STOL aircraft that use these types of device and they can achieve maximum lift coefficients of 10 and above. Some of the known applications are: the C-17 Globemaster with externally blown flaps; the Antonov An 72/74 using over-the-wing blowing; the BAE Systems Harrier with vectored thrust [114].

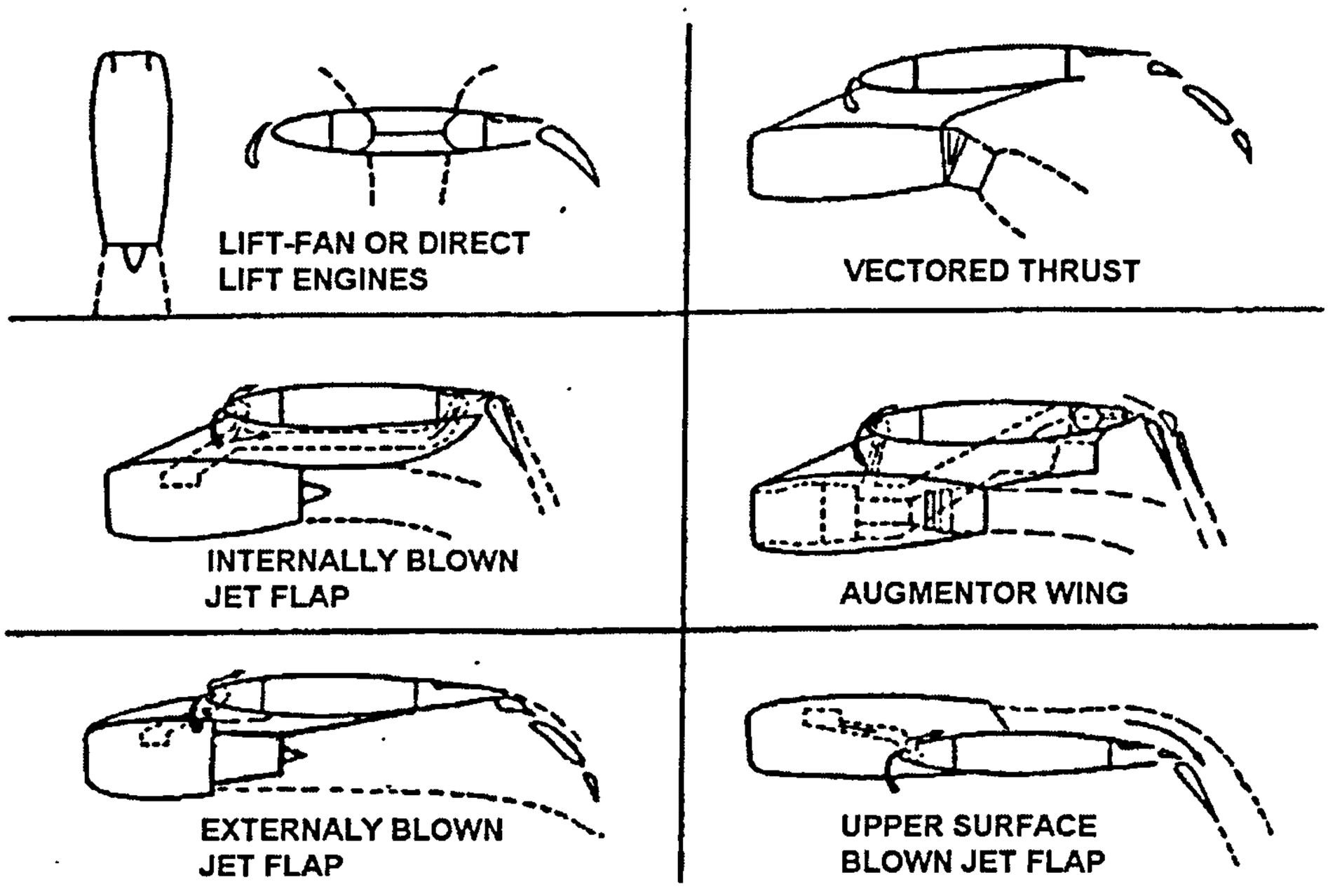

Figure 2.32 – Powered Lift Concepts [16]

2.7. VARIABLE CAMBER WING CONCEPT

The mission profile of current civil transport aircraft is well defined, and the wings are designed to cope with all these phases. The introduction of High-Lift devices in the leading and trailing edge provides the aircraft with the means to adjust and comply with the low speed requirements for take-off and landing. Though, when it comes to cruise, the wing profile is set and there are no variations, meaning that in specific occasions it might not be working in optimum conditions, incurring higher levels of drag and ultimately consuming more fuel.

Variable camber is a concept that looks at changing the profile of the wing during all flight phases, improving the aerodynamic efficiency of the wing by maintaining it working at near optimum conditions. Figure 2.33 show the basic principles of Variable camber operation.

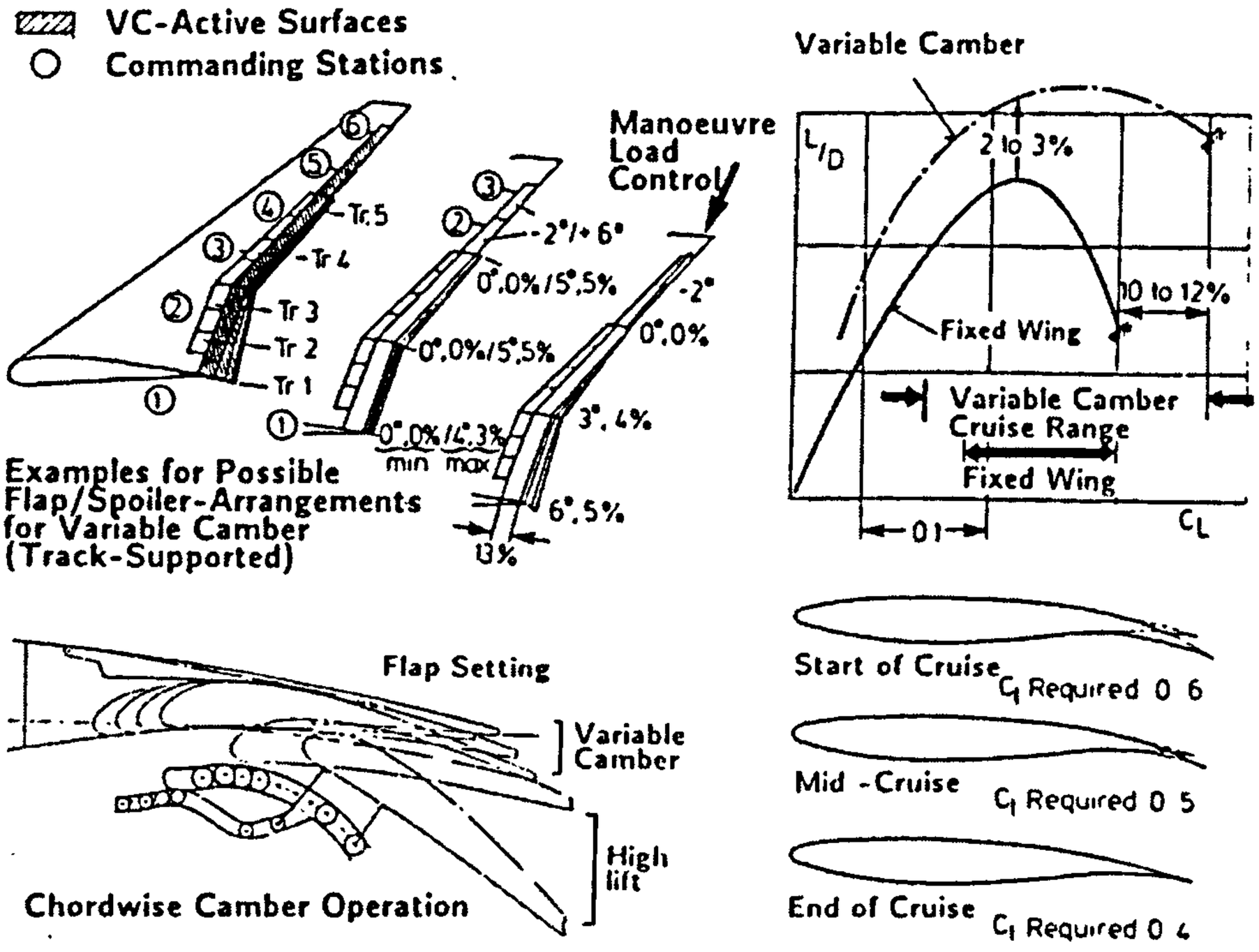

Figure 2.33 – Principle of Variable Camber Operation [40]

The benefits of this concept have been analysed in numerous publications and the most commonly referred advantages of this system are:

- Optimized L/D ratio, reducing fuel consumption (3-5% fuel savings [3])
- Reduce DOC
- Improved operational flexibility
- Increase stretch potential within the aircraft family

However, there are some disadvantages associated with this concept. The requirement for additional flight controls and additional weight associated with the increase in complexity will incur cost and performance penalties. So, when looking

to design a Variable Camber Wing System the main design objectives should be to reduce the systems cost and weight and improve the maintainability and reliability [3].

Cranfield Variable Camber Wing Concept

Initially conceived by Spillman [97][98][99], it has been addressed by several other PhD students from the College of Aeronautics of Cranfield University.
In 1992, Mr. Macci [53] investigated the structural and mechanical feasibility of introducing Variable Camber to super critical airfoil sections of different characteristics, as shown in Figure 2.34. The validation of the research was made in a modern transport aircraft wing and the results showed that it was feasible to apply the VC concept to the trailing edge, but further research was recommended for the leading edge.

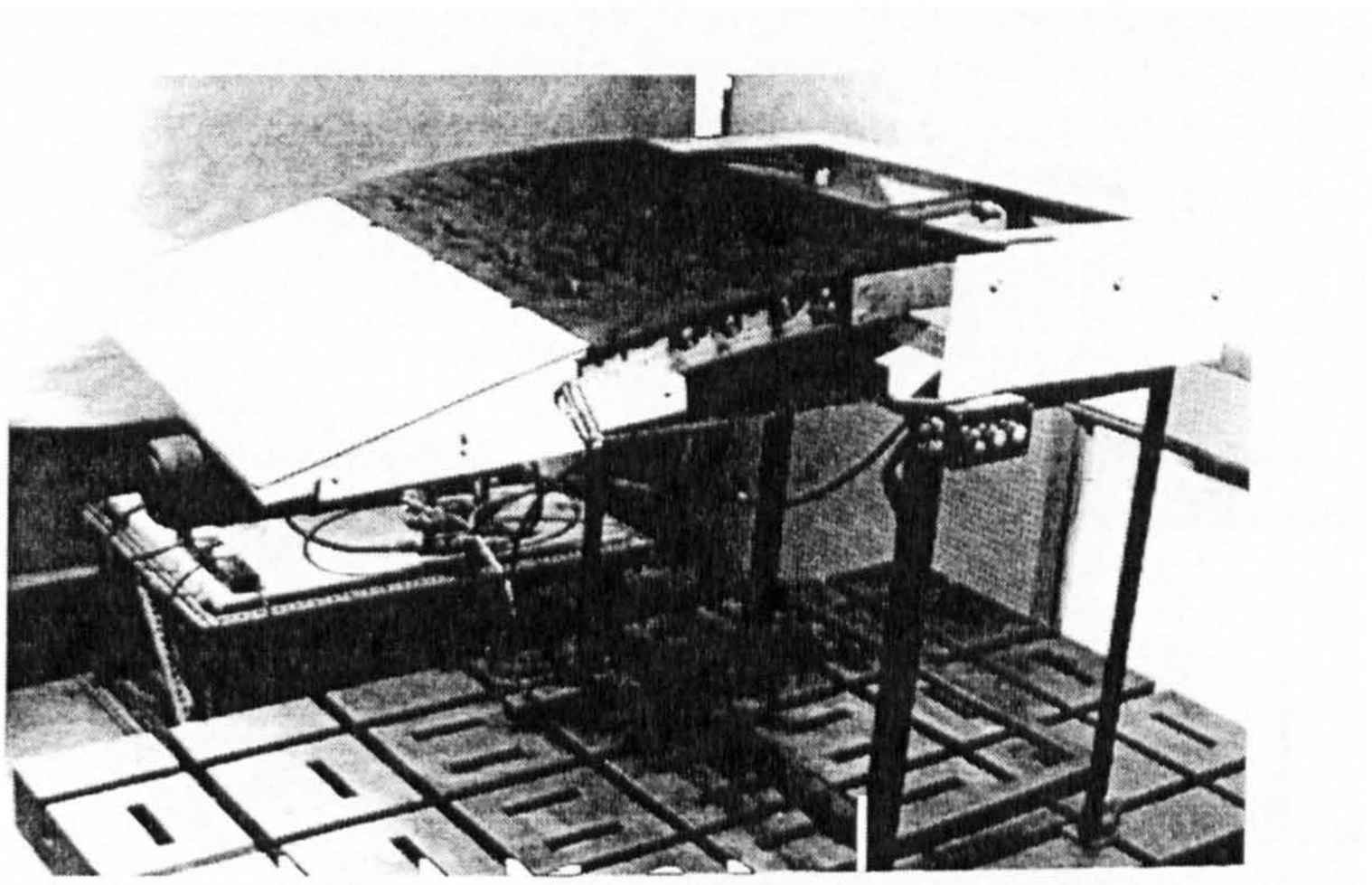

1 - Solid trailing edge device
2 - Flexible Upper surface
3 - Hinged lower surface plate
4 - Grooved extending track
5 - Conforming track
6 - Support track
7 - Rolling pins
8 - Compression spring
9 - Under surface hinge
10 - Wing structural box
11 - Wing rear spar
@ 64.5 % chord
12 - Wing rear spar
@ 54 % chord
(for maximum negative deflections)
13 - Reduced under-side to
retain lower surface continuity

Figure 2.34– MACCI Variable Camber flap concept [53]

The following year, Mr. MacKinnon [55] looked at the application of the novel Variable Camber Wing concept to a supercritical aerofoil and the research included the manufacturing of a 3D half wing wind tunnel model. The tests looked at local and spanwise variation of camber, but only for the trailing edge. The results were not totally satisfactory showing that a bigger wind tunnel model was required.

Later in 1998, Mr. Edi [20] investigated the feasibility of introducing a combined HLFC-VCW concept in the ATRA – Advanced Transport Regional Aircraft, a regional aircraft family, to improve the overall efficiency, flexibility and reduce weight. This research showed that the combined HLFC-VCW concept is feasible for this class and size of aircraft. It was proved that the VCW concept could be optimised to increase the lift to the desired range. Although, Mr. Edi recommended a further multidisciplinary investigation in order to improve the potential of these concepts.

The latest studied was done by Ammoo [1] in 2001 and proposed the use of an extended Fowler kinematic system that allows small deflections for camber variation during the cruise phase of the flight and still perform the flap deflections to meet the required characteristics for takeoff and landing, as can be seen in Figure 2.35.

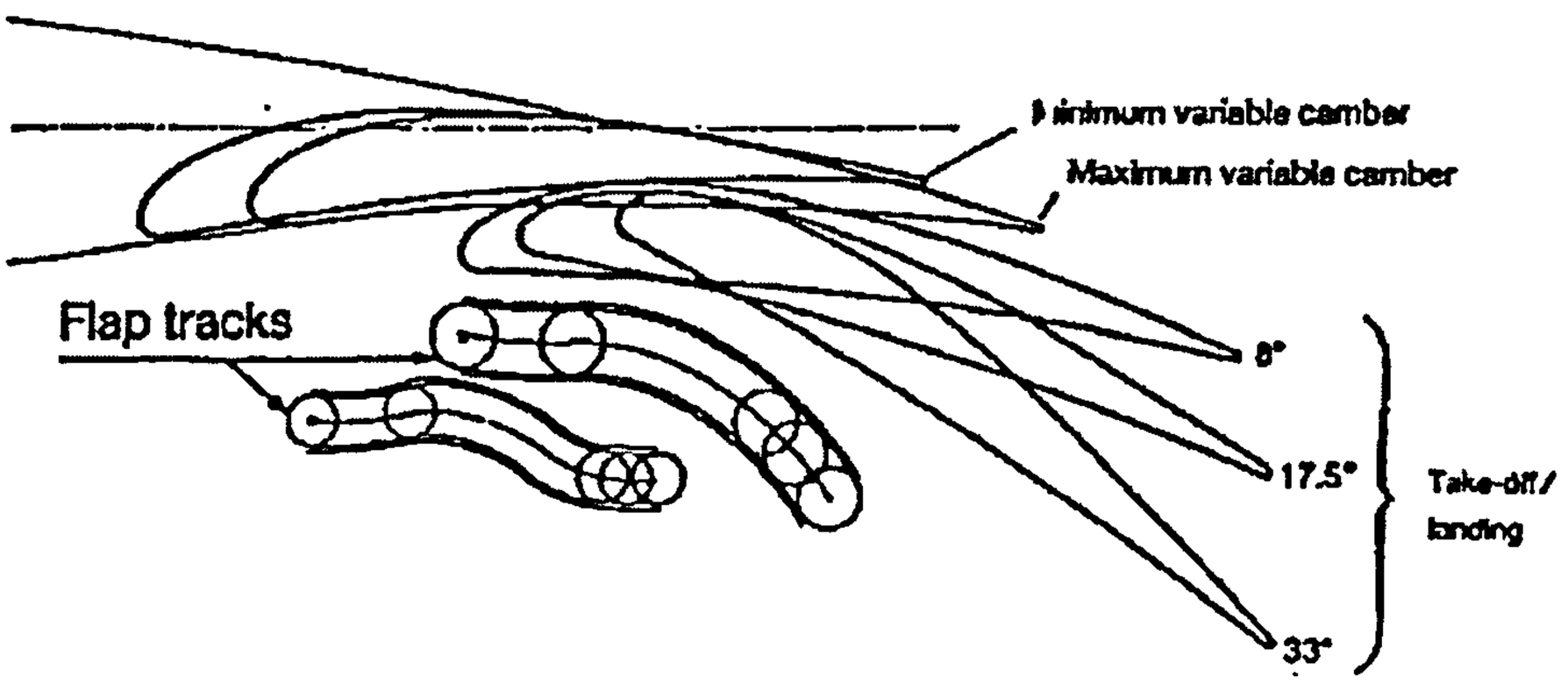

Figure 2.35– Variable Camber flap [1]

MBB Flap Carriage Support Track Concept of Variable Camber

A project sponsored by AIRBUS that looked into the application of the VC concept in to the existing flap systems on the A330/340 family of aircraft. The objective was to create a mechanically simple solution with minimum additional structural weight, that wouldn't change the existing wing box configuration.

The proposed solution consisted of a linkage system actuated by a rotary actuator in a flap carriage support track, as seen in Figure 2.36. Decambering is not possible in this solution.

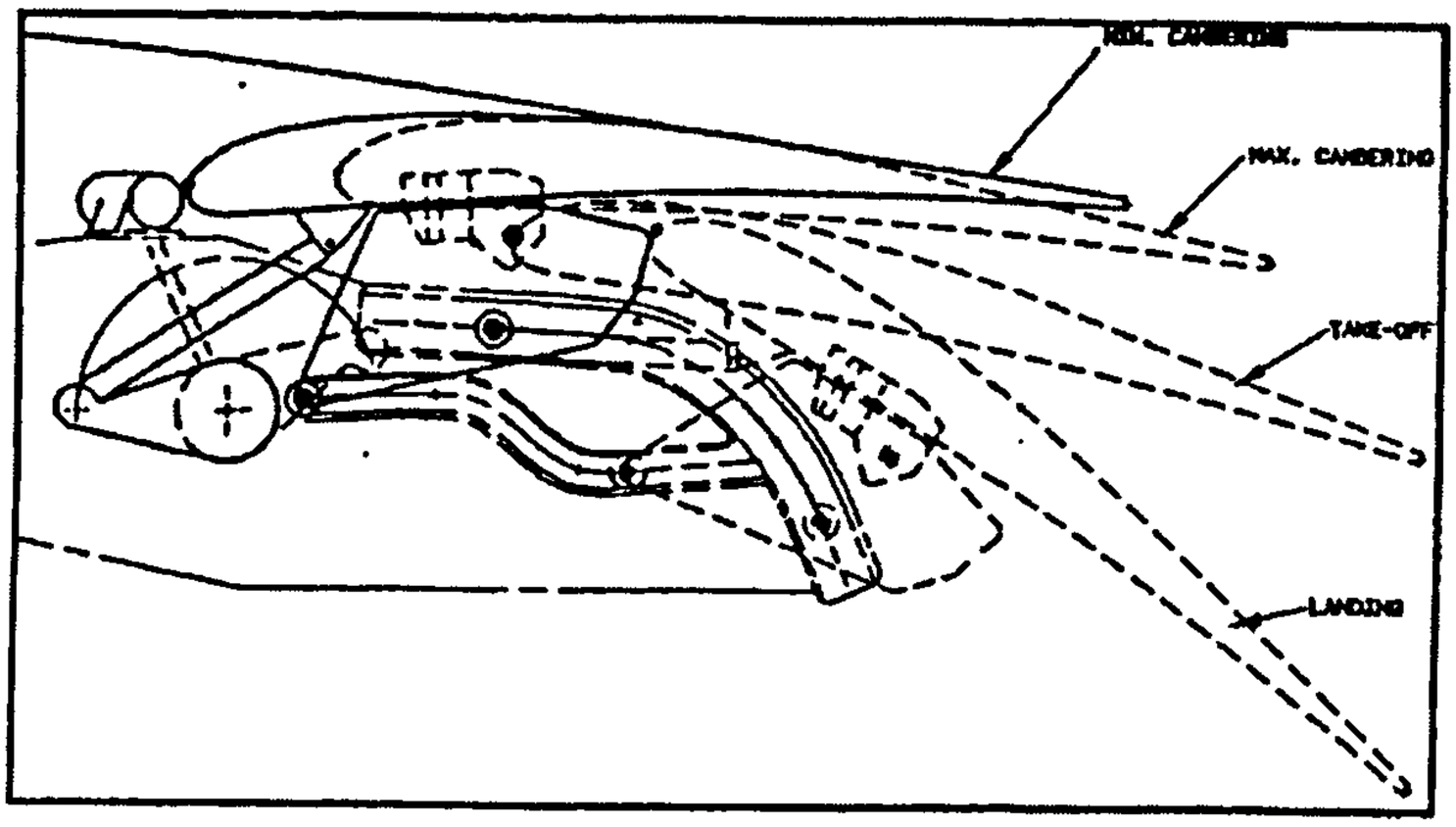

Figure 2.36– MBB Variable Camber Concept [3]

Daimler-Benz R&D "Adaptive Wing" Concept

This approach by Bauer et al. [3] consists of providing the flap with a flexible trailing edge structure capable of adapting its shape to the actual lift and load requirements. The idea behind this concept is a very simple passive trailing edge structure with an external kinematic actuation mechanism, incorporating "smart" technologies to control it. The proposed concept also integrates the flexible flap trailing edge in an extended Fowler kinematic system, as shown in Figure 2.38.

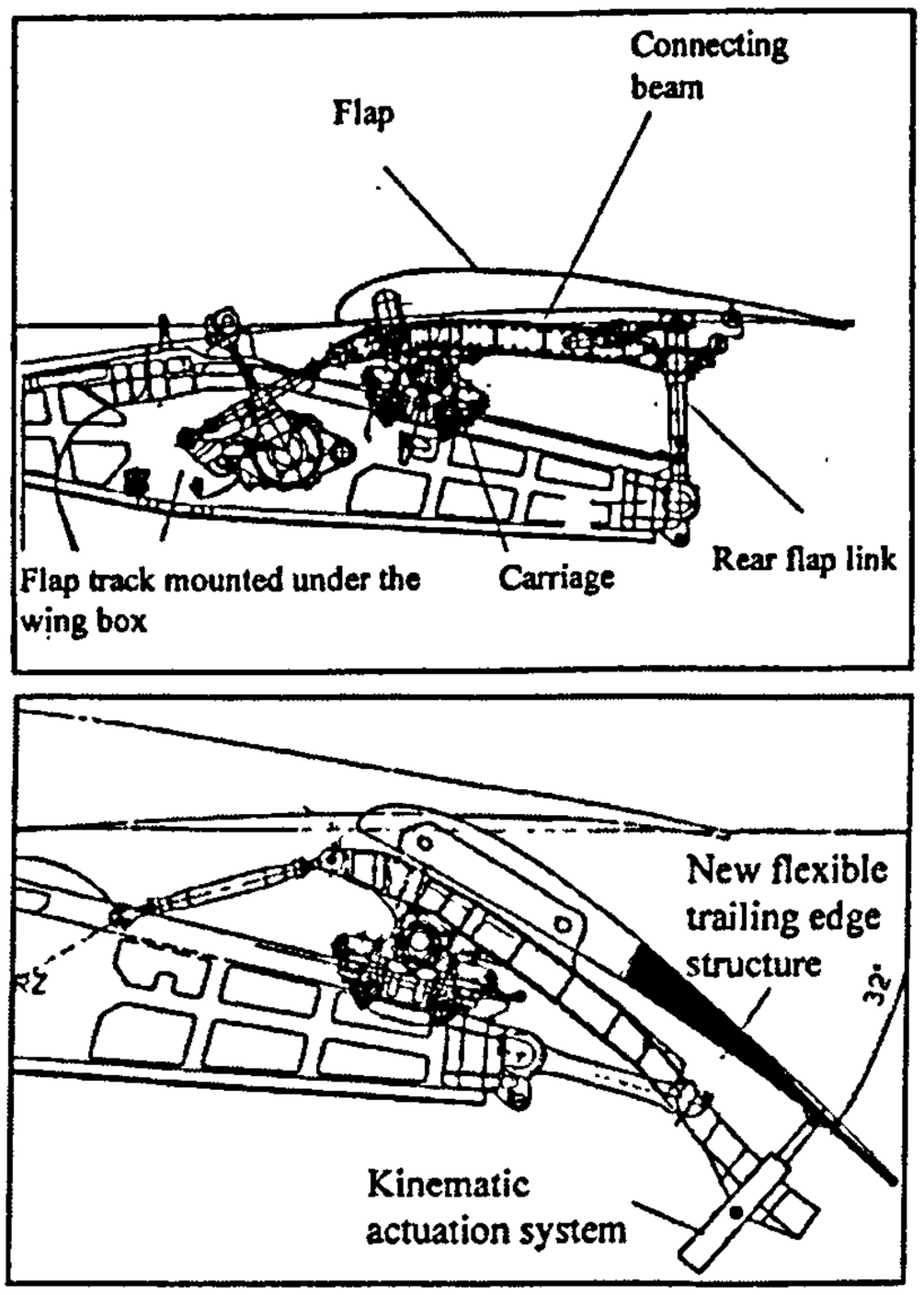

Figure 2.37 – Daimler-Benz "Adaptive Wing" Concept [3]

DaimlerChrysler Research "Adaptive Wing" Concept

Monner et al. [63] developed a concept were the Variable camber is achieve by introducing an adaptive structural system and a bump in the wing trailing edge of the aircraft., as seen in Figure 2.38. The trailing edge flexible structure is able to generate both chordwise and spanwise camber variation, improving the L/d ratio. The bump allows better control over the transonic shock, thus reducing the wave drag and contributing to the improvement the L/D ratio [3].

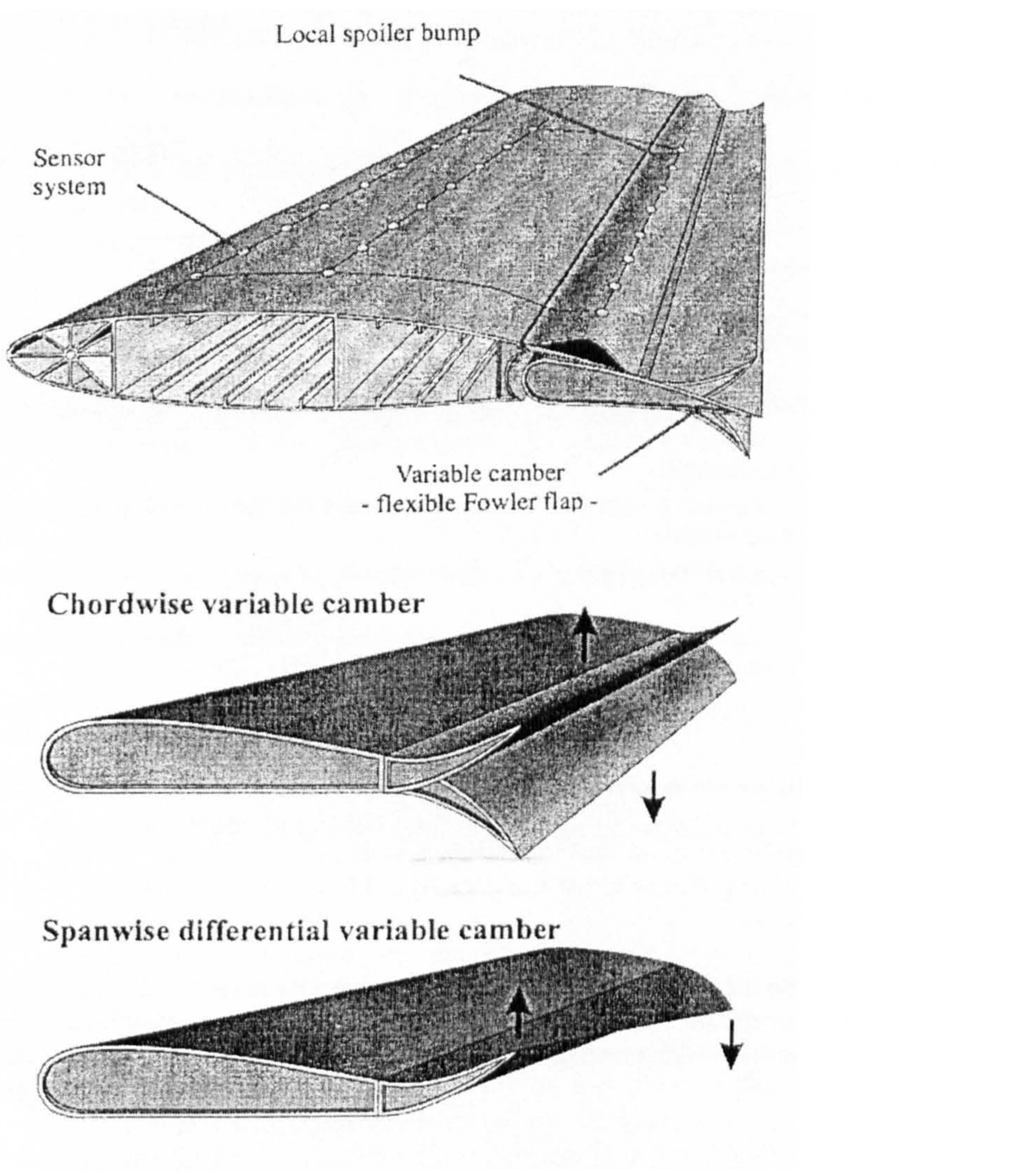

Figure 2.38 – Flexible trailing edge structure [3]

2.8. MECHANISM TYPES

The mechanisms used to operate conventional trailing edge devices are commonly divided in 4 groups, which are [48]:

a) ***Simple Hinges.***

b) ***Linkage systems.***

c) ***Track systems.***

d) ***Link/Track Systems.***

Usually the choice mechanism is a trade-off between cruise drag, flap performance and weight.
Figure 2.39 presents a list of some current applications of the above mechanisms in civil transport aircraft.

Boeing		McDonnell Douglas		Airbus	
707	Internal track	DC-8	Internal four-bar linkage	A300	External straight track
727	External hooked track	DC-9	External hinge	A310	External hooked track
737	External hooked track	DC-10	External hinge	A320	Link/track mechanism 1
747	External hooked track	MD-80	External hinge	A321	Link/track mechanism 1
747SP	Four-bar linkage	MD-81	External hinge	A330	Link/track mechanism 2
757	External hooked track	MD-11	External hinge	A340	Link/track mechanism 2
767	Complex four-bar linkage				
777	Simple four-bar linkage				

Figure 2.39 – Applications of Trailing Edge Flap Mechanisms [85]

2.8.1. Simple Hinge

These mechanisms are characterized by their simplicity and light weight (Figure 2.40). Fairings for these mechanisms can get fairly deep. In some cases they produce additional frontal areas due to motion not aligned with flight which leads to increased drag [85].

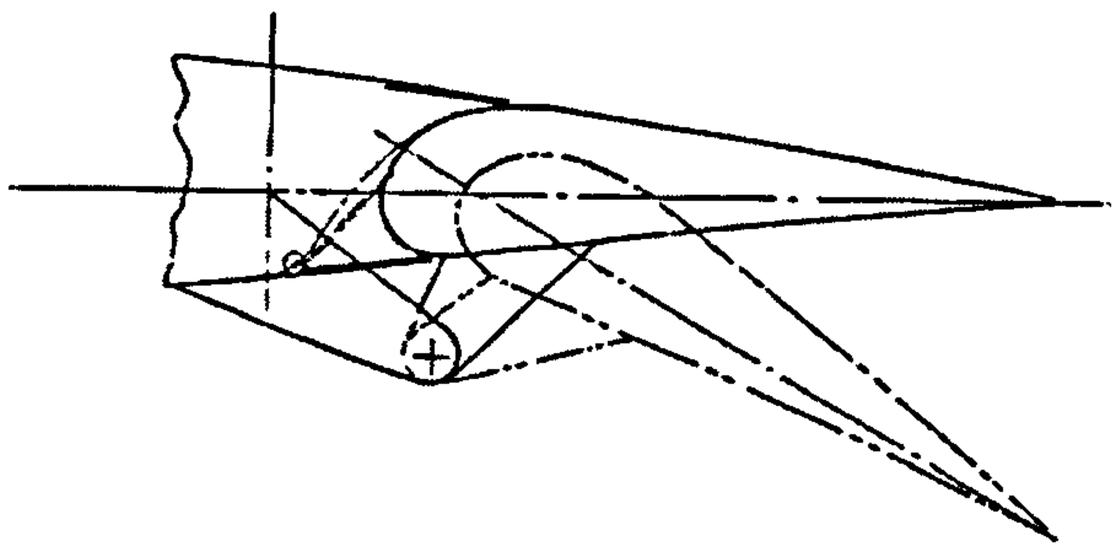

Figure 2.40 – Simple Hinge application [67]

2.8.2. Linkage Systems

These types of arrangements provide a significant aft movement of slotted and Fowler flaps before the main rotation occurs (Figure 2.41 to Figure 2.43). Though, because the motion is normal to the hinge line, when high wing sweeps are associated with large flap travels some difficulties with fairing alignment will arise [60].

Fairing sizes for these types of mechanisms vary and mainly depend on the complexity of the linkage system. They can be shallow on complex 4-bar linkages, but fairly deep on Upside-Down/Upright 4-bar linkages [85].

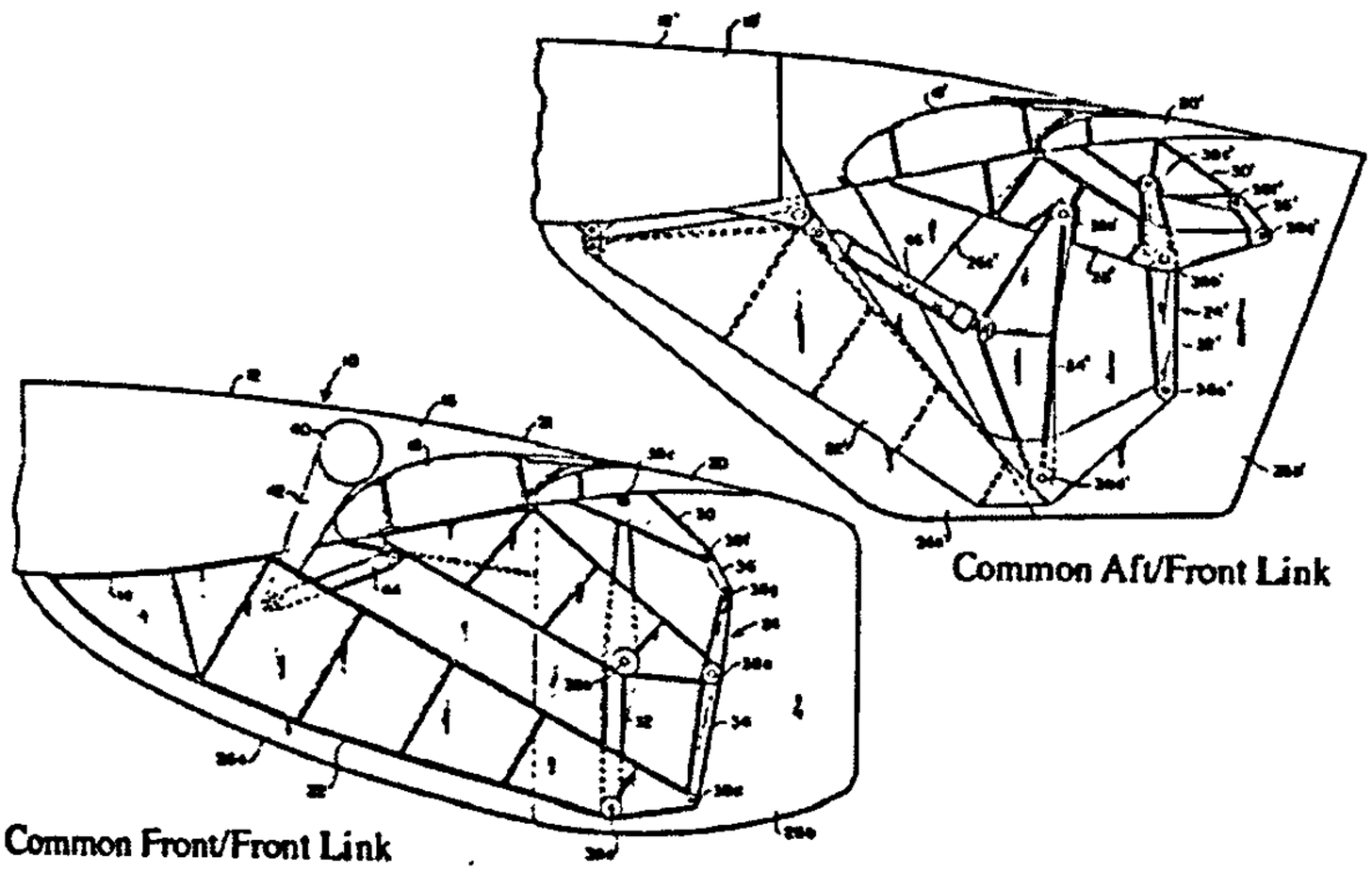

Figure 2.41 – Upright/upright, 4-Bar Linkages [85]

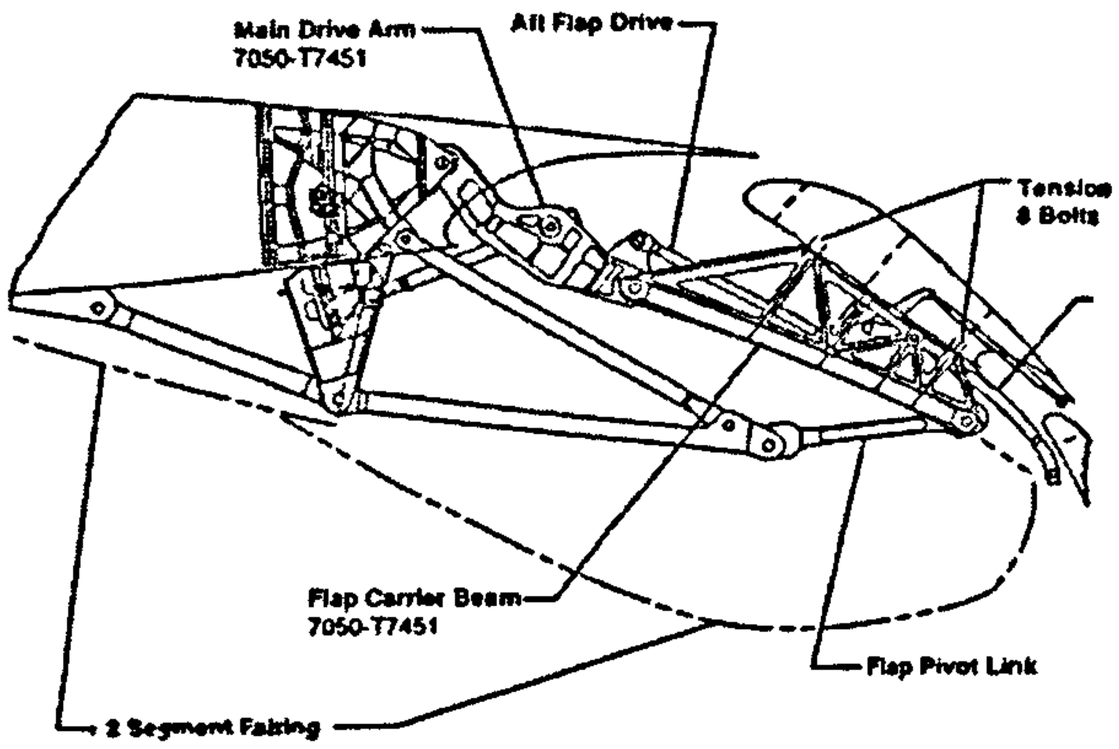

Figure 2.42 – Upside-down/upright, 4-Bar Linkages – Boeing 777 [85]

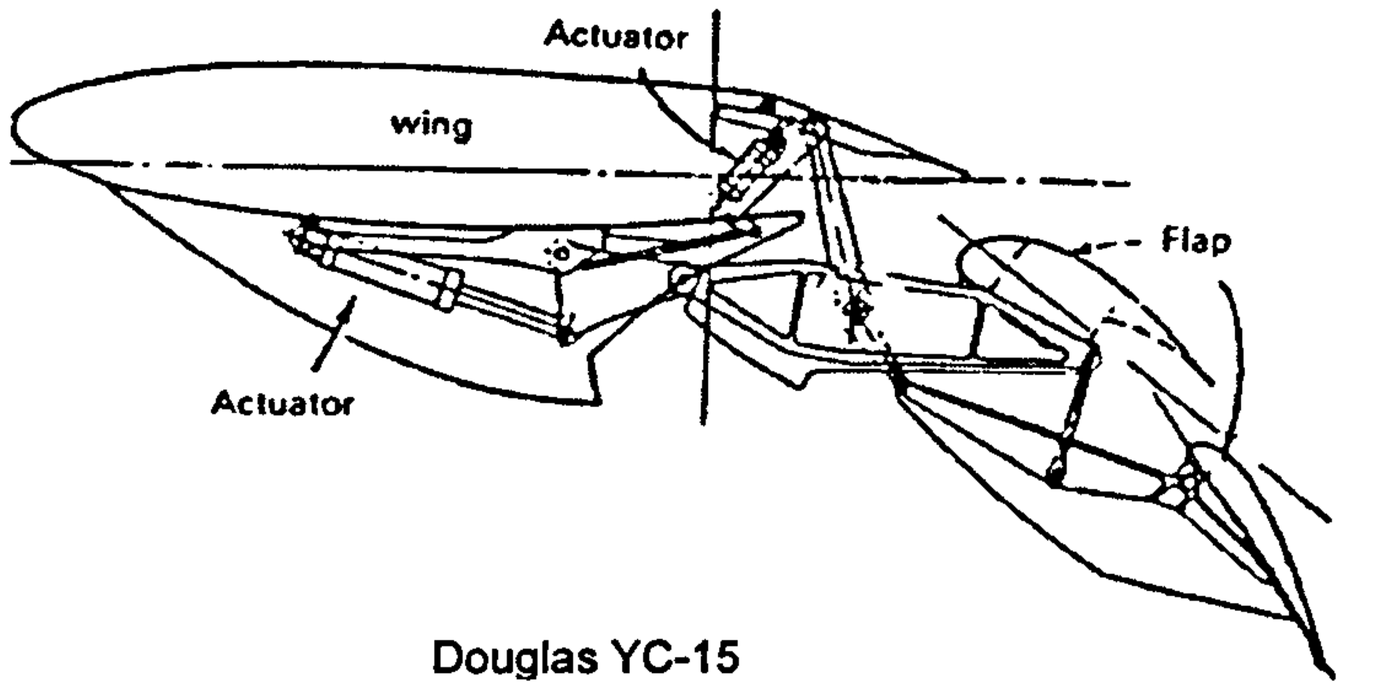

Douglas YC-15

Figure 2.43 – Upside-down/upside-down, 4-Bar Linkages [85]

2.8.3. Track Systems

The flap deployment is controlled by tracks that are shaped for the required flap movement (Figure 2.44 and Figure 2.45). When applied to high swept wings, if aligned with the flight, the track will be subjected to considerably sideloads, making them rather heavy or bulky in order to carry the sideloads in bending. Fairings for these types of mechanisms are medium-sized [85].

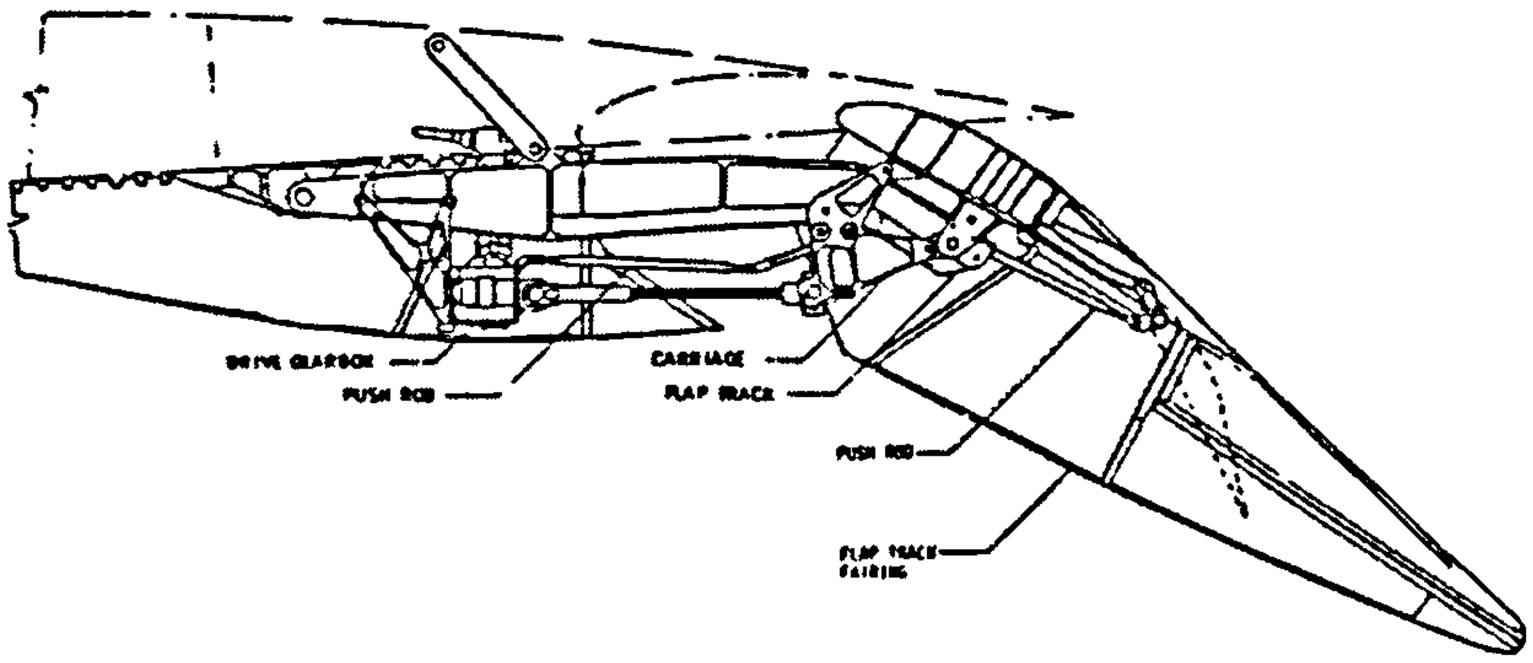

Figure 2.44 – Hooked-track – Boeing 757 [85]

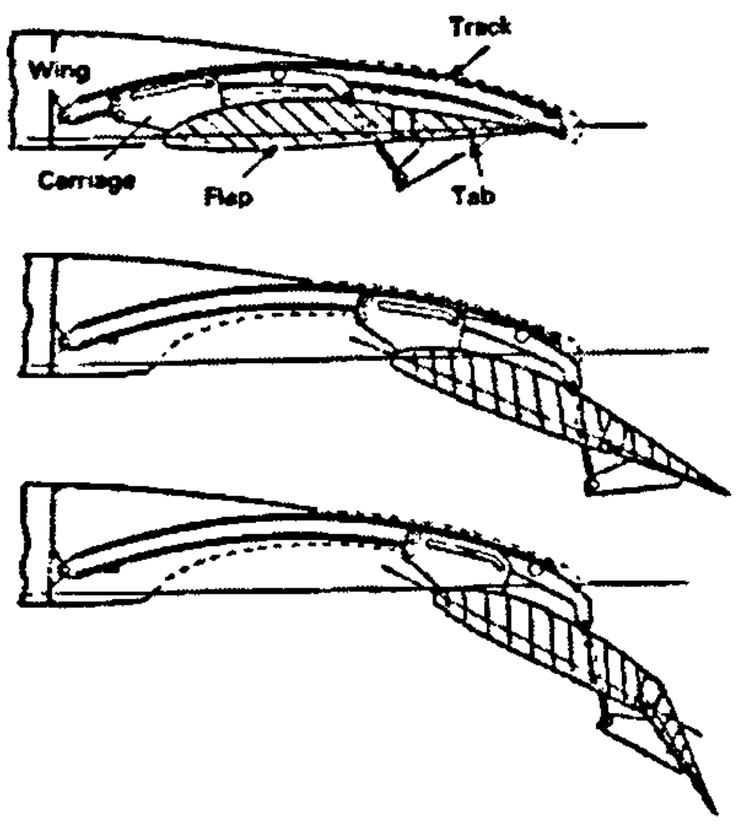

Figure 2.45 – Track Mechanism [67]

2.8.4. Link/Track Mechanisms

These types of mechanisms consist of a straight track on fixed structure and a link arrangement (Figure 2.46 and Figure 2.47). Link/Track mechanisms provide a better fowler motion progression and shallower support fairings than those for linkages systems.

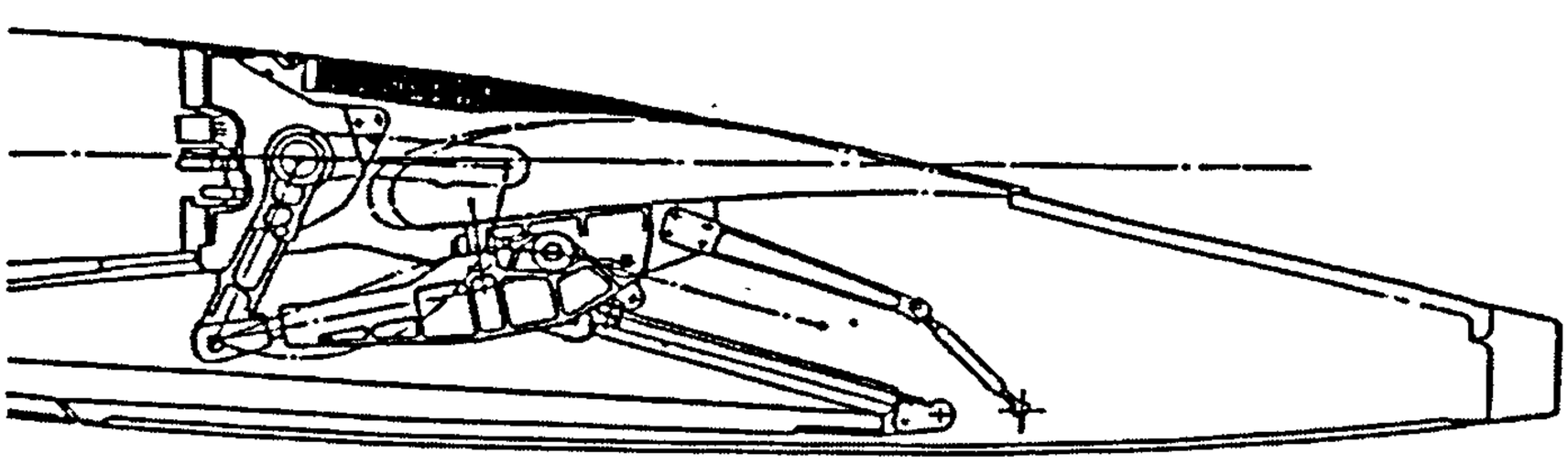

Figure 2.46 – Link/track mechanisms – Airbus A320 [85]

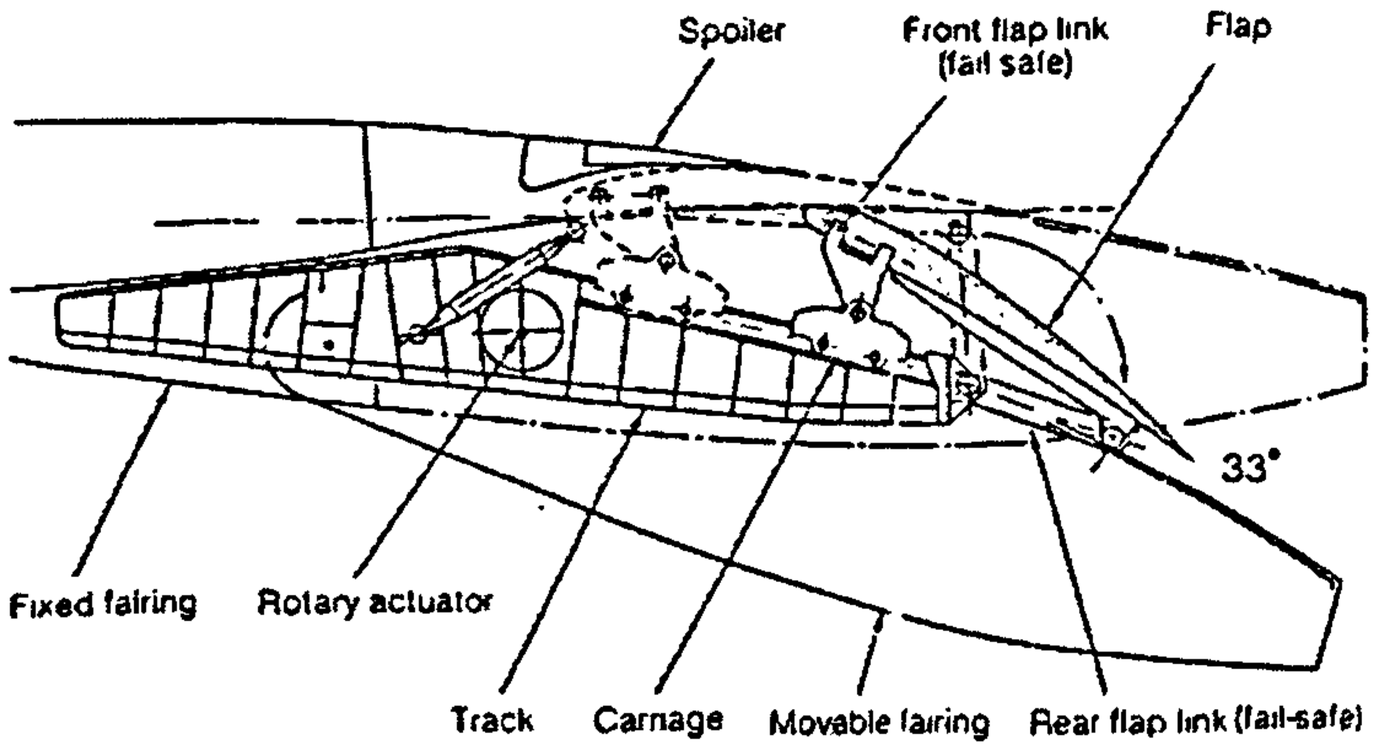

Figure 2.47 – Link/track mechanisms – Airbus A330/340 [85]

2.10. AIRFRAME NOISE

Nowadays aircraft generated noise is a very important issue when it comes to environmental protection. JAR 36 reproduces all the standards and requirements applicable to modern aircraft noise certification. These standards were set by the International Civil Aviation organization (ICAO) for environmental protection.
It has been proven in past and recent research studies that airframe noise is one of the biggest contributors for the overall aircraft generated noise [28] [41] [42] [49] [93]. Other research studies also showed that the most important noise source, from the overall airframe noise, is the Trailing Edge flap tip or side-edge during the Approach/Landing Configuration [41] [42] [91] [93]. During this flight phase, when engines are operated at relatively low power settings, airframe-generated noise becomes very important [28].
The mechanism by which the flap side-edge noise is generated is strongly related to cross flow separation in the sharp edges, which generates strong vortices. This is commonly accepted as the source mechanism for the significant Flap generated noise [42].

The solution used to reduce the noise generated by the flap side-edges is the introduction of Tip Side-Edge Fences. These devices are aerodynamically shaped flat plates fixed perpendicularly to the flaps (or wing structure) and aligned with the free stream velocity of the aircraft [83] [91].
The mechanism through how the tip side-edge fences achieve noise reduction is not yet fully understood, but it has been proven that the use of such devices effectively reduces flap related noise [41] [42] [83] [91].
There are 2 different types of devices that can be applied in part-span flaps [91]:

- Fence type, attached to the main wing

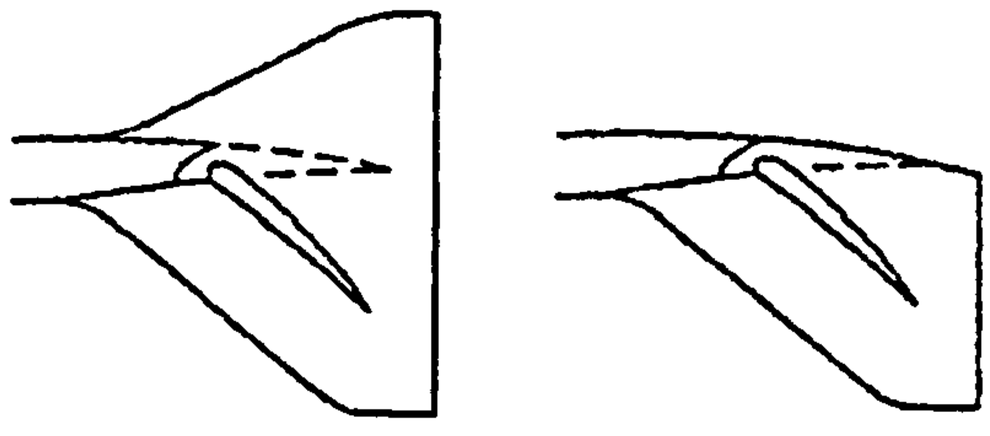

Figure 2.48 – Wing mounted fences [91]

- Winglet type, attached to the tip of the flap (Figure 2.49)

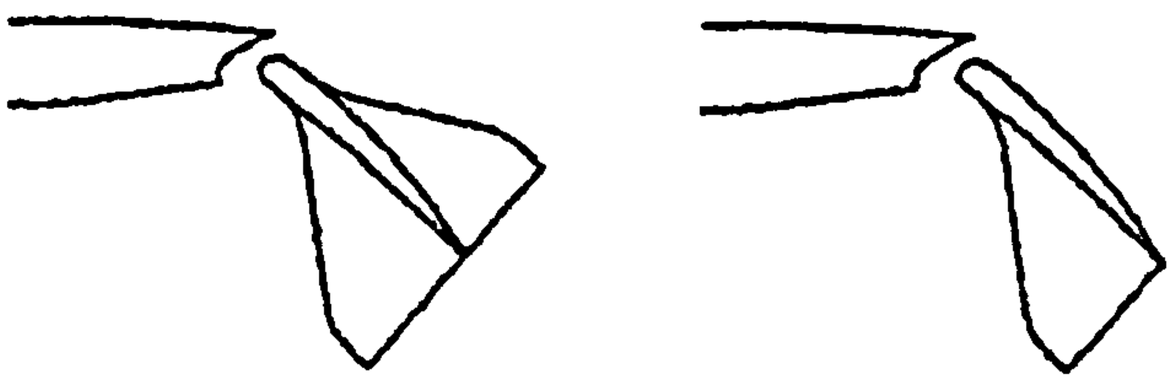

Figure 2.49 – Flap mounted fences [91]

The research studies on these types of devices also show that in addition to decrease the aircraft noise, there is a tendency to increase lift and decrease drag. Its simplicity in design and the easiness of application are also advantages in the use of these devices [83] [91].

2.11. CS-25 AIRWORTHINESS REQUIREMENTS

The work presented in this research study focus on high lift devices of large commercial transport aircraft. The European Aviation Safety Agency (EASA) regulates the airworthiness requirement for these types of aircraft through the document "CS-25 Certification Specifications for Large Aeroplanes" [128]. Listed below are the paragraphs of the CS-25 document that the author considers to be the most relevant to the structural design of High Lift Devices.

CS-25 Amendment 4

BOOK 1 - SUBPART C – STRUCTURE

GENERAL
CS 25.301 Loads
CS 25.303 Factor of Safety
CS 25.305 Strength and Deformation
CS 25.307 Proof of Structure

FLIGHT LOADS
CS 25.321 General

FLIGHT MANOEUVRE AND GUST CONDITIONS
CS 25.335 Design Speeds
CS 25.341 Gusts and turbulent Loads
CS 25.345 High Lift Devices

CONTROL SURFACES AND SYSTEM LOADS
CS 25.457 Wing-Flaps

BOOK 1 - SUBPART D – DESIGN AND CONSTRUCTION

GENERAL
CS 25.601 General
CS 25.603 Materials
CS 25.607 Fasteners
CS25.611 Accessibility provisions
CS25.613 Material strength properties and Material Design Values
CS25.629 Aeroelastic stability requirements

CONTROL SURFACES
CS 25.651 Proof of strength
CS 25.657 Hinges

CONTROL SYSTEMS
CS 25.671 General
CS 25.697 Lift and drag devices, controls

CHAPTER 3

DESIGN METHODOLOGY

3.1. INTRODUCTION

The design methodology for High Lift devices has not changed much in the last few decades, and it is most common to see Aircraft manufactures make use of already in use mechanism types as a quick way to reach a solution.
This chapter will look in to the most commonly used design methodologies and propose requirements for a new one, together with a description of its development

The most commonly accepted High-Lift design methodology is detailed by Flaig & Hilbig [29]. These authors divided the design of High-Lift systems in three successive phases: pre-development, development and pre-flight. The two initial phases are characterized by their highly iterative nature. In the pre-development phase, to find the high-lift concept that complies with the required aerodynamic performances, and in the development phase to improve the C_{LMax} in landing and the L/D in the take-off configurations. Figure 3.1 and Figure 3.2 present a detailed description of this High-Lift device design methodology, along with the design considerations involved [29][66].

A fundamental problem associated with the design of High-lift devices is related to the computational tools available. Not so much nowadays due to recent developments in this area, but there are still issues related with the different software used for the design of High-Lift devices. The design of High-Lift device mechanism focus mainly in three areas: CAD Design, Kinematical Analysis and Structural Design. The mutual interaction between these areas makes the design very complicated, computationally intensive and time consuming. Also, the areas are not usually integrated, making the mechanism design iterative and often a "trial and error" process [101]. The development of alternative types of mechanisms also becomes a challenging task, requiring a great deal of human interaction and creativity.

The objective of this research is to develop a new design methodology that tackles the main problems of the conventional design methodology and improves it by including areas of study not usually considered at that stage. This step-by-step multidisciplinary analysis focus on the pre-development phase, which is characterized by its highly iterative nature, and serves to design and evaluate a wide range of mechanism configurations and select the system that best meets the requirements.

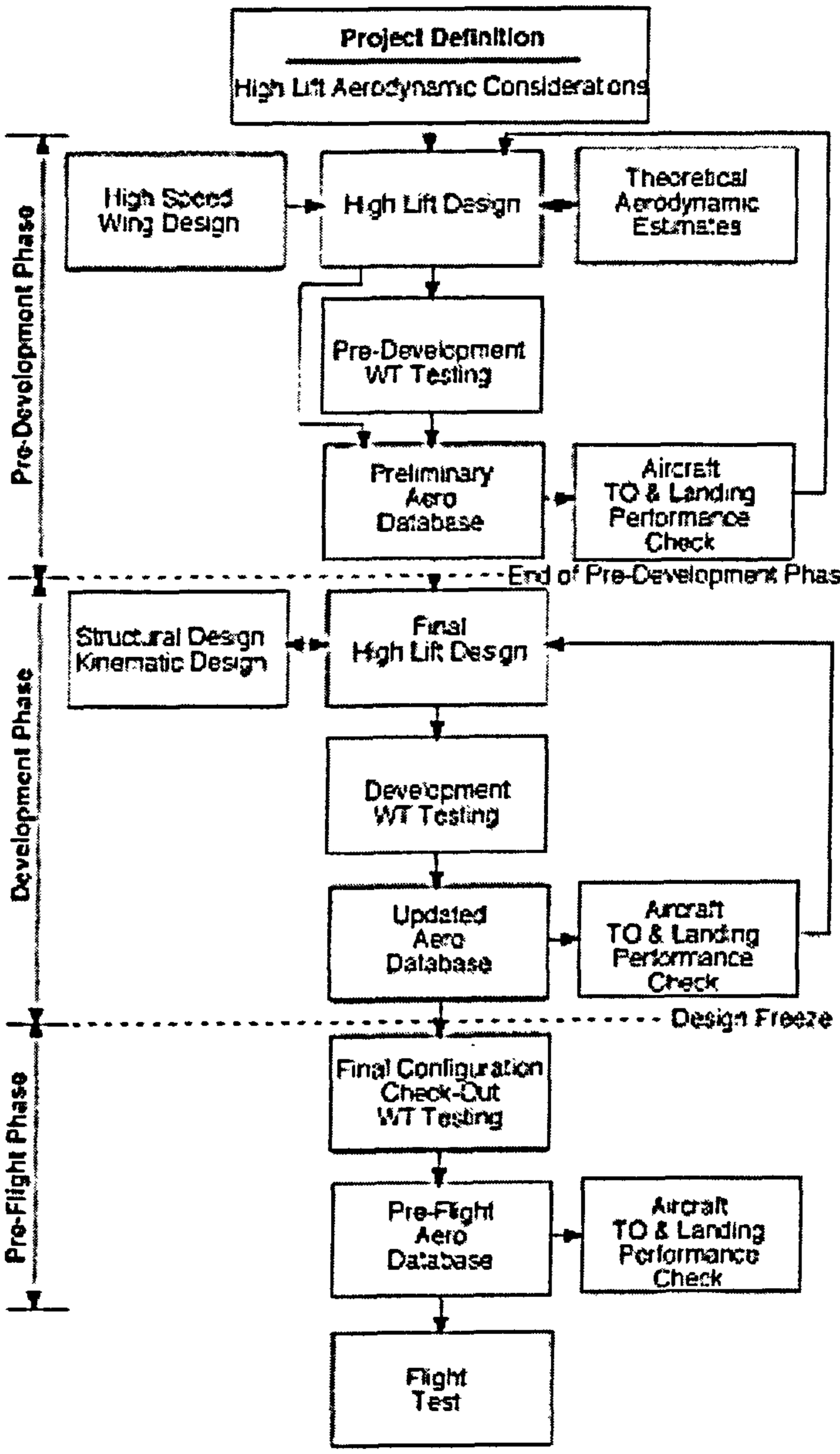

Figure 3.1 – Conventional High Lift Device Design Methodology [29]

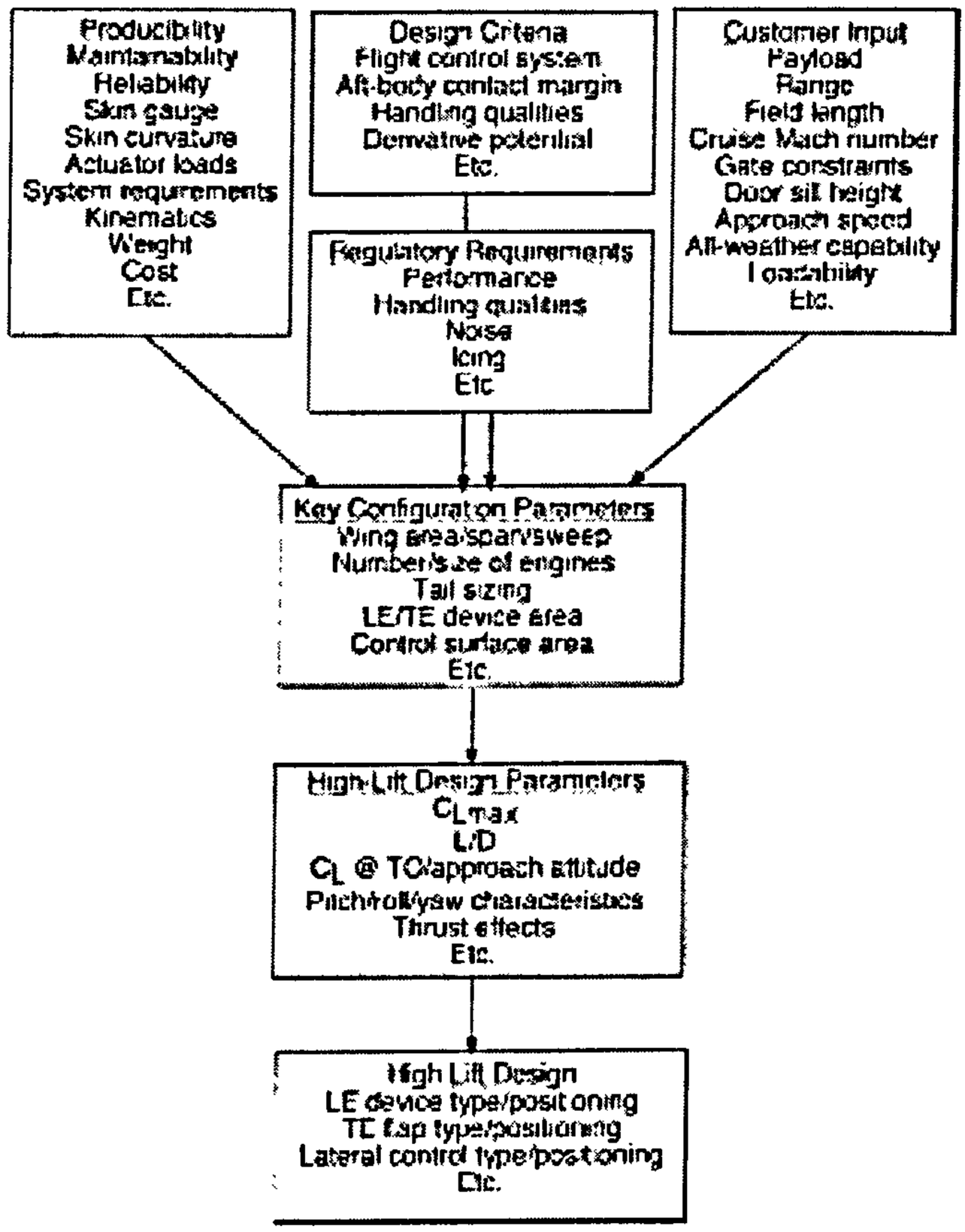

Figure 3.2 – High Lift System Design Considerations [66]

3.2. DEVELOPMENT OF A NEW TRAILING EDGE DEVICE MECHANISM DESIGN METHODOLOGY

Recent progress and improvements in software and computer hardware have permitted a new approach to the design and optimization of High-Lift devices. Integrated CAD/CFD/FE systems have allowed the design process to come away from the "trial and error" process that was followed for many years. It has reached a point were the use of wind tunnel techniques has become complementary [114]. SYNAMEC [101], a recently concluded European Project, which included the participation of Cranfield University, has provided very innovative work of research and development in the area of mechanism type synthesis and design. This work has brought a new approach to the early stages of the mechanism design process. The main objective of the project was to develop a computer-aided design and engineering software system for the synthesis of aeronautical mechanisms. This software was the basic objective for the SYNAMEC project. The work performed had the participation of several Aircraft Manufactures, Software Developers and Research Centres from Europe and South America, with complementary roles. Alberto Cardona [13][14][19][32][78][13], from INTEC, Argentina, a specialist in the area of mechanism design, has developed an innovative computer program called OOFELIE for type synthesis and initial layout of planar mechanisms. This innovative software takes as input a set of nodes, links, joints and fixations of an existing configuration of a given problem and returns a family of mechanisms suitable to describe the desired motion. By integrating this program with SAMCEF FIELD (CAD software), SAMCEF MECANO (Mechanical Analysis Software) and BOSS Quattro (Optimization Software), the SYNAMEC System is capable of covering all the design stages of the mechanism design procedure, from mechanism type synthesis to preliminary and detailed design (see Figure 3.4).

The availability of the SYNAMEC software and the participation of the author in its development led to its inclusion in the development of this new design methodology. The suitability of the SYNAMEC software to this research study was made evident when, in the scope of the European contract, the author had to analyse its application to aeronautical mechanisms and develop a preliminary sizing module. By gathering in the SYNAMEC software a CAD tool, Kinematical Analysis, Structural Design and Optimization made it clear that considerable gains could be achieved by including other areas of the Aircraft Design Process, like R&M and cost. After a review of the traditional design methodologies for High-Lift devices, the author decided to generate a new design methodology that was capable of generating different mechanism solutions and select the most appropriate mechanism for a specific set of initial requirements.

The design methodology presented here is mainly directed at commercial transport aircraft with single slotted flap systems. The decision to contemplate only single slotted flap comes in line with the current trend by aircraft manufacturers to design simpler and lighter high lift devices. This has already been achieved by AIRBUS, where almost all their models have single slotted flaps, without any reduction in landing lift coefficients and making gains in Take-off and landing L/D [85].

3.2.1. Methodology Description

The new design approach and software allows the author to propose a new mechanism design methodology for Wing High Lift Devices. Some of the disadvantages of the current design methodology are targeted for improvement, especially the iterative and often a "trial and error" nature of the process due to the inexistence of an integrated tool. This innovative design approach supports the designer creativity and stimulates the invention of new mechanism concepts. Also, new analysis and optimization methods will support a better and quicker evaluation and simulation of different design variants. Figure 3.3 presents a description of the proposed High Lift device design process and indicates SYNAMEC's part in it.
The methodology is briefly described as having the following process sequence, but more details are shown in paragraphs 3.2.2 to 3.2.7.

SYNAMEC Module (Synthesis & Optimization)

Inputs are taken from High Speed Wing Design and the Aircraft Low Speed Requirements. Mechanism Synthesis and Optimization is performed and several mechanisms can be proposed.

Initial Sizing Module

2D load calculation on mechanism is performed using simple static principles.
The module Calculates element loads for components of 4 types of mechanisms: Simple Hinge, 4-Bar, Link/Track and Hooked Track.
Using the calculated loads and sizing methods of Appendix C, initial sizes are determined for the main dimensions of each component.

Structural/Mechanical Design

CAD modelling in the CATIA Software, using the outputs from the sizing module.

Drag/Aerodynamic Module

Fairing Drag and Take-Off performance calculations are performed for each Mechanisms type. Main parameters are taken from the previously developed CAD model.

Weight Module

Weight calculations are performed for each type of mechanism, followed by an estimation of the total weight of the flap system.

Reliability & Maintainability Module

Reliability predictions are determined for each mechanism type analysis is done using data from NPRD (Nonelectronic Parts Reliability Data) from the Reliability Analysis Center [69]
Maintainability Prediction for each mechanism type is performed using the procedure from MIL-HDBK-472 – Maintainability Prediction [62].

Cost Module

Cost Analysis is performed using simple methods to compare the cost between the different mechanism solutions. It is based in the calculation of the Systems cost and the increment in Drag associated with the fairings

Mechanism Selection

With the results from the previous modules a selection process is used to select the most suitable mechanism.

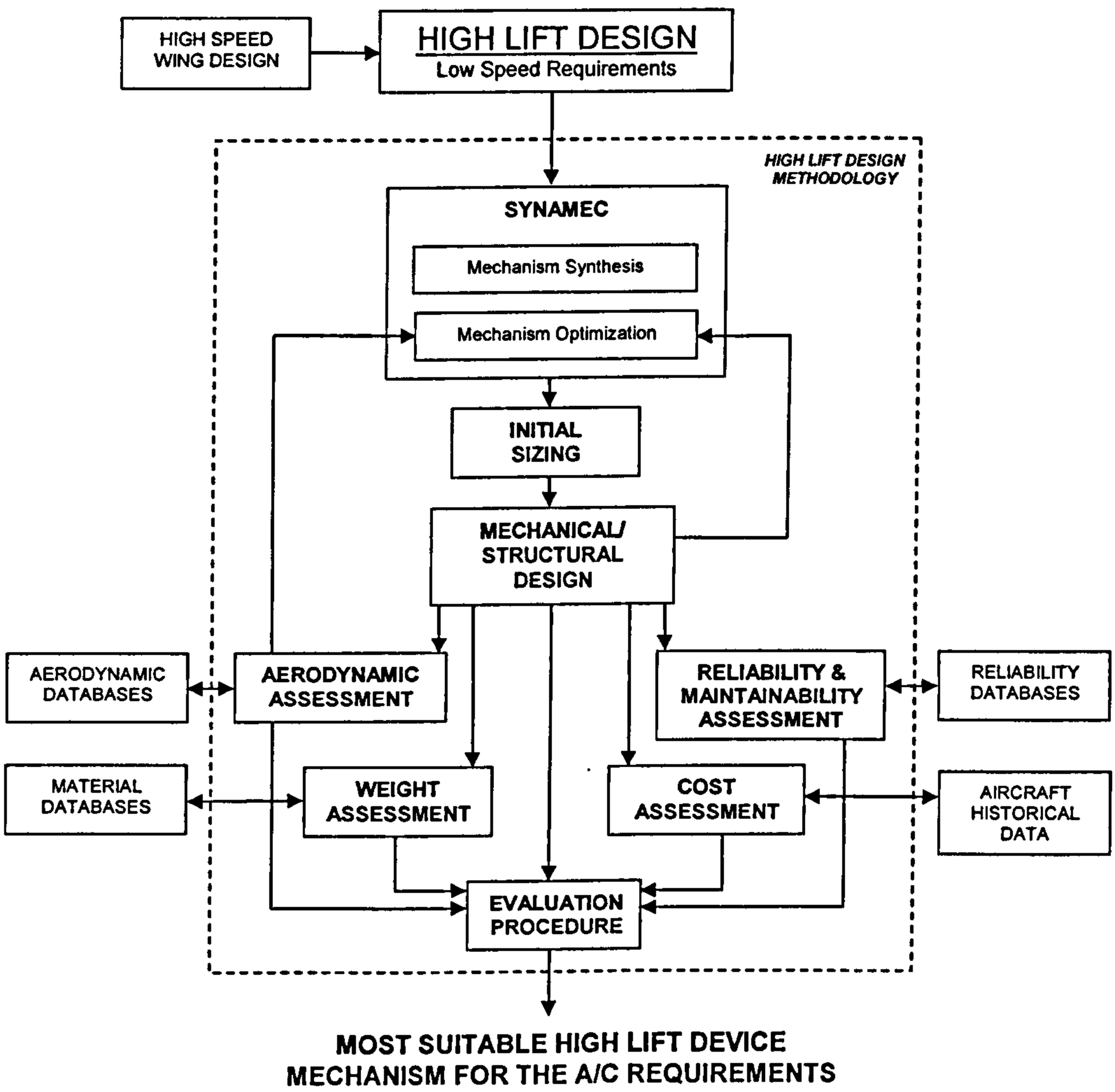

Figure 3.3 – Proposed High Lift Device Design Methodology

3.2.2. SYNAMEC Module

The mechanism design process in the SYNAMEC module is performed in 2 phases (Figure 3.4):

Synthesis

A mechanical simulation and optimization is performed to build a solution for the given problem. The information required is the geometry (known fixation points, rods, etc...), objective trajectory (in the form of 3 points, usually start, middle and end points of the objective trajectory) and an initial and simplified kinematic description (hinges, angles of rotation required, etc...). The result is a parametric mechanism that is able to perform the mechanical motion defined by the specifications, in this case, respecting the 3 trajectory points. Though, it might not pass through all the points of the objective trajectory. The proposed mechanism is composed of elements that have not been sized.

Optimization or Detailed Design

This step consists in the generation of the optimal dimensions (and/or point positions) for the already known configuration in order to allow the mechanism deployment to pass through all the points of the objective curve. Taking as input the parametric model from the previous step, rigid body behaviour is attributed to the mechanism elements and an optimization is performed. As stated before, the result is a mechanism that is able to respect all the points of the objective curve and is now ready for Detailed Design.

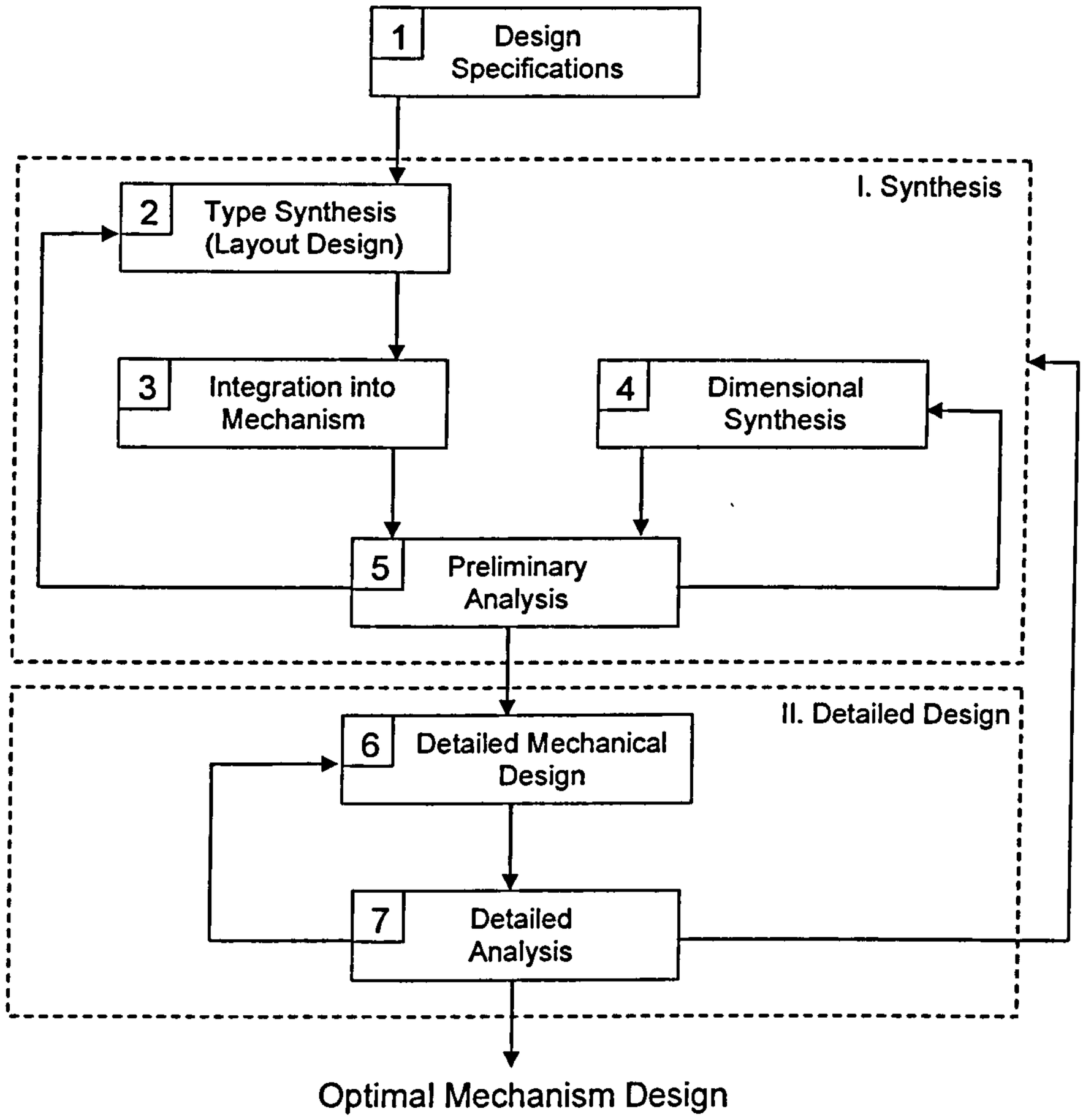

Figure 3.4 – Functional modules of the SYNAMEC system [101]

3.2.3. Initial Sizing Module

The Initial Sizing Module has the purpose of providing the new design methodology with information about preliminary sizes of mechanism components by assuming generic configurations for the different mechanisms. This module performs sizing for components of four 4 generic types of Mechanisms: Simple Hinge (Figure 3.5), 4 Bar Linkage (Figure 3.6), Link Track (Figure 3.7) and Hooked Track (Figure 3.8).

The module calculation procedure is divided in 2 stages:

- ***Component Load Calculation*** – Calculates the loads in each mechanism component using simple static calculations. The inputs are the mechanism coordinates and applied ultimate loads. These calculations are performed using a Visual Basic software application developed by the author.

- ***Component Initial Sizing*** – Calculates the mechanism component sizes. These calculations are done manually using the procedure and methods presented in Appendix C.

Presented in the following pages are the different generic mechanisms and components considered in this research study.

As it can be seen in Figures 3.5 to 3.8, each mechanism has a predetermined configuration with a specific number of components and a single applied load at a specific point of the flap airfoil chord. This point is the flap airfoil centre of pressure at the cruise configuration and it is fixed throughout all the phases of the flap deployment. In reality, as the flap is being deployed, and the centre of pressure of the airfoil changes position, an additional moment should be added to the applied load at the attachment point (Point 5). The author decided not to use this moment in this first iteration of the component load calculation process for two reasons: 1) the moments generated with the single attachment configuration should be much smaller than the moments associated with mechanisms that have the flap attached in two positions. This is due to the fact that the centre of pressure does not move significantly from the initial attachment position, and hence a small moment arm; 2) to decrease the number of variables and to make the component load calculation process simpler and achievable in the time frame available.

The author would like to point out that in normal circumstances this moment has a significant importance in the sizing of the high lift device mechanism components and flap structure itself, and should not be neglected. If the author had included this moment in the sizing calculations it would have increased the loads in the mechanism components and ultimately the mechanism weight.

a.1) Simple Hinge Mechanism Generic Configuration

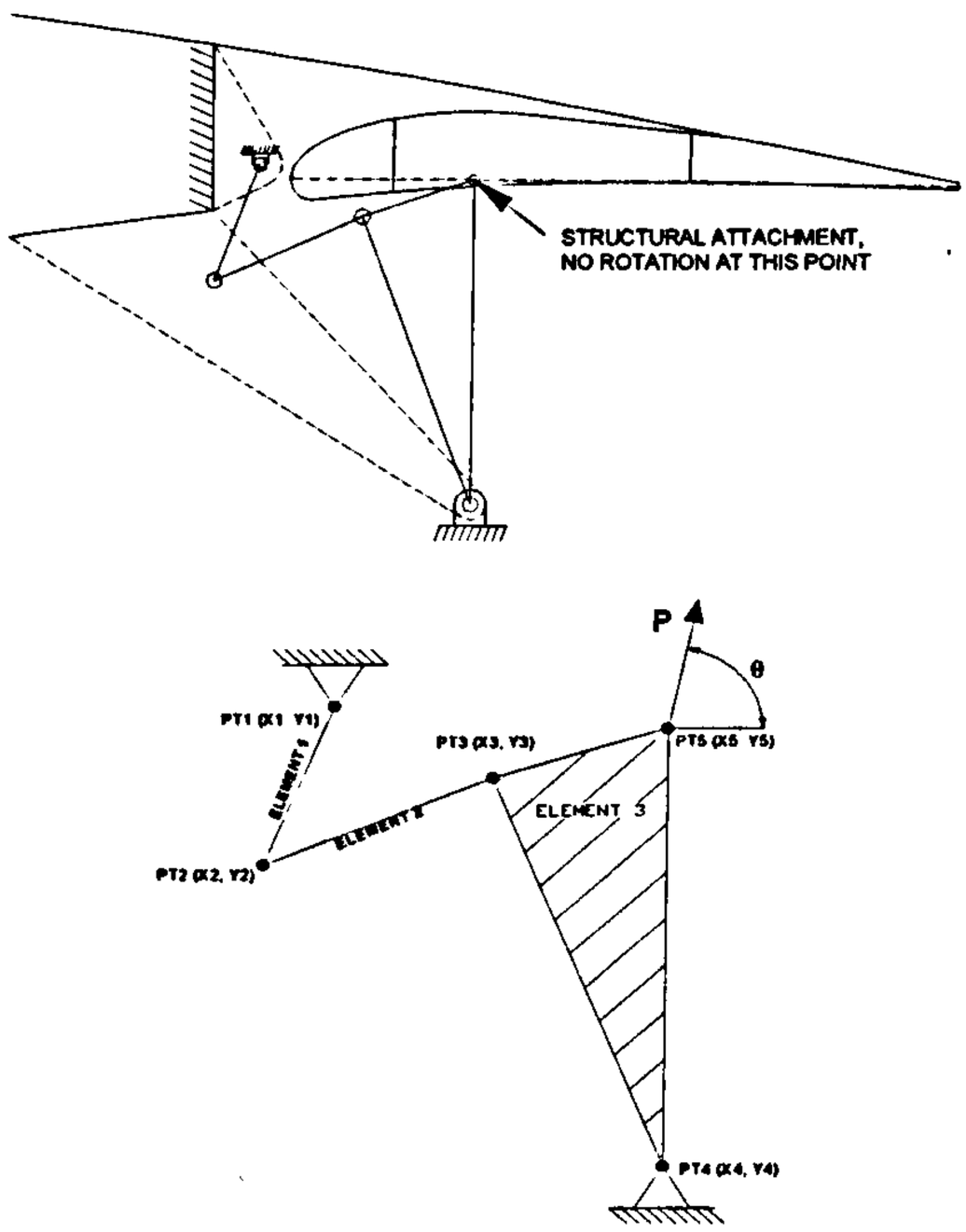

Figure 3.5 – Simple Hinge Mechanism Generic Configuration

a.2) 4 Bar Mechanism Generic Configuration

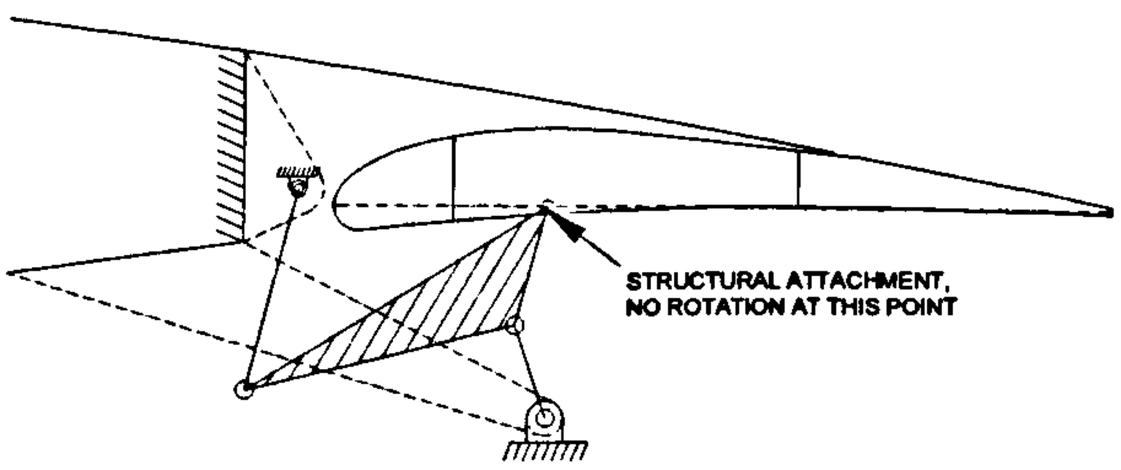

Figure 3.6 – 4 Bar Mechanism Generic Configuration

a.3) Link/Track Mechanism Generic Configuration

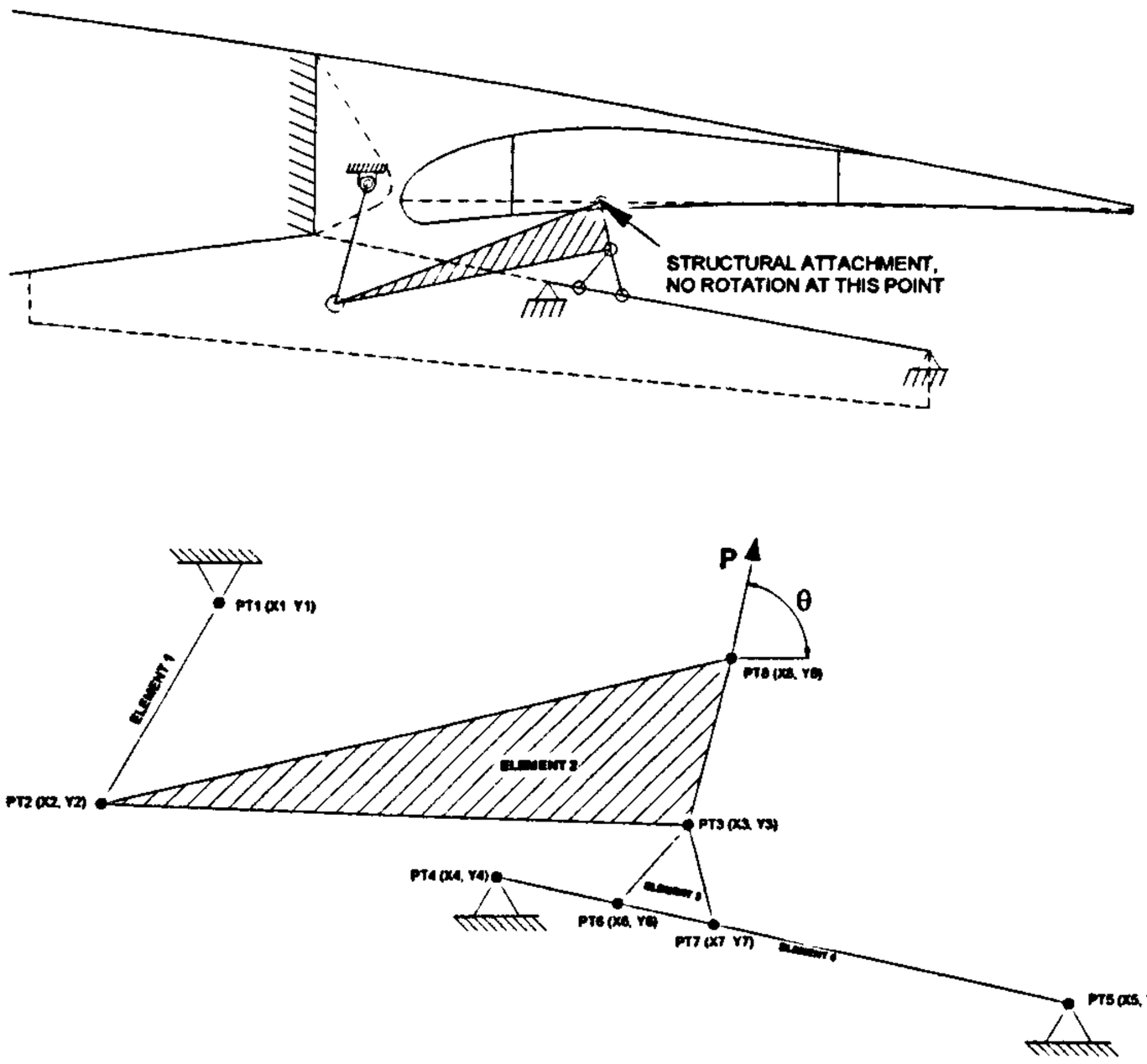

Figure 3.7 – Link/Track Mechanism Generic Configuration

a.4) Hooked Track Mechanism Generic Configuration

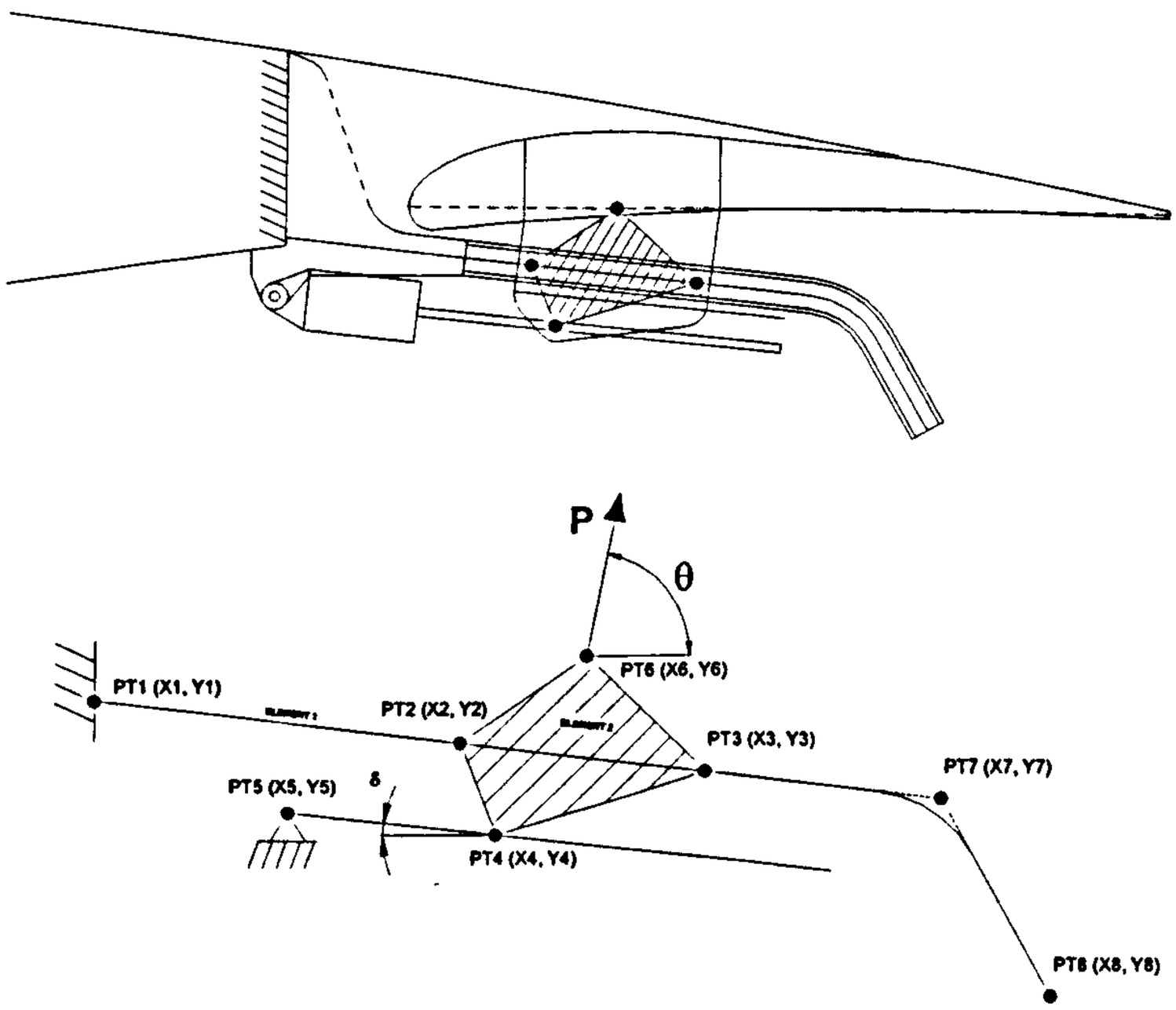

Figure 3.8 – Hooked Track Mechanism Generic Configuration

b) Generic Mechanism Components

Each of the previous mechanisms was decomposed, and generic components defined, such as Links, Hinges, Support Struts, Flap Fittings, and Tracks Struts. To each of the previous elements, a specific sizing method can be created.

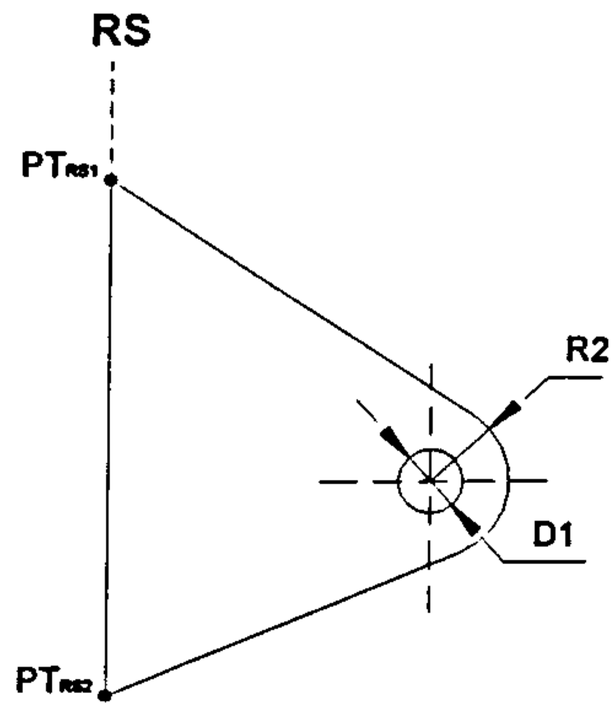

Figure 3.9 – Generic Component - Hinge

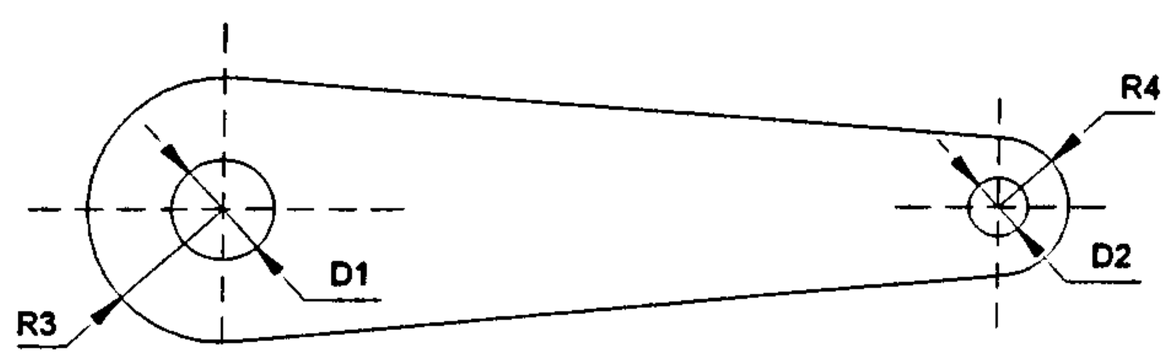

Figure 3.10 – Generic Component - Link

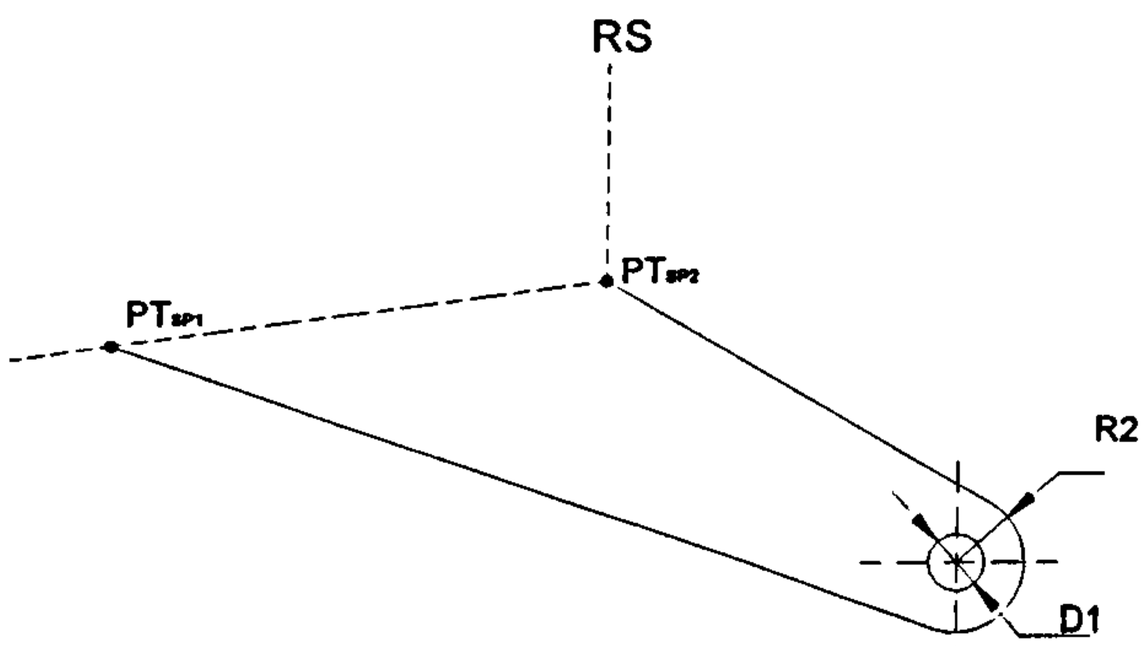

Figure 3.11 – Generic Component – Support Strut

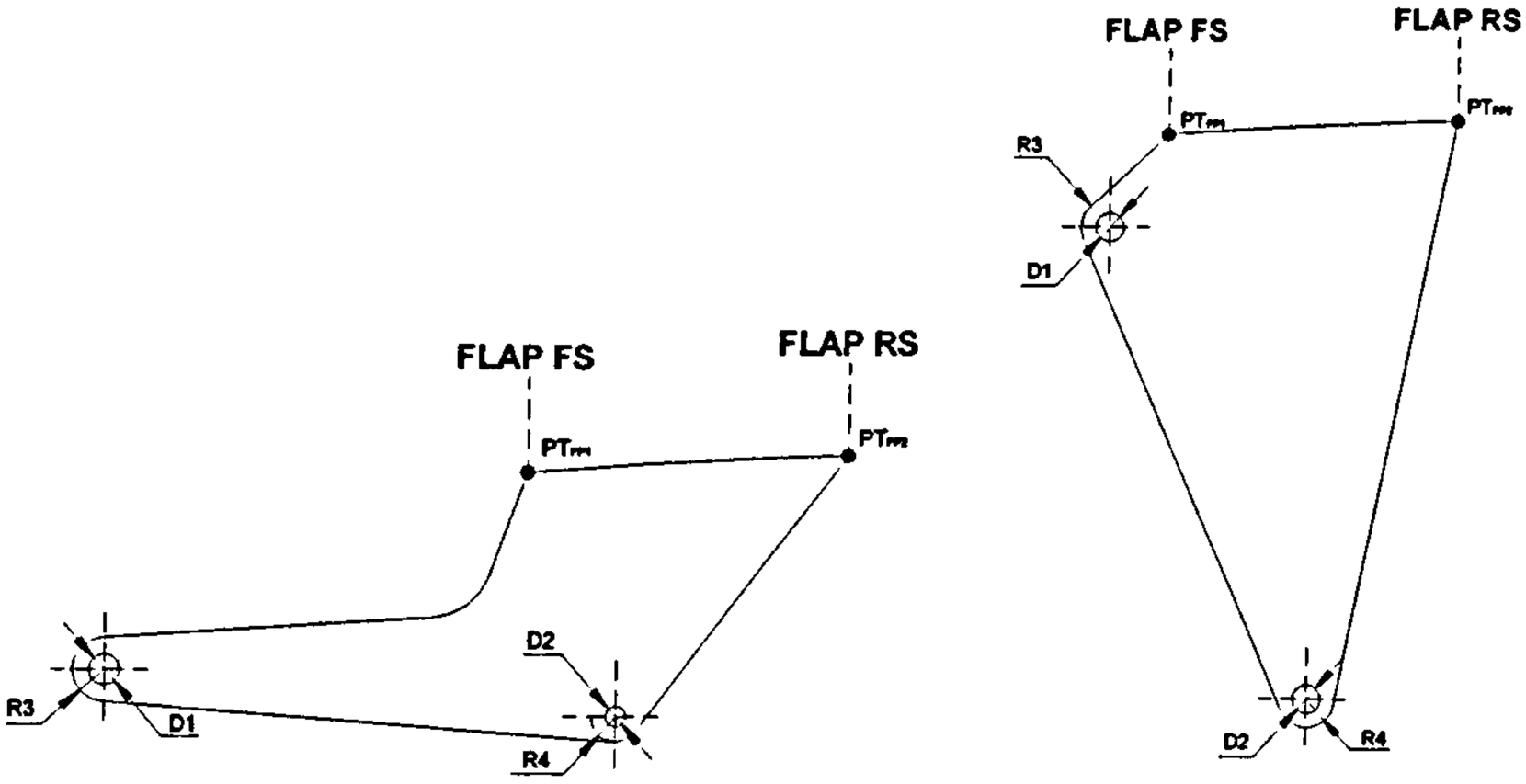

Figure 3.12 – Generic Component – Flap Fitting

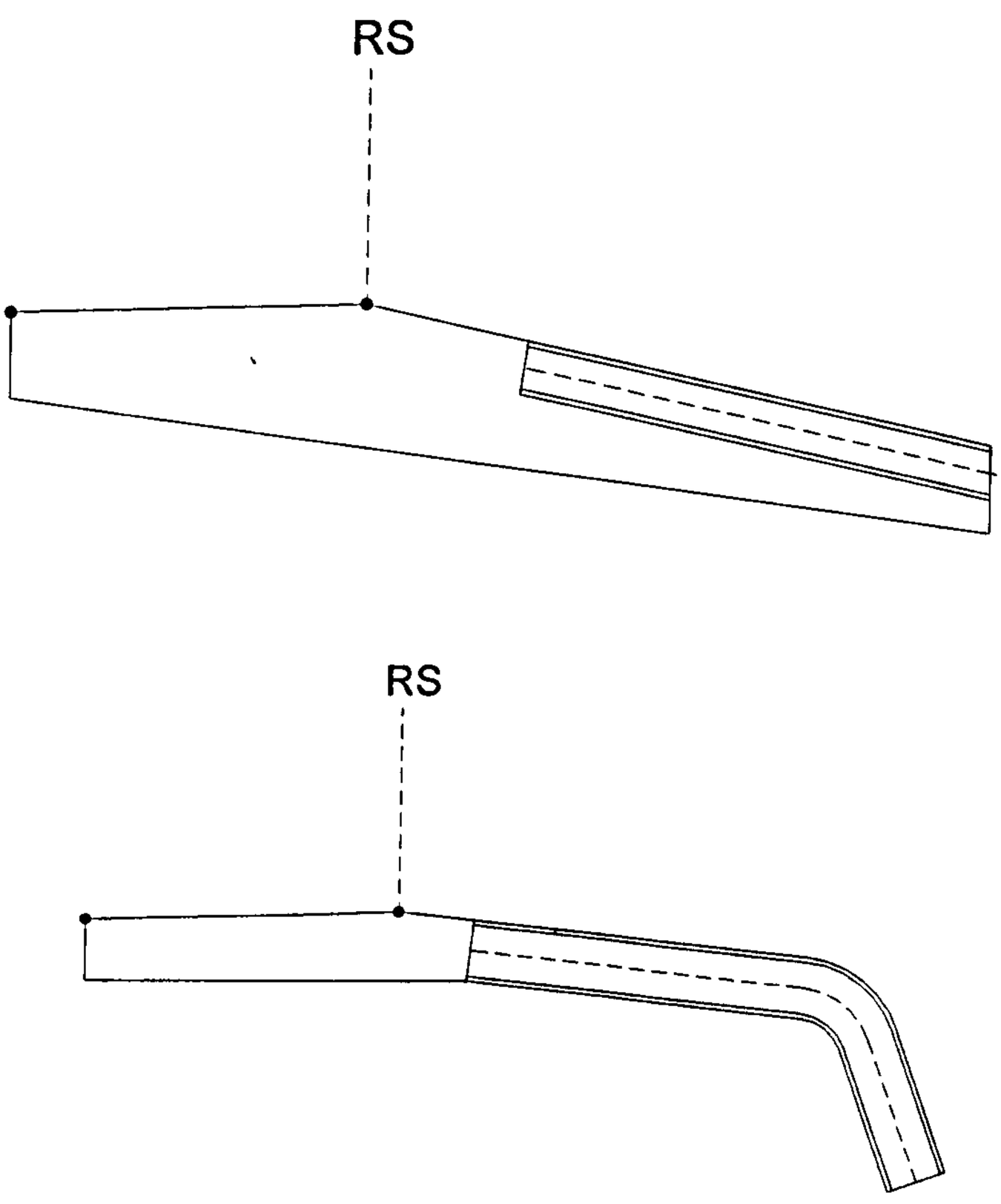

Figure 3.13 – Generic Component – Track Struts (RS – Rear Spar)

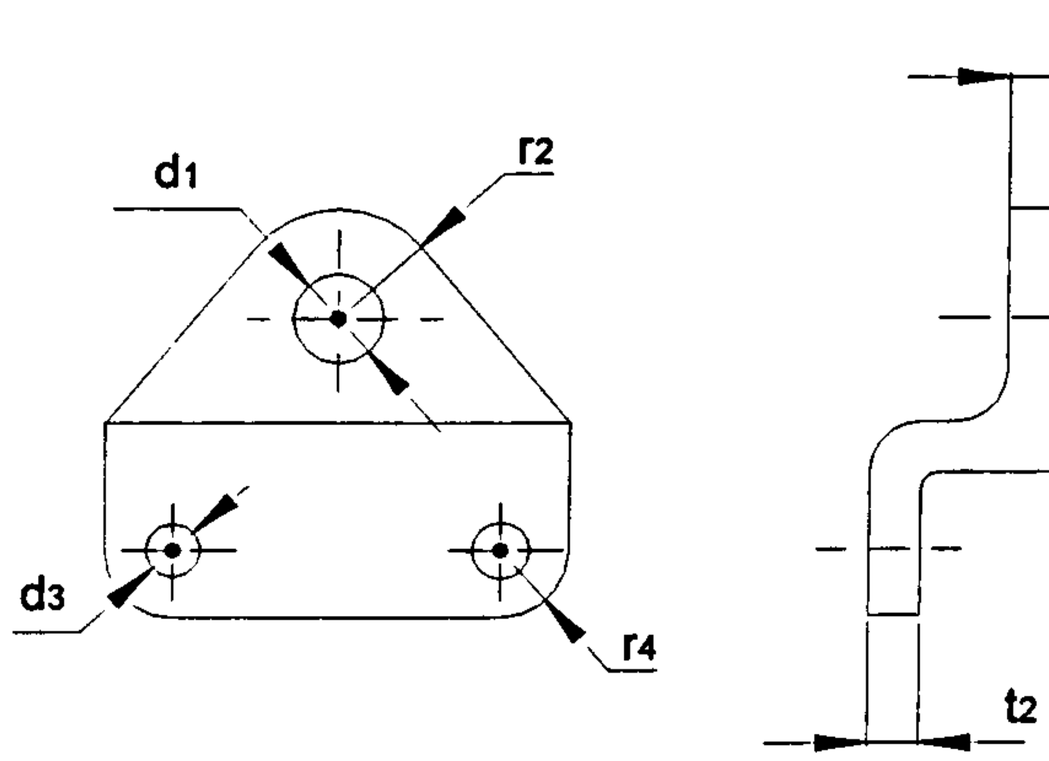

Figure 3.14 – Generic Component – Roller Carriage (Link/Track Mechanism)

c) Program Description

The VB application receives as inputs the mechanism coordinates and applied ultimate load, and using standard static calculations, determines the loads and dimensions for each component. As a key note, for mechanism component sizing all applied loads should be Ultimate loads. Figure 3.15 presents the original idea flow chart for the Initial sizing Module. Due to time constraints, the Visual Basic application was only developed to perform the calculation of the component loads. The initial sizing and weight estimation are performed manually.

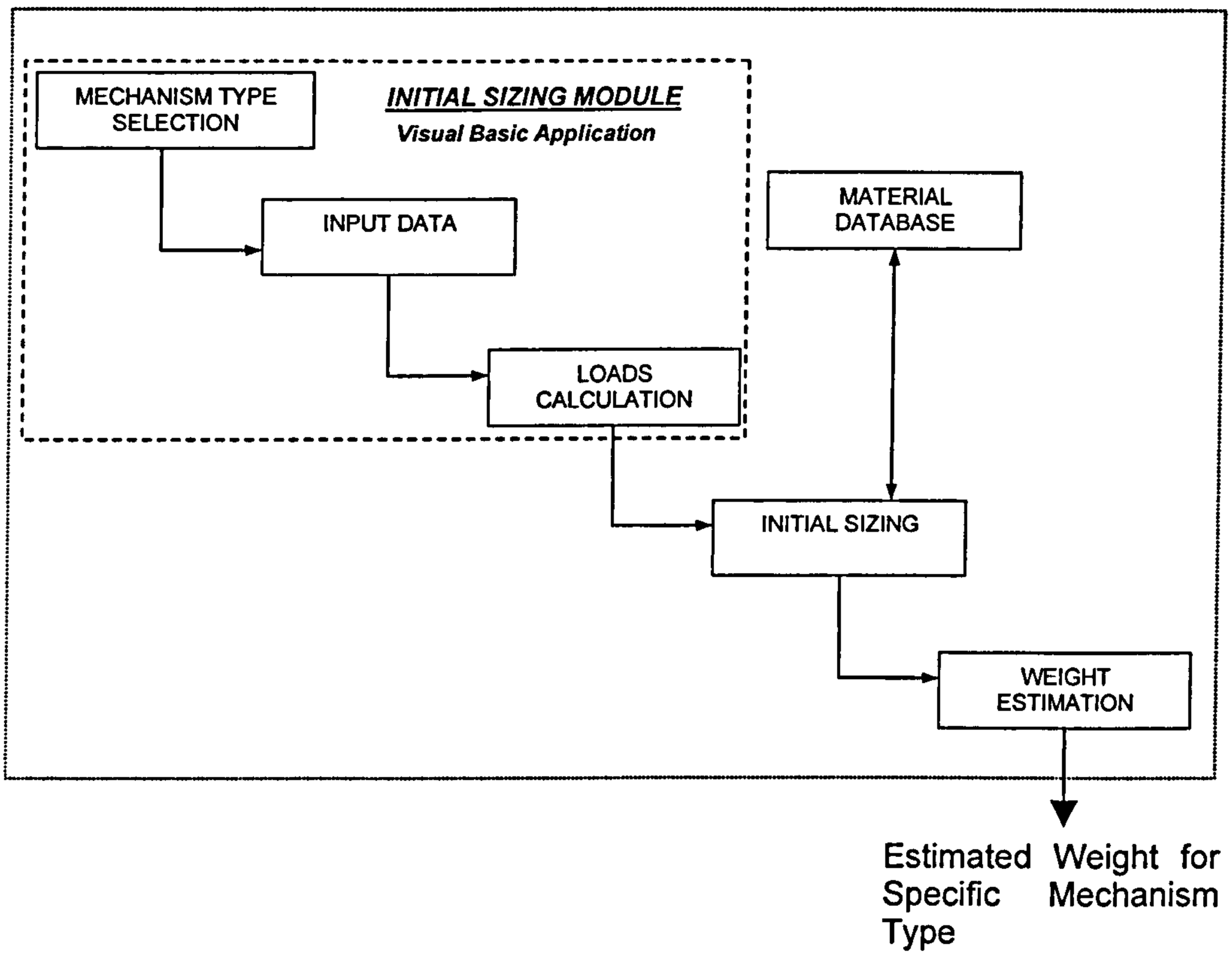

Figure 3.15 – Program Flow Chart

The equations used in the Visual Basic application are function of the mechanism initial points. Once established, the Static equations are solved using MathCAD's Symbolically Calculation functionality, and a set of equations are obtain that are function of the initial mechanism points. The process of obtaining the element loads of the different mechanisms is presented in Appendix C, and the program code for the Visual Basic Application is presented in Appendix D.
The following figures present an example of the programs user interfaces.

Main Menu

In this menu the user will select the type of mechanism required for analysis.

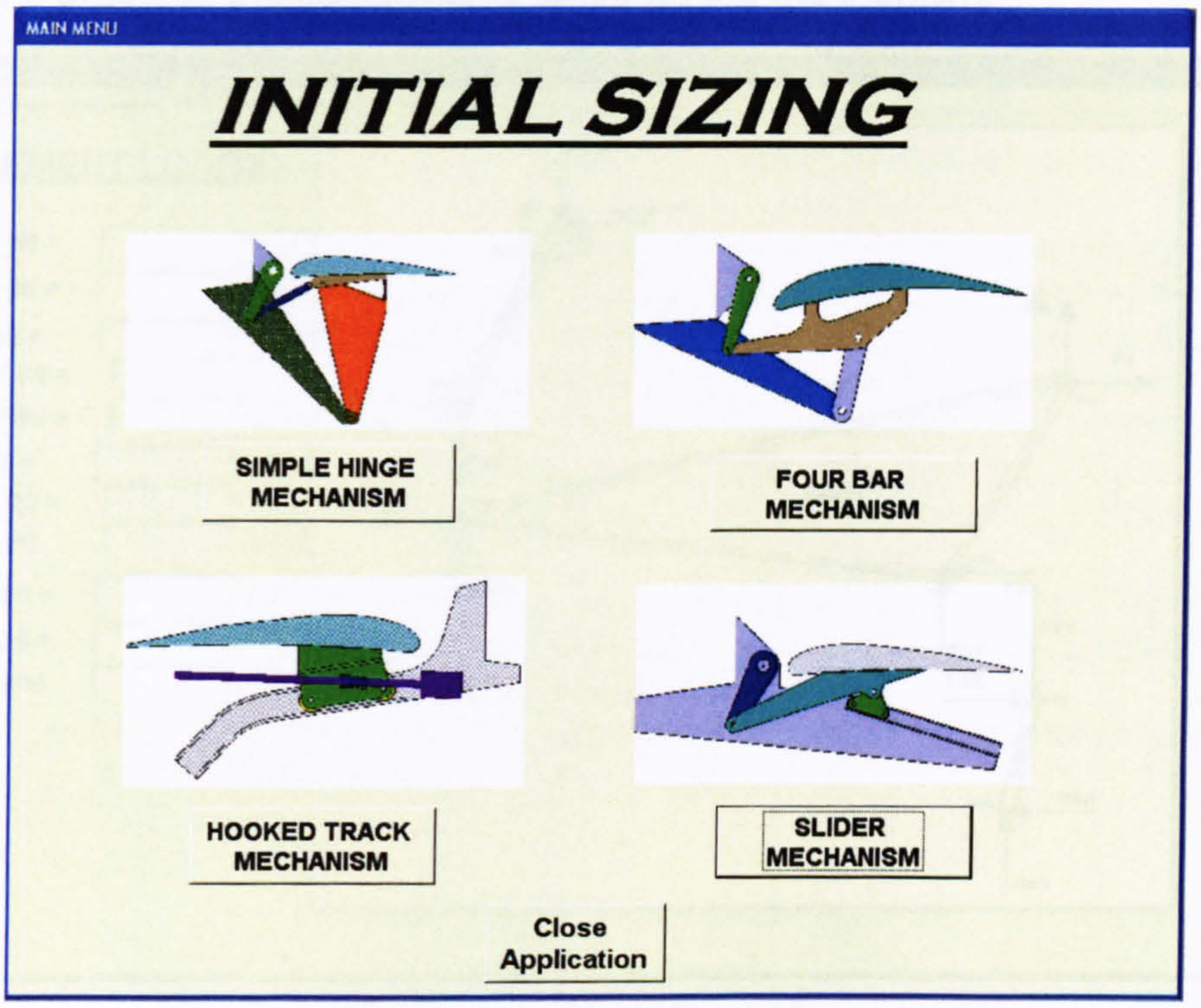

Figure 3.16 – Main Menu

Data Input Menu (similar for every mechanism)

In this menu the user will introduce input data.

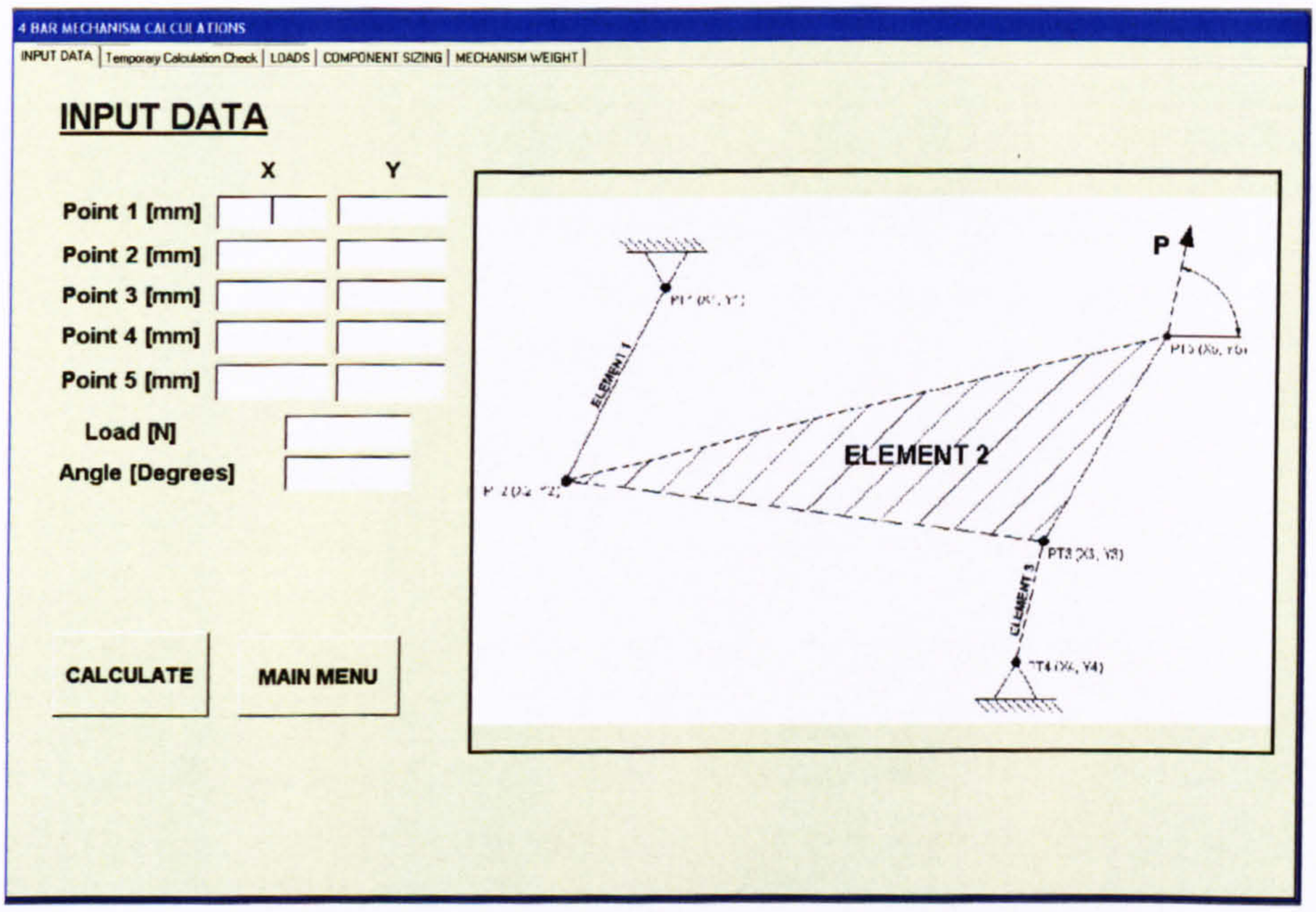

Figure 3.17 – Data Input Menu

Load Results Menu (similar for every mechanism)

This menu presents the components loads for the mechanism.

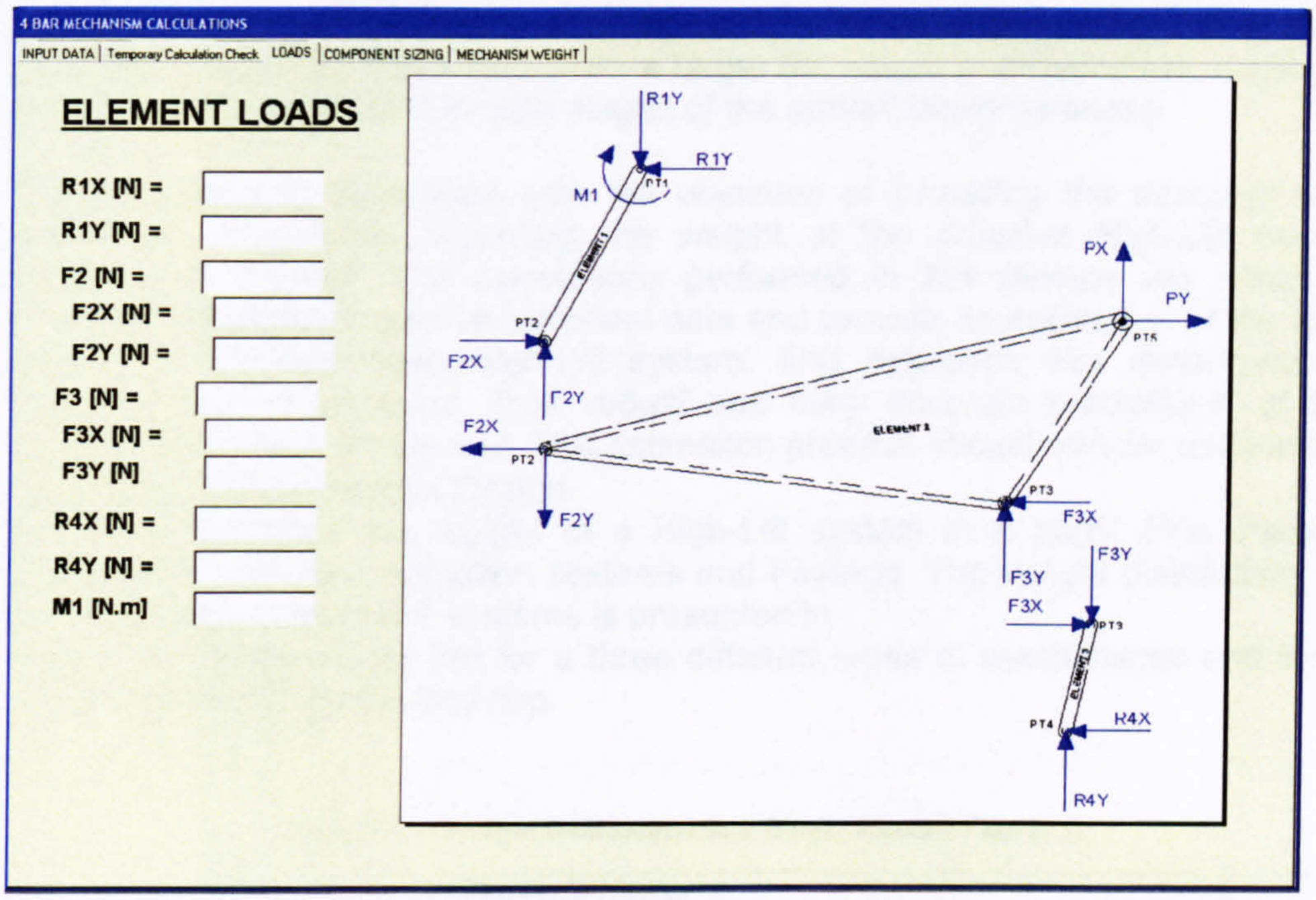

Figure 3.18 – Loads Result Menu

3.2.4. Weight Module

The weight has long been a concern in aircraft design, since it has a great impact in the performance capabilities of an aircraft. As an important part of the aircraft, the High-Lift devices have also been a target for weight improvements, making it an important issue from the initial stages of the aircraft design process.

This module was developed with the objective of providing the designer with preliminary information regarding the weight of the different High-Lift device mechanisms studied. The calculations performed in this module are based in empirical equations based on historical data and provide an estimation of the total weight of a trailing edge High-Lift system. This approach was developed by Pepper [71] and produces *"fast, robust and fairly accurate predictions"* of the trailing edge High-Lift systems. This estimation process should only be used in the initial stages of the Aircraft Design.
Pepper [71] divided the weight of a High-Lift system in 4 parts: Flap Panels, Supports & Linkages; Actuation systems and Fairings. The weight distribution for the 4 different parts of flap systems is presented in
Table 3.1. These values are for a three different types of mechanisms and for a representative Single Slotted flap.

Table 3.1 – Weight Distribution in a Single Slotted Flap [71]

	External hinge Supports	Link/Track	Hooked Track
Supports & Linkages	22%	24%	34%
Actuation Systems	19%	32%	25%
Flap Panels	54%	43%	30%
Fairings	5%	1%	11%

As an example, if the estimated weight of a Link/Track mechanism at one hinge position is 60Kg, and assuming that the aircraft has outboard and inboard flaps, there would be a total of 8 mechanisms with a total of 480 Kg. Since the Supports & Linkages represent 24% of the total High-Lift System with a Link/track mechanism, the total system weight would be (480/24)x100 =2000Kg.

3.2.5. Lift and Fairing Drag Module

This module analyses the aerodynamic performance at the take-off configuration and estimates the increments in drag associated with the fairings of the different types of Trailing Edge High Lift devices. The analysis performed in this module is confined to a theoretical basis as there wasn't scope for the generation of a test prototype. The procedure used the methods provided by ESDU datasheets.

Available from the SYNAMEC Module, the Initial Sizing and Structural/Mechanical Design stages are the depth and width of the flap mechanism, along with the trajectory configuration, making it possible to estimate fairings dimensions and have access to the gap and overlap for the different flight stages.

a) Associated Fairing Drag

Using the procedure presented in ESDU 79015 – UNDERCARRIAGE DRAG PREDICTION METHODS, it is possible to estimate the drag for the fairings of each mechanism. The increment in drag arising from a streamline structure like a fairing depends largely on its Frontal area, the thickness/chord ratio and the Reynolds number.

The drag coefficient for cases where $5.75 \leq \log_{10}Re_{ss} < 7.5$ is given by the following expression:

$$C_{D_{ss}} = 0.00495 \cdot \left[1 + 2 \cdot \frac{t_{ss}}{c_{ss}} + 60 \cdot \left(\frac{t_{ss}}{c_{ss}}\right)^4\right] \qquad \text{[Eq.5.4, ESDU 79015]}$$

where:

$C_{D_{ss}}$ - Drag Coefficient of streamline strut
t_{ss} - Maximum thickness of streamline structure
c_{ss} - Chord of streamline strut normal to its axis

The increment in drag arising from the streamline structure is given by:

$$\frac{D_{ssi}}{q \cdot S} = C_{D_{ss}} \cdot \frac{S_f}{S} \qquad \text{[Eq.5.7, ESDU 79015]}$$

where:

$C_{D_{ss}}$ - Drag coefficient for isolated component free from interference
S_f - Frontal Area of Fairing [m^2]
S - Aircraft Reference Area (Wing Gross Area) [m^2]

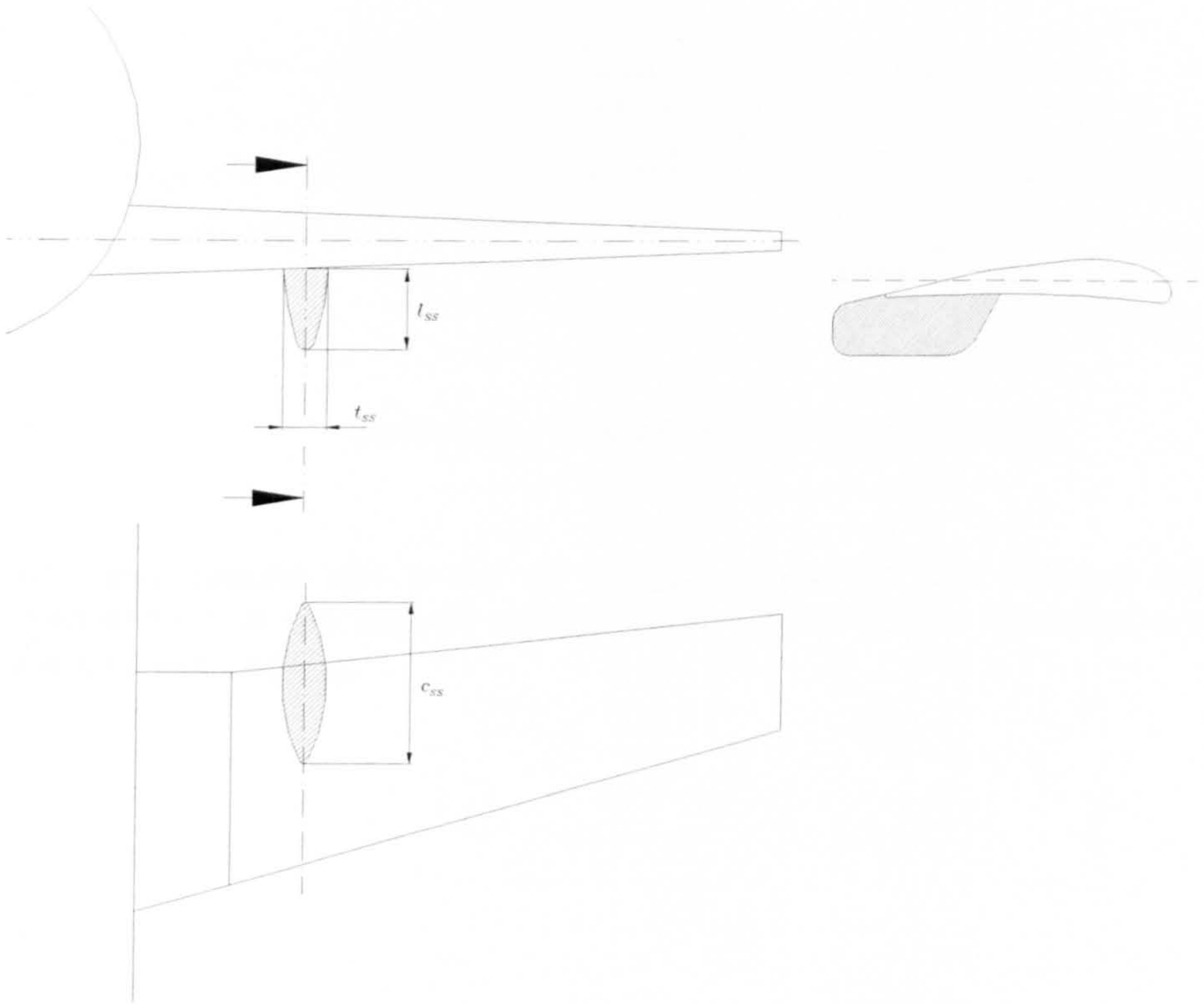

Figure 3.19 – Fairing Drag

The typical drag coefficient of wide body transport aircraft is in the region of 0.02 [126]. Taking that the frontal area of the aircraft fairings is in the region of 1% of the wing reference area, the author assumed that the drag of fairings structures was about 1% of the Aircraft total drag coefficient. Hence, for an aircraft with 3 fairings per wing, the drag coefficient of a single fairing is in the order of 3.0E-5.

b) Aerodynamic Performance in the Take-Off Configuration

During the optimization stage, every mechanism is optimized to guarantee the aerodynamic performance for landing, i.e. they achieve the Fowler motion and gap requirements. Though, for the take-off configuration, the values for Fowler motion and gap vary for each type of mechanism. To access the take-off performance of each mechanism ESDU 94030 (for aerofoil) and ESDU 91014 (for wing) are used to obtain the increment in maximum lift coefficient due to the deployment of the single-slotted fowler flap for each mechanism type.

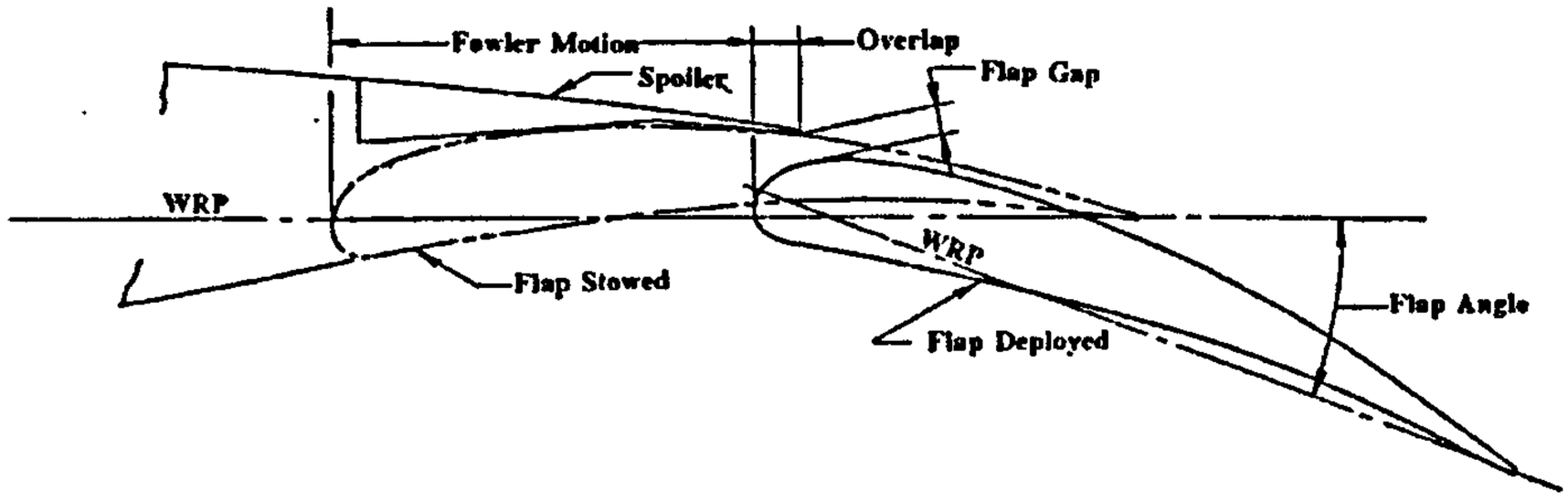

Figure 3.20 – Trailing Edge Flap Nomenclature [86]

The final results are a set of ΔC_{Lmax} values for the different types of flap mechanisms at the take-off configuration. These values represent only a part of the total wing ΔC_{Lmax}..

3.2.6. Reliability & Maintainability Module

The main objective of this module is to provide information about the reliability and maintainability of the different mechanisms analysed, helping the designer in the selection process of the best mechanism, from within a group of viable solutions. The processes on how this information is obtained are presented in the following paragraphs.

Reliability

Reliability has become one of the most important issues in the aircraft Industry. Aircraft operators have recognized its importance and its impact in the Direct Operating Costs. The costs involved with improving the reliability of an in-service aircraft are very high. Improvements and corrections are usually done to make in-service aircraft more reliable, but at a very high cost and only up to a limited extent. However, it would be much more cost effective to include reliability analysis at an early stage in the design process. By doing so, potential failures and weakness can be identified and corrected at a much lower cost.
This module performs just that, applies reliability estimation in the initial stages of the design of High Lift device mechanisms. It estimates the reliability of different mechanisms concepts, providing the designer with comparison values to help in the selection process of the most appropriate mechanisms.
This module uses the 'Part Count' Reliability Prediction [118] and NPRD-95 (Nonelectronic Part Reliability Data) [69] to analyse the different mechanisms in terms of number of parts, and mechanical connections, and assigns a reliability value to the overall mechanism. The NPRD-95 contains data for more than 11000 parts and provides failure rates for a wide variety of component types including mechanical, electromechanical, and discrete electronic parts and assemblies The NPRD reflects field experience in military and commercial applications. Table 3.2 presents a sample reliability result for the Simple Hinge mechanism flap.

Maintainability

Maintainability is also an important issue in aircraft design. The consequences of not considering it from the outset of the design of the aircraft can be very serious and costly. Some of those consequences are [Mansour]:

- Inability to perform maintainability efficiently
- Excessive removal and replacement times
- Inadequate spares holding
- Excessive spare costs
- Low aircraft availability

This module was developed with the main objective of quantifying the maintainability for High-Lift Trailing edge systems. The author used as value of measure the most important measurable parameter on the design for maintainability, the Mean Time to Repair (MTTR).
To determine the MTTR for the different type of mechanisms the author used a maintainability prediction procedure created by the US department of defence

called MIL-HDBK-472. This procedure is very old but its use over the years in many different areas has proved to offer rational results.
The MTTR is assumed to be a function of specific design parameters directly related with:

- Physical Configuration of the system – Check List A
- Facilities available for maintenance – Check List B
- Degree of Maintenance skill required by the personal Check List – C

The designer has to go through these check lists and score each one of them in different categories for each maintenance task. The last step on the calculation of the MTTR is to insert the total check list scores for the analysed maintenance tasks in the equation below.

$$MTTR = 10^{(3.54651 - 0.02512 \cdot A - 0.03055 \cdot B - 0.01093 \cdot C)}$$

A, B and C are the sum of the scores of each maintenance task on Check List A, B and C, respectively.

An example is presented in Table 3.3. The application of this procedure requires adequate knowledge of the system design and operation.

Table 3.2 – Simple Hinge Flap Reliability Result

	SIMPLE HINGE			
	Elements	**QTY**	**Failure Rate/Element (10e6h)**	**Sub-System Failure Rate (10e-6h)**
	HINGE FITTING	1	0.02	0.02
	FLAP FITTING	1	0.02	0.02
	SUPPORT FITTING	1	0.02	0.02
	LINEAR ACTUATOR	1	35.41	35.41
	FWD FAIRING	1	0.20	0.20
	AFT FAIRING	1	0.20	0.20
	Mechanism Connections			
F	SUPPORT FITTING / WING STRUCTURE	1	0.02	0.02
F	HINGE FITTING / FLAP FITTING	1	0.02	0.02
F	LINEAR ACTUATOR / HINGE FITTING	1	0.02	0.02
F	FLAP FITTING / FLAP	1	0.02	0.02
F	FWD FAIRING / WING STRUCTURE	1	0.02	0.02
F	AFT FAIRING / FLAP	1	0.02	0.02
R	SUPPORT FITTING / HINGE FITTING	1	1.00	1.00
R	SUPPORT FITTING / LINEAR ACTUATOR	1	1.00	1.00
R	SUPPORT FITTING / AFT FAIRING	1	1.00	1.00
	Total Nr. Parts	**6**	**Assembly Failure Rate**	**38.99**
	Total Nr. Connections	**9**		

Table 3.3 – Simple Hinge Flap Maintainability Result [82]

MAINTAINABILITY PREDICTION [MIL - HDBK 472]

SIMPLE HINGE FLAP [Fig. 3]

CHECK LIST A - PHISICAL DESIGN FACTORS

		SUPPORTS & LINKAGES			ACTUATION & CONTROLS	FLAP PANEL	FAIRINGS	
	ITEM	HINGE FITTING	FLAP FITTING	SUPPORT FITTING	LINEAR ACTUATOR	FLAP	FWD FAIRING	AFT FAIRING
1	Access	2	2	2	2	4	4	4
2	Latches& Fasteners (external)	2	2	0	2	2	4	4
3	Latches& Fasteners (Internal)	2	0	0	2	0	4	4
4	Access (Internal)	2	2	2	2	4	4	4
5	Packaging	0	0	0	2	0	2	2
6	Units/Parts	2	0	0	2	0	2	2
7	Visual Display	2	2	0	4	2	2	2
8	Fault & Operation Indicators	2	2	0	4	2	0	0
9	Test Point Availability	2	2	2	2	2	2	2
10	Test Point Identification	0	0	0	2	0	0	0
11	Labelling	2	2	2	2	2	2	2
12	Adjustments	2	0	0	2	2	2	2
13	Testing (On Aircraft)	4	4	4	4	4	4	4
14	Protective Devices	2	2	0	2	2	2	2
15	Safety Personal	2	2	2	2	2	2	2
	Total [A]	28	22	14	36	28	36	36

CHECK LIST B - DESIGN FACILITY FACTORS

		SUPPORTS & LINKAGES			ACTUATION & CONTROLS	FLAP PANEL	FAIRINGS	
	ITEM	HINGE FITTING	FLAP FITTING	SUPPORT FITTING	LINEAR ACTUATOR	FLAP	FWD FAIRING	AFT FAIRING
1	External Test Equipment	2	2	2	2	2	4	4
2	Connectors	2	2	2	2	4	4	4
3	Jigs or Fixtures	0	0	0	2	0	2	2
4	Visual Contact	4	4	4	2	2	2	2
5	Assistance (Operations Personal)	4	4	4	2	4	4	4
6	Assistance (Technical Personal)	0	0	0	2	0	2	2
7	Assistance (Supervisory or Contract Personal)	2	2	2	2	4	4	4
	Total [B]	14	14	14	14	16	22	22

CHECK LIST C - MAINTENANCE SKILLS

		SUPPORTS & LINKAGES			ACTUATION & CONTROLS	FLAP PANEL	FAIRINGS	
	ITEM	HINGE FITTING	FLAP FITTING	SUPPORT FITTING	LINEAR ACTUATOR	FLAP	FWD FAIRING	AFT FAIRING
1	Arm, Leg, and Back Strength	2	2	2	2	1	1	1
2	Endurance and Energy	2	2	2	2	1	1	1
3	Eye/Hand Coordination, Dexterity and Neatness	2	2	2	2	2	2	2
4	Visual Acuity	2	2	2	2	4	4	4
5	Logical Analysis	3	3	3	2	3	3	3
6	Memory - Things and Ideas	2	2	2	2	2	3	3
7	Planfulness and Resourcefulness	2	2	2	2	2	2	2
8	Alertness, Cautiousness, and Accuracy	1	1	1	2	1	3	3
9	Concentration, Persistance and Patience	1	1	1	2	1	2	2
10	Initiative and Incisiveness	3	3	3	4	3	4	4
	Total [C]	20	20	20	22	20	25	25
	MTTR [hr]	2.6	3.7	5.9	1.6	2.3	0.8	0.8

TOTAL 17.7

3.2.8. Simple Cost Estimation

It is very difficult to determine the impact of the high-lift system in the total cost of a transport aircraft because it is a complex function of the cost to develop, build, purchase, operate, maintain and dispose of the airplane [71]. Though, simple cost estimation procedures could be used to compare different design solutions and determine which is the most cost effective. This module looks into the costs of the total High-Lift system, as function of the weight and system part count, and the cost of increased drag arising from the different fairing structures of the mechanisms studied. These simple cost estimation procedures are described below.

a) High-Lift Device System Cost

Pepper [71], also proposed the following method for cost evaluation of High-Lift systems. This method is based on Weight and the part count of the different mechanisms of High-Lift devices.

$$Cost = a_1 \cdot W \cdot PC^{x1} \text{ [US Dollar]}$$

$$a_1 = \begin{cases} 1.8881 & \text{Trailing Edge Device} \\ 1.7339 & \text{Leading Edge Device} \end{cases}$$

$$x_1 = 0.7$$

a_1 – Accounts for hourly labour costs and type of material.
PC – Part Count of a system. Part count of a Trailing Edge flap is given by the sum of the parts of the flap panel, support, support fairing and actuation.
W – Total weight of High-Lift system [lb]

Values for the part count of trailing edge devices are given in the following tables.

Table 5 Part Count of Trailing-Edge Flaps with Hooked Track Supports

	Single-Slotted	Fixed Vane/Main	Articulating Vane/Main	Main/Aft	Triple-Slotted
Flap Panel	600	750	820	1400	1620
Support	210	210	230	230	260
Fairing	350	360	370	380	500
Actuation	450	450	450	450	450
Total	1610	1770	1870	2460	2830

Table 6 Part Count of Trailing-Edge Flaps with Link/Track Supports

	Single-Slotted	Fixed Vane/Main	Articulating Vane/Main	Main/Aft	Triple-Slotted
Flap Panel	600	750	820	1400	1620
Support	150	150	164	164	185
Fairing	100	100	105	110	145
Actuation	300	300	300	300	300
Total	1150	1300	1389	1974	2250

Table 7 Part Count of Trailing-Edge Flaps with External Hinge Supports

	Single-Slotted	Fixed Vane/Main	Articulating Vane/Main	Main/Aft
Flap Panel	590	740	810	1380
Support	200	200	220	220
Fairing	200	205	210	220
Actuation	200	200	200	200
Total	1190	1345	1440	2020

Figure 3.21 – Part count for Trailing Edge Devices [71]

b) Cost associated with Fairing Drag

Aircraft efficiency is an important factor for aircraft manufacturers and airline operator, as it relates directly sale price and profit margins. There are several ways of improving aircraft efficiency with the final objective of reducing the direct operating costs. Gilyard [37] stated that a drag reduction of only 1% translates into an equivalent saving in fuel usage and fuel costs. This would bring savings of around £400,000 in the life of a short range category, as shown in the calculations below.

For short range aircraft, like the AIRBUS A320 or BOEING 737, considering:

20 years life, 2500 hours/year at 400 nm/hour = 20,000,000 nm

Actual fuel value = £1.00/US gallon
Fuel consumption = 2.00 US gallon/nm (average Aircraft range/Max fuel capacity for the AIRBUS A320 family)

Total fuel cost over the life of the aircraft would be £40,000,000

1% Fuel saving ⇒ £400,000 saving over the life of the aircraft.

Knowing that the typical drag coefficient of wide body transport aircraft is in the region of 0.02 [126], it can be stated that an increase of 0.2E-3 in drag coefficient could bring additional costs of about £400,000 over the life of the aircraft.

Estimating the increment in drag associated with the fairing structures of the different mechanism allowed the author to determine the cost penalty arising from the difference in drag between the mechanisms.

3.2.9. Mechanism Selection Criteria

A Simple Decision-Making technique, proposed by Fielding [25], was used to help in the selection of the most appropriate mechanism. Pre-selected attributes are gathered and collected in a matrix where points are attributed to each mechanism depending on their performance in each category. The best mechanisms are the ones that achieve the highest score. The attributes to be scored are:

- Weight (lowest weight will receive maximum score)
- Aerodynamic Performance (highest ΔC_{Lmax} will receive maximum score)
- Drag (lowest Drag will receive maximum score)
- Reliability (highest Reliability will receive maximum score)
- Maintainability (highest MTTR will receive maximum score)
- System Cost (lowest associated cost will receive maximum score)
- Fuel Cost Reduction (Highest decrease in cost will receive maximum score)

The highest result in each attribute is scored with a maximum score of 10.0 and the remaining results are factored based on this maximum rating. For example, if a Simple Hinge mechanism has a weight of 50kg and a Link/Track Mechanism a

weight of 100Kg, the Simple Hinge weight attribute would have a score of 10.0 and the Link/Track weight attribute a score of 10 x (50/100) = 5.
All scores are finally added for each mechanism to provide the designer with an overall classification of the different mechanisms analysed.

Trailing Edge High-Lift System Weight [Kg]		
		Score
Mechanism 1		
Mechanism 2		
Mechanism 3		

Aerodynamic Performance ΔC_{LMax}		
		Score
Mechanism 1		
Mechanism 2		
Mechanism 3		

Fairing Drag Coefficient		
		Score
Mechanism 1		
Mechanism 2		
Mechanism 3		

Reliability		
		Score
Mechanism 1		
Mechanism 2		
Mechanism 3		

Maintainability (MTTR)		
		Score
Mechanism 1		
Mechanism 2		
Mechanism 3		

Cost Associated with Fairing Drag		
		Score
Mechanism 1		
Mechanism 2		
Mechanism 3		

Trailing Edge High-Lift System Cost [£]		
		Score
Mechanism 1		
Mechanism 2		
Mechanism 3		

OVERALL SCORES	
Mechanism 1	
Mechanism 2	
Mechanism 3	

CHAPTER 4

VALIDATION OF THE METHODOLOGY

4.1. INTRODUCTION

There was no experimental work or testing involved in this research project, which is the way validation is normally done in research studies. This chapter presents alternative validation results for the main modules of the new methodology. A brief description of the validation process for each of the main modules is presented below, with details in Paras. 4.2 to 4.7.

SYNAMEC Module

The objective of the validation was to check if the SYNAMEC tool was capable of generating different types of mechanisms and optimize them to fulfil the initial requirements. This test was performed in the scope of the SYNAMEC project and had the collaboration of ALENIA, which provided the data required.

Initial Sizing Module

There was no data available from Aircraft manufactures to help in the validation of this module. The author considered this module a fundamental part of the proposed methodology and decided to make a 2D Comparison with an existing trailing edge device of a commercial aircraft. A Link/Track mechanism was sized and a comparison made with the same type of mechanism in the A320 Aircraft.

Reliability & Maintainability Module

Due to the lack of specific reliability and maintainability information regarding high-lift devices of commercial transport, the validation for this Module was performed using the results from the NASA Contractor Report 196709, by Peter K.C. Rudolph [86]. This author is an established Engineering Consultant that has worked for Boeing and has several publications and patents on High-lift devices. A list of his most relevant work is presented below:

Publications:

- ***"Aero-Mechanical Design of High-Lift Systems"***, Aircraft Engineering and Aerospace Technology Journal, Vol. 71. Nr. 5, 1999. pp. 436-443. Other authors: VAN DAM, C., SHAW, S., VANDER, J., KINNEY, D. [105]
- ***"High-Lift Systems on Commercial Subsonic Airliners"***, NASA CR 4746, 1996. [85]
- ***"Mechanical design of high lift systems for high aspect ratio swept wings"***, NASA CR 196709, 1998. [86]

Patents:

- ***"Vortex leading edge flap assembly for supersonic airplanes"*** - US Patent 5681013
- ***"Supersonic airplane with subsonic boost engine means and method of operating the same"*** - US Patent 5529263
- ***"Hinge fairings for control surfaces"*** - US Patent 5388788
- ***"High taper wing tip extension"*** - US Patent 5039032

The publication ***"Mechanical design of high lift systems for high aspect ratio swept wings"*** [86] provides useful information for a range of flap mechanisms that

can be used for comparison with the results of the author-proposed design methodology. Mr. Rudolph compares a variety of mechanisms using common flap geometry and draws a set of conclusions regarding weight, reliability and maintainability for each type of mechanism. Because the work presented in this study makes use of some of the mechanisms studied in Rudolph's work, the author decided to the apply the proposed design methodology to the same mechanisms in the Rudolph's study and compare the results obtained. As in Mr. Rudolph's study, exact or realistic values of the mechanism the mechanisms reliability and maintainability were not achieved. The calculations performed by the author only allow the comparison of the different mechanisms between themselves.

Also, Mr. Rudolph's study was based in a wing planform configuration similar to the A320 aircraft, as was also the ATRA100, which is used as the basis for this author's research. All data relevant for the validation of the Reliability & Maintainability and Lift /Drag Modules is gathered in Appendix E.

Lift and Drag Module

The unavailability of aerodynamic data related with High Lift devices and the fact that CFD was not in the scope of the author's study, makes it almost impossible to validate the Lift and Fairing Drag Module. This module might provide results far from reality, but it will allow the author to compare and classify the different mechanisms between themselves.

In relation to fairing drag, the author will compare the results obtained from the analysis of the Rudolph's work and check if the fairing drag calculated using the procedure proposed by the new design methodology is in the same order of magnitude as the drag associated to fairings of current commercial transport Aircraft. The typical drag of a Wide body transport aircraft is in the region of 0.02 [126], and assuming that the drag of fairings is around 1% of the A/C drag, the typical drag coefficient for a single fairing in an aircraft with 3 fairings per wing is in the order of 3.00 E-5.

4.2. SYNAMEC MODULE

In the scope of the SYNAMEC project, the author performed a test case in conjunction with ALENIA with the objective of generating mechanism solutions for a specific application. This test case concerned a Flap mechanism for a 70 seat commercial aircraft, and all the relevant data was provided by ALENIA. The data provided was a 3D CAD model with all the Flap deployment positions for Takeoff and Landing, including the required trajectories. Due to the fact that the SYNAMEC system type synthesis module only works with 2-Dimensional mechanisms, the test case was performed at one specific wing position corresponding to the Inboard Flap/Inboard Support.

4.2.1. Synthesis

The test cases performed covered only the first phase of the design process provided by the SYNAMEC System, the Mechanism Synthesis.
From the point of view of the SYNAMEC Systems end user, the Mechanism Synthesis process is composed of 2 main stages, the Synthesis and Optimization.

Stage 1 – TYPE SYNTHESIS

The Type Synthesis phase is where a mechanism solution is built. The basic information required for the type synthesis is the following (Figure 4.1):

- 1 Ground Hinge with a Prescribed Rotation
- 1 Rod, connected to the Ground Hinge
- 1 Fixation Point
- 1 Trajectory Point with 3 Prescribed Displacements (from the objective curve, usually start, middle and end)

The final result of this phase is a basic mechanism that is able to perform a mechanical movement that passes through the 3 points of the predefined objective curve, but it may not pass through all the points of the curve.
This basic mechanism is then read back into the SAMCEF Field environment and prepared in accordance with the requirements for a MECANO analysis. This means giving component properties (rod, volume, etc...), defining meshes and analysis parameters. Once this has been done the mechanism analysis is performed and if the mechanism has a working configuration then it is ready for the next phase.

Summarizing, the Type Synthesis phase can be described as the following sequence of actions in the SYNAMEC tool:

a) Preparation of SAMCEF Field file for OOFELIE
b) Perform Synthesis Analysis with OOFELIE
c) Read OOFELIE results into SAMCEF Field
d) Preparation of data for Mechanical analysis with MECANO
e) Perform mechanical analysis with MECANO

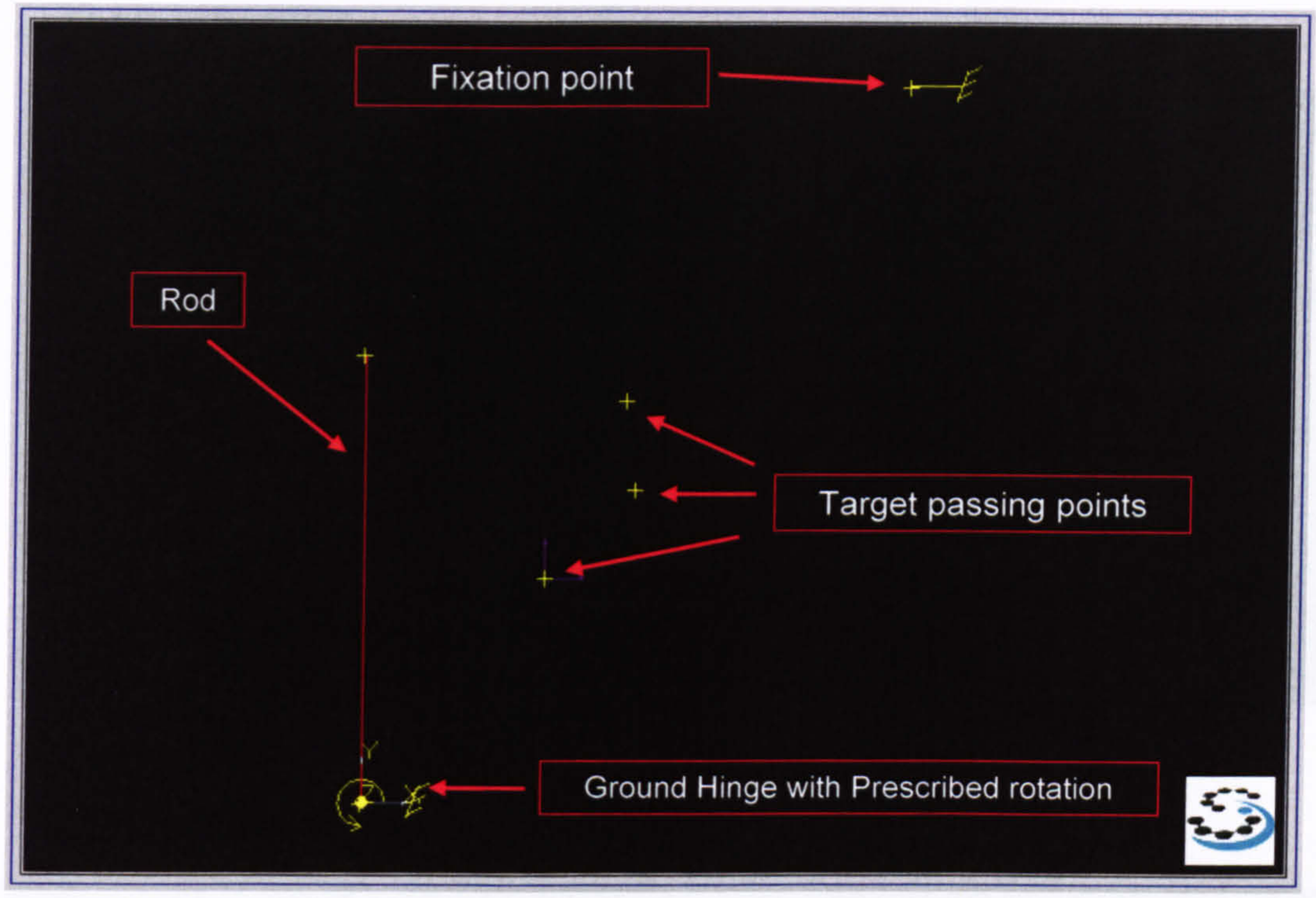

Figure 4.1 – Type Synthesis Input Data

SYNTHESIS RESULTS

The objective of the test cases, performed in the scope of the SYNAMEC contract, was to investigate the capability of the SYNAMEC system to provide solutions that could be compared to flap mechanism concepts already used in commercial aircraft. Due to the numerous types of solutions available for Flap mechanisms, two 4-Bar mechanism concepts were chosen to perform the tests and verify if the system was able to provide similar solutions.
These concepts selected are presented below in Figure 4.2.

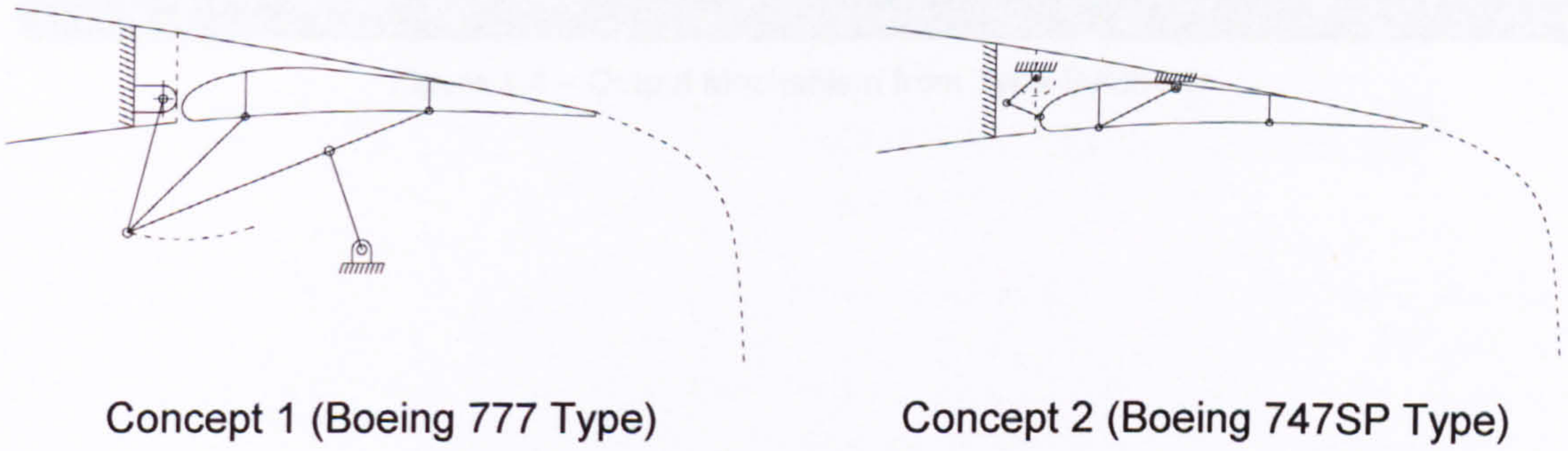

Concept 1 (Boeing 777 Type) Concept 2 (Boeing 747SP Type)

Figure 4.2 – 4-Bar Mechanism concepts

For the first type synthesis applications the rod and second fixing point were positioned in similar orientations and positions, in relation to the airfoil, as the ones from the initial concepts.

a) FLAP CONCEPT 1

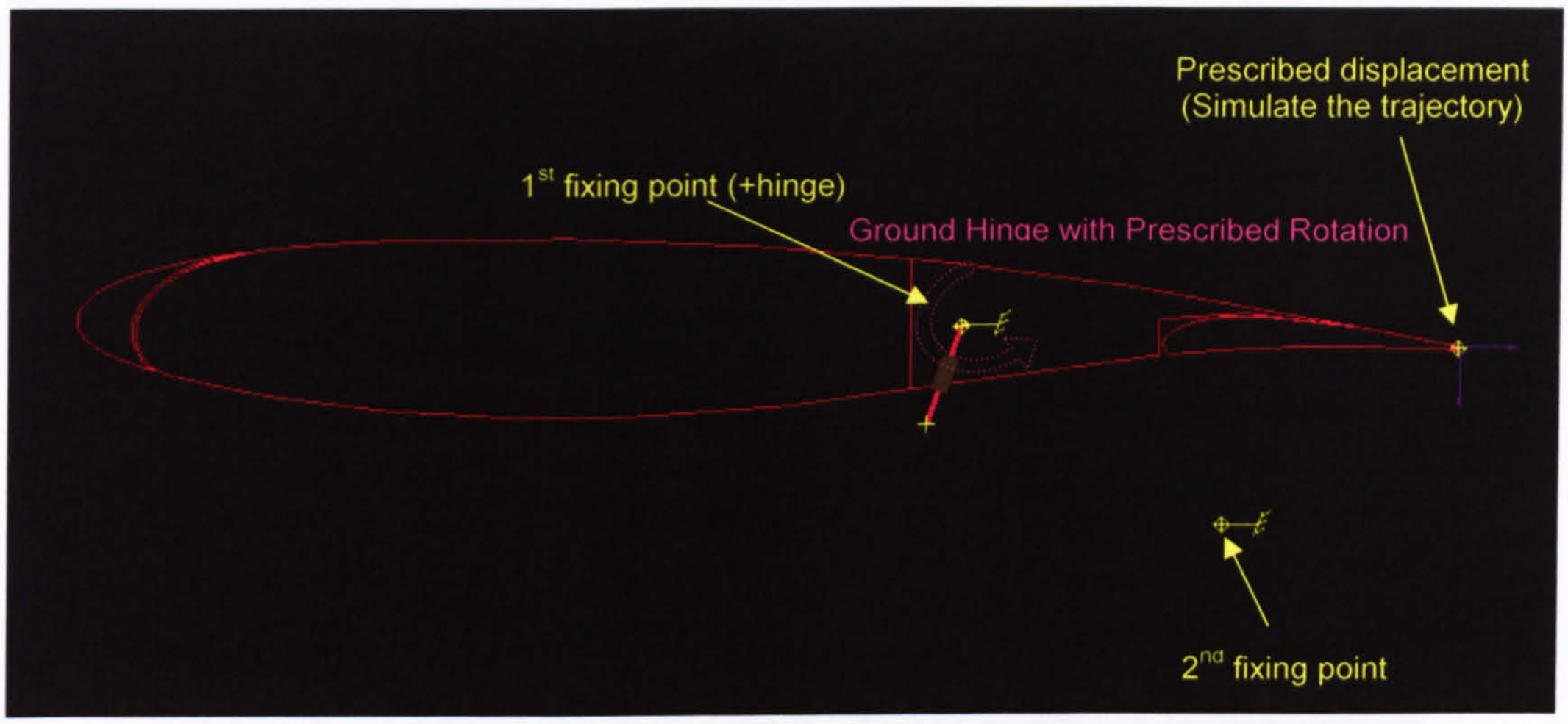

Figure 4.3 – Input Data for Type Synthesis

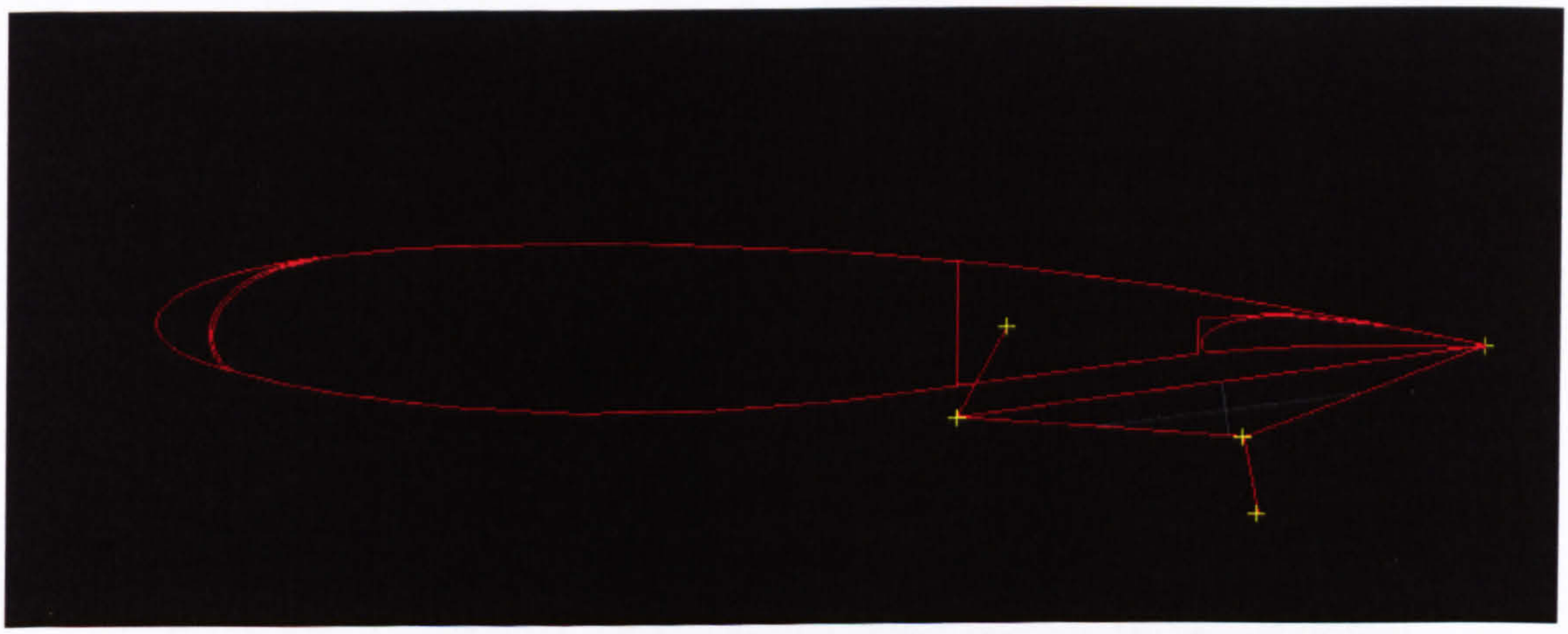

Figure 4.4 – Output Mechanism from Type Synthesis

b) FLAP CONCEPT 2

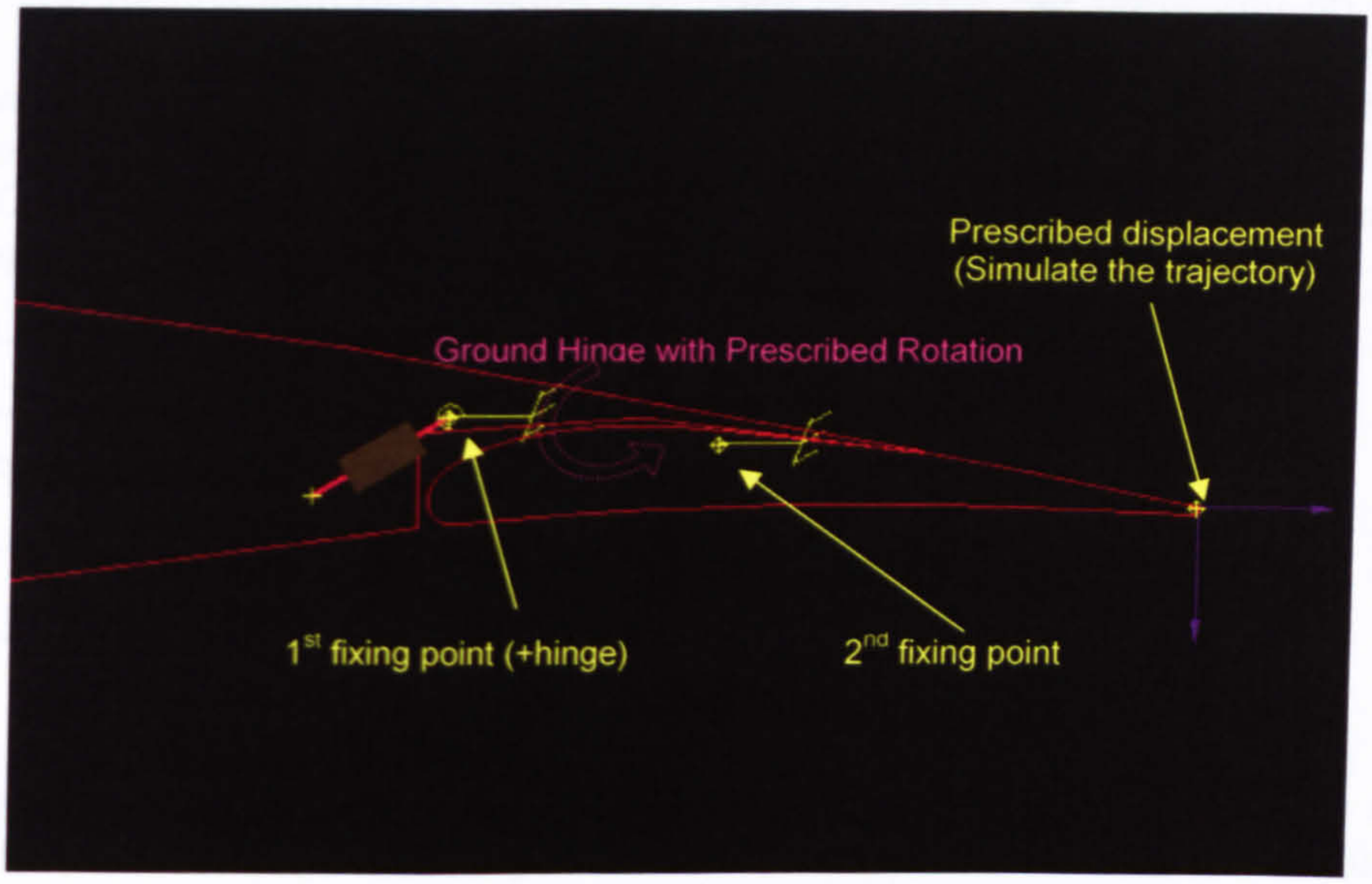

Figure 4.5 – Input Data for Type Synthesis

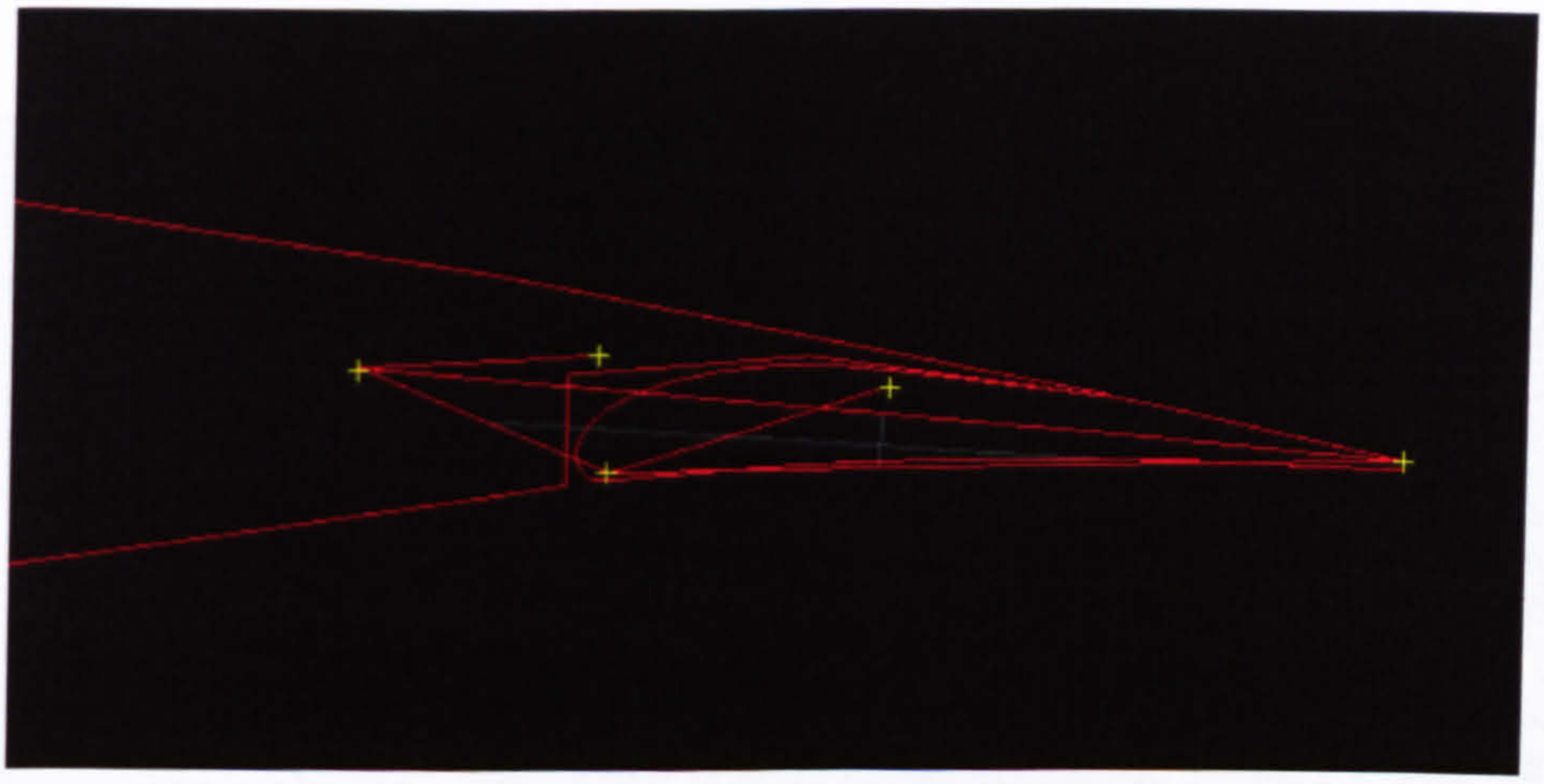

Figure 4.6 – Output Mechanism from Type Synthesis

This phase did not present any major problems. Though, it must be noted that the shape of the mechanism is very sensitive to the prescribed rotations on the ground hinge and the position of the second Fixation point. Small variations on those values may lead to mechanism not proportional to the component sizes involved. Another point to note in the case of the Flap test is that the mechanism returned by the type synthesis process had to be changed in order to better represent the real case. This change is only made to the trajectory point and doesn't influence the rest of the mechanism. This can be seen in Figure 4.7, where the trajectory point of the mechanism (defined from the objective curve) was changed to a point on the Flap structure (which may represent a spar or other fixation structure).

4.2.2. Optimization

Stage 2 deals with the Optimization of the mechanism generated by the Synthesis phase. The mechanism dimensions and point positions are optimized so that the flap LE and TE points coincide with the objective points at cruise and landing. The objective of this validation procedure is to show that the SYNAMEC software is capable of optimizing a mechanism configuration The SAMCEF MECANO and BOSS Quattro packages of the SYNAMEC software are used for the Optimization. The steps used for the SYNAMEC optimization are as follows:

a) Load SAMCEF Field Model and variables

b) Create Bank File to generate input file for MECANO analysis

c) Run MECANO to generate Results and Sensitivities

d) Perform OPTIMIZATION using BOSS Quattro and MECANO

e) Generate SAMCEF Field updated File

For this validation test, the flap trailing and leading edge trajectory were set as objective curves and the flap Leading edge and trailing edge points as the control points for mechanism trajectory verification. At each iteration, the distance between these points and the respective trajectory curves is measured and, if the distance is increasing or decreasing, adjustments are performed to the mechanism points.

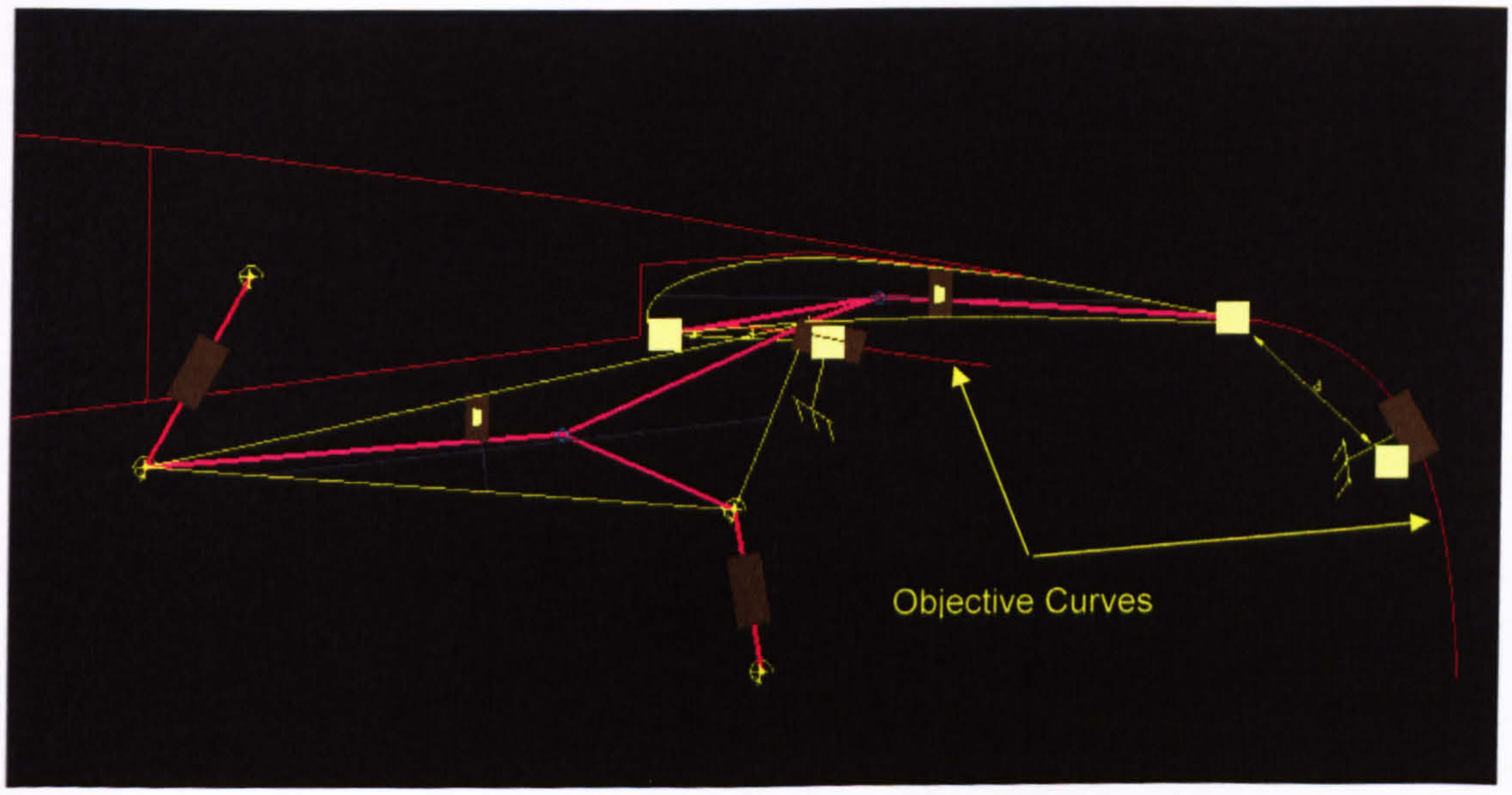

Figure 4.7 – Optimization Problem Definition

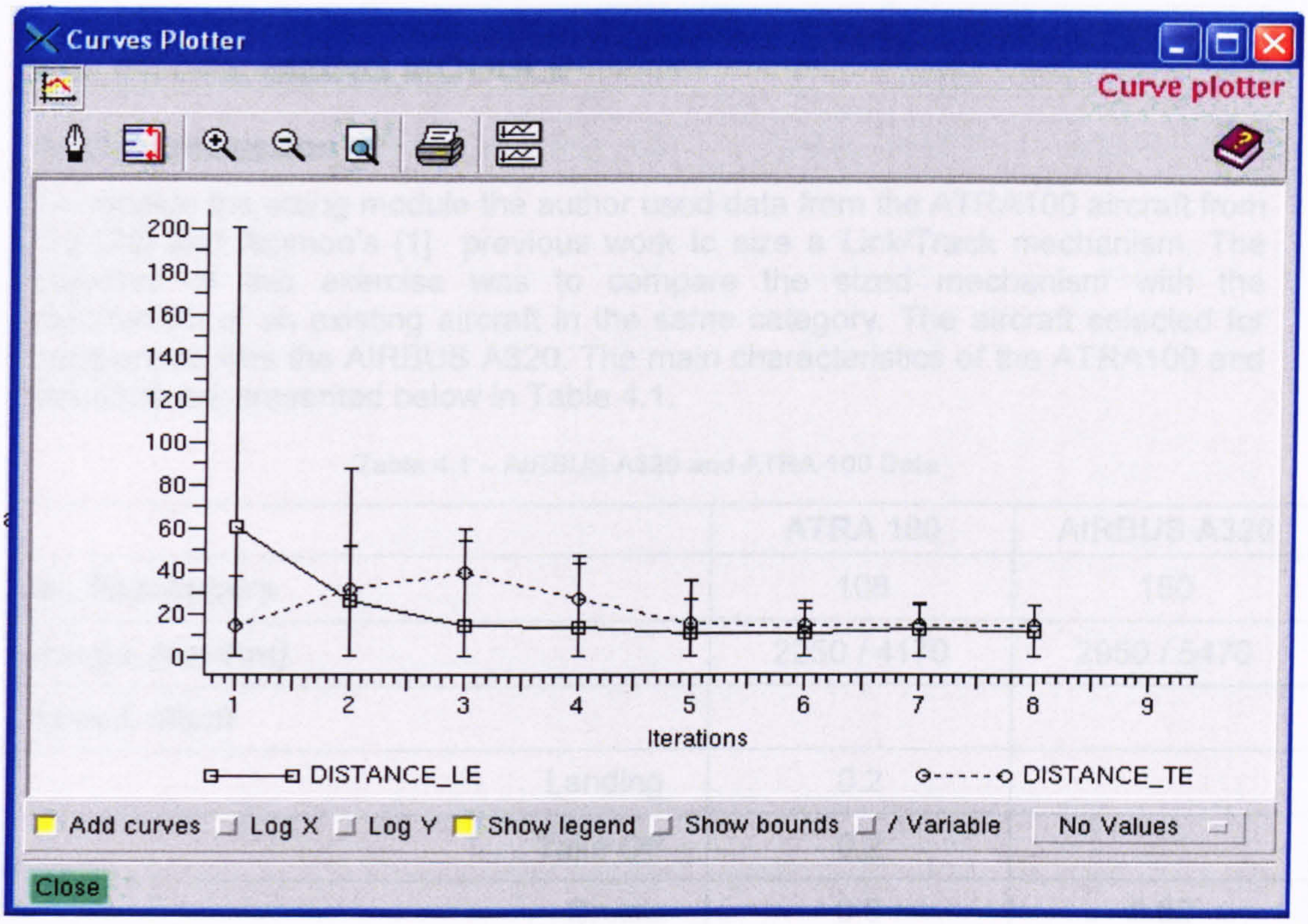

Figure 4.8 – Optimization Result

Figure 4.8 presents the result graph for the mechanism optimization, where we can see the convergence of the distance of the flap leading and trailing edge points to the objective curve.
Although the final result wasn't a total coincidence of the control points to the trajectory curves, this shows that the mechanism was optimized.

4.3. INITIAL SIZING MODULE

4.3.1 Introduction

To validate the sizing module the author used data from the ATRA100 aircraft from Edi [20] and Ammoo's [1] previous work to size a Link/Track mechanism. The objective of this exercise was to compare the sized mechanism with the mechanism of an existing aircraft in the same category. The aircraft selected for comparison was the AIRBUS A320. The main characteristics of the ATRA100 and the A320 are presented below in Table 4.1.

Table 4.1 – AIRBUS A320 and ATRA 100 Data

	ATRA 100	AIRBUS A320
Nr. Passengers	108	150
Range, [nm/Km]	2250 / 4170	2950 / 5470
Speed, Mach		
Landing	0.2	
Take Off	0.2	
Cruise	0.8	0.82
Lift Coefficient, CL		
Landing (Max)	2.9	
Take Off (Max)	2.2	
Cruise	0.51	
Wing (A320 Type)		
Aspect Ratio, A	9.5	9.4
Taper Ratio, l	0.274	
0.25 Sweepback, $\Lambda_{0.25}$	25°	25°
Span, b [m / ft]	32.4 / 9.9	34.1 / 10.4
Area, S [m^2 / ft^2]	110.2 / 1186.3	122.4 / 1318
Inboard Flap Area, S_{Fi} [m^2 / ft^2]	5.25 / 56.5	4.54 / 48.9
Outboard Flap Area, S_{Fo} [m^2 / ft^2]	6.75 / 72.7	5.96 / 64.2
Total Flap Area, S_{Fo} [m^2 / ft^2]	12 / 129.2	10.5 / 113
Design Mass		
Max. Landing Weight, W_L [Kg / Lb]	50635 / 111631	64000 / 141096
Max. Take Off Weight, W_{TO} [Kg / Lb]	56260 / 124032	77000 / 169756

Max. Zero Fuel Weight, W_{ZF} [Kg / Lb]	40738 / 89812	61000 / 134482
Operational Empty Weight, W_{OE} [Kg / Lb]	30425 / 67076	41800 / 92153
Wing Loading, W/S		
Take Off, (W_{TO}/S) [Kg/m^2 / Lb/ft^2]	511/ 105	629 / 129
Landing, (W_L/S) [Kg/m^2 / Lb/ft^2]	459.4 / 94	522.9 / 107
Runway Distances, S		
Take Off, (S_{TO}) [m / ft]	1981/ 6500	2294 / 7526
Landing, (S_L) [m / ft]	1475 / 4840	1442 / 4730
Thrust to Weight Ratio, T/W		
Thrust to Weight Ratio, (T/W)	0.29	0.295

The loads in the A320 are bigger than the loads in the ATRA 100, due to bigger wing area and flap area. To account for this the author scaled the loads from the ATRA to be comparable to the AIRBUS A320 loads. The process used to determine scaling factors for the loads consisted of working back from both aircraft known landing and take-off distances to calculate the increments in Lift due to Flap deployment for Take-off and Landing for both Aircraft. This is done using empirical relationships presented in ref. [25].
The complete calculations are presented in Appendix B and the final results in Table 4.2.

Table 4.2 – Estimated AIRBUS A320 and ATRA 100 Flap Loads

	ATRA	A320	Difference from to A320 to ATRA
Take-Off	53807 N	58082 N	+ 8.0%
Landing	73521 N	81240 N	+10.5%

Difference from to A320 to ATRA in Flap Area = +12.5%

Difference from to A320 to ATRA in Wing Area = +10%

Having in consideration the previous results the author has decided to scale the loads in the ATRA flap use a fixed value of 10%. Also, the ATRA wing, flap chords and airfoils were scaled to coincide with the AIRBUS A320 airfoil dimensions at the wing station where the mechanism was to be designed. The flap ultimate loads provided by Ammoo [1] for the ATRA will be increased 10% for the Sizing validation.

4.3.2 ATRA Link/Track Mechanism Sizing

The sizing validation will be performed for the mechanism at hinge position 2 of the inboard Flap (b/2 = 4563mm), as shown in Figure 4.9.

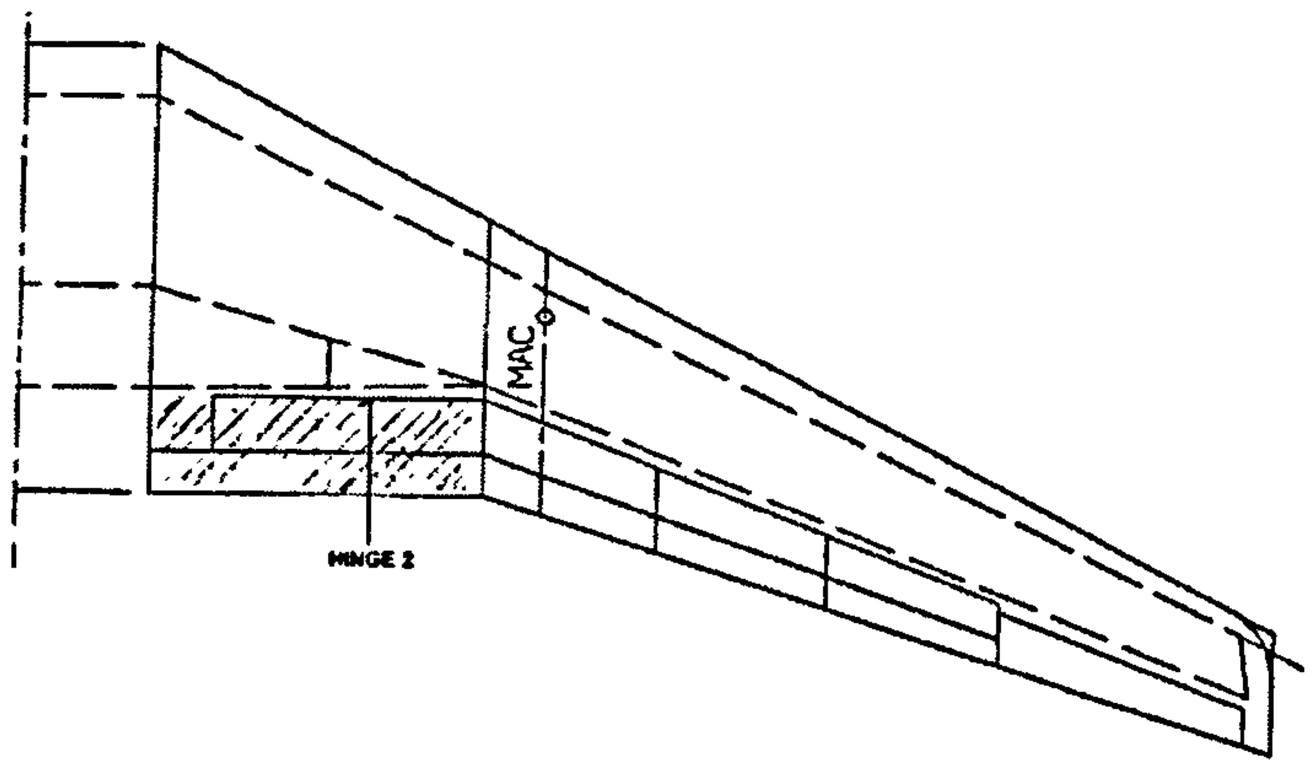

Figure 4.9 – ATRA Link/Track Mechanism Position

The total loads on the flap and the reaction at the hinge were determined and are presented in Appendix B. The values for the hinge loads for the different flight conditions are presented in Table 4.3.

Table 4.3 – Scaled ATRA 100 Hinge Loads

	Reaction @ Hinge 2 [N] (Ult)
Cruise	12740
Take-Off	34200
Landing	32780

The mechanism points to be considered for the calculation of the component loads for each flight condition is presented in
Table **4.4**. The required input data for the calculation of the component loads using the visual basic application developed by the author are shown in Figure 4.10.

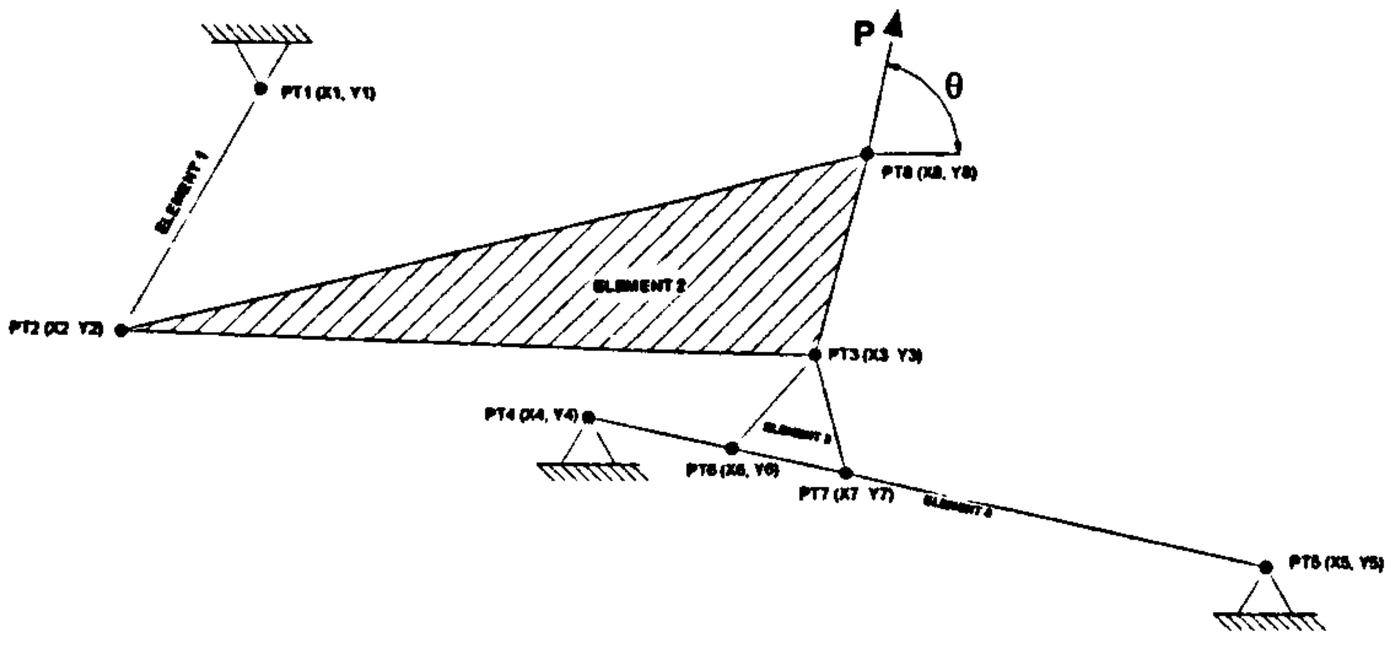

Figure 4.10 – Diagram of Link/Track mechanism

Table 4.4 – Link/Track Mechanism Points

	Cruise		Take-Off		Landing	
	X	Y	X	Y	X	Y
PT1 [mm]	17055.40	2978.13	17055.40	2978.13	17055.40	2978.13
PT2 [mm]	16885.85	2635.55	17361.66	2749.41	17437.30	2994.26
PT3 [mm]	17588.10	2837.40	18092.00	2727.17	18115.38	2722.05
PT4 [mm]	17417.30	2777.37	17417.30	2777.37	17417.30	2777.37
PT5 [mm]	18191.83	2607.94	18191.83	2607.94	18191.83	2607.94
PT6 [mm]	17490.91	2761.27	17994.21	2651.17	18017.60	2646.05
PT7 [mm]	17645.81	2727.38	18149.12	2617.28	18172.50	2612.17
PT8 [mm]	16955.40	3174.21	18159.15	22809.22	18206.67	2775.99

The component loads obtained by the Visual Basic application are presented in Table 4.5.

Table 4.5 –Link/Track Mechanism Component Loads

	Cruise	Take-Off	Landing
R1 [N]	2518	2513	**15067**
R1X [N]	-2517	-2318	**-11984**
R1Y [N]	73	970	9131
F2 [N]	2518	2513	**15067**
F2X [N]	-2517	970	-11984
F2Y [N]	73	-2318	9131
F3 [N]	11779	33113	**37256**
F3X [N]	2517	7076	7962
FY3 [N]	11507	32348	36395
F6 [N]	5935	16561	**26956**
F6X [N]	1268	3539	5761
F6Y [N]	5797	16178	26334
F7 [N]	5845	**16552**	10299
F7X [N]	1249	3537	2201
F7Y [N]	5710	16170	10061
M1 [N.m]	-875	-488	**-4724**

Using the procedures and equations from appendix C, the final dimensions for each mechanism component were calculated and are presented in Table 4.6.

Table 4.6 – ATRA Link/Track Mechanism component sizes

Hinge 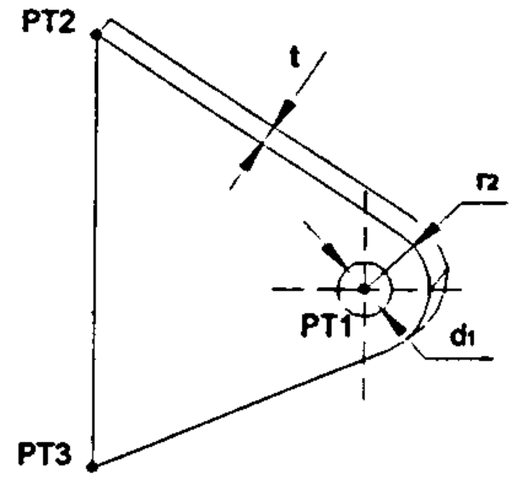	PT1 (17055.40 ; 2978.13) PT2 (16955.40 ; 3174.21) PT3 (16955.40 ; 2862.20) d_1 = 36 mm r_2 = 72 mm t = 18 mm
Drive Link 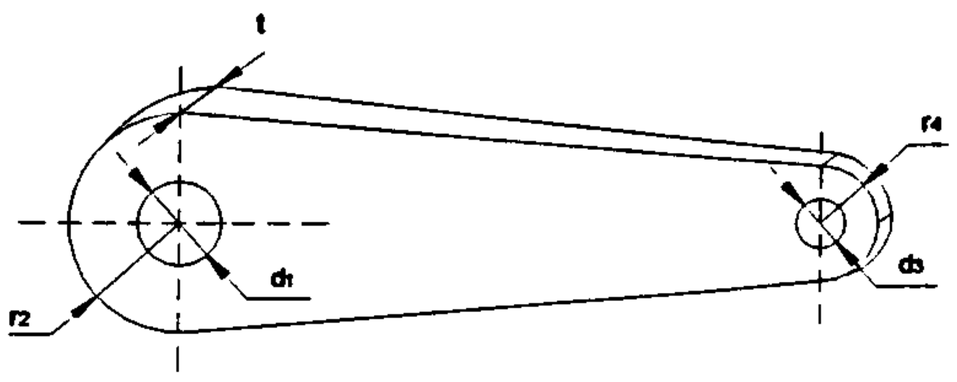	d_1 =36 mm r_2 = 72 mm d_3 = 18 mm r_4 = 36 mm t = 18 mm
Flap Fitting 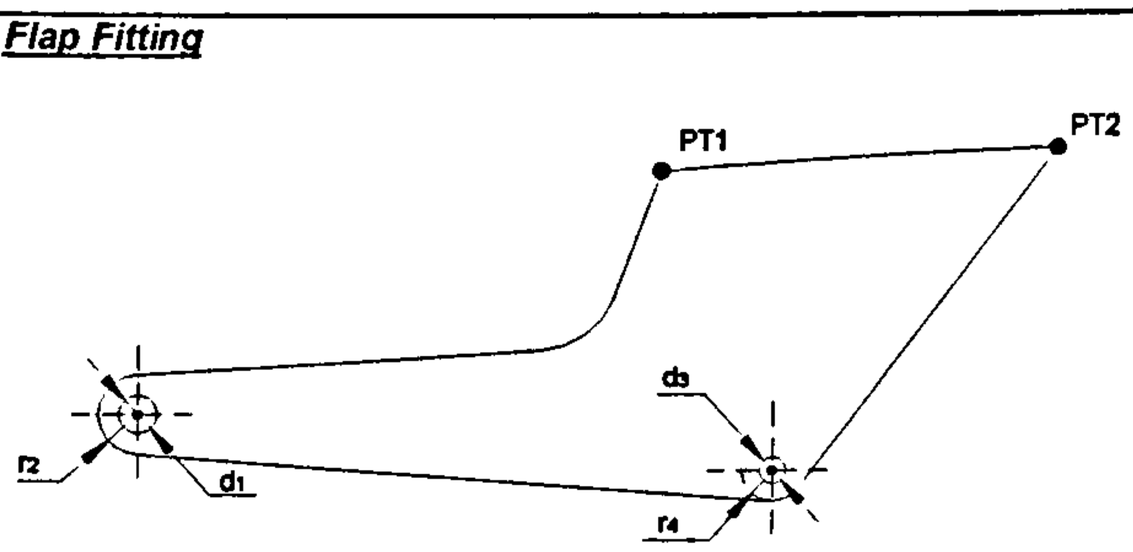	PT1 (17055.40 ; 2978.13) PT2 (16955.40 ; 3174.21) d_1 = 18 mm r_2 = 36 mm d_3 = 15 mm r_4 = 30 mm t = 18 mm
Roller Carriage 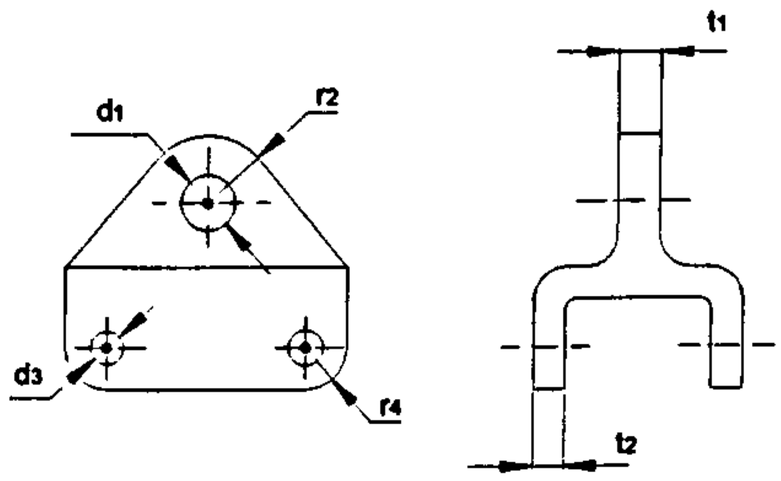	d_1 = 15 mm r_2 = 30 mm t_1 = 7.5 mm d_3 = 10 mm r_4 = 20 mm t_2 = 5 mm

Rollers 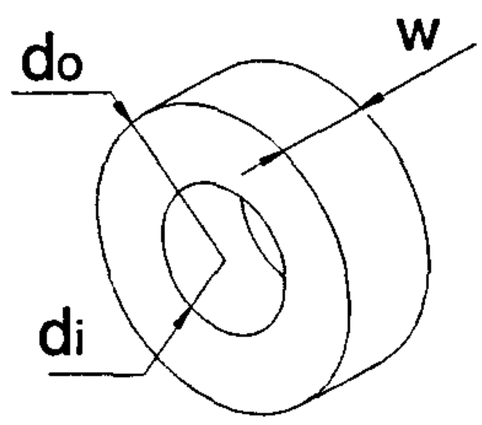 	d_i = 10 mm d_o = 20 mm w = 10 mm
Support Track 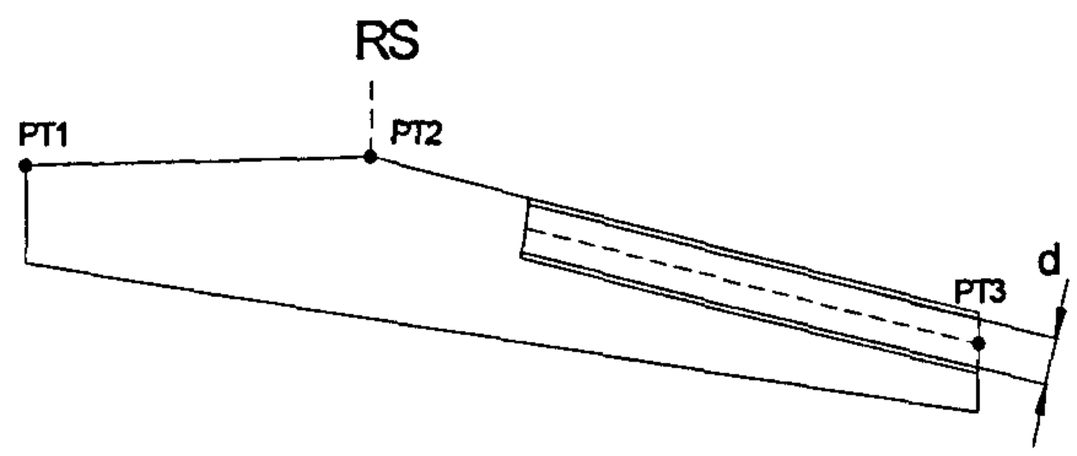 	PT1 (17055.40 , 2978.13) PT2 (16955.40 , 3174.21) PT3 (18191.83 , 2607.44) Track Width: d = 20 mm

4.3.3 ATRA / AIRBUS A320 Mechanism Comparison

The component sizes estimated in the previous paragraph were used to create a 3D CATIA model of the Link/Track mechanism. The 3D CAD model allows the author to make some comparisons with the AIRBUS A320 Link/Track Flap Mechanism. Although it is not possible to compare both mechanisms in detailed terms due to the lack of available information about the AIRBUS Link/Track mechanism, it can be seen from the visual comparison between Figure 4.11, the ATRA Link/Track mechanism, and Figure 4.12, the AIRBUS A320 Link/Track Mechanism, that the mechanism sized using the Initial Sizing procedure isn't very far from the final optimized AIRBUS link track mechanism, which in some ways validates the sizing procedure used by the author in the proposed design methodology.

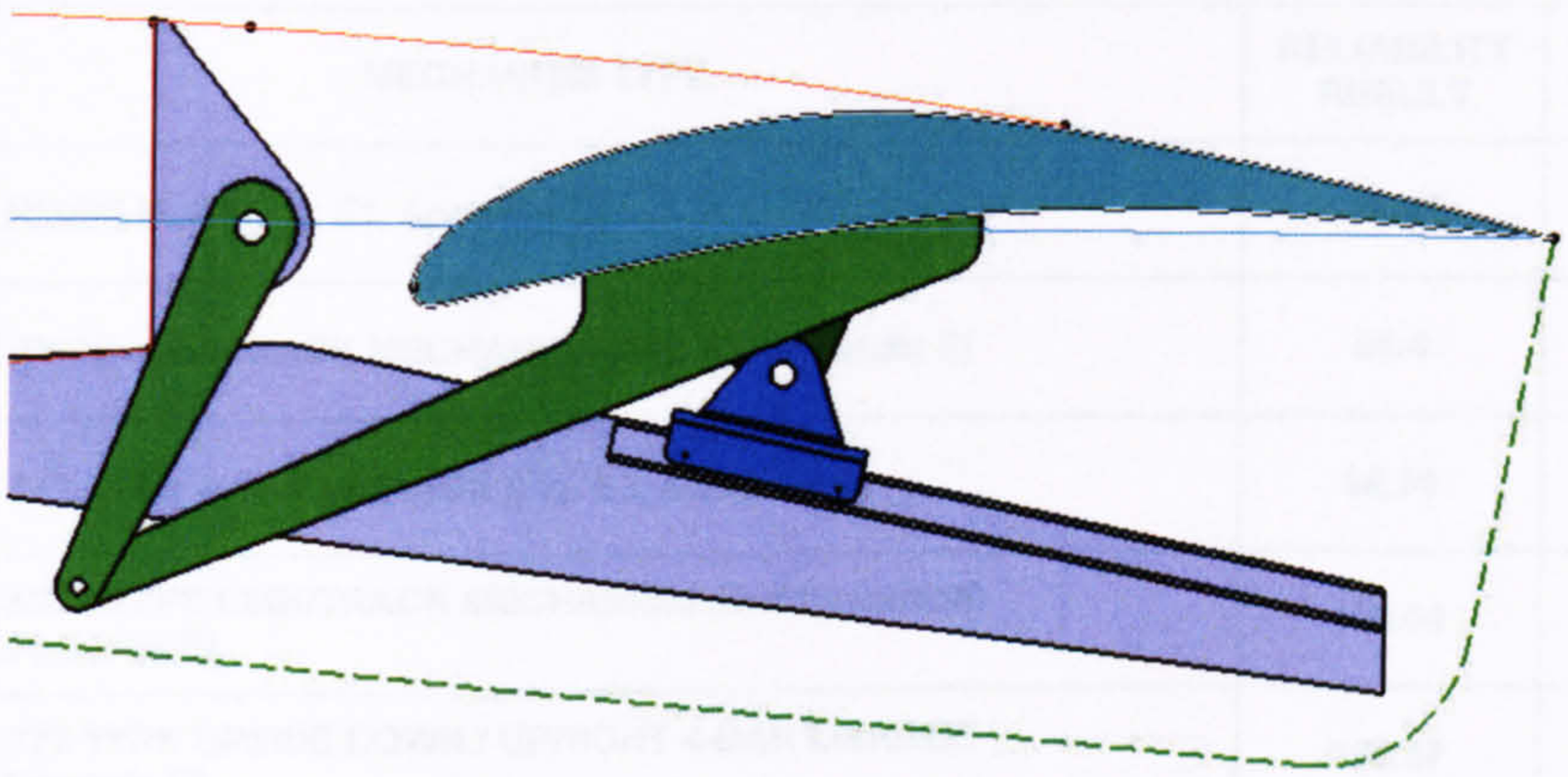

Figure 4.11 – ATRA Link/Track Mechanism

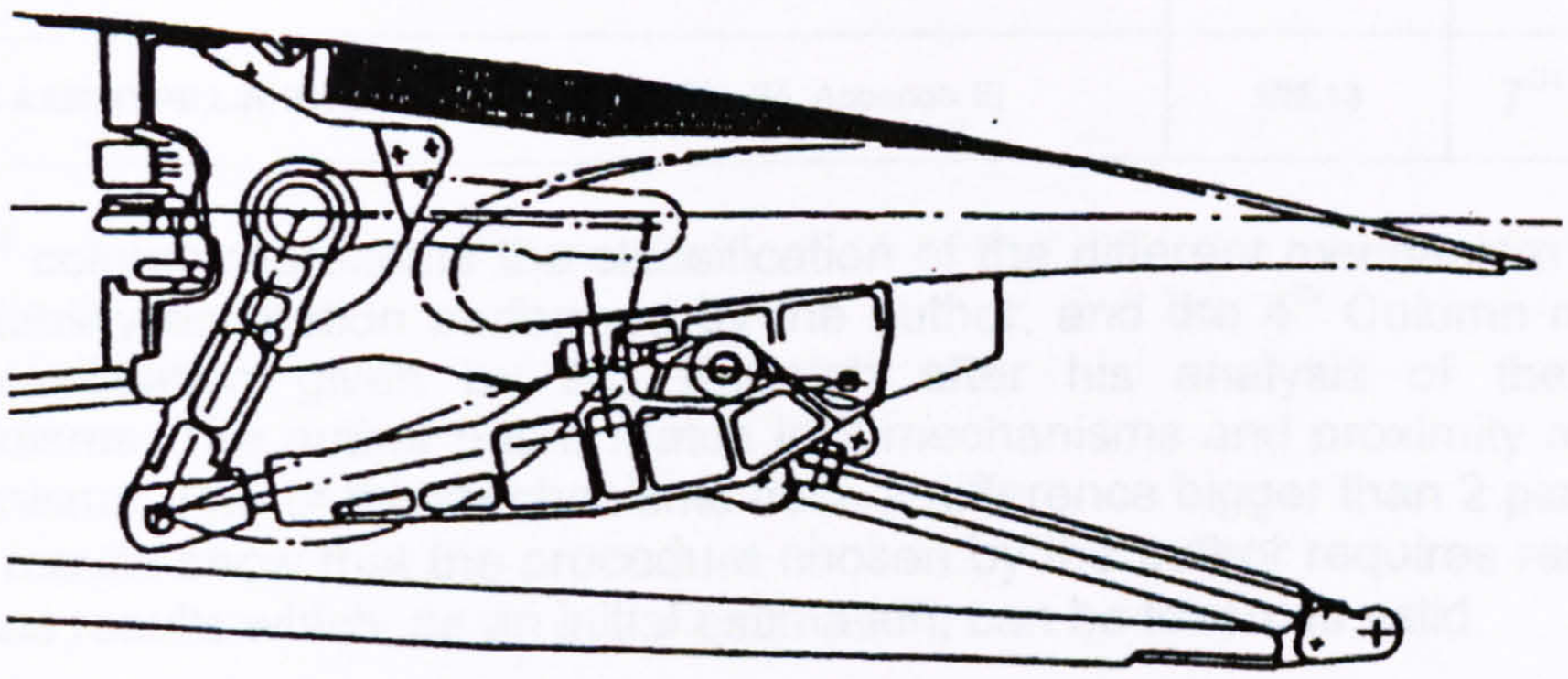

Figure 4.12 – AIRBUS A320 Link/Track Mechanism

Looking at the two mechanisms, we can see that there are some size similarities. By direct measurement it can be assumed that the length, depth and angle of the support track have the same order of measure. The biggest differences come from the Links and Hinge. Both AIRBUS links are 25% smaller than the ATRA ones and the hinge is much bigger. This is certainly due to the 2D nature of the ATRA mechanism design. There is also the fact that the flap trajectories are different.

4.4. RELIABILITY & MAINTAINABILITY MODULES

4.4.1 Reliability

The validation of the Reliability module consisted in comparing the results of the application of the reliability module to the mechanisms studied in Mr. Rudolph's work [86] with the results obtained by Mr. Rudolph himself. The author based the reliability estimation on the Mechanism drawings presented in Appendix E, Figure E1 to E7, taken from Ref. [86].

Table 4.7 presents the final results and comparison to Mr. Rudolph's classification of the different mechanisms. The complete reliability estimation tables are in Appendix F.

Table 4.7 – Reliability Results

MECHANISM TYPE	RELIABILITY RESULT	Author	Rudolph [86]
SIMPLE HINGE FLAP [Fig. E1, Appendix E]	38.99	1st	1st
BOEING TYPE LINK/TRACK MECHANISM [Fig. E7, Appendix E]	98.4	2nd	5th
BOEING 747 TYPE 4-BAR LINKAGE [Fig. E3, Appendix E]	99.35	3rd	2nd
AIRBUS A320 TYPE LINK/TRACK MECHANISM (End Supported) [Fig. E6, Appendix E]	100.04	4th	4th
BOEING 777 TYPE UPSIDE DOWN / UPRIGHT 4-BAR LINKAGE [Fig. E2, Appendix E]	100.37	5th	3rd
AIRBUS A330/340 TYPE LINK/TRACK MECHANISM [Fig. E4, Appendix E]	104.17	6th	7th
AIRBUS A320 TYPE LINK/TRACK MECHANISM [Fig. E5, Appendix E]	106.13	7th	6th

The 3rd column represents the classification of the different mechanism based on the reliability estimation performed by the author, and the 4th Column represents the classification given by Mr. Rudolph after his analysis of the different mechanisms. The author has a match in 2 mechanisms and proximity match in 3 mechanisms. Two of the mechanisms have a difference bigger than 2 places.
These results show that the procedure chosen by the author requires refining but, produces results which, as an initial estimation, can be taken as valid.

4.4.2 Maintainability

Similarly to the Reliability module, the validation of this module consisted in comparing the results of Mr. Rudolph's Study [86] with the results obtained by the authors Maintainability Module. The author based the maintainability estimation on the Mechanism drawings gathered in appendix E, Figure E1 to E7, taken from Ref. [86]. Table 4.8 presents the final results and comparison to Mr. Rudolph's classification of the different mechanisms devices. The complete maintainability estimation tables are in Appendix F.

Table 4.8 – Maintainability Results

MECHANISM TYPE	MAINTAINABILITY RESULT [MTTR] (hrs)	Author	Rudolph
SIMPLE HINGE FLAP [Fig. E1, Appendix E]	17.7	1st	1st
BOEING TYPE LINK/TRACK MECHANISM [Fig. E7, Appendix E]	18.9	2nd	5th
BOEING 747 TYPE 4-BAR LINKAGE [Fig. E3, Appendix E]	19.2	3rd	2nd
AIRBUS A320 TYPE LINK/TRACK MECHANISM (End Supported) [Fig. E6, Appendix E]	22.4	4th	4th
BOEING 777 TYPE UPSIDE DOWN / UPRIGHT 4-BAR LINKAGE [Fig. E2, Appendix E]	25.1	5th	3rd
AIRBUS A320 TYPE LINK/TRACK MECHANISM [Fig. E5, Appendix E]	31.7	6th	6th
AIRBUS A330/340 TYPE LINK/TRACK MECHANISM [Fig. E4, Appendix E]	35.6	7th	7th

Once again, the 3rd column represents the classification of the different mechanism based on the author's calculations, and the 4th Column the classification given by Mr. Rudolph after his analysis of the different mechanisms. In this case, there were closer matches than in the Reliability module. These results also show that the procedure chosen by the author produces results which, as an initial estimation, can also be taken as valid.

4.5. LIFT AND FAIRING DRAG MODULE

As mentioned previously, the validation of this module was not performed due to the lack of available aerodynamic data. Though, a check was made to verify if the results obtained in the Fairing drag module were in the same order of magnitude as the Drag coefficient associated with the fairings of current commercial transport aircraft, which is around 3.0E-5. As before, this was done applying the estimation procedure to the mechanisms studied in Mr. Rudolph's work.
The data presented below are the fairing dimensions for the several different types of trailing edge device mechanisms retrieved from Figure E10 in Appendix E.

Table 4.9 – Flap Support Fairing Sizes [86]

MECHANISM TYPE	Fairing length / Max. Fowler Motion	Fairing Depth / Max. Fowler Motion	Fairing Width (**)
SIMPLE HINGE FLAP [Fig. E1, Appendix E]	**2.93**	**1.74**	**3**
BOEING 777 4-BAR LINKAGE [Fig. E2, Appendix E]	**3.6**	**0.95**	**4**
AIRBUS A320 TYPE LINK/TRACK MECHANISM [Fig. E5, Appendix E]	**4.2**	**0.76**	**3.5**
AIRBUS A330/340 TYPE LINK/TRACK MECHANISM [Fig. E4, Appendix E]	**4.33**	**0.83**	**3**
BOING 747 TYPE 4-BAR LINKAGE [Fig. E3, Appendix E]	**3.68**	**0.62**	**2.5 (Outboard) 1.5 (Middle)**
AIRBUS A320 TYPE LINK/TRACK MECHANISM (END SUPPORTED) [Fig. E6, Appendix E]	**3.26**	**0.55**	**2.5 (Outboard) 1.5 (Middle)**
BOEING TYPE LINK/TRACK MECHANISM [Fig. E7, Appendix E]	**3.06**	**0.53**	**2.5 (Outboard) 1.5 (Middle)**

Max. Fowler Motion =**17.4% C_w** [86]
(**) Counted in Number of Side by Side Structural Members [86]

The author assumed that the ATRA had a single outboard flap and that the Hinge positions 3 and 4 were at 25% and 75% of the flap length. The calculations were based on the wing chord of the ATRA aircraft at hinge positions 3 (b/2 = 7.265m) and (b/2 = 10.998m) and assumed a structural element width of 0.1 m.

Wing Chord C_W at (b/2 = 7.265m) = 3.260m
Wing Chord C_W at (b/2 = 10.998m) = 2.604m

The results from the author's analysis are presented in Table 4.10.

Table 4.10 – Fairing Drag Results

MECHANISM TYPE	Fairing Length (m)		Fairing Depth (m)		Fairing Width (m)		t/c		C_{Dss}		$\frac{D_{ssi}}{q \cdot S}$
	Hinge 3	Hinge 4	Hinge 3	Hinge 4	Hinge 3	Hinge 4	Hinge 3	Hinge 4	Hinge 3	Hinge 4	Total
SIMPLE HINGE FLAP [Fig. E1, Appendix E]	1.66	0.84	0.99	0.50	0.30	0.30	0.18	0.40	0.007	0.016	**3.50E-05**
BOEING 777 4-BAR LINKAGE [Fig E2, Appendix E]	2.04	1.03	0.54	0.27	0.40	0.40	0.20	0.43	0.007	0.020	**2.85E-05**
AIRBUS A320 TYPE LINK/TRACK MECHANISM [Fig. E5, Appendix E]	2.38	1.20	0.43	0.22	0.35	0.35	0.15	0.32	0.007	0.011	**1.45E-05**
AIRBUS A330/340 TYPE LINK/TRACK MECHANISM [Fig E4, Appendix E]	2.46	1.24	0.47	0.24	0.30	0.30	0.12	0.27	0.006	0.009	**1.20E-05**
BOING 747 TYPE 4-BAR LINKAGE [Fig E3, Appendix E]	2.09	1.05	0.35	0.18	0.15	0.25	0.07	0.26	0.006	0.009	**5.38E-06**
AIRBUS A320 TYPE LINK/TRACK MECHANISM (END SUPPORTED) [Fig E6, Appendix E]	1.85	0.93	0.31	0.16	0.15	0.25	0.08	0.30	0.006	0.010	**5.17E-06**
BOEING TYPE LINK/TRACK MECHANISM [Fig E7, Appendix E]	1.74	0.88	0.30	0.15	0.15	0.25	0.09	0.32	0.006	0.011	**5.24E-06**

t/c – Thickness to Chord Ratio of Fairing (Fairing Width / Fairing Length)

C_{Dss} – Drag Coefficient of streamline strut

$\frac{D_{ssi}}{q \cdot S}$ –Increment in drag arising from the streamline structure

The results presented in Table 4.10 show that the estimated drag is indeed in the same order of magnitude of 3.0E-5.
Drag coefficient associated with the fairings of current commercial transport aircraft, which is around 3.0E-5.

The typical drag of Wide body transport aircraft is in the region of 0.02 [126].

CHAPTER 5

CASE STUDY AND RESULTS

5.1. INTRODUCTION

This chapter describes the application of the new design methodology presented in chapter four and is based on work previously done by Edi [20] and Ammoo [1] on the ATRA - Advanced Transport Regional Aircraft.
The main objective of this case study is to apply the design methodology presented in Chapter 3 and determine what is the most appropriate mechanism for the ATRA flap system.
The ATRA or "Advanced Transport Regional Aircraft" was a Cranfield University project design, initially studied by Edi [20] and later by Ammoo [1], with the main objective of studying the application of variable camber wing concepts and hybrid laminar flow control technologies. There were three derivatives of different passenger capacity for the ATRA but they all shared the same wing platform. These are the ATRA-80, ATRA-100 and ATRA-130 (Figure 5.1). For this case study the author used the same wing geometry and flap configurations as in the work performed by Ammoo [1].

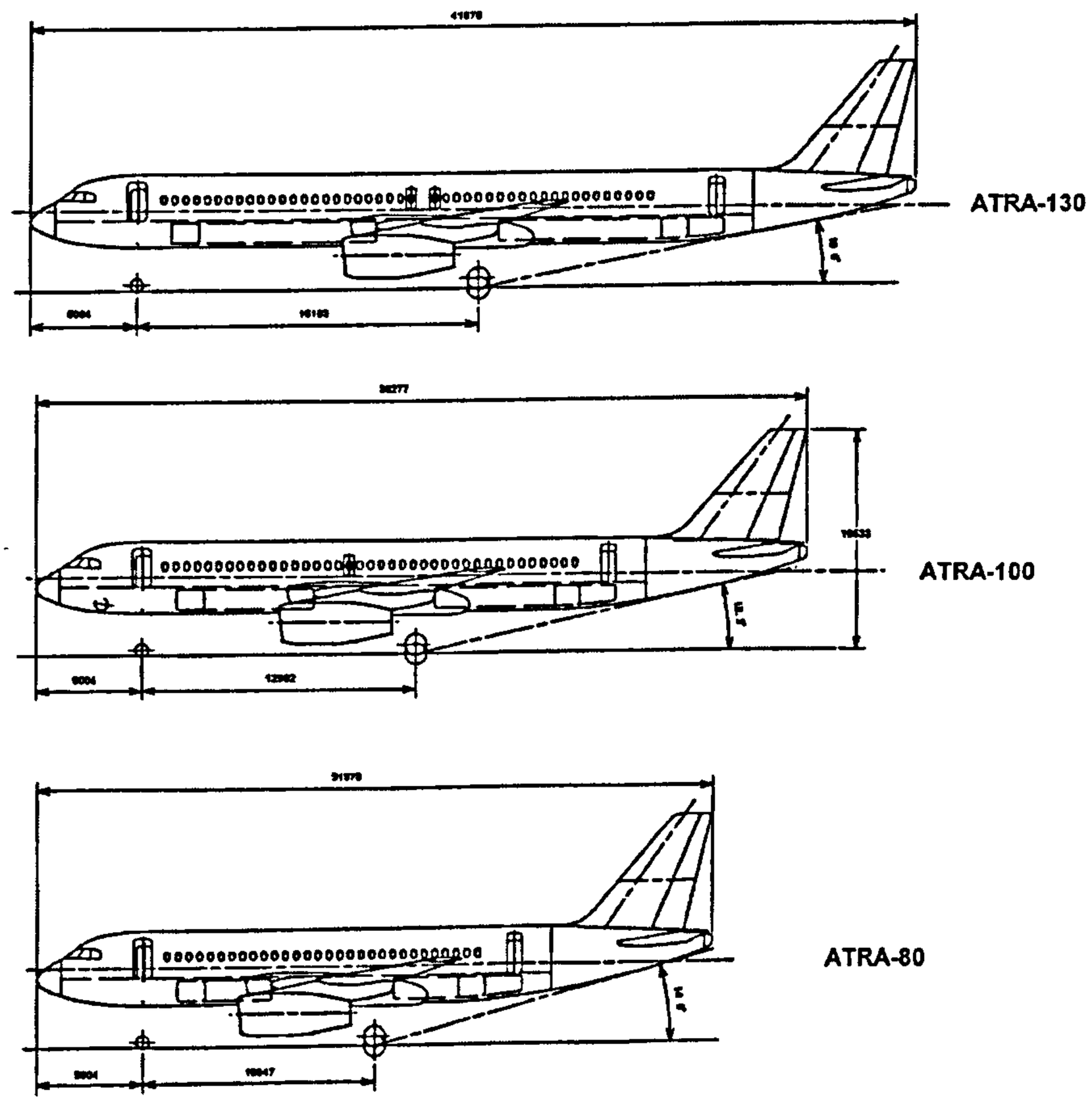

Figure 5.1 – ATRA Family [20]

5.2. MAIN ATRA PARAMETERS

The ATRA main parameters required for this case study were retrieved from Edi's [20] and Ammoo's [1] work and are collected in Appendix A. The most relevant parameters are presented below.

a) Wing Planform Parameters

- ¼ Chord Sweep 25°
- Taper Ratio 0.274
- Aspect Ratio 9.5
- Wing Area 110.21 m^2
- Inboard Section Span 4273 mm
- Outboard Section Span 10192 mm
- Wing Front Spar @ 15% of C_W
- Wing Rear Spar @ 60% of C_W
- Spoiler end @ 85% of C_W
- Flap Front Spar 15 % of C_F
- Flap Rear Spar 55% of C_F

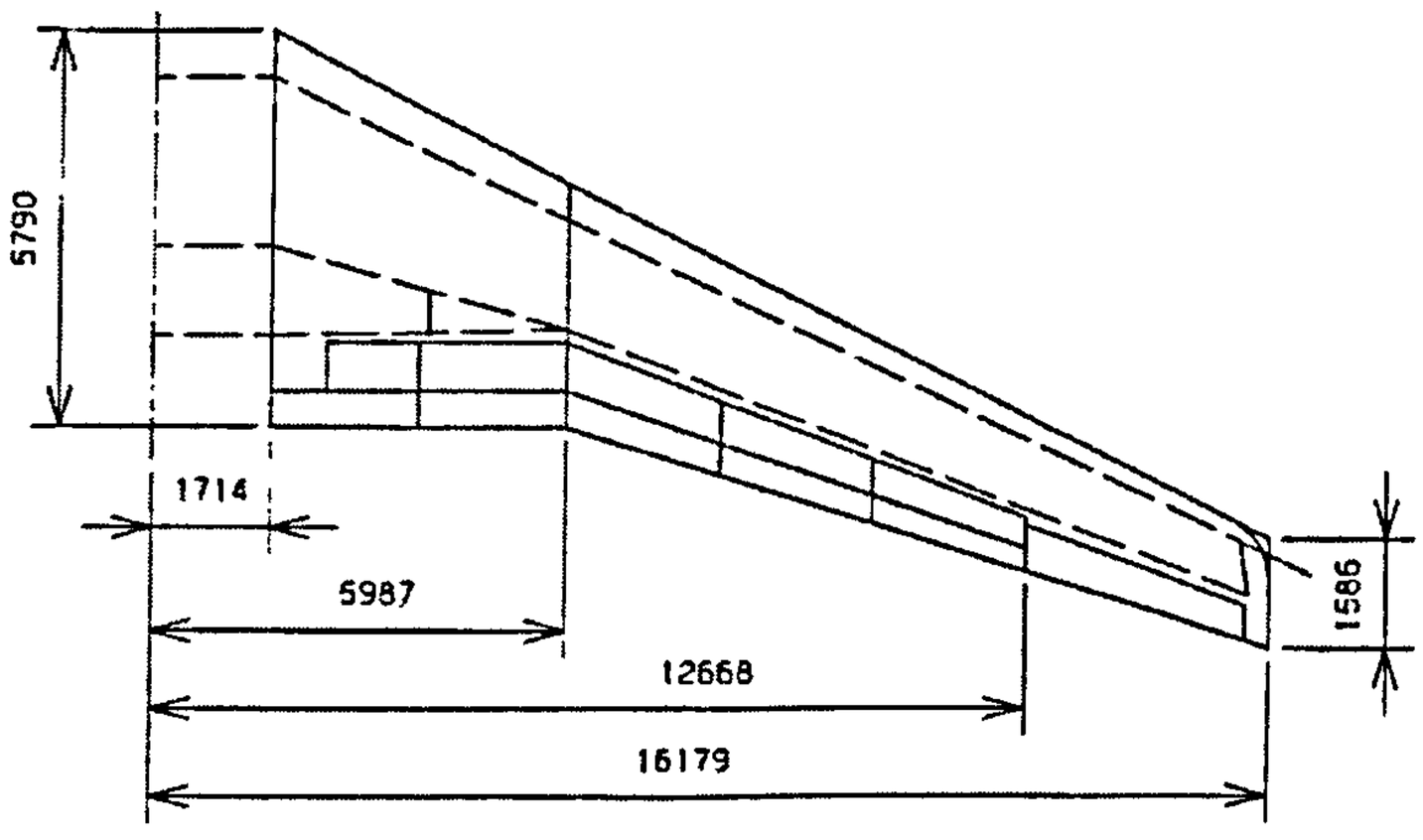

Figure 5.2 – ATRA wing planform [20]

b) Flap Segmentation [1]

As a starting point for this case study, the author maintained the same flap segmentation proposed by Ammoo [1], which was that the ATRA would have 2 inboard flaps and 3 outboard flaps, as shown in Figure 5.2.

c) Flap Type and Variable Camber Definition

The ATRA uses a single slotted flap. This type of flap was selected by Edi [20] with the aim of mechanical simplicity. The selection of this type of flap is also supported by the fact that it is currently considered to be one of the *"biggest weight and cost savers in the area of High-lift devices"* [90].
The maximum flap deflection for variable camber during cruising flight, as defined in Edi's [20] report, is ± 5°. The baseline and deployment data for this case study Variable Camber flap is presented in Figure 5.3 and Table 5.1.

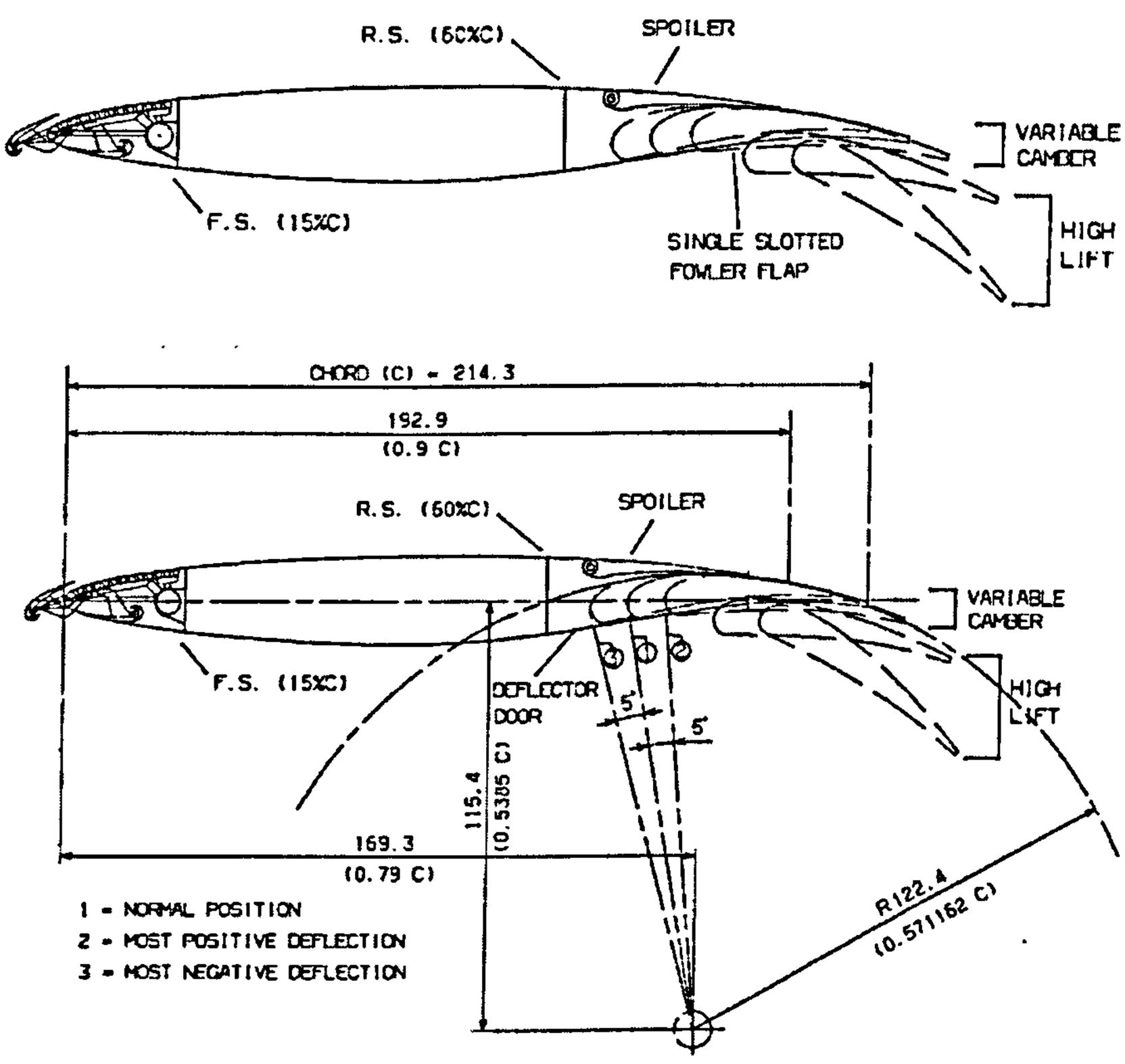

Figure 5.3 – HLFC-VC Section Baseline Configuration [20]

Table 5.1 – VC Flap deployment requirements [1]

	GAP	FOWLER MOTION
-5°	0	2.5 % C_W
0°	0	0
+5°	0	2.5 % C_W

d) Low Speed Requirements

The requirements for take-off and landing were defined on Ammoo's [1] report and are presented in Table 5.2.

Table 5.2 – Low speed flap deployment requirements [1]

		GAP	FOWLER MOTION
Take-Off	+15°	2.5 % C_W	13.5 % C_W
Landing	+35°	1.3 % C_W	17.5 % C_W

5.3. WING CAD DESIGN

A 3D CATIA model of the wing and the flap surfaces was created to allow the author to retrieve the necessary information for the different modules of the design methodology. The CAD models of the Wing and Flap were created using data retrieved from the Ammoo work. All the relevant data for the generation of these CAD models is also presented in Appendix A.

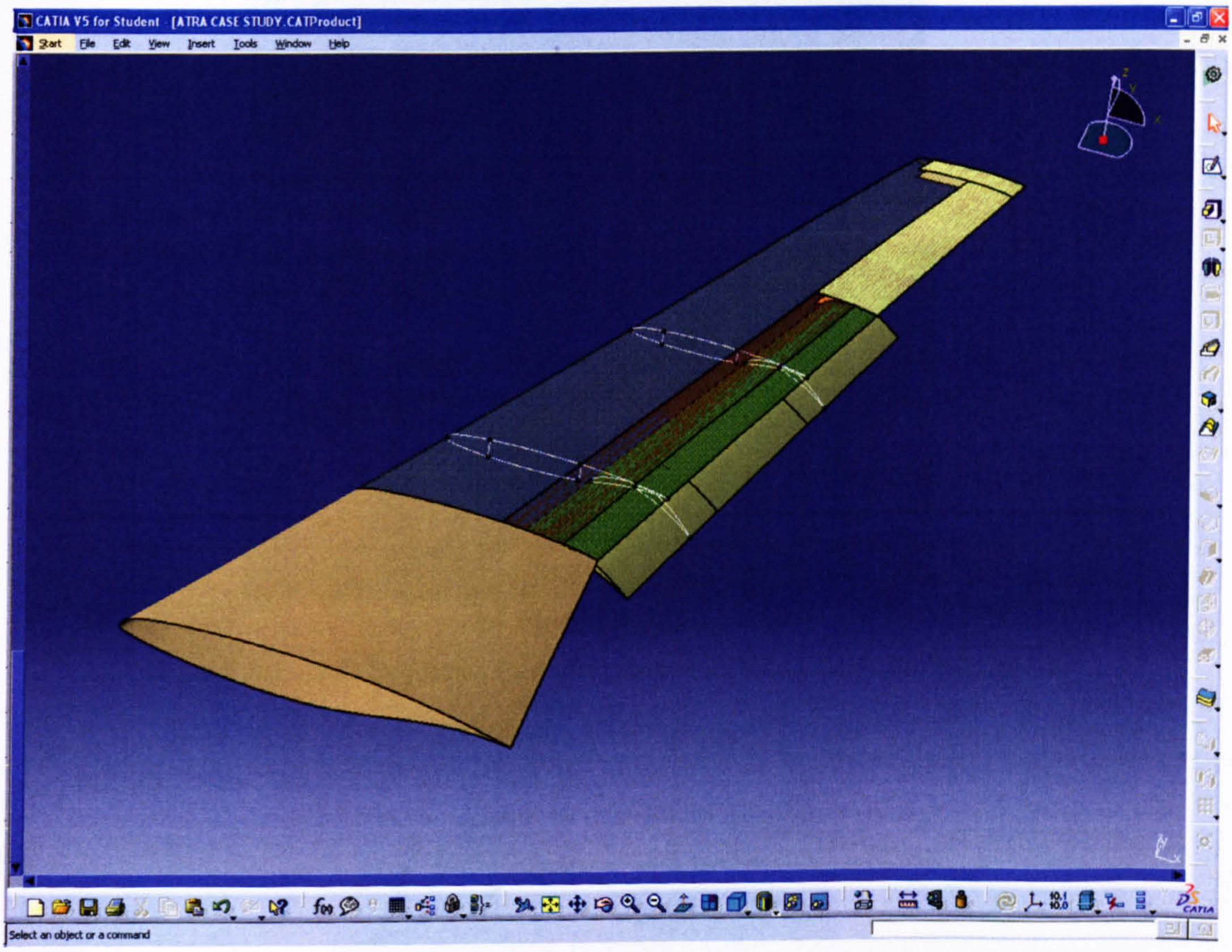

Figure 5.4 – Wing and Flaps CATIA Model

5.4. SYNTHESIS

The mechanism types that are used in the case study are the Simple Hinge Mechanism, the 4 Bar Mechanism and the Link/Track mechanism.
The mechanism synthesis for the case study was performed in 2 different ways. The synthesis of the 4 -Bar mechanism was performed by the SYNAMEC software and the result is presented in Figure 5.5. The results were similar to the ones presented in Chapter 4, section 2.
Due to the limitation of the SYNAMEC Software to perform synthesis of mechanisms other than the 4 Bar Mechanism, the synthesis of the Simple Hinge and Link Track mechanisms was done manually. The mechanism main points were estimated and scaled to the dimensions of the ATRA flap size, from the same type of existing mechanisms, to obtain the configuration shown in Figure 5.6 and Figure 5.7.

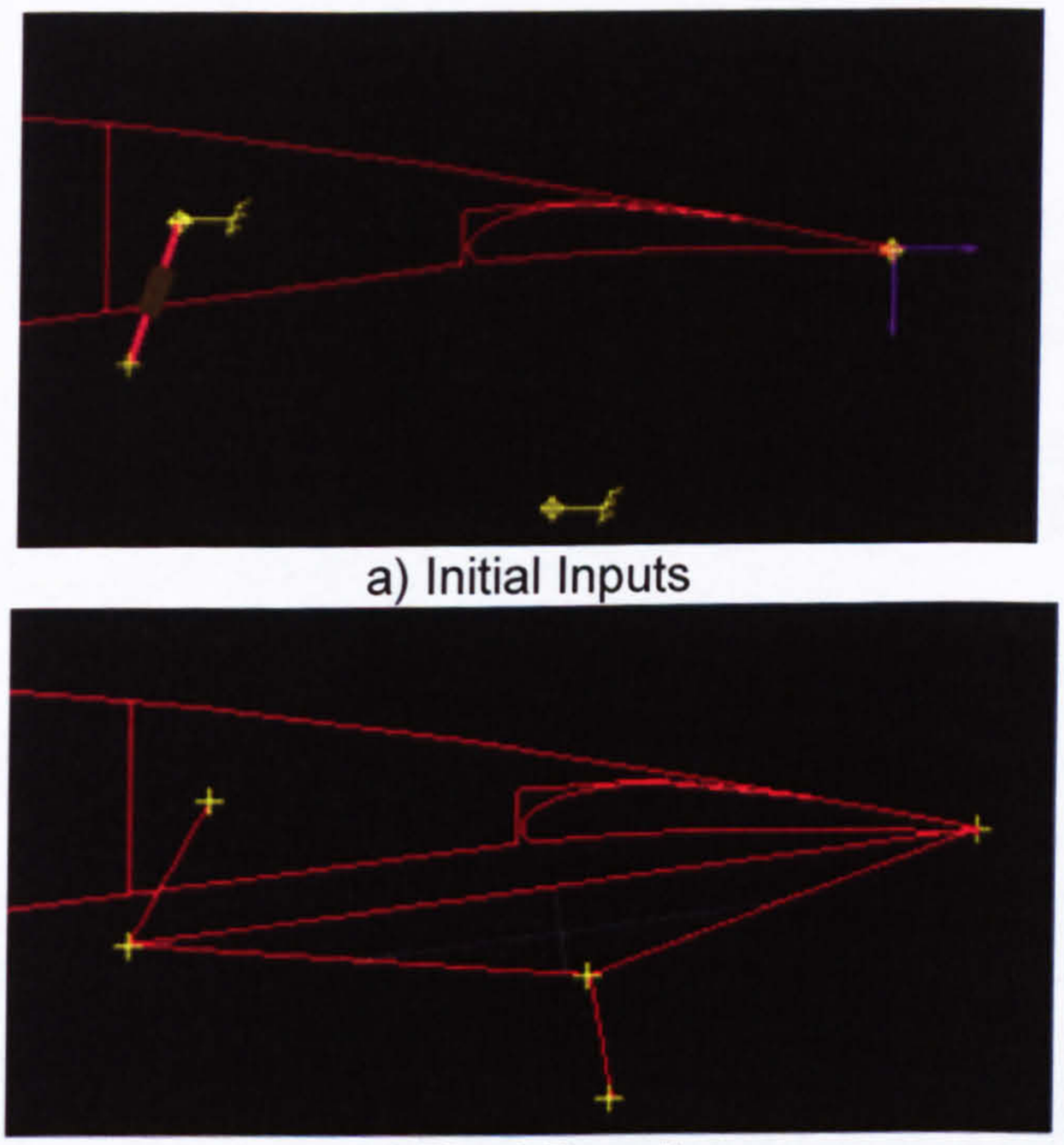

a) Initial Inputs

b) Final Result

Figure 5.5 – 2-D Synthesis Requirements and Result for 4-Bar Mechanism

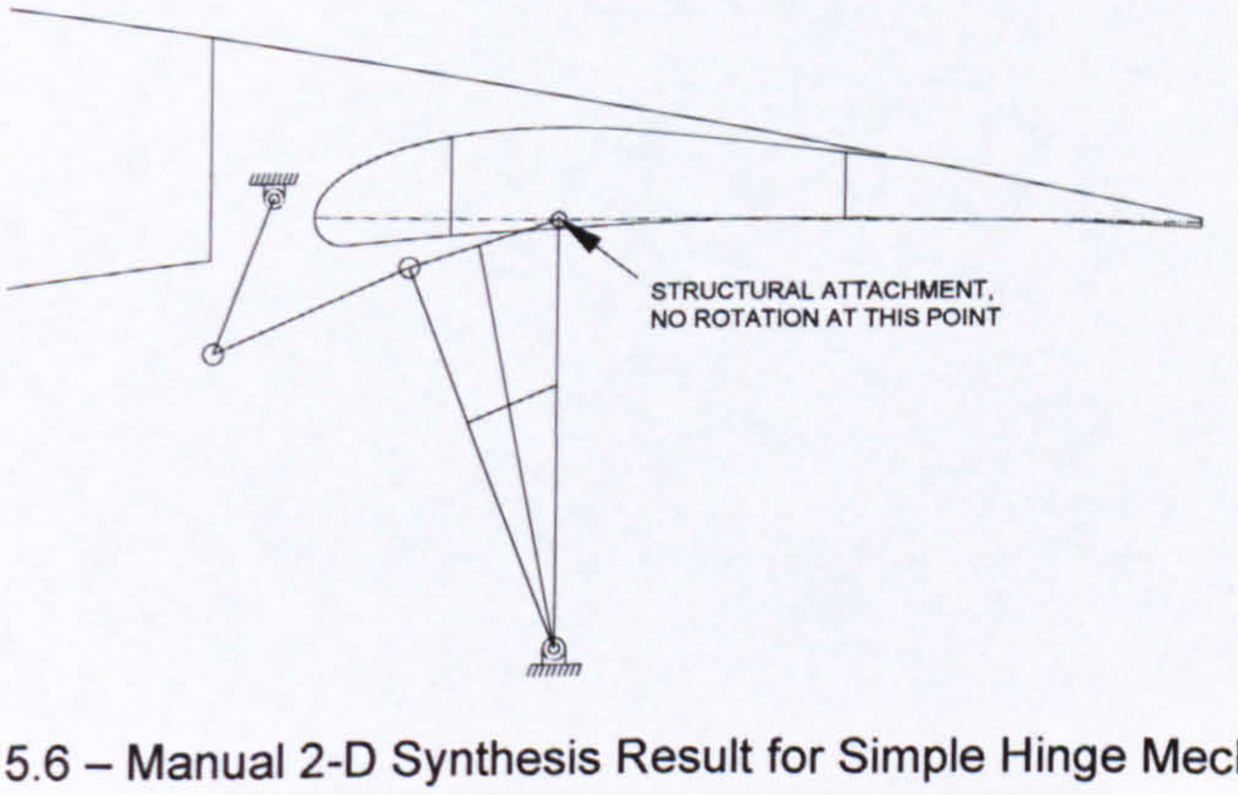

Figure 5.6 – Manual 2-D Synthesis Result for Simple Hinge Mechanism

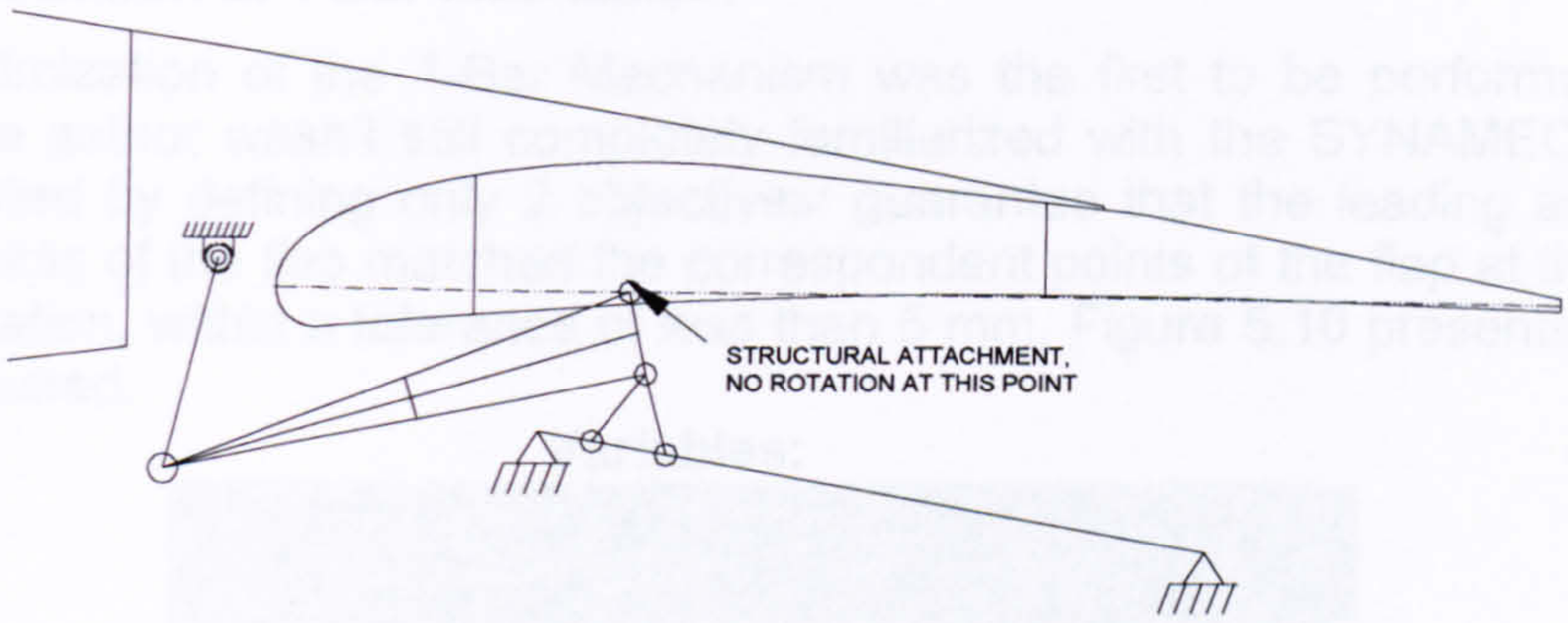

Figure 5.7 – Manual 2-D Synthesis Result for Link/Track Mechanism

5.5. OPTIMIZATION

The optimization process is the most time consuming, when compared with the remaining modules of the Design Methodology. Due to this lengthy process the optimization was only performed for the 4-Bar and the Link/ Track Mechanisms using SYNAMEC.

Due to the simplicity of the Simple Hinge Mechanism, the optimization was done manually. Figure 5.8 depicts the flap configurations for all flight stages along with the objective curves for flap deployment.

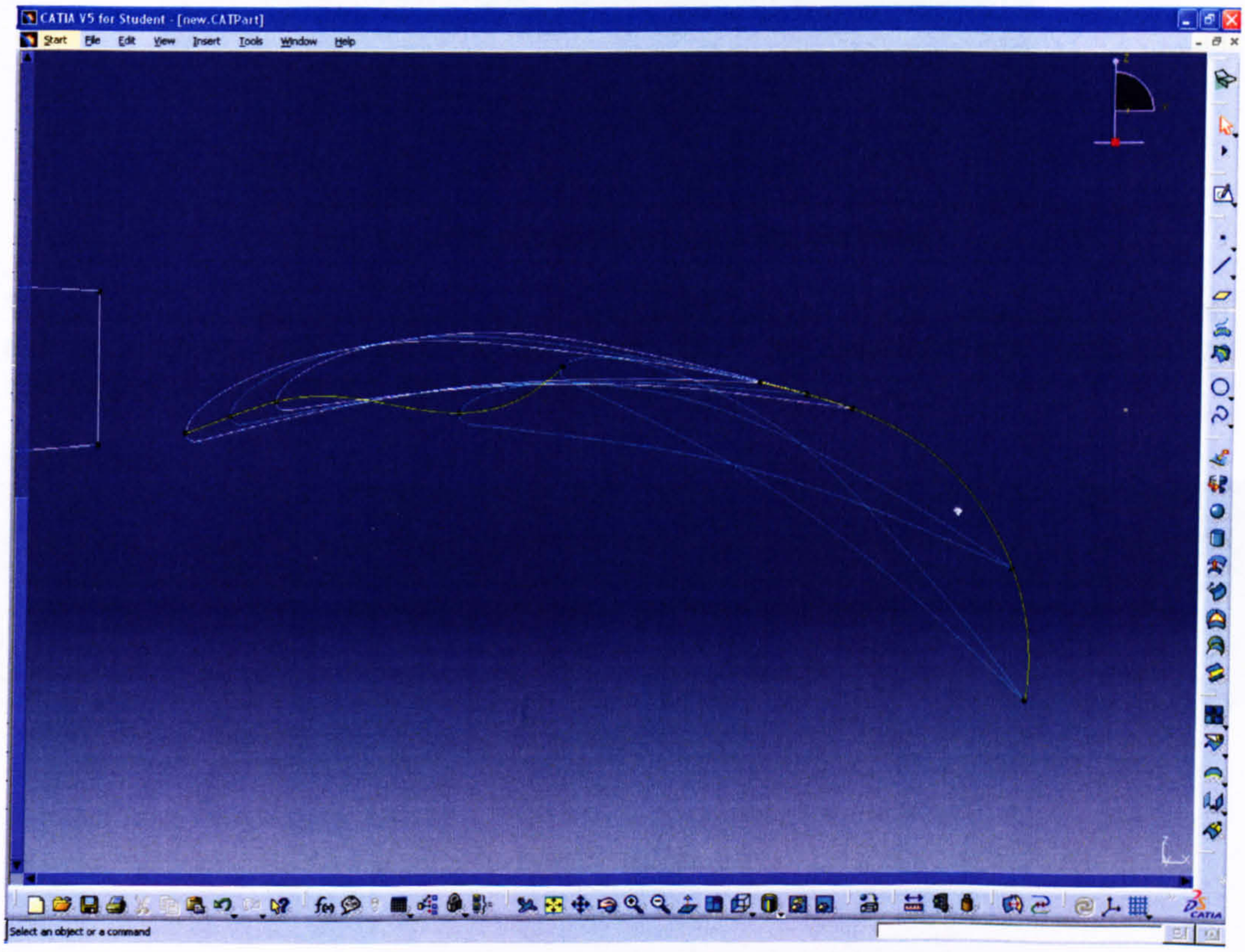

Figure 5.8 – 2-D Flap profile configurations

a) Optimization of 4-Bar Mechanism

The optimization of the 4-Bar Mechanism was the first to be performed. At the time, the author wasn't still completely familiarized with the SYNAMEC software and started by defining only 2 objectives: guarantee that the leading and trailing edge points of the flap matched the correspondent points of the flap at the landing configuration, within a tolerance of less than 5 mm. Figure 5.10 presents the input data required.

Variables:

Name	Lower bound	Initial value	Upper bound
X1	17100	17150	17300
Z1	2900	3000	3100
X2	16800	16950	17100
Z2	2580	2680	2780
X3	17350	17500	17650
Z3	2600	2700	2800
X4	17350	17500	17650
Z4	2300	2400	2500

Functions:

Name	Objective	Initial value	Target value
DISTANCE_TE_PT	Minimize	647.034	1
DISTANCE_LE_PT	Minimize	271.203	1

Figure 5.9 – Optimization Inputs for 4 Bar Mechanism

The SYNAMEC software iteratively changes the values of the variables within the set boundaries until objectives are met. After 39 iterations the optimization converged and presented the following results.

Functions:

Name	Objective	Initial value	Iteration 39	Target value	Variation
DISTANCE_TE_PT	Minimize	647.034	3.51211	1	-99%
DISTANCE_LE_PT	Minimize	271.203	4.19311	1	-98%

Convergence of Objective Curves:

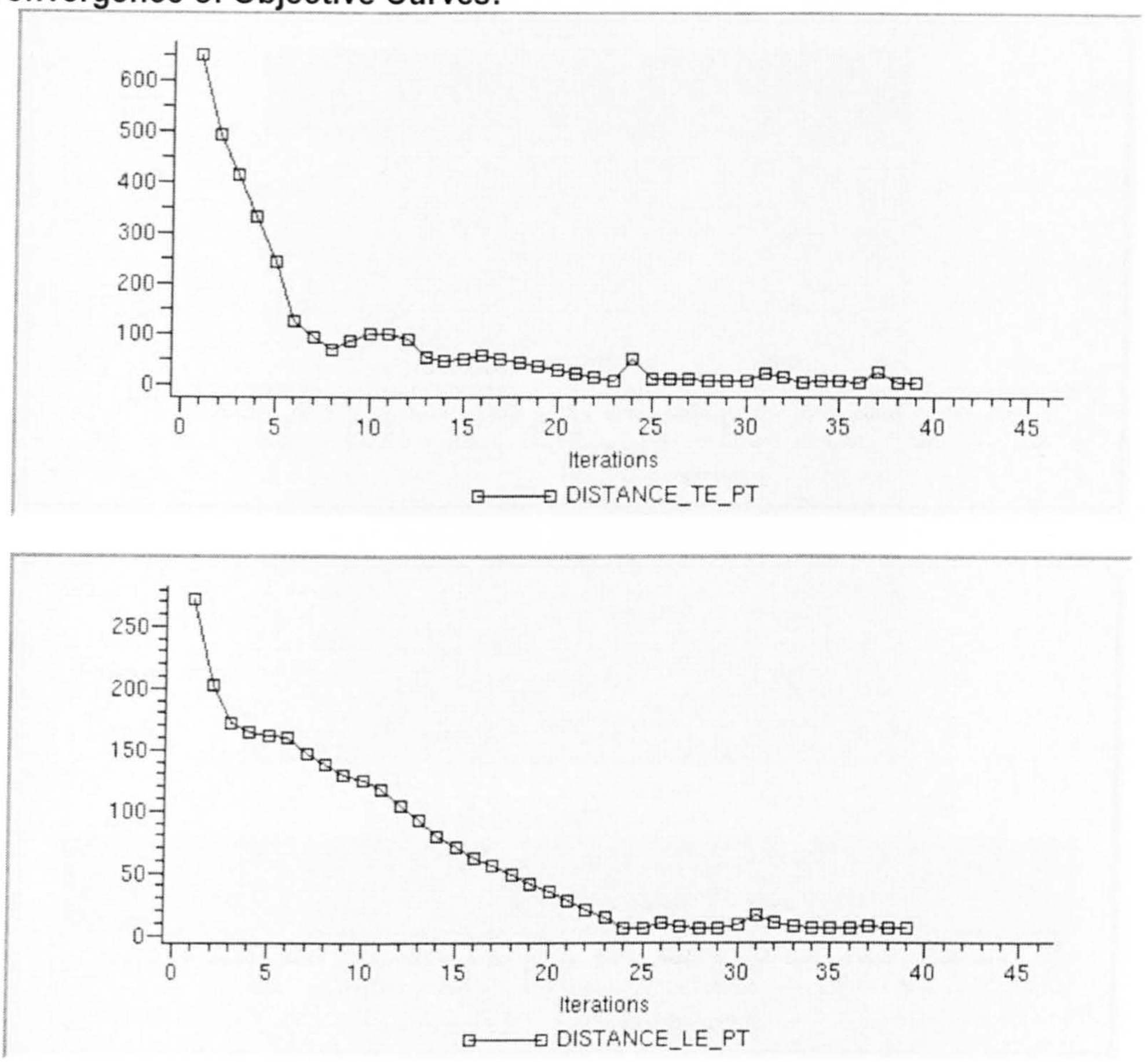

Figure 5.10 – Optimization Results for 4-Bar Mechanism

The complete set of results is presented in Appendix G.

b) Optimization of Link/Track Mechanism

The optimization of the Link Track was performed similarly as the 4-Bar mechanism, but with further more constraints. Along with the Trailing and Leading Edge points distance objective, the author included two constraints (DISTANCE_LE and DISTANCE_TE) to guarantee a proximity to the ideal trajectory curve and a distance constraint to the end of the Support Beam to guarantee that the slider component wouldn't come out of the track. Figure 5.11 presents the input data required.

Variables:

Name	Lower bound	Initial value	Upper bound
X1	16900	17096	17300
Z1	2850	2950	3050
X2	16800	16889	17100
Z2	2580	2680	2780
X7	17300	17504	17700
X8	18050	18252	18450
Z8	2380	2484	2680
a	0.8	0.85	0.9
b	0.15	0.19	0.25
c	0.55	0.6	0.65
Z7	2600	2705	2800

Functions:

Name	Objective	Initial value	Target value	Variation
FINAL_TE_POSITION	Minimize	113.566	0	-99%
FINAL_LE_POSITION	Minimize	72.8256	0	-98%

Constraints:

Name	Lower bound	Initial value	Upper bound
FINAL_TRACK_POSITION	50	78.8161	*****
DISTANCE_LE	*****	0 ... 62.2918	100
DISTANCE_TE	*****	0 ... 89.0834	100

Figure 5.11 – Optimization Inputs for Link/Track Mechanism

After 39 iterations the optimization converged and returned the following results.

Functions:

Name	Objective	Initial value	Iteration 35	Target value	Variation
FINAL_TE_POSITION	Minimize	113.566	0.705226	0	-99%
FINAL_LE_POSITION	Minimize	72.8256	0.978238	0	-98%

Constraints:

Name	Lower bound	Initial value	Iteration 35	Upper bound
FINAL_TRACK_POSITION	50	78.8161	252.085	*****
DISTANCE_LE	*****	0 ... 62.2918	6.3583e-08 ... 38.8136	100
DISTANCE_TE	*****	0 ... 89.0834	2.19636e-07 ... 88.8839	100

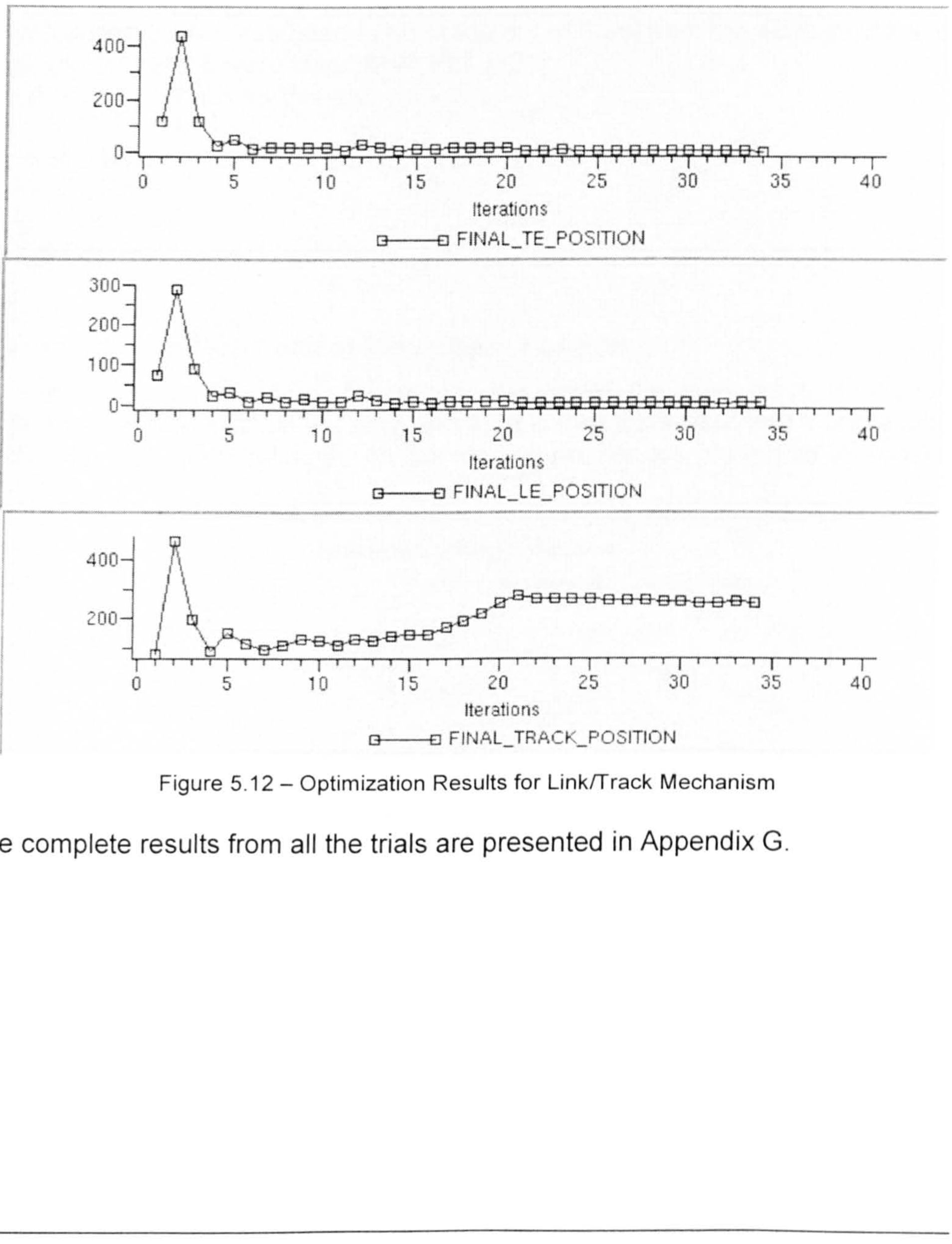

Figure 5.12 – Optimization Results for Link/Track Mechanism

The complete results from all the trials are presented in Appendix G.

5.6. INITIAL SIZING

The next step on the design methodology is the Initial Sizing of the mechanisms components. This step is performed in 3 stages:

a) Calculation of Flap loads at Mechanism Positions
b) Calculation of Component Loads (using Visual Basic Application)
c) Initial Sizing of Components

The Calculation of the Flap Loads is performed assuming the flap as a beam simply supported with a uniform load, as shown in Figure 5.14. The uniform load is calculated from the Flap Loading profiles from Appendix A. The Flap loading profile for the Landing case is presented in Figure 5.13.
All components were assumed to be made out of Steel from the 4000 series and materials properties were taken from Ref. [121].
The most relevant properties are:

f_{tu} = 1240 MPa
f_{su} = 770 MPa
E = $200x10^9$ N/m^2
ρ = 7860 Kg/m^3

a) Calculation of Flap Load at Mechanism Position

For each flap configuration, the author integrated the load curve equation to determine the total load on the flap. This load is then converted into a uniform load by dividing it by the flap length. All flap loading profiles are presented in Appendix A.

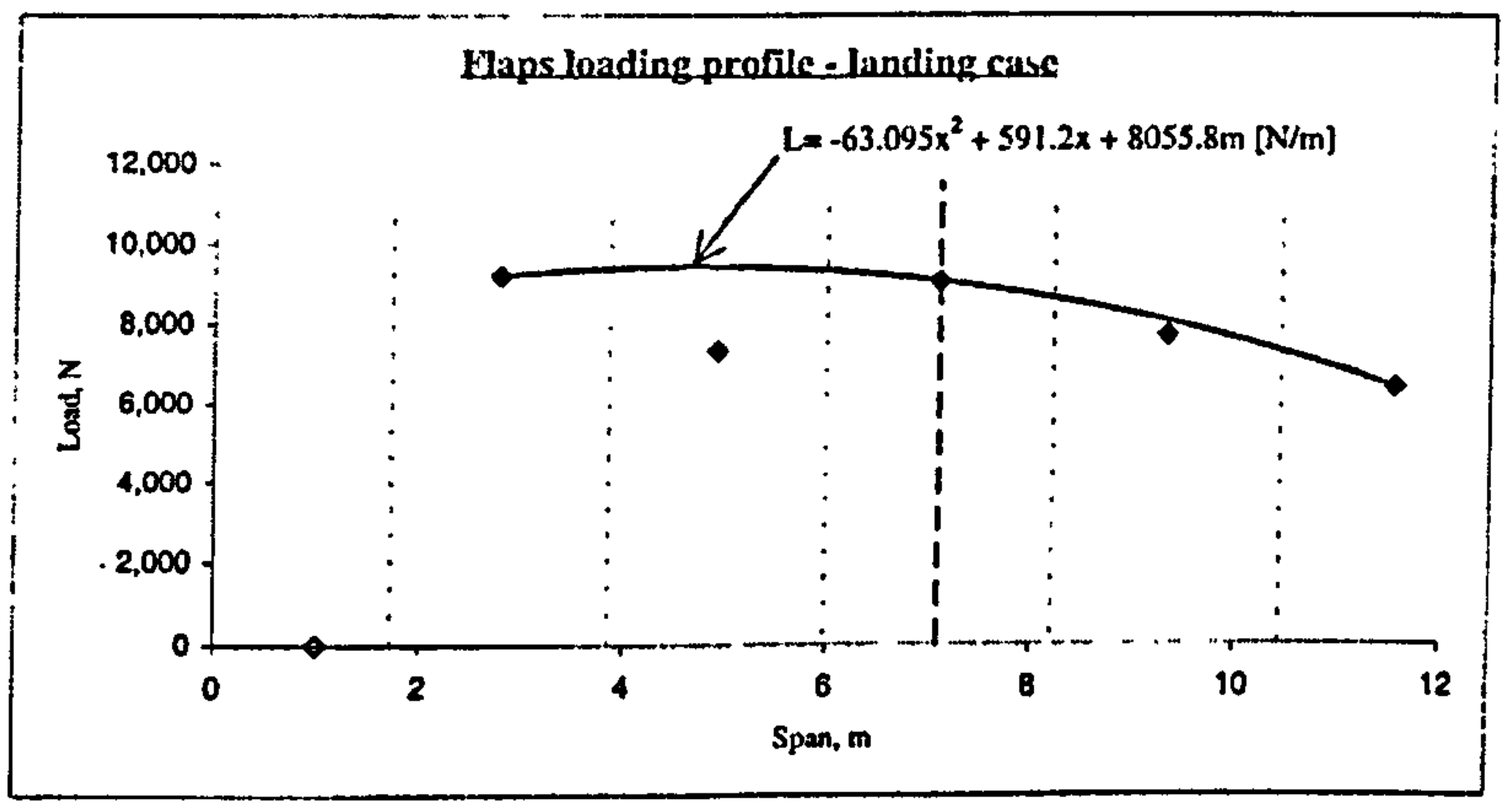

Figure 5.13 – Load per Unit Width (Ultimate) – Landing Case [1]

The calculation of the total loads on the flaps for each flap configuration is presented below.

Cruise Case: $L = -36.063 \cdot x^2 + 435.22 \cdot x + 2527.2$ [N/m]

$$\int_{5.987}^{12.668} L dx = 22150 \text{ [N]}$$

Take-Off Case: $L = -106.97 \cdot x^2 + 1265.1 \cdot x + 6581.3$ [N/m]

$$\int_{5.987}^{12.668} L dx = 57970 \text{ [N]}$$

Landing Case: $L = -63.095 \cdot x^2 + 591.2 \cdot x + 8055.8$ [N/m]

$$\int_{5.987}^{12.668} L dx = 52420 \text{ [N]}$$

The author considered 2 equidistant hinge positions for the three outer flaps at b/2=8214 mm b/2 = 10991 mm. The loads at each hinge were calculated using the following procedure depicted in Figure 5.14.

LOADING	REACTION AND SHEAR
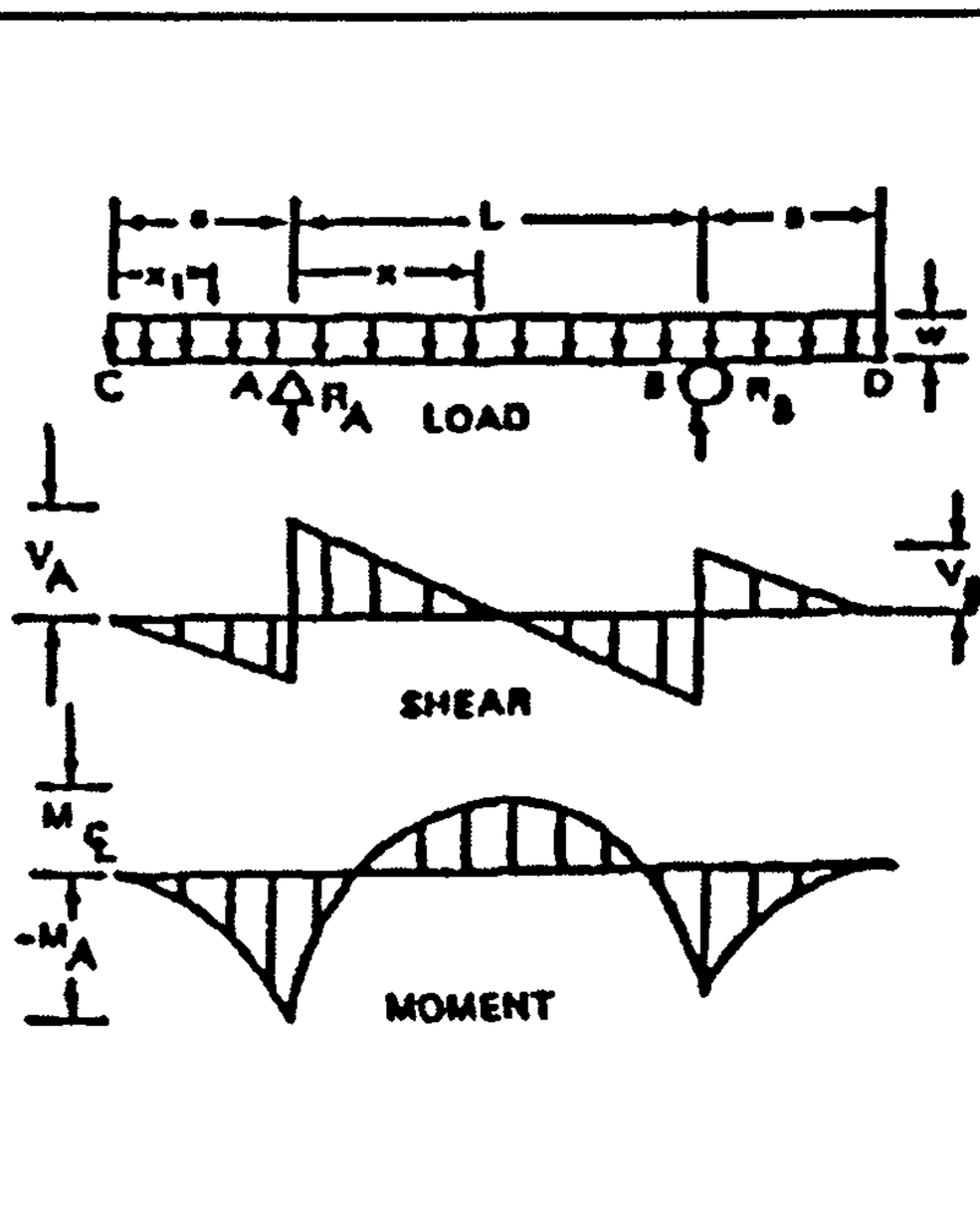	$V_{max} = R_A$ @ $x = 0$ $R_A = R_B - w\left(a + \frac{L}{2}\right)$ $V_{x_1} = -wx_1$ @ $x_1 < a$ $V_x = -w\left(x - \frac{L}{2}\right)$ @ $x < \frac{L}{2}$

Figure 5.14 – Beam Simply Supported with Uniform Load [56]

a = 2.227 m
L = 2.227 m

Cruise

w = 22150 / (12.668-5.987) = 3315 N/m

$$R_A = R_B = w \cdot \left(a + \frac{L}{2}\right) \Rightarrow R_A = R_B = 11075 \text{ N}$$

Take-Off

w = 8677 N/m

$R_A = R_B = 28985$ N

Landing

w = 7846 N/m

$R_A = R_B = 26210$ N

Table 5.3 – Flap Load at Mechanism Position

	P [N]
Cruise	11075
Take-Off	28985
Landing	26210

b) Simple Hinge Mechanism Component Loads

b.1) Simple Hinge Mechanism

To determine the loads in each of the components of the Simple Hinge mechanism the author used the Visual basic application. Figure 5.15 shows the inputs required and what results are obtained from the Visual basic application. The process is equal for all mechanisms.

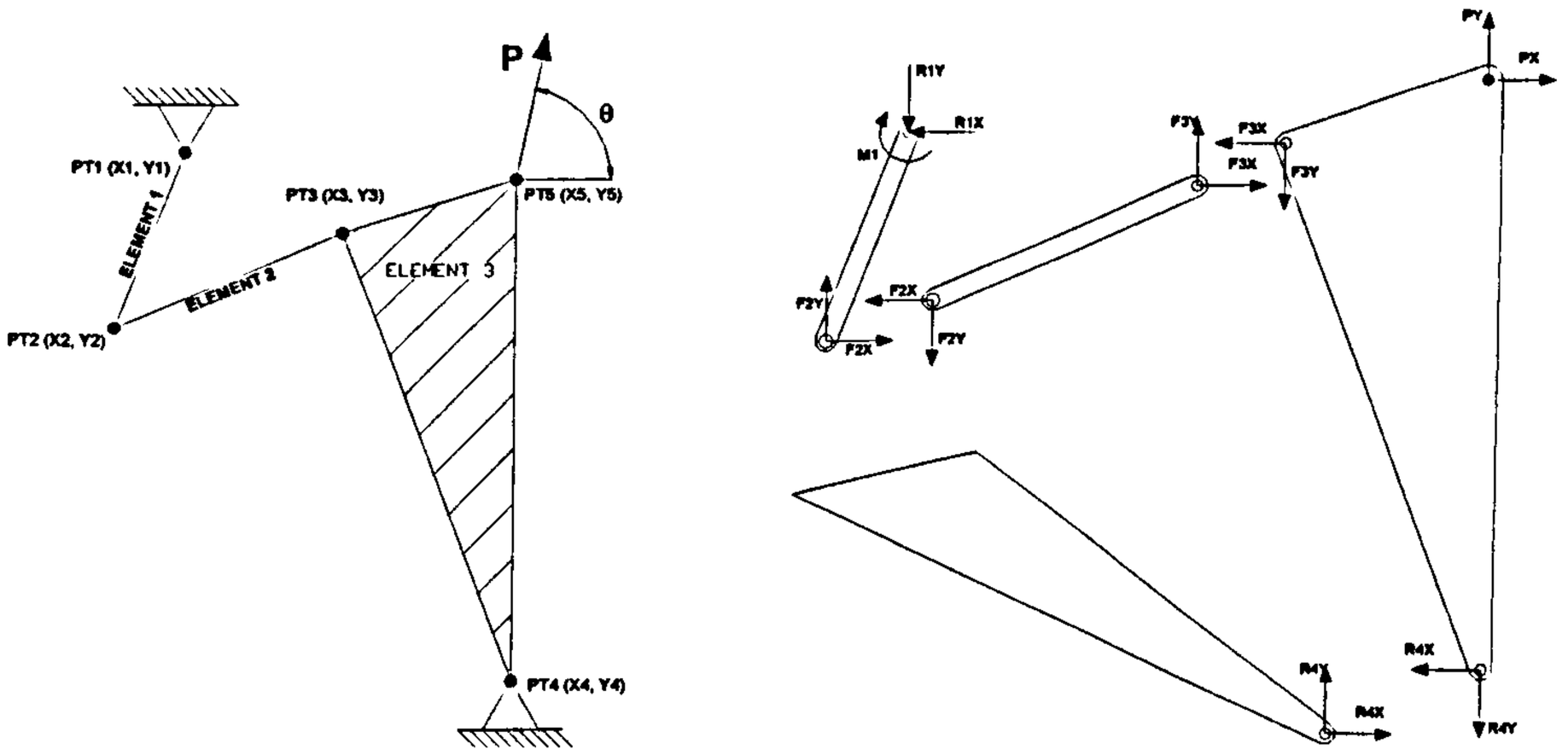

Figure 5.15 – Simple Hinge Mechanism VB input data and Results

Table 5.4 – Simple Hinge Mechanism points

POINTS	CRUISE		TAKE-OFF		LANDING	
	X	Y	X	Y	X	Y
1	17093.21	2956.34	17093.21	2956.34	17093.21	2956.34
2	16910.83	2650.00	17205.80	2618.07	17449.36	2940.05
3	17358.79	2884.90	17598.56	2936.78	17953.34	2897.08
4	17674.18	2007.38	17674.18	2007.38	17674.18	2007.38
5	17627.55	2935.92	17869.536	2916.26	18204.99	2782.29

The results from the Visual Basic program for the Simple Hinge Mechanism Case are presented in Table 5.5.

Table 5.5 – Simple Hinge Mechanism Component Loads

	Cruise	Take-Off	Landing
R1 [N]	560	**1753**	278
R1X [N]	495	1361	277
R1Y [N]	260	1105	-24
F2 [N]	560	**1753**	278
F2X [N]	495	1361	277
F2Y [N]	260	1105	24
F3 [N]	560	**1753**	278
F3X [N]	495	1361	277
FY3 [N]	-260	1105	24
R4 [N]	10827	**27586**	26082
R4X [N]	-495	6141	14762
R4Y [N]	10815	26893	21502
M1 [N.m]	104.3	**584.9**	-3.9

b2) 4-Bar Mechanism

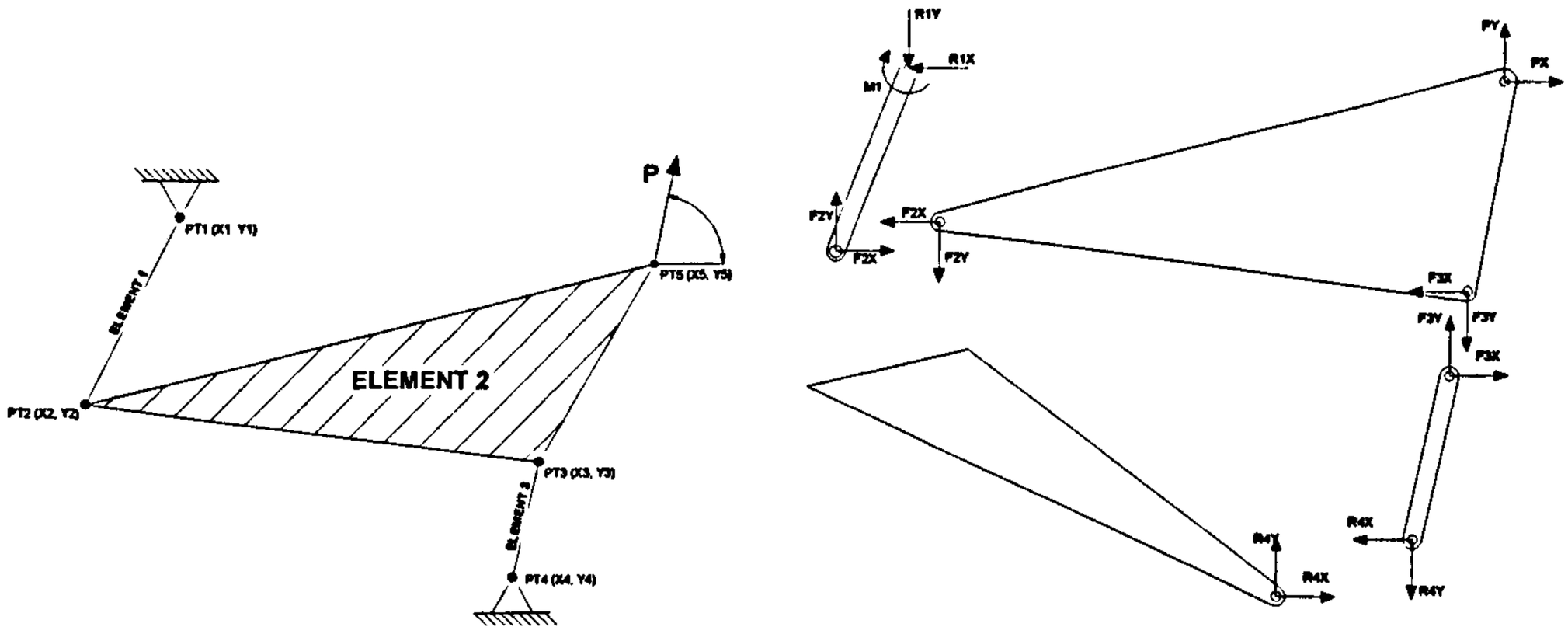

Figure 5.16 – 4 Bar Mechanism VB input data and Results

Table 5.6 – 4-Bar Mechanism points

POINTS	CRUISE		TAKE-OFF		LANDING	
	X [mm]	Y [mm]	X [mm]	Y [mm]	X [mm]	Y [mm]
1	17103.50	3026.27	17103.50	3026.27	17103.50	3026.27
2	16965.00	2644.16	17462.19	2835.14	17503.82	2956.00
3	17350.00	2691.727	17841.67	2754.65	17836.65	2756.73
4	17650.00	2300.00	17650.00	2300.00	17650.00	2300.00
5	17627.55	2935.92	18183.65	2895.08	18204.99	2782.29

The results from the Visual Basic program for the 4-Bar Mechanism Case are presented in Table 5.7.

Table 5.7 – 4-Bar Mechanism Component Loads

	Cruise	**Take-Off**	**Landing**
R1 [N]	10608	23014	20837
R1X [N]	7953	-11273	-3448
R1Y [N]	-7019	-20063	-20550
F2 [N]	10608	23014	**20837**
F2X [N]	7953	-11273	-3448
F2Y [N]	7019	20063	20550
F3 [N]	19765	51598	**45915**
F3X [N]	-7953	18775	18487
FY3 [N]	-18094	-48061	-42028
R4 [N]	19765	51598	**45915**
R4X [N]	-7953	18775	18487
R4Y [N]	-18094	-48061	-42028
M1 [N.m]	1691	-8675	**-9068**

b3) Link/Track Mechanism

Below are the required input data for the calculation of the loads in the Link/Track Mechanism.

Table 5.8 – Link/Track Mechanism points

POINTS	CRUISE		TAKE-OFF		LANDING	
	X [mm]	Y [mm]	X [mm]	Y [mm]	X [mm]	Y [mm]
1	17055.40	2978.13	17055.40	2978.13	17055.40	2978.13
2	16886.50	2635.55	17361.66	2749.41	17437.30	2994.26
3	17588.10	2837.40	18092.00	2727.17	18115.38	2722.05
4	17417.30	2777.37	17417.30	2777.37	17417.30	2777.37
5	18191.83	2607.94	18191.83	2607.94	18191.83	2607.94
6	17490.91	2761.27	17994.21	2651.17	18017.60	2646.05
7	17645.81	2727.38	18149.12	2617.28	18172.50	2612.17
8	17627.55	2935.92	18159.15	2809.22	18206.67	2775.99

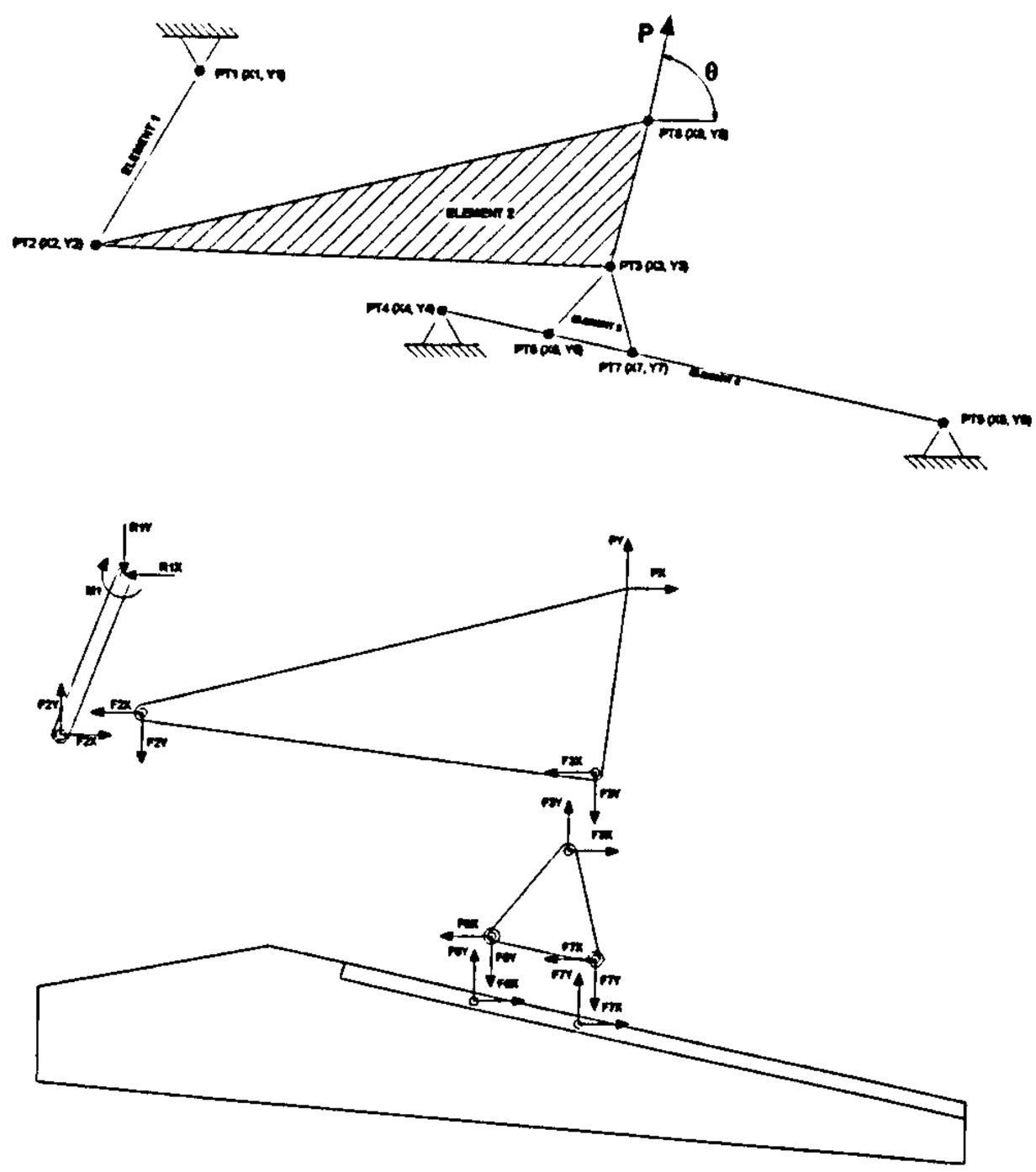

Figure 5.17 – Link/Track Mechanism VB input data and Results

The results from the Visual Basic program for the Link/Track Mechanism Case are presented in Table 5.9.

Table 5.9 – Link/Track Mechanism Loads

	Cruise	Take-Off	Landing
R1 [N]	2518	2513	**15067**
R1X [N]	-2517	-2318	-11984
R1Y [N]	73	970	9131
F2 [N]	2518	2513	**15067**
F2X [N]	-2517	970	-11984
F2Y [N]	73	-2318	9131
F3 [N]	11779	33113	**37256**
F3X [N]	2517	7076	7962
FY3 [N]	11507	32348	36395
F6 [N]	5935	16561	**26956**
F6X [N]	1268	3539	5761
F6Y [N]	5797	16178	26334
F7 [N]	5845	**16552**	10299
F7X [N]	1249	3537	2201
F7Y [N]	5710	16170	10061
M1 [N.m]	-875	-488	**-4724**

c) Mechanism Components Initial Sizing

c1) Simple Hinge Mechanism

HINGE 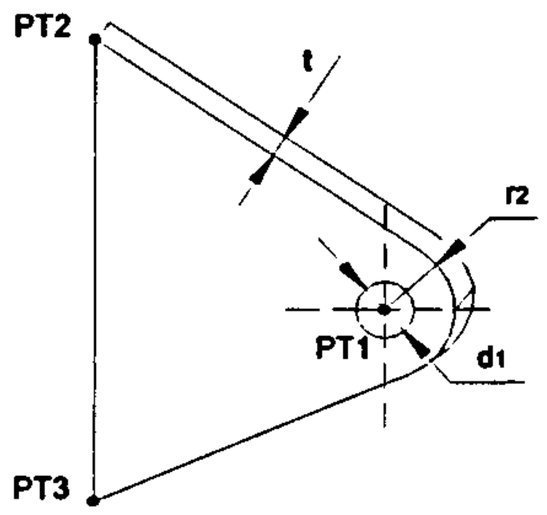	PT1 = (17093.2 ; 2956.3) [mm] PT2 = (16955.4 ; 3174.2) [mm] PT3 = (16955.4 ; 2862.2) [mm] d_1 = 18 mm r_2 = 36 mm t = 9 mm Volume = 3.06E-4 m^3 Weight = 2.4 Kg
DRIVE LINK 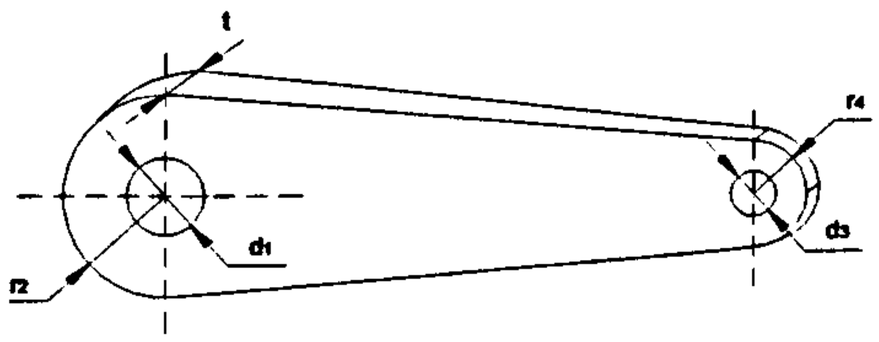	d_1 = 18 mm r_2 = 36 mm d_3 = 9 mm r_4 = 18 mm L = 356.5 mm t = 9 mm Volume = 2.55E-4 m^3 Weight = 2.0 Kg
FWD LINK 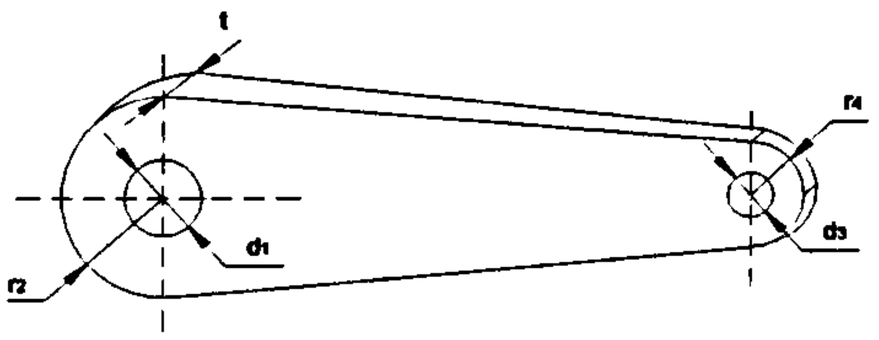	d_1 = 9 mm r_2 = 18 mm d_3 = 9 mm r_4 = 18 mm L = 505.8 mm t = 9 mm Volume = 2.17E-4 m^3 Weight = 1.7 Kg
FLAP FITTING 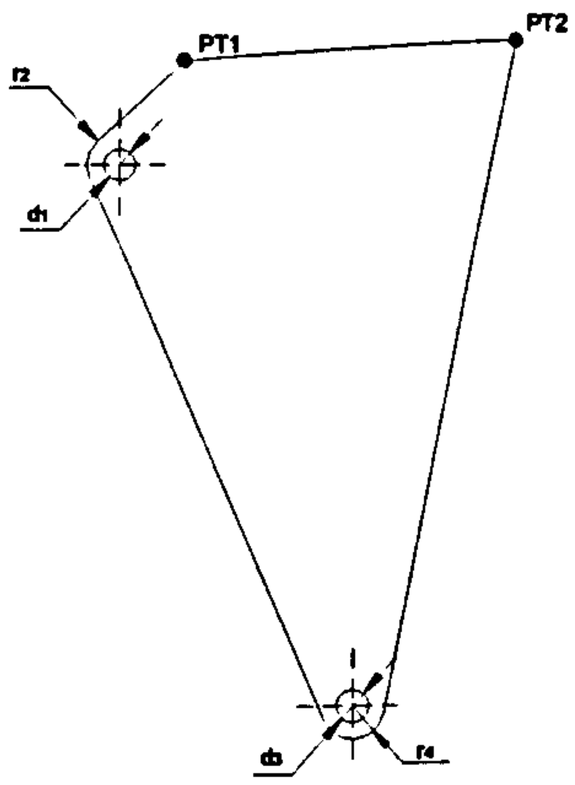	PT1 = (17386.42 ; 2933.51) [mm] PT2 = (17783.77 ; 2988.18) [mm] d_1 = 9 mm r_2 = 18 mm d_3 = 10 mm r_4 = 20 mm t = 9 mm Volume = 2.32E-4 m^3 Weight = 18.2 Kg

SUPPORT BEAM 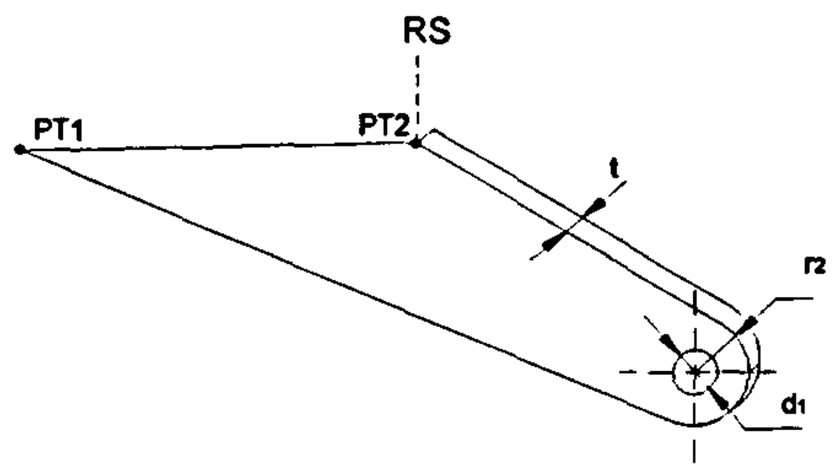	PT1 = (16955.4 ; 2862.20) [mm] PT2 = (16564.93 : 2843.38) [mm] d_1 = 10 mm r_2 = 20 mm t = 10 mm Volume = 4.52E-3 m^3 Weight = 35.5 Kg

c2) 4-Bar Mechanism

HINGE 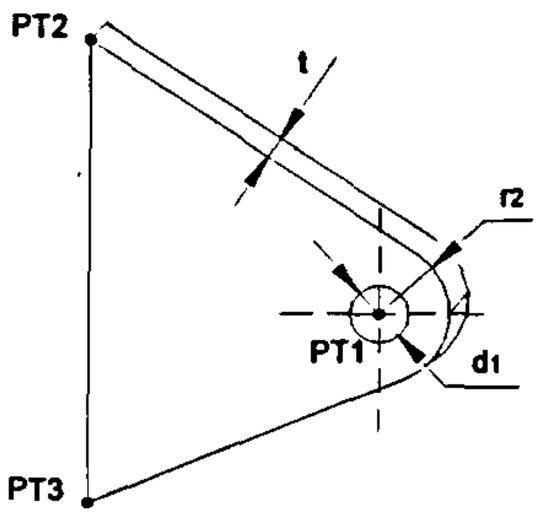	PT1 = (17103.5 ; 3026.27) [mm] PT2 = (16955.4 ; 3174.2) [mm] PT3 = (16955.4 ; 2862.2) [mm] d_1 = 45 mm r_2 = 90 mm t = 22.5 mm Volume = 1.81E-3 m^3 Weight = 14.2 Kg
DRIVE LINK 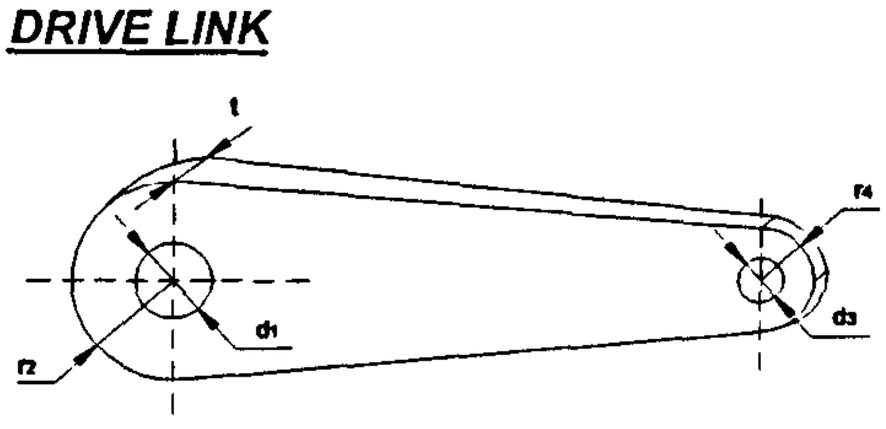	d_1 = 45 mm r_2 = 90 mm d_3 = 22.5 mm r_4 = 45 mm L = 406.4 mm t = 22.5 mm Volume = 0.001 m^3 Weight = 8.5 Kg
FLAP FITTING 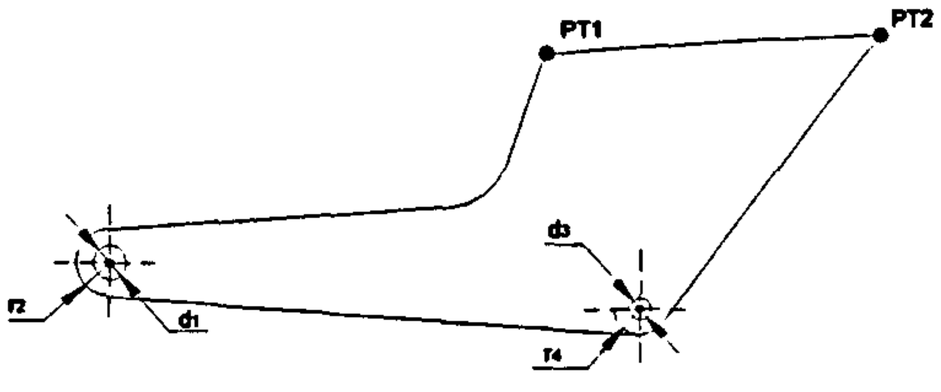	PT1 = (17357.3 ; 2926.26) [mm] PT2 = (17815.18 ; 2984) [mm] d_1 = 22.5 mm r_2 = 45 mm d_3 = 12 mm r_4 = 24 mm t = 11.25 mm Volume = 1.87E-3 m^3 Weight = 14.7 Kg

AFT LINK 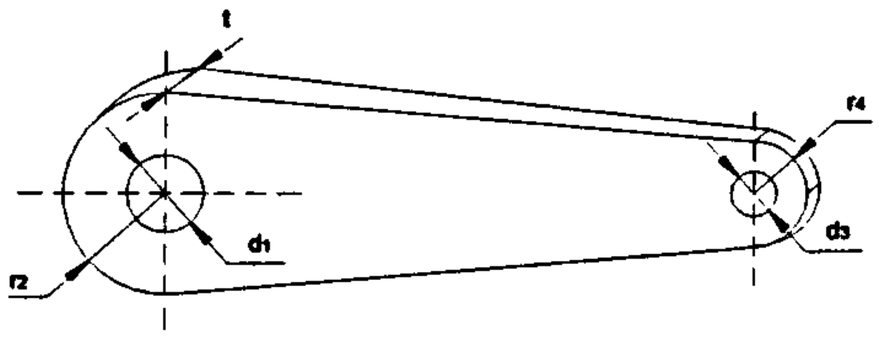 	d_1 = 12 mm r_2 = 24 mm d_3 = 22.5 mm r_4 = 45 mm L = 493.4 mm t = 22.5 mm Volume = 5.86E-4 m^3 Weight = 4.6 Kg
SUPPORT STRUT 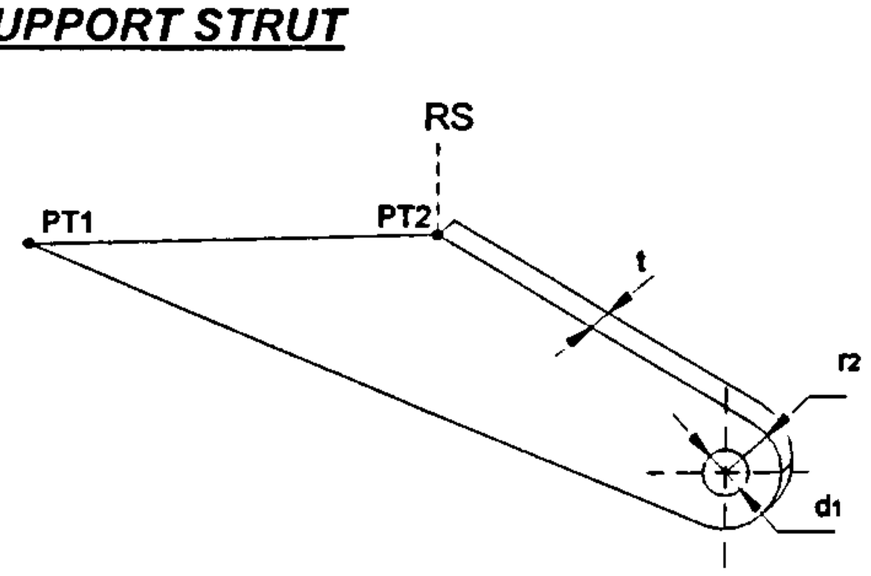 	PT1 = (16561.81;2862.2) [mm] PT2 = 1(6955.40 ; 2862.2) [mm] d_1 = 12 mm r_2 = 24 mm t = 11.25 mm Volume = 1.58E-3 m^3 Weight = 12.4 Kg

c3) Link/Track Mechanism

HINGE 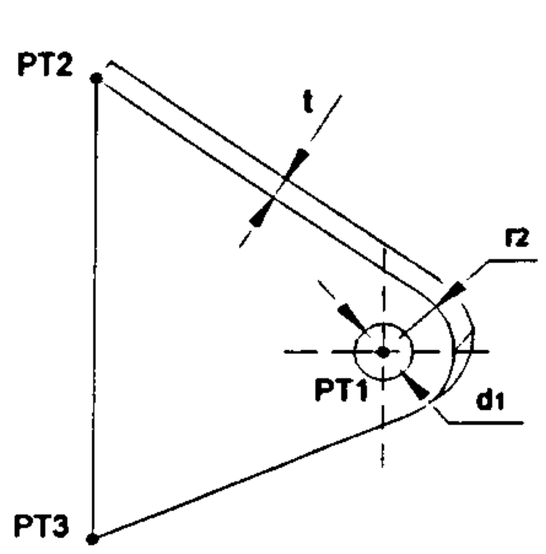 	PT1 = (17055.4 ; 1978.13) [mm] PT2 = (16955.4 ; 3174.2) [mm] PT3 = (16955.4 ; 2862.2) [mm] d_1 = 35 mm r_2 = 70 mm t = 17.5mm Volume = 5.61E-4 m^3 Weight = 4.4 Kg
DRIVE LINK 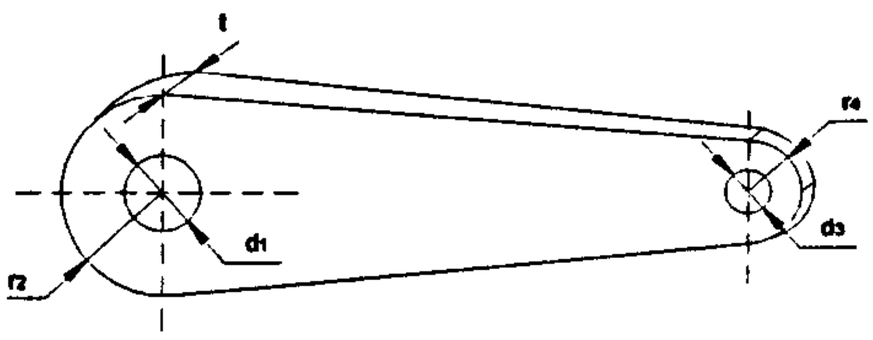 	d_1 = 35 mm r_2 = 70 mm d_3 = 17.5 mm r_4 = 35 mm L = 382.2 mm t = 17.5 mm Volume = 5.99E-4 m^3 Weight = 4.7 Kg

FLAP FITTING 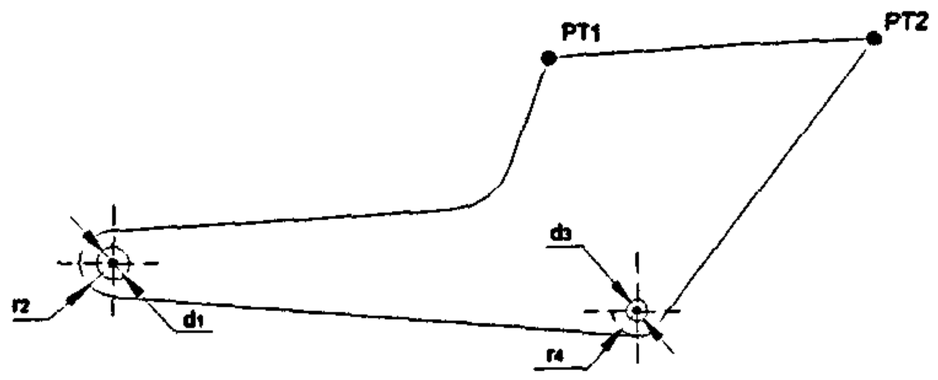	PT1 = (17387.70 ; 2933.67) [mm] PT2 = (17785.16 ; 2987.92) [mm] d_1 = 17.5 mm r_2 = 35 mm d_3 = 15 mm r_4 = 30 mm t = 17.5 mm Volume = 1.31E-3 m^3 Weight = 10.3 Kg
ROLLER CARRIAGE 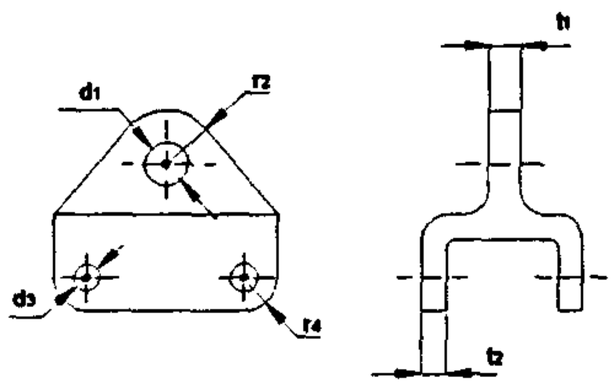	d_1 = 15 mm r_2 = 30 mm d_3 = 10 mm r_4 = 20 mm t_1 = 7.5 mm t_2 = 5 mm Width = 85 mm Volume = 3.82E-4 m^3 Weight = 3 Kg
ROLLERS 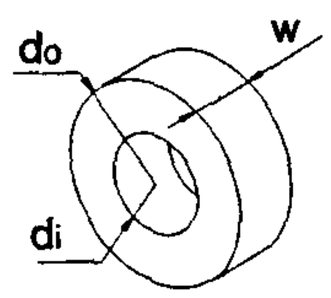	d_i = 10 mm d_o = 20 mm w = 10 mm
SUPPORT TRACK 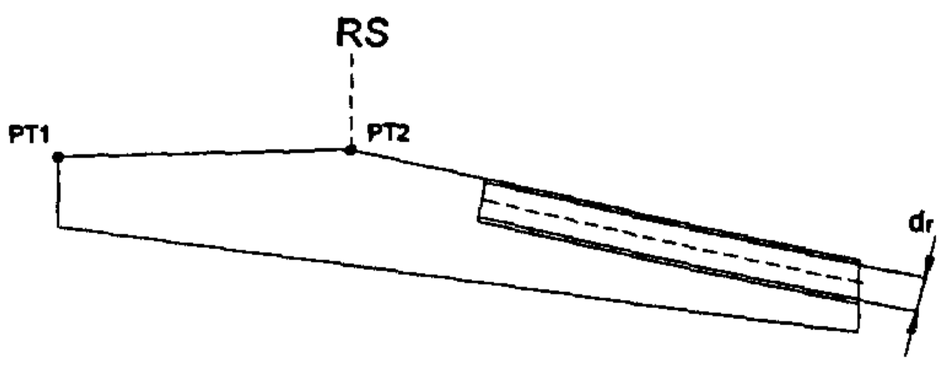	PT1 = (16955.4 ; 2862.2) [mm] PT2 = (16515.8 ; 2838.7) [mm] d_r = 20 mm Width = 50 mm Volume = 5.83E-4 m^3 Weight = 45.8 Kg

5.7. MECHANISM CAD MODEL

The initial sizing of the mechanism components allows the author to generate 3D CATIA models of each mechanism. The following figures present a side view of all three mechanisms analysed, in the Cruise, Take-Off and Landing configurations

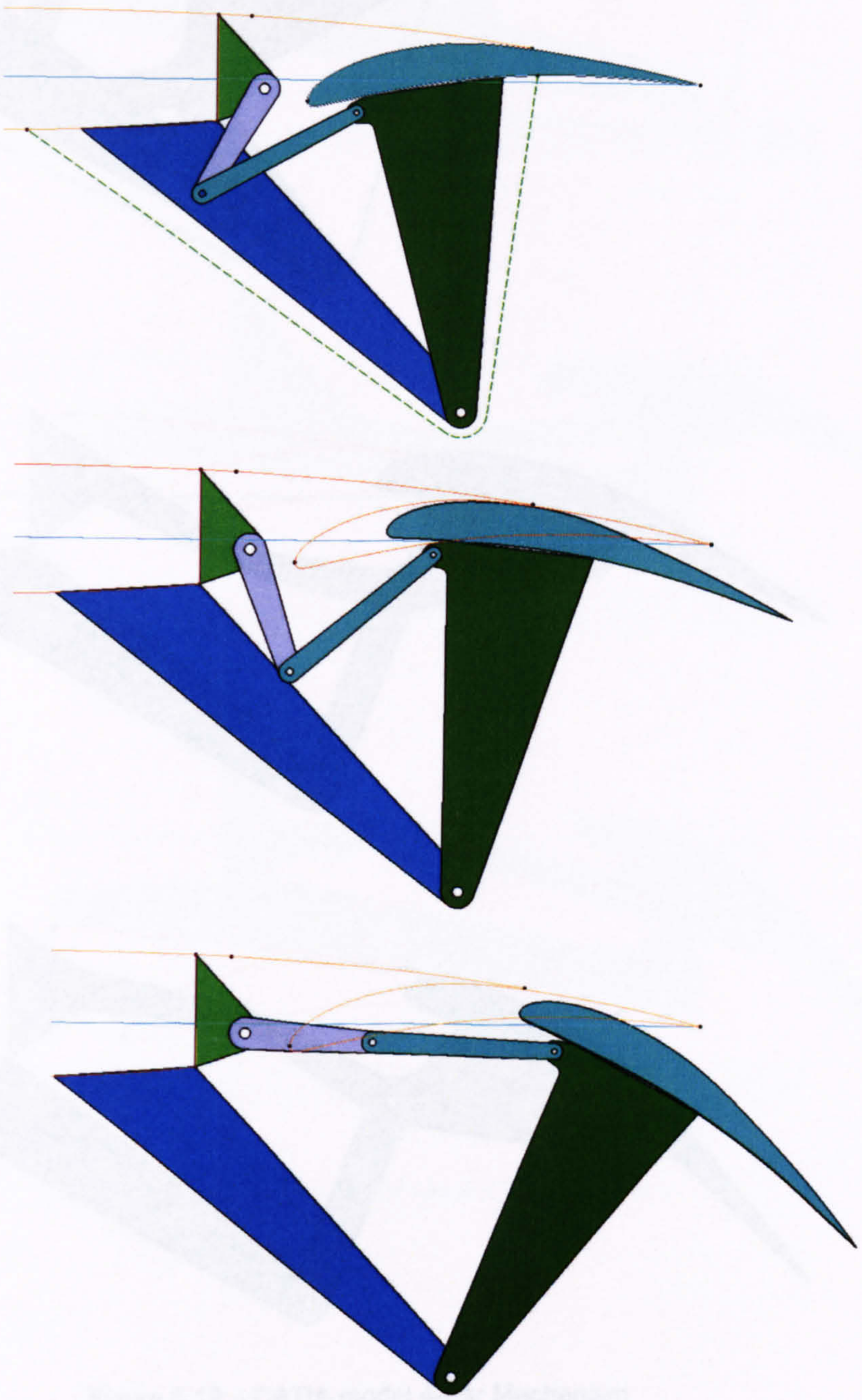

Figure 5.18 – CATIA model of Simple Hinge Mechanism

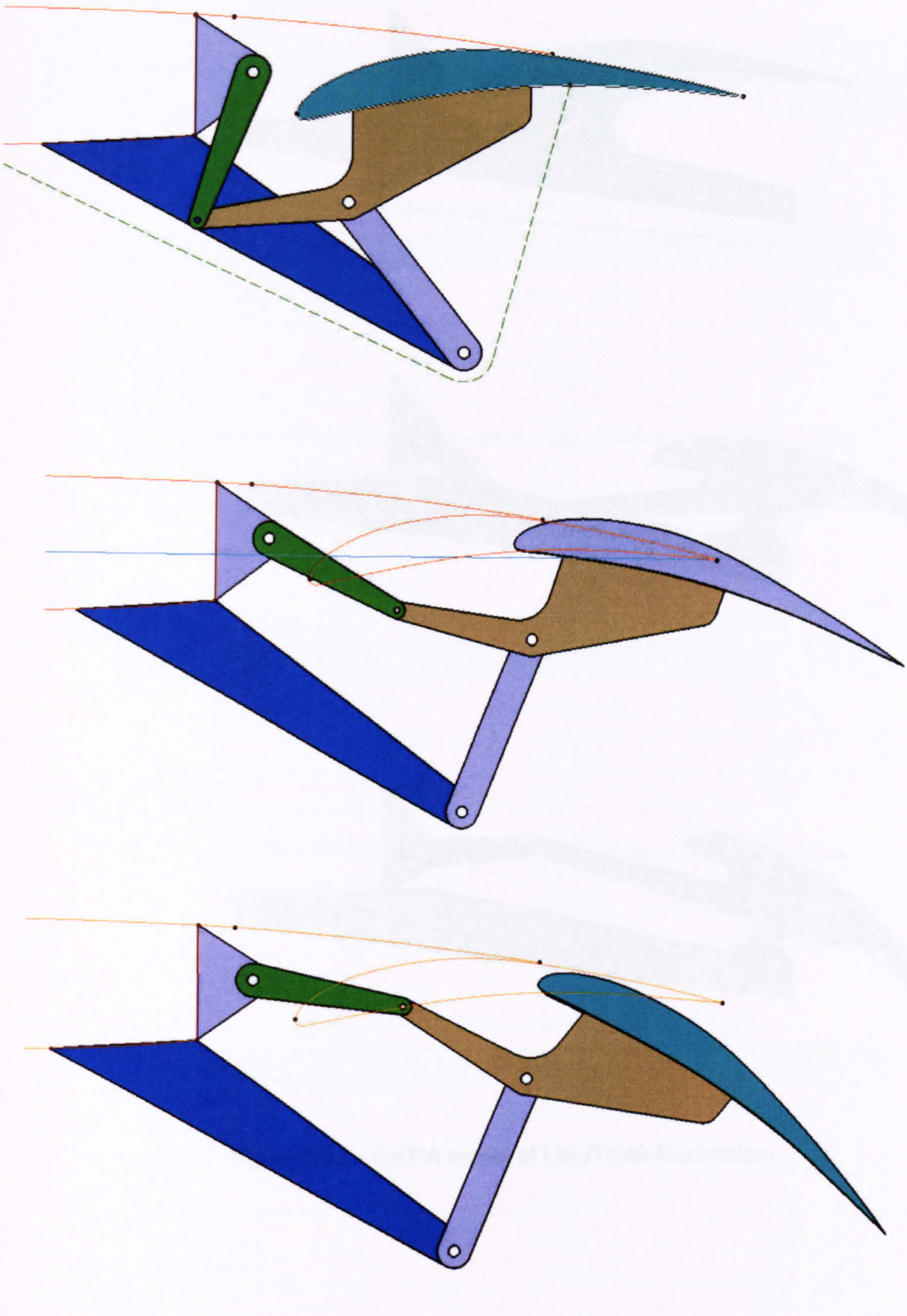

Figure 5.19 – CATIA model 4-Bar Mechanism

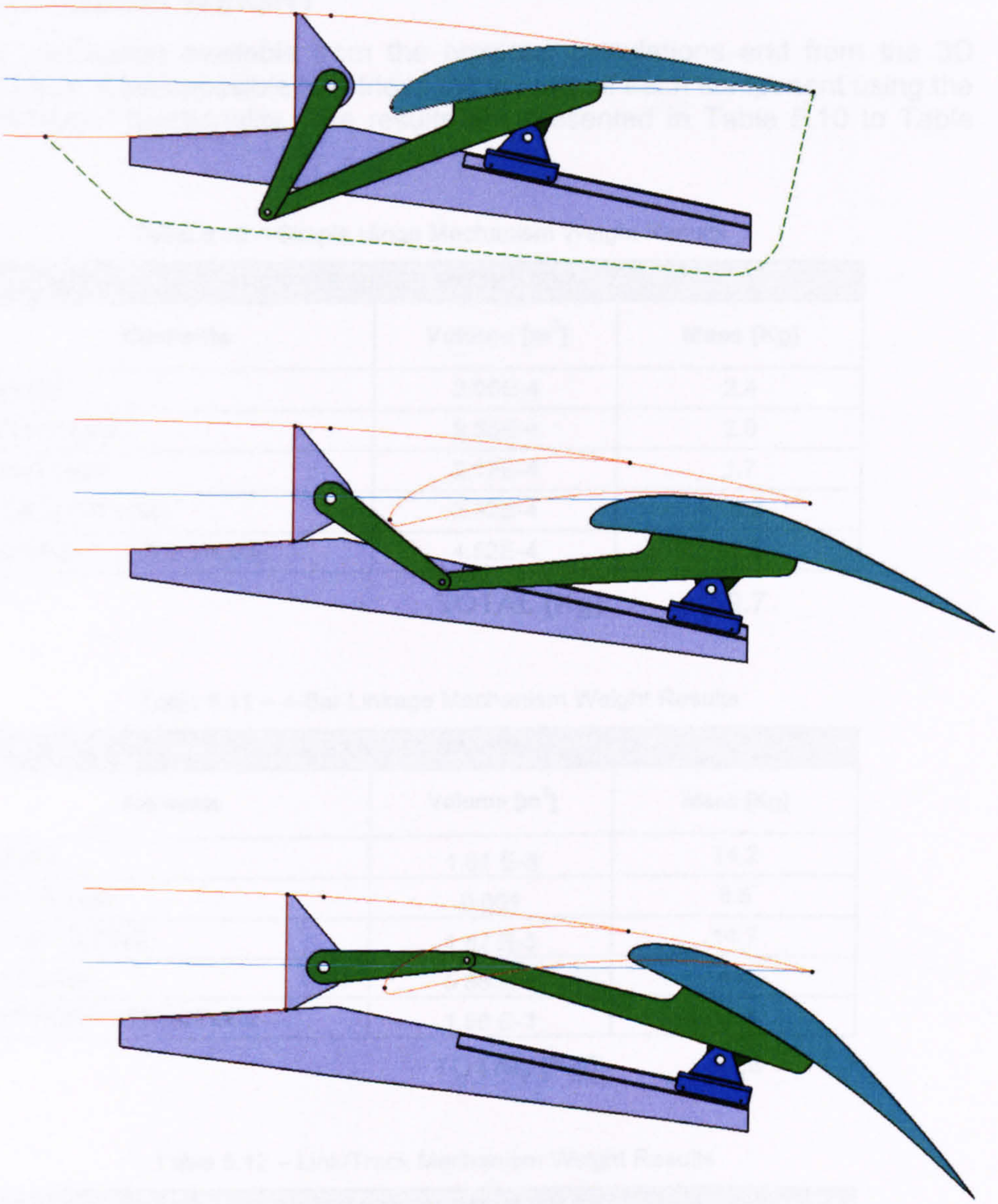

Figure 5.20 – CATIA model of Link/Track Mechanism

5.8. MECHANISM WEIGHT

With the information available from the previous calculations and from the 3D CATIA models, it was possible to retrieve the volume of each component using the CATIA *"Analyse"* functionality. The results are presented in Table 5.10 to Table 5.13.

Table 5.10 – Simple Hinge Mechanism Weight Results

SIMPLE HINGE MECHANISM		
Elements	**Volume [m^3]**	**Mass [Kg]**
HINGE	3.06E-4	2.4
DRIVE LINK	2.55E-4	2.0
FWD LINK	2.17E-4	1.7
HINGE FITTING	2.32E-4	18.2
SUPPORT STRUCTURE	4.52E-4	35.5
	TOTAL [Kg]	**59.7**

Table 5.11 – 4-Bar Linkage Mechanism Weight Results

4-BAR MECHANISM		
Elements	**Volume [m^3]**	**Mass [Kg]**
HINGE	1.81 E-3	14.2
DRIVE LINK	0.001	8.5
FLAP FITTING	1.87 E-3	14.7
AFT LINK	5.86 E-4	4.6
SUPPORT STRUCTURE	1.58 E-3	12.4
	TOTAL [Kg]	**54.4**

Table 5.12 – Link/Track Mechanism Weight Results

LINK/TRACK MECHANISM		
Elements	**Volume [m^3]**	**Mass [Kg]**
ACTUATOR HINGE	5.61E-4	4.4
DRIVE LINK	5.99E-4	4.7
FLAP FITTING	1.31E-3	10.3
ROLLER CARRIAGE	3.82E-4	3
ROLLER	-	0.5
SUPPORT BEAM WITH TRACK	5.83E-4	45.8
	TOTAL [Kg]	**68.7**

Table 5.13 – Trailing Edge High-Lift System Weight Results

Mechanism type	Weight of a Single Support & Linkage Structures [Kg]	Total weight of Support & Linkage Structures [Kg]	Total weight of High-Lift system [Kg]	% of Total Aircraft Weight (ATRA AUM)
Simple Hinge	59.7	477.6	2173	2.8%
4-Bar Linkage	54.5	435.2	1978	2.6%
Link/Track	68.7	549.6	2290	3.0%

5.9. LIFT/FAIRING DRAG

The 3D CATIA models also allow the author to retrieve the data necessary for the assessment of the aerodynamic performance in Landing configuration and Fairing drag of the different mechanisms.

a) Fairing Drag

The data retrieved from the CATIA model for each mechanisms and the results from the calculation of the increment in drag coefficient arising from the fairing ($\frac{D_{ssi}}{q \cdot S}$) are presented in Table 5.14. These results are for one fairing only.

Table 5.14 – Fairing Drag analysis results

MECHANISM TYPE	Fairing Length (m)	Fairing Depth (m)	Fairing Width (m)	t/c	C_{Dss}	$\frac{D_{ssi}}{q \cdot S}$
SIMPLE HINGE MECHANISM	1.48	0.93	0.3	0.20	7.46E-3	1.9E-5
4-BAR MECHANISM	1.56	0.61	0.35	0.22	7.92E-3	1.5E-5
LINK/TRACK MECHANISM	2.07	0.38	0.4	0.19	7.28E-3	1.0E-5

b) Aerodynamic Performance in Take-Off Configuration

As before, all the relevant data required for the calculation of the ΔC_{LMax} for the Landing configuration was taken from the 3D CATIA models.

Table 5.15 – Gap and Overlap for Calculations

MECHANISM TYPE	Fowler Motion (mm)	Gap (mm)	Overlap (mm)
SIMPLE HINGE MECHANISM	251.6	4.6	399.2
4-BAR MECHANISM	572.3	13.1	78.5
LINK/TRACK MECHANISM	545.5	98.1	105.3

The relevant parameters for the calculation of ΔC_{LMax} of the ATRA airfoil at the Wing Station b/2 = 8.214m and for all the mechanism are presented in Table 5.16.

Table 5.16 – ATRA Wing and Flap Parameters

	SIMPLE HINGE MECHANISM	4-BAR MECHANISM	LINK/TRACK MECHANISM
Airfoil			
t/c	0.1085		
C [mm]	3260.26		
$Z_{u1.25}/c$	0.0192		
X_{um}/c	0.422		
c'/c	1.109	1.206	1.205
$(a_1)_0$ [1]	6.18075		
$(C_{LmB})_d$ [1]	4.22		
Flap			
δ_{t1}°	15°		
c_{t1} [mm]	1140		
ΔC_{t1} [mm]	-374.3	-57.3	-59.5
c_{t1}' [mm]	765.7	1082.7	1080.5
X_{ts} [mm]	2849.5		
c' [mm]	3615.2	3932.2	3930
c_{t1}' /c'	0.212	0.275	0.275

The results of the calculation of increment in lift in the landing configuration are presented in Table 5.17. These results are for the outboard flap at one wing span position only. To obtain the total $\Delta C_{L\max}$ of the wing with the specific flap, the above process would have to be repeated on other representative positions of the wing.

Table 5.17 – Take-Off Performance Results

MECHANISM TYPE	$\Delta C_{L\max}$
SIMPLE HINGE MECHANISM	***0.14***
4-BAR MECHANISM	***0.11***
LINK/TRACK MECHANISM	***0.09***

5.10. RELIABILITY & MAINTAINABILITY

As defined in the Design Methodology, each mechanism was assessed in terms of number of components and mechanical connections to ultimately determine its Reliability and Maintainability.
The final results for the Reliability and Maintainability of all mechanism analysed are presented in Table 5.18 to Table 5.23.

a) Reliability

Table 5.18 – Simple Hinge Mechanism Reliability Result

	SIMPLE HINGE MECHANISM			
	Elements	**QTY**	**Failure Rate/Element (10e6h)**	**Sub-System Failure Rate (10e-6h)**
	ACTUATOR HINGE	1	0.02	0.02
	DRIVE LINK	1	9.26	9.26
	FWD LINK	1	0.02	0.02
	HINGE FITTING	1	0.02	0.02
	SUPPORT FITTING	1	0.02	0.02
	ROTARY ACTUATOR	1	87.94	87.94
	Mechanism Connections			
F	ACTUATOR HINGE / ROTARY ACTUATOR	1	0.02	0.02
F	ACTUATOR HINGE / WING STRUCTURE	1	0.02	0.02
F	SUPPORT FITTING / WING STRUCTURE	1	0.02	0.02
F	HINGE FITTING / FLAP	1	0.02	0.02
R	ACTUATOR HINGE / DRIVE LINK	1	1.00	1.00
R	DRIVE LINK/ FWD LINK	1	1.00	1.00
R	FWD LINK / HINGE FITTING	1	1.00	1.00
	Total Nr. Parts	**6**		
	Total Nr. Connections	**7**	**Assembly Failure Rate**	**100.36**

Table 5.19 – 4-Bar Linkage Mechanism Reliability Result

	4-BAR MECHANISM			
	Elements	**QTY**	**Failure Rate/Element (10e6 hr)**	**Sub-System Failure Rate (10e-6 hr)**
	ACTUATOR HINGE	1	0.02	0.02
	DRIVE LINK	1	9.26	9.26
	FLAP FITTING	1	0.02	0.02
	SUPPORT FITTING	1	0.02	0.02
	AFT LINK	1	0.02	0.02
	ROTARY ACTUATOR	1	87.94	87.94
	Mechanism Connections			
F	ACTUATOR HINGE / ROTARY ACTUATOR	1	0.02	0.02
F	ACTUATOR HINGE / WING STRUCTURE	1	0.02	0.02
F	FLAP FITTING / FLAP	1	0.02	0.02
F	SUPPORT FITTING / WING STRUCTURE	1	0.02	0.02
R	ACTUATOR HINGE / DRIVE LINK	1	1.00	1.00
R	DRIVE LINK / FLAP FITTING	1	1.00	1.00
R	FLAP FITTING / AFT LINK	1	1.00	1.00
R	SUPPORT FITTING / AFT LINK	1	1.00	1.00
	Total Nr. Parts	**6**		
	Total Nr. Connections	**8**	**Assembly Failure Rate**	**101.36**

Table 5.20 – Link/Track Mechanism Reliability Result

	LINK/TRACK MECHANISM			
	Elements	**QTY**	**Failure Rate/Element (10e6 hr)**	**Sub-System Failure Rate (10e-6 hr)**
	ACTUATOR HINGE	1	0.02	0.02
	DRIVE LINK	1	9.26	9.26
	FLAP FITTING	1	0.02	0.02
	SUPPORT BEAM WITH TRACK	1	0.02	0.02
	ROLLER CARRIAGE	1	0.02	0.02
	ROLLER	4	0.69	2.76
	ROTARY ACTUATOR	1	87.94	87.94
	Mechanism Connections			
F	ACTUATOR HINGE / ROTARY ACTUATOR	1	0.02	0.02
F	ACTUATOR HINGE / WING STRUCTURE	1	0.02	0.02
F	FLAP FITTING / FLAP	1	0.02	0.02
F	SUPPORT BEAM WITH TRACK / WING STRUCTURE	1	0.02	0.02
F	ROLLER CARRIAGE / ROLLER	1	0.02	0.02
R	ACTUATOR HINGE / DRIVE LINK	1	1.00	1.00
R	DRIVE LINK / FLAP FITTING	1	1.00	1.00
R	FLAP FITTING / ROLLER CARRIAGE	1	1.00	1.00
	Total Nr. Parts	**10**		
	Total Nr. Connections	**8**	**Assembly Failure Rate**	**103.14**

b) Maintainability

Table 5.21 – Simple Hinge Mechanism Maintainability Result

MAINTAINABILITY PREDICTION [MIL - 472]

SIMPLE HINGE MECHANISM

CHECK LIST A - PHISICAL DESIGN FACTORS

		SUPPORTS & LINKAGES					ACTUATION & CONTROLS	FLAP PANEL
	ITEM	ACTUATOR HINGE	DRIVE LINK	FWD LINK	HINGE FITTING	SUPPORT FITTING	ROTARY ACTUATOR	FLAP
1	Access	2	2	2	2	2	2	4
2	Latches& Fasteners (external)	0	2	2	2	0	2	2
3	Latches& Fasteners (Internal)	0	2	2	2	0	2	0
4	Access (Internal)	2	4	4	4	2	2	4
5	Packaging	0	0	0	0	0	2	0
6	Units/Parts	0	2	2	2	0	2	0
7	Visual Display	0	2	2	2	0	4	2
8	Fault & Operation Indicators	0	2	2	2	0	4	2
9	Test Point Availability	2	2	2	2	2	2	2
10	Test Point Identification	0	0	0	0	0	2	0
11	Labelling	2	2	2	2	2	2	2
12	Adjustments	0	2	2	2	0	2	2
13	Testing (On Aircraft)	4	4	4	4	4	4	4
14	Protective Devices	0	2	2	2	0	2	2
15	Safety Personal	2	2	2	2	2	2	2
	Total	14	30	30	30	14	36	28

CHECK LIST B - DESIGN FACILITY FACTORS

		SUPPORTS & LINKAGES					ACTUATION & CONTROLS	FLAP PANEL
	ITEM	ACTUATOR HINGE	DRIVE LINK	FWD LINK	HINGE FITTING	SUPPORT FITTING	ROTARY ACTUATOR	FLAP
1	External Test Equipment	2	2	2	2	2	2	2
2	Connectors	2	2	2	2	2	2	4
3	Jigs or Fixtures	0	0	0	0	0	2	0
4	Visual Contact	4	4	4	4	4	2	2
5	Assistance (Operations Personal)	4	4	4	4	4	2	4
6	Assistance (Technical Personal)	0	0	0	0	0	2	0
7	Assistance (Supervisory or Contract Personal)	2	4	4	4	2	2	4
	Total	14	16	16	16	14	14	16

CHECK LIST C - MAINTENANCE SKILLS

		SUPPORTS & LINKAGES					ACTUATION & CONTROLS	FLAP PANEL
	ITEM	ACTUATOR HINGE	DRIVE LINK	FWD LINK	HINGE FITTING	SUPPORT FITTING	ROTARY ACTUATOR	FLAP
1	Arm, Leg, and Back Strength	2	2	2	2	2	2	1
2	Endurance and Energy	2	2	2	2	2	2	1
3	Eye/Hand Coordination, Dexterity and Neatness	2	2	2	2	2	2	2
4	Visual Acuity	2	2	2	2	2	2	4
5	Logical Analysis	3	3	3	3	3	2	3
6	Memory - Things and Ideas	2	2	2	2	2	2	2
7	Planfulness and Resourcefulness	2	2	2	2	2	2	2
8	Alertness, Cautiousness, and Accuracy	1	1	1	1	1	2	1
9	Concentration, Persistance and Patience	1	1	1	1	1	2	1
10	Initiative and Incisiveness	3	3	3	3	3	4	3
	Total	20	20	20	20	20	22	20

MTTR [hr]	5.9	2.0	2.0	2.0	5.9	1.6	2.3

TOTAL **21.7**

Table 5.22 – 4-Bar Mechanism Maintainability Result

MAINTAINABILITY PREDICTION [MIL - 472]

FOUR-BAR MECHANISM

CHECK LIST A - PHISICAL DESIGN FACTORS

		SUPPORTS & LINKAGES					ACTUATION & CONTROLS	FLAP PANEL
	ITEM	ACTUATOR HINGE	DRIVE LINK	FLAP FITTING	SUPPORT FITTING	AFT LINK	ROTARY ACTUATOR	FLAP
1	Access	2	2	2	2	2	2	4
2	Latches& Fasteners (external)	0	2	2	0	2	2	2
3	Latches& Fasteners (Internal)	0	2	0	0	2	2	0
4	Access (Internal)	2	4	2	2	4	2	4
5	Packaging	0	0	0	0	0	2	0
6	Units/Parts	0	2	0	0	2	2	0
7	Visual Display	0	2	2	0	2	4	2
8	Fault & Operation Indicators	0	2	2	0	2	4	2
9	Test Point Availability	2	2	2	2	2	2	2
10	Test Point Identification	0	0	0	0	0	2	0
11	Labelling	2	2	2	2	2	2	2
12	Adjustments	0	2	0	0	2	2	2
13	Testing (On Aircraft)	4	4	4	4	4	4	4
14	Protective Devices	0	2	2	0	2	2	2
15	Safety Personal	2	2	2	2	2	2	2
	Total	14	30	22	14	30	36	26

CHECK LIST B - DESIGN FACILITY FACTORS

		SUPPORTS & LINKAGES					ACTUATION & CONTROLS	FLAP PANEL
	ITEM	SIMPLE HINGE	DRIVE LINK	FLAP FITTING	SUPPORT FITTING	AFT LINK	ROTARY ACTUATOR	FLAP
1	External Test Equipment	2	2	2	2	2	2	2
2	Connectors	2	2	2	2	2	2	4
3	Jigs or Fixtures	0	0	0	0	0	2	0
4	Visual Contact	4	4	4	4	4	2	2
5	Assistance (Operations Personal)	4	4	4	4	4	2	4
6	Assistance (Technical Personal)	0	0	0	0	0	2	0
7	Assistance (Supervisory or Contract Personal)	2	4	2	2	4	2	4
	Total	14	16	14	14	16	14	16

CHECK LIST C - MAINTENANCE SKILLS

		SUPPORTS & LINKAGES					ACTUATION & CONTROLS	FLAP PANEL
	ITEM	SIMPLE HINGE	DRIVE LINK	FLAP FITTING	SUPPORT FITTING	AFT LINK	ROTARY ACTUATOR	FLAP
1	Arm, Leg, and Back Strength	2	2	2	2	2	2	1
2	Endurance and Energy	2	2	2	2	2	2	1
3	Eye/Hand Coordination, Dexterity and Neatness	2	2	2	2	2	2	2
4	Visual Acuity	2	2	2	2	2	2	4
5	Logical Analysis	3	3	3	3	3	2	3
6	Memory - Things and Ideas	2	2	2	2	2	2	2
7	Planfulness and Resourcefulness	2	2	2	2	2	2	2
8	Alertness, Cautiousness, and Accuracy	1	1	1	1	1	2	1
9	Concentration, Persistance and Patience	1	1	1	1	1	2	1
10	Initiative and Incisiveness	3	3	3	3	3	4	3
	Total	20	20	20	20	20	22	20

MTTR [hr]	5.9	2.0	3.7	5.9	2.0	1.6	2.3

TOTAL 23.4

Table 5.23 – Link/Track Mechanism Maintainability Result

MAINTAINABILITY PREDICTION [MIL - 472]

LINK/TRACK MECHANISM

CHECK LIST A - PHISICAL DESIGN FACTORS

		SUPPORTS & LINKAGES						ACTUATION & CONTROLS	FLAP PANEL
	ITEM	ACTUATOR HINGE	DRIVE LINK	FLAP FITTING	SUPPORT BEAM WITH TRACK	ROLLER CARRIAGE	ROLLER	ROTARY ACTUATOR	FLAP
1	Access	2	2	2	2	2	2	2	4
2	Latches& Fasteners (external)	0	2	2	0	2	0	2	2
3	Latches& Fasteners (Internal)	0	2	0	0	2	0	2	0
4	Access (Internal)	2	4	2	2	2	2	2	4
5	Packaging	0	0	0	0	0	0	2	0
6	Units/Parts	0	2	0	0	2	2	2	0
7	Visual Display	0	2	2	0	2	0	4	2
8	Fault & Operation Indicators	0	2	2	0	2	2	4	2
9	Test Point Availability	2	2	2	2	2	4	2	2
10	Test Point Identification	0	0	0	0	0	4	2	0
11	Labelling	2	2	2	2	2	2	2	2
12	Adjustments	0	2	0	0	2	2	2	2
13	Testing (On Aircraft)	4	4	4	4	4	4	4	4
14	Protective Devices	0	2	2	0	2	2	2	2
15	Safety Personal	2	2	2	0	2	2	2	2
	Total	14	30	22	12	28	28	36	28

CHECK LIST B - DESIGN FACILITY FACTORS

		SUPPORTS & LINKAGES						ACTUATION & CONTROLS	FLAP PANEL
	ITEM	ACTUATOR HINGE	DRIVE LINK	FLAP FITTING	SUPPORT BEAM WITH TRACK	ROLLER CARRIAGE	ROLLER	ROTARY ACTUATOR	FLAP
1	External Test Equipment	2	2	2	2	2	4	2	2
2	Connectors	2	2	2	2	2	4	2	4
3	Jigs or Fixtures	0	0	0	0	0	0	2	0
4	Visual Contact	4	4	4	2	2	2	2	2
5	Assistance (Operations Personal)	4	4	4	2	4	4	2	4
6	Assistance (Technical Personal)	0	0	0	0	2	2	2	0
7	Assistance (Supervisory or Contract Personal)	2	4	2	2	4	4	2	4
	Total	14	16	14	10	16	20	14	16

CHECK LIST C - MAINTENANCE SKILLS

		SUPPORTS & LINKAGES						ACTUATION & CONTROLS	FLAP PANEL
	ITEM	ACTUATOR HINGE	DRIVE LINK	FLAP FITTING	SUPPORT BEAM WITH TRACK	ROLLER CARRIAGE	ROLLER	ROTARY ACTUATOR	FLAP
1	Arm, Leg, and Back Strength	2	2	2	1	2	2	2	1
2	Endurance and Energy	2	2	2	1	2	2	2	1
3	Eye/Hand Coordination, Dexterity and Neatness	2	2	2	2	2	2	2	2
4	Visual Acuity	2	2	2	2	2	2	2	4
5	Logical Analysis	3	3	3	3	3	3	2	3
6	Memory - Things and Ideas	2	2	2	2	2	2	2	2
7	Planfulness and Resourcefulness	2	2	2	2	2	2	2	2
8	Alertness, Cautiousness, and Accuracy	1	1	1	1	1	1	2	1
9	Concentration, Persistance and Patience	1	1	1	1	1	1	2	1
10	Initiative and Incisiveness	3	3	3	2	3	3	4	3
	Total	20	20	20	16	20	20	22	20

MTTR [hr]	5.9	2.0	3.7	9.7	2.3	1.7	1.6	2.3

TOTAL 29.2

5.11. SIMPLE COST ESTIMATION

Presented below is the cost estimation for the different mechanism analysed in this case study. The final results are presented in Table 5.24 and Table 5.25.

a) High-Lift Device System Cost

As defined in the design methodology in page 68, the total cost of the High-Lift system is given by:

$$Cost = a_1 \cdot W \cdot PC^{x1} \quad [71]$$

$a_1 = 1.8881$ for Trailing Edge devices and $x_1 = 0.7$.

Where:
a_1 accounts for hourly labour costs and type of material.
PC – Part Count of a system. Part count of a Trailing Edge flap is given by the sum of the parts of the flap panel, support, support fairing and actuation.
W – Flap System weight.

Table 5.24 – High-Lift System Total Cost

Mechanism type	Total Weight of High-Lift System	Parts Count [71]	Total System Cost
Simple Hinge	2173Kg / 4790lb	1190	***£643,000***
4-Bar Linkage	1978Kg / 4360lb	1190	***£585,000***
Link/Track	2290Kg / 5049lb	1150	***£662,000***

b) Cost associated with Fairing Drag

Using the procedure defined in section 3.2.8, page 68, and the results from Table 5.17, it is possible to calculate the additional cost due to the different mechanism fairings.

Table 5.25 – Cost associated with Fairing Drag over the Aircraft Life

MECHANISM TYPE	Drag of one Fairing	Drag of all Wing Fairings	Additional Costs due to Fairing Drag
Link/Track	9.04E-6	5.42E-05	***£108,480***
4-Bar Linkage	1.38E-5	8.28E-05	***£165,600***
Simple Hinge	1.7E-5	1.02E-04	***£204,000***

5.12. SELECTION PROCESS

The final stage of the design methodology is the selection process. All the results from the previous modules are gathered and weighed so that a final score can be assigned to each mechanism. Table 5.26 presents the final results.

Table 5.26 – Selection Process Results

Trailing Edge High-Lift System Weight [Kg]		
		Score
Simple Hinge Mechanism	2173	***9.1***
4-Bar Mechanism	1978	***10***
Link/Track Mechanism	2290	***8.6***

Aerodynamic Performance ΔC_{LMax}		
		Score
Simple Hinge Mechanism	0.14	***10***
4-Bar Mechanism	0.11	***7.9***
Link/Track Mechanism	0.09	***6.4***

Fairing Drag Coefficient		
		Score
Simple Hinge Mechanism	1.70E-05	***5.2***
4-Bar Mechanism	1.38E-05	***6.1***
Link/Track Mechanism	9.04E-06	***10***

Reliability		
		Score
Simple Hinge Mechanism	100.36	***10***
4-Bar Mechanism	101.36	***9.9***
Link/Track Mechanism	103.14	***9.7***

Maintainability (MTTR)		
		Score
Simple Hinge Mechanism	21.7	***10***
4-Bar Mechanism	23.4	***9.3***
Link/Track Mechanism	29.2	***7.4***

Cost Associated with Fairing Drag		
		Score
Simple Hinge Mechanism	£204,000	***5.3***
4-Bar Mechanism	£165,600	***6.6***
Link/Track Mechanism	£108,480	***10***

Trailing Edge High-Lift System Cost [£]		
		Score
Simple Hinge Mechanism	643,000	***9.5***
4-Bar Mechanism	608,000	***10***
Link/Track Mechanism	662,000	***9.2***

OVERALL SCORES	
Simple Hinge Mechanism	***59.1***
4-Bar Mechanism	***59.8***
Link/Track Mechanism	***61.3***

The selection process is complete and the overall scores show that the mechanism most appropriate for the ATRA Variable camber Wing concept is the Link/Track mechanism. However, the other two mechanisms came very close in the final overall scores, maybe suggesting that more accurate data is required for validation and/or more accurate calculation and estimation procedures are required.

CHAPTER 6

DISCUSSION

6.1. INTRODUCTION

The objective of this research study was to develop a new design methodology for Trailing Edge High Lift device mechanisms. This research is to be used in the initial stages of the design process to improve it and to allow a more detailed selection of the mechanisms used in Trailing Edge High Lift devices. The author used different technical areas of investigation, including the use of the SYNAMEC software, an innovative computational design tool, and the application of the methodology in a case study applied to the Variable Camber Concept.
The different areas of investigation also included were:

- Development of the design methodology
- Development of Initial Sizing and Weight estimation methods
- Aerodynamic studies (lift and fairing drag analysis)
- Development of Reliability and Maintainability prediction methods
- Basic cost estimation
- Software development (Visual Basic application)
- 3D CAD modelling of mechanisms

This chapter gathers all the most relevant aspects of the development of the design methodology and the work developed, including the difficulties encountered.

6.2. DESIGN METHODOLOGY

The first step on the development of this design methodology was to revise conventional high-lift device design methods. This has allowed the author to target possible areas of improvement. The research into the High-Lift device topic showed that there are several areas of great importance that are not considered from the outset of the design process. These areas are Maintainability & Reliability and Weight considerations. The advantage of having the SYNAMEC software available allowed the author to introduce these areas in the design methodology. By using SYNAMEC the author was able to have access, at an earlier stage, to mechanism configurations not far from the kinematic optimum, and hence perform a more effective preliminary sizing of the different mechanisms. Once the preliminary sizing and CAD modelling of the mechanisms was complete, the estimation of Weight, Reliability and Maintainability could be looked at, having available more information than usual at the initial stages of the design process.
The new design methodology is characterized by several advances in the way the design of High-Lift devices is approached. These advances are:

1) The use of the SYNAMEC software, a state-of-the-art engineering tool capable of covering all the design stages of the mechanism design procedure, from mechanism type synthesis to preliminary and detailed design.
2) The inclusion in the initial stages of design process of engineering disciplines not common at that stage of design, like weight, reliability and maintainability and cost,
3) Extensive use of a new software application for the initial sizing of mechanism components, developed by the author.

The following paragraphs present discussions regarding the main modules of this research study.

SYNAMEC

SYNAMEC is a computer-aided design and engineering software tool for the synthesis of aeronautical mechanisms. It was developed by the SYNAMEC team where the author was a member. This software integrates in one application three other software design tools: SAMCEF FIELD (CAD software), SAMCEF MECANO (Mechanical Analysis Software) and BOSS Quattro (Optimization Software). By doing so, the SYNAMEC System is capable of covering all the design stages of the mechanism design procedure, from mechanism type synthesis to preliminary and detailed design, targeting the reduction of the time to design and making it easier for designers to evaluate different solutions.
The SYNAMEC software has some limitations. At the time of this research study, some of the software functionalities were not available. The author points out the main limitations:

- ***Limited mechanical components available for Type Synthesis*** – Only links, hinges and prismatic joints can be used to perform a mechanism synthesis;
- ***Limited Solutions from Type Synthesis*** – at the time of this study, the solutions provided were limited to 4-Bar and Simple Hinge mechanisms;
- ***The software only deals with 2D problems*** – only deals with planar mechanisms.

The extensive use of SYNAMEC in the new design methodology requires a great amount of computational time. The most time-consuming part of the study was the optimization process. To effectively and efficiently use this design methodology it is required that from the outset the designer has access to powerful computational resources.

Initial Sizing of Mechanism Components

The author developed a very useful tool for calculation of the mechanism component loads. Despite not being a software developer, the author has created an application that is simple and intuitive to use. This software was developed using Visual Basic and initially was supposed to cover calculation of the component loads and also perform weight estimation, but it was decided to limit the development to the calculation of loads. The amount of time involved in the expansion to weight estimation would have been very high, time that was required for other areas of study.
The application is limited to 2D analysis of mechanisms and receives as input all the information made available by the SYNAMEC software, plus preliminary hinge loads and the angles of the low speed flap configurations, and calculates the loads in each component in a matter of seconds. These loads are then used to manually determine all the components dimensions. These dimensions are the first iteration of the design process and they are very crude and clearly oversized. This was the main reason why, for example, the Euler buckling stress check wasn't performed after obtaining the initial sizes. In later stages of the design process this check and other more precise and accurate sizing procedures must be performed.

The author would also like to point out that the load cases used in this research were the only ones available from the ATRA aircraft and they are not the only ones relevant to the sizing of a High Lift Device mechanism. Cases like the maximum stall force of the actuator under a mechanism jam condition or when the aircraft is subjected to vertical gusts and turbulent conditions might also be of great importance for the sizing of a High Lift Device mechanism.
The main characteristic of this software are its simplicity of use and its scope for further development. The main areas of development that should be considered are the calculation of component sizes and Weight estimation within the program, extension of the calculations to Leading edge devices and improvement of the component load calculation methods, allowing the analysis of 3D mechanisms. It can also be further developed to generate output files capable of being read by CATIA to generate the 3D CAD models of the mechanism components.
The literature research in the High-Lift topic by the author found no reference to an application similar to the one developed for this research study.

Weight Estimation

There is almost no information available to the general public about weight estimation for High-Lift systems. The only one found was by Pepper [71] and it was used in the new design methodology. This method is bases its calculations in empirical equations based in historic aircraft data.
This module receives information from the preliminary 3D models of the mechanism components and initially determines the weight of the mechanism by adding the individual weight of each component. The total weight of the mechanism is then used to determine the total weight of the flap system. The process of determining the total Trailing Edge Flap System is presented in Section 3.9.2 and it provides results that are within reason. Though, the author considers that the estimated total weight of the flap cannot be taken as an accurate measure of real mechanisms weight. This is mainly because of the 2 dimensional nature of this initial study. There are many more parameters involved in the design of a 3D Trailing Edge flap device. At this stage of the design process the results obtained are only representative within the different mechanisms analysed.

Lift and Fairing Drag

Once again, information regarding the estimation of the Drag of flap system fairing structures was very limited. There was the possibility of using CFD to perform the calculations of the values required, but due to the fact that the author had never used CFD and was already involved it the learning process of the SYNAMEC software, it was decided to use other methods. This module analysis the aerodynamic performance at the take-off configuration and estimates the increments in drag associated with the fairings of the different types of Trailing Edge High Lift devices. The analysis performed in this module is confined to a theoretical basis and is performed using methods provided by ESDU datasheets.
The fairing preliminary dimensions were obtained from the 3D mechanism CAD model dimensions and used to calculate an associated Drag coefficient. Also from the 3D CAD model, the gap and overlap for the landing phase was measured and the ΔC_{LMax} calculated. The results obtained are within the range of values expected but it is impossible to guarantee that they are 100 % correct. But as in

the Weight estimation module, these values are perfect to perform comparisons between the different mechanisms analysed.

Reliability

Reliability assessment is not typically performed at the early stages of design process. Because of this there isn't available a known methods of doing it at this stage. To estimate the reliability in this new design methodology a variation of the 'Part Count' Reliability Prediction method [118] with data from NPDR-95 (Nonelectronic Part Reliability Data) [69] was used.
Every mechanism type has a characteristic and specific number of components, this module analyses the different mechanisms in terms of number of parts, and mechanical connections and assigns a reliability value to the overall mechanism. The results of this assessment are used as a measure of comparison between the different types of mechanism. The results might not be totally accurate but are enough to allow the designer to select the most reliable from within a group of viable mechanisms.

Maintainability

Maintainability assessment in the design methodology was performed using the procedure from MIL-HDBK-472. This method is supposed to be performed by experienced designers in Maintainability with adequate knowledge of the system design and operation, which isn't the case in this study, as the author lacks experience in maintainability of High-Lift Systems. The author tried to use engineering common sense and tried to be consistent in the analysis of the problem, but some errors might have been made inadvertently. This means that any result obtained by the author has to be used with caution. Once again, the results were used only to compare the different mechanisms under analysis between themselves, and classify them in terms of their MTTR.

Cost Estimation

This module uses simple cost estimation methods to look into the costs of the Trailing Edge Flap systems, as function of the weight and system part count, and the cost of increased drag arising from the different fairing structures of the mechanisms studied. Some assumptions were made due to the lack of information available about this subject. The results obtained, once again, might not be the most accurate but will allow the author to compare the costs of the different design solutions.

Selection Process

The selection process used in this research study is a simple and quick method to classify the different mechanisms analysed. The process focused on a set of attributes that were relevant for this research study and did not look at relative importance between them. In reality each attribute has different significance when looking at the design requirements. The requirements and specs for the different aircraft can be defined by numerous sources, but they have to fundamentally look at the needs of the aircraft operator, whether it's an airline company or the air forces. If the end user is an airline, then the weight and direct operational costs

might be the driving attributes. This is also valid for other aircraft types. Military aircraft, depending on the role, have a different set of attributes, like takeoff and landing distances, manoeuvrability and Maintainability & Reliability.
In more advance stages of the conceptual design process and based on the design requirements, different weights (multiplication factors) should be assigned to the different attributes and used to obtain the final weighted scores for each mechanism design. The fact that the author did not assigned weights to the different attributes might have been the reason why the results between the different mechanisms were so close.

6.3. VALIDATION AND CASE STUDY

The biggest problem encountered during the development of this research study was where to obtain information for the validation of the design methodology. Unsuccessful contacts were made with a Manufacturer and several Airlines in order to try to have access to some form of information related with the several topics of the study. This has lead to limited validation of the design methodology, but a limited number of validation exercises were performed, based on results and conclusions available from experts in the design of High-Lift devices, and other areas of relevant importance, and gave some confidence in the methodology. The author is quite sure that if more information was available, the results could have been more realistic.

The main objective of this research was achieved in the form of a validated multidisciplinary design methodology for mechanisms of wing trailing edge High-Lift devices. A case study was carried out using the design methodology and looked at the application of the innovative VCW concept to the ATRA – Advanced Transport Regional Aircraft, showing that the application of the methodology in the design of aeronautical mechanisms is viable.

In this study the author performed all the tasks in the different modules of the methodology. The lack of experience in the design of Trailing Edge High Lift device made it initially difficult for the author to fully grasp the real problems of the design of these devices. For this methodology to be used in an optimum way, it requires that each module to be run by a specialist on that area, but integrated in a single team. The designer has to be familiar with the variety of tools from the different disciplines, and have full knowledge of the aircraft design process and the impact of the different disciplines in the design process. This is a very different approach to the current trend, where each engineering discipline is a separate team in the design organization. This might be one of the difficulties in the implementation of this design methodology in an aircraft design office. The methodology could be expanded to incorporate more expert knowledge in integrated help functions to aid designers.

Although some approaches are simplistic, the main objective was to provide an innovative design methodology that would include from the outset disciplines not common at the initial stages of the design. This objective has been achieved and could be used as the basis for further developments.

CHAPTER 7

CONCLUSIONS & FUTURE WORK

7.1. CONCLUSIONS

The aim of this research study was to develop an innovative design methodology for the design of trailing edge high lift device mechanisms for commercial transport aircraft. This was achieved, and the design methodology was validated and demonstrated by performing a case study on the Cranfield University ATRA project.
The following conclusions can be drawn taken from the development of the new design methodology:

- The synthesis and optimization capabilities provided by the SYNAMEC design tool allow the study of more solutions in a given time and there is the scope for the development of new ideas and concepts.
- The methodology allows the designer to assess different solutions, taking in to consideration issues not usually accessible at the initial stages of the design, such as Weight, R&M and Cost.
- It allows a faster design process by removing the human "trial and error" characteristic of traditional design methodologies, and has the potential to proportionately decrease the amount of time and money spent in the preliminary design of aeronautical mechanisms. It is thus possible to get better results earlier in the design process
- The use of the new Visual Basic application for the sizing of mechanism components has improved the speed and the accuracy of the design process.
- The methodology allows the designer to have more information available to help in the selection of the most appropriate mechanisms for a specific application.
- The case study has shown that in comparison with other viable mechanism solutions, the Link/Track mechanism stands out as the most appropriate for the ATRA VCW concept.
- The different modules of the methodology can be used individually for improvement of current mechanism applications.
- Due to the increased influence of HL devices on the A/C performance, it is important that issues like Reliability & Maintainability, Weight Estimation and Cost, be included at the earliest stages of the design process.
- It is possible to create with success a methodology that incorporates from the outset R&M, Weight estimation and Cost.
- It is very important to be able to have access to aircraft data in the realization of a project of this type, in order to obtain more accurate results.

Finally, the author would like to point out that the Design Methodology developed in this research study represents a simplistic approach when compared with the complex design process of High Lift Devices and a great number of assumptions were made in order for the author to complete the study on time. The author had to make these assumptions mainly due to the limited amount of data and information on High Lift device mechanisms available from previous research studies and from aircraft manufacturers.

7.2. RESEARCH CONTRIBUTIONS

The research developed by the author contributes to the current body of knowledge in 4 different areas.

7.2.1. Contribution to academic theory

This research study provides a new design approach using the innovative SYNAMEC software and a program developed by the author for Initial Sizing of Mechanism Components. There were also contributions on the innovative subject of Variable Camber Wing concepts, through the application of the methodology in a Case Study.

7.2.2. Contribution to the High Lift Device topic

The review of traditional design methodologies and current High-Lift device systems carried out by the author contributes to the existing knowledge of High-Lift devices. Also, it presents an innovative design process that positively adds to the current research and development on the design of High-Lift device mechanisms. The case study has proven the suitability of the new design methodology in helping the author in the process of selecting the most appropriate mechanism from a group of viable solutions.

7.2.3. Contribution to aircraft design practice

The traditional aircraft design methodologies researched by the author were found to miss the inclusion of R&M and cost from the outset of the design process. The new design methodology looks into Reliability & Maintainability and cost from the outset of the design process and provides a platform for further developments and its implementation at higher levels of the aircraft design process.

7.2.4. Contribution to initial sizing topic

The development of the new sizing methodology with Software application applicable to mechanism components has helped the author by making the process quicker and more accurate, making it a valuable contribution for this topic.

7.3. RECOMMENDATIONS FOR FUTURE WORK

Further developments can be pursued as a continuing research effort towards the development and improvement of the High-Lift Devices Design process.
Regarding the methodology itself, the author has the following recommendations:

1) Apply the methodology to military aircraft and other types of aeronautical mechanisms.
2) Update the methodology to cope with 3D flap configurations.
3) Update the methodology to include the analysis and design of mechanisms with linear actuation systems.
4) Include in the methodology the analysis of the electronics and other systems that are part of a flap system.
5) Expand the methodology to include the manufacturing of prototypes. This can be done using the capabilities of the CATIA software to generate Machining programs and directly transfer them to different types on CNC machines for component manufacturing and ultimately mechanism assembly and testing.

The next recommendations are directed at each of the individual modules of the design methodology and target all the aspects that could be further developed or improved.

SYNAMEC Software

- Revisit the design methodology using the most recent version of the software with improved synthesis and optimization functionalities.
- Perform optimization of 3D mechanism model and look at interference between aircraft structures

Initial Sizing of Mechanism Components

- Develop more accurate sizing methods, accounting for 3D Mechanisms.
- Include Weight Estimation in the Initial Sizing Software application.
- Extend the Initial Sizing Software application to include LE device mechanism Load Calculations.
- Include FE analysis of mechanisms.

Reliability and Maintainability

- Improve estimation process by looking into more adequate processes of determining the reliability and maintainability of whole flap systems at the early stages of the design process.
- Revisit Reliability & Maintainability estimation if access to Aircraft relevant data is made available.

Lift & Fairing Drag

- Use CFD to perform the Lift and Fairing Drag calculations

Cost Estimation

- Improve estimation process by looking into more adequate processes of determining the cost of whole flap systems at the early stages of the design process.
- Develop a tool to analyse the cost of manufacturing components having in consideration the different manufacturing process.

Selection Process

- Assign different weights to the different attributes to obtain a weighted score for each mechanism design.

REFERENCES

REFERENCES

[1] AMMOO, M.S., "Development of a Design Methodology for Transport Aircraft Variable Camber Flaps Suitable for Cruise and Low-Speed Operations". PhD Thesis, Cranfield University, 2001.

[2] ANHALT, C., BREITBACH, E., SASHAU, D., "Realization of a Shape Variable Fowler Flap for Transport Aircraft". AIAA-2000-01-5572.

[3] BAUER, C., MARTIN, W., SIEGLING, H-F., "A New Structural Approach to Variable Camber Wing Technology of Transport Aircraft". AIAA-98-1756.

[4] BESNARD, E., SCHMITZ, A., BOSCHER, E., GARCIA, N. AND CEBECI, T., "Two-Dimensional Aircraft High Lift System Design and Optimisation". AIAA-98-0123, 1998.

[5] BEZY, O., "Investigation into a novel Flap and Slot Mechanism Concept". MSc Thesis, Cranfield University, 2003.

[6] BOLOKIN, A., GILYARD, G., "Estimated Benefits of Variable-Geometry Wing Camber Control for Transport Aircraft". NASA/TM-1999-206586, 1999.

[7] BRANDT, S.A., STILES, R.J., BERTIN, J. ., WHITFORD, R., "Introduction to aeronautics: A design perspective". Reston, VA: AIAA, 1997.

[8] BROOKS, T.F., POPE, D.S., MARCOLINI, M.A., "Airfoil Self-Noise and Prediction". NASA RP-1218, July 1989.

[9] BROSSEAU, J., "A-94 Red Aircraft Variable Camber Flap Design". MSc Thesis, Cranfield University, 1995.

[10] BUTTER, D.J., "Recent Progress on Development and Understanding of High-Lift Systems". AGARD CP-365 "Improvement of Aerodynamic Performance Through Boundary Layer Control and High-Lift Systems".

[11] CAHILL, J.P., "Summary of Section Data on Trailing Edge High Lift Devices". NACA, 1949.

[12] CALLAHAM, J.G., "Aerodynamic Prediction Methods for Aircraft at Low Speeds with Mechanical High-Lift Devices". AGARD LS - 67 "Prediction Methods for Aircraft Aerodynamic Characteristics".

[13] CARDONA, A, REMOUCHAMPS, A., SCHILS, P., "Integrated Software: SYNAMEC Validator". SYNAMEC Report Nr. D5.3, 2003.

[14] CARDONA, A., PUCHETA, M., LENS, E., "Software for Type Synthesis and Initial Sizing of Mechanisms". SYNAMEC Report Nr. D.2.3, 2004.

[15] DECOSTA, A.L., Ishimisu, K.K., Pickrel, C.R., Miller, D.S., Zierten, T.A., "Analytical investigation of variable camber concepts (Aerodynamic characteristics of two dimensional airfoils with variable camber and performance of Whitcomb supercritical airfoil). Report Nr. AD-740369, 1971

[16] DILLNER, B., MAY, F.W., McMASTERS, J.H., "Aerodynamic Issues in the Design of High-Lift Systems for Transport Aircraft". AGARD CP-365 "Improvement of Aerodynamic Performance Through Boundary Layer Control and High-Lift Systems".

[17] DOBRZYNSKI, W., "Trailing Edge Airframe Noise Source Studies on Aircraft Wings". Journal of Aircraft, Vol. 18, Nr. 5, 1981. pp. 397-402.

[18] DOBRZYNSKI, W., NAGAKURA, K., BUSCHBAUM, A., "Airframe Noise Studies on Wings with Deployed High-Lift Devices". AIAA Paper 98-2337. June 1998.

[19] DUYSENS, C., CARDONA, A., REMOUCHAMPS, A., "Synthesis Tool for Aeronautical Mechanisms Design (SYNAMEC European Project)", 2003.

[20] EDI, P., "Investigation of the Application of Hybrid Laminar Flow Control and Variable Camber Wing Design for Regional Aircraft". PhD Thesis, Cranfield University, 1998.

[21] ELMER, K., JOSHI, M., "Noise Impact of Advanced High Lift Systems". NASA CR-195028, 1995.

[22] FERRIS, J.C., "The Effect of a Variable Camber and Twist Wing at Transonic Mach Numbers". NASA TM-86281, December 1984.

[23] FIELDING, J.P., "Design Investigation of Variable Camber Flaps for High Subsonic Airliners". In: 22nd Congress of the International Council of Aeronautical Sciences (ICAS), Harrogate,UK, 27th August - 1st September 2000, pp. 0124.1-0124.11. Washington: AIAA, 2000.

[24] FIELDING, J.P., "Design Investigation of Variable Camber Flaps for High-Subsonic Airliners. ICAS 2000.

[25] FIELDING, J.P., "Introduction to Aircraft Design". Cambridge: Cambridge University Press, 2000.

[26] FIELDING, J.P., MACCI, S.H.M., MACKINNON, A.V., STOLLERY, J.L., "The Aerodynamic and Structural Design of a Variable Camber Wing". In: 18th Congress of the International Council of Aeronautical Sciences (ICAS), Vol. 2, Beijing, China, 20th - 25th June 1992, pp. 1098a-1098k. Washington: AIAA, 1992.

[27] FIELDING, J.P., VAZIRY-ZANJANY, M.A.F., "Reliability, Maintainability and Development Cost Implications of Variable Camber Wings". The Aeronautical Journal, Vol. 100, Nr. 995, May 1996, pp. 183-195.

[28] FINK, M.R., SCHLINKER, R.H., "Airframe Noise Component Interaction Studies". NASA CR-3110, March 1979.

[29] FLAIG A., HILBIG R., "High-lift design for large civil aircraft". High-Lift System Aerodynamics, AGARD CP 515, Sep. 1993. pp. 31-1–31-12.

[30] FOSTER, D.N., "A Review of the Low Speed Aerodynamic Characteristics of Aircraft with Powered-Lift Systems". AGARD LS - 67 "Prediction Methods for Aircraft Aerodynamic Characteristics".

[31] FROST, Richard C., GOMEZ, W. Eduardo, McANALLY, Robert W.: "Airfoil Variable Cambering Device and Method". US-Patent 4,247,066, 1981.

[32] GERADIN, M., CARDONA, A., "Kinematics and Dynamics of Rigid and Flexible Mechanisms using Finite Elements and Quaternion Algebra". Computational Mechanics, Vol. 4, 1989, pp115-135.

[33] GILBERT, William W., "Development of a Mission Adaptive Wing System for a Tactical Aircraft". 1980. AIAA-1886.

[34] GILBEY, R.W., "Information on the use of Data Items on High-Lift Devices". ESDU-97002. London, 1997.

[35] GILYARD, G., Cited in "Aerospace Technology Innovation", Volume 5, Number 4. July/August 1997.

[36] GILYARD, G., ESPAÑA, M., "On the Use of Controls for Subsonic Transport Performance Improvement: Overview and Future Directions". NASA/TM – 4605.

[37] GILYARD,G., BARNICKI, J., "Flight Test of an Adaptive Configuration Optimization System for Transport Aircraft". NASA/TM-1999-206569,Edwards, California, 1999.

[38] GREFF, E., "Aerodynamic design and technology concepts for a new ultra high capacity aircraft". ICAS-96-4.6.3, 1996.

[39] GREFF, E., "Aerodynamic Design for a New Regional Aircraft". In: 17th Congress of the International Council of Aeronautical Sciences (ICAS), Vol. 2, Stockholm, Sweden, 9th-14th Sept. 1990. New York: ICAS, 1990.

[40] GREFF, E., "The Development and Design Integration of a Variable Camber Wing for a Long/Medium Range Aircraft". The Aeronautical Journal, Vol. 94, Nr. 939, Nov. 1990, pp. 301-312.

[41] GUO, Y.P., JOSHI, M.C., "Noise Characteristics of Aircraft High Lift Systems". AIAA Journal, Vol. 41, Nr. 7, 2003. pp. 1247-1256

[42] GUO, Y.P., YAMAMOTO, K.J., STOKER, R.W., "Component-Based Empirical Model for High-Lift System Noise Prediction". Journal of Aircraft, Vol. 40, Nr. 5, 2003. pp. 914-922.

[43] HARDIN, POTTER, VAN DAM, YIP, "2 Dimensional Computational Analysis of a Transport High-Lift System and Comparison with Flight-Test Results". AIAA-93-3533.

[44] HERFRIED, HENRY, "Wing with Extendable Flap and Variable Camber". Patent Nr. US-4725026.

[45] HILBIG, H., WAGNER, H., "Variable Camber Control for Civil Transport Aircraft". In: 14th Congress of the International Council of Aeronautical Sciences (ICAS), Vol. 1, Toulouse, France, 9-14 Sept. 1984. New York : AIAA, 1984.

[46] HILBIG, SZODRUCH, "The intelligent Wing – Aerodynamic Developments for Future Transport Aircraft". AIAA-89-0534.

[47] HOLT, D.R., PROBERT, B., "Some Particular Configuration Effects on a Thin Supercritical Variable Camber Wing". In: AGARD Congress on "Subsonic/Transonic Configuration Aerodynamics", Munich, Germany, 5th-7th May 1980. London: AGARD, 1980.

[48] HOWE, D., "Aircraft conceptual design synthesis", Professional Engineering Publishing, London, 2000.

[49] HOWE, M.S., "A Review of the Theory of Trailing Edge Noise". NASA CR-3021, June 1978.

[50] HOWE, M.S., "On the Generation of Side-Edge Flap Noise". NASA CR-3437, June 1981.

[51] LAJUX, V., FIELDING, J.P., "Development of the SYNAMEC – A Design Tool for Aeronautical Mechanisms Applied to Leading Edge Devices". ICAS 2004.

[52] MACCI, S.H.M., "Aircraft Wing Weight Prediction". MSc Thesis, Cranfield University, 1988.

[53] MACCI, S.H.M., "Structural and Mechanical Feasibility Study of a Variable Camber Wing (VCW) for a Transport Aircraft". PhD Thesis, Cranfield University, 1992.

[54] MACEY, P., "A Feasibility Study on the Application of Variable Camber Flaps on a Military Tactical Transport Aircraft". MSc Thesis, Cranfield University, 1993.

[55] MACKINNON, A.V., "An Experimental Study of a Variable Camber Wing (VCW)". PhD Thesis, Cranfield University, 1993.

[56] MARSHALL AEROSPACE STRESS MANUAL, Unpublished, 2002.

[57] MARTIN, G.H., "Kinematics and Dynamics of Machines", 2nd Edition. New York: McGraw-Hill, 1982.

[58] MASON, W., "Leading Edge – Trailing Edge Airfoil Interactions". AIAA-95-0436.

[59] MCMASTERS, J.H., "Rethinking the Airplane Design Process – An Early 21st Century Perspective". AIAA-2004-0693.

[60] MCRAE, D.M., "Aerodynamics of Mechanical High-Lift Devices". AGARD LS - 43 "Assessment of Lift Augmentation Devices".

[61] MEADOW, L.J., "A85 Project Design – Trailing Edge Flap System". MSc Thesis, Cranfield University, 1986.

[62] MIL-HDBK-472, "Maintainability Prediction". Department of Defence, Washingthon D.C., 1966.

[63] MONNER, H., BREITBACH, E., HANSELICA, T., "Design Aspects of the Adaptive Wing – The Elastic Trailing Edge and the Local Spoiler Bump".

[64] MONNER, H.P., BREITBACH, E., BEIN, T., HANSELKA, H., "Design Aspects of the Adaptive Wing – the Elastic Trailing Edge and the Local Spoiler Bump". The Aeronautical Journal, Vol. 104, Nr. 1032, February 2000, pp.89-95.

[65] NASH, S.M., ROGER, S.E., "Numerical Study of a Trapezoidal Wing High-Lift Configuration". AIAA 1999-01-5559.

[66] NIELD, B.N., "An overview of the Boeing 777 high-lift aerodynamic design". Aeronautical Journal, Vol. 99, Nr. 989, Nov.1995, pp.361-371.

[67] NIU, M.C.Y., "Airframe Structural Design". Hong Kong: CONMILIT PRESS Ltd., 1991.

[68] NIYOMTHAI, "A97 Project Design – Trailing Edge Flap". MSc Thesis, Cranfield University, 1998.

[69] NPRD-95 - Nonelectronic Parts Reliability Data. RAC - Reliability Analysis Center, 1994.

[70] PEPPER, R.S., VAN DAM, C.P., "Design Methodology for Multi-Element High-Lift Systems on Subsonic Civil Transport Aircraft (Final Report)". NASA-CR-202365, 1996.

[71] PEPPER, R.S., VAN DAM, C.P., GELHAUSEN, P.A., "Design Methodology for High-Lift Systems on Subsonic Aircraft". In: 6th AIAA/NASA/ISSMO Symposium on Multidisciplinary Analysis and Optimization, AIAA Paper 96-4056-CP, Bellevue, WA, 4th-6th Sept. 1996. Reston, VA: AIAA, 1996.

[72] PIRES, R.M.M., LAJUX, V., FIELDING, J.P., "Methodology for the Design and Evaluation of Wing Leading and Trailing Edge Devices". ICAS 2006

[73] PROBERT, B., "Aspect of Wing Design for Transonic and Supersonic Combat Aircraft".

[74] PROBERT, B., "High Lift Devices-Aerodynamic Design". MSc. Course Lecture Notes in Aircraft Engineering, Cranfield University, 2000.

[75] Proceedings of "Evolution of A/C wing design symposium", AIAA, 1980.

[76] RAO, A.J., "Variable Camber Wings for Transport Aircraft". PhD Thesis, Cranfield University, 1989.

[77] RAYMER, D.P., "Aircraft Design: A conceptual Approach". 3rd Edition. AIAA Education Series. 1999.

[78] REMOUCHAMPS, A., CARDONA, A., GLIZE, P., "Validation by Simulation on Generic Models". SYNAMEC Report Nr. D4.3, 2004.

[79] RENEAUX, J., "Overview on Drag Reduction Technologies for Civil Transport Aircraft". ECCOMAS 2004. July 2004

[80] RENKEN, J.H., "Integration of a Variable Wing Camber Function into an EFCS of a Transport Aircraft". AIAA-87-2879.

[81] ROSENAUER, N, WILLIES, A.H., "Kinematics of Mechanisms". New York: Dove Publications, 1967.

[82] ROSKAM, J., "Airplane Design – Part III". University of Kansas, 1986.

[83] ROSS, J.C., STORMS, B.L., "Tip Fence for Reduction of Lift-Generated Airframe Noise". NASA nr 1999000858. 1999.

[84] RUDNIK, R., ELIASSON, P., PERRAUD, J., "Evaluation of CFD Methods for Transport Aircraft High Lift Systems". The Aeronautical Journal, Volume 109, Number 1092, February 2005.

[85] RUDOLPH, P.K.C., "High-Lift Systems on Commercial Subsonic Airliners". NASA/CR-4746, 1996.

[86] RUDOLPH, P.K.C., Mechanical Design of High-Lift Systems for High Aspect Ratio Swept Wings". NASA/CR-196709, 1998.

[87] SELLARS, N., "High Lift Lecture". BAe Systems. Cranfield University Lecture, 2003.

[88] SERGHIDES, V.C., "Development of a Reliability and Maintainability Prediction Methodology for the Aircraft Conceptual Design Process". MSc THESIS, Cranfield University, 1985.

[89] SIEWERT, R.F., WHITEHEAD, R.E., "Analysis of Advanced Variable Camber Concepts". In: AGARD Conference on "Fighter Aircraft Design", Florence, Italy, 3rd-6th October 1977. London: AGARD, 1978.

[90] SIEWERT, R.F., WHITEHEAD, R.E., "Analysis of Advanced Variable Camber Concepts". AGARD CP-241 "Fighter Aircraft Design".

[91] SLOOFF, J.W., WOLF, W.B., VAN DER WAL, H.M.M., MASELAND, J.E.J., "Aerodynamic and Aero-Acoustic Effects of Flap Tip Fences". AIAA Paper 2002-0848, January 2002.

[92] SMITH, "Aerodynamics of High-Lift Airfoil Systems". AGARD CP-102 "Fluid Dynamics of Aircraft Stalling".

[93] SMITH, M.G., CHOW, L.C., "Aerodynamic Noise Sources on High Lift Slats and Flaps". AIAA Paper 2003-3226, May 2003.

[94] SMITH, S.B., NELSON, D.W., "Determination of Aerodynamic Characteristics of the Mission Adaptive Wing". In: 6th AIAA Applied Aerodynamics Conference, Virginia, USA, 6th-8th June 1988. Washington: AIAA, 1988.

[95] SOMMERER, A., LUTZ, T., WAGNER, S., "Numerical optimisation of adaptive transonic airfoils with variable camber". In: 22nd Congress of the International Council of Aeronautical Sciences, Harrogate, UK, 27th Aug. - 1st Sept. 2000, ICA2111.1-10. Washington: AIAA, 2000.

[96] SOMMERER, A., LUTZ, W., "Numerical Optimization of Adaptive Transonic Airfoils with Variable Camber". ICAS 2000.

[97] SPILLMAN, J.J., "The Potential of Using Variable Camber Across the Span of an Aircraft". CoA Report Nr. 8801. Cranfield University, 1988.

[98] SPILLMAN, J.J., "The Use of Variable Camber to Reduce Drag, Weight and Costs of Transport Aircraft". The Aeronautical Journal, Vol. 96, Nr. 951, Jan. 1992, pp. 1-9.

[99] SPILLMAN, J.J., "Variable Camber Geometry for Transport Aircraft Wings". In: Proceedings of "Aerotech 92" Conference, London, UK, 14th-17th Jan. 1992. London: Institution of Mechanical Engineers, 1992.

[100] STOCKING, P., "Introduction to Stress Analysis". Cranfield University Lecture Notes. 2005.

[101] SYNAMEC – Synthesis Tool for Aeronautical Mechanism Design. Final Report. SAMTECH, Liege, Belgium, 2004

[102] SZODRUCH, J., HILBIG, R., "Variable Camber for Transport Aircraft". Progress in Aerospace Sciences, Vol. 25, Nr. 3, 1988, pp. 297-328.

[103] SZODRUCH, J., SCHNIEDER, H., "High Lift Aerodynamics for Transport Aircraft by Interactive Experimental and Theoretical Tool Development". In: AIAA 27th Aerospace Sciences Meeting, Reno, Nevada, 9th-12th January 1989. Washington, D.C: AIAA, 1989.

[104] TORENBEEK, E., "Synthesis of Subsonic Airplane Design". Delft: Delft University Press, 1982.

[105] VAN DAM, C., SHAW, S., VANDER, J., RUDOLPH, P.K.C., KINNEY, D., "Aero-Mechanical Design of High-Lift Systems". Aircraft Engineering and Aerospace Technology Journal, Vol. 71. Nr. 5, 1999. pp. 436-443.

[106] VAN DAM, C.P., "The Aerodynamic Design of Multi-Element High-Lift Systems for Transport Aircraft". Elsevier Science Ltd. Progression in Aerospace Sciences, Nr 38, 2002, pp. 101-144.

[107] VAN DAM, C.P., KAM, J.C.V., PARIS, J.K., "Design-oriented high-lift methodology for general aviation and civil transport aircraft". Journal of Aircraft, Vol. 38, Nr. 6, Nov.-Dec. 2001, pp. 1076-1084.

[108] VAN DER DECKEN, J., "Aerodynamics of Pneumatic High-Lift Devices". AGARD LS - 43 "Assessment of Lift Augmentation Devices".

[109] VARIZY-Z, M.A.F., FIELDING, J.P., "Computer Aided Conceptual Aircraft Design (CACAD) for Transport Aircraft". CU/COA/R-9608 Report. Cranfield University, 1996.

[110] VAZIRY-ZANJANY, "Aircraft Conceptual Design Modelling Incorporating Reliability and Maintainability Predictions". PhD Thesis. Cranfield University, 1996.

[111] WEDDERSPOON, J.R., "High lift research and its application to aircraft design". In: 12th Congress of the International Council of the Aeronautical Sciences, Munich, Germany, 12th-17th Oct. 1980, pp. 480-493. New York: AIAA, 1980.

[112] WILLIAMS, J., "Aircraft Performance Consideration for Noise Reduction". AGARD LS - 67 "Prediction Methods for Aircraft Aerodynamic Characteristics".

[113] WILLIAMS, J., "General Technical Introduction". AGARD LS - 67 "Prediction Methods for Aircraft Aerodynamic Characteristics".

[114] . "Advanced Topics on Aerodynamics" Website http://aerodyn.org/

[115] . "Aircraft Mass Prediction – Structural Components" – DAeT 9317 Lecture Note. College of Aeronautics, Cranfield University, 2000.

[116] . "Design of Auxiliary Surfaces". DAeT 9574 Lecture Note. College of Aeronautics, Cranfield University, 2000.

[117] . "Mechanization and Utilization of Variable Camber in Fighter and Attack Airplanes", BOEING – D180-15377-1.

[118] . "Parts Count' Reliability Prediction" – AVD 0405, Lecture Note. Cranfield University

[119] . "Quest for Performance: The Evolution of Modern Aircraft" – Website. http://www.hq.nasa.gov/office/pao/History/SP-468/contents.htm

[120] . "Reliability Prediction Methods for Use in Aircraft Design" – DAeT 9542 Lecture Note. Cranfield University.

[121] . "Stressing Data Sheets". AVT-AVD 9632 -Lecture Note. College of Aeronautics, School of Engineering, Cranfield University, 1999.

[122] . "V/STOL Aircraft Structures", Cranfield University Lecture Note AVD0014. 2001.

[123] . "Wing Design Requirements and Construction Methods". DAeT 9573 Lecture Note. College of Aeronautics, Cranfield University, 2000.

[124] . Desktop Aeronautics, INC. Website.
"http://www.desktopaero.com"

[125] . WIKIPEDIA Website
"http://www.wikipedia.com"

[126] . .School of Aerospace, Mechanical & Mechatronic Engineering – University of Sidney
"http://www.aeromech.usyd.edu.au"

[127] ."A320 Briefing" – AIRBUS INDUSTRIES Catalogue.

[128] Certification Specifications for Large Aeroplanes CS-25. Amendment 4. European Aviation Safety Agency. December 2007.

APPENDIX A

ATRA SPECIFICATIONS

TABLE OF CONTENTS

A1 – ATRA GENERAL SPECIFICATIONS

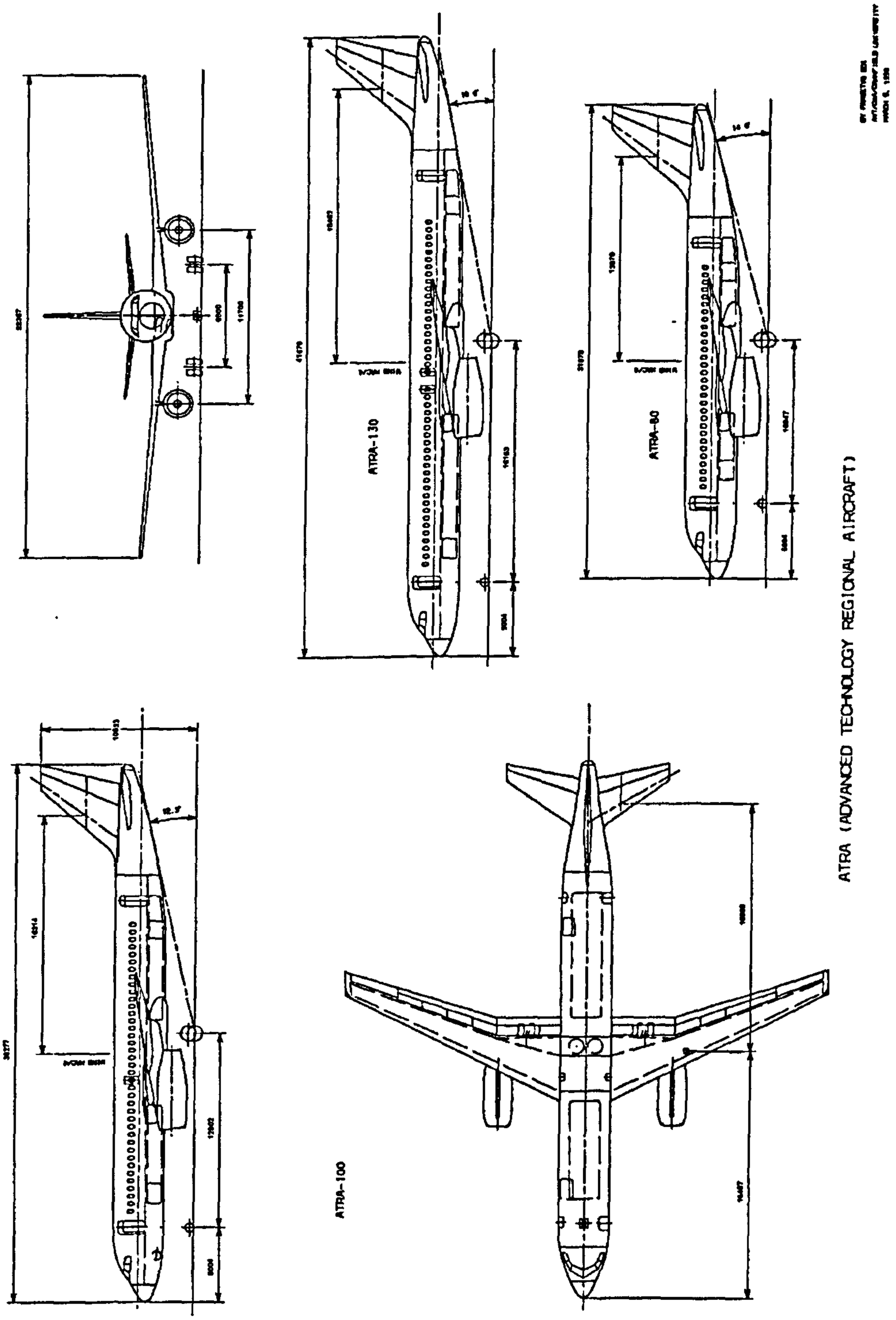

Figure A21 – ATRA (Advanced Technology Regional Aircraft) [20]

	ATRA-80	ATRA-100	ATRA-130
Number of Passenger	83	108	133
Range, nm/km	2000/3706	2250/4170	2500/4633
Speed, Mach			
landing	0.2	0.2	0.2
take-off	0.2	0.2	0.2
cruise	0.8	0.8	0.8
Lift Coefficient, C_L			
landing (max.)	2.9	2.9	2.9
take-off (max.)	2.2	2.2	2.2
cruise	0.49	0.51	0.53
Wing (A320 Type)			
aspect ratio, A	9.5	9.5	9.5
taper ratio, l	0.274	0.274	0.274
0.25 sweepback, $\Lambda_{0.25}$	25	25	25
span, b (m)	32.357	32.357	32.357
area, S (m^2)	110.21	110.21	110.21
mass, m (kg)	5811.13	5811.13	5811.13
root chord, cr (m)	6.673	6.673	6.673
tip chord, ct (m)	1.586	1.586	1.586
mean aero. chord, MAC	3.439	3.439	3.439
t/c root	13%	13%	13%
t/c tip	9%	9%	9%
trailing-edge flap	single-slotted	single-slotted	single-slotted
leading-edge flap	vented Kruger	vented Kruger	vented Kruger

Figure A22 – ATRA Family Specifications [20]

MAC = 3.439 M
ROOT CHORD (CR) = 6.673 M
TIP CHORD (CT) = 1.586 M
SOB CHORD (CSOB) = 5.790 M
TAPER RATIO = CT/CSOB = 0.274
C/4 SWEEP ANGLE = 25 DEG
SPAN = 32.357 M
ASPECT RATIO = 9.5
AREA = 110.21 SQ.M

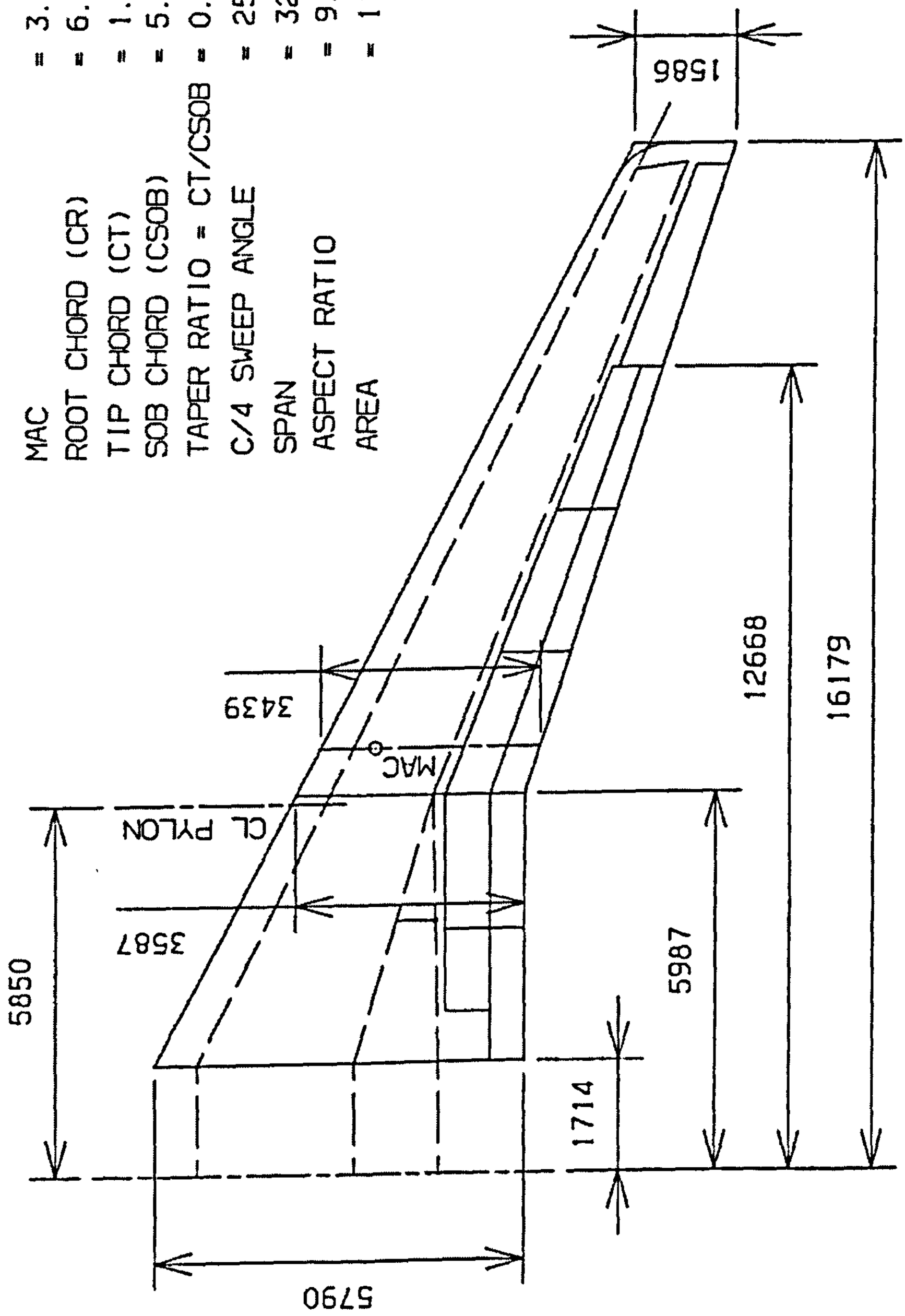

Figure A23 - ATRA Wing Concept [20]

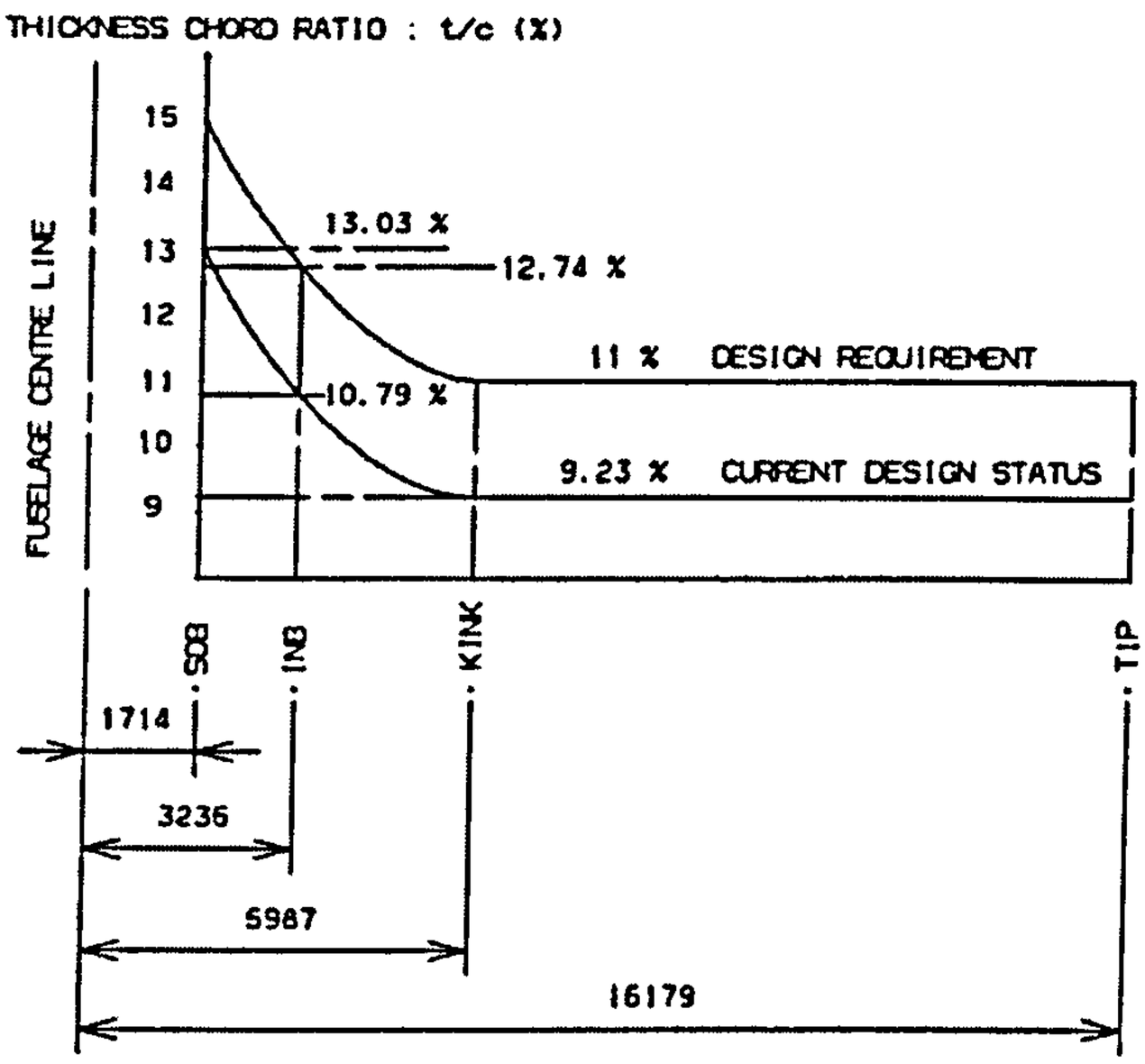

Figure A24 - ATRA wing Thickness Distributions [20]

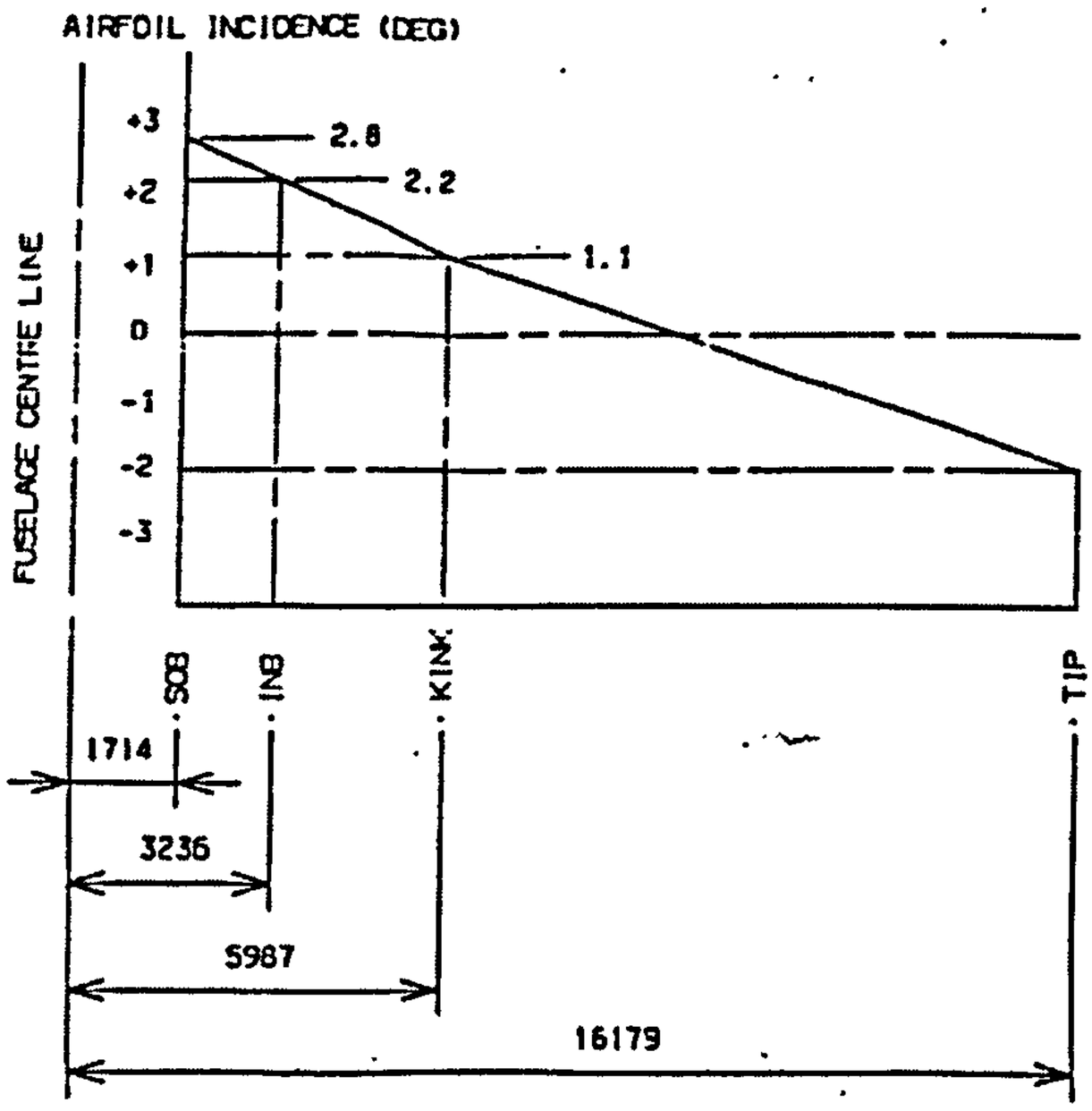

Figure A25 - ATRA wing Twist [20]

	W.Sta.2782	W.Sta.4920	W.Sta.7100	W.Sta.9328	W.Sta.11555
chord, mm	5240	4138	3369	2932	2494
0.0125c	65.50	51.73	42.11	36.65	31.18
t/c	0.135	0.118	0.109	0.107	0.103
$z_{u1.25}$, mm	124.71	88.55	65.36	54.54	44.14
$z_{u1.25}/c$	0.0238	0.0214	0.0194	0.0186	0.0177
x_{um}, mm	2214	1749	1418	1243	1067
z_{um}, mm	387	269	206	177	147
x_{um}/c	0.4226	0.4226	0.4209	0.4238	0.4278
z_{um}/c	0.0739	0.065	0.0611	0.0602	0.0589
x_{ts}, mm	4716	3600	2864	2492	2120
c_{tl}, mm	1228	1228	1179	1024	872
y_{90}, mm	95.9	70.8	51.9	44.9	37.9
y_{99}, mm	7.9	8.3	7.1	5.9	5.0
y_{90}/c	0.0183	0.0171	0.0154	0.0153	0.0152
y_{99}/c	0.0015	0.002	0.0021	0.002	0.002
τ, degree	6.99	6.43	6.03	5.97	5.88

Figure A26 - ATRA Wing Airfoil Parameters [20]

A2 – ATRA WING AND FLAP GEOMETRIC DATA

A2.1 - Wing Airfoil Data [1]

Wing Airfoil SOB

(b/2=1714mm)

X	Z
5239.597	1.473
4940.311	74.949
4578.826	156.056
4217.341	222.482
3855.855	275.586
3494.368	316.130
3132.882	344.791
2771.396	362.263
2409.909	370.932
2048.423	371.263
1686.936	362.713
1325.450	344.717
963.964	316.730
602.477	274.044
240.991	200.568
80.330	133.284
0.000	0.000
80.330	-78.368
240.991	-132.042
602.477	-210.860
963.964	-266.127
1325.450	-304.036
2048.423	-335.695
2409.909	-325.204
2771.396	-293.758
3132.882	-236.923
3494.368	-160.402
3855.855	-79.021
4217.341	-11.825
4578.826	26.910
4940.311	26.270
5239.597	1.473

Wing Airfoil Inboard

(b/2=3235.8 mm)

X	Z
4138.319	0.817
4069.974	18.720
3888.249	61.918
3580.381	123.495
3254.874	175.509
2929.367	215.003
2603.860	243.078
2278.352	260.744
1952.845	268.960
1627.338	269.768
1301.831	262.893
976.324	246.633
650.816	219.251
325.309	174.432
72.137	101.269
0.000	0.000
72.137	-69.618
325.309	-130.679
650.816	-173.051
976.324	-200.134
1301.831	-215.756
1627.338	-219.199
1952.845	-209.683
2278.352	-183.364
2603.860	-134.949
2929.367	-69.381
3254.874	-9.306
3580.381	22.667
3888.249	202.730
4069.974	5.798
4138.319	0.817

Wing Airfoil Kink

(b/2=5987 mm)

X	Z
3369.118	0.000
3176.822	47.476
2888.020	100.437
2599.218	141.786
2310.416	171.963
2021.614	191.793
1732.812	202.244
1444.010	206.146
1155.208	203.039
1058.941	200.194
866.406	191.460
673.871	178.291
481.337	160.230
192.535	116.170
96.267	89.342
0.000	0.000
96.267	-75.245
192.535	-97.059
481.337	-132.996
673.871	-146.840
866.406	-155.115
1058.941	-159.835
1155.208	-161.123
1444.010	-159.046
1732.812	-144.782
2021.614	-113.778
2310.416	-60.171
2599.218	-4.769
2888.020	23.233
3176.822	16.068
3369.118	0.000

Wing Airfoil Outboard

(Between b/2=5987 mm and b/2=16178.5 mm)

X	Z
2931.792	0.000
2722.378	49.264
2471.082	92.923
2219.785	126.763
1968.489	151.097
1717.192	166.613
1465.896	174.348
1214.600	176.587
963.303	172.568
712.007	161.048
460.710	140.757
209.414	107.306
125.648	87.818
83.765	75.314
41.883	57.760
0.000	0.000
41.883	-48.116
83.765	-64.134
125.648	-74.834
209.414	-88.800
460.710	-115.989
712.007	-129.573
963.303	-135.444
1214.600	-134.908
1465.896	-124.745
1717.192	-101.410
1968.489	-59.438
2219.785	-11.715
2471.082	17.554
2722.378	16.648
2931.792	0.000

Wing Airfoil Tip

(b/2=16178.5 mm)

X	Z
2494.324	0.000
2351.791	34.055
2137.992	72.141
1924.193	101.793
1710.394	123.363
1496.594	137.422
1282.795	144.656
1068.996	147.056
855.197	144.414
641.398	135.636
427.598	119.727
213.799	94.487
142.533	80.645
71.266	61.320
35.633	46.784
0.000	0.000
35.633	-40.155
71.266	-53.094
142.533	-67.937
213.799	-77.676
427.598	-97.331
641.398	-106.782
855.197	-110.633
1068.996	-108.900
1282.795	-98.938
1496.594	-77.869
1710.394	-42.220
1924.193	-5.034
2137.992	15.310
2351.791	11.104
2494.324	0.000

A2.2 - Flap Airfoil Data [1]

Flap Airfoil @ b/2=2782mm

X	Z
1257.535	1.473
1122.535	34.767
923.587	83.281
621.776	141.569
421.776	147.797
321.776	137.354
221.776	118.214
121.776	84.474
100.108	74.354
80.108	63.939
60.108	52.026
40.108	37.659
30.336	29.523
21.776	21.326
15.096	13.737
5.096	-1.598
0.000	-21.187
16.000	-44.384
40.108	-45.425
60.108	-41.661
80.108	-37.965
100.108	-34.337
121.776	-30.489
221.776	-13.906
321.776	0.533
421.776	12.546
621.776	28.203
923.587	27.953
1122.535	13.939
1257.535	14.730

Flap Airfoil @ b/2=4920mm

X	Z
1257.535	0.817
1120.0	27.777
920.0	367.309
620.0	112.154
500.0	115.609
420.0	110.634
320.0	96.199
220.0	72.979
120.0	34.990
100.0	24.738
80.0	13.409
60.0	0.621
40.0	-14.703
30.0	-23.571
25.0	-28.464
20.0	-33.843
16.0	-38.633
10.0	-46.995
5.0	-55.928
0.0	-77.411
5.0	-90.565
10.0	-95.750
16.0	-99.453
20.0	-100.868
25.0	-101.699
30.0	-101.699
40.0	-100.111
60.0	-95.433
80.0	-90.819
100.0	-86.267
120.0	-81.795
220.0	-60.607
320.0	-41.615
420.0	-25.096
500.0	-13.882
620.0	-0.562
920.0	12.405
1120.0	7.169
1257.535	0.817

Flap Airfoil @ b/2=7100mm

X	Z
1093.2	0.0000
900.0	47.6700
800.0	67.5190
700.0	85.5300
500.0	111.9490
400.0	112.5500
300.0	101.6050
200.0	81.0020
105.0	46.6600
85.0	36.6270
65.0	25.3570
45.0	12.1400
25.0	-4.3310
15.0	-14.8230
5.0	-29.4740
0.0	-47.7240
5.0	-60.1700
15.0	-63.7410
25.0	-62.1390
45.0	-58.0140
65.0	-53.8860
85.0	-49.7650
105.0	-45.6600
200.0	-26.7060
300.0	-8.5960
400.0	6.4250
500.0	17.1950
700.0	24.4300
800.0	22.2740
900.0	16.1450
1093.2	0.0000

Flap Airfoil @ b/2=9328mm

X	Z
951.602	0.000
870.0	21.470
770.0	43.696
670.0	62.812
620.0	71.639
520.0	88.355
370.0	98.386
270.0	89.660
170.0	69.765
70.0	30.586
50.0	18.926
40.0	12.174
30.0	4.465
20.0	-43.240
10.0	-15.585
0.0	-40.234
5.0	-51.641
20.0	-53.227
30.0	-51.256
40.0	-49.283
50.0	-47.309
70.0	-45.335
170.0	-24.094
270.0	-6.727
370.0	7.238
520.0	18.829
620.0	20.455
670.0	19.661
770.0	14.695
870.0	6.517
951.602	0.000

Flap Airfoil @ b/2=11555mm

X	Z
809.3620	0.000
770.0	10.501
720.0	22.552
670.0	33.401
620.0	43.291
470.0	69.422
270.0	80.595
220.0	74.836
170.0	65.854
120.0	52.613
70.0	32.336
35.0	1.221
25.0	4.613
15.0	-43.640
5.0	-17.053
0.0	-32.700
5.0	-42.933
15.0	-44.135
25.0	-42.300
35.0	-40.448
70.0	-33.967
120.0	-24.842
170.0	-16.090
220.0	-7.951
270.0	-0.660
470.0	15.826
620.0	14.201
670.0	10.858
720.0	6.889
770.0	2.823
809.3620	0.000

A2.3 – Flap Pressure Distributions [1]

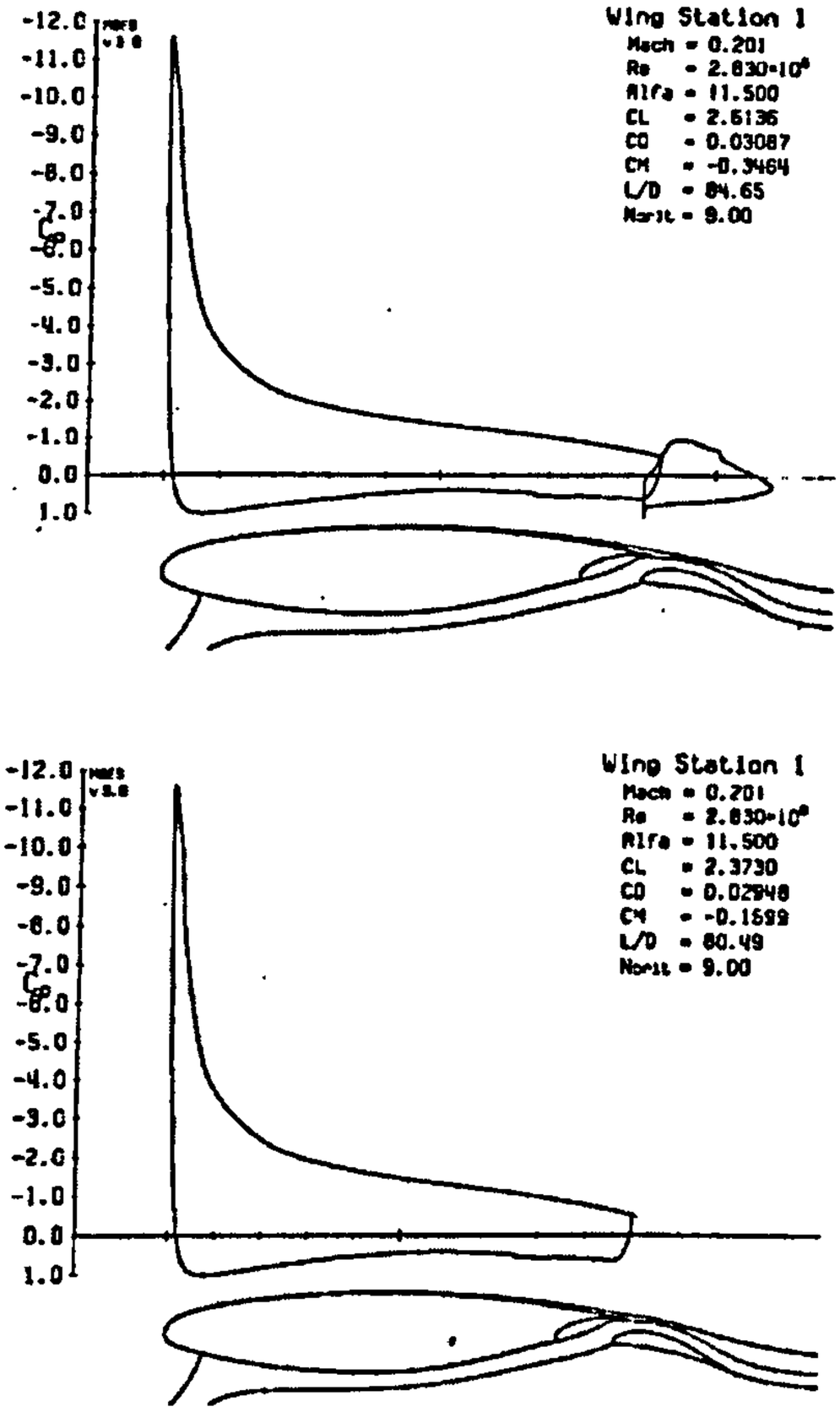

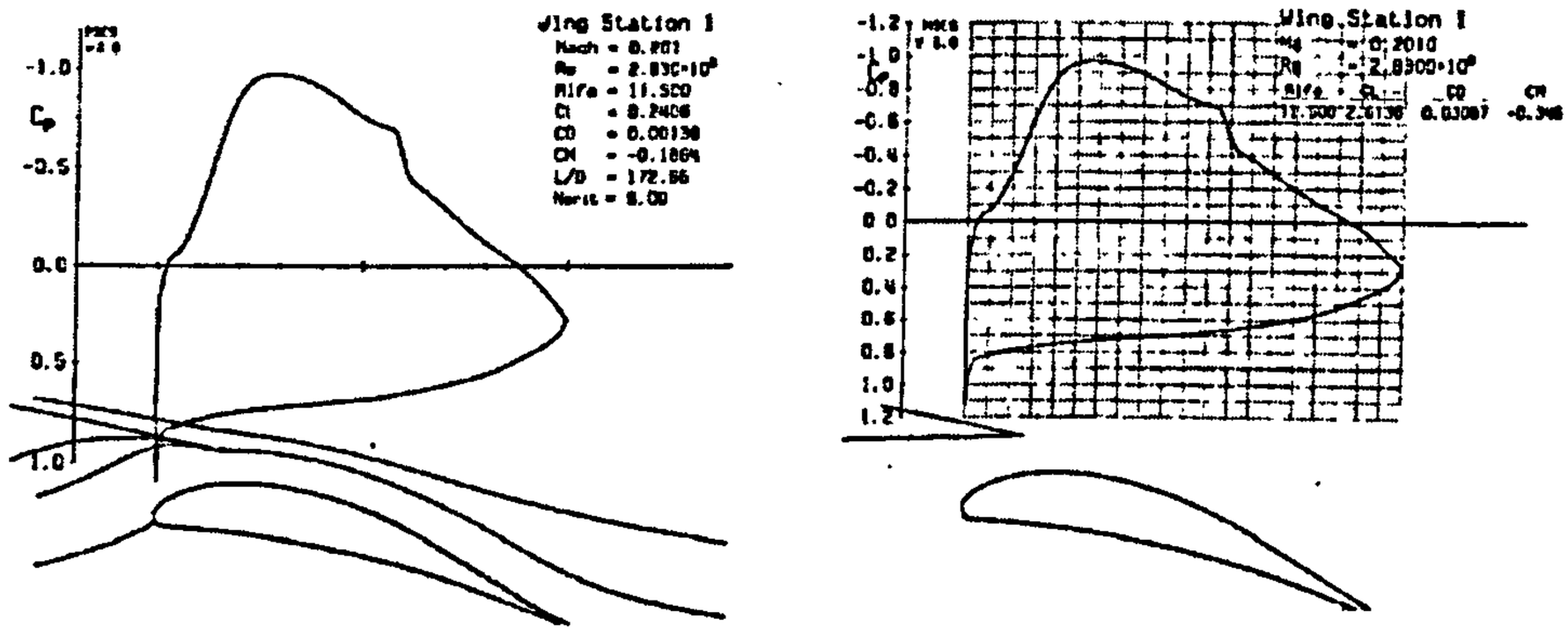

Figure 7.12 Calculated inviscid pressure distribution of wing airfoil at station 1 (or at b/2 = 2782mm) with 15^0 flap deflection for take-off configuration.

Figure A27 - Pressure Distribution (15° - b/2=2782mm)

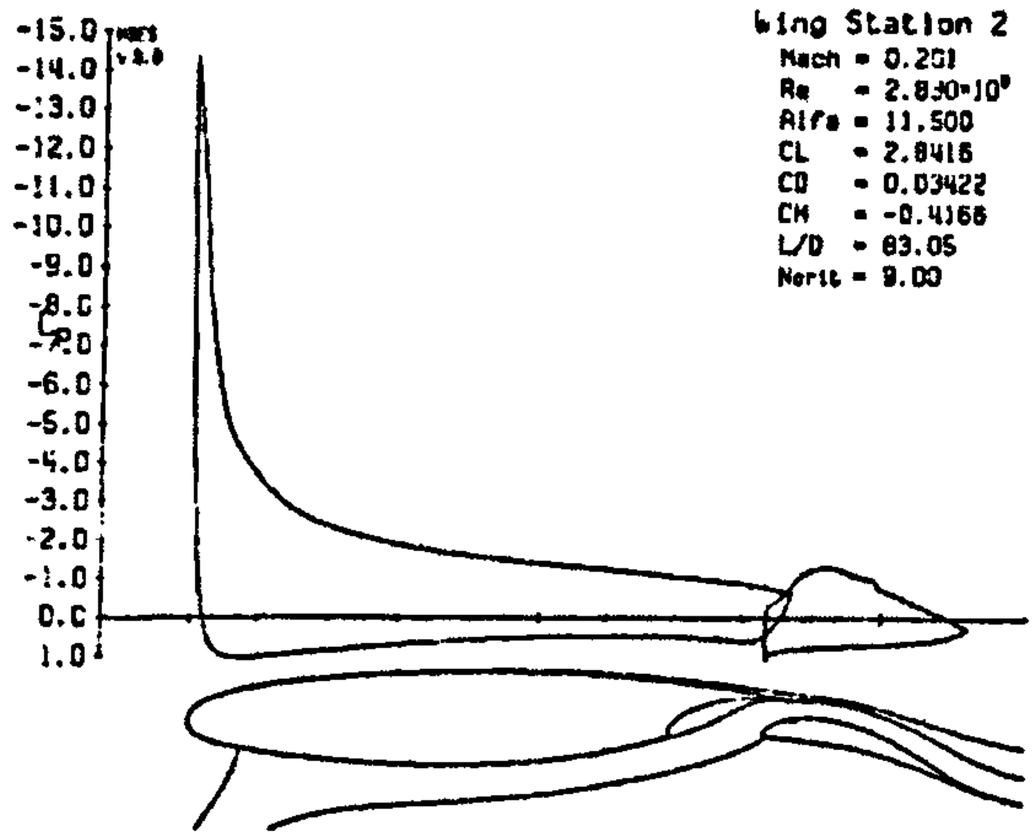

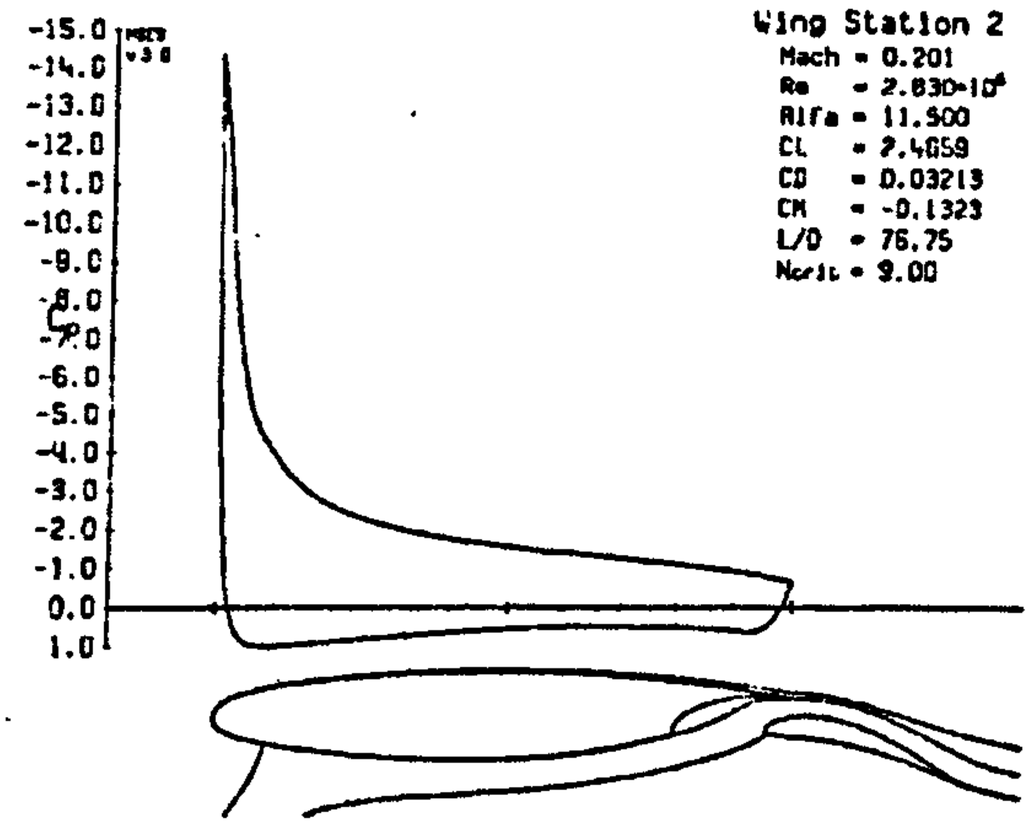

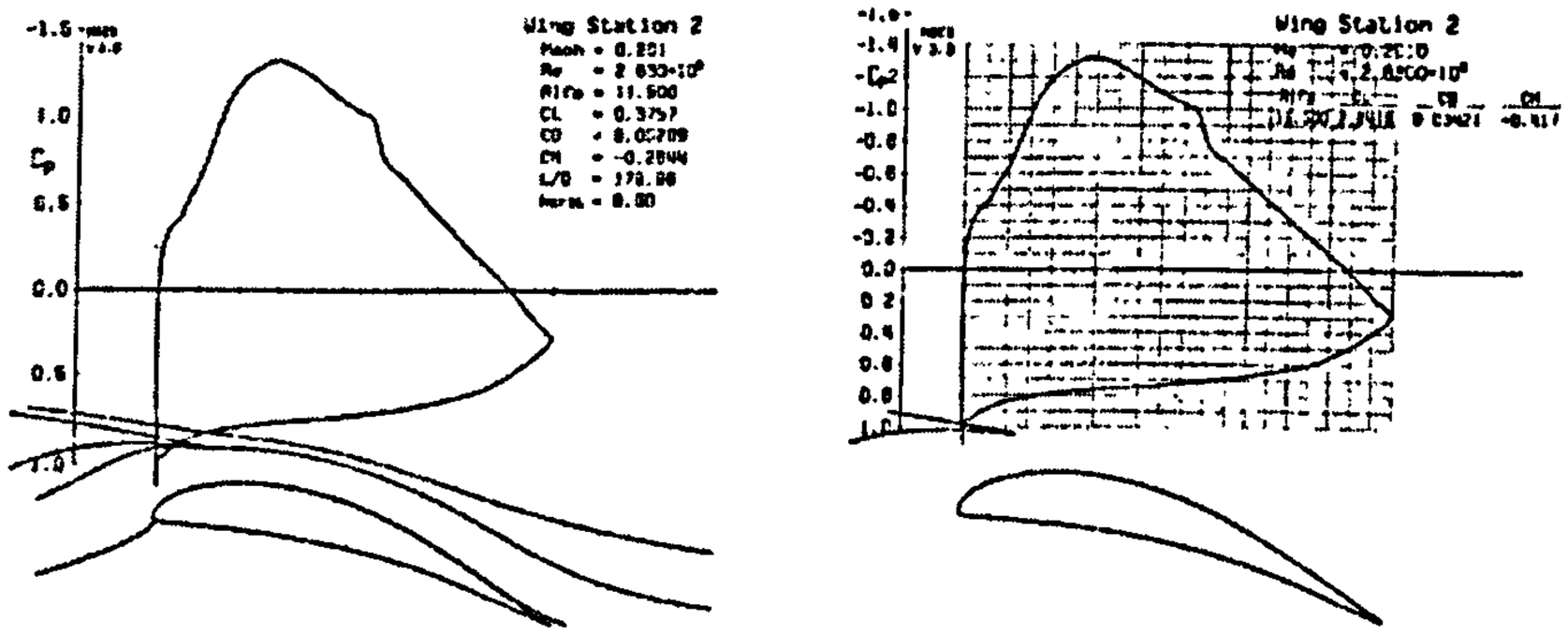

Figure 7.13 Calculated inviscid pressure distribution of wing airfoil at station 2 (or at b/2 = 4920mm) with 15^0 flap deflection for take-off configuration.

Figure A28 – Pressure Distribution (15° - b/2=4920mm)

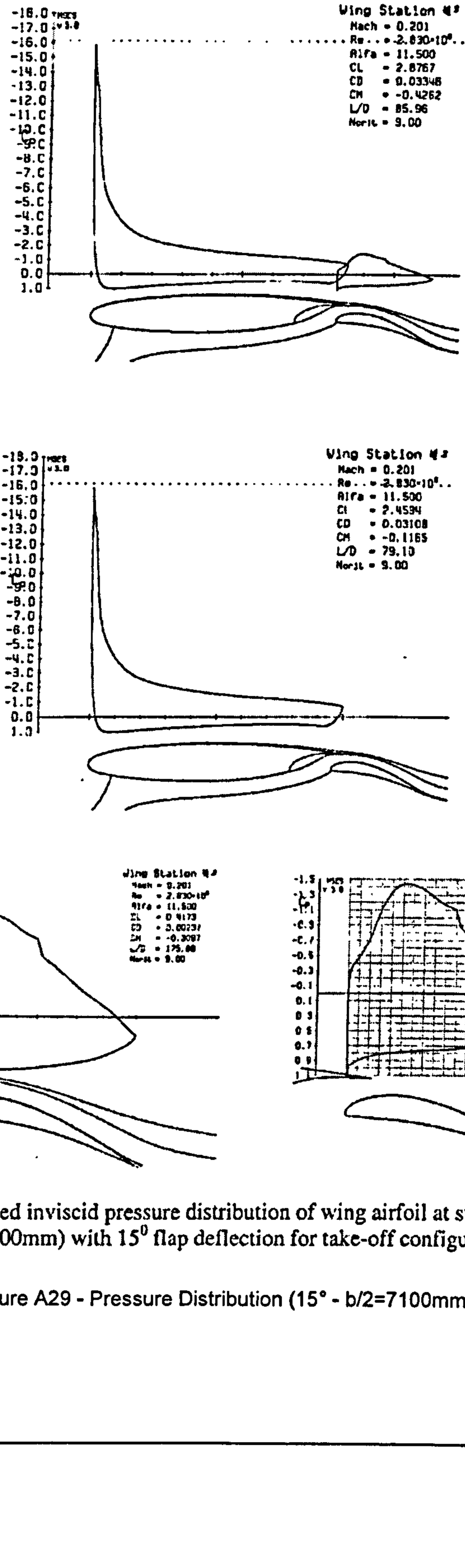

Figure 7.14 Calculated inviscid pressure distribution of wing airfoil at station 3 (or at b/2 = 7100mm) with 15^0 flap deflection for take-off configuration.

Figure A29 - Pressure Distribution (15° - b/2=7100mm)

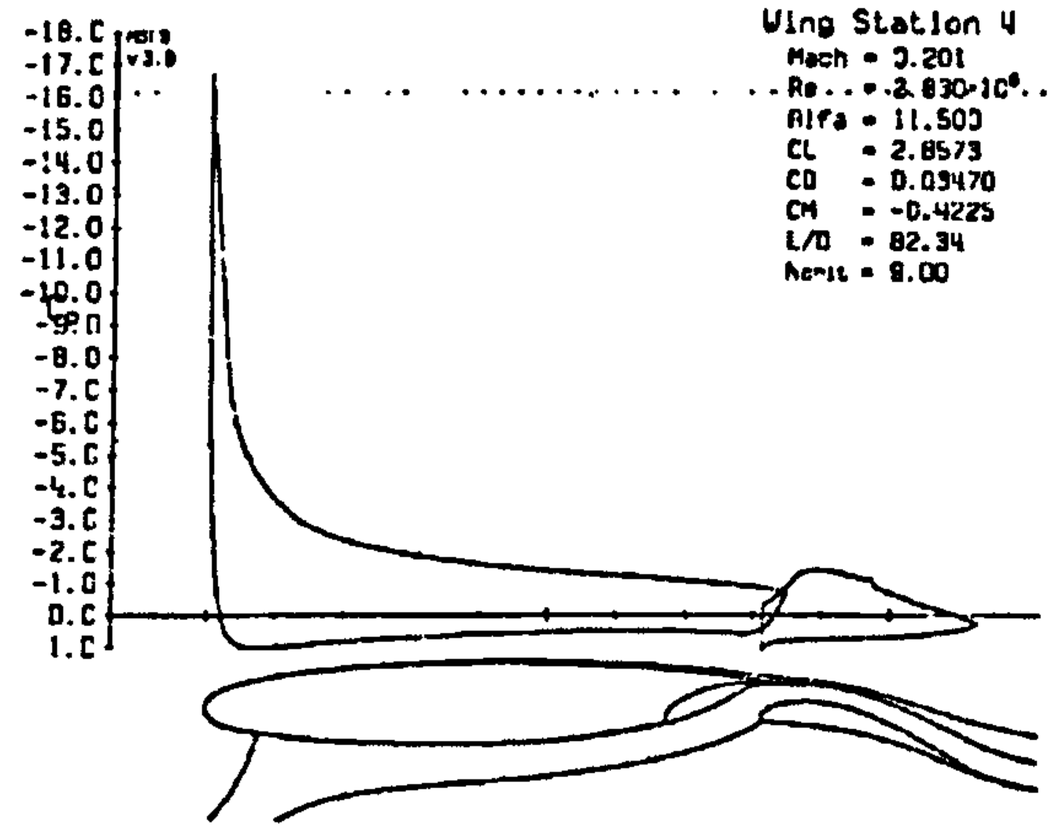

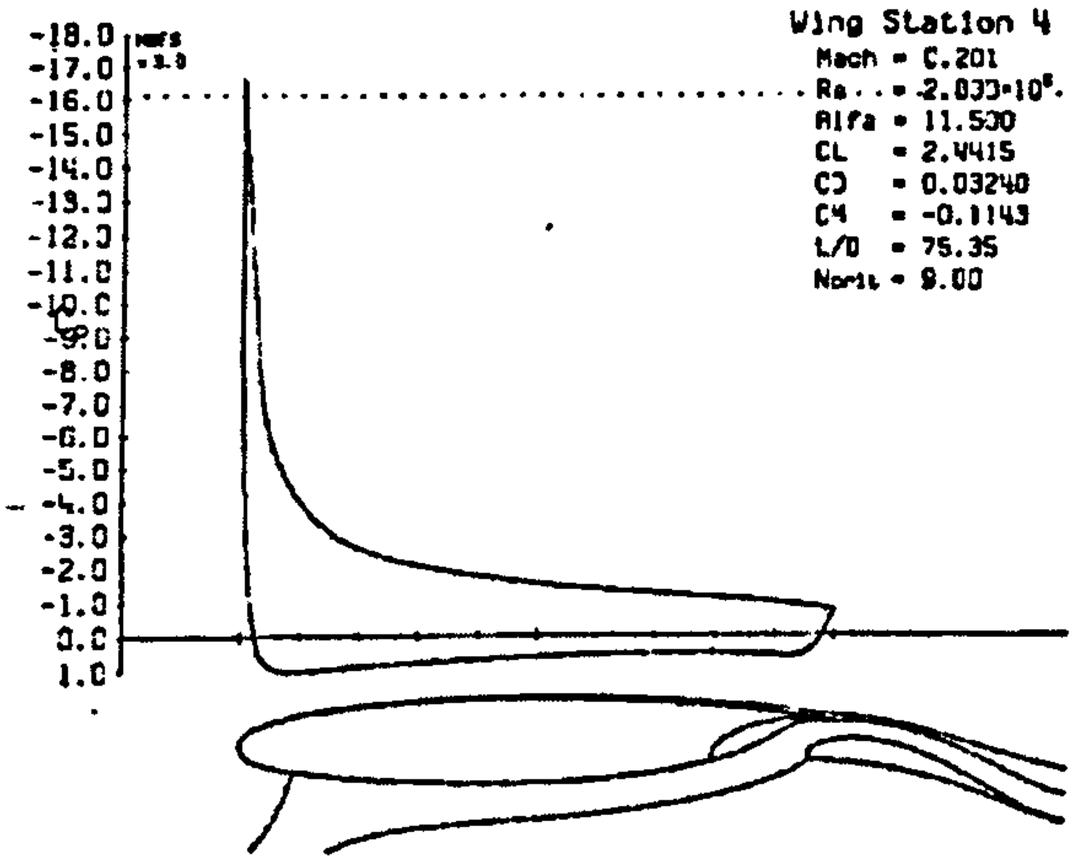

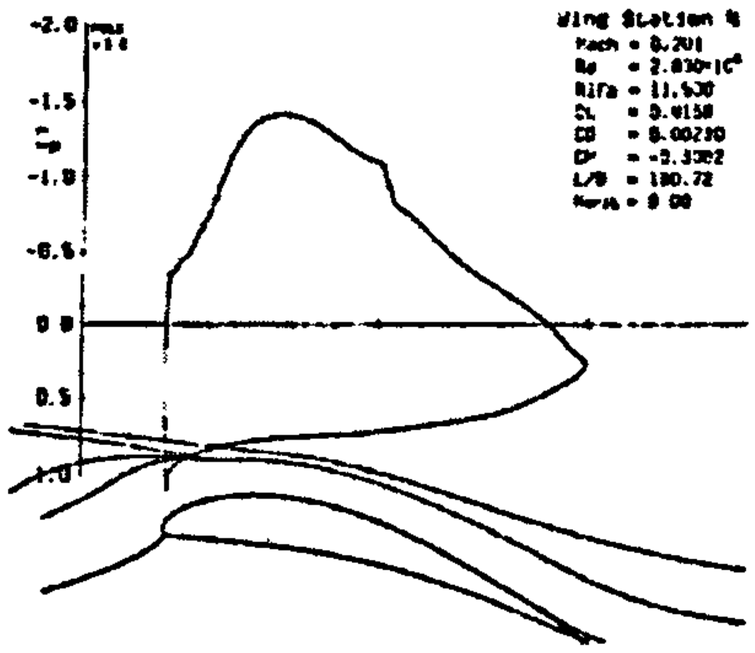

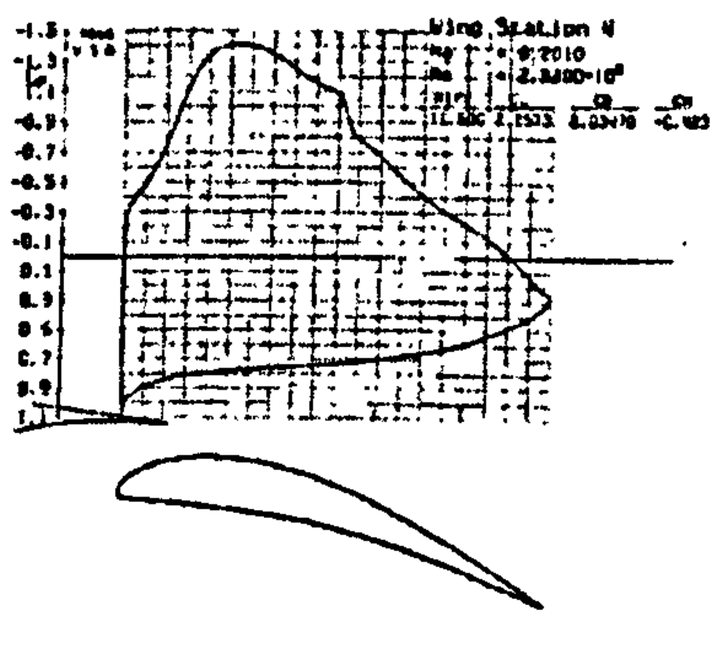

Figure 7.15 Calculated inviscid pressure distribution of wing airfoil at station 4 (or at b/2 = 9328mm) with 15^0 flap deflection for take-off configuration.

Figure A30 - Pressure Distribution (15° - b/2=9328mm)

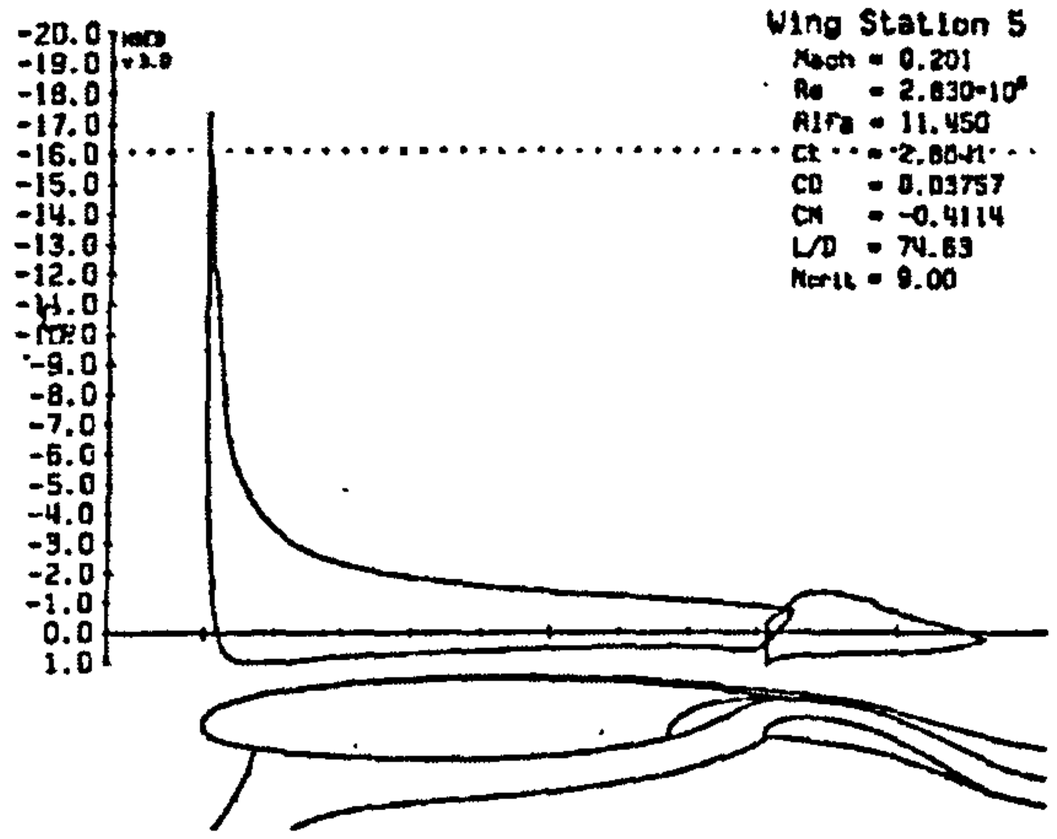

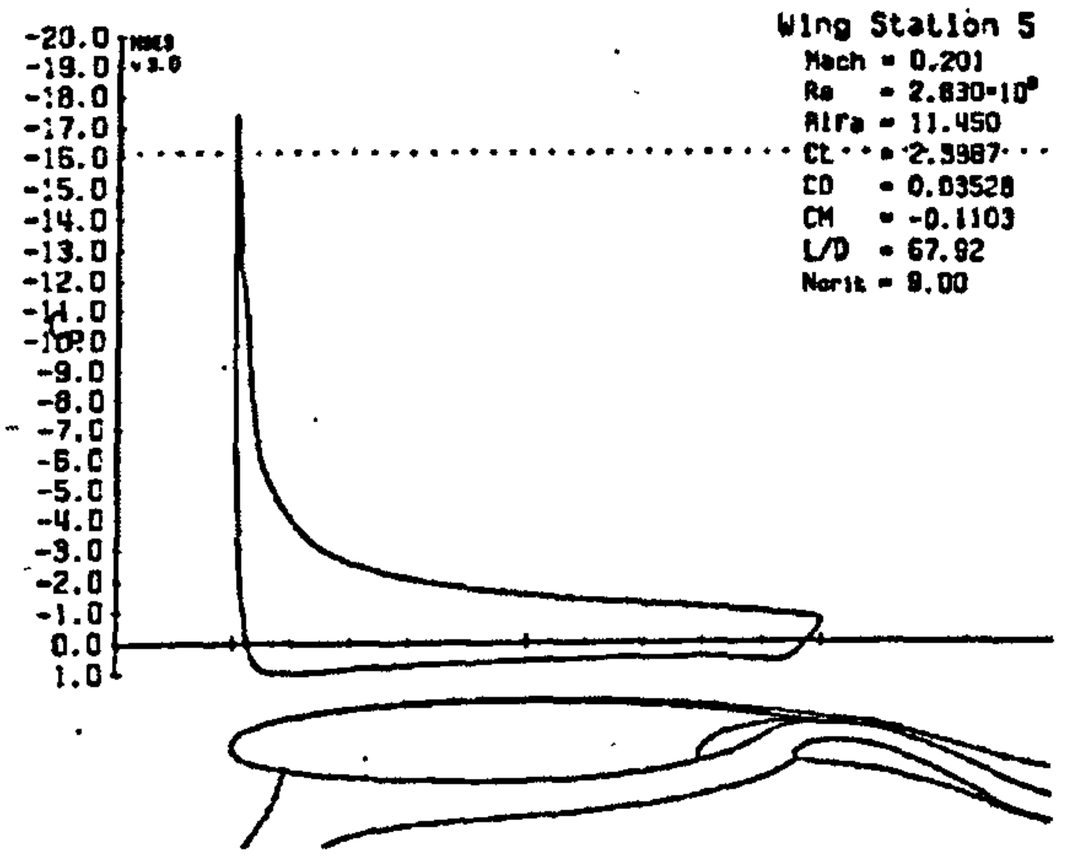

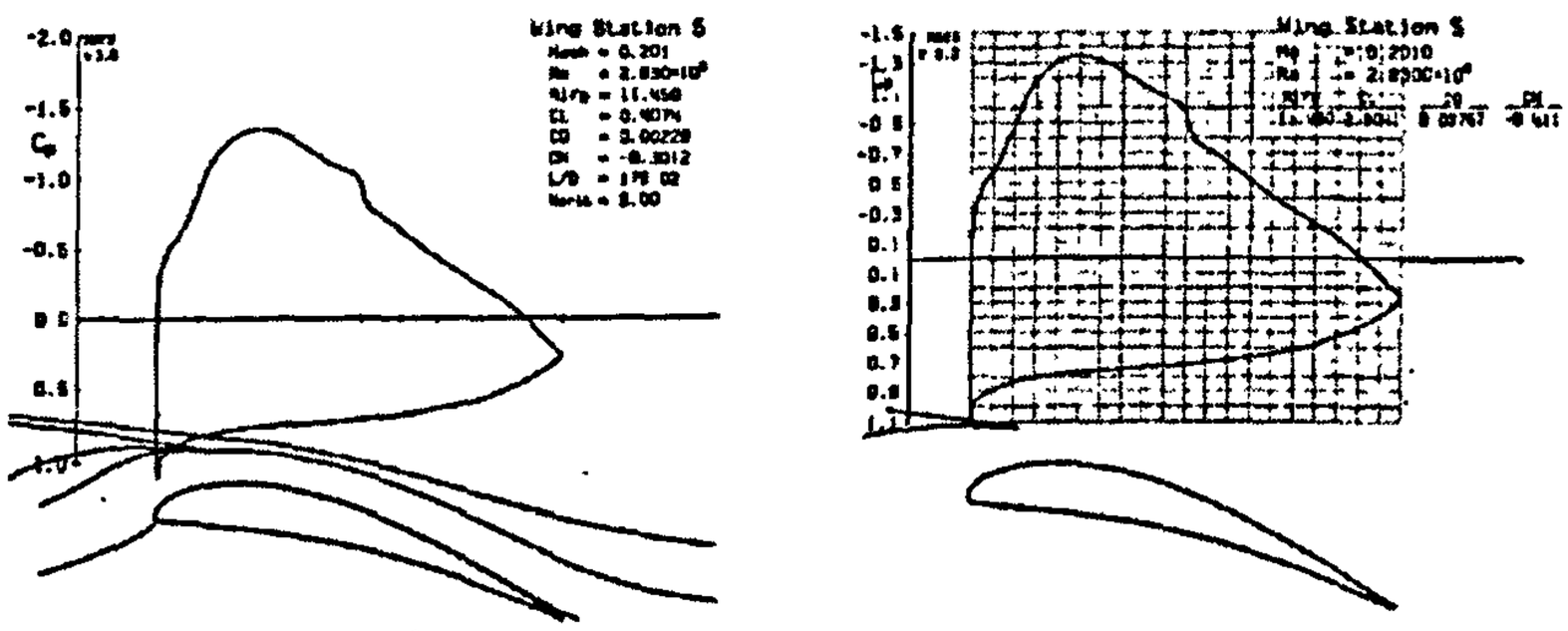

Figure 7.16 Calculated inviscid pressure distribution of wing airfoil at station 5 (or at b/2 = 11555mm) with 15^0 flap deflection for take-off configuration.

Figure A31 - Pressure Distribution (15° - b/2=11555mm)

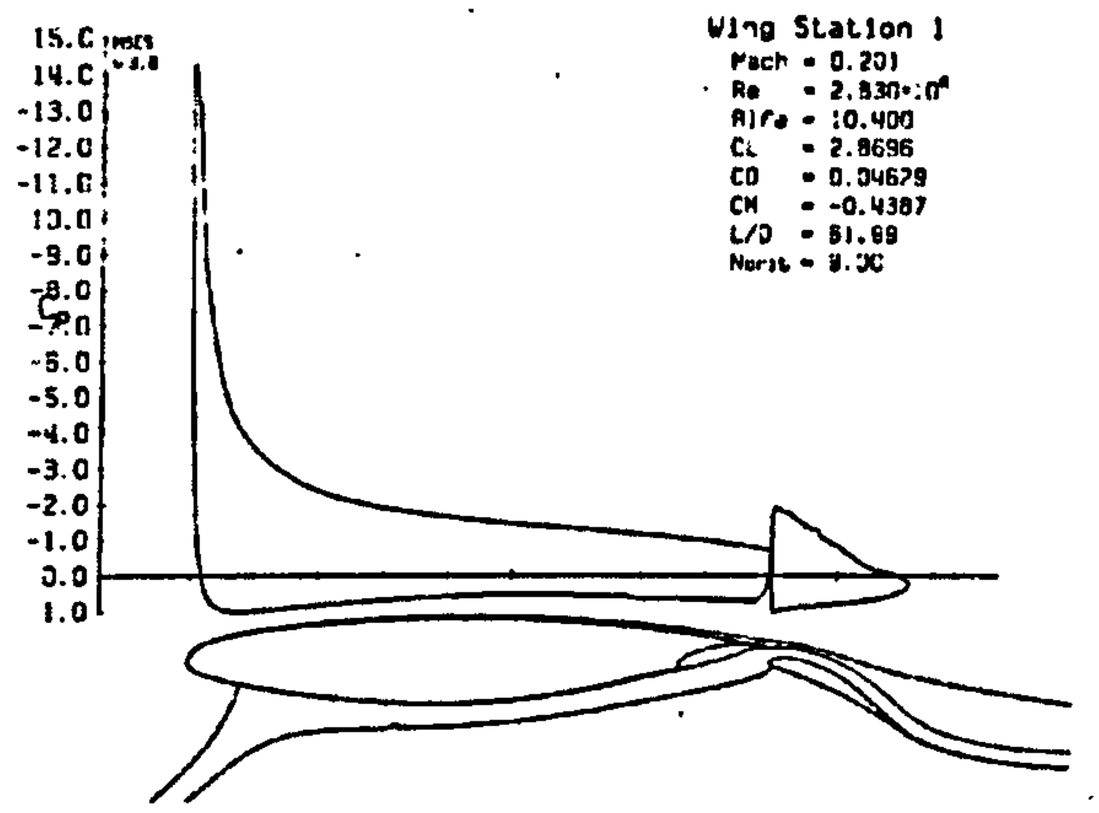

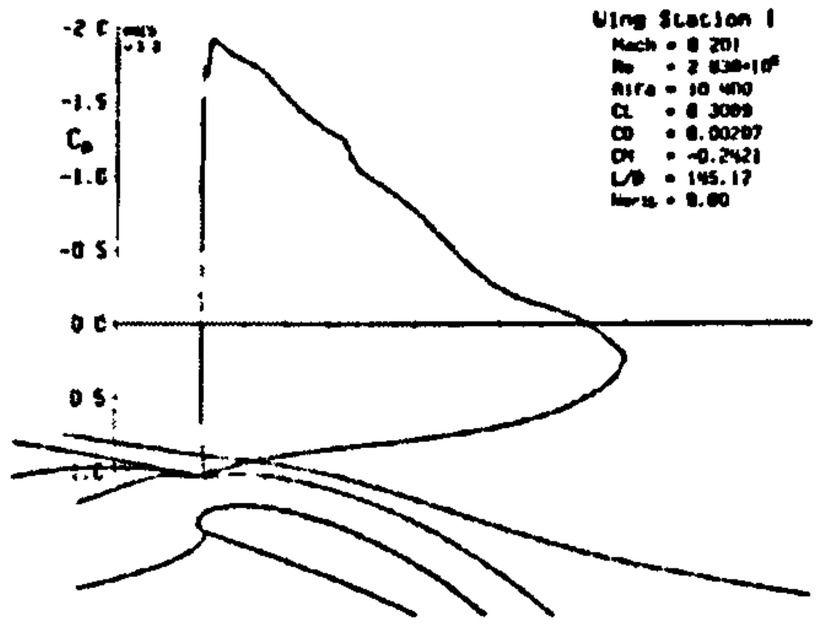

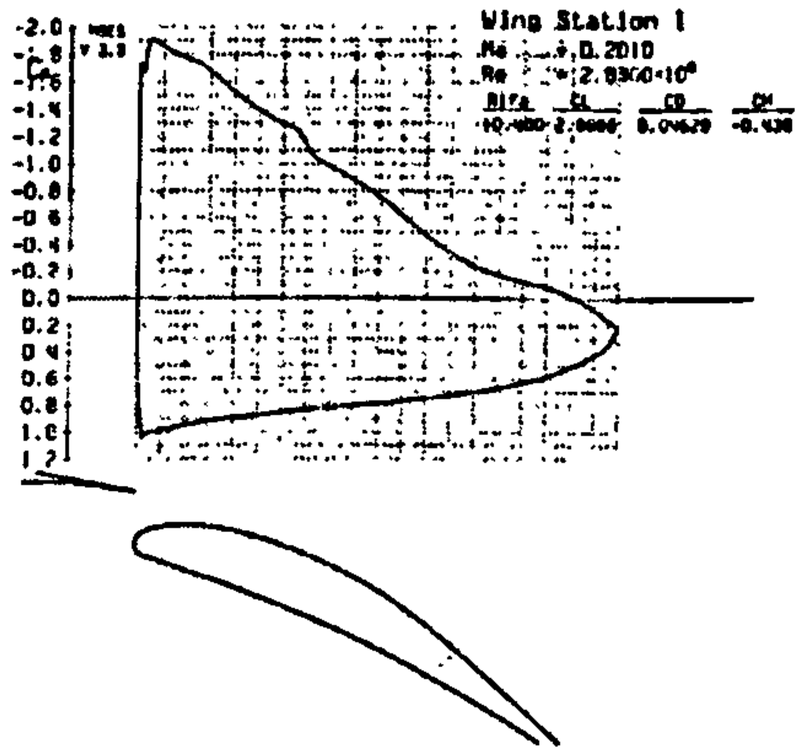

Figure 7.17 Calculated inviscid pressure distribution of wing airfoil at station 1 (or at b/2 = 2782mm) with 35^0 flap deflection for landing configuration.

Figure A32 - Pressure Distribution (35° - b/2=2782mm)

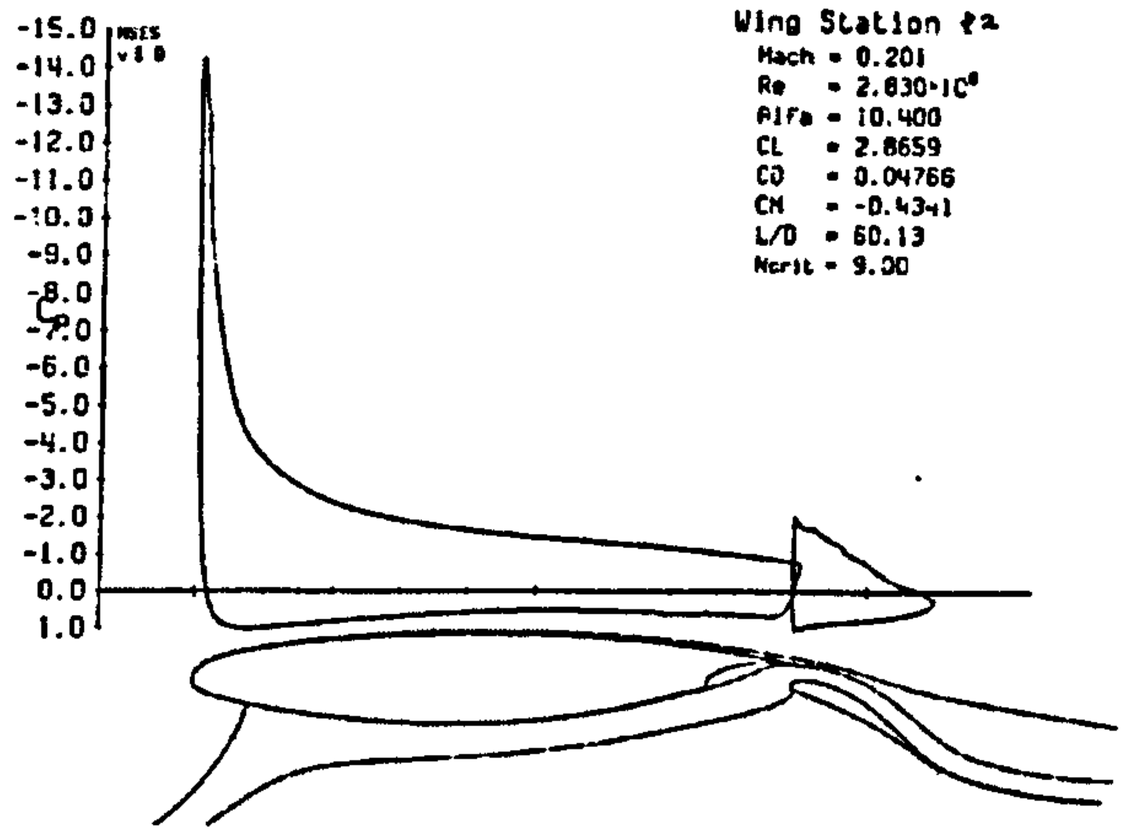

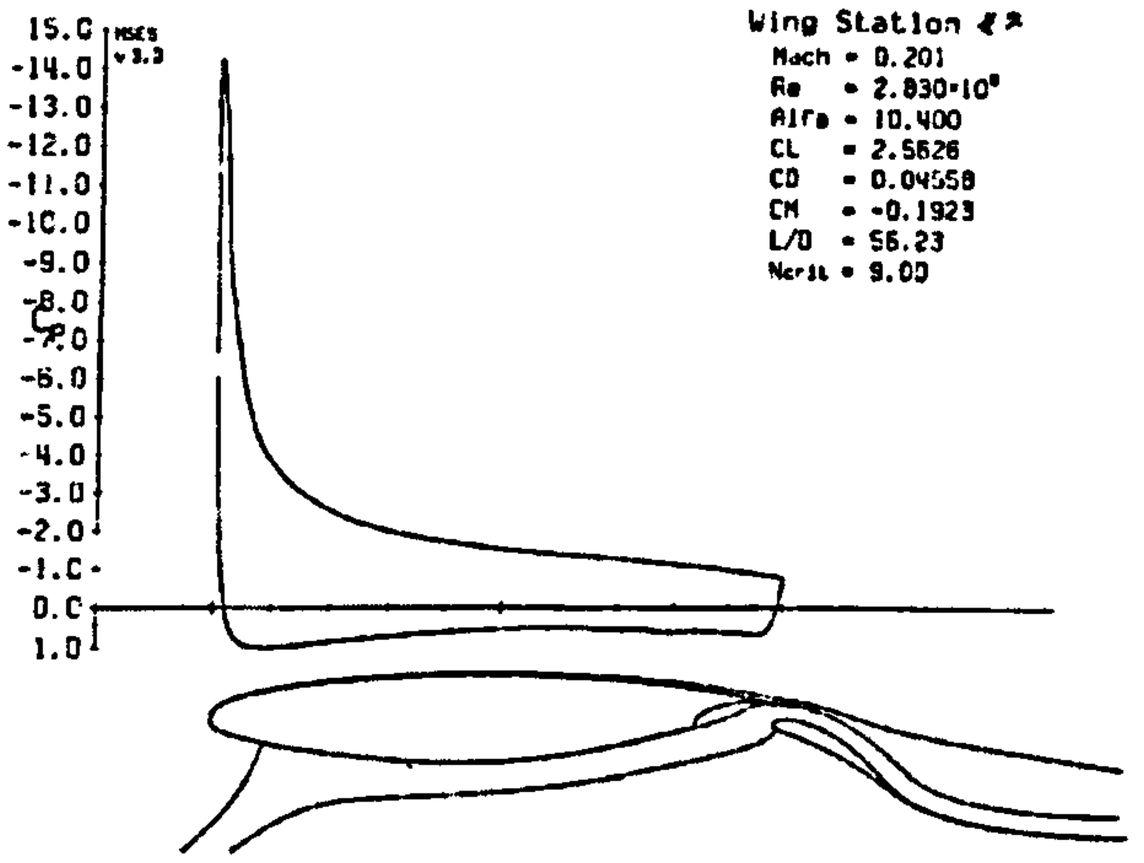

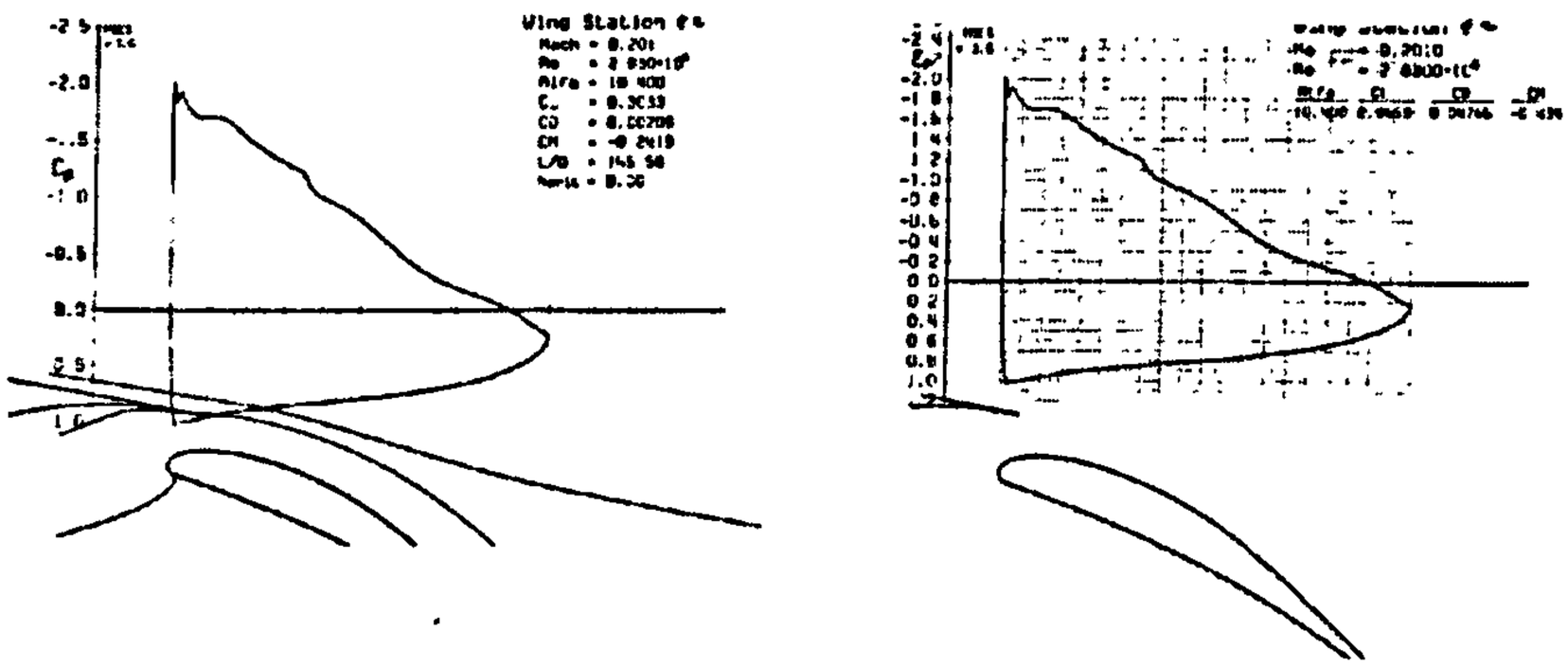

Figure 7.18 Calculated inviscid pressure distribution of wing airfoil at station 2 (or at b/2 = 4920mm) with 35^0 flap deflection for landing configuration.

Figure A33 - Pressure Distribution (35° - b/2=4920mm)

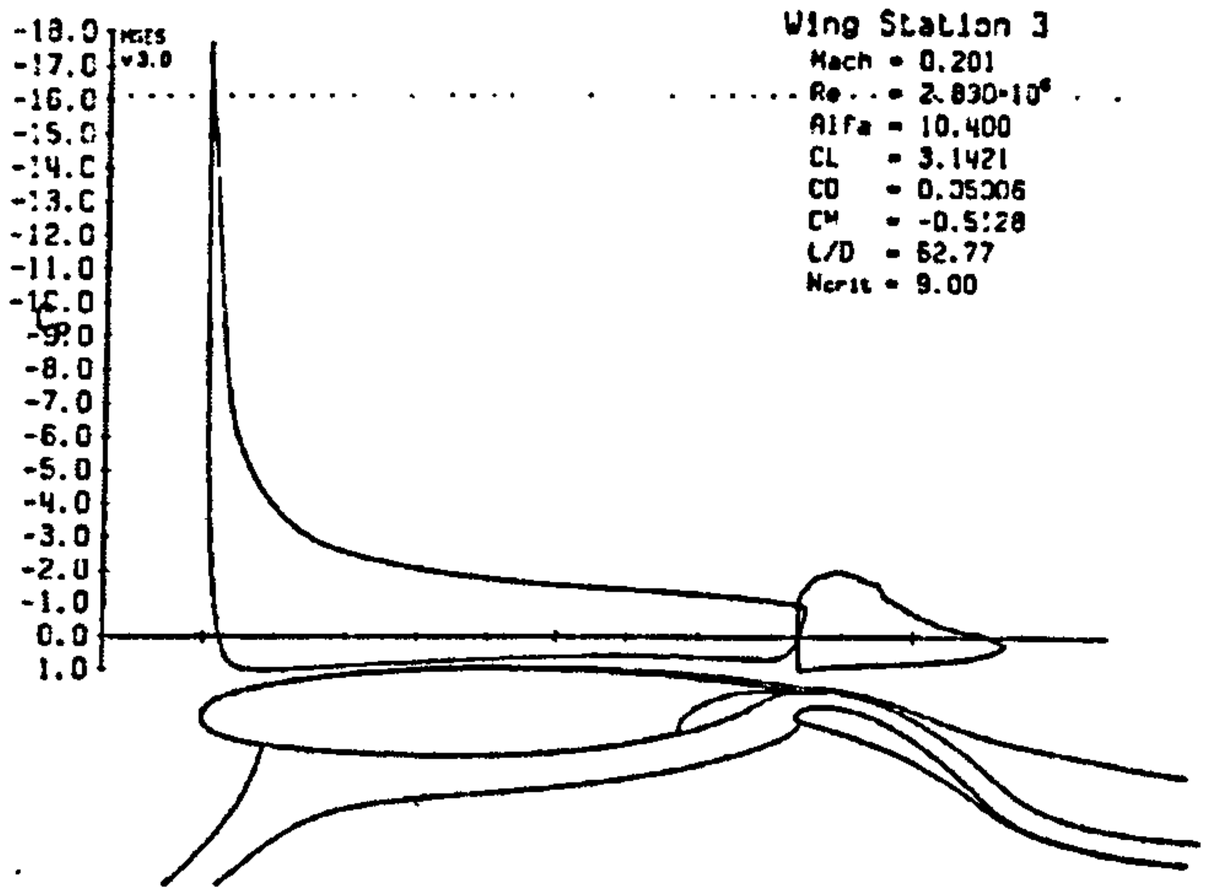

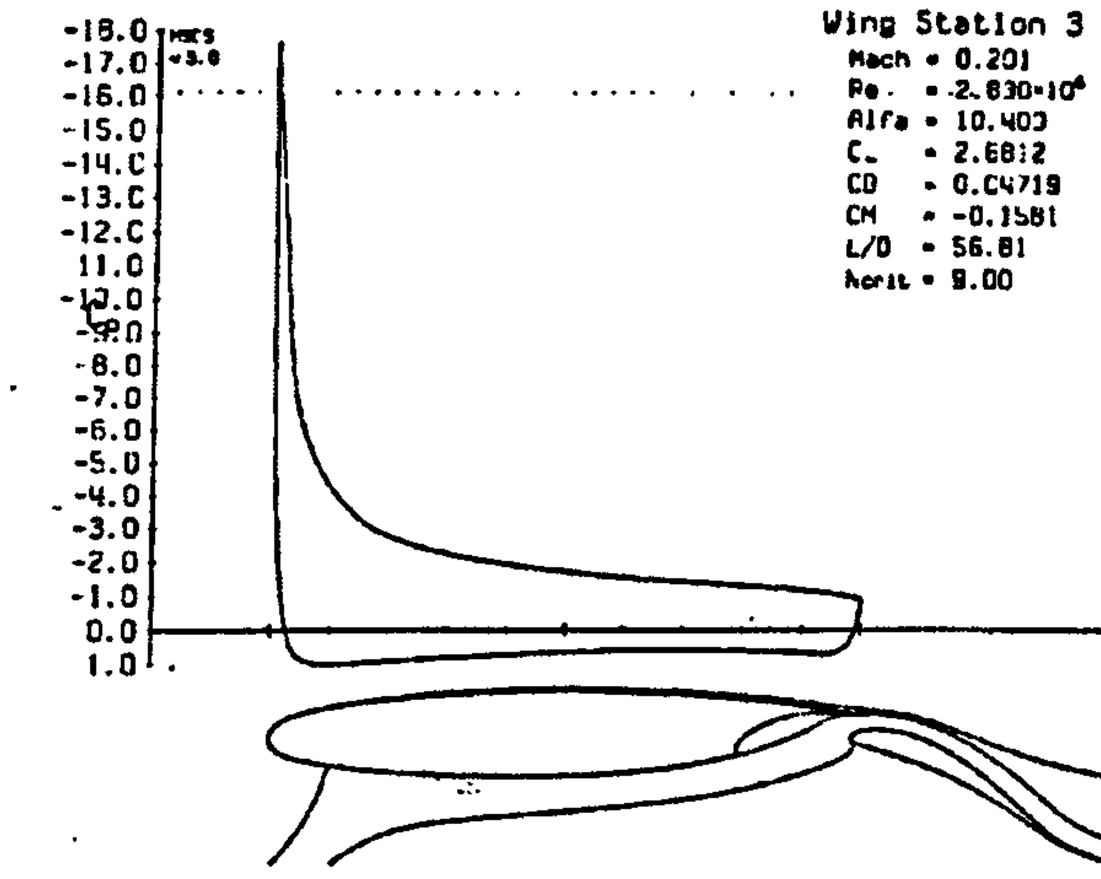

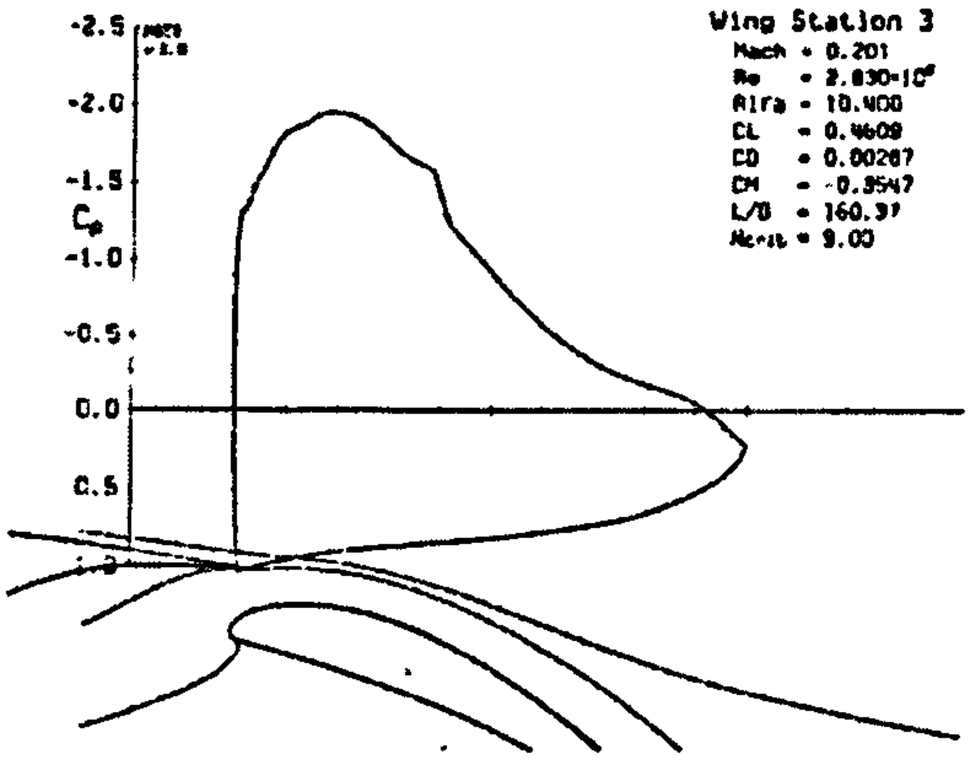

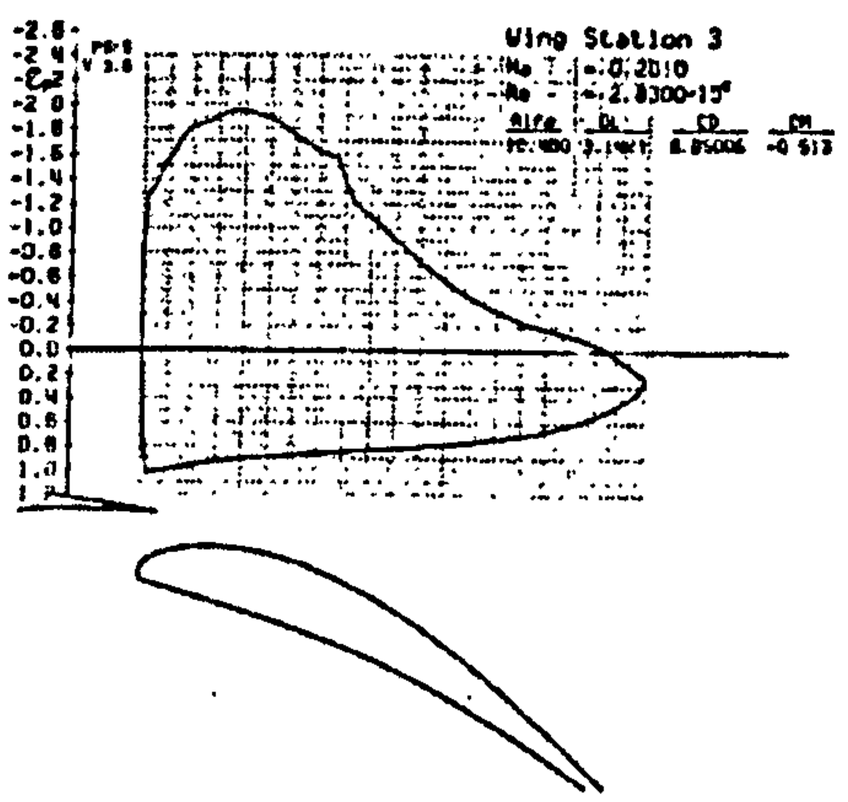

Figure 7.19 Calculated inviscid pressure distribution of wing airfoil at station 3 (or at b/2 = 7100mm) with 35^0 flap deflection for landing configuration.

Figure A34 – Pressure Distribution (35° - b/2=7100mm)

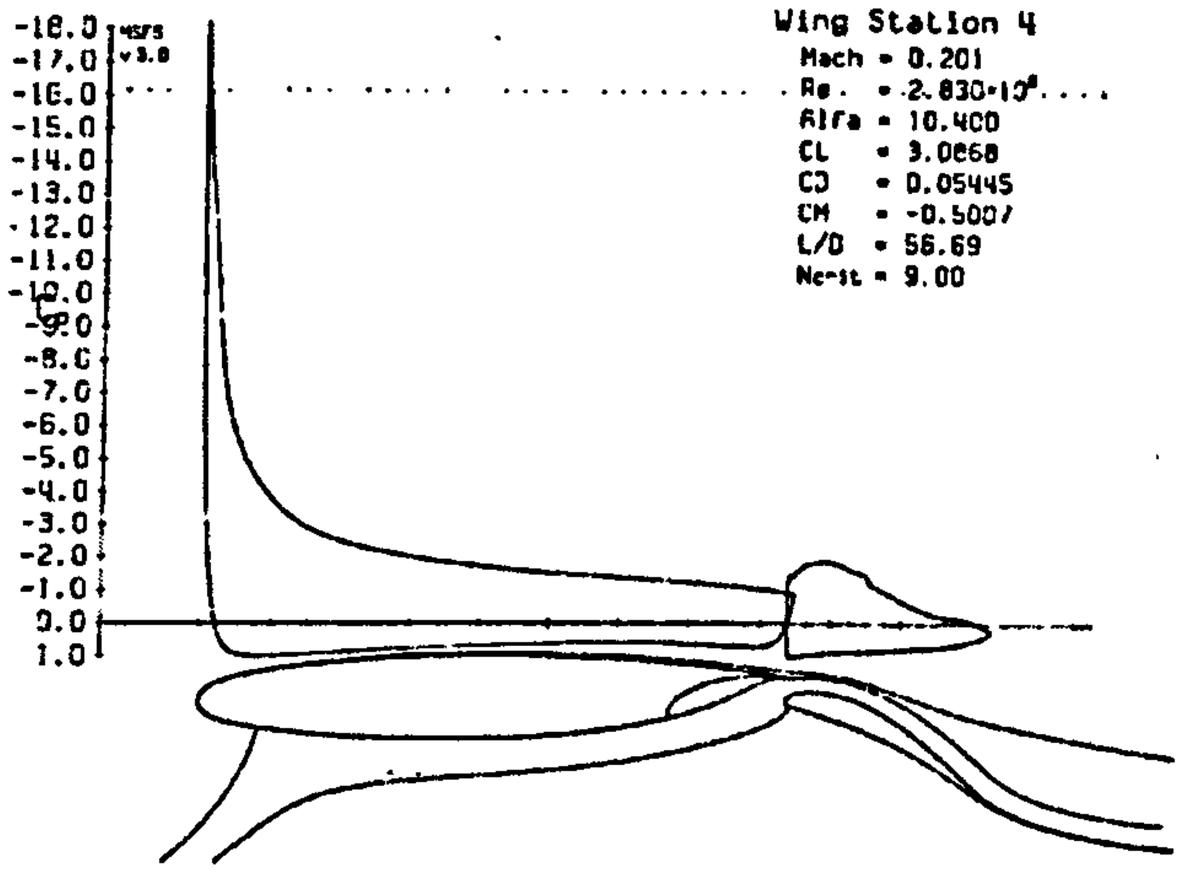

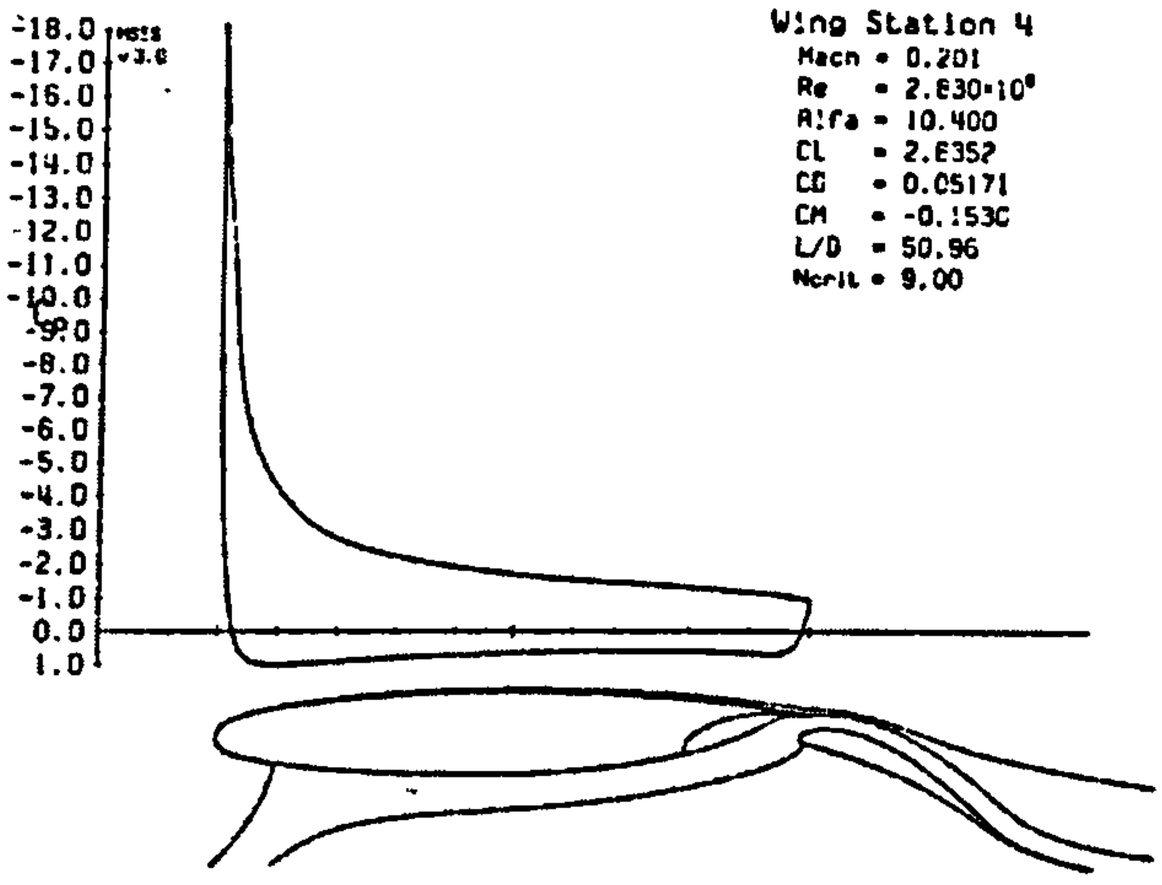

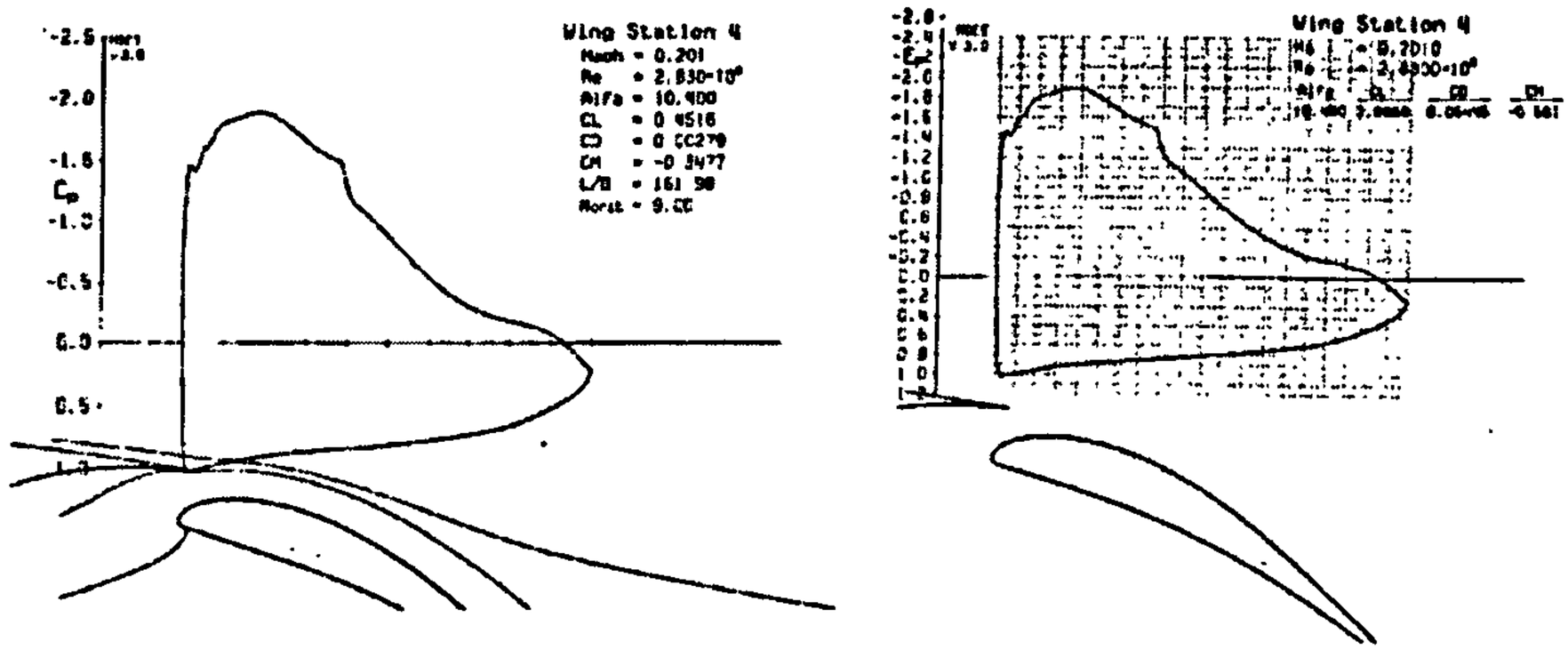

Figure 7.20 Calculated inviscid pressure distribution of wing airfoil at station 4 (or at b/2 = 9328mm) with 35^0 flap deflection for landing configuration.

Figure A35 - Pressure Distribution (35° - b/2=9328mm)

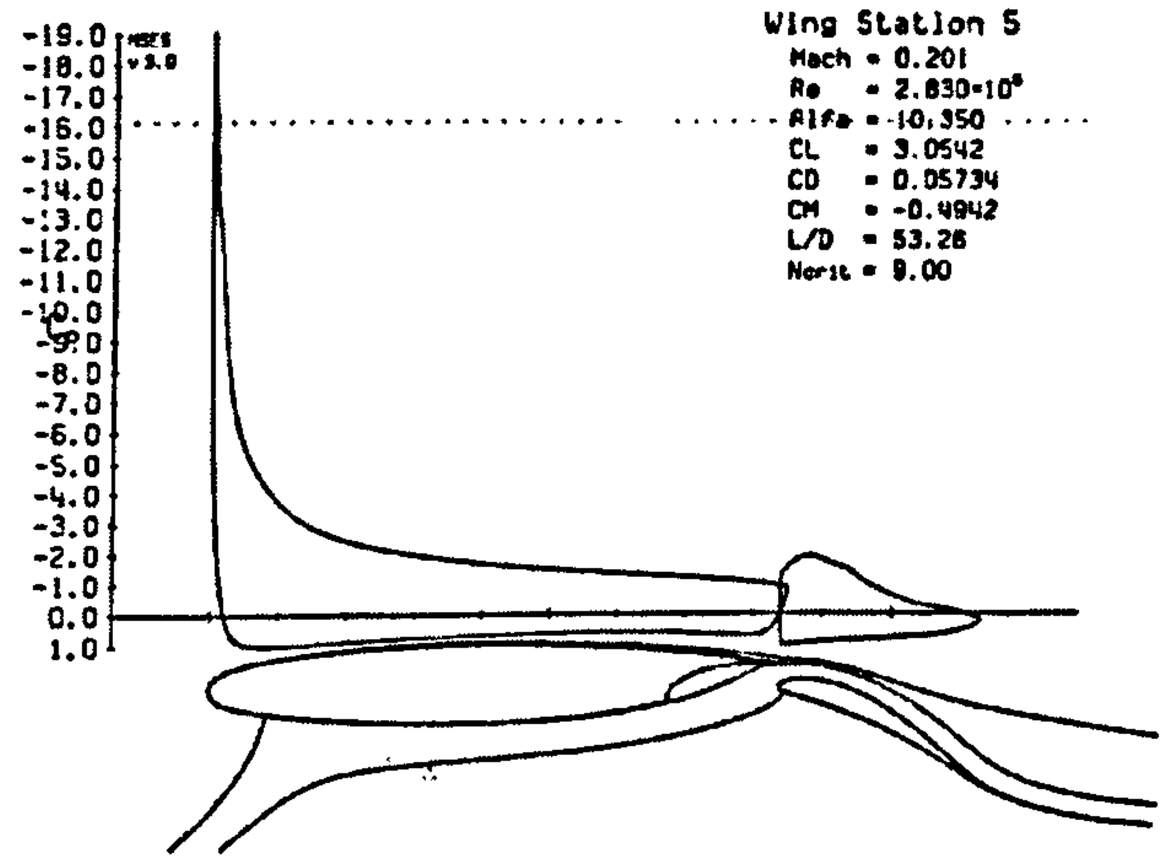

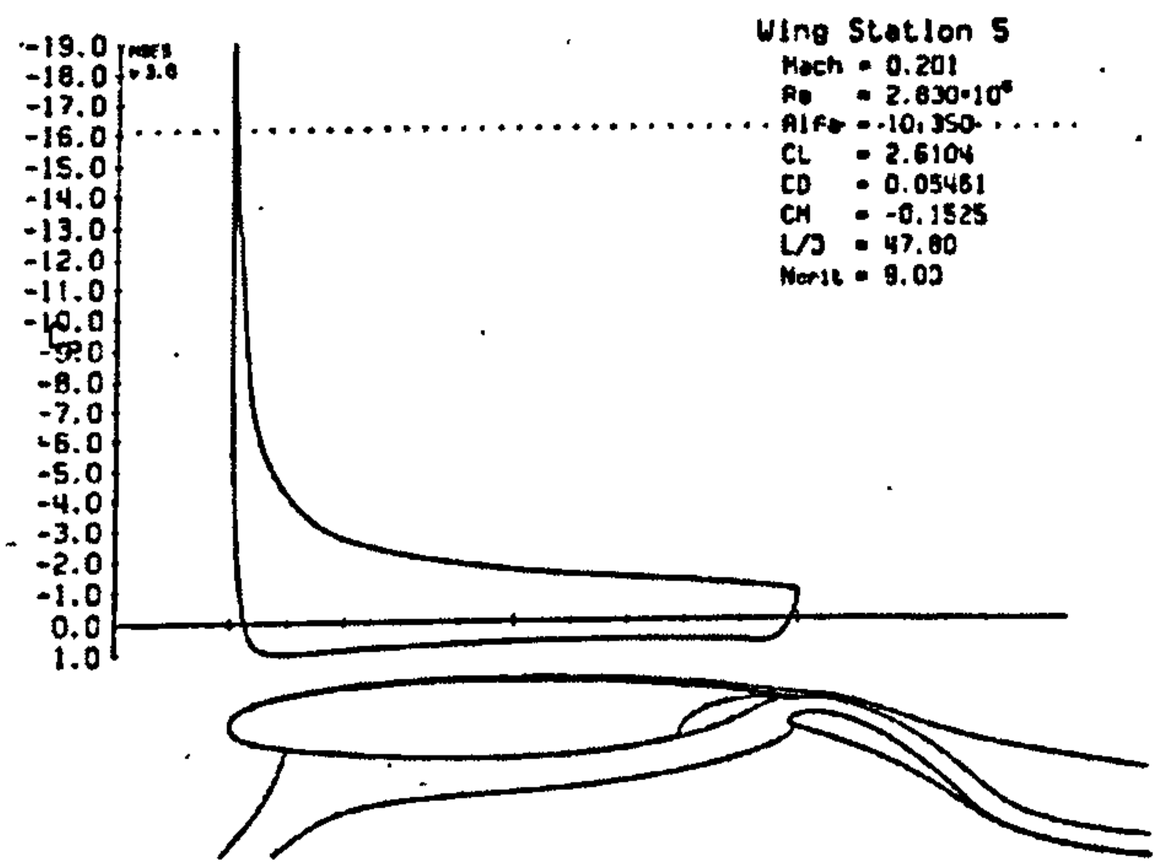

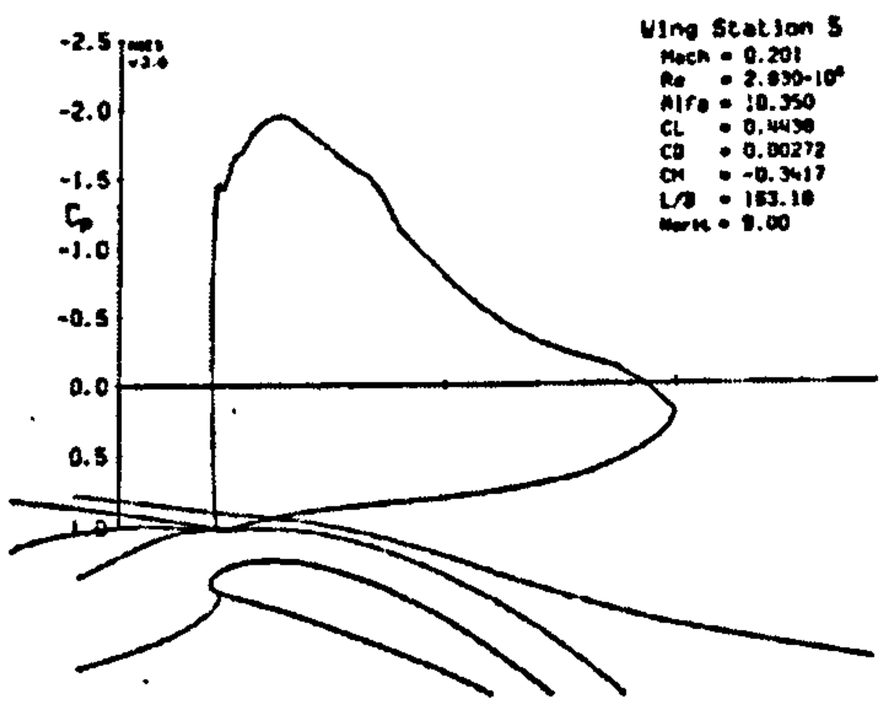

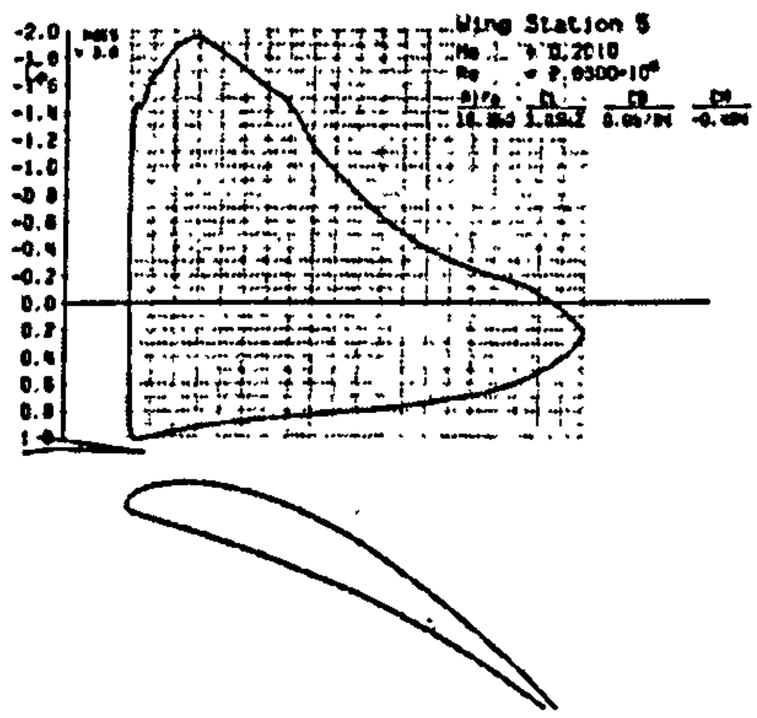

Figure 7.21 Calculated inviscid pressure distribution of wing airfoil at station 5 (or at b/2 = 11555mm) with 35^0 flap deflection for landing configuration.

Figure A36 - Pressure Distribution (35° - b/2=11555mm)

A2.4 – Spanwise Load Distributions [1]

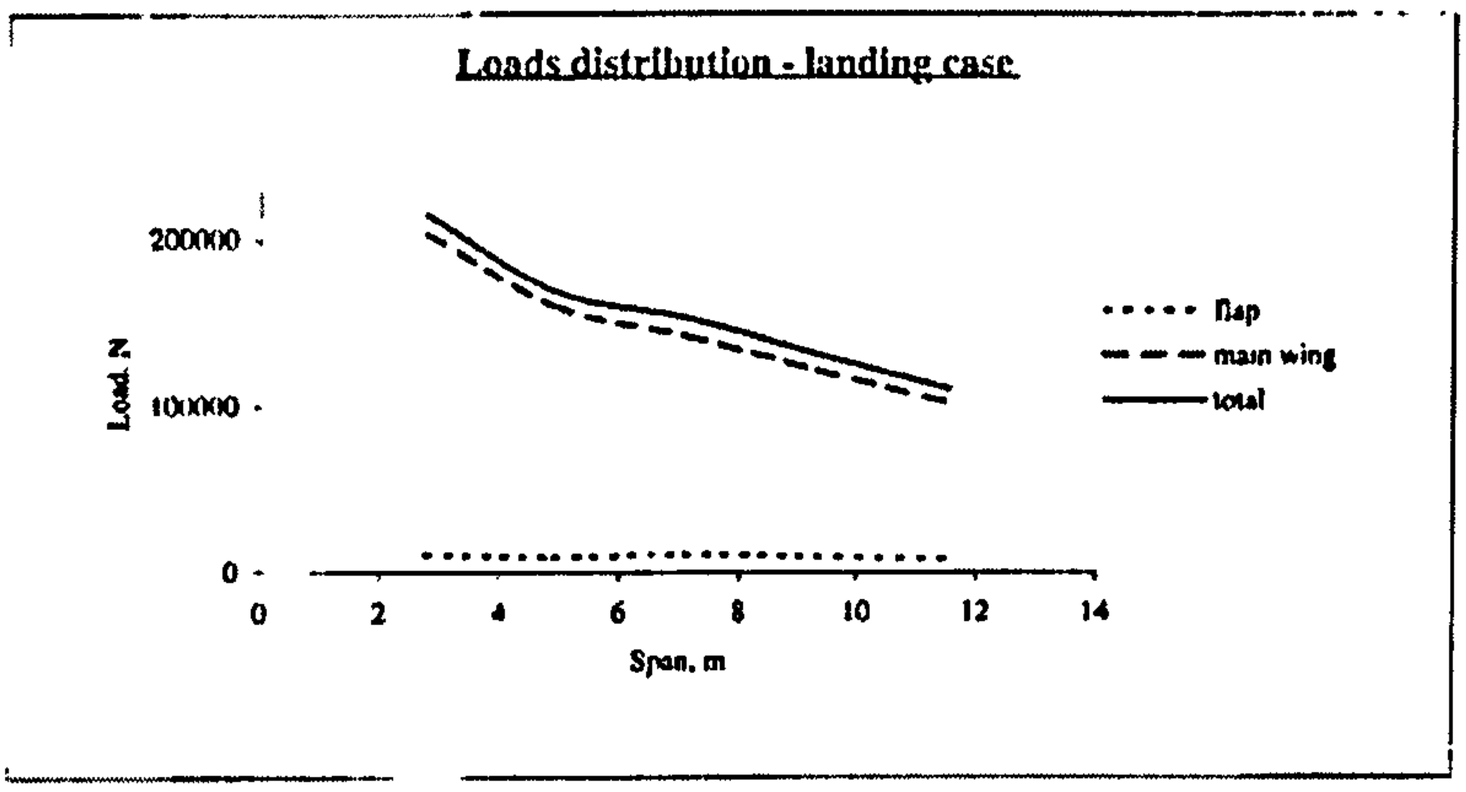

Figure A37 - ATRA Overall Spanwise Load per Unit Width Distribution – Landing Case

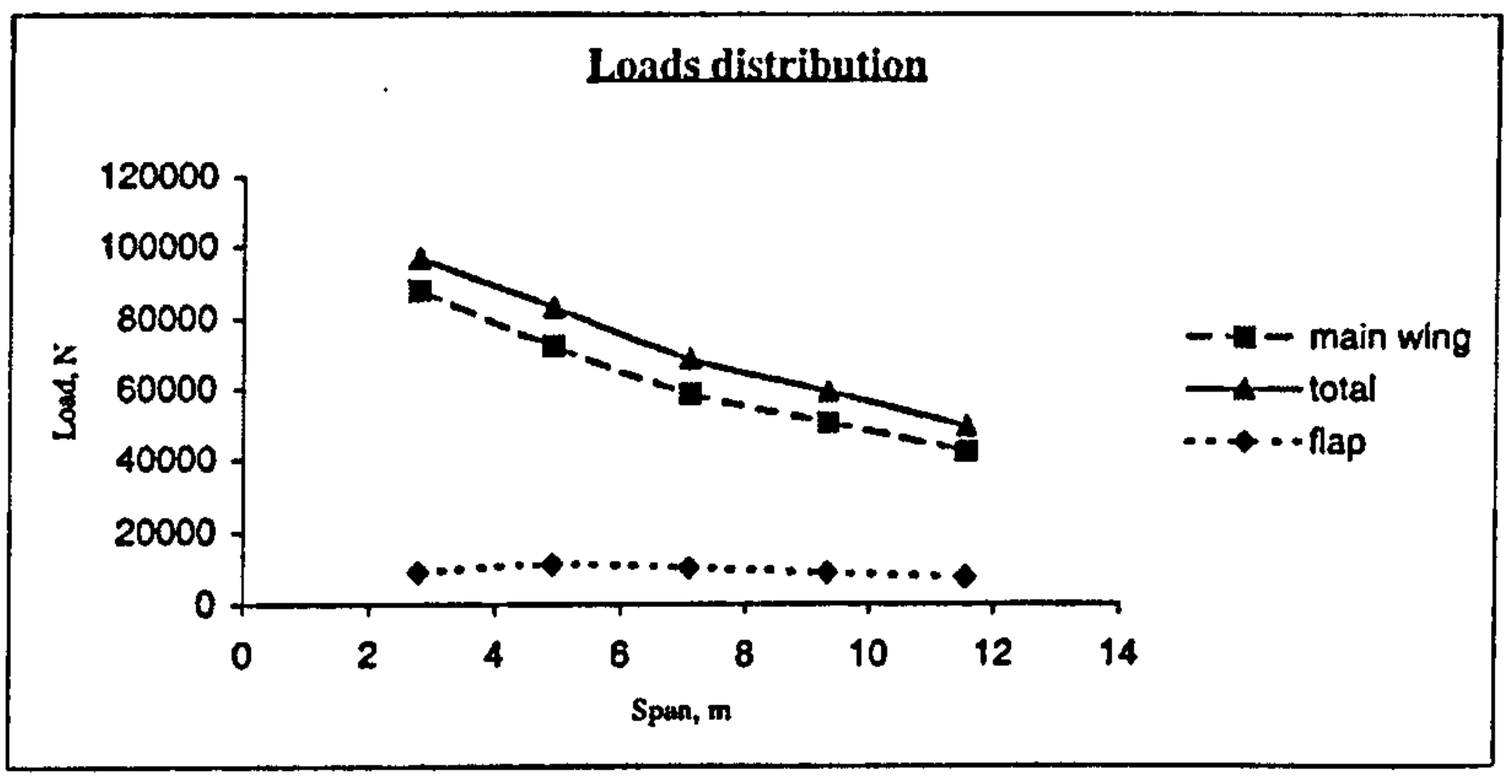

Figure A38 - ATRA Overall Spanwise Load per Unit Width Distribution – Take-Off Case

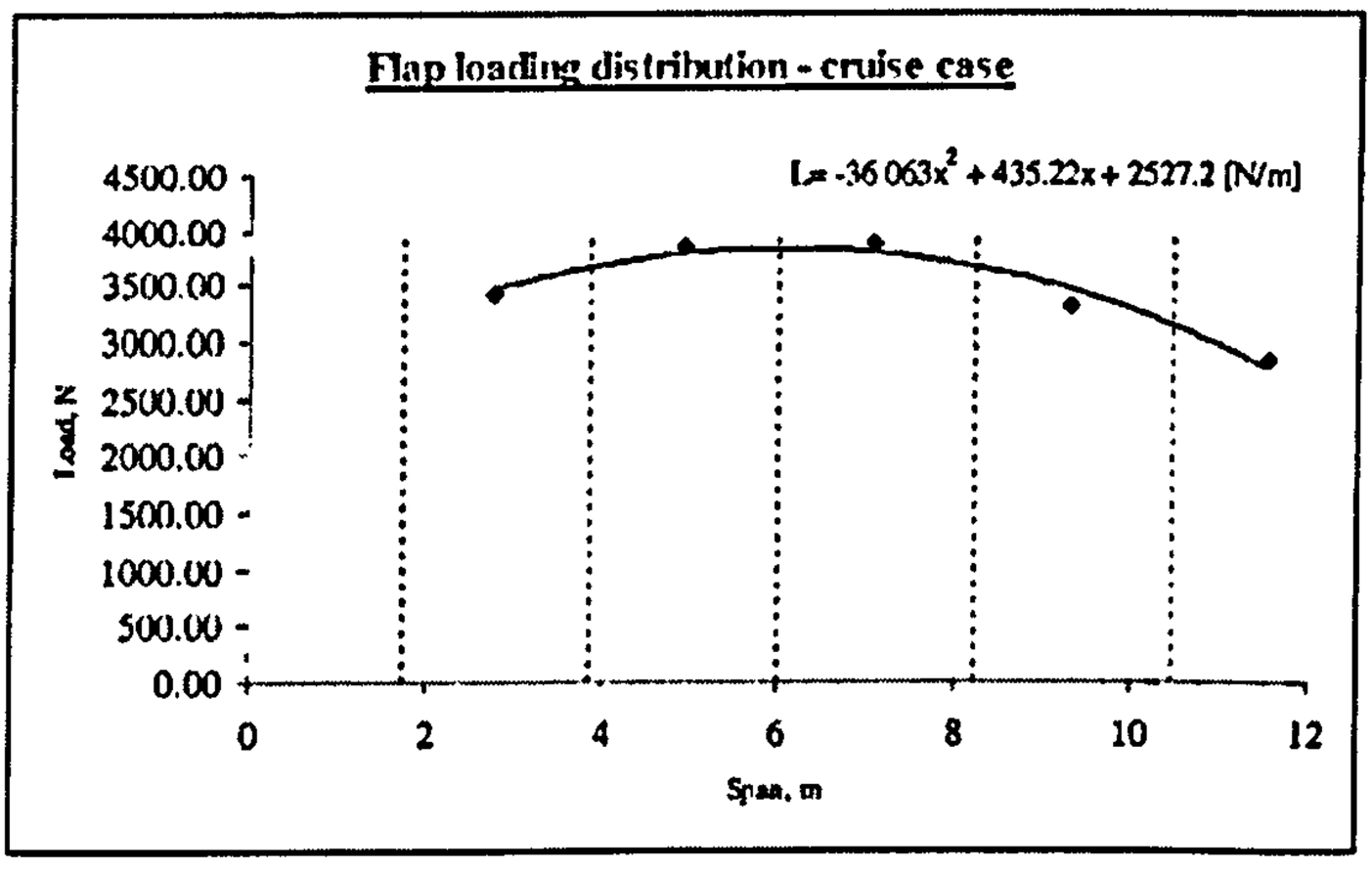

Figure A39 – ATRA Flap Spanwise Load per Unit Width Distribution (Ultimate) – Cruise Case

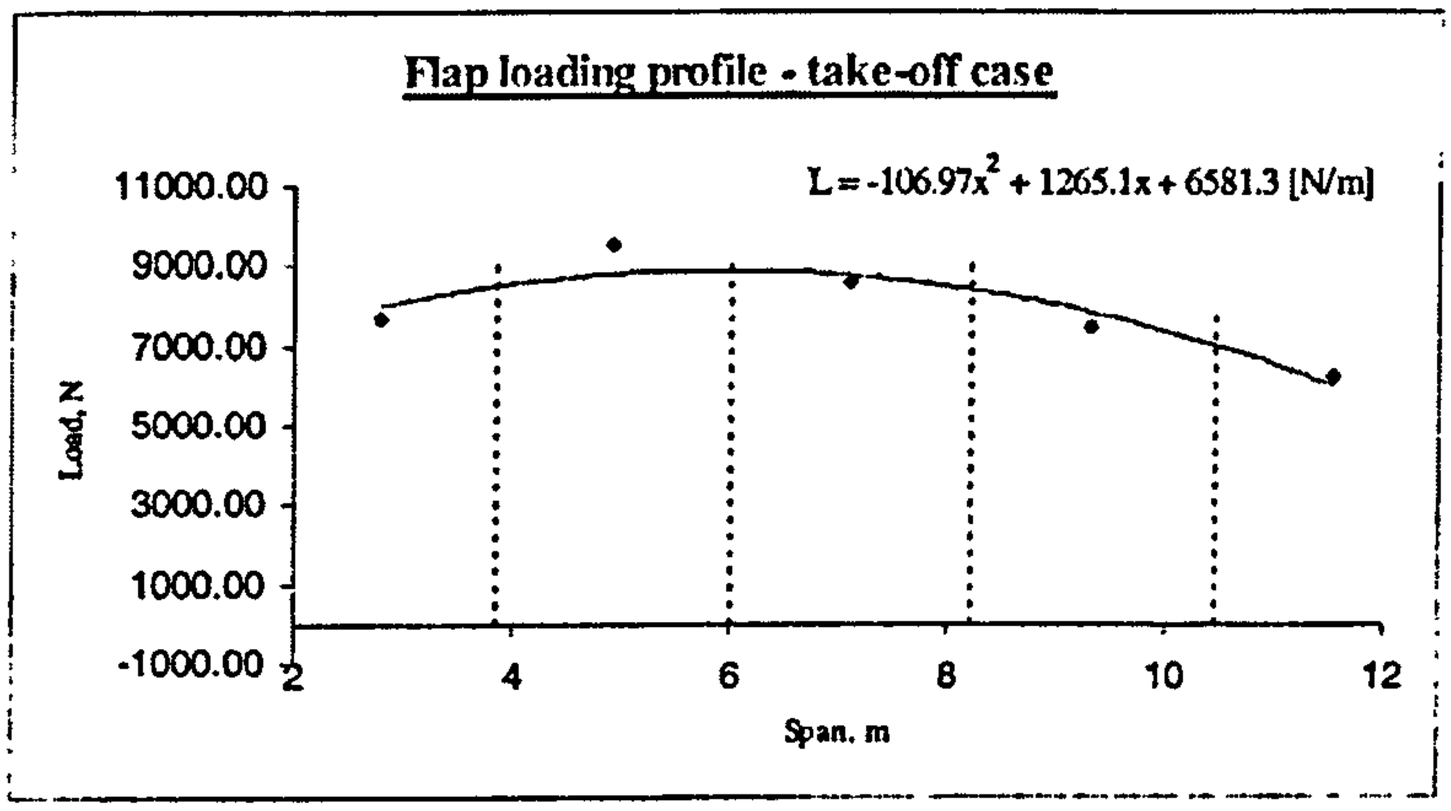

Figure A40 - ATRA Flap Spanwise Load per Unit Width Distribution (Ultimate) – Take-Off Case

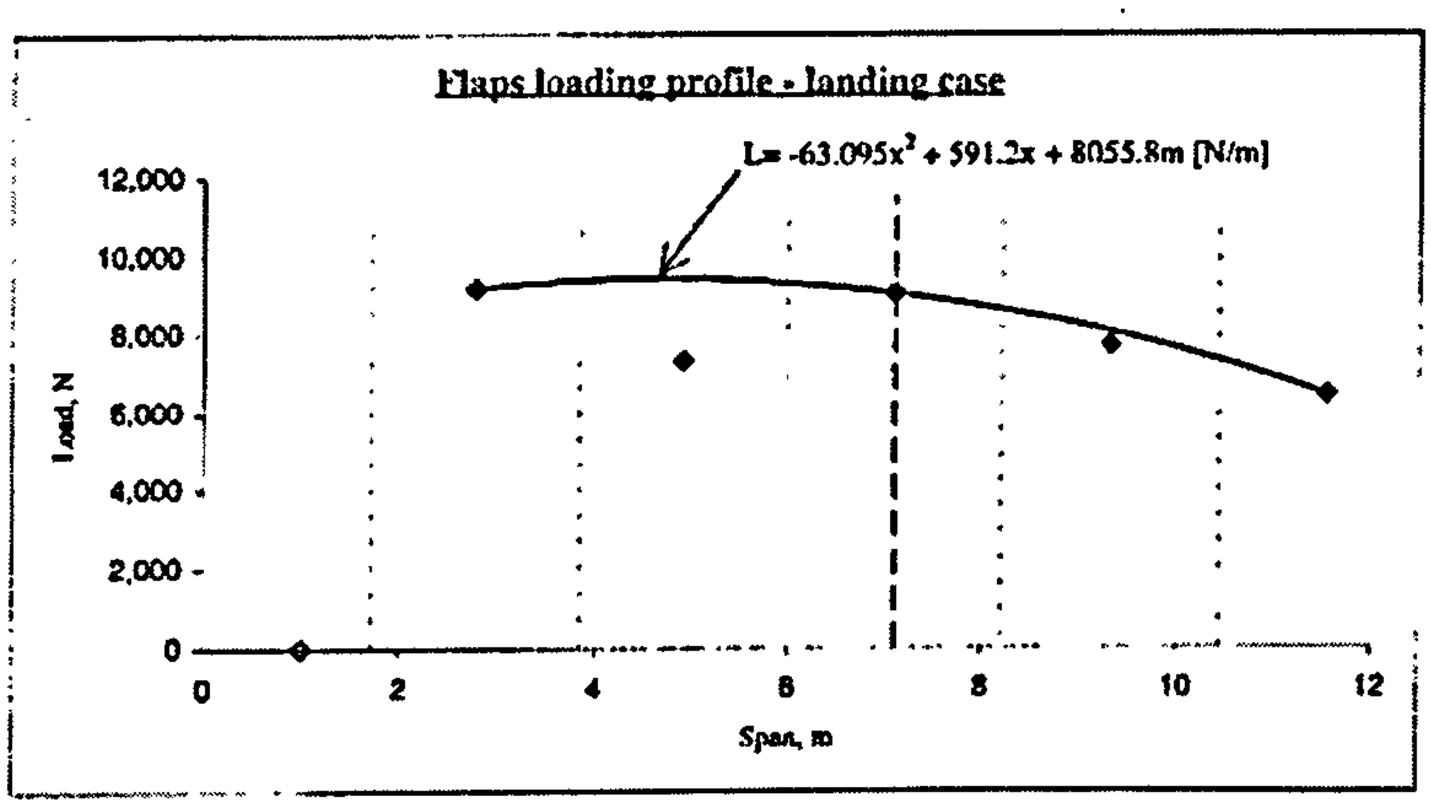

Figure A41 - ATRA Flap Spanwise Load per Unit Width Distribution (Ultimate) – Landing Case

APPENDIX B

ATRA/AIRBUS A320 LOADS COMPARISON

TABLE OF CONTENTS

B1 – ATRA 100/AIRBUS A320 COMPARISON DATA

Table B.1 – AIRBUS A320 and ATRA 100 Data [20]

	ATRA 100	AIRBUS A320
Nr. Passengers	108	150
Range, [nm/Km]	2250 / 4170	2950 / 5470
Speed, Mach		
Landing	0.2	
Take Off	0.2	
Cruise	0.8	0.82
Lift Coefficient, C_L		
Landing (Max)	2.9	
Take Off (Max)	2.2	
Cruise	0.51	
Wing (A320 Type)		
Aspect Ratio, A	9.5	9.4
Taper Ratio, l	0.274	
0.25 Sweepback, $\Lambda_{0.25}$	25°	25°
Span, b [m / ft]	32.4 / 9.9	34.1 / 10.4
Area, S [m^2 / ft^2]	110.2 / 1186.3	122.4 / 1318
Inboard Flap Area, S_{Fi} [m^2 / ft^2]	5.25 / 56.5	4.54 / 48.9
Outboard Flap Area, S_{Fo} [m^2 / ft^2]	6.75 / 72.7	5.96 / 64.2
Total Flap Area, S_{Fo} [m^2 / ft^2]	12 / 129.2	10.5 / 113
Design Mass		
Max. Landing Weight, W_L [Kg / Lb]	50635 / 111631	64000 / 141096
Max. Take Off Weight, W_{TO} [Kg / Lb]	56260 / 124032	77000 / 169756
Max. Zero Fuel Weight, W_{ZF} [Kg / Lb]	40738 / 89812	61000 / 134482
Operational Empty Weight, W_{OE} [Kg / Lb]	30425 / 67076	41800 / 92153
Wing Loading, W/S		
Take Off, (W_{TO}/S) [Kg/m^2 / Lb/ft^2]	511/ 105	629 / 129
Landing, (W_L/S) [Kg/m^2 / Lb/ft^2]	459.4 / 94	522.9 / 107

Runway Distances, S		
Take Off, (S_{TO}) [m / ft]	1981/ 6500	2294 / 7526
Landing, (S_L) [m / ft]	1475 / 4840	1442 / 4730
Thrust to Weight Ratio, T/W		
Thrust to Weight Ratio, (T/W)	0.29	0.295
Flap area, S		
Inboard Flap , [m^2]	5.25	4.54(*)
Outboard Flap, [m^2]	6.75	6.75(*)
Total Flap, [m^2]	12.00	10.50 (*)

(*) Estimated Value

B2 – ATRA 100/AIRBUS A320 FLAP LOADS ESTIMATION

B2.1 - ESTIMATION OF FLAP LIFT CONTRIBUTION – ATRA 100

The lift contribution due to the deployment of single slotted trailing edge flaps for the ATRA was estimated in ref. [1]. For Take-Off, 35% of the total lift coefficient was due to the deployment of the trailing edge flaps, while for Landing this value increased to around 42%. These percentages are used to determine the lift coefficient associated with the flap deployment and ultimately the increment in lift due to flap deployment.

a) Calculation of Take-Off Maximum Lift Coefficient ($C_{L_{MAX\_TO}}$)

From Ref. [25] retrieve take-off parameter for the ATRA100 take-off distance S_{TO}.

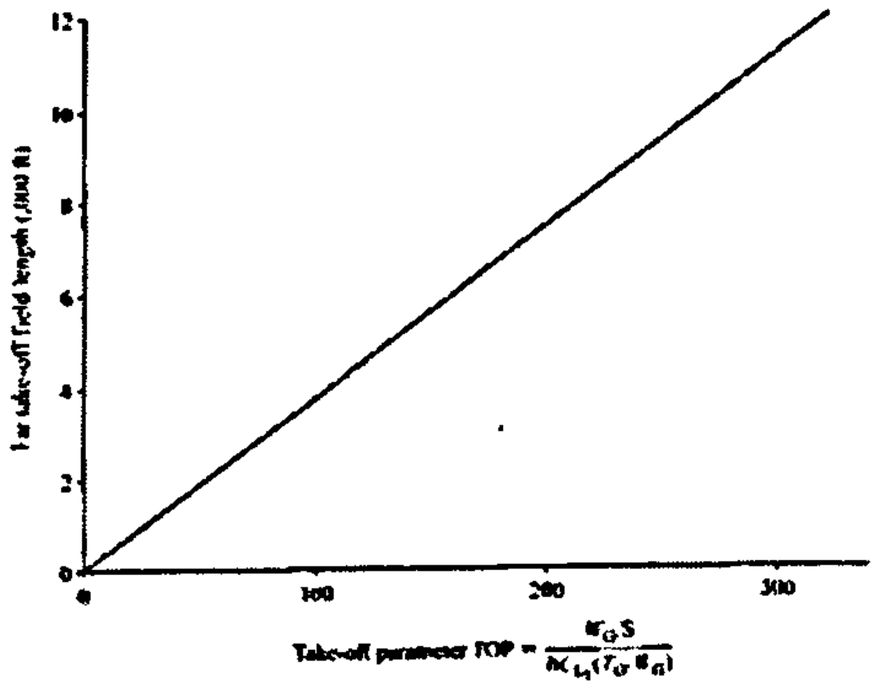

Figure B.1 – Simple Take-Off Estimation method [25]

For S_{TO}=6500ft (from Table 1 – Aircraft Data) the Take-Off Parameter is:

$$TOP = 173.4 \quad \text{and}$$

$$TOP = \frac{W_G / S}{\delta \cdot C_{L_{TO}} \cdot (T / W_G)} \qquad \text{[Equation B.1]}$$

where:

δ - Density Ratio ; W_G – Gross Take-Off Weight [lb]; S – Gross Wing Area [ft^2]; $C_{L_{TO}}$ – Max Lift Coefficient at Take-Off Configuration (not C_L at Take-Off Speed).

Rearranging Equation 1:

$$C_{L_{TO}} = \frac{W_G / S}{TOP \cdot \delta \cdot (T / W_G)} \qquad \text{[Equation B.2]}$$

From Table B.1:
W_G = 124032 lb
S = 1186.2 ft^2
(T/W_G) = 0.29

$$C_{L_{MAX\_TO}} = 2.1 \text{ (2.2 in Table B.1)}$$

b) Calculation of Maximum Landing Lift Coefficient ($C_{L_{MAX\_LD}}$)

1st Step – Approach Speed

From Ref. [25] retrieve square Approach Speed for the ATRA 100 landing distance SL.

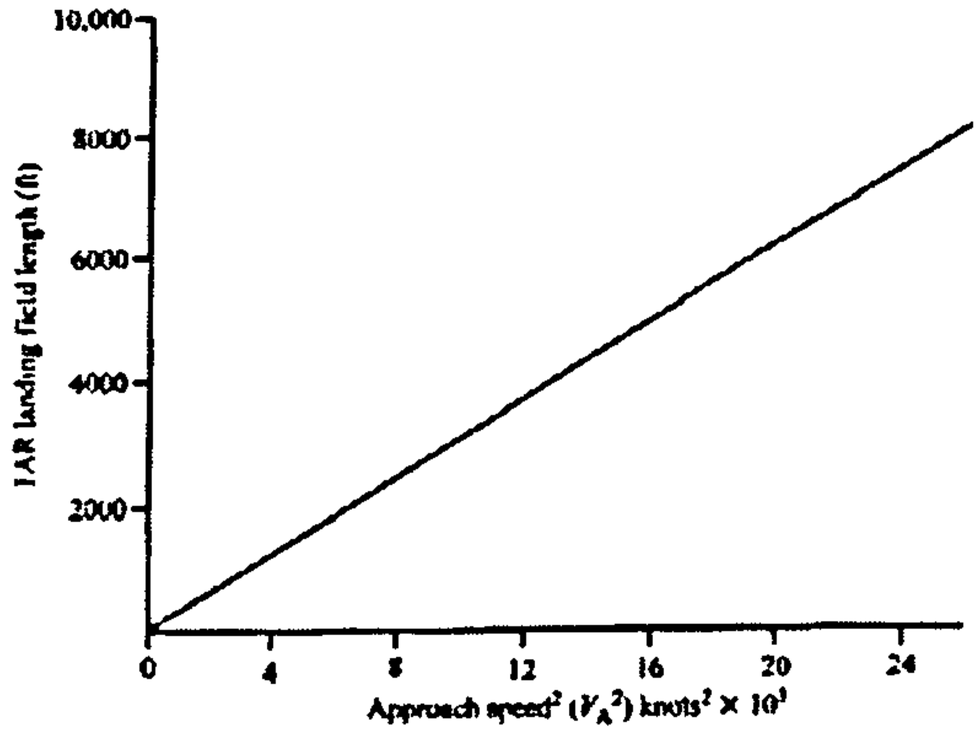

Figure B.2 – Landing Field Length [25]

For S_L=4840ft (Table 1 – Appendix A) the Take-Off Parameter is:

$$V_A^2 = 15600 \text{ knot}^2 \quad \Rightarrow \quad V_A = 124.9 \text{ knot}$$

2nd Step – Approach Lift Coefficient CLA

From Ref. [25] retrieve approach lift coefficient for the ATRA 100 approach speed V_A and Landing Parameter.

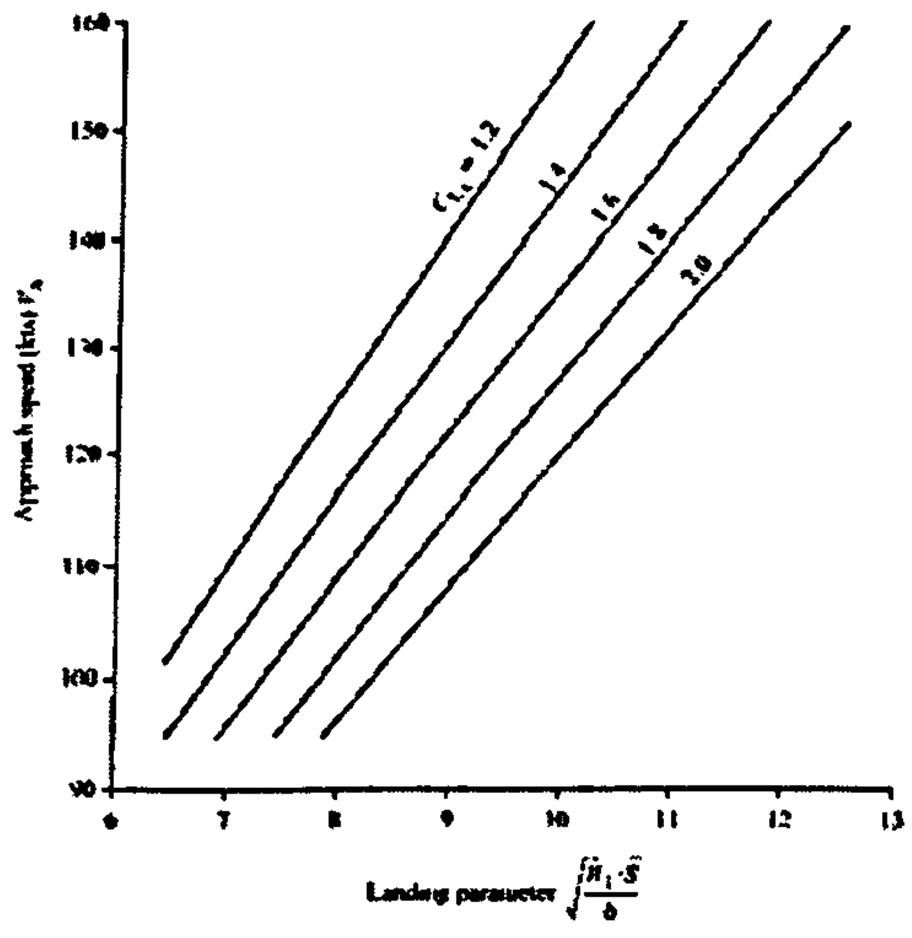

Figure B.3 – Approach speed [25]

where:

Landing Parameter = $\sqrt{\frac{W_L/S}{\delta}} = 9.7$

Approach Lift Coefficient $C_{LA} = 1.8$

$C_{LA} = C_{L_{MAX}} / 1.3^2$ [25]

[Equation B.3]

Rearranging Equation B.3: $C_{L_{MAX\_LD}} = 1.69 \cdot C_{L_A}$

$$C_{L_{MAX\_LD}} = 3.0 \text{ (2.9 in Table B.1)}$$

The values previously calculated for the Maximum Lift Coefficients are very similar to the ones presented in Table B.1. This means that the calculations to be performed for the Airbus A320 will not be far from the real lift coefficients.

c) Calculation of Flap Design Speeds (V_F)

FLAP SPEED, V_F

Landing: $V_{F_L} = 1.8 \cdot V_{S1}$

[Equation B.4]

Take-Off: $V_{F_{TO}} = 1.6 \cdot V_{S1}$

[Equation B.5]

Where:

V_{S1} – Stall Speed

$$V_{S1} = \sqrt{\frac{M \cdot g}{\frac{1}{2} \cdot \rho_0 \cdot S \cdot C_{L_{MAX}}}}$$

[Equation B.6]

Case 1 – Flap at Landing Position @ Max Design Landing Weight

From Table B.1:

M = 50635 kg ; g = 9.80665 kg/m^2 ; ρ_0 = 1.2250 kg/m^3 ; S = 110.2 m^2 ; C_{LMAX} = 3.0

$V_{S1} = 49.5$ **m/s** ⇒ $V_{F_L} = 89.1$ **m/s**

Case 2 – Flap at Take-Off Position @ Max Design Landing Weight

From Table B.1:

M = 56260 kg ; g = 9.80665 kg/m^2 ; ρ_0 = 1.2250 kg/m^3 ; S = 110.2 m^2 ; C_{LMAX} = 2.1

$V_{S1} = 62.5$ **m/s** ⇒ $V_{F_L} = 99.8$ **m/s**

d) *Increment in Lift Force due to Flap @V_F*

The increment in Lift Coefficient is given by the following equation:

$$\Delta C_{L_F} = \frac{\Delta L_F}{\frac{1}{2} \cdot \rho \cdot V_F^2 \cdot S_F}$$

[Equation B.7]

where:

ΔC_{L_F} - Increment in Lift Coefficient due to Flap deployment

ΔL_F - Increment in Lift due to Flap deployment

V_F - Flap Speed [m/s]

S_F - Flap Area [m^2]

ρ - Air Density [kg/m^3]

Rearranging Equation 5:

$$\Delta L_F = \frac{1}{2} \cdot \Delta C_{L_F} \cdot \rho \cdot V_F^2 \cdot S_F$$

Case 1 – Flap at Landing Position @ Max Design Landing Weight

ΔC_{L_F} - 1.2 (42% of calculated Max Lift Coefficient @ landing)

V_F - 89.1 [m/s]

S_F - 12 m^2

ρ - 1.2250 kg/m^3

$$\Delta L_F = 73521 \text{ N}$$

Case 2 – Flap at Take-Off Position @ Max Design Landing Weight

ΔC_{L_F} - 0.77 (35% of calculated Max Lift Coefficient @ take-off)

V_F - 99.8 [m/s]

S_F - 12 m^2

ρ - 1.2250 kg/m^3

$$\Delta L_F = 53807 \text{ N}$$

B2.2 - ESTIMATION OF FLAP LIFT CONTRIBUTION – AIRBUS A320

Applying the same procedure to the Airbus A320 we obtain the following results:

a) Calculation of Take-Off Maximum Lift Coefficient ($C_{L_{MAX\_TO}}$)

From Figure B.1: TOP = 202.5 $\Rightarrow$

$$C_{L_{MAX\_TO}} = 2.2$$

b) Maximum Landing Lift Coefficient ($C_{L_{MAX\_LD}}$)

1st Step – Approach Speed

From Figure B.2, with S_L=4730ft (Table B.1), the Take-Off Parameter is:

$$V_A^2 = 15280 \text{ knot}^2 \quad \Rightarrow \quad V_A = 123.6 \text{ knot}$$

2nd Step – Approach Lift Coefficient CLA

From Figure B.3, with $\sqrt{\frac{W_L / S}{\delta}} = 10.4$ and V_A, the Approach Lift Coefficient C_{LA} is:

$$C_{LA} = 2.07 \quad \Rightarrow$$

$$\boxed{C_{L_{MAX\_LD}} = 3.5}$$

c) Flap Design Speeds (V_F)

Case 1 – Flap at Landing Position @ Max Design Landing Weight

From Table B.1,

M = 64000 kg
S = 122.4 m^2
C_{LMAX} = 3.5

$$V_{S1} = 48.9 \text{ m/s} \quad \Rightarrow \quad V_{FL} = 88.0 \text{ m/s}$$

Case 2 – Flap at Take-Off Position @ Max Design Landing Weight

From Table 1 – Aircraft Data
M = 77000 kg
S = 122.4 m^2
C_{LMAX} = 2.2

$$V_{S1} = 67.7 \text{ m/s} \quad \Rightarrow \quad V_{FL} = 108.3 \text{ m/s}$$

d) Increment in Lift Force due to Flap @V_F

Case 1 – Flap at Landing Position @ Max Design Landing Weight

ΔC_{L_F} - 1.47 (42% of calculated Max Lift Coefficient @ landing)

V_F - 92.7 [m/s]

S_F - 10.5 m^2

$$\Delta L_F = 81240 \ \mathbf{N}$$

Case 2 – Flap at Take-Off Position @ Max Design Landing Weight

ΔC_{L_F} - 0.77 (35% of calculated Max Lift Coefficient @ take-off)

V_F - 108.3 [m/s]

S_F - 10.5 m^2

$$\Delta L_F = 58082 \ \mathbf{N}$$

B2.3 - FINAL RESULTS

	ATRA	A320	Difference from to A320 to ATRA
Take Off	53807 N	58082 N	+ 7.945%
Landing	73521 N	81240 N	+10.5%

Difference from to A320 to ATRA in Flap Area = +12.5%

Difference from to A320 to ATRA in Wing Area = +10%

The flap loads provided by Ammoo [1] for the ATRA will be increased 10%.

B2.4 – ATRA LOADS FOR VALIDATION

Total loads on the Flap (Figure A17, Appendix A)

Cruise Case – $L = -36.063 \cdot x^2 + 435.22 \cdot x + 2527.2$ [N/m] *(from Figure A17, Appendix A)*

$$\int_{1.714}^{5.987} L\,dx = 15440 \text{ [N]}$$

Take Off Case – $L = -106.97 \cdot x^2 + 1265.1 \cdot x + 6581.3$ [N/m] *(from Figure A18, Appendix A)*

$$\int_{1.714}^{5.987} L\,dx = 41460 \text{ [N]}$$

Landing Case – $L = -63.095 \cdot x^2 + 591.2 \cdot x + 8055.8$ [N/m] *(from Figure A19, Appendix A)*

$$\int_{1.714}^{5.987} L\,dx = 39740 \text{ [N]}$$

Reactions at hinge positions (Hinge 1 is assumed inside the fuselage and Hinge 2 at 67% of flap span).

LOADING	REACTION AND SHEAR	BENDING MOMENTS
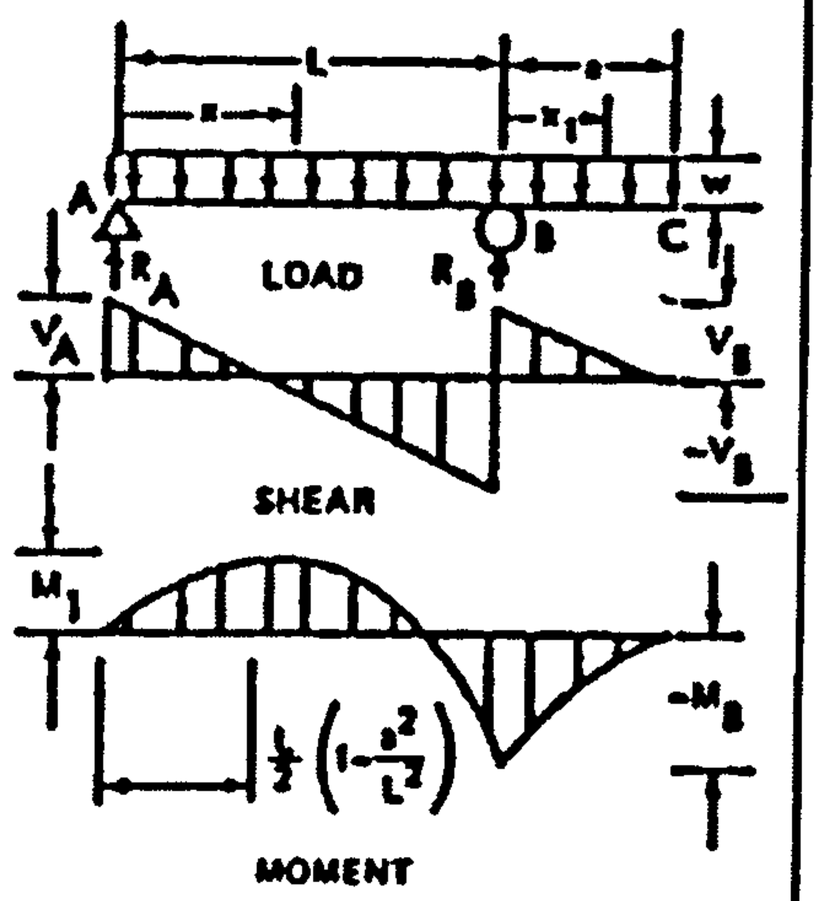	$R_A = \frac{w}{2L}(L^2 - a^2)$ $R_B = \frac{w}{2L}(L + a)^2$ $V_{max} = \frac{w}{2L}(L^2 + a^2)$ @ $x = L$ $V_x = R_A - wx$ @ $x < L$ $V_{x_1} = w(a - x_1)$ @ $x_1 \leq a$	$M_{max} = \frac{w}{8L^2}(L + a)^2(L - a)^2$ @ $x = \frac{L}{2}\left(1 - \frac{a^2}{L^2}\right)$ $M_{max_1} = \frac{-wa^2}{2}$ @ $x_1 = 0$ $M_x = \frac{wx}{2L}(L^2 - a^2 - xL)$ @ $x \leq L$ $M_{x_1} = \frac{-w}{2}(a - x_1)^2$ @ $x_1 \leq a$

Figure 4.4 – Hinge Reaction load Calculation [56]

a = 1.424 m
L = 2.849 m

Cruise

w = 15440 / (5.987-1.714) = 3613 N/m

$$R_A = \frac{w}{2 \cdot L} \cdot \left(L^2 - a^2\right) \Rightarrow R_A = 3860 \text{ N}$$

$$R_B = \frac{w}{2 \cdot L} \cdot (L + a)^2 \Rightarrow R_B = 11580 \text{ N}$$

Scaled Load - R_B= 12740 N

Take-Off

w = 9703 N/m

R_A= 10370 N

R_B= 31090 N

Scaled Load - R_B= 34200 N

Landing

w = 39740 / (5.987-1.714) = 9300 N/m

R_A= 9940 N

R_B= 29800 N

Scaled Load - R_B= 32780 N

APPENDIX C

INITIAL SIZING METHODS

TABLE OF CONTENTS

C1 – Mechanism Load Calculation Procedure

C1.1 Simple Hinge Mechanism Load Calculation Procedure

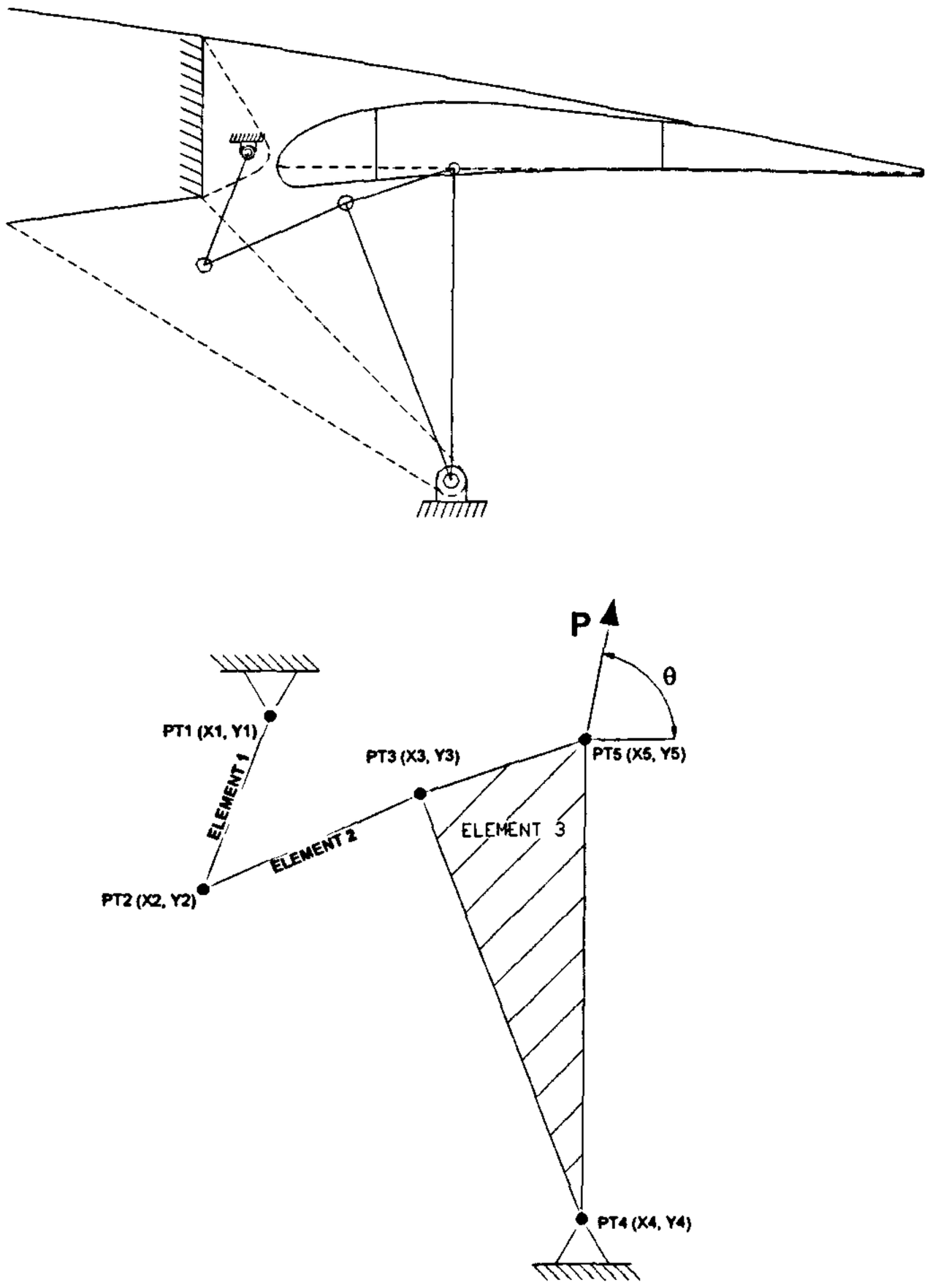

INPUTS

Mechanism points (mm):

PT1 (X1,Y1) PT2 (X2,Y2) PT3 (X3,Y3) PT4 (X4,Y4)
PT5 (X5,Y5)

Load and Angle:

P [N]
θ [°]

LOADS CALCULATIONS

Free Body Diagram – Whole System

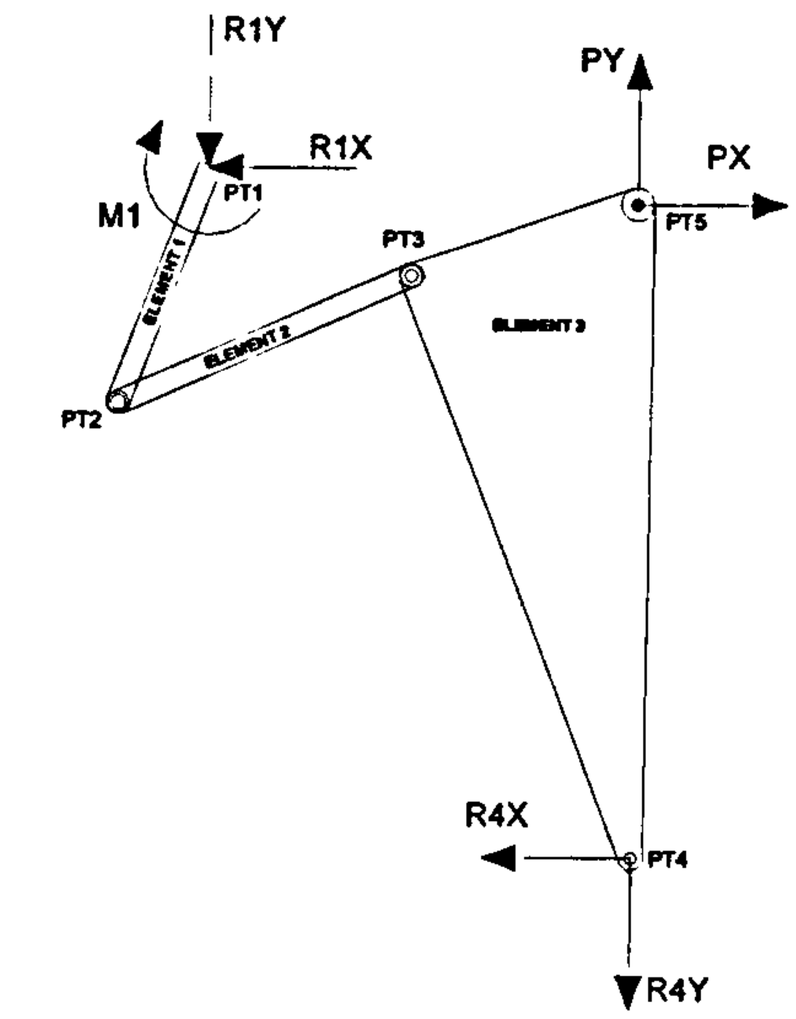

$$\rightarrow + \sum F_X = 0:$$

$$(R1X) + (R4X) - (PX) = 0 \qquad [1]$$

$$\uparrow + \sum F_Y = 0:$$

$$(PY) - (R1Y) - (R4Y) = 0 \qquad [2]$$

$$+) \sum M_{PT1} = 0:$$

$$-(R4X)\cdot(Y1 - Y4) - (R4Y)\cdot(X4 - X1) + (PX)\cdot(Y1 - Y5) + (PY)\cdot(X5 - X1) - M1 = 0 \qquad [3]$$

Free Body Diagram – Element 1

$$\rightarrow + \sum F_X = 0:$$

$$(F2X) - (R1X) = 0 \Leftrightarrow (F2X) = (R1X) \qquad [4]$$

$$\uparrow + \sum F_Y = 0:$$

$$(F2Y) - (R1Y) = 0 \Leftrightarrow (F2Y) = (R1Y) \qquad [5]$$

$$+) \sum M_{PT1} = 0:$$

$$(F2X)\cdot(Y1 - Y2) - (F2Y)\cdot(X1 - X2) - M1 = 0 \qquad [6]$$

Free Body Diagram – Element 2

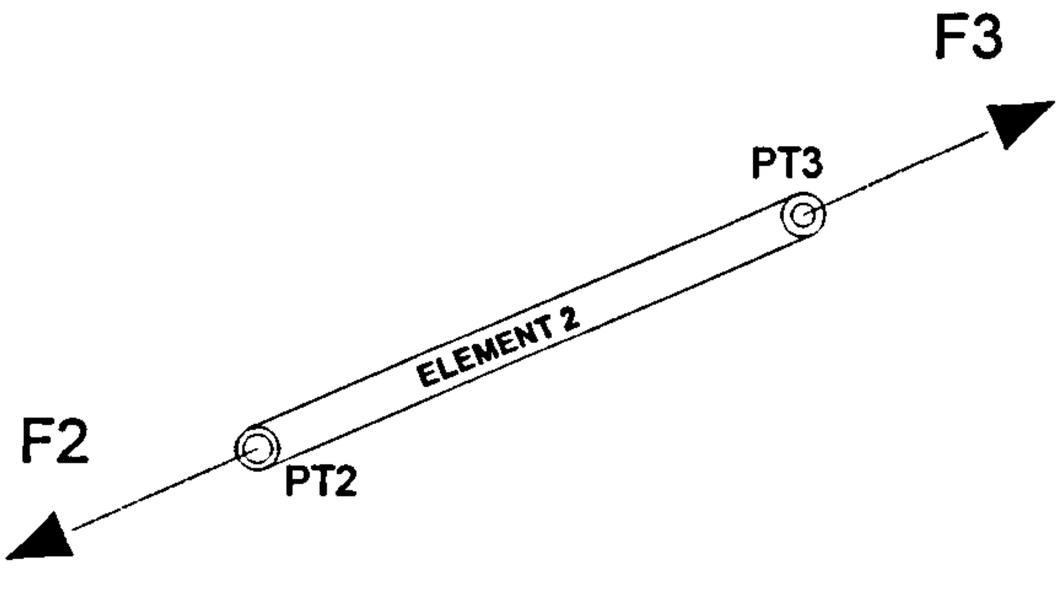

$$\rightarrow + \sum F = 0:$$

$$F2 = F3$$

Free Body Diagram – Element 3

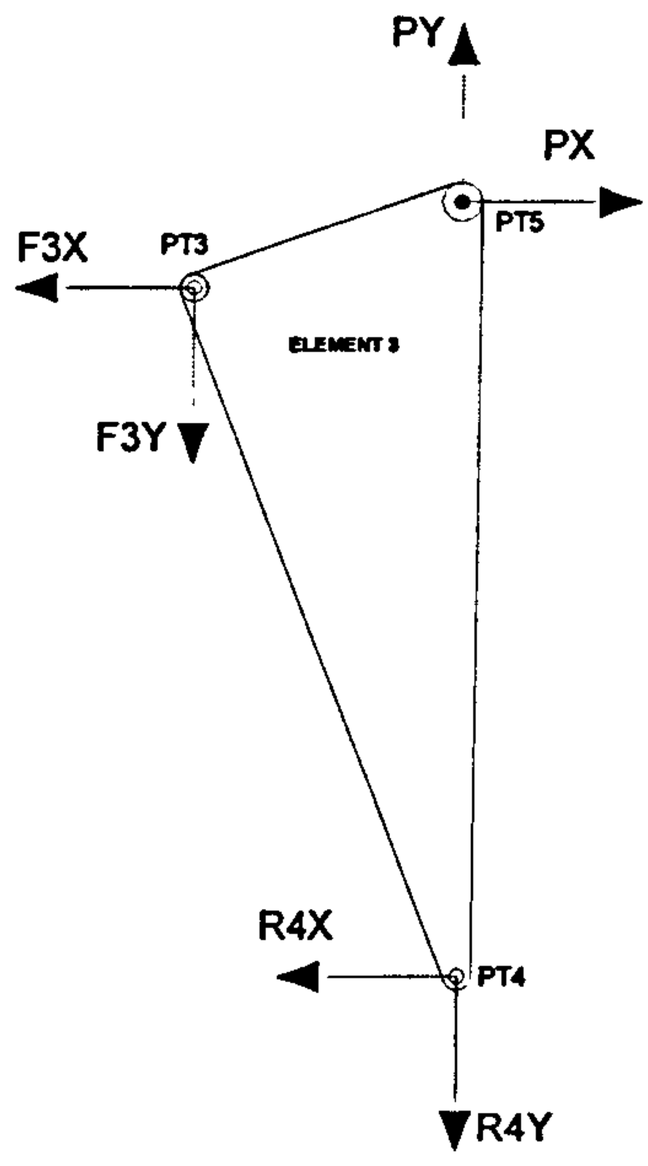

$$\rightarrow + \sum F_X = 0:$$

$$(PX) - (F3X) - (R4X) = 0 \qquad [10]$$

$$\uparrow + \sum F_Y = 0:$$

$$(PY) - (F3Y) - (R4Y) = 0 \qquad [11]$$

$$+) \sum M_{PT3} = 0:$$

$$-(R4X)\cdot(Y3 - Y4) - (R4Y)\cdot(X4 - X3)$$
$$-(PX)\cdot(Y5 - Y3) + (PY)\cdot(X5 - X3) = 0 \qquad [12]$$

Equations to Consider

$$(PX) - (R1X) - (R4X) = 0 \qquad [1]$$

$$(PY) + (R1Y) - (R4Y) = 0 \qquad [2]$$

$$-(R4X)\cdot(Y1 - Y4) - (R4Y)\cdot(X4 - X1) +$$
$$(PX)\cdot(Y1 - Y5) + (PY)\cdot(X5 - X1) - M1 = 0 \qquad [3]$$

$$(R1X)\cdot(Y1 - Y2) - (R1Y)\cdot(X1 - X2) - M1 = 0 \qquad [6]$$

$$-(R4X)\cdot(Y3 - Y4) - (R4Y)\cdot(X4 - X3)$$
$$-(PX)\cdot(Y5 - Y3) + (PY)\cdot(X5 - X3) = 0 \qquad [12]$$

Simplifying for MathCAD

$$PX - R4X - R1X = 0 \qquad [1]$$

$$PY + R4Y - R1Y = 0 \qquad [2]$$

$$-(R4X)\cdot a - (R4Y)\cdot b + c - (M1) = 0 \qquad [3]$$

$$(R1X)\cdot d - (R1Y)\cdot f - (M1) = 0 \qquad [6]$$

$$-(R4X)\cdot g - (R4Y)\cdot h + j = 0 \qquad [9]\ [12]$$

$a = Y1 - Y4$; $b = X4 - X1$; $c = (PX)\cdot(Y1 - Y5) + (PY)\cdot(X5 - X1)$; $d = Y1 - Y2$;

$f = X1 - X2$; $g = Y3 - Y4$; $h = X4 - X3$; $j = -(PX)\cdot(Y5 - Y3) + (F3Y)\cdot(X5 - X3)$

Using the symbolical calculation form MathCAD we obtain the following results:

$$R1X = \frac{(PX\cdot g\cdot f + a\cdot PX\cdot h + b\cdot g\cdot PX - f\cdot PY\cdot h - f\cdot j - b\cdot j - c\cdot h)}{(-d\cdot h + g\cdot f + g\cdot b + a\cdot h)}$$

$$R1Y = \frac{(-PY\cdot d\cdot h + a\cdot PY\cdot h + g\cdot b\cdot PY + d\cdot g\cdot PX - c\cdot g - j\cdot d + j\cdot a)}{(-d\cdot h + g\cdot f + g\cdot b + a\cdot h)}$$

$$R4X = \frac{(-d\cdot PX\cdot h + f\cdot PY\cdot h + f\cdot j + b\cdot j + c\cdot h)}{(-d\cdot h + g\cdot f + g\cdot b + a\cdot h)}$$

$$R4Y = \frac{(-d\cdot g\cdot PX + g\cdot f\cdot PY + c\cdot g + j\cdot d - j\cdot a)}{(-d\cdot h + g\cdot f + g\cdot b + a\cdot h)}$$

$$M1 = \frac{(a\cdot d\cdot PX\cdot h - a\cdot f\cdot PY\cdot h - a\cdot f\cdot j + b\cdot d\cdot g\cdot PX - b\cdot g\cdot f\cdot PY - b\cdot j\cdot d - c\cdot d\cdot h + c\cdot g\cdot f)}{(-d\cdot h + g\cdot f + g\cdot b + a\cdot h)}$$

C1.2. Four Bar Mechanism Load Calculation Procedure

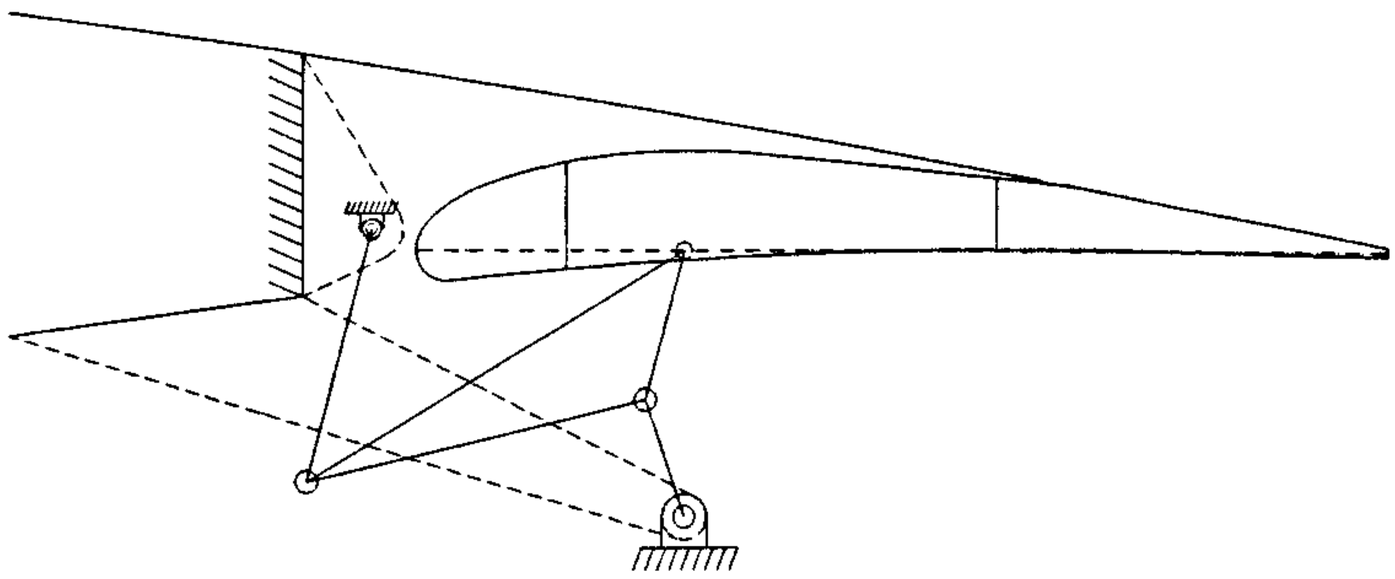

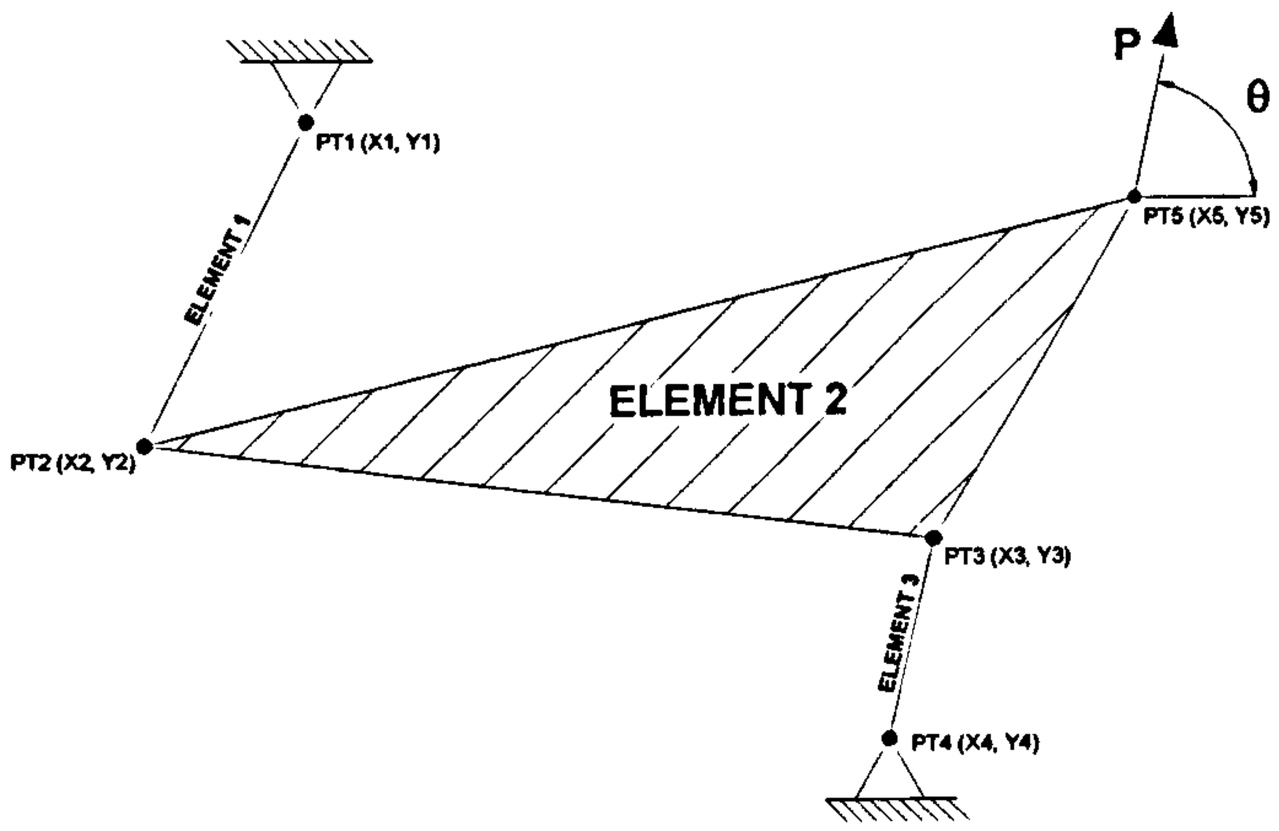

INPUTS

Mechanism points (mm):

PT1 (X1,Y1) PT2 (X2,Y2) PT3 (X3,Y3) PT4(X4,Y4)
PT5 (X5,Y5)

Load and Angle:

P [N]
θ [°]

LOADS CALCULATIONS

Free Body Diagram – Whole System

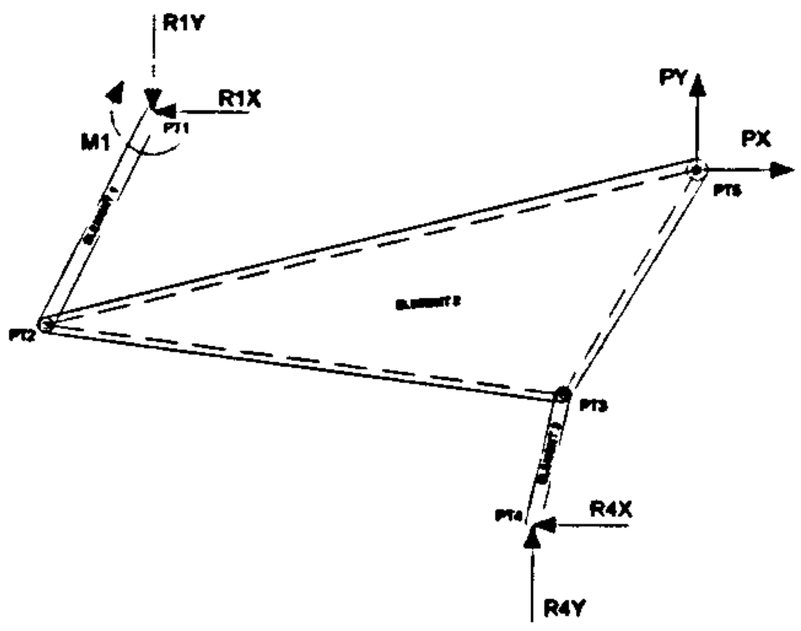

$$\rightarrow + \sum F_X = 0:$$

$$(R1X) + (R4X) - (PX) = 0 \quad [1]$$

$$\uparrow + \sum F_Y = 0:$$

$$(PY) + (R4Y) - (R1Y) = 0 \quad [2]$$

$$+) \sum M_{PT1} = 0:$$

$$-(R4X)\cdot(Y1 - Y4) + (R4Y)\cdot(X4 - X1) + (PX)\cdot(Y1 - Y5) + (PY)\cdot(X5 - X1) - M1 = 0 \quad [3]$$

Free Body Diagram – Element 1

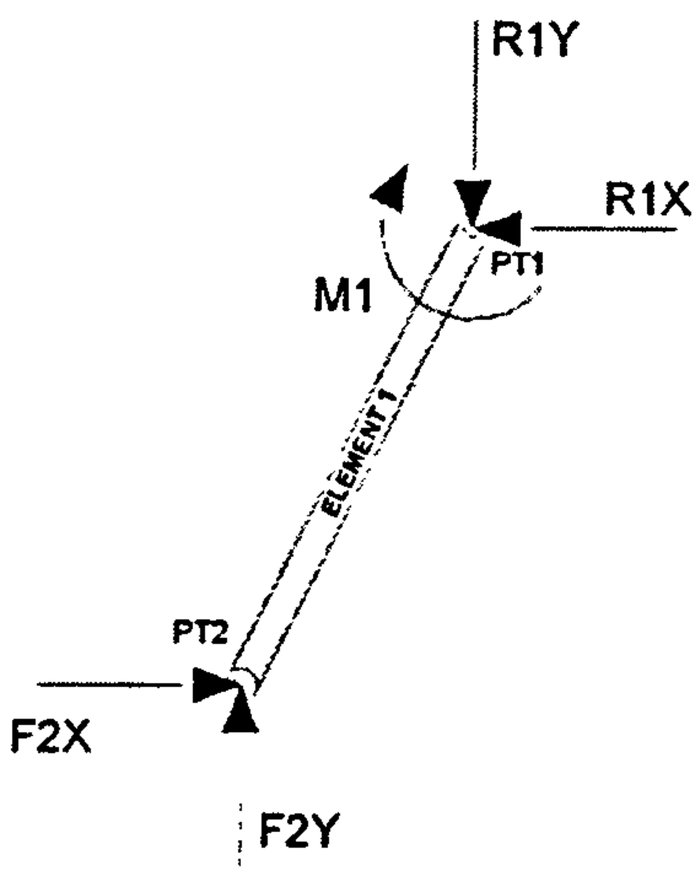

$$\rightarrow + \sum F_X = 0:$$

$$(F2X) - (R1X) = 0 \Leftrightarrow (F2X) = (R1X) \quad [4]$$

$$\uparrow + \sum F_Y = 0:$$

$$(F2Y) - (R1Y) = 0 \Leftrightarrow (F2Y) = (R1Y) \quad [5]$$

$$+) \sum M_{PT1} = 0:$$

$$(F2X)\cdot(Y1 - Y2) - (F2Y)\cdot(X1 - X2) - M1 = 0 \quad [6]$$

Free Body Diagram – Element 2

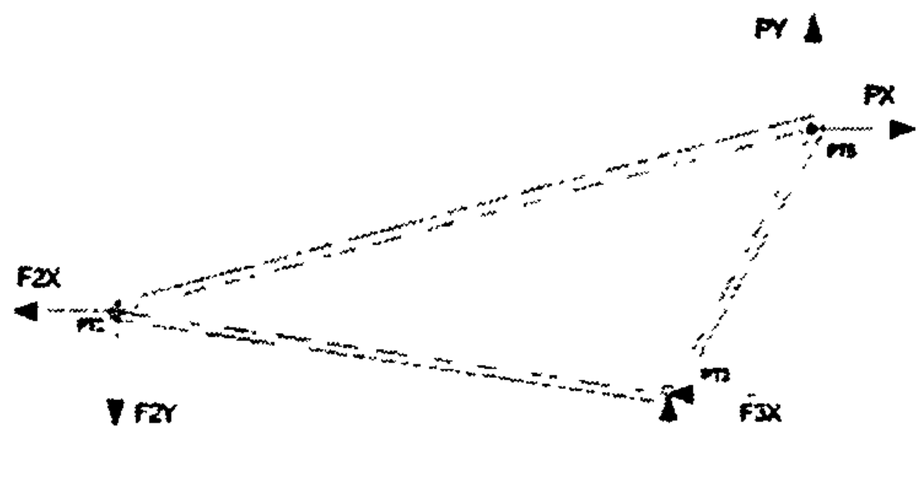

$$\rightarrow + \sum F_X = 0:$$

$$(F2X) - (PX) + (F3X) = 0 \Leftrightarrow$$
$$(R1X) - (PX) + (F3X) = 0 \quad [7]$$

$$\uparrow + \sum F_Y = 0:$$

$$(PY) + (F3Y) - (F2Y) = 0 \Leftrightarrow$$
$$(PY) + (F3Y) - (R1Y) = 0 \quad [8]$$

$$+) \sum M_{PT2} = 0:$$

$$(F3X) \cdot (Y3 - Y2) + (F3Y) \cdot (X3 - X2)$$
$$-(PX) \cdot (Y5 - Y2) + (PY) \cdot (X5 - X2) = 0 \quad [9]$$

Free Body Diagram – Element 3

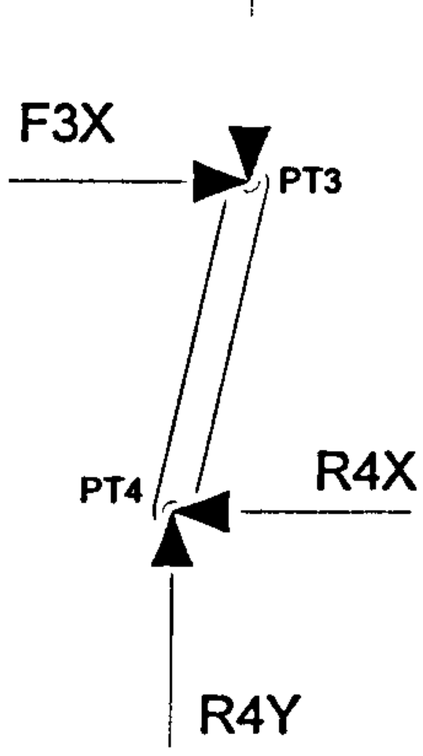

$$\rightarrow + \sum F_X = 0:$$

$$(F3X) - (R4X) = 0 \Leftrightarrow (F3X) = (R4X) \quad [10]$$

$$\uparrow + \sum F_Y = 0:$$

$$(F3Y) - (R4Y) = 0 \Leftrightarrow (F3Y) = (R4Y) \quad [11]$$

$$+) \sum M_{PT4} = 0:$$

$$(F3Y) \cdot (X3 - X4) - (F3X) \cdot (Y3 - Y4) = 0 \quad [12]$$

Simplifications

[4] & [5] into [6]

+) $\sum M_{PT1}=0$: $(R1X)\cdot(Y1-Y2)-(R1Y)\cdot(X1-X2)-M1=0$ [6]

[10] & [11] into [12]

+) $\sum M_{PT4}=0$: $(-R4Y)\cdot(X3-X4)-(R4X)\cdot(Y3-Y4)=0$ [12]

[10] & [11] into [9]

+) $\sum M_{PT2}=0$: $(PY)\cdot(X5-X2)-(PX)\cdot(Y5-Y2)+$
$(R4Y)\cdot(X3-X2)+(R4X)\cdot(Y3-Y2)=0$ [9]

Equations to Consider

$(R1X)+(R4X)-(PX)=0$ [1]

$(PY)+(R4Y)-(R1Y)=0$ [2]

$(R4Y)\cdot(X4-X1)-(R4X)\cdot(Y1-Y4)+$
$(PX)\cdot(Y1-Y5)+(PY)\cdot(X5-X1)-M1=0$ [3]

$(R1X)\cdot(Y1-Y2)-(R1Y)\cdot(X1-X2)-M1=0$ [6]

$(PY)\cdot(X5-X2)-(PX)\cdot(Y5-Y2)+$
$(R4Y)\cdot(X3-X2)+(R4X)\cdot(Y3-Y2)=0$ [9]

Simplifying for MathCAD

$PX-R4X-R1X=0$ [1]

$PY+R4Y-R1Y=0$ [2]

$-(R4X)\cdot a+(R4Y)\cdot b+c-(M1)=0$ [3]

$(R1X)\cdot d-(R1Y)\cdot f-(M1)=0$ [6]

$(R4X)\cdot g+(R4Y)\cdot h+j=0$ [9]

$a=Y1-Y4$; $b=X4-X1$; $c=(PX)\cdot(Y1-Y5)+(PY)\cdot(X5-X1)$; $d=Y1-Y5$;

$f=X1-X2$; $g=Y3-Y2$; $h=X3-X2$; $j=(PY)\cdot(X5-X2)-(PX)\cdot(Y5-Y2)$;

Using the symbolical calculation form MathCAD we obtain the following results:

$$R1X = \frac{(-h \cdot f \cdot PY - h \cdot c + j \cdot f + j \cdot b + PX \cdot g \cdot f + b \cdot PX \cdot g + a \cdot h \cdot PX)}{(-d \cdot h + g \cdot f + g \cdot b + a \cdot h)}$$

$$R1Y = \frac{(d \cdot j + d \cdot PX \cdot g - a \cdot j - c \cdot g - PY \cdot d \cdot h + b \cdot PY \cdot g + a \cdot h \cdot PY}{(-d \cdot h + g \cdot f + g \cdot b + a \cdot h)}$$

$$R4X = \frac{(-h \cdot d \cdot PX + h \cdot f \cdot PY + h \cdot c - j \cdot f - j \cdot b)}{(-d \cdot h + g \cdot f + g \cdot b + a \cdot h)}$$

$$R4Y = \frac{(d \cdot j + d \cdot PX \cdot g - f \cdot PY \cdot g - a \cdot j - c \cdot g)}{(-d \cdot h + g \cdot f + g \cdot b + a \cdot h)}$$

$$M1 = \frac{(b \cdot d \cdot j + b \cdot d \cdot PX \cdot g - b \cdot f \cdot PY \cdot g + a \cdot h \cdot d \cdot PX - a \cdot h \cdot f \cdot PY + a \cdot j \cdot f - c \cdot d \cdot h + c \cdot g \cdot f)}{(-d \cdot h + g \cdot f + g \cdot b + a \cdot h)}$$

Other Equations

$(F2X) = (R1X)$ [4]

$(F2Y) = (R1Y)$ [5]

$(F3X) = (R4X)$ [10]

$(F3Y) = (R4Y)$ [11]

C1.3. Link/Track Mechanism Load Calculation Procedure

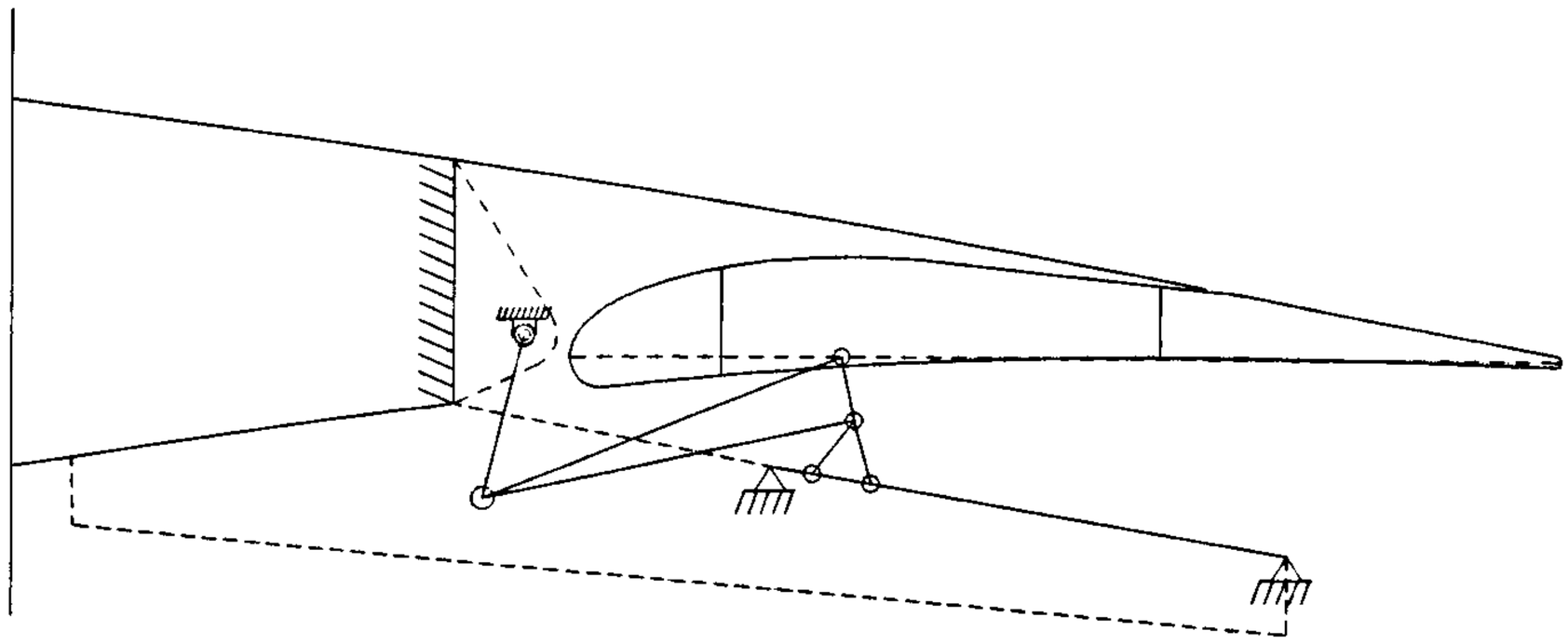

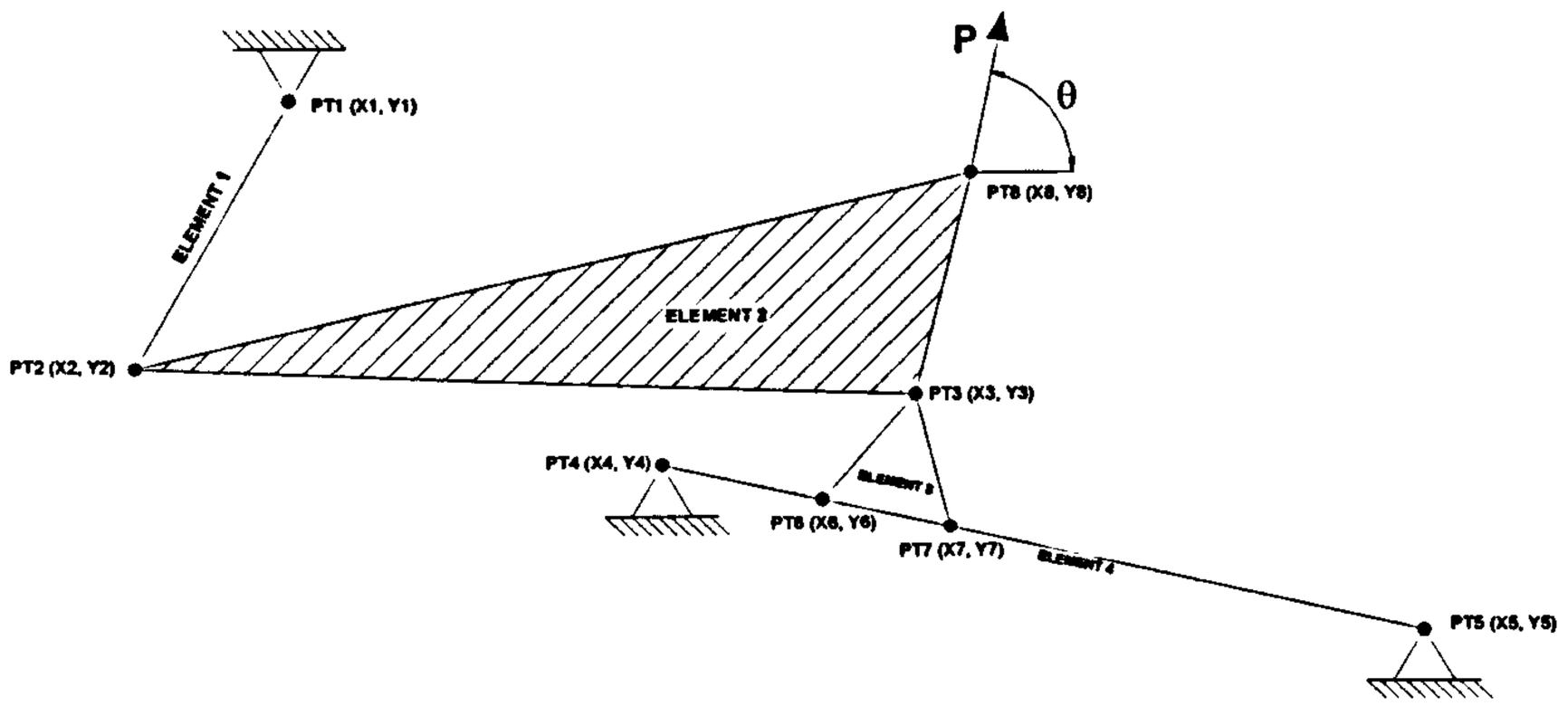

INPUTS

Mechanism points (mm):

PT1 (X1,Y1)	PT2 (X2,Y2)	PT3 (X3,Y3)	PT4(X4,Y4)
PT5 (X5,Y5)	PT6 (X6,Y6)	PT7 (X7,Y7)	PT8 (X8,Y5)

Load and Angle:

P [N]
θ [°]

LOADS CALCULATIONS

Free Body Diagram – Whole System

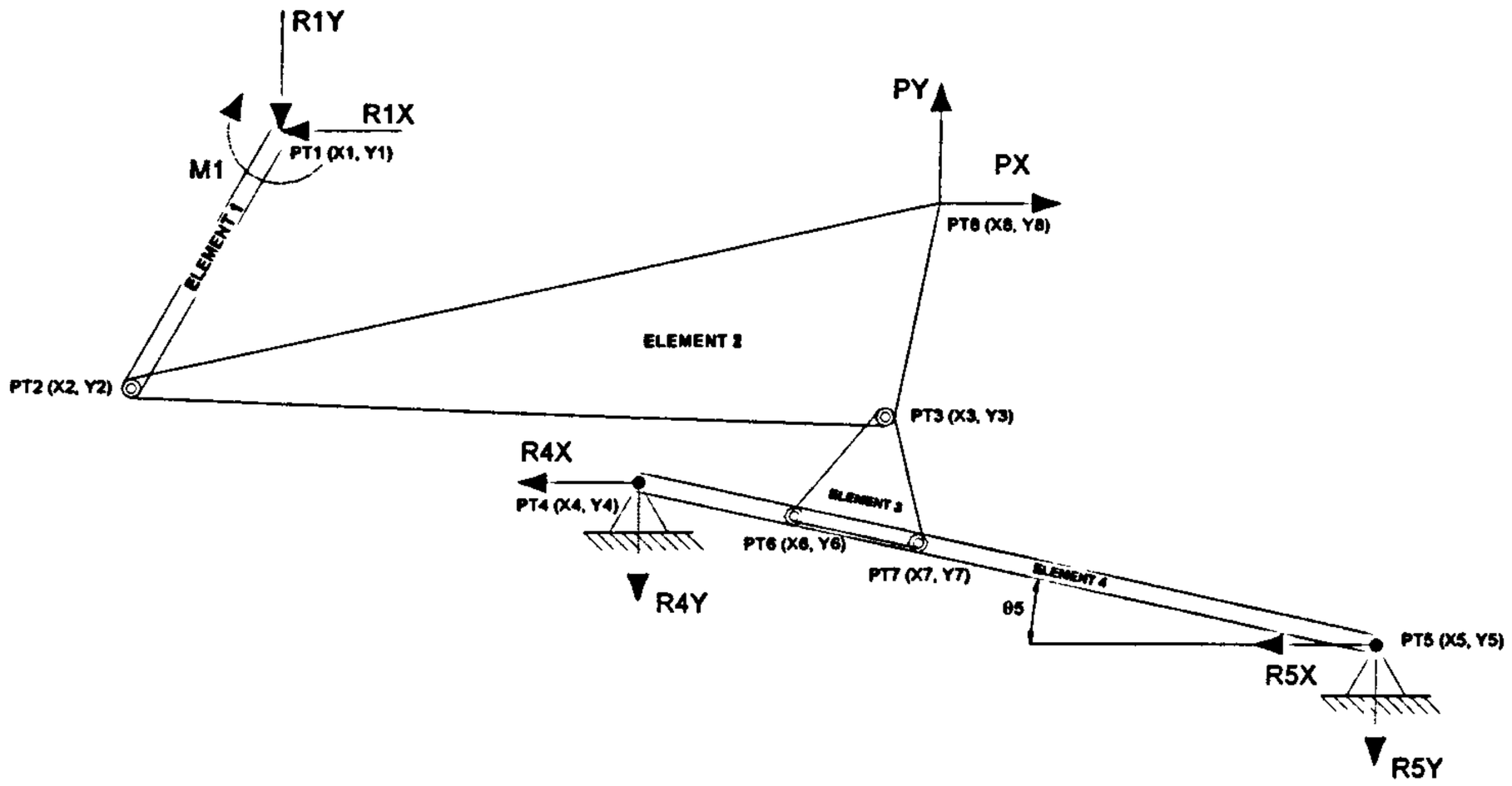

$$\rightarrow + \sum F_X = 0: \qquad (PX) - (R1X) - (R4X) - (R5X) = 0 \qquad [1]$$

$$\uparrow + \sum F_Y = 0: \qquad (PY) - (R1Y) - (R4Y) - (R5Y) = 0 \qquad [2]$$

$$+) \sum M_{PT1} = 0: \qquad (PX)\cdot(Y1 - Y8) + (PY)\cdot(X8 - X1) -$$
$$(R4X)\cdot(Y1 - Y4) - (R4Y)\cdot(X4 - X1) -$$
$$(R5X)\cdot(Y1 - Y5) - (R5Y)\cdot(X5 - X1) - M1 = 0 \qquad [3]$$

Free Body Diagram – Element 1

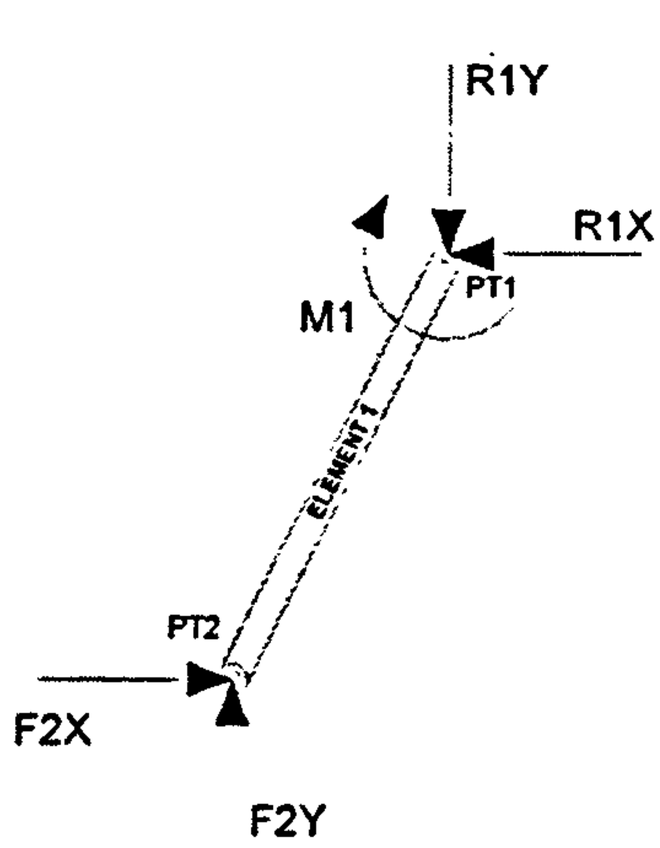

$$\rightarrow + \sum F_X = 0:$$

$$(F2X) - (R1X) = 0 \Leftrightarrow (F2X) = (R1X) \qquad [4]$$

$$\uparrow + \sum F_Y = 0:$$

$$(F2Y) - (R1Y) = 0 \Leftrightarrow (F2Y) = (R1Y) \qquad [5]$$

$$+) \sum M_{PT1} = 0:$$

$$(F2X)\cdot(Y1 - Y2) - (F2Y)\cdot(X1 - X2) - M1 = 0 \qquad [6]$$

Free Body Diagram – Element 2

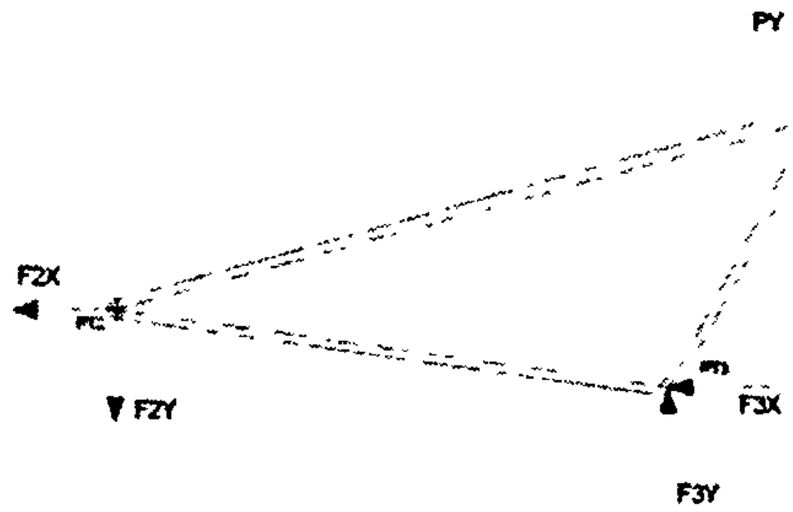

$$\rightarrow + \sum F_X = 0:$$

$$(PX) - (F2X) - (F3X) = 0 \qquad [7]$$

$$\uparrow + \sum F_Y = 0:$$

$$(PY) - (F2Y) - (F3Y) = 0 \qquad [8]$$

$$+) \sum M_{PT2} = 0:$$

$$(F3X)\cdot(Y2 - Y3) - (F3Y)\cdot(X3 - X2) - (PX)\cdot(Y8 - Y2) + (PY)\cdot(X8 - X2) = 0 \qquad [9]$$

Free Body Diagram – Element 3

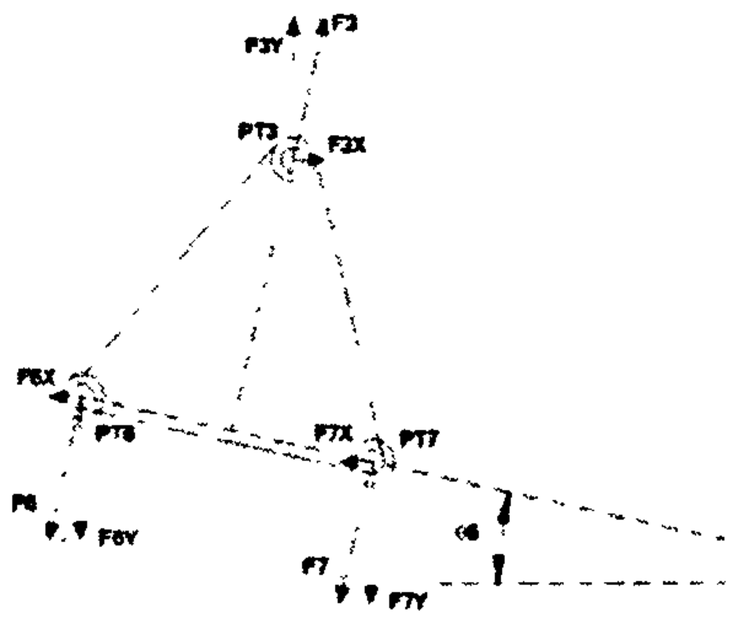

$$\rightarrow + \sum F_X = 0:$$

$$(F3X) - (F6X) - (F7X) = 0 \qquad [10]$$

$$\uparrow + \sum F_Y = 0:$$

$$(F3Y) - (F6Y) - (F7Y) = 0 \qquad [11]$$

$$+) \sum M_{PT3} = 0:$$

$$-(F6X)\cdot(Y3 - Y6) + (F6Y)\cdot(X3 - X6) - (F7X)\cdot(Y3 - Y7) - (F7Y)\cdot(X7 - X3) = 0 \qquad [12]$$

Free Body Diagram - Element 4

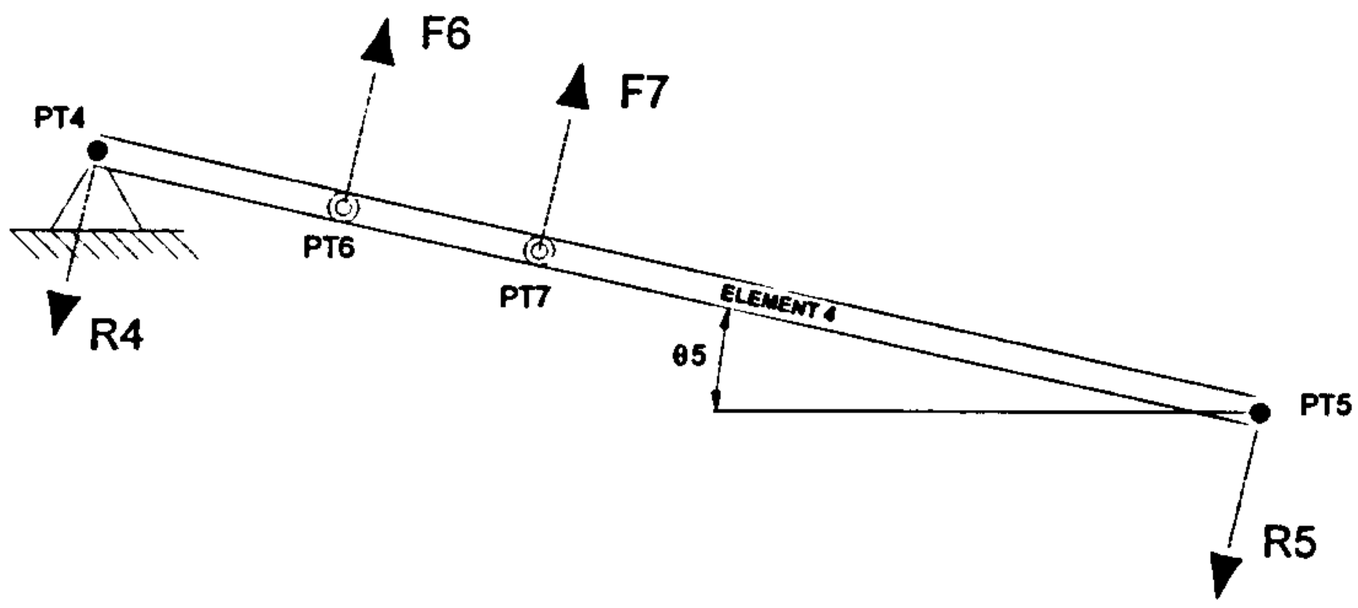

$$\rightarrow + \sum F_Y = 0 \quad : \quad F6 + F7 - R4 - R5 = 0 \qquad [13]$$

$$+) \sum M_{PT4} = 0 : \quad F6 \cdot \frac{(X6 - X4)}{Cos(\theta 5)} + F7 \cdot \frac{(X7 - X4)}{Cos(\theta 5)} - R5 \cdot c = 0 \qquad [14]$$

Equations to Consider For MathCAD

$h \cdot R1X - j \cdot R1Y - M1 = 0$ [6]

$PX - R1X - p \cdot F3 = 0$ [7]

$PY - R1Y - q \cdot F3 = 0$ [8]

$F3 \cdot (k \cdot p - l \cdot q) + m = 0$ [9]

$F3 - F6 - F7 = 0$ [10]

$n \cdot F6 - o \cdot F7 = 0$ [12]

$R4 + R5 - F6 - F7 = 0$ [13]

$R5 \cdot c - t \cdot F6 - u \cdot F7 = 0$ [14]

Simplifications

$a = Y1 - Y4$; $b = X4 - X1$; $c = \frac{X5 - X4}{\cos(\theta 5)}$; $d = Y1 - Y5$; $f = X5 - X1$;

$g = (PX) \cdot (Y1 - Y8) + (PY) \cdot (X8 - X1)$; $h = Y1 - Y2$; $j = X1 - X2$; $k = Y2 - Y3$;

$l = X3 - X2$; $m = -(PX) \cdot (Y8 - Y2) + (PY) \cdot (X8 - X2)$;

$n = -\sin(\theta 5) \cdot (Y3 - Y6) + \cos(\theta 5) \cdot (X3 - X6)$;

$o = \sin(\theta 5) \cdot (Y3 - Y7) + \cos(\theta 5) \cdot (X3 - X7)$; $p = \sin(\theta 5)$; $q = \cos(\theta 5)$;

$t = \frac{(X6 - X4)}{q}$; $u = \frac{(X7 - X4)}{q}$: $\theta 5 = a\tan\left(\frac{Y4 - Y5}{X5 - X4}\right)$.

MathCAD Solution

$$R1X = \frac{(PX \cdot k \cdot p - PX \cdot l \cdot q + p \cdot m)}{(k \cdot p - l \cdot q)}$$

$$R1Y = \frac{(PY \cdot k \cdot p - PY \cdot l \cdot q - q \cdot m)}{(k \cdot p - l \cdot q)}$$

$$F3 = \frac{-m}{(k \cdot p - l \cdot q)}$$

$$F6 = -o \cdot \frac{m}{(n \cdot k \cdot p - n \cdot l \cdot q + o \cdot k \cdot p - o \cdot l \cdot q)}$$

$$F7 = -n \cdot \frac{m}{(n \cdot k \cdot p - n \cdot l \cdot q + o \cdot k \cdot p - o \cdot l \cdot q)}$$

$$R4 = -m \cdot \frac{(-n \cdot u + t \cdot o - o \cdot c - n \cdot c)}{c \cdot (n \cdot k \cdot p - n \cdot l \cdot q + o \cdot k \cdot p - o \cdot l \cdot q)}$$

$$R5 = -m \cdot \frac{(n \cdot u + t \cdot o)}{c \cdot (n \cdot k \cdot p - n \cdot l \cdot q + o \cdot k \cdot p - o \cdot l \cdot q)}$$

$$M1 = \frac{(h \cdot PX \cdot k \cdot p - h \cdot PX \cdot l \cdot q + h \cdot p \cdot m - j \cdot PY \cdot k \cdot p + j \cdot PY \cdot l \cdot q - j \cdot q \cdot m)}{(k \cdot p - l \cdot q)}$$

Other Equations

$$F2X = R1X$$

$$F2Y = R1Y$$

$$R4X = R4 \cdot \sin(\theta 5)$$

$$R4Y = R4 \cdot \cos(\theta 5)$$

$$R5X = R5 \cdot \sin(\theta 5)$$

$$R5Y = R5 \cdot \cos(\theta 5)$$

$$F3X = F3 \cdot \sin(\theta 5)$$

$$F3Y = F3 \cdot \cos(\theta 5)$$

$$F6X = F6 \cdot \sin(\theta 5)$$

$$F6Y = F6 \cdot \cos(\theta 5)$$

$$F7X = F7 \cdot \sin(\theta 5)$$

$$F7Y = F7 \cdot \cos(\theta 5)$$

C1.4. Hooked Track Mechanism Load Calculation Procedure

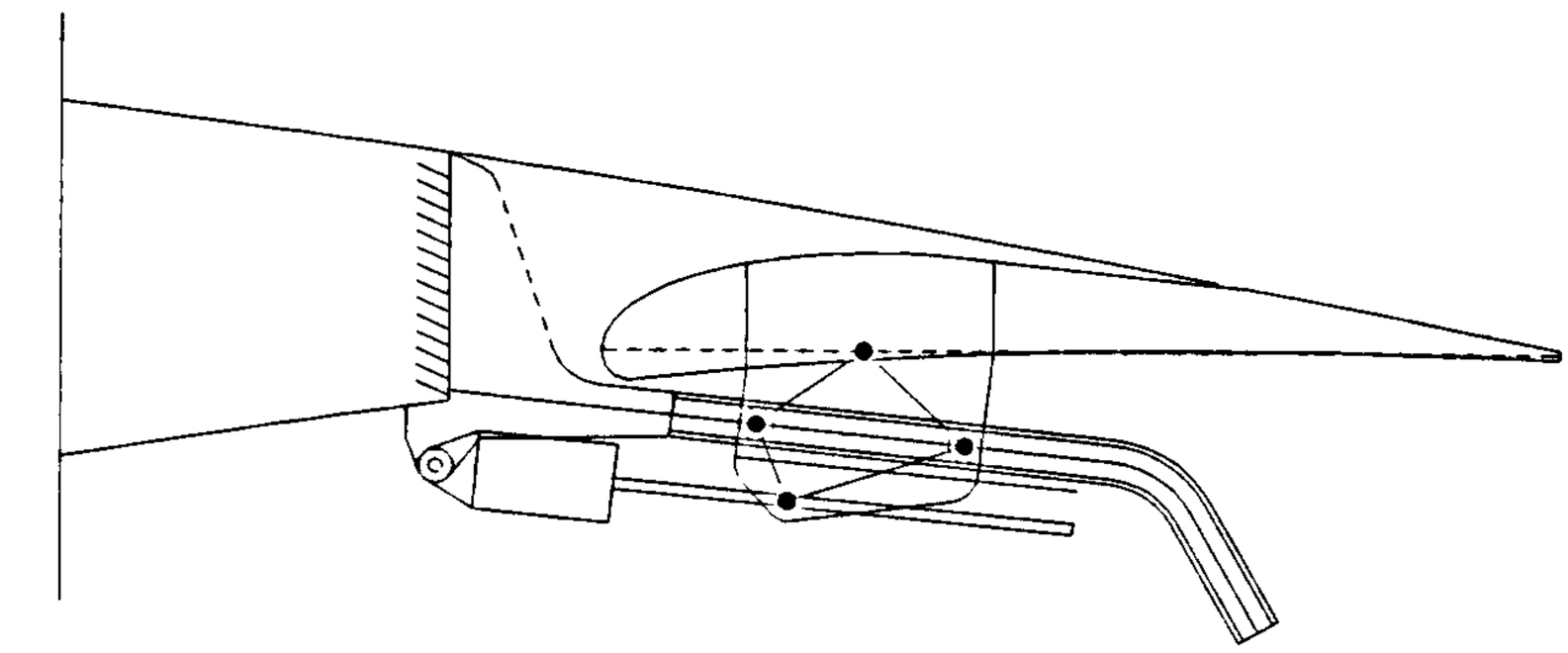

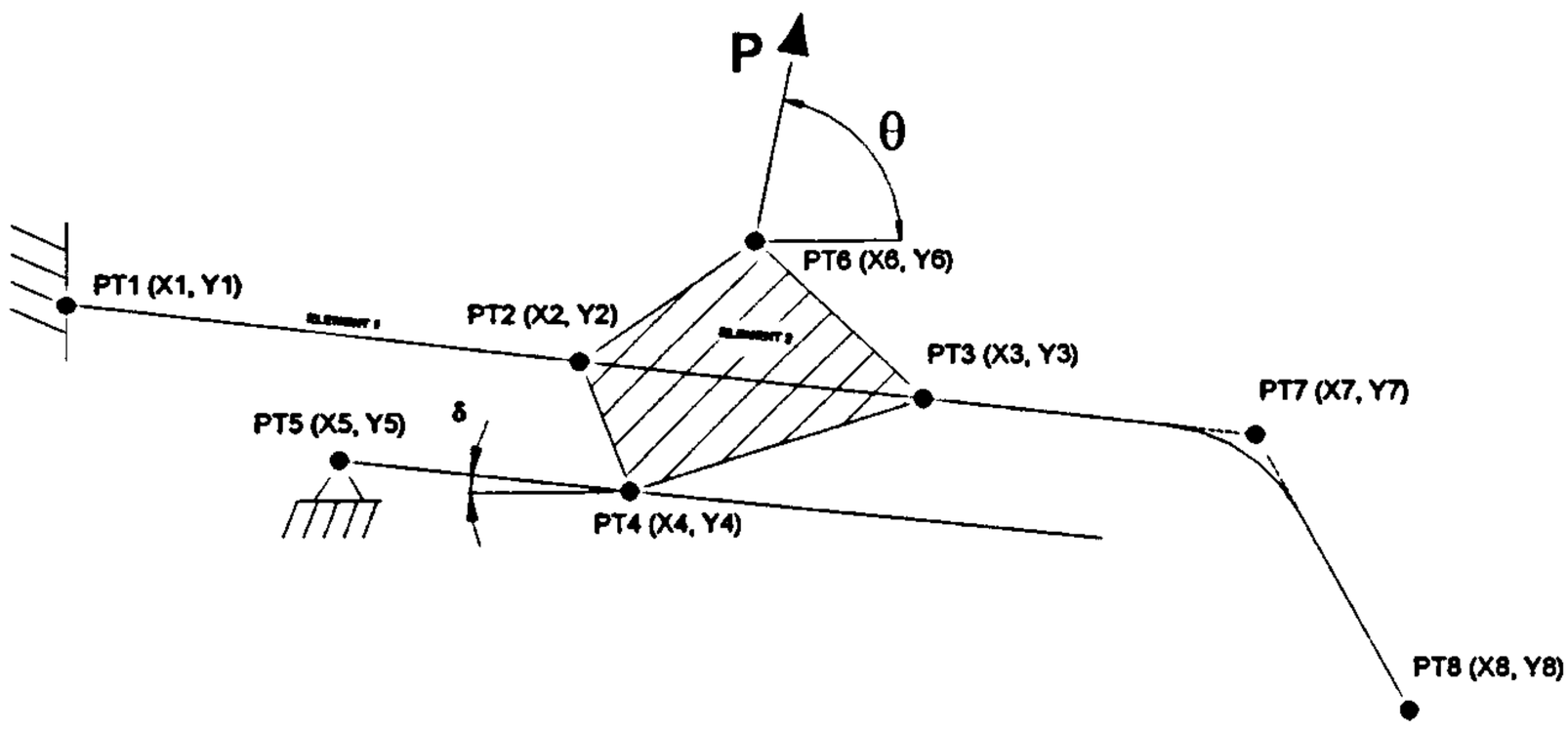

INPUTS

Mechanism points (mm):

PT1 (X1,Y1)	PT2 (X2,Y2)	PT3 (X3,Y3)	PT4(X4,Y4)
PT5 (X5,Y5)	PT6 (X6,Y6)	PT7 (X7,Y7)	PT8(X8,Y8)

Load and Angle:

P [N]
θ [°]

LOADS CALCULATIONS

Free Body Diagram – Whole System

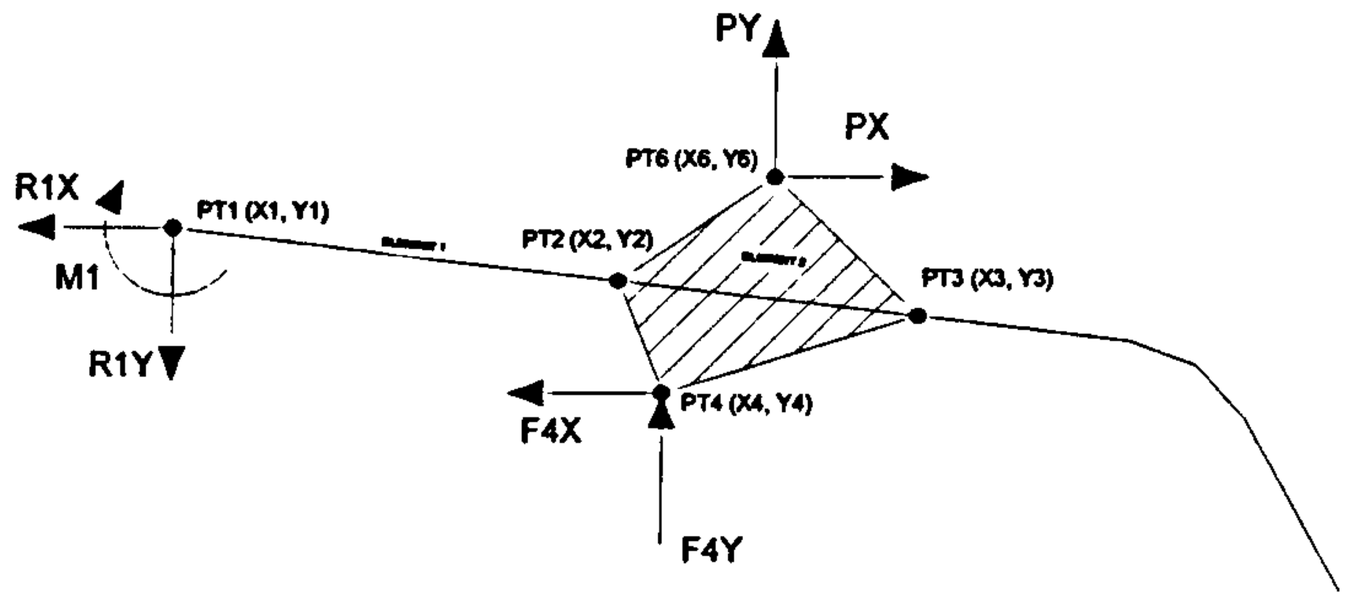

$$\delta = a\tan\frac{(Y5-Y4)}{(X4-X5)}$$

$$\rightarrow + \sum F_X = 0: \qquad (PX)-(R1X)-(F4X)=0 \qquad [1]$$

$$\uparrow + \sum F_Y = 0: \qquad (PY)-(R1Y)-(F4Y)=0 \qquad [2]$$

$$+) \sum M_{PT1} = 0: \qquad (PX)\cdot(Y6-Y1)+(PY)\cdot(X6-X1)-$$
$$(F4X)\cdot(Y1-Y4)+(F4Y)\cdot(X4-X1)-M1=0 \qquad [3]$$

Free Body Diagram – Roller Carriage

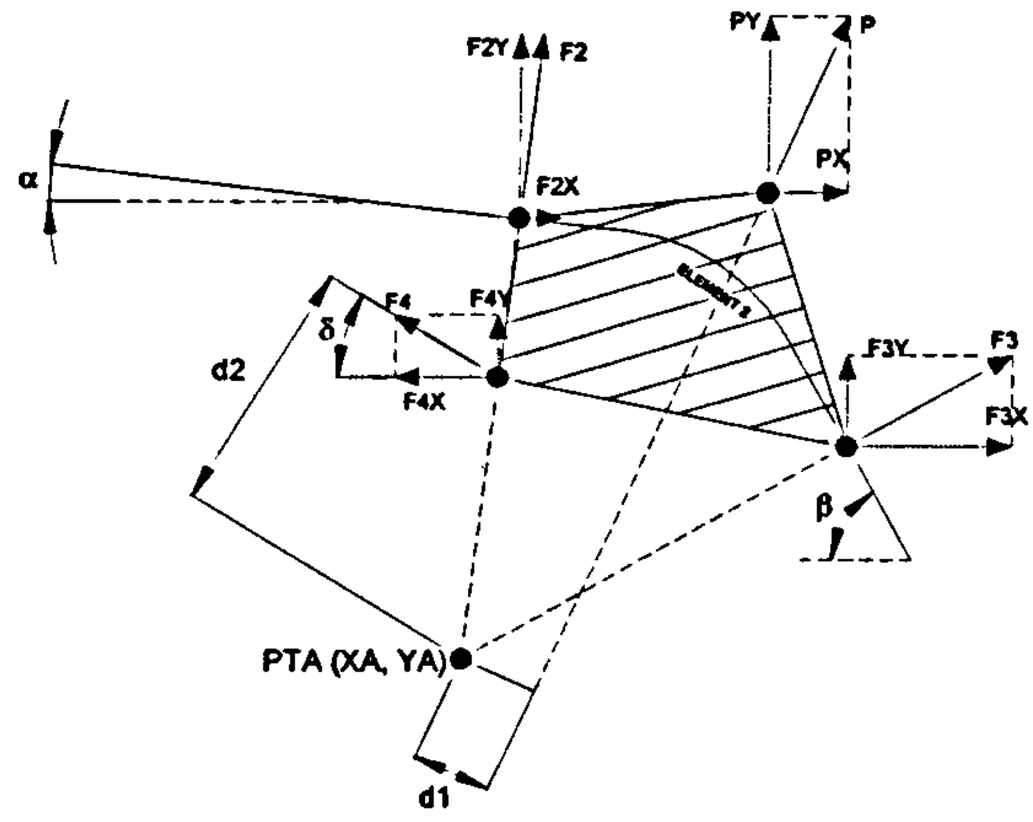

$$\alpha = a\tan\frac{(Y1-Y7)}{(X7-X1)} \; ; \; \beta = a\tan\frac{(Y7-Y8)}{(X8-X7)}$$

$$XA = \frac{n\cdot X3 - Y3 - m\cdot X2 + Y2}{n-m}$$

$$YA = \frac{-m\cdot X2\cdot n + m\cdot n\cdot X3 - m\cdot Y3 + n\cdot Y2}{n-m}$$

where

$m = \tan(90° - \alpha)$ *and* $n = \tan(90° - \beta)$.

$$d1 = \left| \frac{-m_1 \cdot XA + YA + (m_1 \cdot X6 - Y6)}{\pm\sqrt{m_1^2 + 1}} \right|$$

$$d2 = \left| \frac{-m_2 \cdot XA + YA + (m_2 \cdot X4 - Y4)}{\pm\sqrt{m_2^2 + 1}} \right|$$

where

$m_1 = \tan(\theta)$ *and* $m_2 = \tan(180° - \delta)$.

$$\rightarrow + \sum F_X = 0 \quad : \quad (PX) + (F2X) + (F3X) - (F4X) = 0 \qquad [4]$$

$$\uparrow + \sum F_Y = 0 \quad : \quad (PY) + (F2Y) + (F3Y) - (F4Y) = 0 \qquad [5]$$

$$+) \sum M_{PTA} = 0 : \quad P \cdot d1 + F4 \cdot d2 = 0$$

$$F4 = -\frac{d1}{d2} \cdot P \qquad [6]$$

Simplifications

$F2X = F2 \cdot \cos(90 - \alpha) = F2 \cdot b$

$F2Y = F2 \cdot \sin(90 - \alpha) = F2 \cdot g$

$F3X = F3 \cdot \cos(90 - \beta) = F3 \cdot c$

$F3Y = F3 \cdot \sin(90 - \beta) = F3 \cdot h$

$F4X = F4 \cdot \cos(\delta) = F4 \cdot d$

$F4Y = F4 \cdot \sin(\delta) = F4 \cdot j$

$PX = P \cdot \cos(\theta) = P \cdot a$

$PY = P \cdot \sin(\theta) = P \cdot f$

$a = \cos(\theta)$

$b = \cos(90 - \alpha)$

$c = \cos(90 - \beta)$

$d = \cos(\delta)$

$f = \sin(\theta)$

$g = \sin(90 - \alpha)$

$h = \sin(90 - \beta)$

$j = \sin(\delta)$

$$k = \frac{d1}{d2}$$

Equations to Consider For MathCAD

$P \cdot a + F2 \cdot b + F3 \cdot c - F4 \cdot d = 0$ [4]

$P \cdot f + F2 \cdot g + F3 \cdot h - F4 \cdot j = 0$ [5]

$F4 + k \cdot P = 0$ [6]

MathCAD Solution

$$F2 = -P \cdot \frac{(-f \cdot c + h \cdot a + h \cdot k \cdot d - j \cdot k \cdot c)}{(b \cdot h - c \cdot g)}$$

$$F3 = P \cdot \frac{(a \cdot g - f \cdot b - j \cdot k \cdot b + k \cdot d \cdot g)}{(b \cdot h - c \cdot g)}$$

$$F4 = -k \cdot P$$

Other Equation

$$(R1X) = (PX) - (F4X) \quad [1]$$

$$(R1Y) = (PY) - (F4Y) \quad [2]$$

$$M1 = (PX) \cdot (Y6 - Y1) + (PY) \cdot (X6 - X1) - (F4X) \cdot (Y1 - Y4) + (R4Y) \cdot (X4 - X1) \quad [3]$$

C2 – Initial Sizing Methods

C2.1 - ASSUMPTIONS

The formulae presented in this document assumes that :

- Materials are Isotropic;
- Initial effect of applying loads is ignored;
- Equilibrium is assumed;
- Loads are static.

C2.2 - FORMULAE FOR INITIAL SIZING

The objective of this section is to provide a set of equations that will allow the designer to calculate initial sizing values for a component of a specific material subjected to a load.

Tension/Compression

When an axial load (tension or compression) is applied to a component of uniform cross section the basic induced stress is given by:

$$\sigma_{applied} = \frac{P}{A}$$

Equation C2.1

The minimum cross sectional dimensions area of the component is given by:

$$A = \frac{P}{\sigma_{allowable}}$$

Equation C2.2

Direct Shear

When a transverse load is applied to a component the basic induced stress is given by:

$$\tau_{applied} = \frac{P}{A_S}$$

Equation C2.3

The minimum cross section area of the component to resist shear is given by:

$$A_S = \frac{P}{\tau_{allowable}}$$

Equation C2.4

Bearing Pressure

Bearing stress is a limiting condition for pin, rivet and shear bolts when loaded transversely. The contact stress is given by:

$$\sigma_{applied} = \frac{P}{d \cdot L} = \frac{P}{A_b}$$

Equation C2.5

where d – Common diameter
L – Length of bearing surface
A_b – Projected area (rectangle)

The minimum diameter for a component to resist the Bearing Stress is given by:

$$d = \frac{P}{L \cdot \sigma_{allowable}}$$

Equation C2.6

Bending

When a bending moment is applied to a component the stress due to bending is given by:

$$\sigma = \frac{M}{Z} = \frac{M \cdot c}{I}$$

Equation C2.7

where σ – Bending stress
M – Applied bending moment
Z – Section Modulus
I – Second Moment of Area of the cross-section
c – Distance from the Neutral axis to the point on the cross section at which the bending stress is to be determined (c = radius for cylindrical elements)

The minimum cross sectional dimensions can be determined using the following equations:

$$Z = \frac{M}{\sigma_{allowable}} \quad \text{or} \quad \frac{I}{c} = \frac{M}{\sigma_{allowable}}$$

Equation C2.8

Torsion

When a Torque is applied to a component of circular cross section the induced stress τ is given by:

$$\tau_{applied} = \frac{T}{J} \cdot r$$

Equation C2.9

where τ – Shear stress at radius r
T – Applied torque
J – Polar second moment of area of cross-section

The minimum cross sectional dimensions are given by:

$$\frac{J}{r} = \frac{T}{\tau_{allowable}}$$

Equation C2.10

Section Properties

Cross Section	Area A	Second Moment of Area I	Section Modulus Z	Torsional Constant J
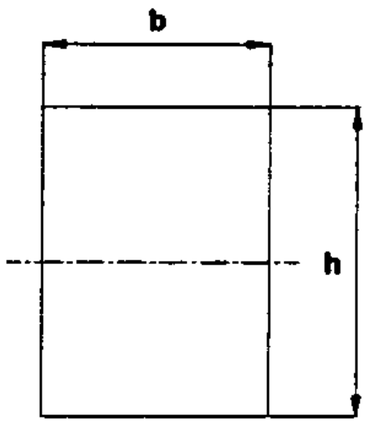	$b \cdot h$	$\frac{b \cdot h^3}{12}$	$\frac{b \cdot h^2}{6}$	-
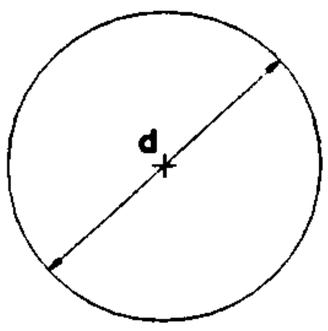	$\frac{\pi \cdot d^2}{4}$	$\frac{\pi \cdot d^4}{64}$	$\frac{\pi \cdot d^3}{32}$	$\frac{\pi \cdot d^4}{32}$
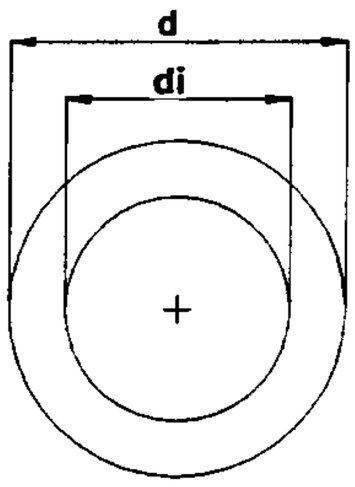	$\frac{\pi \cdot (d^4 - d_i^4)}{4}$	$\frac{\pi \cdot (d^4 - d_i^4)}{64}$	$\frac{\pi \cdot (d^4 - d_i^4)}{32 \cdot d}$	$\frac{\pi \cdot \left(d^4 - d_i^4\right)}{32}$

C2 – Stability of Components

If a component is subjected to loads as in the Figure below there is the chance of it failing by elastic instability. This might happen if the component is sufficiently slender. In this case the maximum unit stress sustained is less than the proportional limit of the material; it depends on the modulus of elasticity, the slenderness ratio, and the end conditions and is independent of the strength of the material.

Nomenclature:
$P_{applied}$ – Applied Load [N]
n – Coefficient of end condition
L – Length of column [mm]
E – Modulus of elasticity [Mpa]
I – Moment of Inertia of Area [mm4]

	Both Guided	Both Fixed	Guided/Fixed	Fixed/Free
n	**1**	**4**	**2**	**0.25**

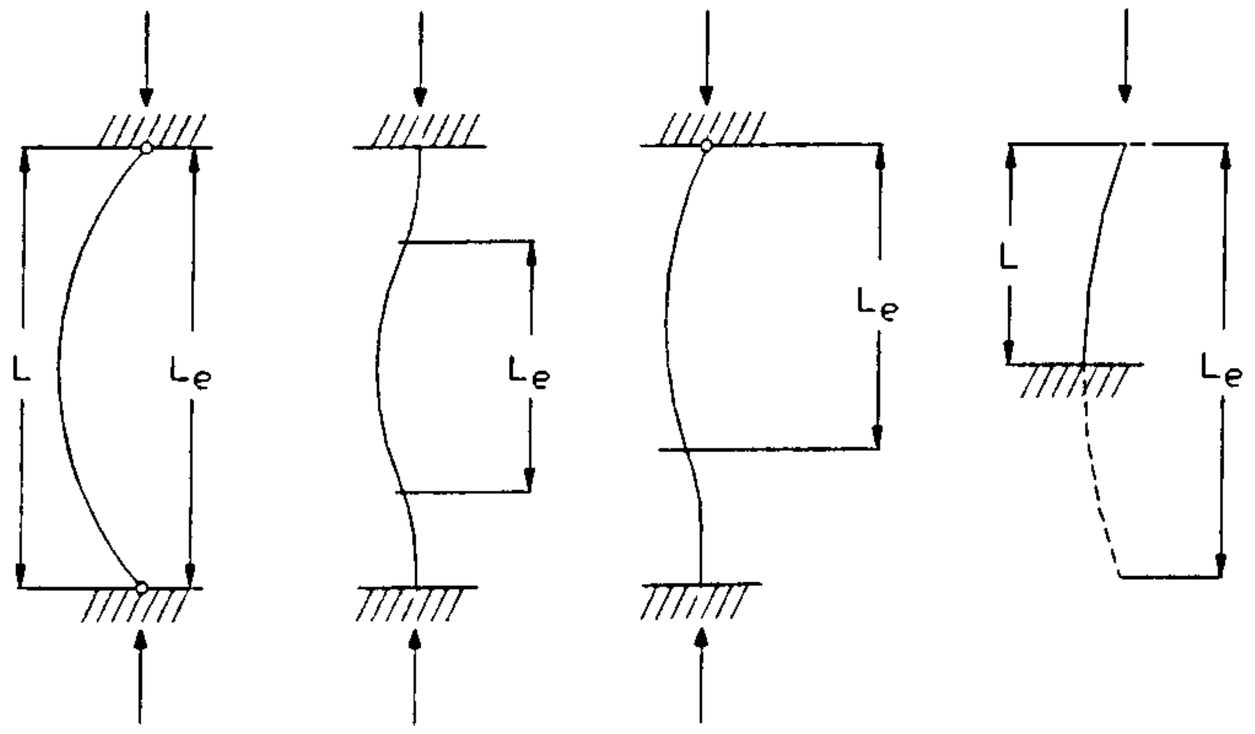

The critical load for a component in those conditions is given by the EULER equation:

$$P_{cr} = \frac{n \cdot \pi^2 \cdot E \cdot I}{L^2}$$

Equation C3.1

Hence, the minimum cross sectional dimensions can be determined using the following equation:

$$I = \frac{P_{applied} \cdot L^2}{n \cdot \pi^2 \cdot E}$$

Equation C3.2

Once the final dimensions of the component are determined a check has to be made on the allowable Euler buckling stress to verify if it does not exceed the 0.2% Proof Stress for the material.

C4 – Lug Design

The geometry of the lug should satisfy the following conditions [121]:

$d/t < 8.0$

$r/d > 1.5$

For initial sizing calculations the following values were assumed by the author:

$d/t = 2$ *Equation C4.1*

$r/d = 2$ *Equation C4.2*

$c=(a - d/2)$ *Equation C4.3*

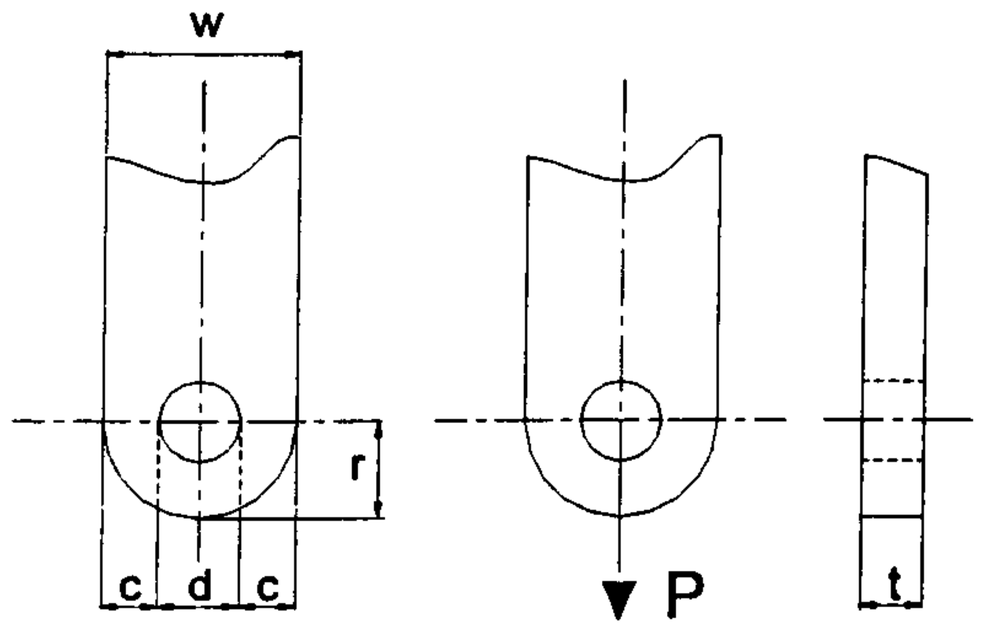

The previous geometrical conditions defined for the lug are driven by the pin diameter, which is calculated using the equations for Tension or Shear Tear Out failure shown below:

Tension across Net Section

$$f_{tu} = \frac{P}{A_t} \text{ where } A_t = (w - d)\cdot t \Rightarrow A_t = \frac{3}{2}\cdot d^2$$

Rearranging

$$d = \sqrt{\frac{2\cdot P}{3\cdot f_{tu}}}$$ *Equation C4.3*

40° Shear Tear Out

$$f_{su} = \frac{P}{A_{shr}} \text{ where } A_{shr} = 2\cdot x\cdot t \text{ and } x = (4 - \cos 40°)\cdot \frac{d}{2}$$

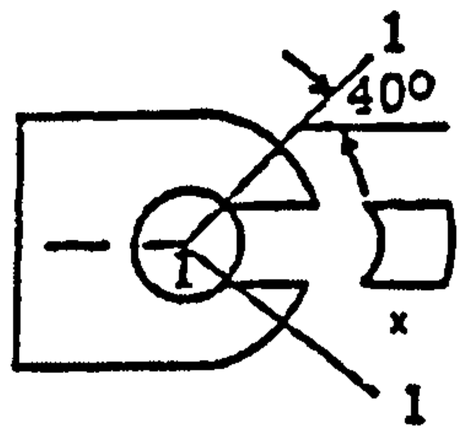

Rearranging

$$d = \sqrt{\frac{2\cdot P}{(4 - \cos 40°)\cdot f_{su}}}$$ *Equation C4.4*

C5 – Component Sizing

a) HINGE TYPE

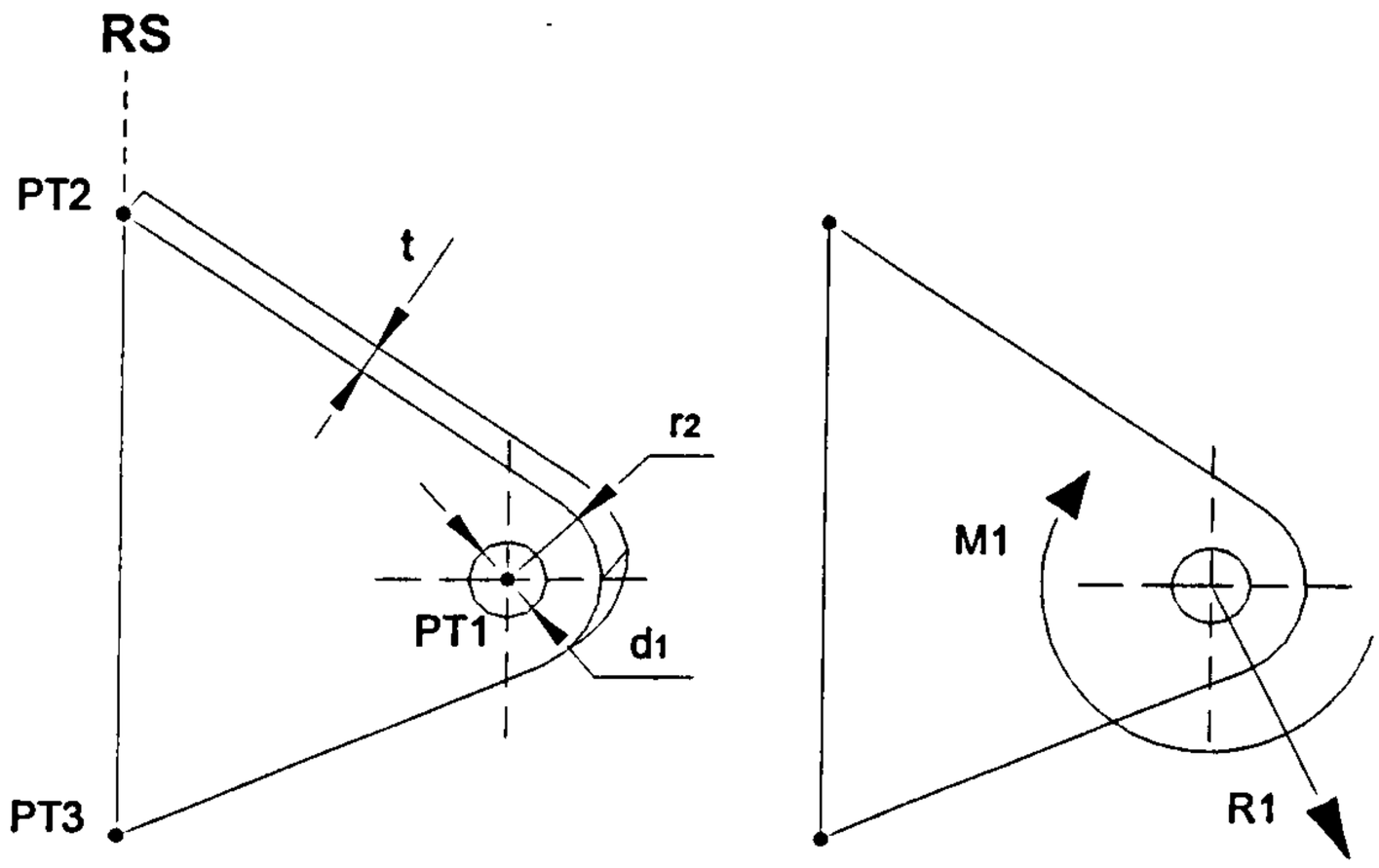

Initial Assumptions:

$$t = \frac{d_1}{2} \quad ; r_2 = 2 \cdot d_1$$

Inputs:

PT1(X_1,Y_1); PT2(X_2,Y_2); PT3(X_3,Y_3) - Points for CAD Modelling
P[N]; M1[N.m]

Sizing

Actuator Shaft in Torsion

$$d_1 = \sqrt{\frac{16 \cdot M}{\pi \cdot f_{su}}}$$

Lug - 40° Shear Tear Out (Oblique load)

$$d_1 = \sqrt{\frac{2 \cdot P}{3.234 \cdot f_{su}}} \cdot 1.15$$

b) LINK TYPE

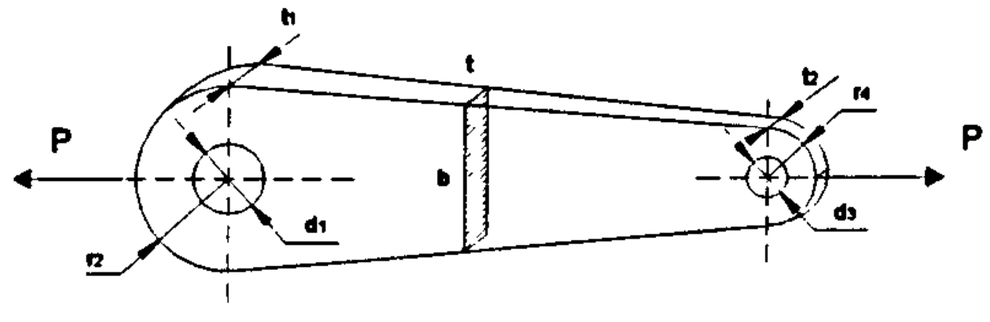

Initial Assumptions:

$$t_1 = \frac{d_1}{2} \quad ; \quad t_2 = \frac{d_3}{2} \quad ; \quad r_2 = 2 \cdot d_1 \; ; \quad r_4 = 2 \cdot d_3 \quad ; \quad d_3 \geq \frac{d_1}{2}$$

Inputs:

PT1(X_1,Y_1); PT2(X_2,Y_2) – Points for CAD Modelling
P[N]

Calculations:

$$L = \sqrt{(X_2 - X_1)^2 + (Y_2 - Y_1)^2}$$

Sizing

Both d_1 and/or d_3 can be given by the previous or adjacent element dimensions.

Lug – Tension Across Net Section

$$d = \sqrt{\frac{2 \cdot P}{3 \cdot f_{tu}}}$$

Lug - 40° Shear Tear Out

$$d = \sqrt{\frac{2 \cdot P}{3.234 \cdot f_{su}}}$$

Check for Euler Buckling

$$P_{cr} = \frac{\pi \cdot E \cdot I}{L^2} \qquad I = \frac{t \cdot b^3}{12} \qquad b = r_2 + r_4 \qquad t = \frac{t_1 - t_2}{2}$$

OK if $P_{cr} \geq P$

c) FLAP FITTING COMPONENTS

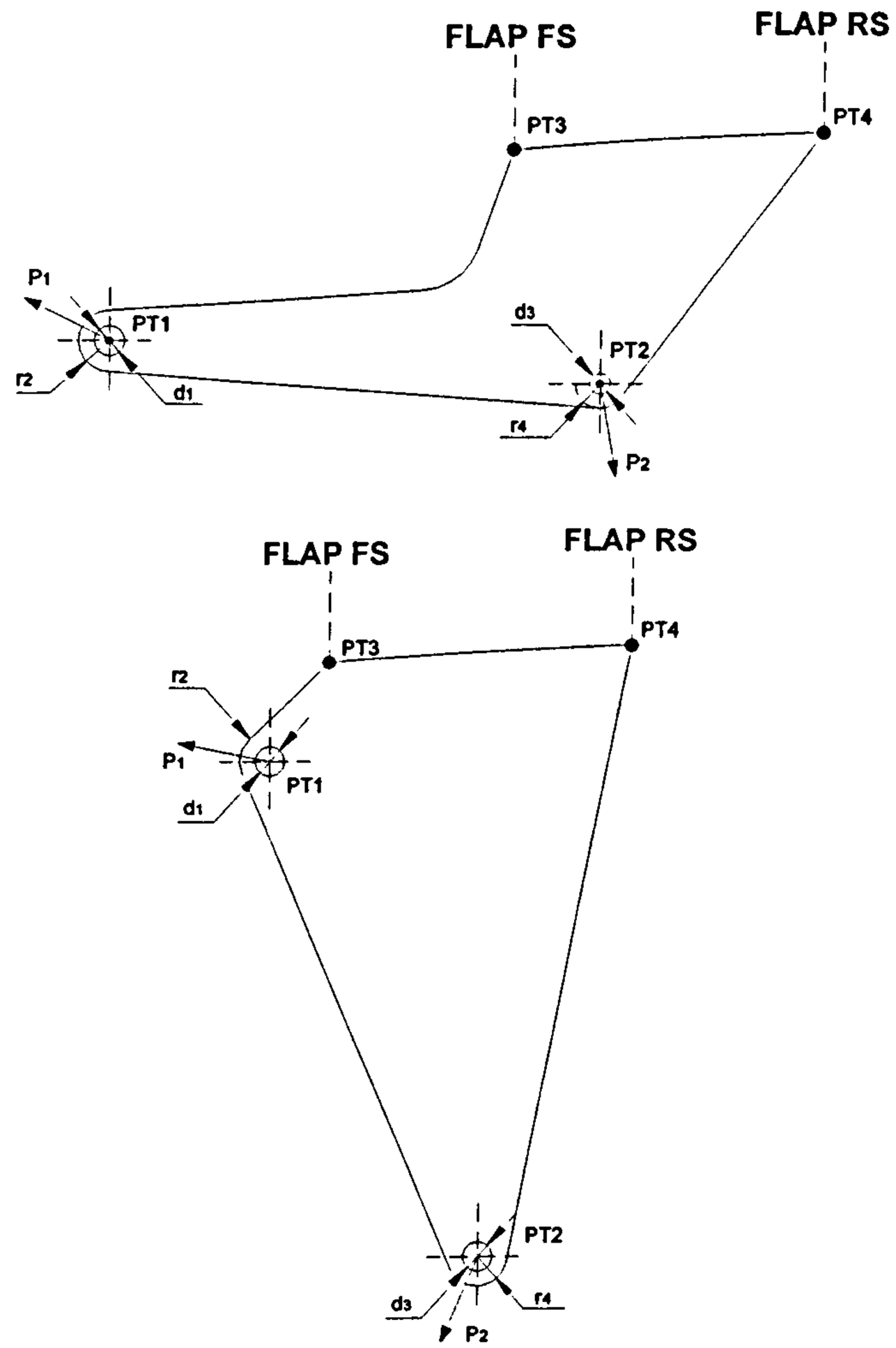

Initial Assumptions:

t = the biggest of $d_1/2$ or $d_3/2$

$$r_2 = 2 \cdot d_1 \;\; ; \;\; r_4 = 2 \cdot d_3 \;\; ; \;\; d_3 \geq \frac{d_1}{2}$$

Inputs:

PT1(X_1,Y_1); PT2(X_2,Y_2); PT3(X_3,Y_3); PT4(X_4,Y_4); P_1; P_2[N]

Sizing

Both d_1 and/or d_3 can be given by the previous or adjacent element dimensions.

Lug – Tension Across Net Section

$$d = \sqrt{\frac{2 \cdot P}{3 \cdot f_{tu}}}$$

Lug - 40° Shear Tear Out (Oblique Loads)

$$d = \sqrt{\frac{2 \cdot P}{3.234 \cdot f_{su}}} \cdot 1.15$$

d) SUPPORT STRUTS COMPONENTS

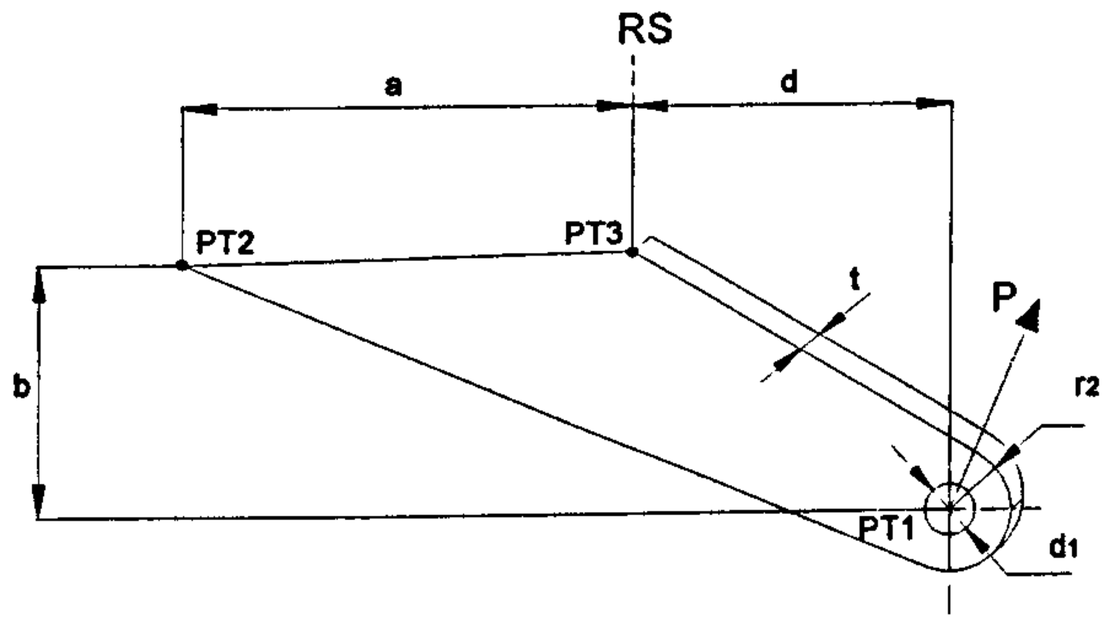

Initial Assumptions:

$$t_1 = \frac{d_1}{2} \quad ; \quad r_2 = 2 \cdot d_1$$

Inputs:

PT1(X_1,Y_1); PT3(X_3,Y_3); PT3(X_3,Y_3); P_X; P_Y [N]

Sizing

d_1 can be given by the previous or adjacent element dimensions.

Lug - 40° Shear Tear Out (Oblique Loads)

$$d_1 = \sqrt{\frac{2 \cdot P}{3.234 \cdot f_{su}}} \cdot 1.15$$

e) TRACK STRUT COMPONENTS

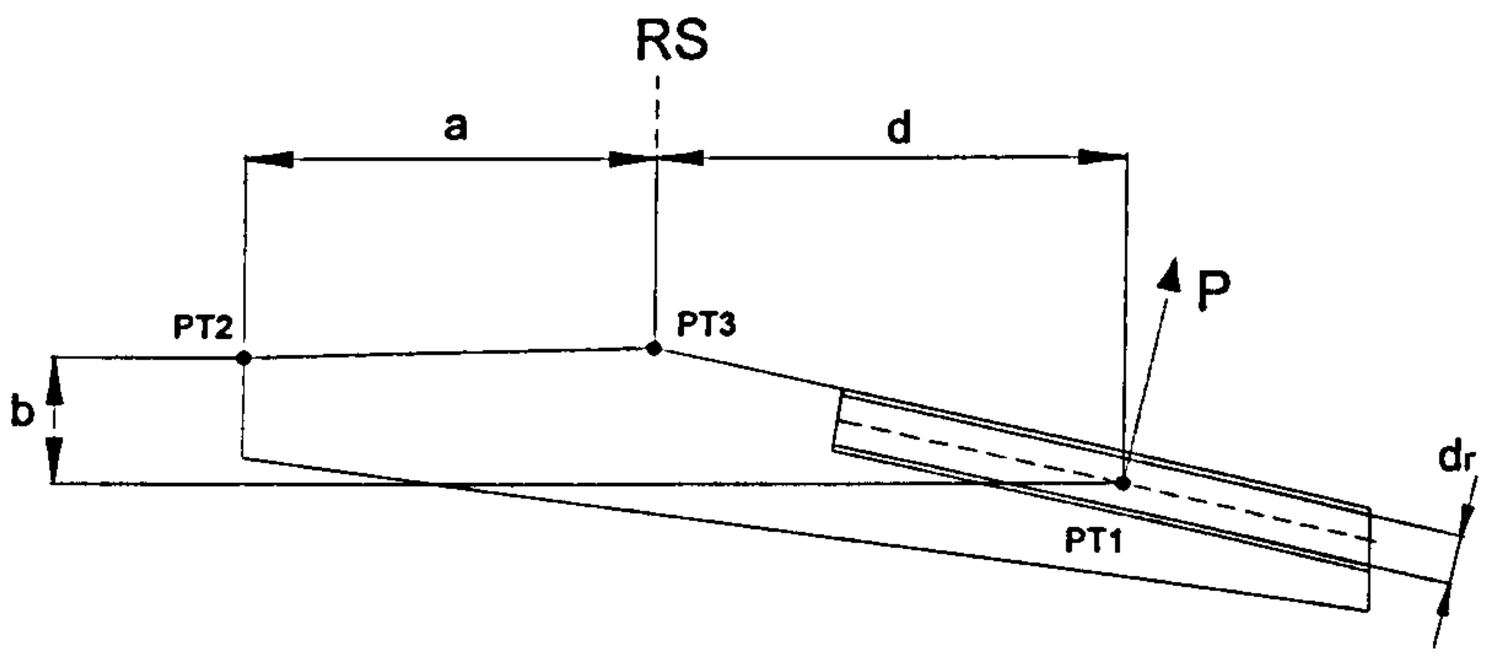

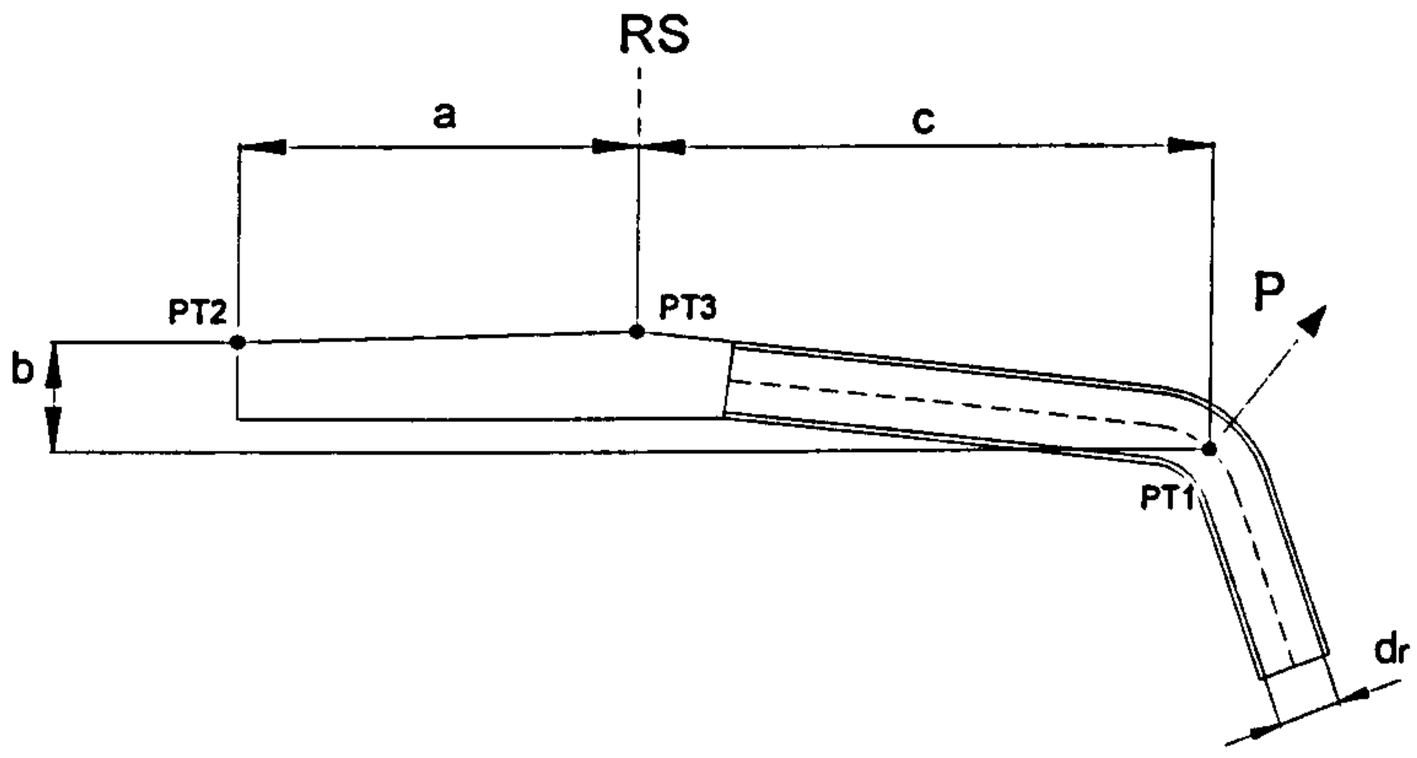

Inputs:

PT1(X_1,Y_1); PT2(X_2,Y_2); PT3(X_3,Y_3)
P_X; P_Y [N]

Dimensions ruled by Roller dimensions

f) ROLLER CARRIAGE COMPONENTS

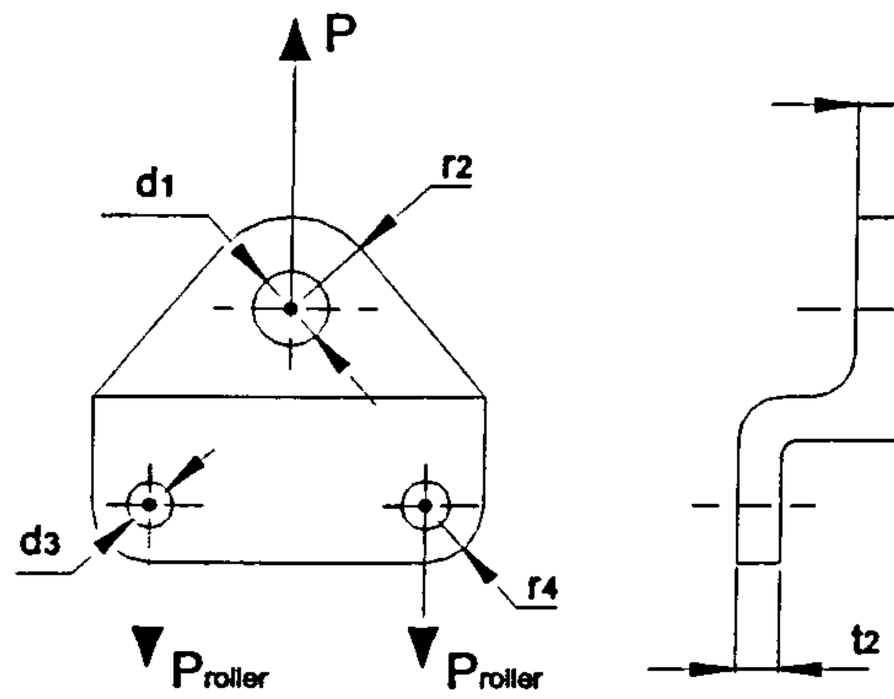

Assumptions:

$$t_1 = \frac{d_1}{4} \quad ; \quad t_2 = \frac{d_3}{4} \quad ; \quad r_2 = 2 \cdot d_1 \quad ; \quad r_4 = 2 \cdot d_3$$

Sizing

d_1 can be given by the previous or adjacent element dimensions.

Lug - 40° Shear Tear Out (Flap Fitting Attachment)

$$d_1 = \sqrt{\frac{2 \cdot P}{3.234 \cdot f_{su}}}$$

Lug – Tension Across Net Section (Roller Attachment)

$$d_3 = \sqrt{\frac{2 \cdot P_{Roller}}{3 \cdot f_{tu}}}$$

Lug - 40° Shear Tear Out

$$d_3 = \sqrt{\frac{2 \cdot P_{Roller}}{3.234 \cdot f_{su}}}$$

g) ROLLERS

Assumptions:

Outer diameter = 2 x Bore

Width = Bore

APPENDIX D

VISUAL BASIC PROGRAM

TABLE OF CONTENTS

D1 – Example Code for Four Bar Mechanism Menu

```
Option Compare Database
Option Explicit
Dim fb_x1, fb_x2, fb_x3, fb_x4, fb_x5, fb_y1, fb_y2, fb_y3, fb_y4, fb_y5 As Double
Dim fb_theta As Double
Dim fb_P, fb_PX, fb_PY, fb_M1, fb_R1X, fb_R1Y, fb_R4X, fb_R4Y  As Double
Dim fb_F2, fb_F2X, fb_F2Y, fb_F3, fb_F3X, fb_F3Y As Double
Dim fb_a, fb_b, fb_c, fb_d, fb_f, fb_g, fb_h, fb_j, fb_Denominator As Double
Const pi = 3.14159265358979
Private Sub Additional_Points_Click()
DoCmd.OpenForm "ADDITIONAL POINTS"
End Sub
Private Sub FB_Calculation_Click()
'Auxiliary Calculations
 fb_PX = fb_P * Cos(radians(fb_theta))
 fb_PX_txt.SetFocus
 fb_PX_txt.Text = fb_PX
 fb_PY = fb_P * Sin(radians(fb_theta))
 fb_PY_txt.SetFocus
 fb_PY_txt.Text = fb_PY
 fb_a = fb_y1 - fb_y4
 fb_a_txt.SetFocus
 fb_a_txt.Text = fb_a
 fb_b = fb_x4 - fb_x1
 fb_b_txt.SetFocus
 fb_b_txt.Text = fb_b
 fb_c = (fb_PX) * (fb_y1 - fb_y5) + (fb_PY) * (fb_x5 - fb_x1)
 fb_c_txt.SetFocus
 fb_c_txt.Text = fb_c
 fb_d = fb_y1 - fb_y5
 fb_d_txt.SetFocus
 fb_d_txt.Text = fb_d
 fb_f = fb_x1 - fb_x2
 fb_f_txt.SetFocus
 fb_f_txt.Text = fb_f
 fb_g = fb_y3 - fb_y2
 fb_g_txt.SetFocus
 fb_g_txt.Text = fb_g
 fb_h = fb_x3 - fb_x2
 fb_h_txt.SetFocus
 fb_h_txt.Text = fb_h
 fb_j = (fb_PY) * (fb_x5 - fb_x2) - (fb_PX) * (fb_y5 - fb_y2)
 fb_j_txt.SetFocus
 fb_j_txt.Text = fb_j
 'Loads Calculations
 fb_Denominator = (-fb_d * fb_h + fb_g * fb_f + fb_g * fb_b + fb_a * fb_h)
 fb_Denominator_txt.SetFocus
 fb_Denominator_txt.Text = fb_Denominator
 fb_R1X = (-fb_h * fb_f * fb_PY - fb_h * fb_c + fb_j * fb_f + fb_j * fb_b + fb_PX * fb_g * fb_f + fb_b * fb_PX * fb_g + fb_a *
fb_h * fb_PX) / fb_Denominator
 value_fb_R1X.SetFocus
 value_fb_R1X.Text = fb_R1X
 fb_R1Y = (fb_d * fb_j + fb_d * fb_PX * fb_g - fb_a * fb_j - fb_c * fb_g - fb_PY * fb_d * fb_h + fb_b * fb_PY * fb_g + fb_a *
fb_h * fb_PY) / fb_Denominator
 value_fb_R1Y.SetFocus
 value_fb_R1Y.Text = fb_R1Y
 fb_R4X = (-fb_h * fb_d * fb_PX + fb_h * fb_f * fb_PY + fb_h * fb_c - fb_j * fb_f - fb_j * fb_b) / fb_Denominator
 value_fb_R4X.SetFocus
 value_fb_R4X.Text = fb_R4X
 fb_R4Y = (fb_d * fb_j + fb_d * fb_PX * fb_g - fb_f * fb_PY * fb_g - fb_a * fb_j - fb_c * fb_g) / fb_Denominator
 value_fb_R4Y.SetFocus
 value_fb_R4Y.Text = fb_R4Y
 fb_M1 = (fb_b * fb_d * fb_j + fb_b * fb_d * fb_PX * fb_g - fb_b * fb_f * fb_PY * fb_g + fb_a * fb_h * fb_d * fb_PX - fb_a * fb_h
* fb_f * fb_PY + fb_a * fb_j * fb_f - fb_c * fb_d * fb_h + fb_c * fb_g * fb_f) / fb_Denominator
 value_fb_M1.SetFocus
 value_fb_M1.Text = fb_M1
 fb_F2X = fb_R1X
 value_fb_F2X.SetFocus
 value_fb_F2X.Text = fb_F2X
 fb_F2Y = -fb_R1Y
 value_fb_F2Y.SetFocus
 value_fb_F2Y.Text = fb_F2Y
  fb_F2 = Sqr((fb_F2X) ^ 2 + (fb_F2Y) ^ 2)
```

```
    value_fb_F2.SetFocus
    value_fb_F2.Text = fb_F2
    fb_F3X = fb_R4X
    value_fb_F3X.SetFocus
    value_fb_F3X.Text = fb_F3X
    fb_F3Y = fb_R4Y
    value_fb_F3Y.SetFocus
    value_fb_F3Y.Text = fb_F3Y
    fb_F3 = Sqr((fb_F3X) ^ 2 + (fb_F3Y) ^ 2)
    value_fb_F3.SetFocus
    value_fb_F3.Text = fb_F3
End Sub
'Initialize Data Values
Private Sub txt_fb_P_Change()
    fb_P = txt_fb_P.Text
End Sub
Private Sub txt_fb_x1_Change()
    fb_x1 = txt_fb_x1.Text
End Sub
Private Sub txt_fb_x2_Change()
    fb_x2 = txt_fb_x2.Text
End Sub
Private Sub txt_fb_x3_Change()
    fb_x3 = txt_fb_x3.Text
End Sub
Private Sub txt_fb_x4_Change()
    fb_x4 = txt_fb_x4.Text
End Sub
Private Sub txt_fb_x5_Change()
    fb_x5 = txt_fb_x5.Text
End Sub
Private Sub txt_fb_y1_Change()
    fb_y1 = txt_fb_y1.Text
End Sub
Private Sub txt_fb_y2_Change()
    fb_y2 = txt_fb_y2.Text
End Sub
Private Sub txt_fb_y3_Change()
    fb_y3 = txt_fb_y3.Text
End Sub
Private Sub txt_fb_y4_Change()
    fb_y4 = txt_fb_y4.Text
End Sub
Private Sub txt_fb_y5_Change()
    fb_y5 = txt_fb_y5.Text
End Sub
Private Sub txt_fb_theta_Change()
    fb_theta = txt_fb_theta.Text
End Sub
'FUNCTIONS
'Convert Radians to Degrees
Private Function degrees(rad_value)
    degrees = rad_value * 180 / pi
End Function
'Convert Degrees to Radians
Private Function radians(deg_value)
    radians = deg_value * pi / 180
End Function
'Program Buttons
Private Sub fb_Return_1_Click()
    DoCmd.Close
End Sub
Private Sub fb_Create_Geo_Click()
    MsgBox "Under Development"
End Sub
Private Sub fb_Save_Results_Click()
    Dim Message, Title, CaseName  'Default,
    Message = "Enter Case Name"    ' Set prompt.
    Title = "Case Name"    ' Set title.
    'Default = "1"    ' Set default.
    ' Display message, title, and default value.
    CaseName = InputBox(Message, Title)
    MsgBox "Under Development"
End Sub
Private Sub fb_New_Test_Click()
```

```
    Dim stDocName As String
    Dim stLinkCriteria As String
        DoCmd.Close
    stDocName = "4 BAR MECHANISM"
        DoCmd.OpenForm stDocName, , , stLinkCriteria
End Sub
Private Sub ADD_NEW_MATERIAL_Click()
MsgBox "Under Development"
End Sub
Private Sub fb_Return_Click()
    DoCmd.Close
End Sub
```

APPENDIX E

DATA FOR VALIDATION

TABLE OF CONTENTS

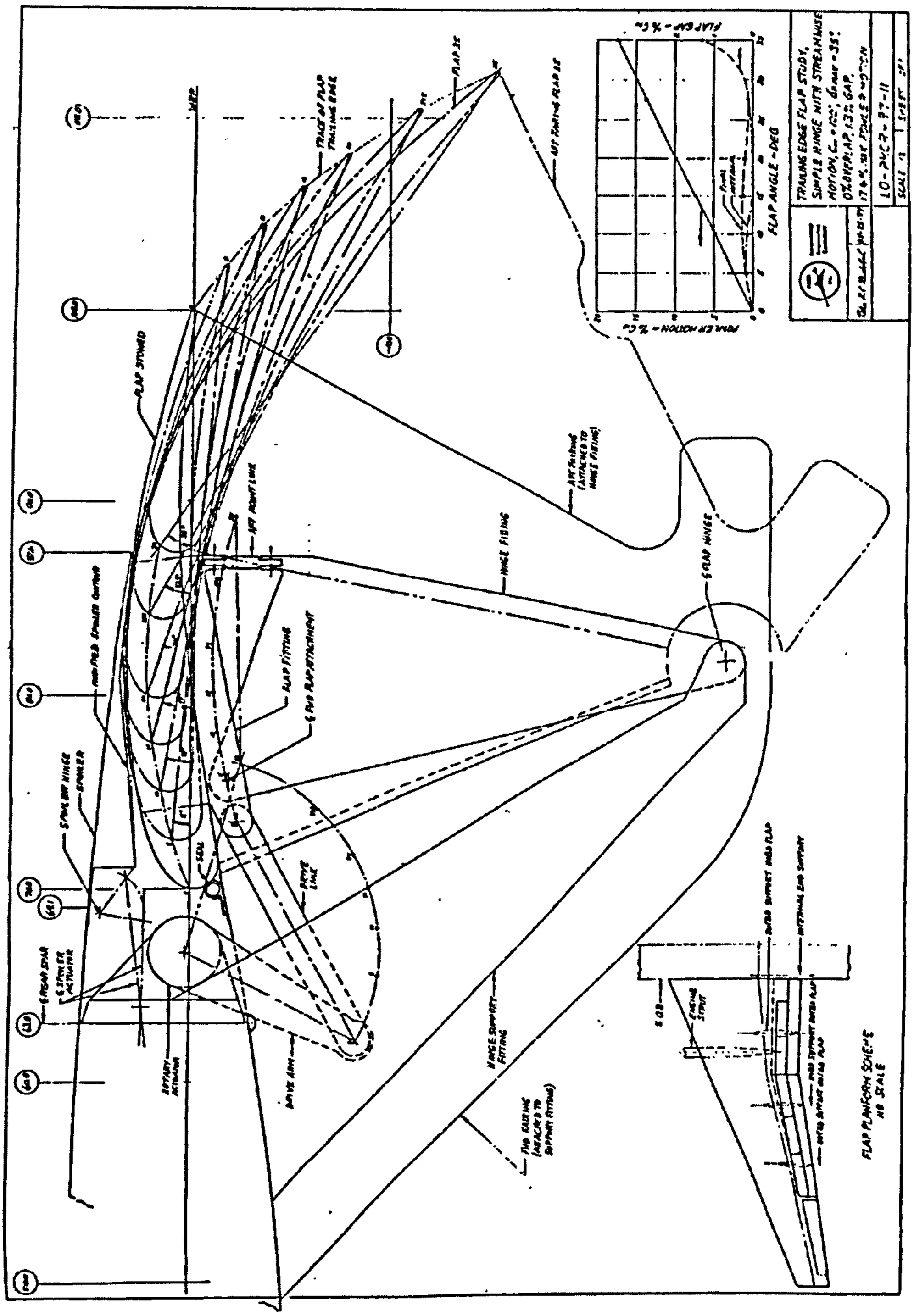

Figure 3 Simple Hinge Flap with Streamwise Motion

Figure E1 – Simple Hinge Flap with Streamwise Motion [86]

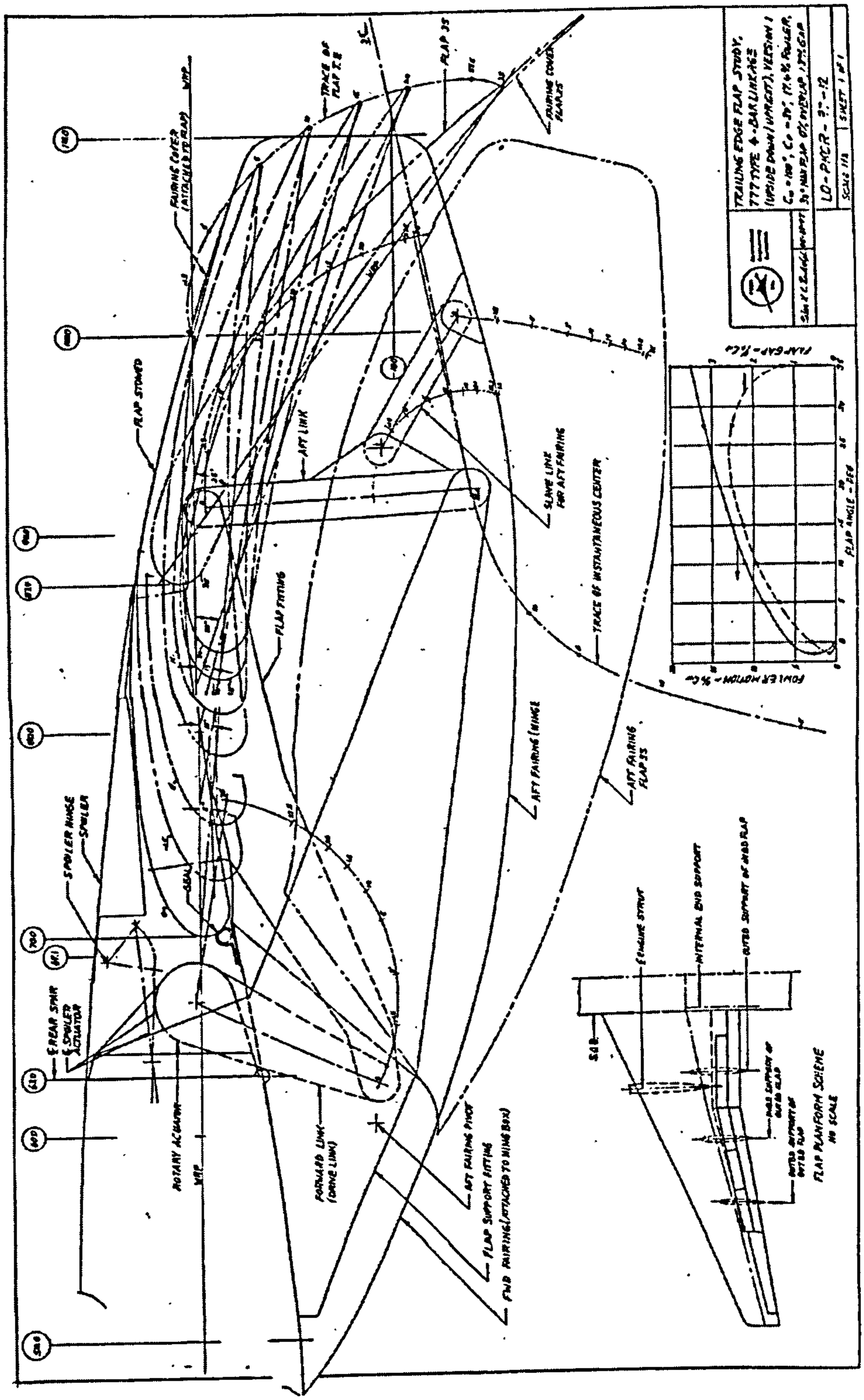

Figure 5 Boeing 777 Type Upside Down/Upright Four Bar Linkage (Aggressive)

Figure E2 – Boeing 777 Type Four Bar Linkage [86]

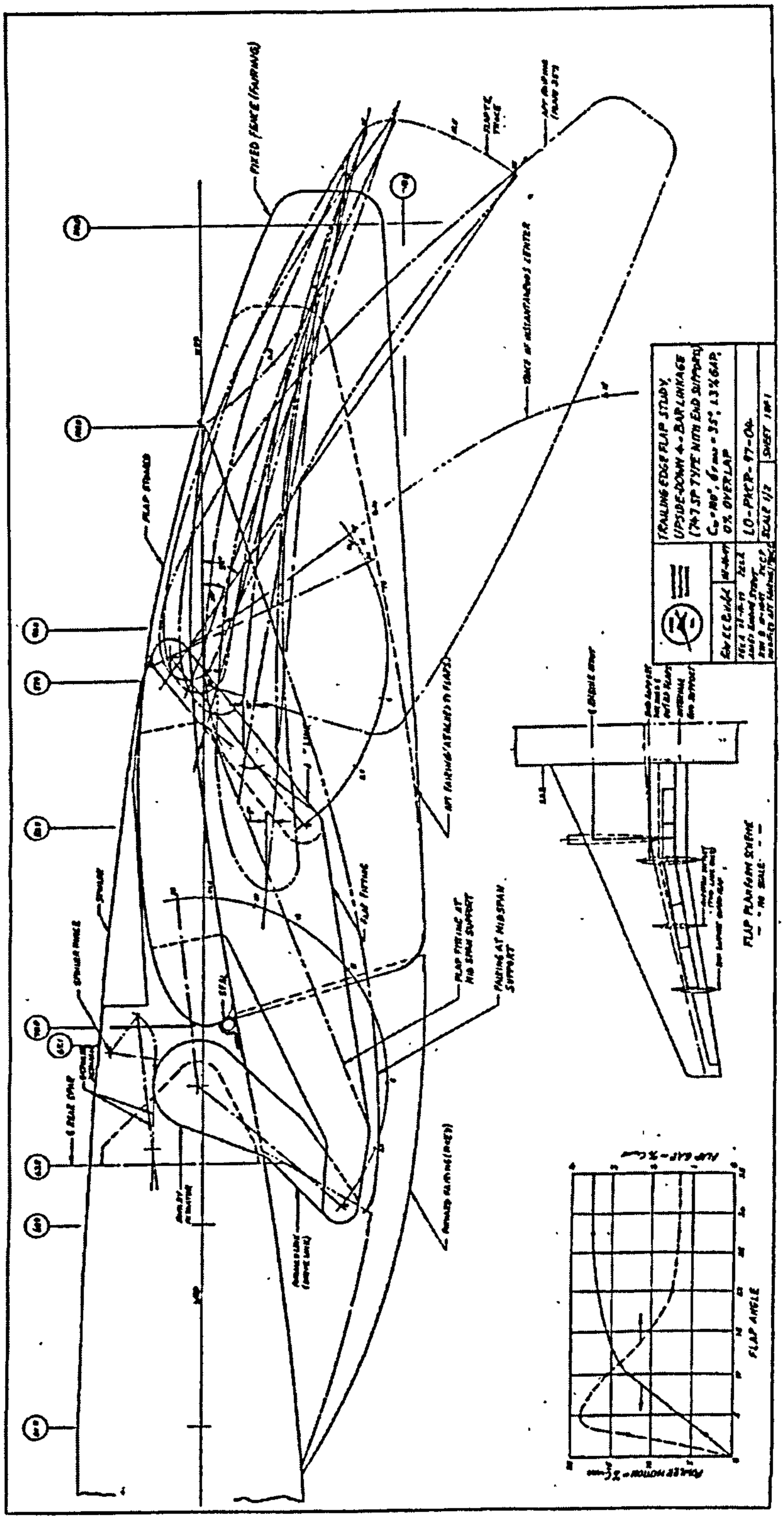

Figure 8 Boeing 747 Type Four Bar linkage

Figure E3 – Boeing 747 Type Four Bar Linkage [86]

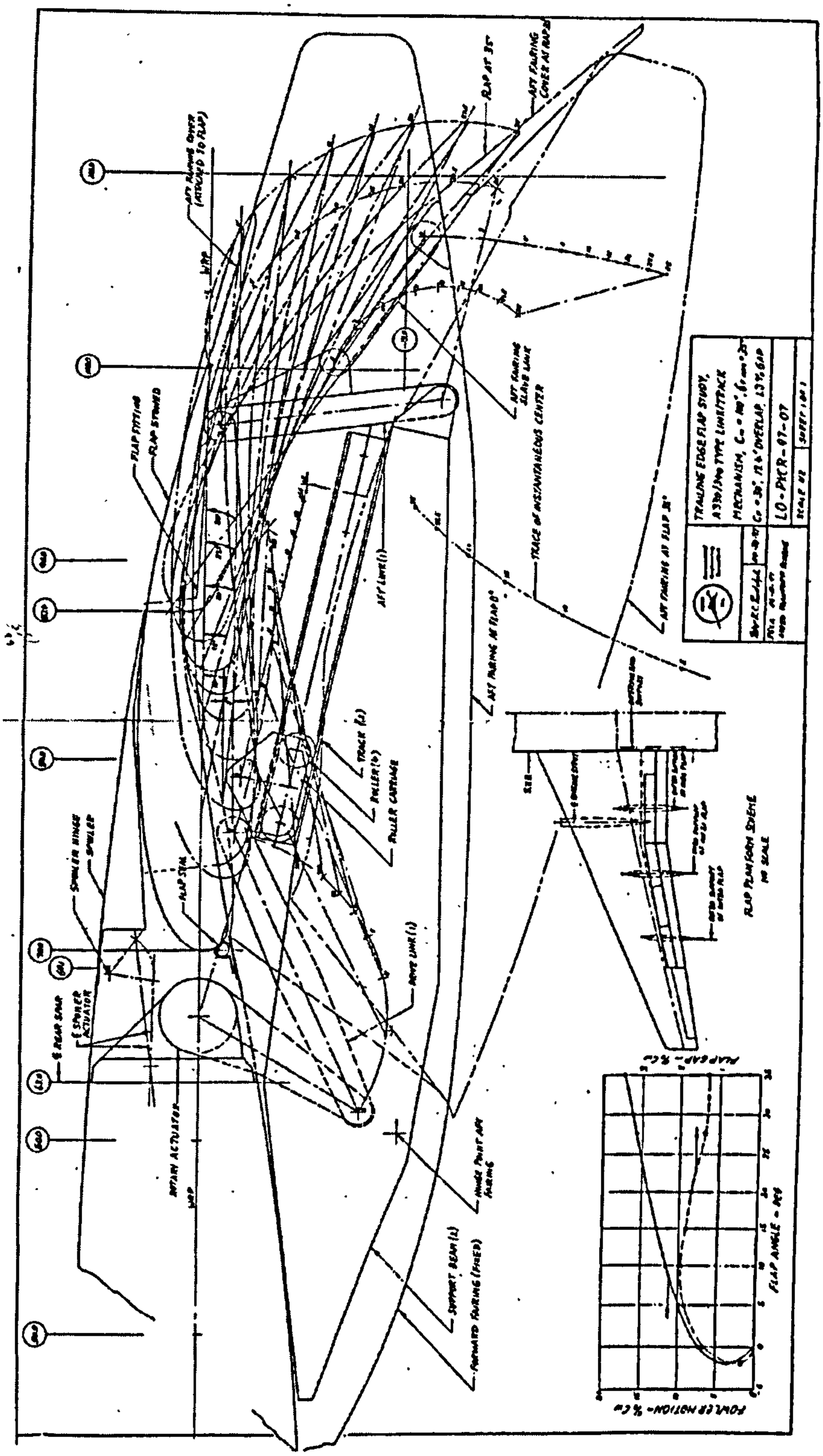

Figure 9 Airbus A330/340 Type Link/Track Mechanism

Figure E4 – AIRBUS A330/340 Type Link/Track Mechanism [86]

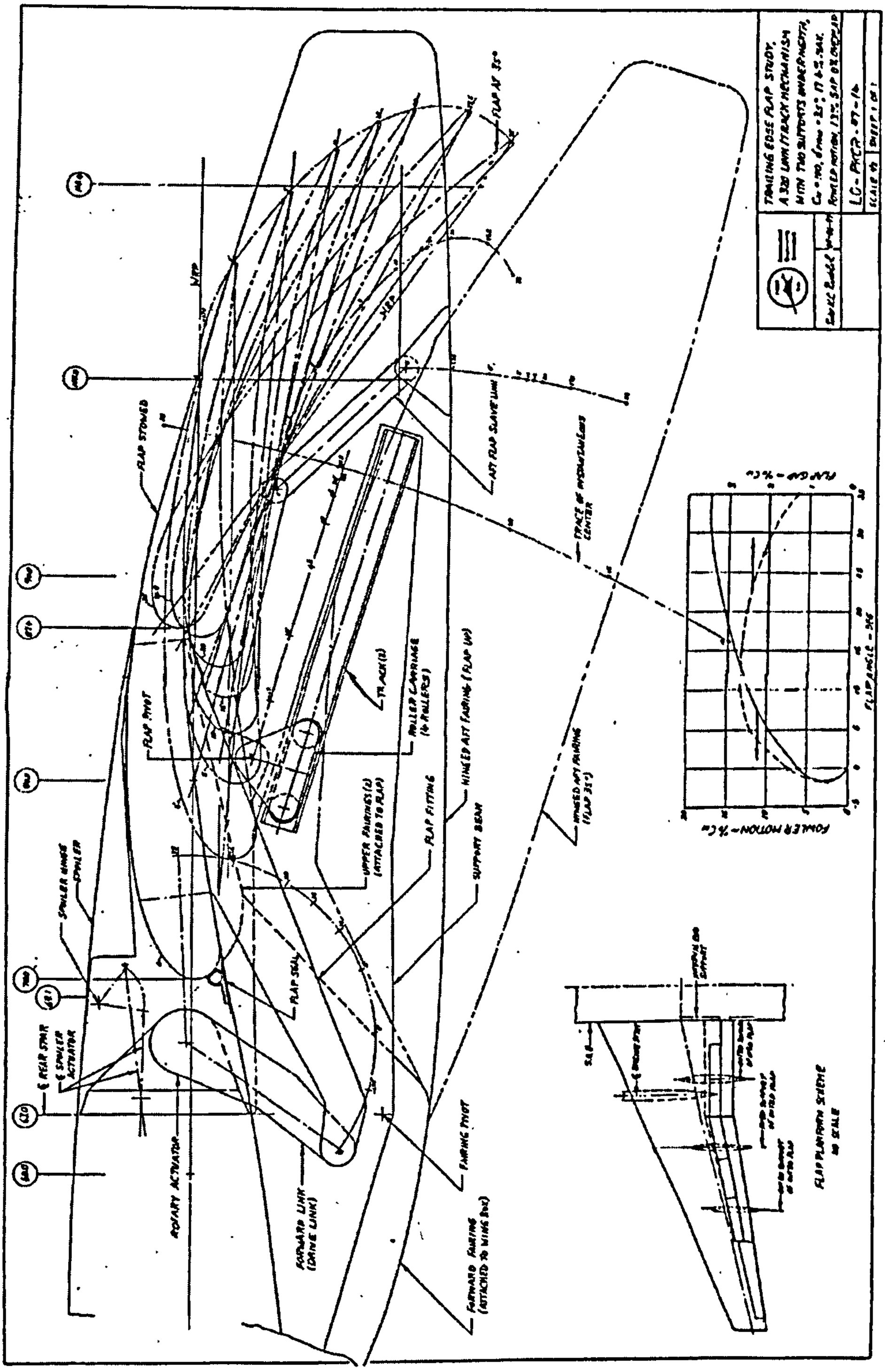

Figure 10 Airbus A320 Type Link/Track Mechanism (Conservative)

Figure E5 – AIRBUS A320 Type Link/Track Mechanism [86]

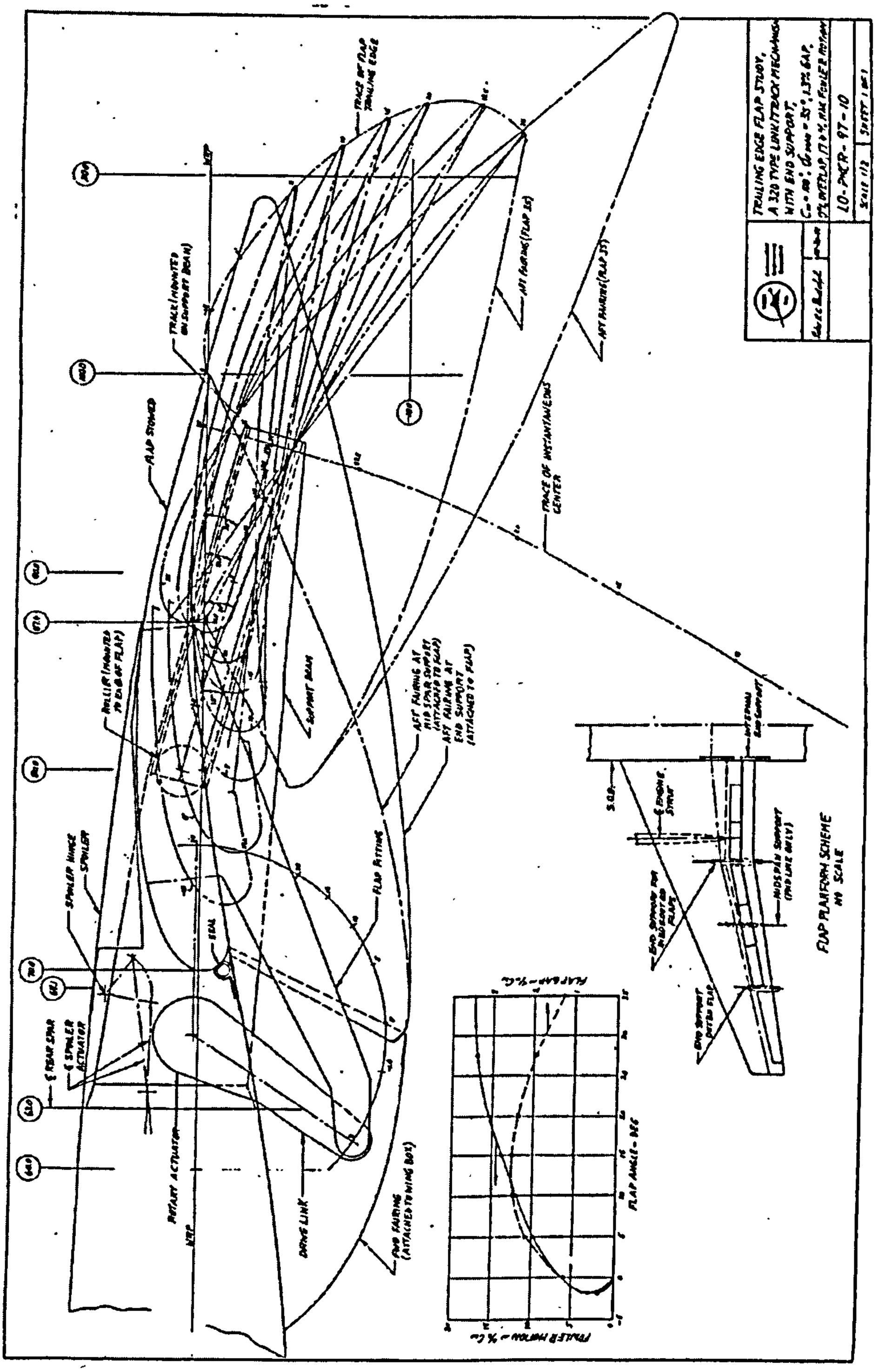

Figure 11 Airbus A320 Type Link/Track Mechanism (End Supported)

Figure E6 – AIRBUS A320 Type Link/Track Mechanism (End Supported) [86]

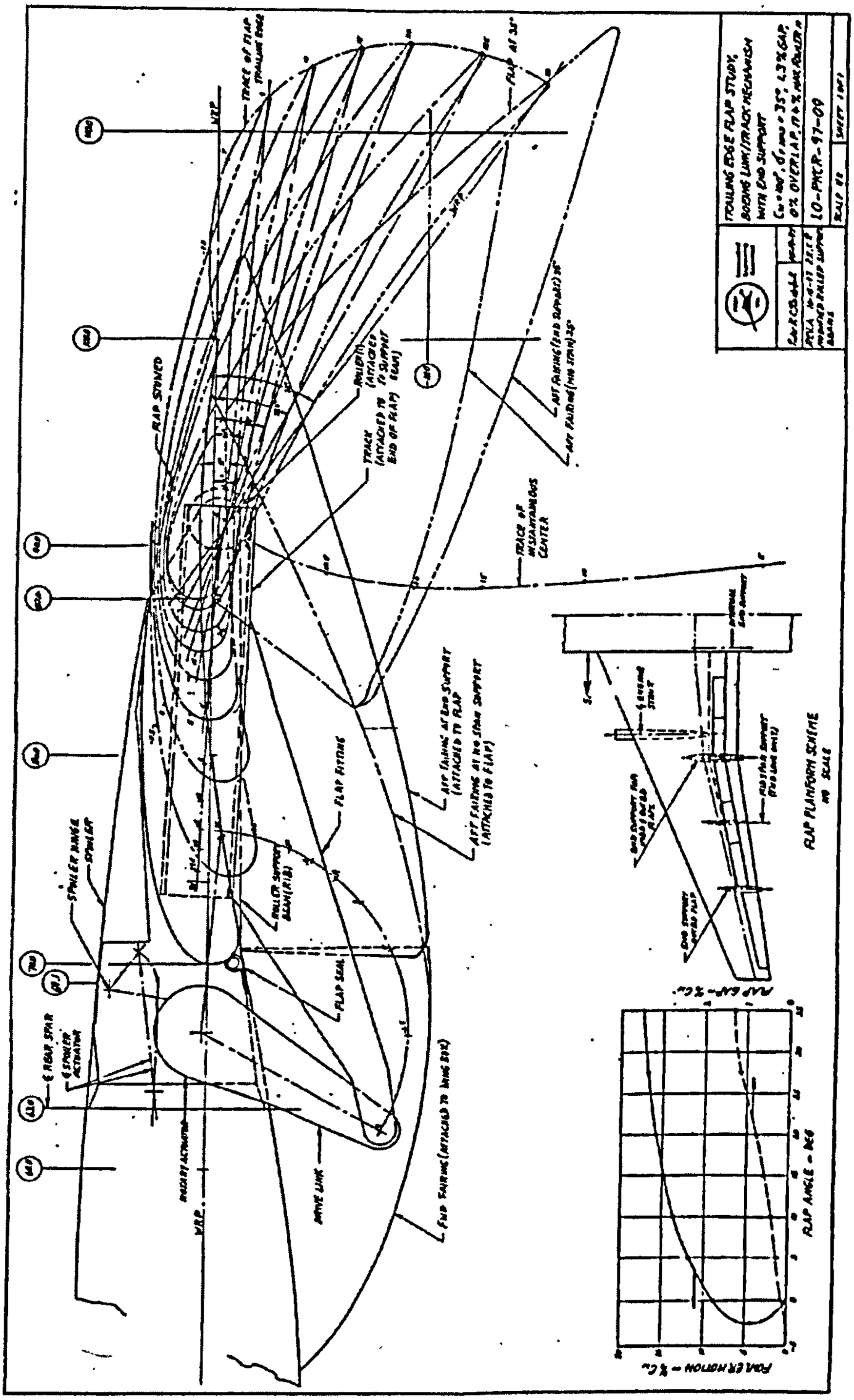

Figure 13 Boeing Type Link/Track Mechanism (End Supported)

Figure E7 – Boeing Type Link/Track Mechanism (End Supported) [86]

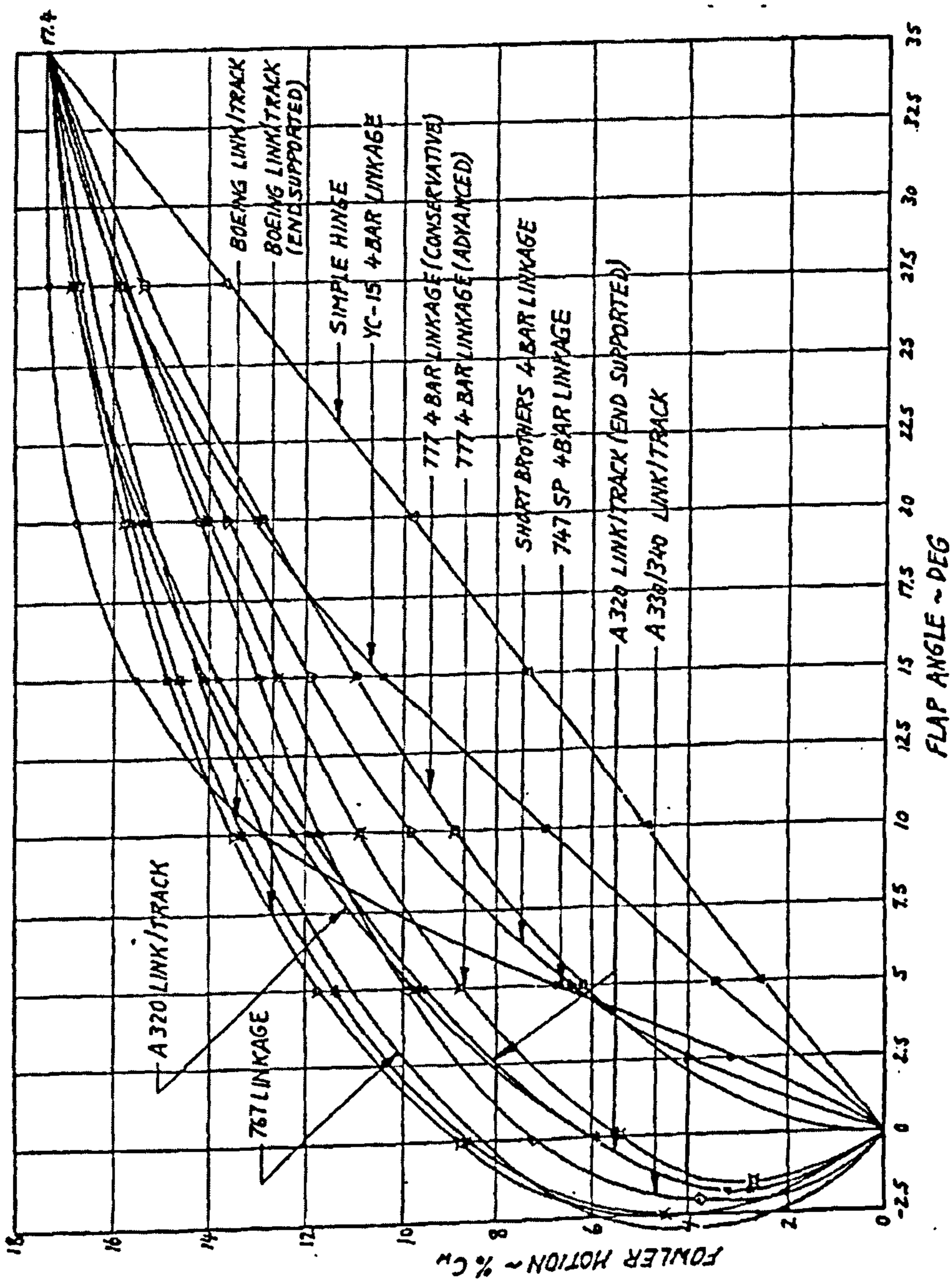

Figure 17 Fowler Motion Progression Comparison

Figure E8 – Fowler Motion Progression Comparison [86]

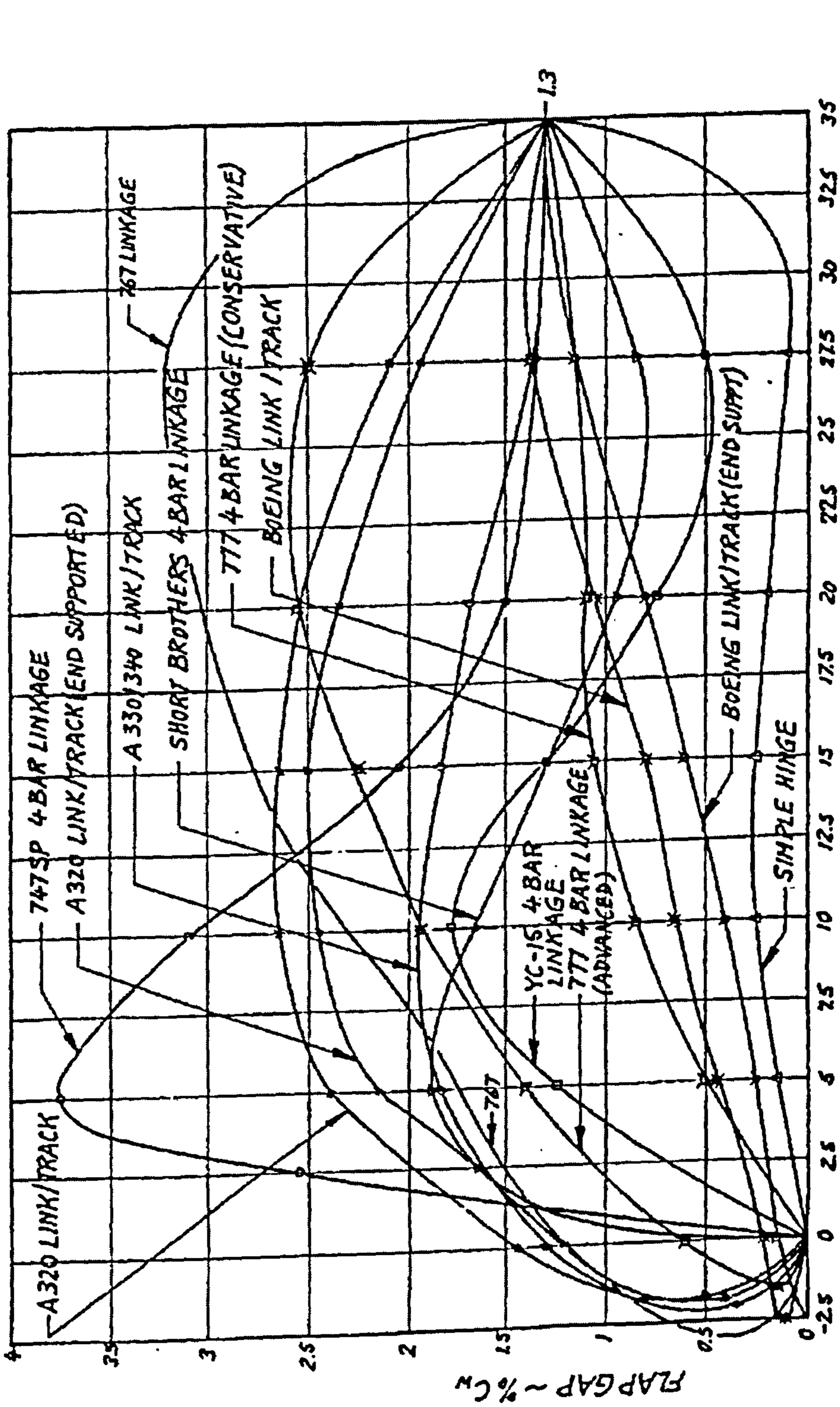

Figure 19 Flap Gap Development Comparison

Figure E9 – Flap Gap Development Comparison [86]

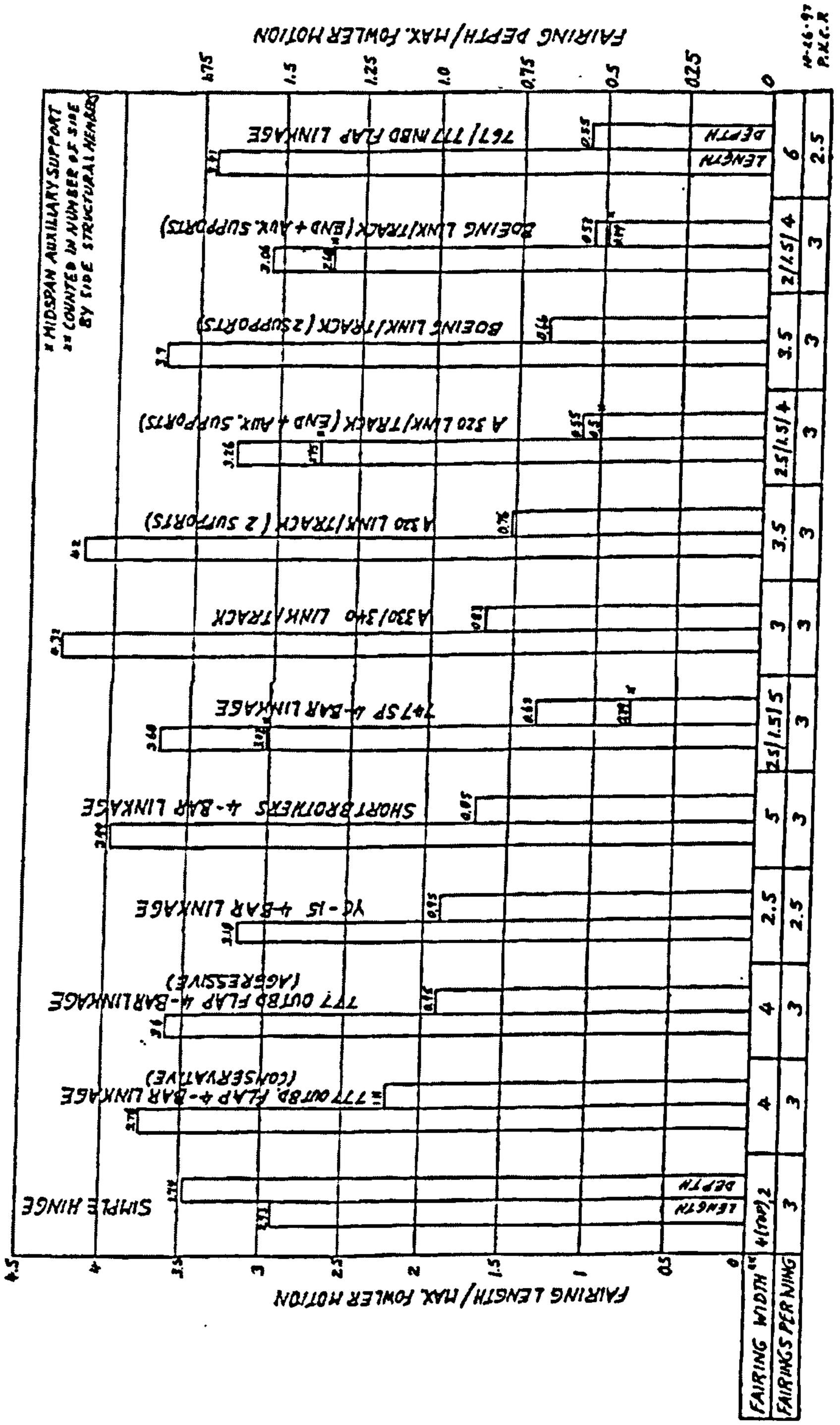

Figure 20 Flap Support Fairing Size Comparison

Figure E10 – Flap Support Fairing Size Comparison [86]

APPENDIX F

RELIABILITY & MAINTAINABILITY VALIDATION RESULTS

TABLE OF CONTENTS

F.1 - RELIABILITY VALIDATION TABLES

F.1.1 - SIMPLE HINGE FLAP *(Appendix E, Fig.E1)*

	SIMPLE HINGE			
	Elements	**QTY**	**Failure Rate/Element (10e6h)**	**Sub-System Failure Rate (10e-6h)**
	HINGE FITTING	1	0.02	0.02
	FLAP FITTING	1	0.02	0.02
	SUPPORT FITTING	1	0.02	0.02
	LINEAR ACTUATOR	1	35.41	35.41
	FWD FAIRING	1	0.20	0.20
	AFT FAIRING	1	0.20	0.20
	Mechanism Connections			
F	SUPPORT FITTING / WING STRUCTURE	1	0.02	0.02
F	HINGE FITTING / FLAP FITTING	1	0.02	0.02
F	LINEAR ACTUATOR / HINGE FITTING	1	0.02	0.02
F	FLAP FITTING / FLAP	1	0.02	0.02
F	FWD FAIRING / WING STRUCTURE	1	0.02	0.02
F	AFT FAIRING / FLAP	1	0.02	0.02
R	SUPPORT FITTING / HINGE FITTING	1	1.00	1.00
R	SUPPORT FITTING / LINEAR ACTUATOR	1	1.00	1.00
R	SUPPORT FITTING / AFT FAIRING	1	1.00	1.00
	Total Nr. Parts	**6**	**Assembly Failure Rate**	**38.99**
	Total Nr. Connections	**9**		

F1.2 - BOEING 777 TYPE FOUR-BAR LINKAGE *(Appendix E, Fig.E2)*

	BOEING 777 TYPE UPSIDE DOWN / UPRIGHT FOUR-BAR LINKAGE			
	Elements	**QTY**	**Failure Rate/Element (10e6 hr)**	**Sub-System Failure Rate (10e-6 hr)**
	ACTUATOR HINGE	1	0.02	0.02
	DRIVE LINK	1	9.26	9.26
	FLAP FITTING	1	0.02	0.02
	SUPPORT FITTING	1	0.02	0.02
	AFT LINK	1	0.02	0.02
	ROTARY ACTUATOR	1	87.935	87.935
	SLAVE LINK	1	0.20	0.20
	FWD FAIRING	1	0.20	0.20
	AFT FAIRING	1	0.20	0.20
	Mechanism Connections			
F	ACTUATOR HINGE / ROTARY ACTUATOR	1	0.02	0.02
F	ACTUATOR HINGE / WING STRUCTURE	1	0.02	0.02
F	FLAP FITTING / FLAP	1	0.02	0.02
F	SUPPORT FITTING / WING STRUCTURE	1	0.02	0.02
F	FWD FAIRING / WING STRUTURE	1	0.02	0.02
R	ACTUATOR HINGE / DRIVE LINK	1	1.00	1.00
R	DRIVE LINK / FLAP FITTING	1	1.00	1.00
R	FLAP FITTING / AFT LINK	1	1.00	1.00
R	SUPPORT FITTING / AFT LINK	1	1.00	1.00
R	SUPPORT FITTING / AFT FAIRING	1	1.00	1.00
R	SLAVE LINK / AFT LINK	1	1.00	1.00
R	SLAVE LINK / AFT FAIRING	1	1.00	1.00
	Total Nr. Parts	**9**	**Assembly Failure Rate**	**100.37**
	Total Nr. Connections	**12**		

F1.3 - AIRBUS A320 TYPE LINK/TRACK MECHANISM *(Appendix E, Fig.E5)*

	AIRBUS A320 TYPE LINK/TRACK MECHANISM			
	Elements	**QTY**	**Failure Rate/Element (10e6 hr)**	**Sub-System Failure Rate (10e-6 hr)**
	ACTUATOR HINGE	1	0.02	0.02
	DRIVE LINK	1	9.26	9.26
	FLAP FITTING	1	0.02	0.02
	SUPPORT BEAM WITH TRACK	1	0.02	0.02
	ROLLER CARRIAGE	1	0.02	0.02
	ROLLER	4	0.6854	2.74
	ROTARY ACTUATOR	1	87.935	87.935
	SLAVE .LNK	1	0.020	0.02
	FWD FAIRING	1	0.20	0.20
	AFT FAIRING	1	0.20	0.20
	Mechanism Connections			
F	ACTUATOR HINGE / ROTARY ACTUATOR	1	0.02	0.02
F	ACTUATOR HINGE / WING STRUCTURE	1	0.02	0.02
F	FLAP FITTING / FLAP	1	0.02	0.02
F	SUPPORT BEAM WITH TRACK / WING STRUCTURE	1	0.02	0.02
F	ROLLER CARRIAGE / ROLLER	1	0.02	0.02
F	FWD FAIRING / WING STRUCTURE	1	0.02	0.02
R	ACTUATOR HINGE / DRIVE LINK	1	1.00	1.00
R	DRIVE LINK / FLAP FITTING	1	1.00	1.00
R	FLAP FITTING / ROLLER CARRIAGE	1	1.00	1.00
R	SUPPORT BEAM WITH TRACK / AFT FAIRING	1	1.00	1.00
R	AFT FAIRING / SLAVE LINK	1	1.00	1.00
R	FLAP FITTING / SLAVE LINK	1	1.00	1.00
	Total Nr. Parts	**13**	**Assembly Failure Rate**	**106.13**
	Total Nr. Connections	**12**		

F1.4 - AIRBUS A330/340 TYPE LINK/TRACK MECHANISM *(Appendix E, Fig.E4)*

	AIRBUS A330/340 TYPE LINK/TRACK MECHANISM			
	Elements	**QTY**	**Failure Rate/Element (10e6 hr)**	**Sub-System Failure Rate (10e-6 hr)**
	ACTUATOR HINGE	1	0.02	0.02
	DRIVE LINK	1	9.26	9.26
	FWD LINK	1	0.02	0.02
	FLAP FITTING	1	0.02	0.02
	SUPPORT BEAM WITH TRACK	1	0.02	0.02
	AFT LINK	1	0.02	0.02
	ROLLER CARRIAGE	1	0.02	0.02
	ROLLER	4	0.6854	2.74
	ROTARY ACTUATOR	1	87.935	87.93
	SLAVE .LNK	1	0.02	0.02
	FWD FAIRING	1	0.20	0.20
	AFT FAIRING	1	0.20	0.20
	Mechanism Connections			
F	ACTUATOR HINGE / ROTARY ACTUATOR	1	0.02	0.02
F	ACTUATOR HINGE / WING STRUCTURE	1	0.02	0.02
F	FLAP FITTING / FLAP	1	0.02	0.02
F	SUPPORT BEAM WITH TRACK / WING STRUCTURE	1	0.02	0.02
F	ROLLER CARRIAGE / ROLLER	1	0.02	0.02
F	FWD FAIRING / WING STRUCTURE	1	0.02	0.02
R	ACTUATOR HINGE / DRIVE LINK	1	1.00	1.00
R	DRIVE LINK / FWD LINK	1	1.00	1.00
R	FWD LINK / FLAP FITTING	1	1.00	1.00
R	FLAP FITTING / AFT LINK	1	1.00	1.00
R	SUPPORT BEAM WITH TRACK / AFT LINK	1	1.00	1.00
R	SUPPORT BEAM WITH TRACK / AFT FAIRING	1	1.00	1.00
R	AFT FAIRING / SLAVE LINK	1	1.00	1.00
R	AFT LINK / SLAVE LINK	1	1.00	1.00
	Total Nr. Parts	**15**	**Assembly Failure Rate**	**104.17**
	Total Nr. Connections	**14**		

F1.5 - BOEING 747 TYPE FOUR-BAR LINKAGE *(Appendix E, Fig.E3)*

	BOING 747 TYPE FOUR-BAR LINKAGE			
	Elements	**QTY**	**Failure Rate/Element (10e6 hr)**	**Sub-System Failure Rate (10e-6 hr)**
	SUPPORT FITTING	1	0.02	0.02
	DRIVE LINK	1	9.26	9.26
	FLAP FITTING	1	0.02	0.02
	AFT LINK	1	0.02	0.02
	ROTARY ACTUATOR	1	87.935	87.93
	FWD FAIRING	1	0.20	0.20
	AFT FAIRING	1	0.20	0.20
	Mechanism Connections			
F	SUPPORT FITTING / ROTARY ACTUATOR	1	0.02	0.02
F	SUPPORT FITTING / WING STRUCTURE	1	0.02	0.02
F	FLAP FITTING / FLAP	1	0.02	0.02
F	FWD FAIRING / WING STRUCTURE	1	0.02	0.02
F	AFT FAIRING / FLAP	1	0.02	0.02
R	SUPPORT FITTING / DRIVE LINK	1	1.00	1.00
R	SUPPORT FITTING / AFT LINK	1	1.00	1.00
R	DRIVE LINK / FLAP FITTING	1	1.00	1.00
R	FLAP FITTING AFT LINK	1	1.00	1.00
	Total Nr. Parts	**7**	**Assembly Failure Rate**	**99.35**
	Total Nr. Connections	**9**		

F1.6 - AIRBUS A320 TYPE LINK/TRACK MECHANISM *(Appendix E, Fig.E6)*

	AIRBUS A320 TYPE LINK/TRACK MECHANISM			
	Elements	**QTY**	**Failure Rate/Element (10e6 hr)**	**Sub-System Failure Rate (10e-6 hr)**
	SUPPORT BEAM WITH TRACK	1	0.02	0.02
	DRIVE LINK	1	9.26	9.26
	FLAP FITTING	1	0.02	0.02
	ROLLER	1	0.6854	0.69
	ROTARY ACTUATOR	1	87.935	87.93
	FWD FAIRING	1	0.20	0.20
	AFT FAIRING	1	0.20	0.20
	Mechanism Connections			
F	SUPPORT BEAM WITH TRACK / ROTARY ACTUATOR	1	0.02	0.02
F	SUPPORT BEAM WITH TRACK / WING STRUCTURE	1	0.02	0.02
F	FLAP FITTING / FLAP	1	0.02	0.02
F	FLAP / ROLLER	1	0.02	0.02
F	FWD FAIRING / WING STRUCTURE	1	0.02	0.02
F	AFT FAIRING / FLAP	1	0.02	0.02
R	SUPPORT BEAM WITH TRACK / DRIVE LINK	1	1.00	1.00
R	DRIVE LINK / FLAP FITTING	1	1.00	1.00
	Total Nr. Parts	**7**	**Assembly Failure Rate =**	**100.04**
	Total Nr. Connections	**8**		

F1.7 - BOEING TYPE LINK/TRACK MECHANISM *(Appendix E, Fig.E7)*

	BOEING TYPE LINK/TRACK MECHANISM			
	Elements	**QTY**	**Failure Rate/Element (10e6h)**	**Sub-Sytem Failure Rate (10e-6h)**
	SUPPORT FITTING	1	0.02	0.02
	DRIVE LINK	1	9.26	9.26
	FLAP FITTING WITH TRACK	1	0.02	0.02
	ROLLER	1	0.6854	0.69
	ROTARY ACTUATOR	1	87.935	87.93
	FWD FAIRING	1	0.20	0.20
	AFT FAIRING	1	0.20	0.20
	Mechanism Connections			
F	SUPPORT FITTING / ROTARY ACTUATOR	1	0.02	0.02
F	SUPPORT FITTING / WING STRUCTURE	1	0.02	0.02
F	SUPPORT FITTING / ROLLER	1	0.02	0.02
F	FLAP FITTING WITH TRACK / FLAP	1	0.02	0.02
F	FWD FAIRING / WING STRUCTURE	1	0.02	0.02
F	AFT FAIRING / FLAP	1	0.02	0.02
R	SUPPORT FITTING / DRIVE LINK	1	1.00	1.00
R	DRIVE LINK / FLAP FITTING WITH TRACK	1	1.00	1.00
	Total Nr. Parts	**7**	**Assembly Failure Rate =**	**98.04**
	Total Nr. Connections	**8**		

F2 - MAINTANABILITY VALIDATION TABLES

F1.1 - SIMPLE HINGE FLAP *(Appendix E, Fig.E1)*

MAINTAINABILITY PREDICTION [MIL - HDBK 472]

SIMPLE HINGE FLAP [Fig. 3]

CHECK LIST A - PHISICAL DESIGN FACTORS

		SUPPORTS & LINKAGES			ACTUATION & CONTROLS	FLAP PANEL	FAIRINGS	
	ITEM	HINGE FITTING	FLAP FITTING	SUPPORT FITTING	LINEAR ACTUATOR	FLAP	FWD FAIRING	AFT FAIRING
1	Access	2	2	2	2	4	4	4
2	Latches& Fasteners (external)	2	2	0	2	2	4	4
3	Latches& Fasteners (Internal)	2	0	0	2	0	4	4
4	Access (Internal)	2	2	2	2	4	4	4
5	Packaging	0	0	0	2	0	2	2
6	Units/Parts	2	0	0	2	0	2	2
7	Visual Display	2	2	0	4	2	2	2
8	Fault & Operation Indicators	2	2	0	4	2	0	0
9	Test Point Availability	2	2	2	2	2	2	2
10	Test Point Identification	0	0	0	2	0	0	0
11	Labelling	2	2	2	2	2	2	2
12	Adjustments	2	0	0	2	2	2	2
13	Testing (On Aircraft)	4	4	4	4	4	4	4
14	Protective Devices	2	2	0	2	2	2	2
15	Safety Personal	2	2	2	2	2	2	2
	Total	28	22	14	36	28	36	36

CHECK LIST B - DESIGN FACILITY FACTORS

		SUPPORTS & LINKAGES			ACTUATION & CONTROLS	FLAP PANEL	FAIRINGS	
	ITEM	HINGE FITTING	FLAP FITTING	SUPPORT FITTING	LINEAR ACTUATOR	FLAP	FWD FAIRING	AFT FAIRING
1	External Test Equipment	2	2	2	2	2	4	4
2	Connectors	2	2	2	2	4	4	4
3	Jigs or Fixtures	0	0	0	2	0	2	2
4	Visual Contact	4	4	4	2	2	2	2
5	Assistance (Operations Personal)	4	4	4	2	4	4	4
6	Assistance (Technical Personal)	0	0	0	2	0	2	2
7	Assistance (Supervisory or Contract Personal)	2	2	2	2	4	4	4
	Total	14	14	14	14	16	22	22

CHECK LIST C - MAINTENANCE SKILLS

		SUPPORTS & LINKAGES			ACTUATION & CONTROLS	FLAP PANEL	FAIRINGS	
	ITEM	HINGE FITTING	FLAP FITTING	SUPPORT FITTING	LINEAR ACTUATOR	FLAP	FWD FAIRING	AFT FAIRING
1	Arm, Leg, and Back Strength	2	2	2	2	1	1	1
2	Endurance and Energy	2	2	2	2	1	1	1
3	Eye/Hand Coordination, Dexterity and Neatness	2	2	2	2	2	2	2
4	Visual Acuity	2	2	2	2	4	4	4
5	Logical Analysis	3	3	3	2	3	3	3
6	Memory - Things and Ideas	2	2	2	2	2	3	3
7	Planfulness and Resourcefulness	2	2	2	2	2	2	2
8	Alertness, Cautiousness, and Accuracy	1	1	1	2	1	3	3
9	Concentration, Persistance and Patience	1	1	1	2	1	2	2
10	Initiative and Incisiveness	3	3	3	4	3	4	4
	Total	20	20	20	22	20	26	26

MTTR [hr]	2.6	3.7	6.9	1.6	2.3	0.8	0.8

TOTAL 17.7

F1.2 - BOEING 777 TYPE FOUR-BAR LINKAGE *(Appendix E, Fig.E2)*

MAINTAINABILITY PREDICTION [MIL - HDBK 472]

BOEING 777 TYPE UPSIDE DOWN / UPRIGHT FOUR-BAR LINKAGE [Fig. 5]

CHECK LIST A - PHISICAL DESIGN FACTORS

		SUPPORTS & LINKAGES					ACTUATION & CONTROLS	FLAP PANEL	FAIRINGS		
	ITEM	ACTUATOR HINGE	DRIVE LINK	FLAP FITTING	SUPPORT FITTING	AFT LINK	ROTARY ACTUATOR	FLAP	FWD FAIRING	AFT FAIRING	SLAVE LINK
1	Access	2	2	2	2	2	2	4	4	4	2
2	Latches& Fasteners (external)	0	2	2	0	2	2	2	4	4	2
3	Latches& Fasteners (Internal)	0	2	0	0	2	2	0	4	4	2
4	Access (Internal)	2	4	2	2	4	2	4	4	4	4
5	Packaging	0	0	0	0	0	2	0	2	2	2
6	Units/Parts	0	2	0	0	2	2	0	2	2	2
7	Visual Display	0	2	2	0	2	4	2	2	2	2
8	Fault & Operation Indicators	0	2	2	0	2	4	2	0	0	2
9	Test Point Availability	2	2	2	2	2	2	2	2	2	2
10	Test Point Identification	0	0	0	0	0	2	0	0	0	0
11	Labelling	2	2	2	2	2	2	2	2	2	2
12	Adjustments	0	2	0	0	2	2	2	2	2	2
13	Testing (On Aircraft)	4	4	4	4	4	4	4	4	4	4
14	Protective Devices	0	2	2	0	2	2	2	2	2	2
15	Safety Personal	2	2	2	2	2	2	2	2	2	2
	Total	14	30	22	14	30	36	28	36	36	32

CHECK LIST B - DESIGN FACILITY FACTORS

		SUPPORTS & LINKAGES					ACTUATION & CONTROLS	FLAP PANEL	FAIRINGS		
	ITEM	ACTUATOR HINGE	DRIVE LINK	FLAP FITTING	SUPPORT FITTING	AFT LINK	ROTARY ACTUATOR	FLAP	FWD FAIRING	AFT FAIRING	SLAVE LINK
1	External Test Equipment	2	2	2	2	2	2	2	4	4	4
2	Connectors	2	2	2	2	2	2	4	4	4	4
3	Jigs or Fixtures	0	0	0	0	0	2	0	2	2	2
4	Visual Contact	4	4	4	4	4	2	2	2	2	4
5	Assistance (Operations Personal)	4	4	4	4	4	2	4	4	4	4
6	Assistance (Technical Personal)	0	0	0	0	0	2	0	2	2	2
7	Assistance (Supervisory or Contract Personal)	2	4	2	2	4	2	4	4	4	4
	Total	14	16	14	14	16	14	16	22	22	24

CHECK LIST C - MAINTENANCE SKILLS

		SUPPORTS & LINKAGES					ACTUATION & CONTROLS	FLAP PANEL	FAIRINGS		
	ITEM	ACTUATOR HINGE	DRIVE LINK	FLAP FITTING	SUPPORT FITTING	AFT LINK	ROTARY ACTUATOR	FLAP	FWD FAIRING	AFT FAIRING	SLAVE LINK
1	Arm, Leg, and Back Strength	2	2	2	2	2	2	1	1	1	1
2	Endurance and Energy	2	2	2	2	2	2	1	1	1	1
3	Eye/Hand Coordination, Dexterity and Neatness	2	2	2	2	2	2	2	2	2	2
4	Visual Acuity	2	2	2	2	2	2	4	4	4	4
5	Logical Analysis	3	3	3	3	3	2	3	3	3	3
6	Memory - Things and Ideas	2	2	2	2	2	2	2	3	3	3
7	Planfulness and Resourcefulness	2	2	2	2	2	2	2	2	2	2
8	Alertness, Cautiousness, and Accuracy	1	1	1	1	1	2	1	3	3	3
9	Concentration, Persistance and Patience	1	1	1	1	1	2	1	2	2	2
10	Initiative and Incisiveness	3	3	3	3	3	4	3	4	4	4
	Total	20	20	20	20	20	22	20	25	25	26

	MTTR [hr]	5.9	2.0	3.7	5.9	2.0	1.6	2.3	0.8	0.8	0.9

TOTAL 26.0

F1.3 - AIRBUS A320 TYPE LINK/TRACK MECHANISM *(Appendix E, Fig.E5)*

MAINTAINABILITY PREDICTION [MIL - HDBK 472]

AIRBUS A320 TYPE LINK/TRACK MECHANISM [Fig. 10]

CHECK LIST A - PHISICAL DESIGN FACTORS

		SUPPORTS & LINKAGES						ACTUATION & CONTROLS	FLAP PANEL	FAIRINGS		
	ITEM	ACTUATOR HINGE	DRIVE LINK	FLAP FITTING	SUPPORT BEAM WITH TRACK	ROLLER CARRIAGE	ROLLER	ROTARY ACTUATOR	FLAP	FWD FAIRING	AFT FAIRING	SLAVE LINK
1	Access	2	2	2	2	2	2	2	4	4	4	2
2	Latches& Fasteners (external)	0	2	2	0	2	0	2	2	4	4	2
3	Latches& Fasteners (Internal)	0	2	0	0	2	0	2	0	4	4	2
4	Access (Internal)	2	4	2	2	2	2	2	4	4	4	4
5	Packaging	0	0	0	0	0	0	2	0	2	2	2
6	Units/Parts	0	2	0	0	2	2	2	0	2	2	2
7	Visual Display	0	2	2	0	2	0	4	2	2	2	2
8	Fault & Operation Indicators	0	2	2	0	2	2	4	2	0	0	2
9	Test Point Availability	2	2	2	2	2	4	2	2	2	2	2
10	Test Point Identification	0	0	0	0	0	4	2	0	0	0	0
11	Labelling	2	2	2	2	2	2	2	2	2	2	2
12	Adjustments	0	2	0	0	2	2	2	2	2	2	2
13	Testing (On Aircraft)	4	4	4	4	4	4	4	4	4	4	4
14	Protective Devices	0	2	2	0	2	2	2	2	2	2	2
15	Safety Personal	2	2	2	0	2	2	2	2	2	2	2
	Total	14	30	22	12	28	28	36	28	36	36	32

CHECK LIST B - DESIGN FACILITY FACTORS

		SUPPORTS & LINKAGES						ACTUATION & CONTROLS	FLAP PANEL	FAIRINGS		
	ITEM	ACTUATOR HINGE	DRIVE LINK	FLAP FITTING	SUPPORT BEAM WITH TRACK	ROLLER CARRIAGE	ROLLER	ROTARY ACTUATOR	FLAP	FWD FAIRING	AFT FAIRING	SLAVE LINK
1	External Test Equipment	2	2	2	2	2	4	2	2	4	4	4
2	Connectors	2	2	2	2	2	4	2	4	4	4	4
3	Jigs or Fixtures	0	0	0	0	0	0	2	0	2	2	2
4	Visual Contact	4	4	4	2	2	2	2	2	2	2	4
5	Assistance (Operations Personal)	4	4	4	2	4	4	2	4	4	4	4
6	Assistance (Technical Personal)	0	0	0	0	2	2	2	0	2	2	2
7	Assistance (Supervisory or Contract Personal)	2	4	2	2	4	4	2	4	4	4	4
	Total	14	16	14	10	16	20	14	16	22	22	24

CHECK LIST C - MAINTENANCE SKILLS

		SUPPORTS & LINKAGES						ACTUATION & CONTROLS	FLAP PANEL	FAIRINGS		
	ITEM	ACTUATOR HINGE	DRIVE LINK	FLAP FITTING	SUPPORT BEAM WITH TRACK	ROLLER CARRIAGE	ROLLER	ROTARY ACTUATOR	FLAP	FWD FAIRING	AFT FAIRING	SLAVE LINK
1	Arm, Leg, and Back Strength	2	2	2	1	2	2	2	1	1	1	1
2	Endurance and Energy	2	2	2	1	2	2	2	1	1	1	1
3	Eye/Hand Coordination, Dexterity and Neatness	2	2	2	2	2	2	2	2	2	2	2
4	Visual Acuity	2	2	2	2	2	2	2	4	4	4	4
5	Logical Analysis	3	3	3	3	3	3	2	3	3	3	3
6	Memory - Things and Ideas	2	2	2	2	2	2	2	2	3	3	3
7	Planfulness and Resourcefulness	2	2	2	2	2	2	2	2	2	2	2
8	Alertness, Cautiousness, and Accuracy	1	1	1	1	1	1	2	1	3	3	3
9	Concentration, Persistance and Patience	1	1	1	1	1	1	2	1	2	2	2
10	Initiative and Incisiveness	3	3	3	2	3	3	4	3	4	4	4
	Total	20	20	20	16	20	20	22	20	26	26	25
	MTTR [hr]	5.9	2.0	3.7	9.7	2.3	1.7	1.6	2.3	0.8	0.8	0.9

TOTAL 31.7

F1.4 - AIRBUS A330/340 TYPE LINK/TRACK MECHANISM *(Appendix E, Fig.E4)*

MAINTAINABILITY PREDICTION [MIL - HDBK 472]

AIRBUS A330/340 TYPE LINK/TRACK MECHANISM [Fig. 9]

CHECK LIST A - PHISICAL DESIGN FACTORS

		SUPPORTS & LINKAGES								ACTUATION & CONTROLS	FLAP PANEL	FAIRINGS		
	ITEM	ACTUATOR HINGE	DRIVE LINK	FWD LINK	FLAP FITTING	SUPPORT BEAM WITH TRACK	AFT LINK	ROLLER CARRIAGE	ROLLER	ROTARY ACTUATOR	FLAP	FWD FAIRING	AFT FAIRING	SLAVE LNK
1	Access	2	2	2	2	2	2	2	2	2	4	4	4	2
2	Latches& Fasteners (external)	0	2	2	2	0	2	2	0	2	2	4	4	2
3	Latches& Fasteners (Internal)	0	2	2	0	0	2	2	0	2	0	4	4	2
4	Access (Internal)	2	4	4	2	2	4	2	2	2	4	4	4	4
5	Packaging	0	0	0	0	0	0	0	0	2	0	2	2	2
6	Units/Parts	0	2	2	0	0	2	2	2	2	0	2	2	2
7	Visual Display	0	2	2	2	0	2	2	0	4	2	2	2	2
8	Fault & Operation Indicators	0	2	2	2	0	2	2	2	4	2	0	0	2
9	Test Point Availability	2	2	2	2	2	2	2	4	2	2	2	2	2
10	Test Point Identification	0	0	0	0	0	0	0	4	2	0	0	0	0
11	Labelling	2	2	2	2	2	2	2	2	2	2	2	2	2
12	Adjustments	0	2	2	0	0	2	2	2	2	2	2	2	2
13	Testing (On Aircraft)	4	4	4	4	4	4	4	4	4	4	4	4	4
14	Protective Devices	0	2	2	2	0	2	2	2	2	2	2	2	2
15	Safety Personal	2	2	2	2	0	2	2	2	2	2	2	2	2
	Total	14	30	30	22	12	30	28	28	36	28	36	36	32

CHECK LIST B - DESIGN FACILITY FACTORS

		SUPPORTS & LINKAGES								ACTUATION & CONTROLS	FLAP PANEL	FAIRINGS		
	ITEM	ACTUATOR HINGE	DRIVE LINK	FWD LINK	FLAP FITTING	SUPPORT BEAM WITH TRACK	AFT LINK	ROLLER CARRIAGE	ROLLER	ROTARY ACTUATOR	FLAP	FWD FAIRING	AFT FAIRING	SLAVE LNK
1	External Test Equipment	2	2	2	2	2	2	2	4	2	2	4	4	4
2	Connectors	2	2	2	2	2	2	2	4	2	4	4	4	4
3	Jigs or Fixtures	0	0	0	0	0	0	0	0	2	0	2	2	2
4	Visual Contact	4	4	4	4	2	4	2	2	2	2	2	2	4
5	Assistance (Operations Personal)	4	4	4	4	2	4	4	4	2	4	4	4	4
6	Assistance (Technical Personal)	0	0	0	0	0	0	2	2	2	0	2	2	2
7	Assistance (Supervisory or Contract Personal)	2	4	4	2	2	4	4	4	2	4	4	4	4
	Total	14	16	16	14	10	16	16	20	14	16	22	22	24

CHECK LIST C - MAINTENANCE SKILLS

		SUPPORTS & LINKAGES								ACTUATION & CONTROLS	FLAP PANEL	FAIRINGS		
	ITEM	ACTUATOR HINGE	DRIVE LINK	FWD LINK	FLAP FITTING	SUPPORT BEAM WITH TRACK	AFT LINK	ROLLER CARRIAGE	ROLLER	ROTARY ACTUATOR	FLAP	FWD FAIRING	AFT FAIRING	SLAVE LNK
1	Arm, Leg, and Back Strength	2	2	2	2	1	2	2	2	2	1	1	1	1
2	Endurance and Energy	2	2	2	2	1	2	2	2	2	1	1	1	1
3	Eye/Hand Coordination, Dexterity and Neatness	2	2	2	2	2	2	2	2	2	2	2	2	2
4	Visual Acuity	2	2	2	2	2	2	2	2	2	4	4	4	4
5	Logical Analysis	3	3	3	3	3	3	3	3	2	3	3	3	3
6	Memory - Things and Ideas	2	2	2	2	2	2	2	2	2	2	3	3	3
7	Planfulness and Resourcefulness	2	2	2	2	2	2	2	2	2	2	2	2	2
8	Alertness, Cautiousness, and Accuracy	1	1	1	1	1	1	1	1	2	1	3	3	3
9	Concentration, Persistance and Patience	1	1	1	1	1	1	1	1	2	1	2	2	2
10	Initiative and Incisiveness	3	3	3	3	2	3	3	3	4	3	4	4	4
	Total	20	20	20	20	17	20	20	20	22	20	25	25	25

	MTTR [hr]	5.9	2.0	2.0	3.7	9.5	2.0	2.3	1.7	1.6	2.3	0.8	0.8	0.9

TOTAL 35.6

F1.5 - BOEING 747 TYPE FOUR-BAR LINKAGE *(Appendix E, Fig.E3)*

MAINTAINABILITY PREDICTION [MIL - HDBK 472]

BOEING 747 TYPE FOUR-BAR LINKAGE [Fig. 8]

CHECK LIST A - PHISICAL DESIGN FACTORS

		SUPPORTS & LINKAGES				ACTUATION & CONTROLS	FLAP PANEL	FAIRINGS	
	ITEM	SUPPORT FITTING	DRIVE LINK	FLAP FITTING	AFT LINK	ROTARY ACTUATOR	FLAP	FWD FAIRING	AFT FAIRING
1	Access	2	2	2	2	2	4	4	4
2	Latches& Fasteners (external)	0	2	2	2	2	2	4	4
3	Latches& Fasteners (Internal)	0	2	0	2	2	0	4	4
4	Access (Internal)	2	4	2	4	2	4	4	4
5	Packaging	0	0	0	0	2	0	2	2
6	Units/Parts	0	2	0	2	2	0	2	2
7	Visual Display	0	2	2	2	4	2	2	2
8	Fault & Operation Indicators	0	2	2	2	4	2	0	0
9	Test Point Availability	2	2	2	2	2	2	2	2
10	Test Point Identification	0	0	0	0	2	0	0	0
11	Labelling	2	2	2	2	2	2	2	2
12	Adjustments	0	2	0	2	2	2	2	2
13	Testing (On Aircraft)	4	4	4	4	4	4	4	4
14	Protective Devices	0	2	2	2	2	2	2	2
15	Safety Personal	2	2	2	2	2	2	2	2
	Total	14	30	22	30	36	28	36	36

CHECK LIST B - DESIGN FACILITY FACTORS

		SUPPORTS & LINKAGES				ACTUATION & CONTROLS	FLAP PANEL	FAIRINGS	
	ITEM	SUPPORT FITTING	DRIVE LINK	FLAP FITTING	AFT LINK	ROTARY ACTUATOR	FLAP	FWD FAIRING	AFT FAIRING
1	External Test Equipment	2	2	2	2	2	2	4	4
2	Connectors	2	2	2	2	2	4	4	4
3	Jigs or Fixtures	0	0	0	0	2	0	2	2
4	Visual Contact	4	4	4	4	2	2	2	2
5	Assistance (Operations Personal)	4	4	4	4	2	4	4	4
6	Assistance (Technical Personal)	0	0	0	0	2	0	2	2
7	Assistance (Supervisory or Contract Personal)	2	4	2	4	2	4	4	4
	Total	14	16	14	16	14	16	22	22

CHECK LIST C - MAINTENANCE SKILLS

		SUPPORTS & LINKAGES				ACTUATION & CONTROLS	FLAP PANEL	FAIRINGS	
	ITEM	SUPPORT FITTING	DRIVE LINK	FLAP FITTING	AFT LINK	ROTARY ACTUATOR	FLAP	FWD FAIRING	AFT FAIRING
1	Arm, Leg, and Back Strength	2	2	2	2	2	1	1	1
2	Endurance and Energy	2	2	2	2	2	1	1	1
3	Eye/Hand Coordination, Dexterity and Neatness	2	2	2	2	2	2	2	2
4	Visual Acuity	2	2	2	2	2	4	4	4
5	Logical Analysis	3	3	3	3	2	3	3	3
6	Memory - Things and Ideas	2	2	2	2	2	2	3	3
7	Planfulness and Resourcefulness	2	2	2	2	2	2	2	2
8	Alertness, Cautiousness, and Accuracy	1	1	1	1	2	1	3	3
9	Concentration, Persistance and Patience	1	1	1	1	2	1	2	2
10	Initiative and Incisiveness	3	3	3	3	4	3	4	4
	Total	20	20	20	20	22	20	25	25

	MTTR [hr]	5.9	2.0	3.7	2.0	1.6	2.3	0.8	0.8

TOTAL 19.2

F1.6 - AIRBUS A320 TYPE LINK/TRACK MECHANISM *(Appendix E, Fig.E6)*

MAINTAINABILITY PREDICTION [MIL - HDBK 472]

AIRBUS A320 TYPE LINK/TRACK MECHANISM [Fig. 11]

CHECK LIST A - PHISICAL DESIGN FACTORS

		SUPPORTS & LINKAGES				ACTUATION & CONTROLS	FLAP PANEL	FAIRINGS	
	ITEM	SUPPORT BEAM WITH TRACK	DRIVE LINK	FLAP FITTING	ROLLER	ROTARY ACTUATOR	FLAP	FWD FAIRING	AFT FAIRING
1	Access	2	2	2	2	2	4	4	4
2	Latches& Fasteners (external)	0	2	2	0	2	2	4	4
3	Latches& Fasteners (Internal)	0	2	0	0	2	0	4	4
4	Access (Internal)	2	4	2	2	2	4	4	4
5	Packaging	0	0	0	0	2	0	2	2
6	Units/Parts	0	2	0	2	2	0	2	2
7	Visual Display	0	2	2	0	4	2	2	2
8	Fault & Operation Indicators	0	2	2	2	4	2	0	0
9	Test Point Availability	2	2	2	4	2	2	2	2
10	Test Point Identification	0	0	0	4	2	0	0	0
11	Labelling	2	2	2	2	2	2	2	2
12	Adjustments	0	2	0	2	2	2	2	2
13	Testing (On Aircraft)	4	4	4	4	4	4	4	4
14	Protective Devices	0	2	2	2	2	2	2	2
15	Safety Personal	0	2	2	2	2	2	2	2
	Total	12	30	22	28	36	28	36	36

CHECK LIST B - DESIGN FACILITY FACTORS

		SUPPORTS & LINKAGES				ACTUATION & CONTROLS	FLAP PANEL	FAIRINGS	
	ITEM	SUPPORT BEAM WITH TRACK	DRIVE LINK	FLAP FITTING	ROLLER	ROTARY ACTUATOR	FLAP	FWD FAIRING	AFT FAIRING
1	External Test Equipment	2	2	2	4	2	2	4	4
2	Connectors	2	2	2	4	2	4	4	4
3	Jigs or Fixtures	0	0	0	0	2	0	2	2
4	Visual Contact	2	4	4	2	2	2	2	2
5	Assistance (Operations Personal)	2	4	4	4	2	4	4	4
6	Assistance (Technical Personal)	0	0	0	2	2	0	2	2
7	Assistance (Supervisory or Contract Personal)	2	4	2	4	2	4	4	4
	Total	10	16	14	20	14	16	22	22

CHECK LIST C - MAINTENANCE SKILLS

		SUPPORTS & LINKAGES				ACTUATION & CONTROLS	FLAP PANEL	FAIRINGS	
	ITEM	SUPPORT BEAM WITH TRACK	DRIVE LINK	FLAP FITTING	ROLLER	ROTARY ACTUATOR	FLAP	FWD FAIRING	AFT FAIRING
1	Arm, Leg, and Back Strength	1	2	2	2	2	1	1	1
2	Endurance and Energy	1	2	2	2	2	1	1	1
3	Eye/Hand Coordination, Dexterity and Neatness	2	2	2	2	2	2	2	2
4	Visual Acuity	2	2	2	2	2	4	4	4
5	Logical Analysis	3	3	3	3	2	3	3	3
6	Memory - Things and Ideas	2	2	2	2	2	2	3	3
7	Planfulness and Resourcefulness	2	2	2	2	2	2	2	2
8	Alertness, Cautiousness, and Accuracy	1	1	1	1	2	1	3	3
9	Concentration, Persistance and Patience	1	1	1	1	2	1	2	2
10	Initiative and Incisiveness	2	3	3	3	4	3	4	4
	Total	17	20	20	20	22	20	25	25

MTTR [hr]	9.5	2.0	3.7	1.7	1.6	2.3	0.8	0.8

TOTAL 22.4

F1.7 - BOEING TYPE LINK/TRACK MECHANISM *(Appendix E, Fig.E7)*

MAINTAINABILITY PREDICTION [MIL - HDBK 472]

BOEING TYPE LINK/TRACK MECHANISM [Fig. 13]

CHECK LIST A - PHISICAL DESIGN FACTORS

		SUPPORTS & LINKAGES				ACTUATION & CONTROLS	FLAP PANEL	FAIRINGS	
	ITEM	SUPPORT FITTING	DRIVE LINK	FLAP FITTING WITH TRACK	ROLLER	ROTARY ACTUATOR	FLAP	FWD FAIRING	AFT FAIRING
1	Access	2	2	2	2	2	4	4	4
2	Latches& Fasteners (external)	0	2	2	0	2	2	4	4
3	Latches& Fasteners (Internal)	0	2	0	0	2	0	4	4
4	Access (Internal)	2	4	2	2	2	4	4	4
5	Packaging	0	0	0	0	2	0	2	2
6	Units/Parts	0	2	0	2	2	0	2	2
7	Visual Display	0	2	2	0	4	2	2	2
8	Fault & Operation Indicators	0	2	2	2	4	2	0	0
9	Test Point Availability	2	2	2	4	2	2	2	2
10	Test Point Identification	0	0	0	4	2	0	0	0
11	Labelling	2	2	2	2	2	2	2	2
12	Adjustments	0	2	0	2	2	2	2	2
13	Testing (On Aircraft)	4	4	4	4	4	4	4	4
14	Protective Devices	0	2	2	2	2	2	2	2
15	Safety Personal	2	2	2	2	2	2	2	2
	Total	14	30	22	28	36	28	36	36

CHECK LIST B - DESIGN FACILITY FACTORS

		SUPPORTS & LINKAGES				ACTUATION & CONTROLS	FLAP PANEL	FAIRINGS	
	ITEM	SUPPORT FITTING	DRIVE LINK	FLAP FITTING WITH TRACK	ROLLER	ROTARY ACTUATOR	FLAP	FWD FAIRING	AFT FAIRING
1	External Test Equipment	2	2	2	4	2	2	4	4
2	Connectors	2	2	2	4	2	4	4	4
3	Jigs or Fixtures	0	0	0	0	2	0	2	2
4	Visual Contact	4	4	4	2	2	2	2	2
5	Assistance (Operations Personal)	4	4	4	4	2	4	4	4
6	Assistance (Technical Personal)	0	0	0	2	2	0	2	2
7	Assistance (Supervisory or Contract Personal)	2	4	2	4	2	4	4	4
	Total	14	16	14	20	14	16	22	22

CHECK LIST C - MAINTENANCE SKILLS

		SUPPORTS & LINKAGES				ACTUATION & CONTROLS	FLAP PANEL	FAIRINGS	
	ITEM	SUPPORT FITTING	DRIVE LINK	FLAP FITTING WITH TRACK	ROLLER	ROTARY ACTUATOR	FLAP	FWD FAIRING	AFT FAIRING
1	Arm, Leg, and Back Strength	2	2	2	2	2	1	1	1
2	Endurance and Energy	2	2	2	2	2	1	1	1
3	Eye/Hand Coordination, Dexterity and Neatness	2	2	2	2	2	2	2	2
4	Visual Acuity	2	2	2	2	2	4	4	4
5	Logical Analysis	3	3	3	3	2	3	3	3
6	Memory - Things and Ideas	2	2	2	2	2	2	3	3
7	Planfulness and Resourcefulness	2	2	2	2	2	2	2	2
8	Alertness, Cautiousness, and Accuracy	1	1	1	1	2	1	3	3
9	Concentration, Persistance and Patience	1	1	1	1	2	1	2	2
10	Initiative and Incisiveness	3	3	3	3	4	3	4	4
	Total	20	20	20	20	22	20	25	25

MTTR [hr]	5.9	2.0	3.7	1.7	1.6	2.3	0.8	0.8

TOTAL **18.9**

APPENDIX G

OPTIMIZATION RESULTS

TABLE OF CONTENTS

G1 – 4-BAR CASE STUDY – Optimization report

Report date: Tue Apr 4 20:23:36 2006
Settings:

Type of study	Optimization
Algorithm	GCM
Convergence Precision	0.01
Convergence Criteria	Variation on variables -
Global perturbation	0.0001 (based on current value)
Move limit	No limit
Scaling of Variables	By individual factor
Scaling of Functions	Also when Multi-Objective
Check	Check Standard
Switch	Switch On
Listing	Delete
Moving Variables Bounds	10% of Range
External Relaxation	Relaxation Disabled
Cut	Cut=10
Degressive Relaxation	DRelax Inactive

Variables:

Name	Lower bound	Initial value	Iteration 39	Upper bound
X1	17100	17150	17103.5	17300
Z1	2900	3000	3026.27	3100
X2	16800	16950	16965	17100
Z2	2580	2680	2644.16	2780
X3	17350	17500	17350	17650
Z3	2600	2700	2691.72	2800
X4	17350	17500	17650	17650
Z4	2300	2400	2300	2500

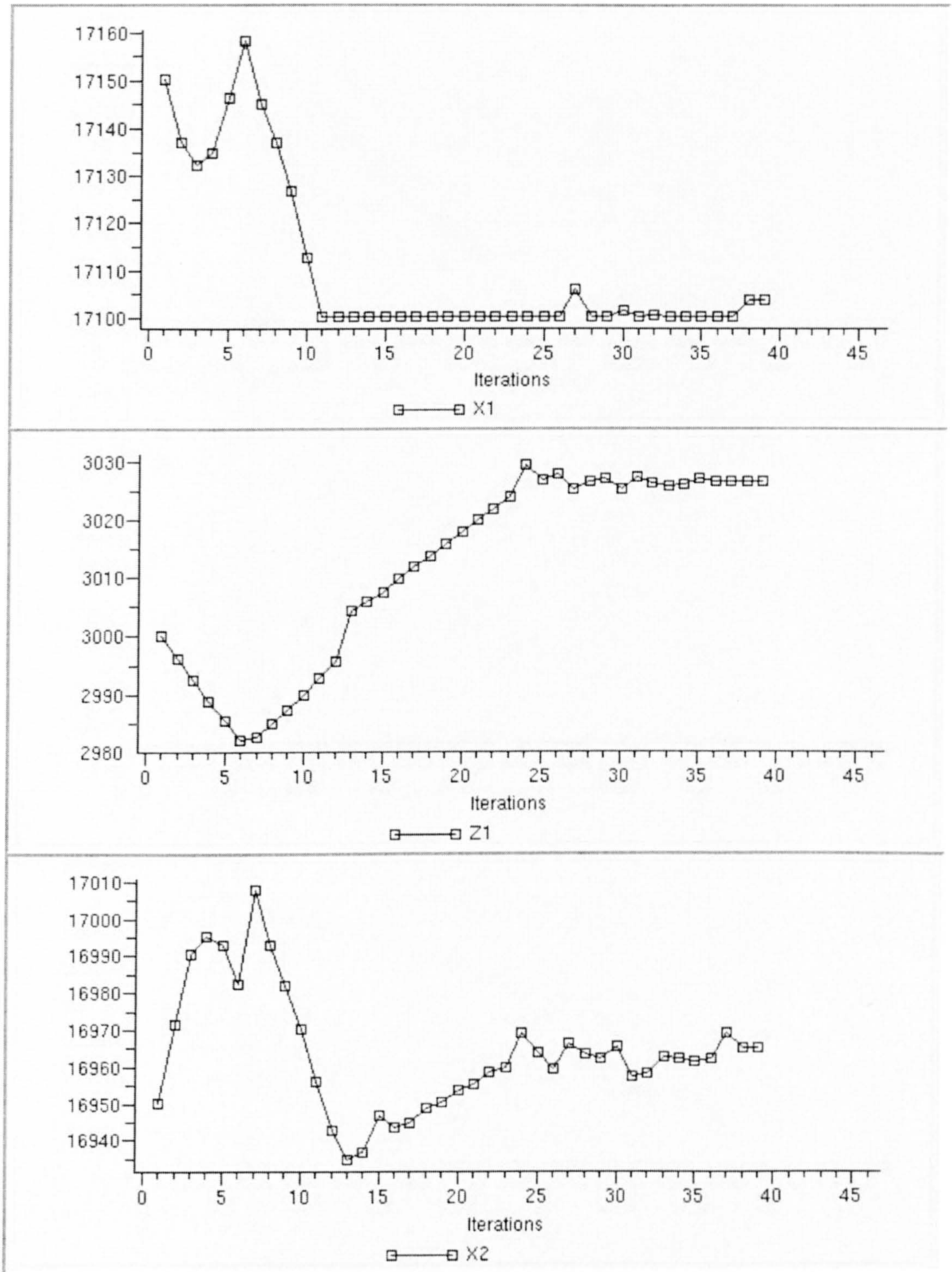
17160
17150
17140
17130
17120
17110
17100
0 5 10 15 20 25 30 35 40 45
Iterations
X1
3030
3020
3010
3000
2990
2980
0 5 10 15 20 25 30 35 40 45
Iterations
Z1
17010
17000
16990
16980
16970
16960
16950
16940
0 5 10 15 20 25 30 35 40 45
Iterations
X2

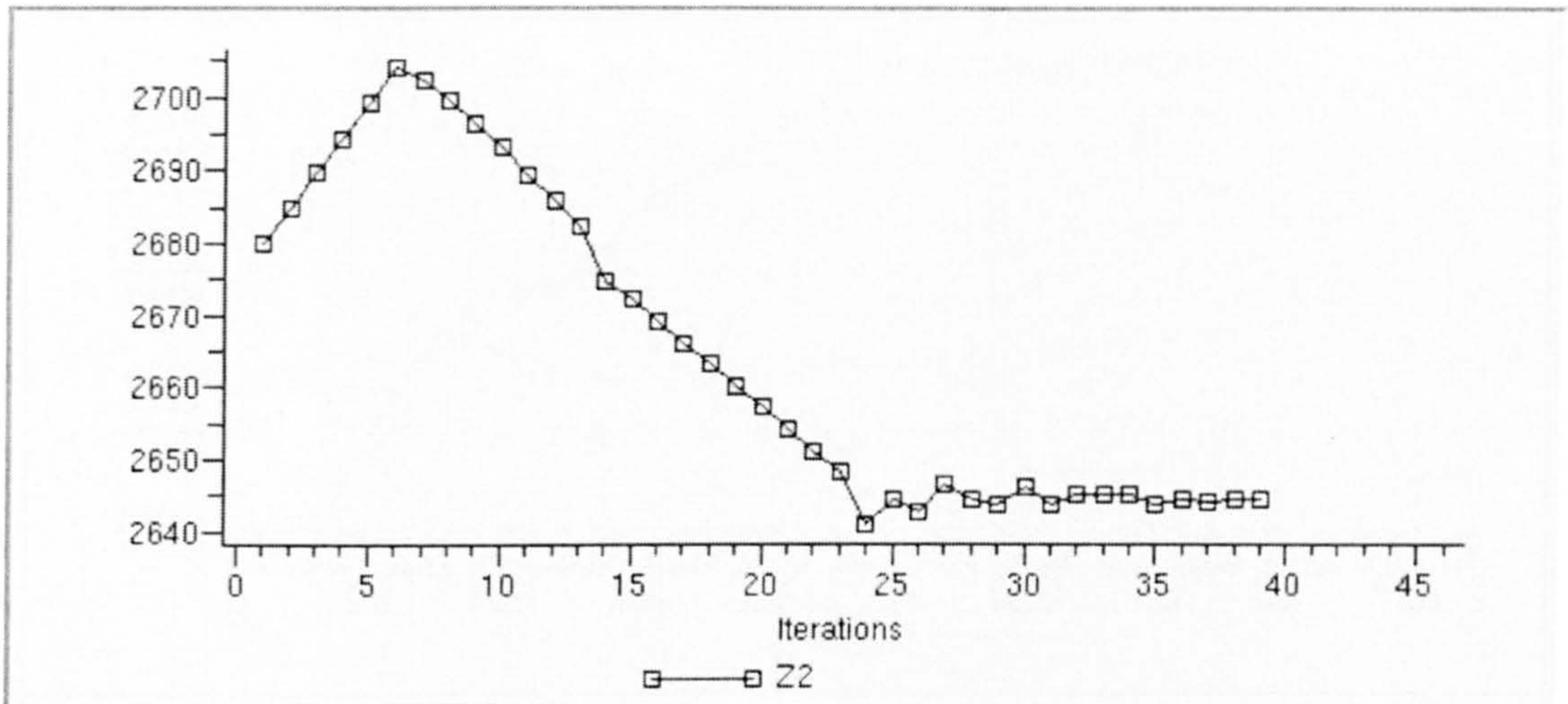
2700
2690
2680
2670
2660
2650
2640
0
5
10
15
20
25
30
35
40
45
Iterations
Z2

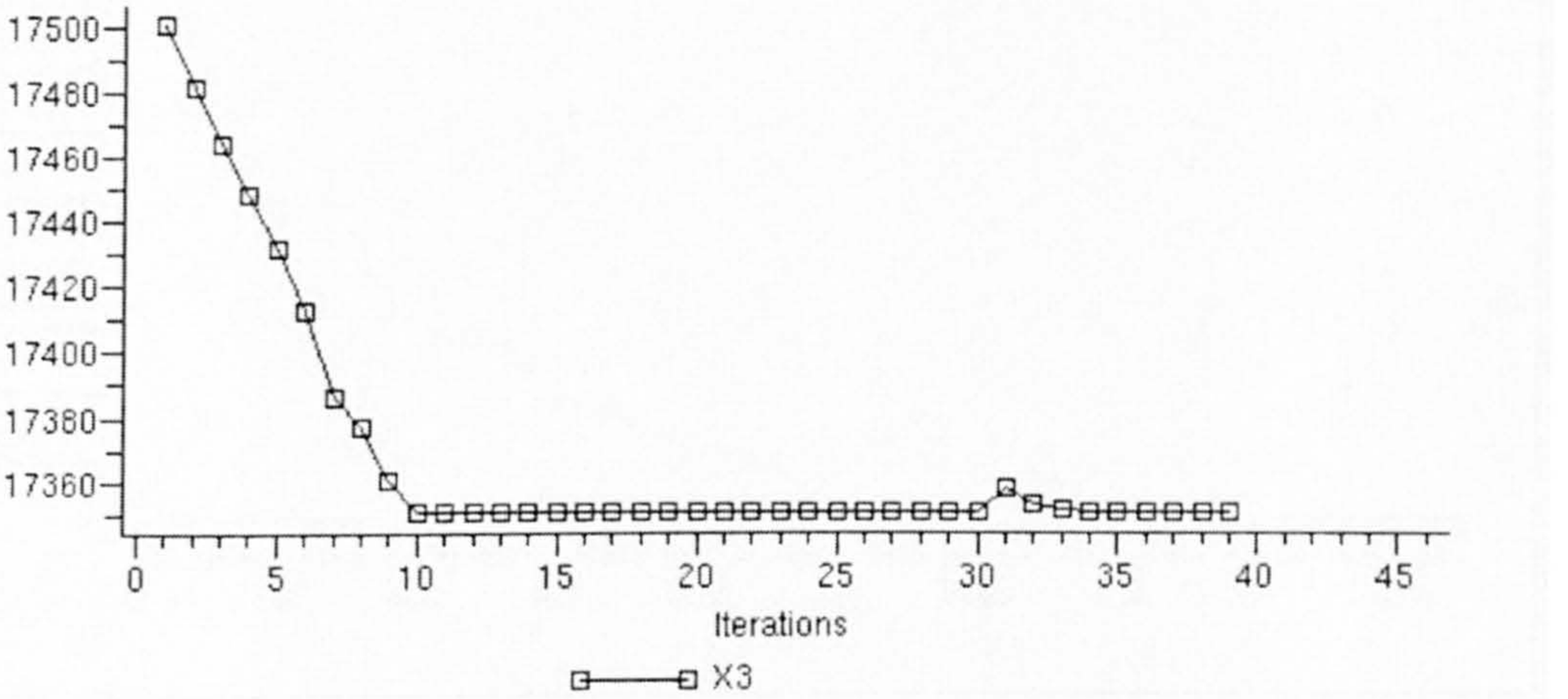
17500
17480
17460
17440
17420
17400
17380
17360
0
5
10
15
20
25
30
35
40
45
Iterations
X3

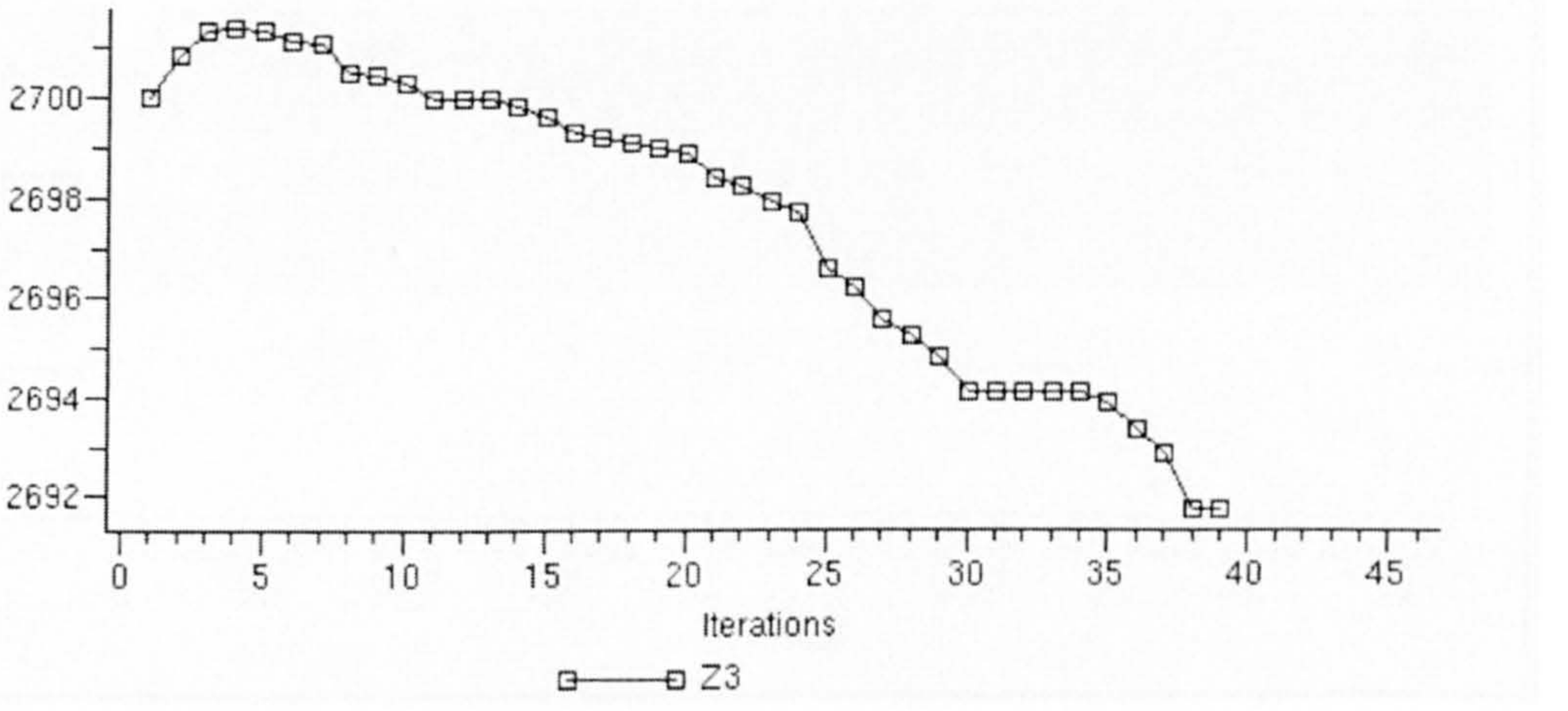
2700
2698
2696
2694
2692
0
5
10
15
20
25
30
35
40
45
Iterations
Z3

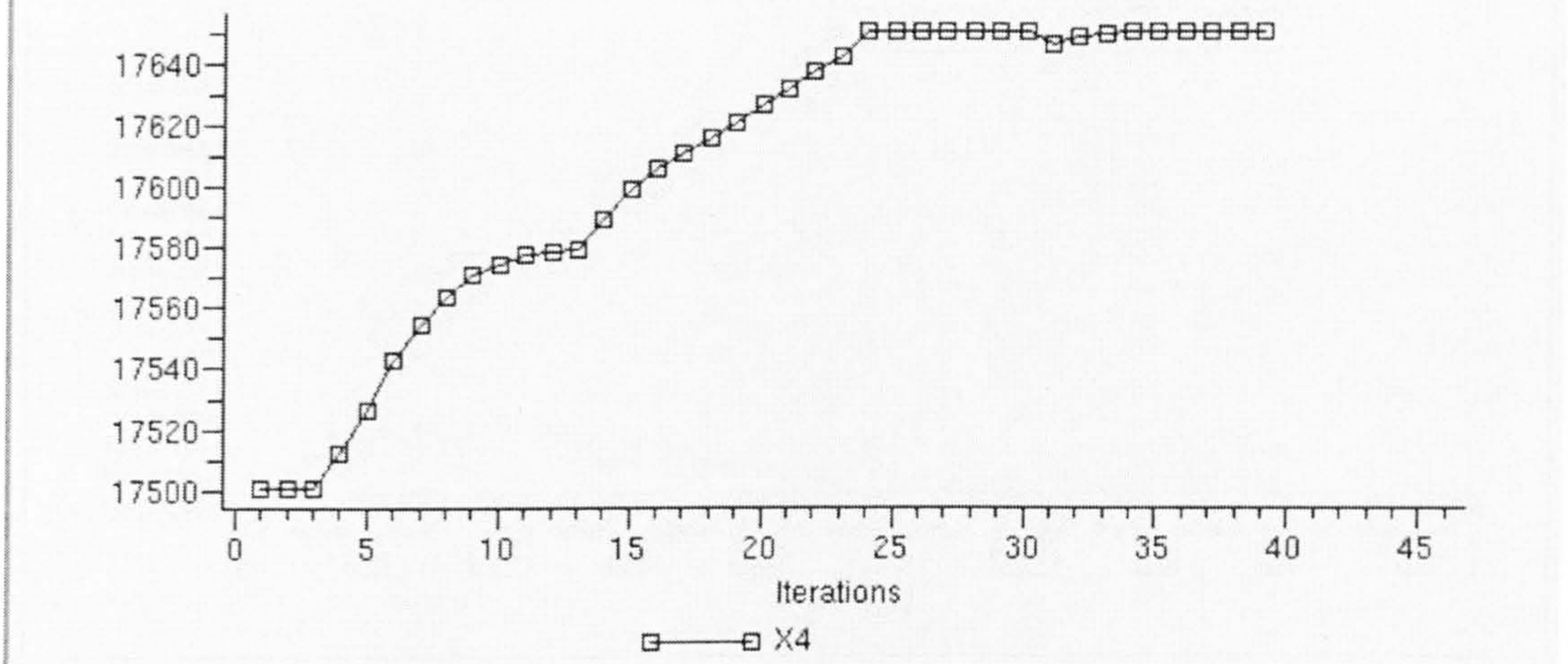

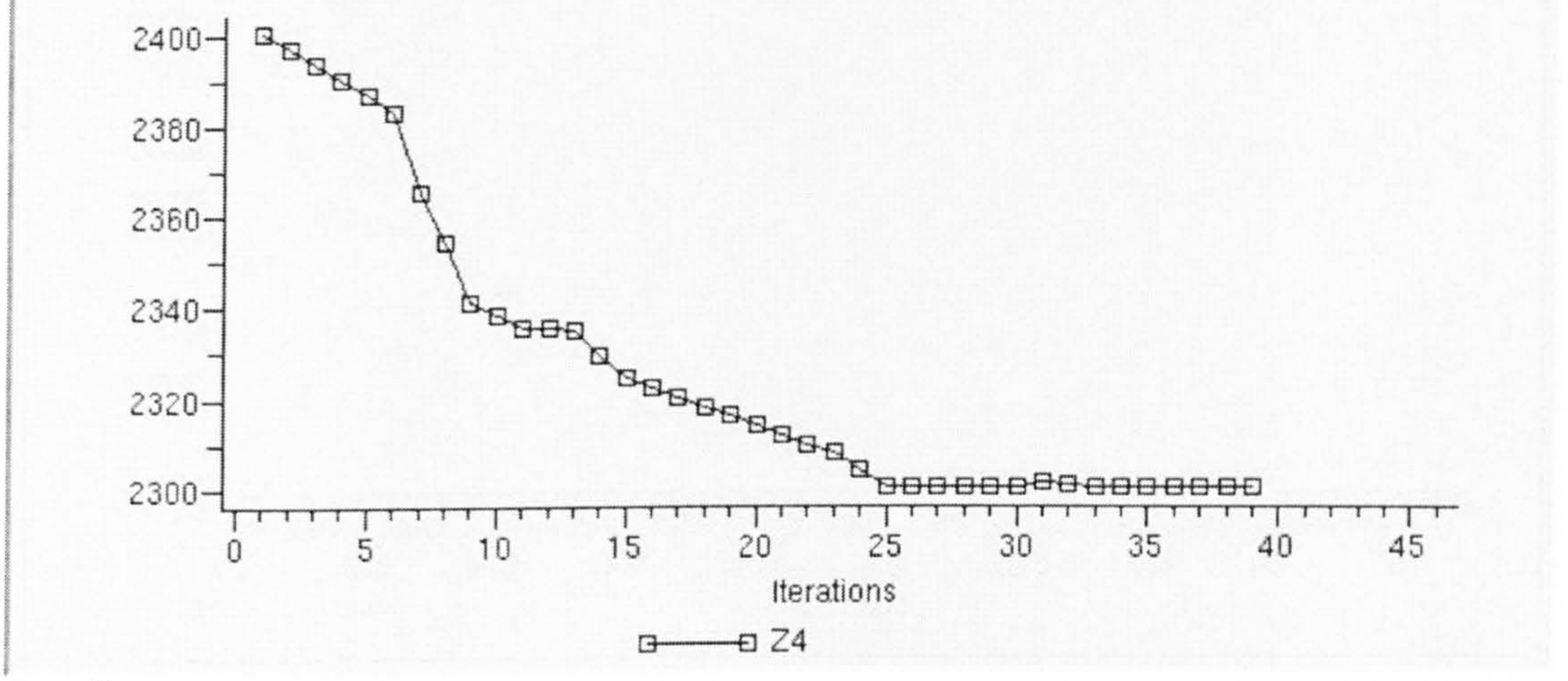

Functions:

Name	Objectif	Initial value	Iteration 39	Target value	Variation
DISTANCE_TE_PT	Minimize	647.034	3.51211	1	-99%
DISTANCE_LE_PT	Minimize	271.203	4.19311	1	-98%

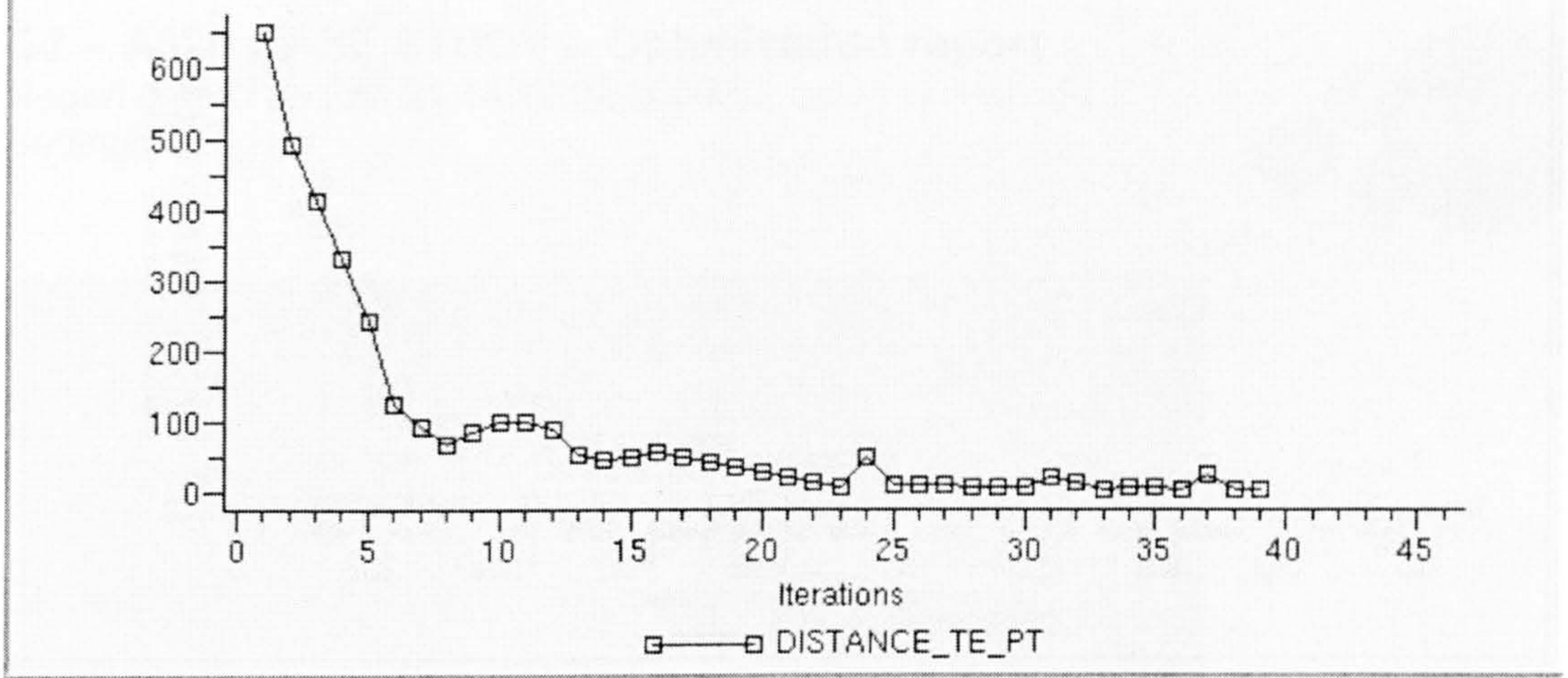
600
500
400
300
200
100
0
0
5
10
15
20
25
30
35
40
45
Iterations
DISTANCE_TE_PT

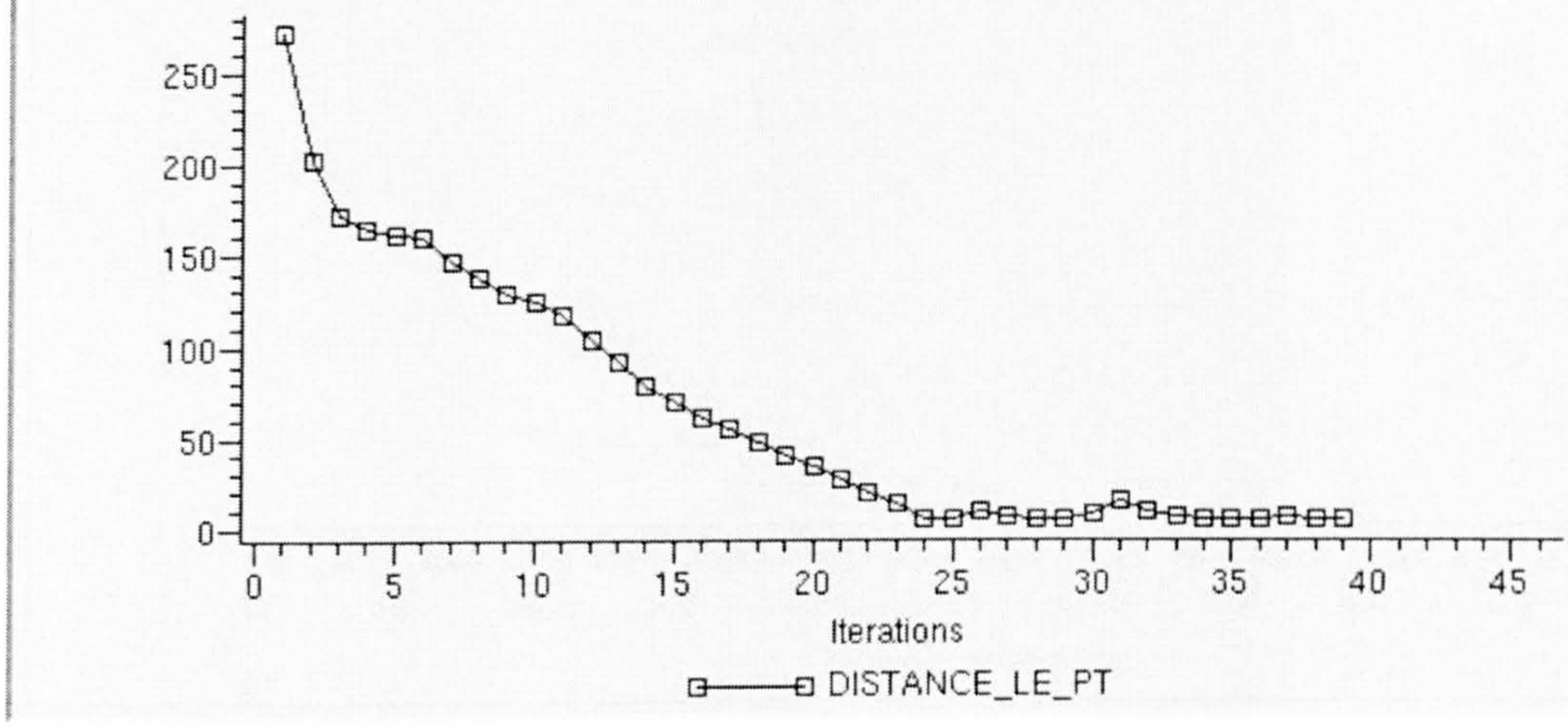
250
200
150
100
50
0
0
5
10
15
20
25
30
35
40
45
Iterations
DISTANCE_LE_PT

G2 – A320 CASE STUDY – Optimization report

Report date: Tue Feb 21 14:10:02 2006
Settings:

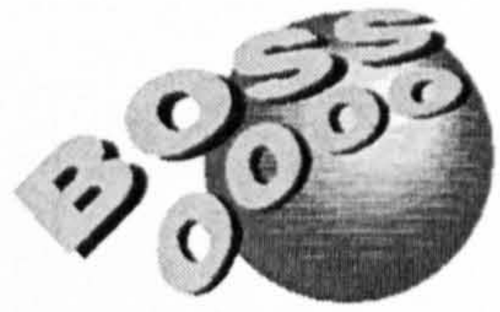

Type of study	Optimization
Algorithm	GCM
Convergence Precision	0.01
Convergence Criteria	Variation on variables -
Global perturbation	0.0001 (based on current value)
Move limit	No limit
Scaling of Variables	By individual factor
Scaling of Functions	Also when Multi-Objective
Check	Check Standard
Switch	Switch On
Listing	Delete
Moving Variables Bounds	Full Range
External Relaxation	Relaxation Disabled
Cut	Cut=10
Degressive Relaxation	DRelax Inactive

Variables:

Name	Lower bound	Initial value	Iteration 28	Upper bound
X1	16900	17096	16993.6	17300
Z1	2850	2950	3020.62	3050
X2	16700	16889	16916.2	17100
Z2	2580	2680	2585.93	2780
X7	17300	17504	17393	17700
X8	18050	18252	18450	18450
Z8	2380	2484	2523.05	2680
a	0.8	0.85	0.856061	0.9
b	0.15	0.19	0.189898	0.25
c	0.55	0.6	0.59974	0.65

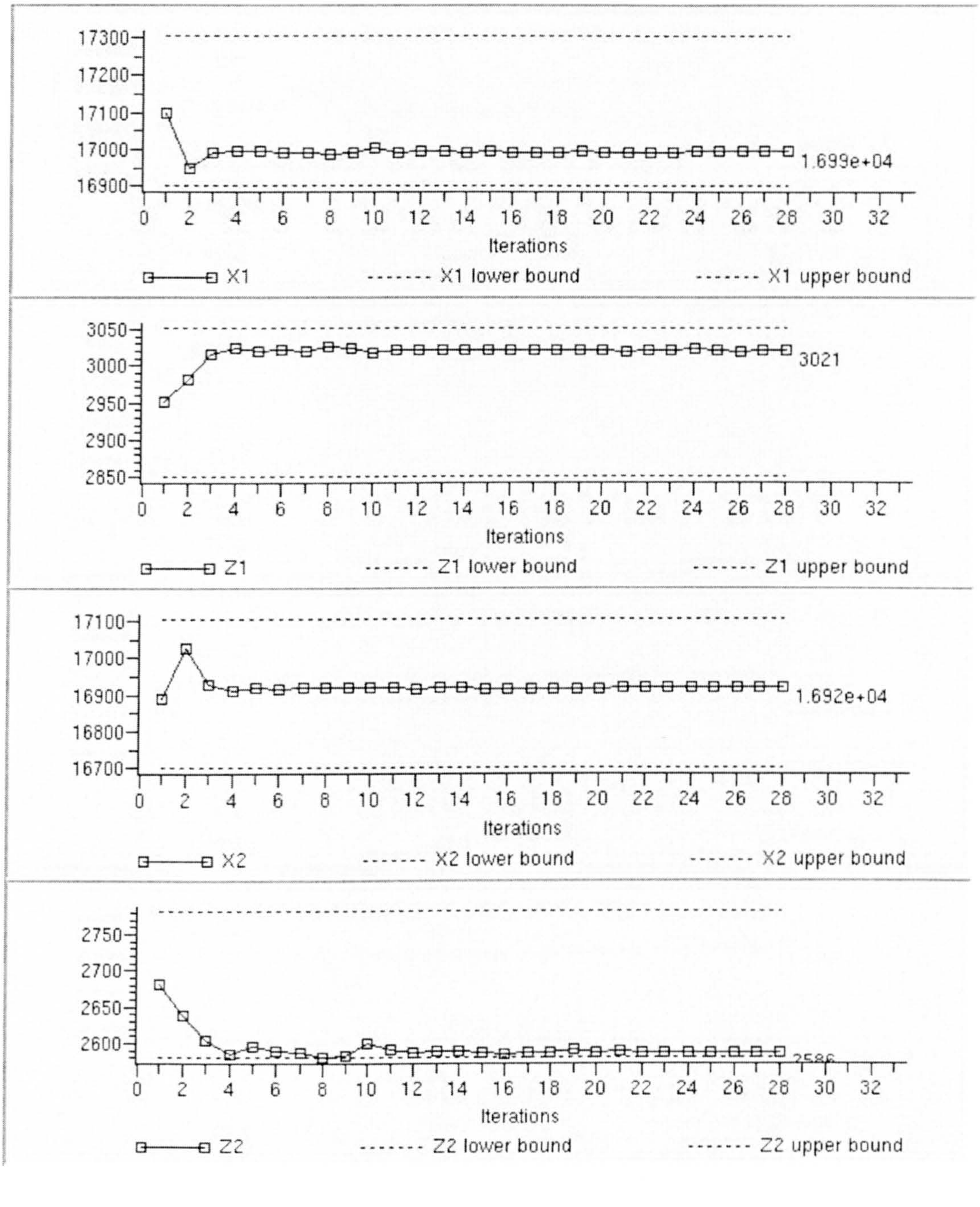
17300
17200
17100
17000
16900
1.699e+04
0 2 4 6 8 10 12 14 16 18 20 22 24 26 28 30 32
Iterations
X1
X1 lower bound
X1 upper bound
3050
3000
2950
2900
2850
3021
0 2 4 6 8 10 12 14 16 18 20 22 24 26 28 30 32
Iterations
Z1
Z1 lower bound
Z1 upper bound
17100
17000
16900
16800
16700
1.692e+04
0 2 4 6 8 10 12 14 16 18 20 22 24 26 28 30 32
Iterations
X2
X2 lower bound
X2 upper bound
2750
2700
2650
2600
0 2 4 6 8 10 12 14 16 18 20 22 24 26 28 30 32
Iterations
Z2
Z2 lower bound
Z2 upper bound

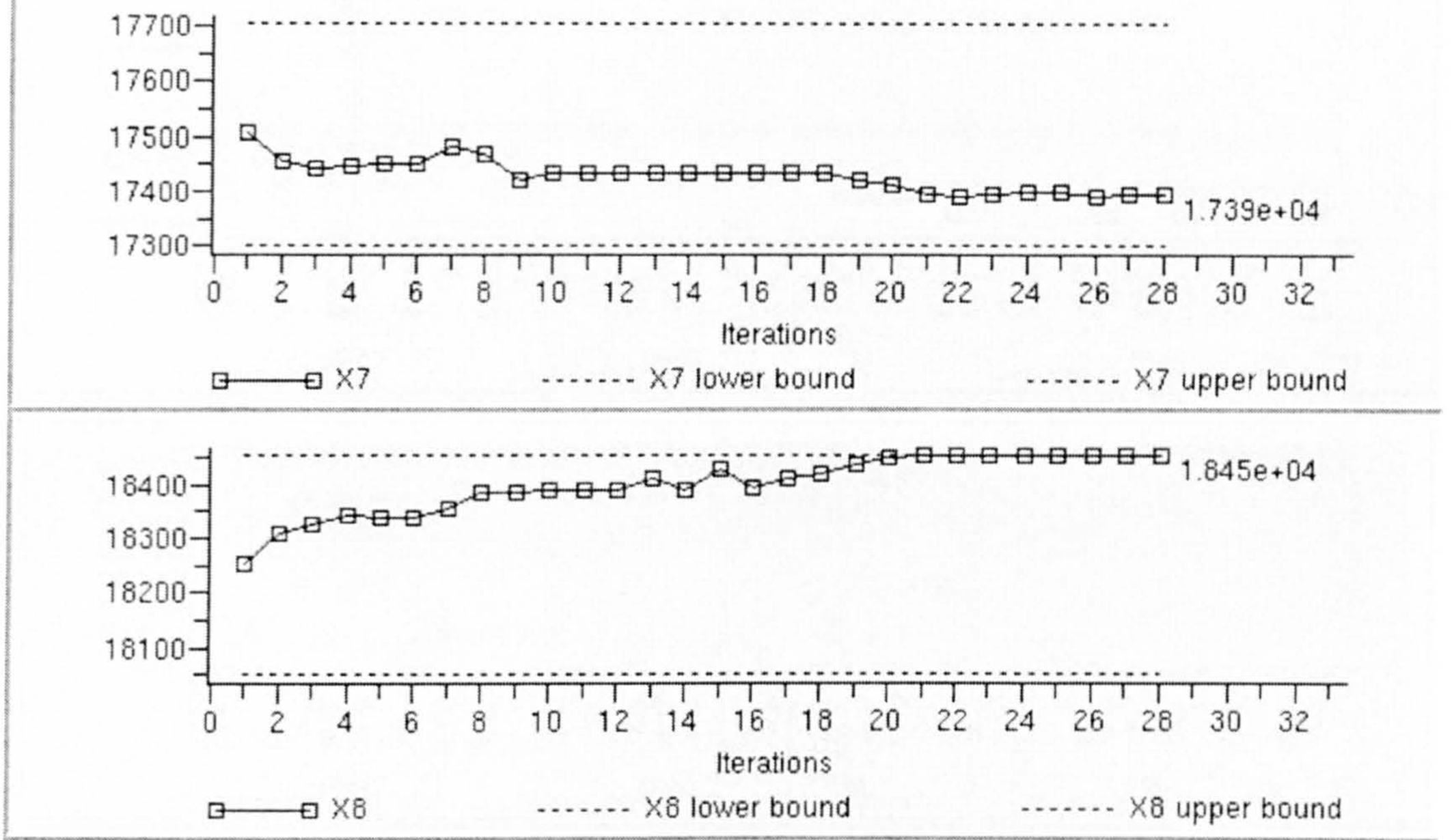
17700
17600
17500
17400
17300
1.739e+04
0 2 4 6 8 10 12 14 16 18 20 22 24 26 28 30 32
Iterations
X7
X7 lower bound
X7 upper bound
18400
18300
18200
18100
1.845e+04
0 2 4 6 8 10 12 14 16 18 20 22 24 26 28 30 32
Iterations
X8
X8 lower bound
X8 upper bound
2600
2500
2400
2523
0 2 4 6 8 10 12 14 16 18 20 22 24 26 28 30 32
Iterations
Z8
Z8 lower bound
Z8 upper bound
0.9
0.85
0.8
0.8561
0 2 4 6 8 10 12 14 16 18 20 22 24 26 28 30 32
Iterations
a
a lower bound
a upper bound
0.25
0.2
0.15
0.1899
0 2 4 6 8 10 12 14 16 18 20 22 24 26 28 30 32
Iterations
b
b lower bound
b upper bound

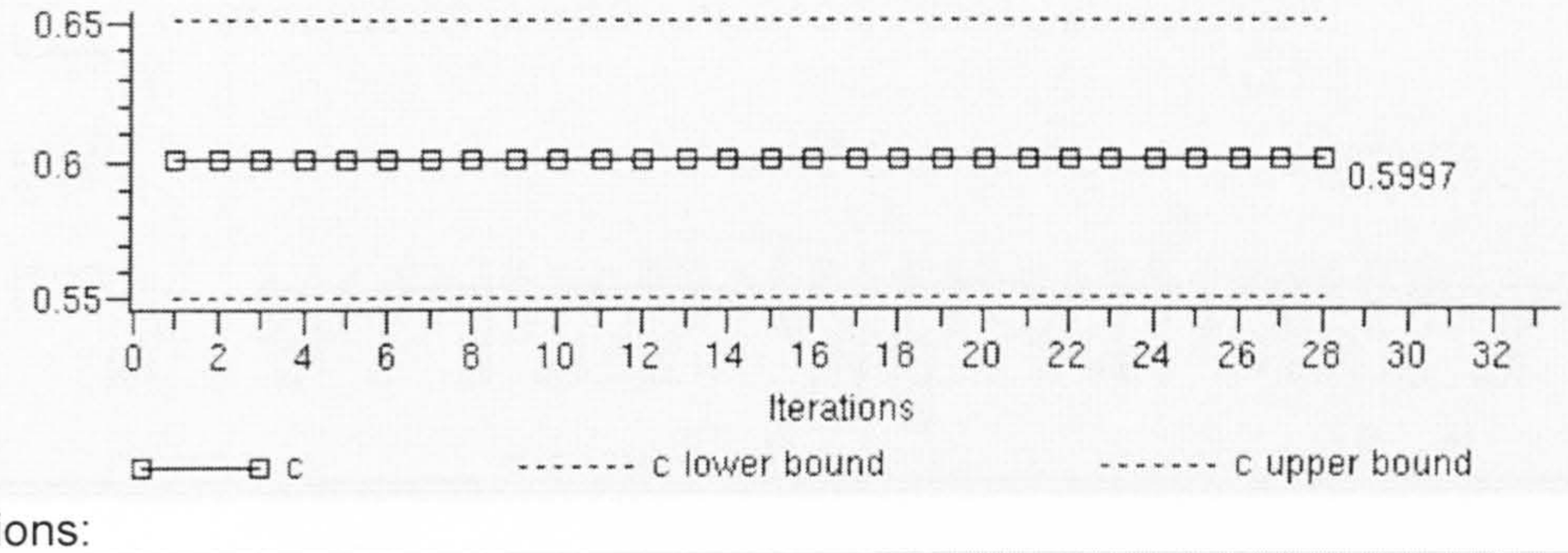

Functions:

Name	Objectif	Initial value	Iteration 28	Target value	Variation
DISTANCE_LE	Minimize	0 ... 62.2918	2.82909e-08 ... 17.3898	20	-72%
FINAL_TE_POSITION	Minimize	279.45	0.80451	0	-99%
FINAL_LE_POSITION	Minimize	184.64	1.1909	0	-99%
DISTANCE_TE	Minimize	0 ... 86.9302	9.36525e-08 ... 47.5571	50	-45%

Constraints:

Name	Lower bound	Initial value	Iteration 28	Upper bound
FINAL_TRACK_POSITION	20	98.2077	302.892	*****

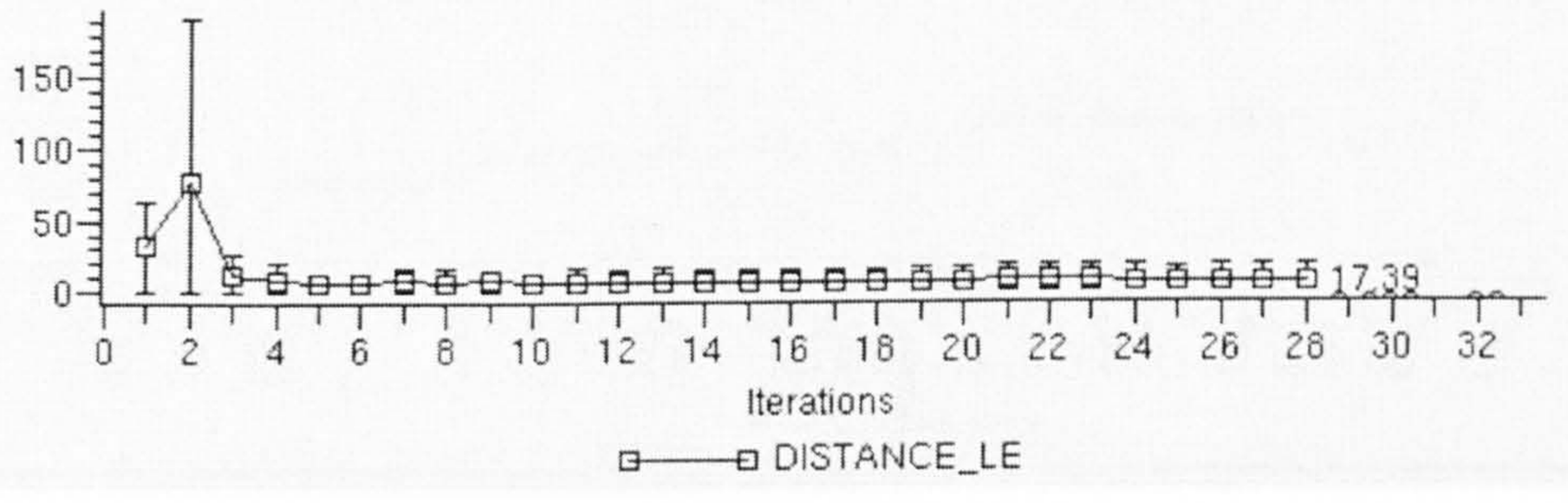

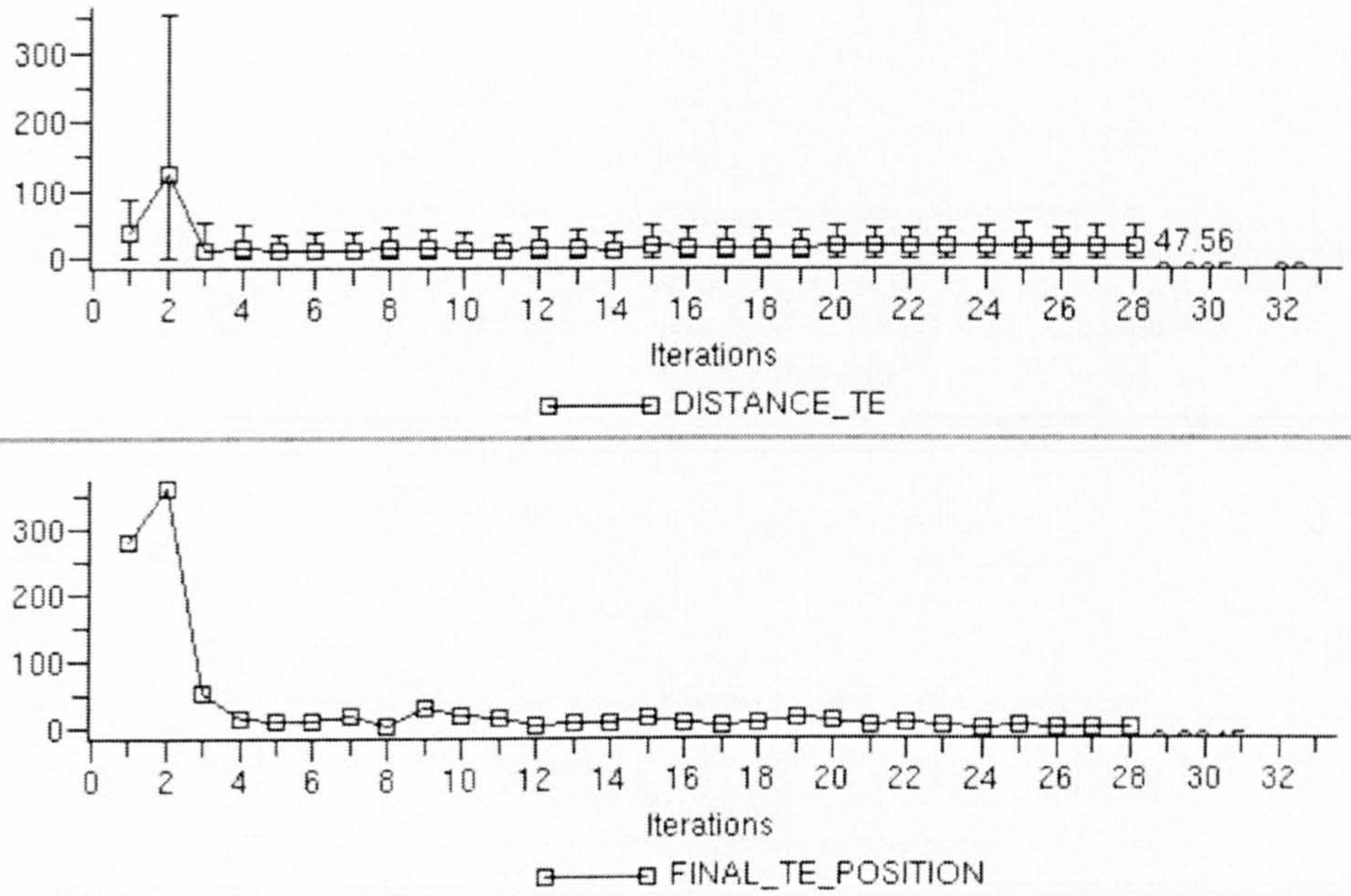
300
200
100
0
0 2 4 6 8 10 12 14 16 18 20 22 24 26 28 30 32
47.56
Iterations
DISTANCE_TE

300
200
100
0
0 2 4 6 8 10 12 14 16 18 20 22 24 26 28 30 32
Iterations
FINAL_TE_POSITION

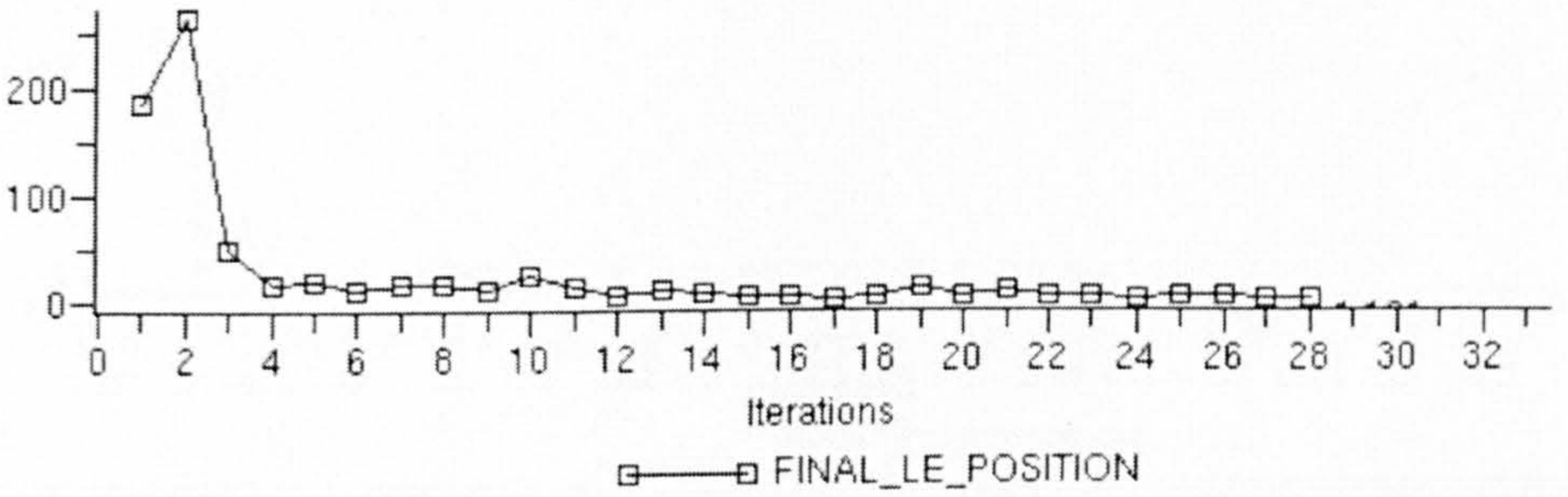
200
100
0
0 2 4 6 8 10 12 14 16 18 20 22 24 26 28 30 32
Iterations
FINAL_LE_POSITION

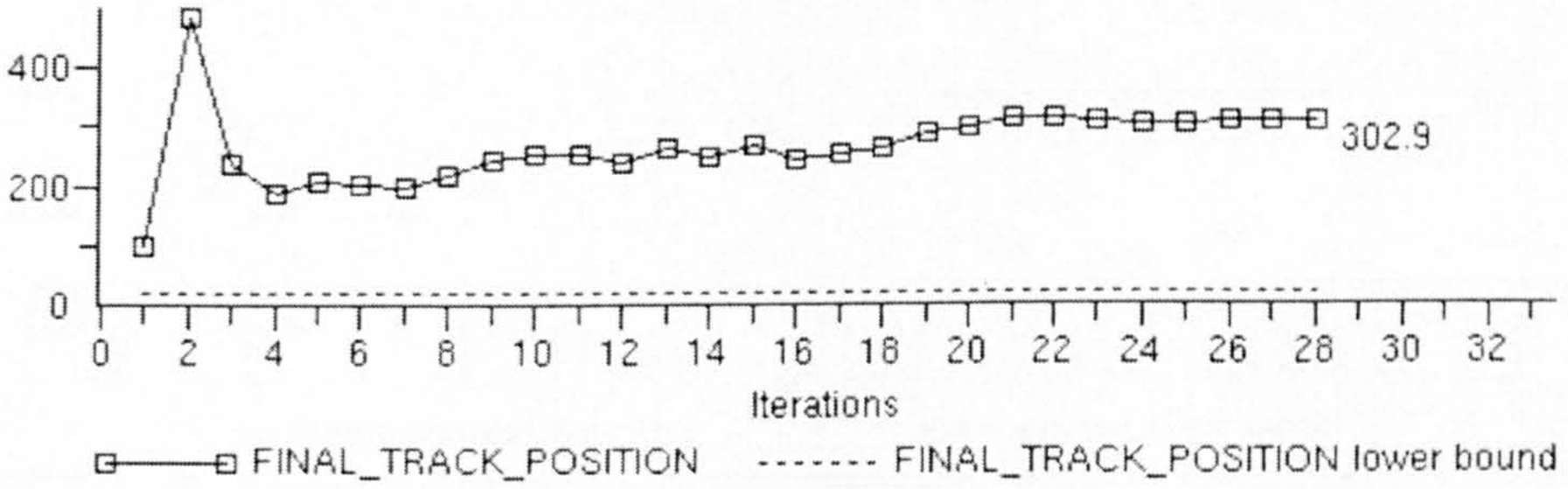
400
200
0
0 2 4 6 8 10 12 14 16 18 20 22 24 26 28 30 32
302.9
Iterations
FINAL_TRACK_POSITION
FINAL_TRACK_POSITION lower bound